The erosional and Cainozoic depositional history of the Lower Orange River, southwestern Africa

Volume 2

Roger Jürgen Jacob

BSc. (Hons.) (Rhodes, RSA)

A thesis presented for the degree of Ph.D.

University of Glasgow

Division of Earth Sciences

January 2005

© R. Jürgen Jacob 2005

Volume 1

Chapters 1 to 8

References

Volume 2

All Tables and Figures

Appendices A to D

List of Tables

Table 2.1 Distribution of the annual water resources within the Orange River drainage basin (after Everson 1999)..... 2

Table 2.2 Orange River gradient per reach..... 13

Table 2.3 Vaal River gradient per reach until the Orange River confluence..... 13

Table 3.1 Summary of tributary and Orange River characteristics per Geomorphic Reach..... 56

List of Figures

Figure 1.1 a) Drainage basin of the Orange/Vaal River system. b) Study area between Noordoewer and the Atlantic Ocean..... 1

Figure 2.1 Mean annual rainfall in the Orange River catchment..... 2
Figure 2.2 Simplified geological map of southern Africa. Stratigraphic table after SACS (1980). Geological GIS-based data acquired from the South African Council for Geoscience..... 3
Figure 2.3 Tectonic Provinces of southern Africa (after Shirley *et al.* 2001)..... 4
Figure 2.4 Digital terrain model of southern Africa showing elevated central plateau with the fringing "Great Escarpment" and low-lying coastal plain..... 4
Figure 2.5 Partridge & Maud's Cainozoic uplift areas and amounts (after Partridge 1998)..... 5
Figure 2.6 Burke's geomorphological development of Africa (after Burke 1996)..... 5
Figure 2.7 a) Estimated denudation amounts for southern Africa from apatite fission track thermochronology (AFTT, after Gallagher & Brown 1999). b) AFTT ages vs frequency (after Brown *et al.* 1990)..... 6
Figure 2.8 Reconstructions of the evolution of the Namibian margin (after Aizawa et al. 2000)..... 7
Figure 2.9 Summary of pre-1990 work on southwestern African drainage evolution in Post-Gondwana times (after de Wit 1993, 1999)..... 8
Figure 2.10 Summary of post-1990 work on southwestern African drainage evolution in Post-Gondwana times (after de Wit *et al.* 2000). 9
Figure 2.11 Longitudinal profiles of the Orange and Vaal River channels and topographic profiles for landscape 30 km north of the channels..... 10
Figure 2.12 Longitudinal profiles of the Orange and Vaal Rivers from source to the Atlantic Ocean showing the geology traversed..... 11
Figure 2.13 Semi-logarithmic longitudinal profiles of the Orange and Vaal Rivers..... 12
Figure 2.14 DS Plots of Orange and Vaal River longitudinal profiles..... 12
Figure 2.15 Gradient analysis of Reaches defined in figure 2.12..... 14

Figure 3.1 Satellite image of study area. 15
Figure 3. 2a Colour-coded DTM of study area (100 m intervals) showing topography and drainage 16
Figure 3. 2b Solid-shaded DTM of study area highlighting the topographic relief. Letters refer to section lines in figure 3.9 A-P..... 17
Figure 3.3 Simplified geological map of the study area. South African data, after de Villiers & Sohnge (1958). Namibian GIS-based data acquired from the Geological Survey of Namibia..... 18
Figure 3.4 Oblique aerial photos illustrating the incision of the Orange River into a landscape with a consistent summit level (500-600m) of the NMC basement rocks. Note the pre-Nama quartzite ridge in c)..... 19
Figure 3.5 The Fish River canyon to the northeast of the study area. a) Upstream canyon reach b) Mid-canyon reach c) Downstream canyon reach with Nama Group sedimentary cover removed from the underlying NMC basement..... 20

Figure 3.6 Satellite image showing superimposed route A as opposed to easier route A_1 and the short reach B occupying a Carboniferous age (Dwyka) glacial valley..... 21
Figure 3.7 Superimposed meanders (A and B) and reaches influenced by basement structures (C exploits path followed by dyke and D exploits regional foliation)..... 22
Figure 3.8 Photos illustrating the striated and polished surfaces and Dwyka tillite remnants present in the valley sidewalls of a short reach near Noordoewer..... 23
Figure 3.9 A-P Valley cross sections looking downstream (location of cross sections in figure 3.3)..... 24-27
Figure 3.10 Satellite image showing tributary network and their drainage basins. 28
Figure 3.11 Oblique aerial photograph showing Orange River (bottom right) and different sized tributaries. Large meandering tributary is the Fish River..... 28
Figure 3.12 Satellite image of study area showing Reaches 1-7..... 29
Figure 3.13 Comparison of overall characteristics per geomorphic reach. 30
Figure 3.14 Rotated 3-dimensional view of the Orange River channel and its tributary network in the study area..... 31
Figure 3.15 Figure 3.15 Longitudinal profiles of tributaries in relation to the Orange River profile..... 31
Figure 3.16 Figure 3.16 All tributary profiles in the study area. Low gradient tributary is the Fish River..... 31
Figure 3.17 Tributary drainage area vs gradient..... 32
Figure 3.18 Drainage area analysis of the tributary catchments for Reaches 1-7..... 32
Figure 3.19 Tributary gradient analysis per reach for equivalent drainage basin areas..... 33
Figure 3.20 Drainage area vs tributary gradient per Geomorphic Reach..... 34
Figure 3.21 Comparison between DGPS profiles and digitised profiles from the 1:50 000 scale topographic maps with a 20m contour interval..... 35
Figure 3.22 A-L Tributary profiles colour-coded per reach..... 36-39
Figure 3.23 Knickpoints in tributaries from Reach 7; a-d) Tributary No.57 (Fig.3.22H); e) Tributary No.61 (Fig.3.22F); f) Bar EQ tributary (Fig.3.22E); g-h) Bar EM tributary (Fig.3.22J)..... 40
Figure 3.24 Profiles along selected tributaries in Reach 2..... 41
Figure 3.25 Photos illustrating the flat-topped nature of the Rosyntjieberg mountains. Deeply incised tributary in a) is the Bar AH tributary in (Fig.3.24c)..... 42
Figure 3.26 Comparison of longitudinal profiles of the modern Orange River in the study area obtained by different means..... 43
Figure 3.27 Differential global positioning system (DGPS) equipment used in measuring Orange River surface profile..... 43
Figure 3.28 Echo sounding equipment used in measuring Orange River bottom profile..... 43
Figure 3.29 Surface and bottom profiles of the modern Orange River in the study area..... 44
Figure 3.30 Surface and bottom profiles of the modern Orange River colour-coded per Geomorphic Reach. 45
Figure 3.31 Surface and bottom profiles with underlying geological reaches (Geological units identified in figure 3.32)..... 46
Figure 3.32 a) Location and b) data from the geological reaches of the profile presented in figure 3.31..... 47

Figure 3.33 Plot of tensile strength vs rock erodability for various lithologies (after Sklar & Dietrich 2001)..... 48
Figure 3.34 Analysis of the effect of flow direction on gradient for north-south and east-west reaches..... 48
Figure 3.35 Surface profile showing geological contacts (green) and tributary input deltas (red) responsible for steps in the profile..... 49
Figure 3.36 Example of the Boom River tributary input bar. a) In rare flood during April 2002 - note the dark, sediment laden water and large boulder being tumbled down the channel (photo courtesy of J.Botes). b) Aerial view of the same tributary in December 2002. Note the channel constriction and turbulence at point of constriction and the presence of bedrock in the rapid..... 50
Figure 3.37 Surface and bottom profile showing the effect of coarse gravel bars on the profile (areas of interest are within oval shapes). Red lines above the profile are tributary input deltas..... 51
Figure 3.38 Surface and bottom profile showing the effect of tributary fans on the profile (areas of interest are within oval shapes). Red lines above the profile are tributary input deltas..... 52
Figure 3.39 Inner channels with flanking straths in the study reach (flow direction indicated)..... 53
Figure 3.40 Inner channel in the Sambok area displaying abundant features indicating recent incision..... 54
Figure 3.41 Schematic diagram illustrating the effect of tributaries on the trunk stream..... 55

Figure 4.1 Figure 4.1 Satellite image of study area showing the distribution of Proto and Meso Orange River terrace suites..... 57
Figure 4.2 a) Oblique aerial view showing Proto and Meso Terraces at Daberas b) Oblique aerial view showing Pre-Proto1, Proto and Meso terraces at Sendelingsdrif. Note that terrace labelled as P2 is a lower terrace than P1, however they are underlain by the same bedrock strath, hence both are classified as Proto terraces..... 58
Figure 4.3 Sequence of Orange River deposits at one locality..... 59
Figure 4.4 Satellite image showing Proto-Orange deposits between Reuning Mine and Arrisdrif and the Proto-Orange and Meso-Orange River courses..... 60
Figure 4.5 a) Type 1 terrace preserved by meander cutoff on straightening of channel. b) Type 2 terraces preserved by lateral erosion of meander prior to incision. c) Type 3 terraces preserved downstream of tributary input delta. d) Type 4 terrace formed by dissection of modern channel, leaving paired terraces..... 61
Figure 4.6 Analysis of terrace types per reach for Proto and Meso terraces..... 62
Figure 4.7 Survey data from Noordoewer to the river mouth used to construct longitudinal profiles..... 63
Figure 4.8 Pre-Proto and Proto longitudinal profiles of bedrock straths from Noordoewer to the mouth..... 64
Figure 4.9a Bedrock surface of the Sendelingsdrif deposit obtained from percussion drilling data..... 65
Figure 4.9b Bedrock surface of the Daberas Proto deposit obtained from percussion drilling data..... 66
Figure 4.9c Bedrock surface of the Auchas Major Proto deposit obtained from percussion drilling data..... 67
Figure 4.9d Bedrock surface of the Auchas Lower deposit obtained from percussion drilling data..... 68

Figure 4.9e Bedrock surface of the Arrisdrif Proto deposit obtained from percussion drilling data..... 69
Figure 4.10 Oblique aerial views of Proto Orange River bedrock surface at Daberas showing straths, scours and inner channels. Surface was based on drilling data, created using Vulcan modelling software..... 70
Figure 4.11 Various features of the bedrock surface at Auchas Major, exposed by mining operations..... 71
Figure 4.12 Figure 4.12 Scour filling of Pre-Proto 2 scours a) Xarries North, where Meso gravel overlies scour filled by Pre-Proto 2 gravel b) Lorelei East Pre-Proto c) Close-up of Lorelei East gravel face - note the large bedrock rafts..... 72
Figure 4.13 Pre-Proto and Proto longitudinal profiles from Noordoewer to the mouth..... 73
Figure 4.14 Pre-Proto and Proto longitudinal profiles from Noordoewer to the mouth showing sections through some deposits along the profile..... 74
Figure 4.15 Intermediate terrace longitudinal profile. Note the restricted longitudinal occurrence of this group of terraces..... 75
Figure 4.16 Upper Meso terrace longitudinal profile from Noordoewer to the river mouth..... 76
Figure 4.17 Upper Meso terrace longitudinal profile from Noordoewer to the river mouth showing sections through some deposits along the profile..... 77
Figure 4.18 Lower Meso terrace longitudinal profile from Noordoewer to the river mouth..... 78
Figure 4.19 Longitudinal profiles of the terraces from Renosterkop (near Augrabies Falls) to the river mouth..... 79
Figure 4.20 Interpretation 1 of the sequence of Type 2 unpaired terraces. Progressive incision and valley widening on meander bends, punctuated by periods of alluviation..... 80
Figure 4.21 Interpretation 2 of the sequence of type 2 unpaired terraces. Initial incision and valley widening, followed by long period of alluviation and gradual incision into valley fill..... 81
Figure 4.22 Cainozoic sea level curves (modified after Siesser & Dingle 1981)... 82
Figure 4.23 Longitudinal profiles and gradients of all bedrock strath surfaces in study area..... 83

Figure 5.1 Figure 5.1 a) Typical bar surface sampled on modern riverbars. b) Typical gravel face sampled from terrace deposits. Ranging rod is 2 m long. c) Chart used to visually estimate clast roundness after Powers (1953)..... 84
Figure 5.2 Bar categories a) Tributary input bar b) Strath bar c) Normal bar..... 85
Figure 5.3 Modern river maximum clast size (MCS) measuring locations, colour-coded per bar type..... 86
Figure 5.4 Figure 5.4 Simplified stratigraphic table illustrating clast types found in the Orange River deposits and clast provenance, adapted from (SACS, 1980)..... 87
Figure 5.5 a-k Clast types of the MCS dataset..... 88-91
Figure 5.6 Figure 5.6 a-c) Modern river average maximum clast size (MCS) and d) Clast length standard deviation per bar from Modderdrif to Hohenfels..... 92
Figure 5.7 Controls on tributary input bar clast size a) Tributary gradient b) Tributary drainage basin area c) Clast lithology..... 93

Figure 5.8 a-b Position of the 4 major downstream fining sedimentary links as defined in dataset c) Position of Links 1-4 within the study reach.... 94
Figure 5.9 Clast length vs distance downstream for Links 1 to 4 with composition % vs distance downstream for all normal and strath bars in study reach. Link changes coincide with the addition of resistant lithologies to the normal bar population..... 95
Figure 5.10 Pie charts showing composition of the MCS population on the normal and strath bars in the study reach. Links 1 to 4 are shown. Note the dominance of different lithologies in the MCS composition in each Link (cf. Fig.5.11)..... 96
Figure 5.11 Figure 5.11 Pie charts showing the composition of the MCS population on the tributary input bars in the study reach (cf. Fig.5.10)..... 97
Figure 5.12 Comparison between the maximum clast size (MCS) population composition of tributary input and normal bars (comprising normal and strath bars) for the entire dataset in the study reach..... 98
Figure 5.13 Comparison between the MCS population composition of tributary input and normal bars for Link 1. 99
Figure 5.14 Comparison between the MCS population composition of tributary input and normal bars for Link 2..... ..100
Figure 5.15 Comparison between the MCS population composition of tributary input and normal bars for Link 3..... ..101
Figure 5.16 Comparison between the MCS population composition of tributary input and normal bars for Link 4..... ..102
Figure 5.17 a-d Comparison between the MCS population composition of tributary input and normal bars for Reaches 1 to 4..... ..103
Figure 5.18 a-c Comparison between the MCS population composition of tributary input and normal bars for Reaches 5 to 7..... ..104
Figure 5.19 Clast length reduction percentage per lithology for each link - calculated by difference between average tributary input and normal bar clast size..... ..105
Figure 5.20 Average clast length per normal bar vs distance downstream for prominent lithologies in the study reach..... ..106
Figure 5.21 Average clast roundness per normal bar vs distance downstream for prominent lithologies in the study reach..... ..107
Figure 5.22 Figure 5.22 Average clast length per bar vs distance downstream for tributary and normal bars for prominent lithologies in the study reach. 108
Figure 5.23 Clast roundness differences in proximal and distal normal bars in Link 4, mainly due to the decrease in rounding with decreasing clast size..... ..109
Figure 5.24 Clast size and roundness differences between adjacent point and strath bars..... ..110
Figure 5.25 a) Location of selected bar measure sites. b) MCS decline on individual bars in a downstream direction. c) MCS decline on individual bars with MCS data per bar for the entire study reach..... ..111
Figure 5.26 MCS vs distance along channel per gravel age. a) Along entire study reach (Noordoewer to the mouth) b) Along Link 4 (Boom River to the mouth) for Nama quartzite population c) Photos illustrating values in b) at the Boom River, Sendelingsdrif and Arrisdrif..... ..112
Figure 5.27 Pie charts showing the comparison of the MCS assemblage through time per site..... ..113

Figure 6.1	Figure 6.1 a) Typical face of gravel that was sampled for clast assemblage analysis. Ranging rod is 2m long. b) Close-up view of face illustrating area which was excavated and sieved. c) Sampling equipment used.....	..114
Figure 6.2	Clasts assemblage analysis per size fraction: amount of clasts sorted per size fraction.....	..115
Figure 6.3	Regional satellite image from Augrabies Falls to the mouth showing the location of the clast assemblage samples taken in this study.....	..116
Figure 6.4a	Clast assemblage samples analysed in the study reach between Noordoewer and the mouth.....	..117
Figure 6.4b	Clast assemblage samples analysed in the Augrabies Falls area.....	..118
Figure 6.4c	Clast assemblage samples analysed in the Buntfeldschuh/Bogenfels Area.....	..119
Figure 6.5	a-i Clast types limited to the finer size fractions.....	120-122
Figure 6.6	Distribution of Proto and Meso terraces in the Noordoewer area.....	..123
Figure 6.7	Clast type proportions per size fraction and average clast roundness per size fraction for samples in the Noordoewer area.	..124
Figure 6.8	Distribution of Meso terraces in the Seven Pillars area.....	..125
Figure 6.9	Clast type proportions per size fraction and average clast roundness per size fraction for samples in the Seven Pillars area.	..126
Figure 6.10	Distribution of Proto, Intermediate and Meso terraces in the Grasdrif/Aussenkjer area.....	..127
Figure 6.11a	Clast type proportions per size fraction and average clast roundness per size fraction for samples in the Grasdrif/Aussenkjer area.....	..128
Figure 6.11b	Clast type proportions per size fraction and average clast roundness per size fraction for samples in the Grasdrif/Aussenkjer area including the +2 and +1mm sand fractions.....	...129
Figure 6.12	Distribution of the Meso terrace in the Gamkab River area.....	..130
Figure 6.13	Clast type proportions per size fraction and average clast roundness per size fraction for samples in the Gamkab River area.....	..131
Figure 6.14	Distribution of the Meso terraces in the Block 6 area.	..132
Figure 6.15	Clast type proportions per size fraction and average clast roundness per size fraction for samples in the Block 6 area.....	..133
Figure 6.16	Distribution of the Meso terraces in the Fish River area.....	..134
Figure 6.17	Clast type proportions per size fraction and average clast roundness per size fraction for samples in the Fish River area.....	..135
Figure 6.18	Distribution of Proto and Meso terraces in the Boom River and Dabimub areas.....	..136
Figure 6.19	Clast type proportions per size fraction and average clast roundness per size fraction for samples in the Boom River area.....	..137
Figure 6.20	Distribution of Proto and Meso terraces in the Lorelei East area.....	..138
Figure 6.21	Clast type proportions per size fraction and average clast roundness per size fraction for samples in the Lorelei East area.....	..139
Figure 6.22	Distribution of Proto, Intermediate and Meso terraces in the Lorelei West area.....	..140
Figure 6.23	Clast type proportions per size fraction and average clast roundness per size fraction for samples in the Lorelei West area.....	..141
Figure 6.24	Distribution of Pre-Proto 1, Proto and Meso terraces in the Sendelingsdrif area.....	..142
Figure 6.25	Clast type proportions per size fraction and average clast roundness per size fraction for samples in the Sendelingsdrif area.....	..143
Figure 6.26	Distribution of Proto and Meso terraces in the Daberas area.....	..144

Figure 6.27	Clast type proportions per size fraction and average clast roundness per size fraction for samples in the Daberas area.....	..145
Figure 6.28	Distribution of Proto and Meso terraces in the Auchas Major area...	..146
Figure 6.29a	Clast type proportions per size fraction and average clast roundness per size fraction for samples in the Auchas Major area.....	..147
Figure 6.29b	Clast type proportions per size fraction and average clast roundness per size fraction for samples in the Auchas Major area including the +2 and +1mm sand fractions.....	..148
Figure 6.30	Distribution of Proto and Meso terraces in the Auchas Lower area...	..149
Figure 6.31	Clast type proportions per size fraction and average clast roundness per size fraction for samples in the Auchas Lower area.....	..150
Figure 6.32	Distribution of Proto and Meso terraces in the Arrisdrif area.....	..151
Figure 6.33	Clast type proportions per size fraction and average clast roundness per size fraction for samples in the Arrisdrif area.....	..152
Figure 6.34	Distribution of Proto and Meso terraces in the Oranjemund area.....	..153
Figure 6.35	Clast type proportions per size fraction and average clast roundness per size fraction for samples in the Oranjemund area.....	..154
Figure 6.36	Clast type proportions per size fraction and average clast roundness per size fraction for samples in the Buntfeldschuh/Bogenfels area....	..155
Figure 6.37	Clast type proportions per size fraction and average clast roundness per size fraction for samples in the Augrabies Falls area.....	..156
Figure 6.38	Figure 6.38 Summary of clast assemblages per gravel suite in the study area.....	..157
Figure 6.39	Clast assemblage and roundness changes in the Eocene suite of gravels.....	..158
Figure 6.40	Clast assemblage and roundness changes in the Pre-Proto deposits...	..159
Figure 6.41	Clast assemblage and roundness changes and longitudinal profile of the Proto lower gravels.....	..160
Figure 6.42	A-Q Clast assemblage and roundness changes in the Meso suite of deposits.....	161-162
Figure 6.43	Clast assemblage and roundness changes in the Modern deposits.	..163
Figure 6.44	Summary of clast assemblage changes per terrace suite within the study area, grouped into upstream, mid and downstream reaches.	..164
Figure 6.45	Changes in clast assemblage maturity downstream for Proto, Meso and modern deposits, using the ratio of quartzite and quartz to more labile lithologies.....	..165
Figure 6.46	Nama quartzite roundness vs distance downstream for Proto, Meso and modern deposits between the Boom River and the mouth.....	..166
Figure 6.47	Summary of clast asemblage changes in the Lower Orange River from Eocene to modern, for the exotic suite of clasts.....	..167
Figure 6.48	Breakdown of the BIF types in the samples analysed.....	..168
Figure 6.49	Distribution of BIF types in the a) Eocene b) Pre-Proto c) Proto d) Meso and e) Modern samples (legend is in figure 6.48).....	..169
Figure 6.50	Downstream changes in the BIF assemblages of the Proto, Meso and modern deposits within the study reach (legend is in figure 6.48).....	..170
Figure 6.51	Stratigraphy of the iron formations in the Asbestos Hills Subgroup of the Ghaap Group (after Beukes 1986).....	..171
Figure 6.52	a-f Gravel composition, based on the weight percentage of gravel....	172-173
Figure 6.53	Summary of clast assemblage changes through time in the study reach.....	..174

Figure 7.1 Distribution of kimberlites and alluvial deposits in southern Africa with outline of the Kaapvaal Craton shown..... ..175
Figure 7.2 Fixed and mixed and mobile trapsites and their depositional environments in the Lower Orange River deposits..... ..176
Figure 7.3 Satellite image showing the average diamond size per deposit where available..... ..177
Figure 7.4 a) Grade vs average stone size plot at Auchas Major locality. b) Size frequency distribution of Auchas bar and channel samples..... ..178
Figure 7.5 Auchas Mine actual bedrock surface with grades and stones size obtained from gravel directly overlying the bedrock 179
Figure 7.6 Sections through the Auchas Mine deposit showing grades obtained from mining operations in the upper units of the deposit..... ..180
Figure 7.7 Summary of grade and stone size changes in the study area. Grade data in deposits older than Pre-Proto 2 not comparable, hence the uncertainty..... ..181

List of Appendices

Appendix A	Surface and bottom profile survey of the modern Orange River.....	182
Appendix B	Terrace levels data.....	183-184
Appendix C	Maximum clast size dataset.....	185
Appendix D	Clast Assemblage with grain size data	186-265

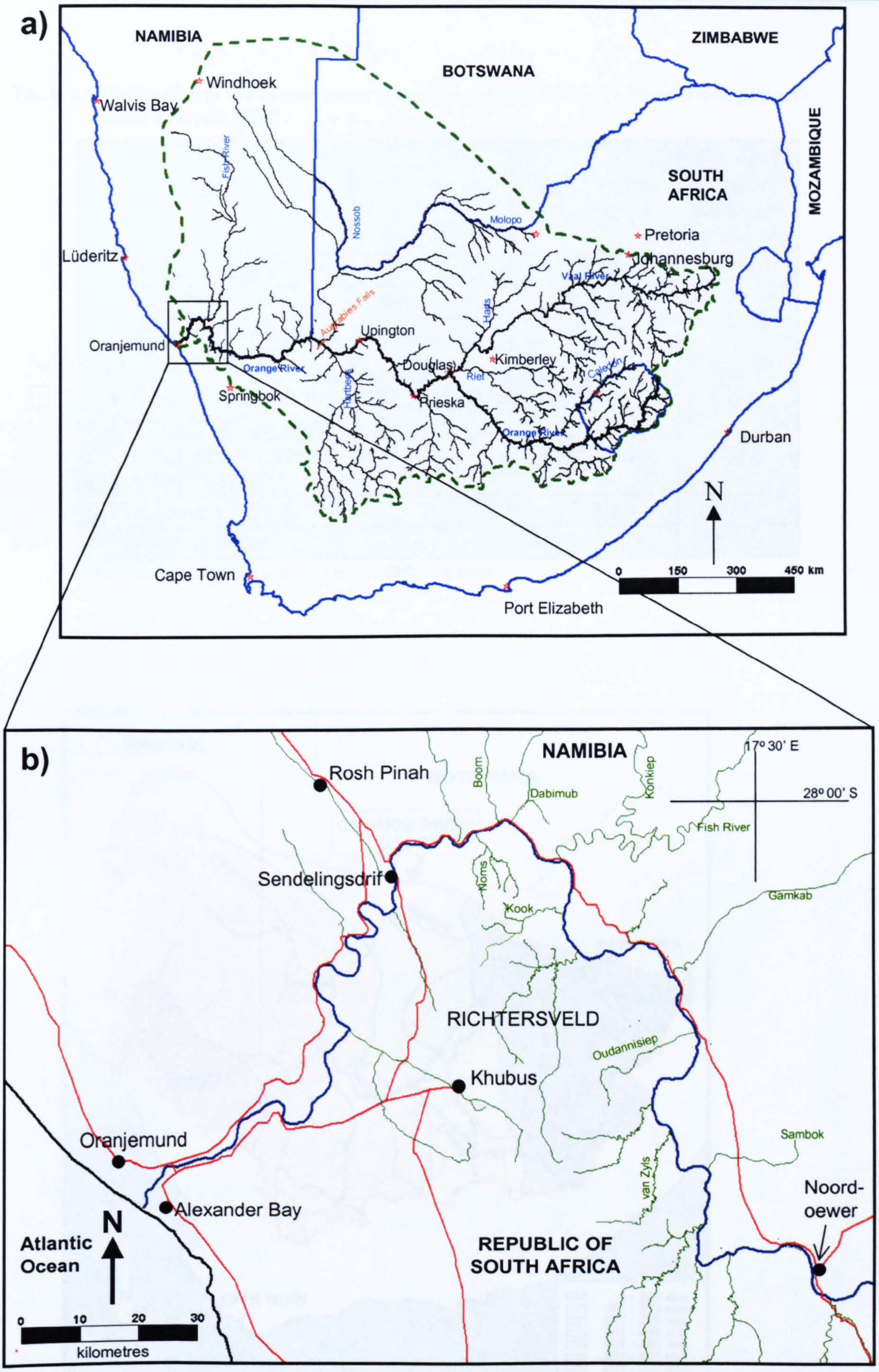

Figure 1.1 a) Drainage basin of the Orange/Vaal River system. b) Study area between Noordoewer and the Atlantic Ocean.

Table 2.1 Distribution of the annual water resources within the Orange River drainage basin (after Everson 1999)

Description	Catchment Area (km^2)	Natural run-off (million m^3/year)
1. Vaal River basin	196 290	4300
2. Senqu/Orange to SA/Lesotho border	24 680	4 010
3. Caledon River basin to Welbedacht Dam	15 270	1 240
4. Remainder of Orange River upstream of Orange/Vaal confluence	~59 400*	1 300
5. Remainder of lower Orange basin excluding Fish River basin	~670 000+	420
6.Fish River basin	76 000	480
Total	~1 000 000	11 750

+Estimate including pan and other non-contributing areas

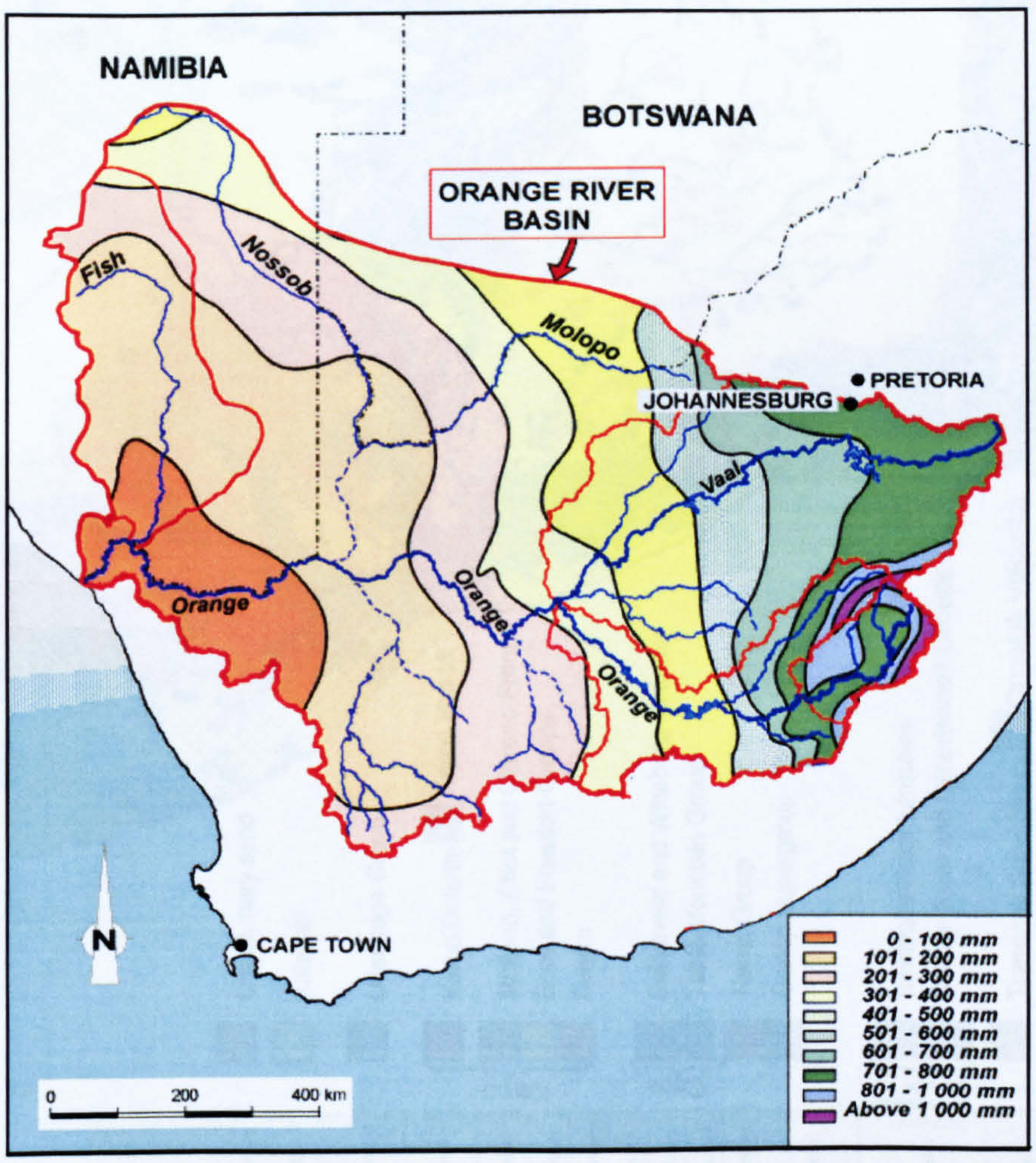

Figure 2.1 Mean annual rainfall in the Orange River catchment.

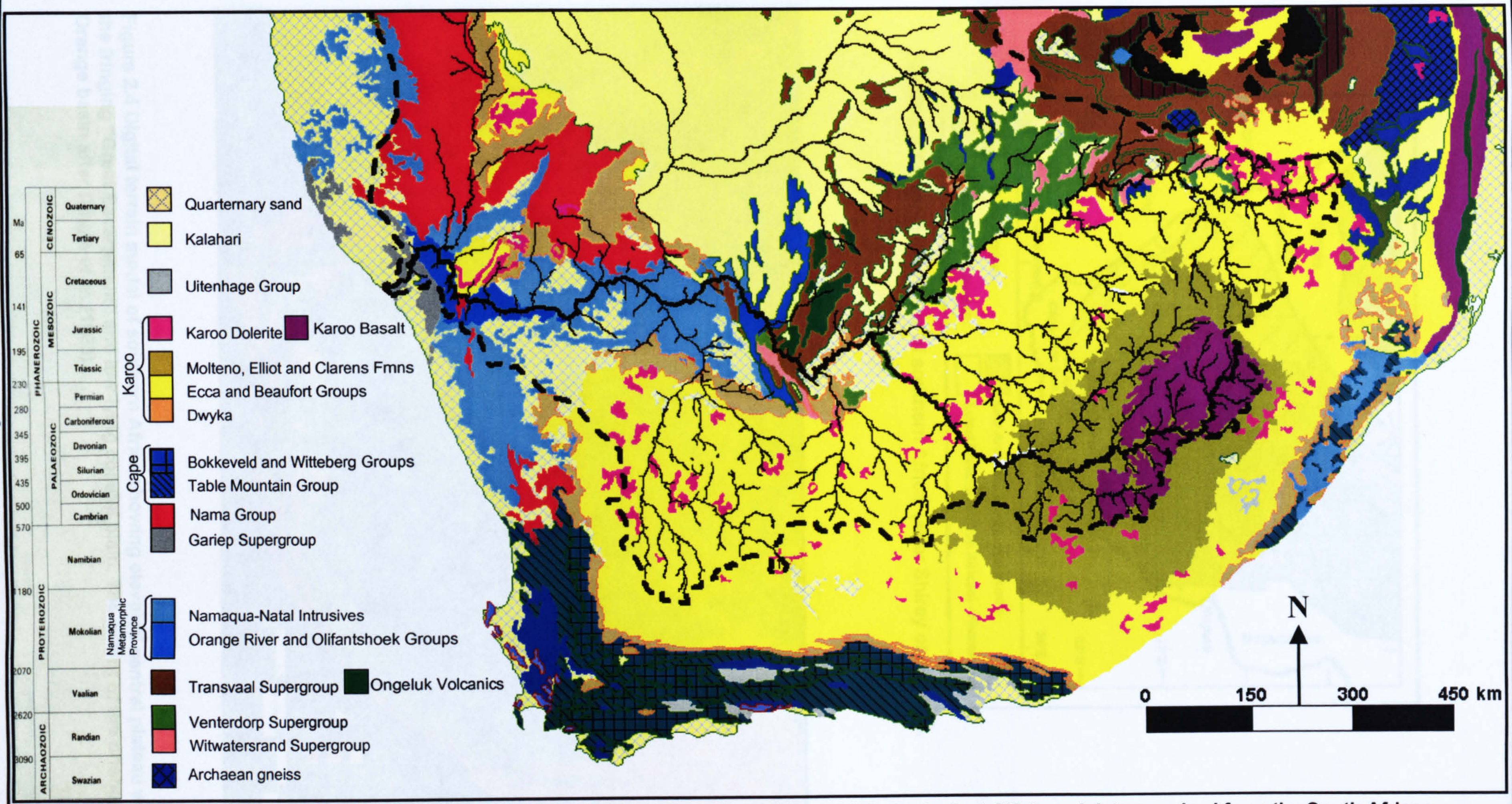

Figure 2.2 Simplified geological map of southern Africa. Stratigraphic table after SACS (1980). Geological GIS-based data acquired from the South African Council for Geoscience.

R. Jürgen Jacob 2005

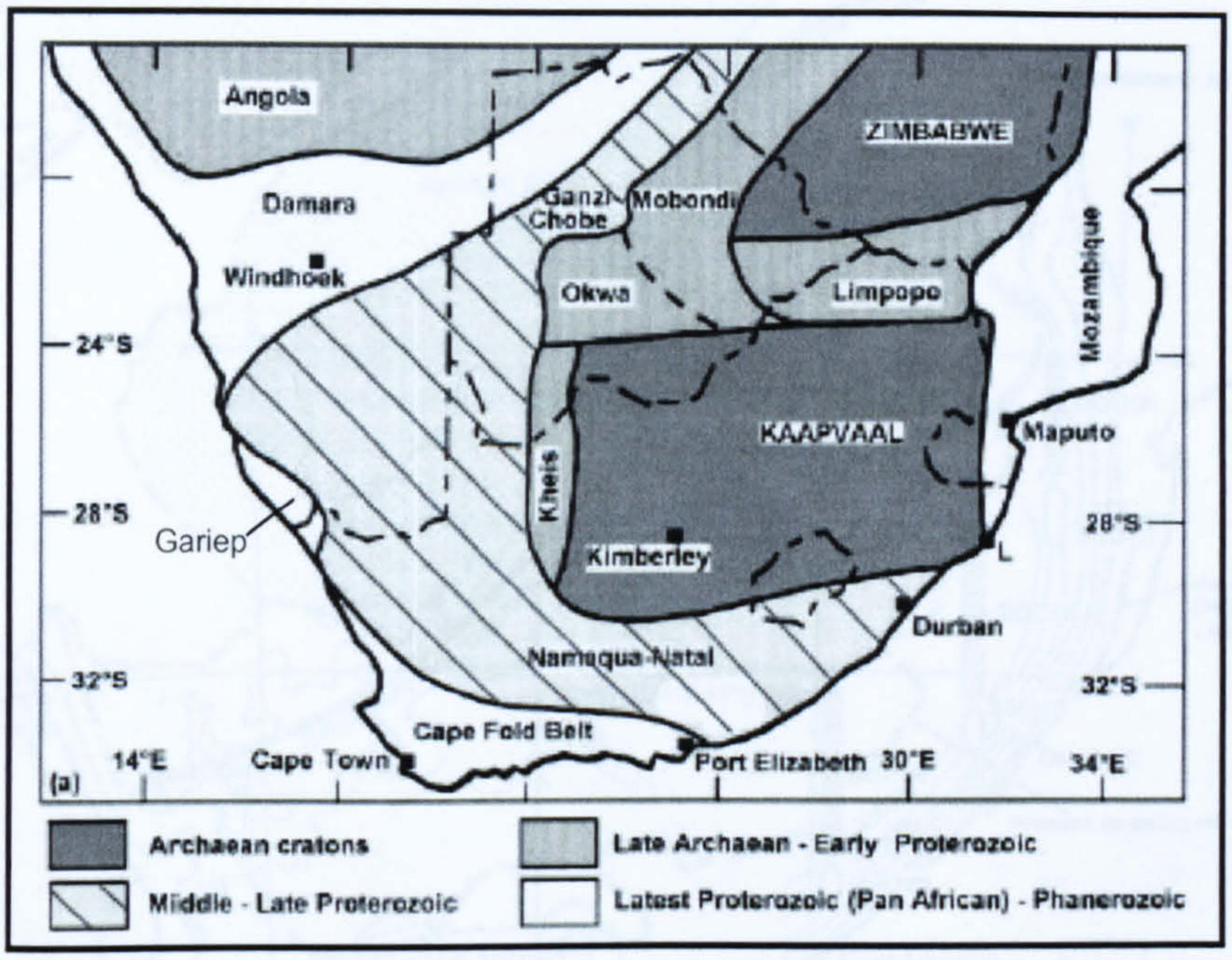

Figure 2.3 Tectonic Provinces of southern Africa (after Shirey *et al.* 2001).

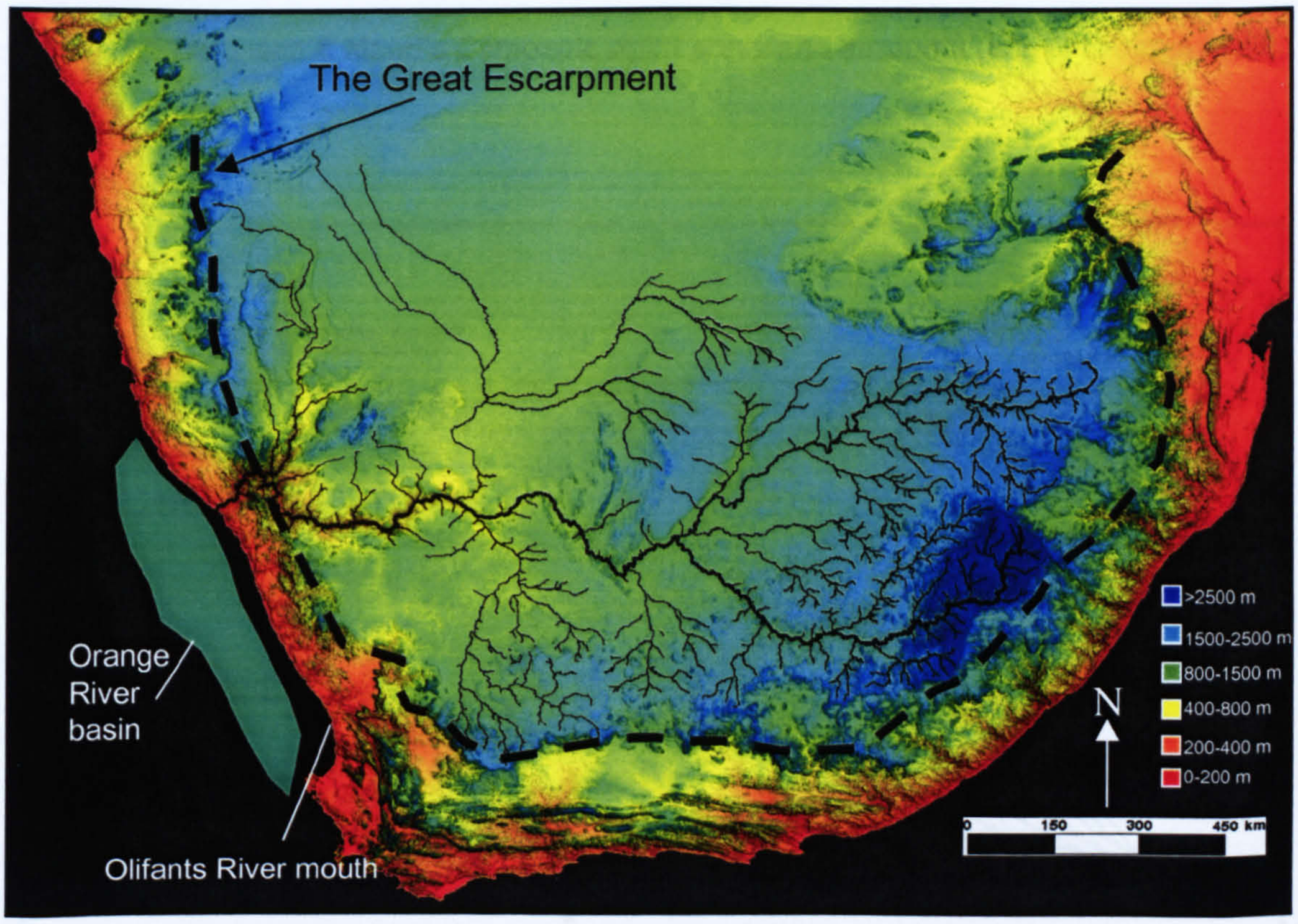

Figure 2.4 Digital terrain model of southern Africa showing elevated central plateau with the fringing "Great Escarpment" and low-lying coastal plain. The extent of the offshore Orange basin after Dingle *et al.* (1983).

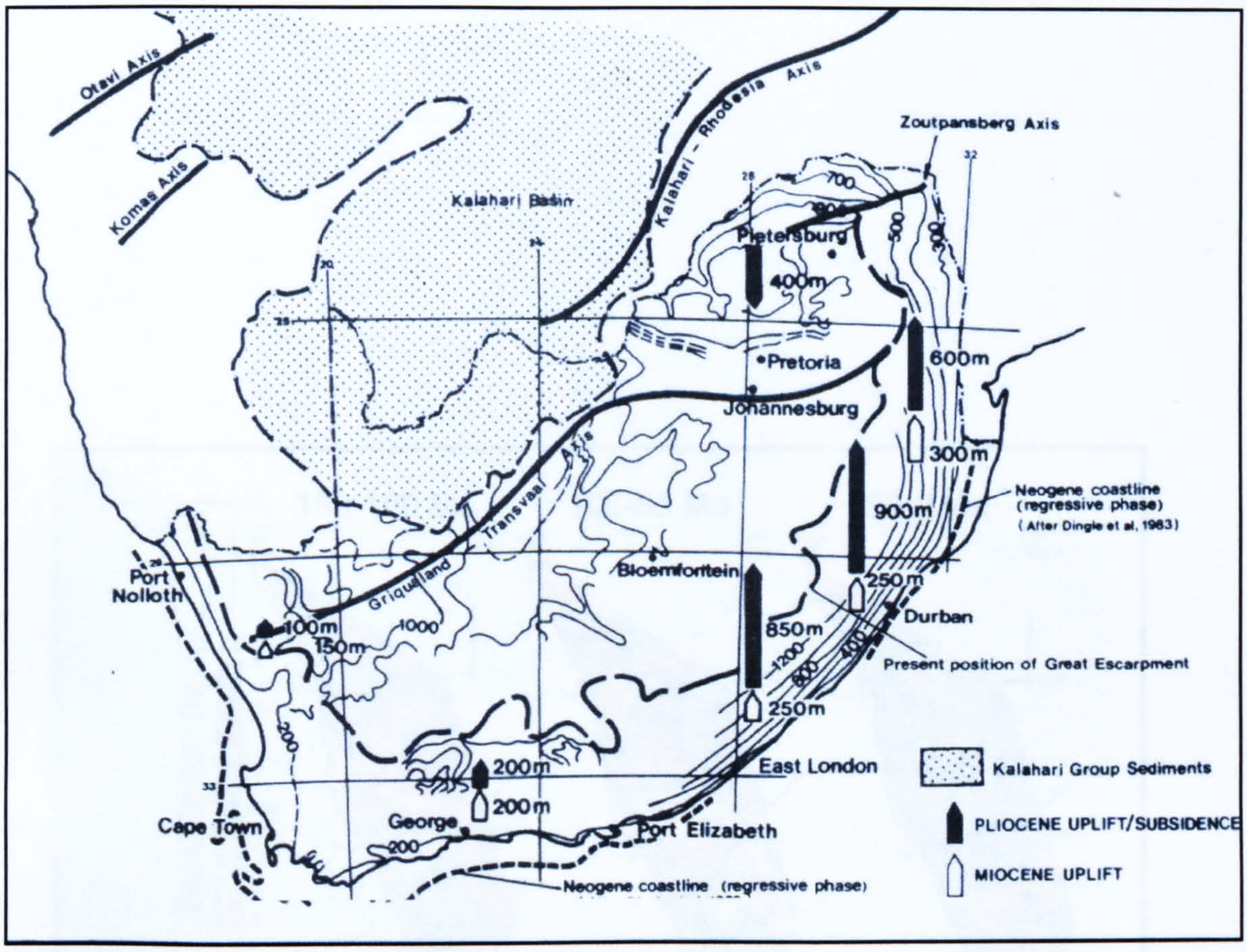

Figure 2.5 Partridge & Maud's Cainozoic uplift areas and amounts (after Partridge 1998).

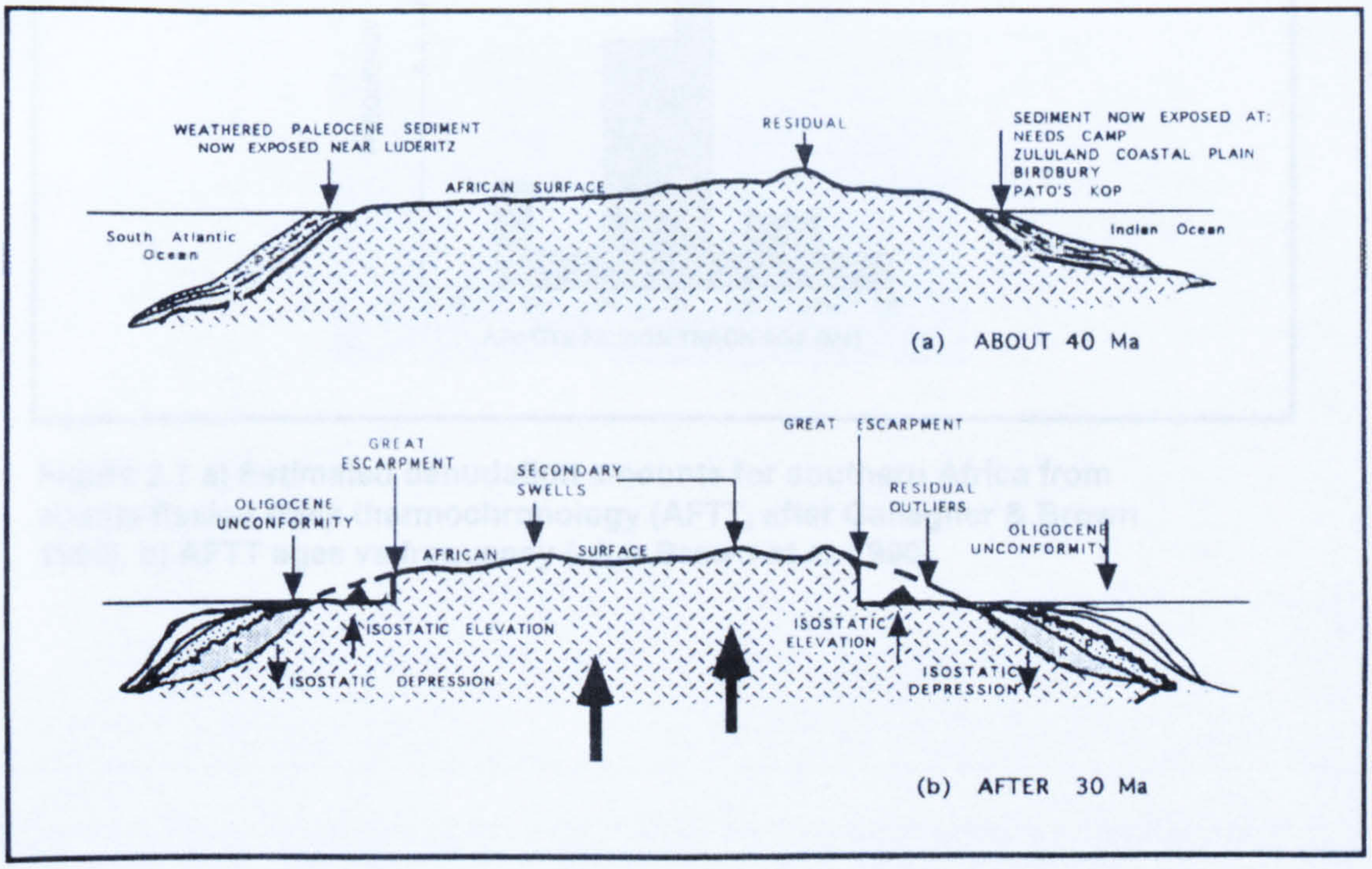

Figure 2.6 Burke's geomorphological development of Africa (after Burke 1996).

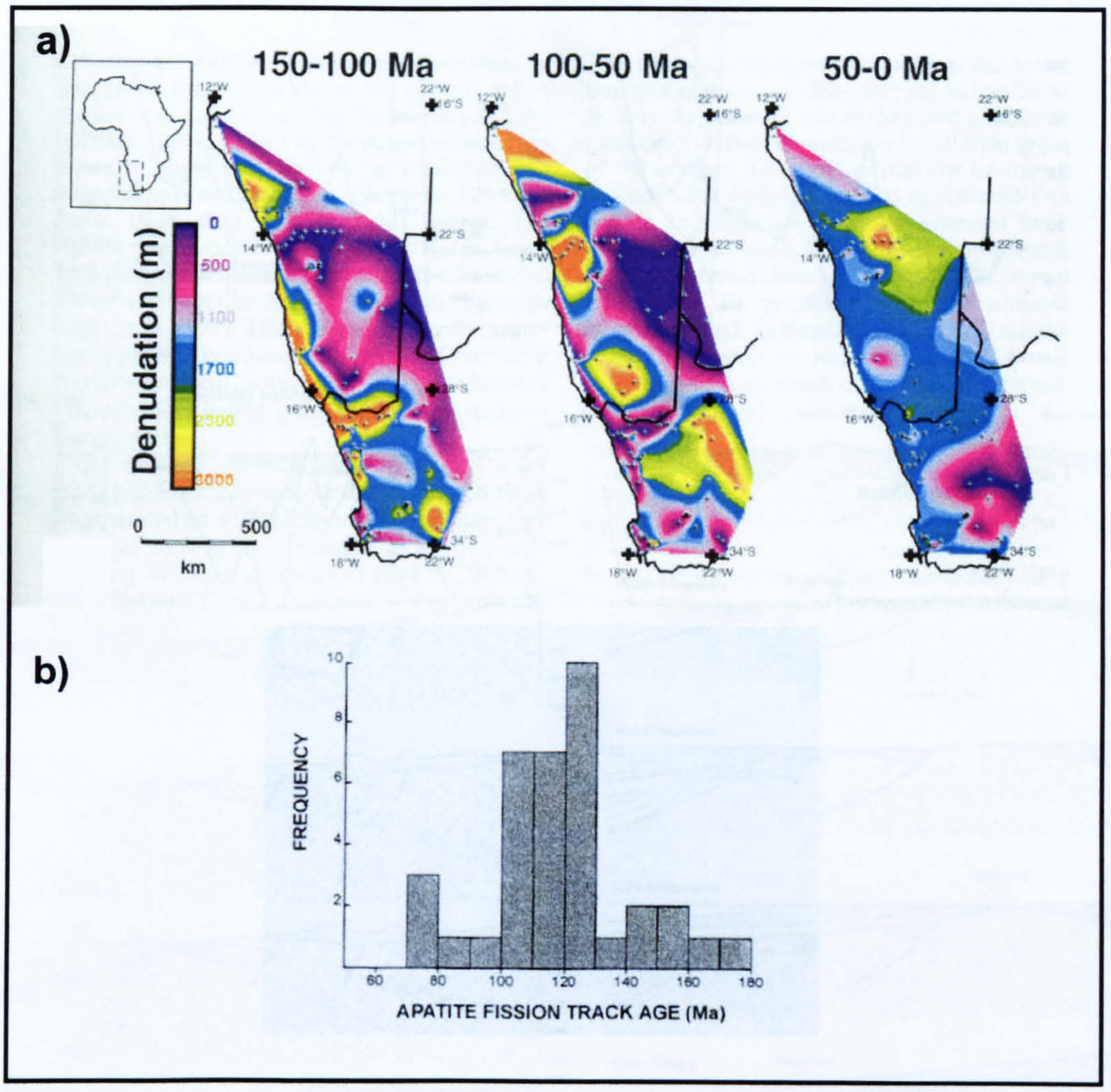

Figure 2.7 a) Estimated denudation amounts for southern Africa from apatite fission track thermochronology (AFTT, after Gallagher & Brown 1999). b) AFTT ages vs frequency (after Brown *et al.* 1990).

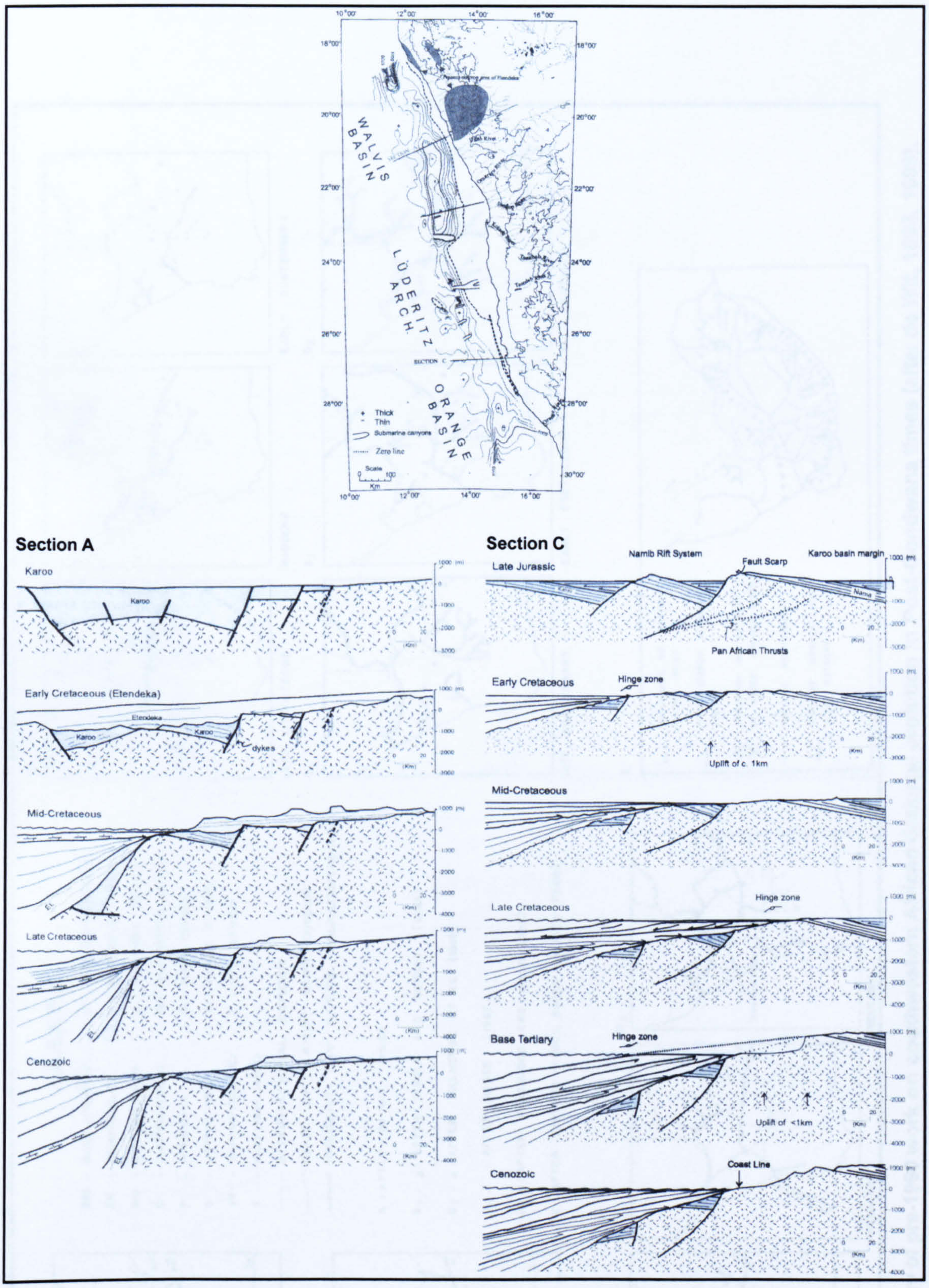

Figure 2.8 Reconstructions of the evolution of the Namibian margin (after Aizawa *et al.* 2000).

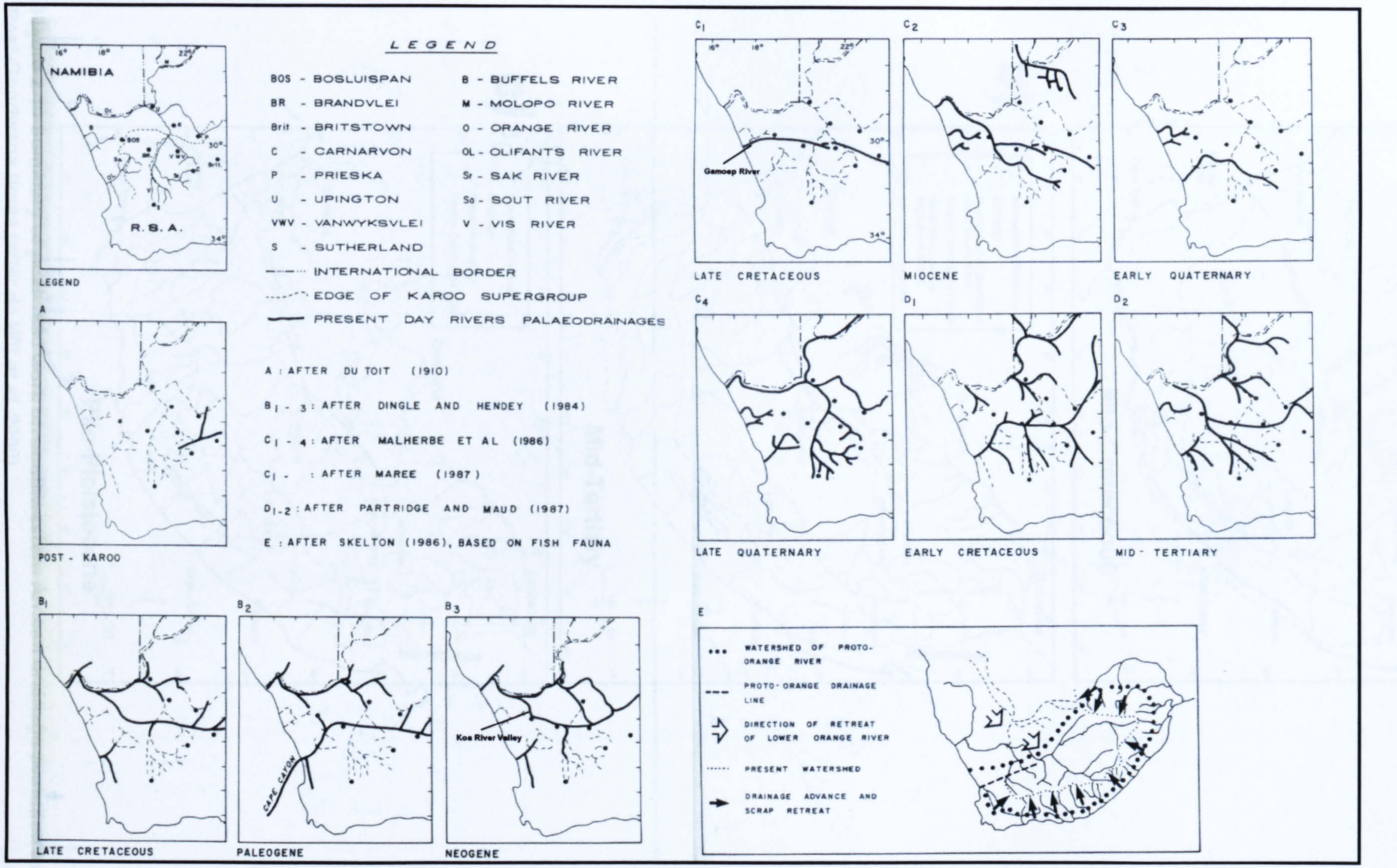

Figure 2.9 Summary of pre-1990 work on southwestern African drainage evolution in Post-Gondwana times (after de Wit, 1993, 1999).

a)

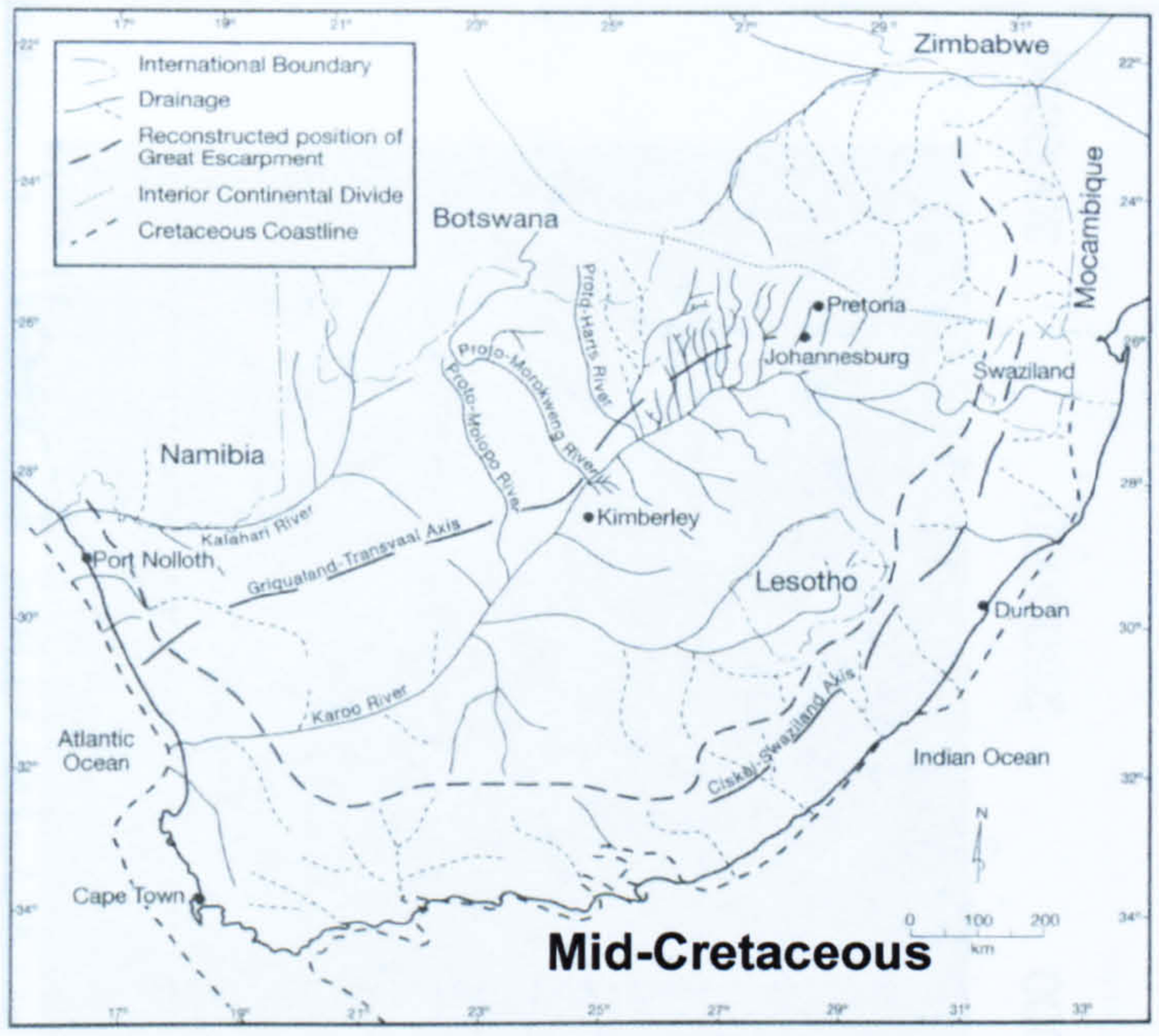

b)

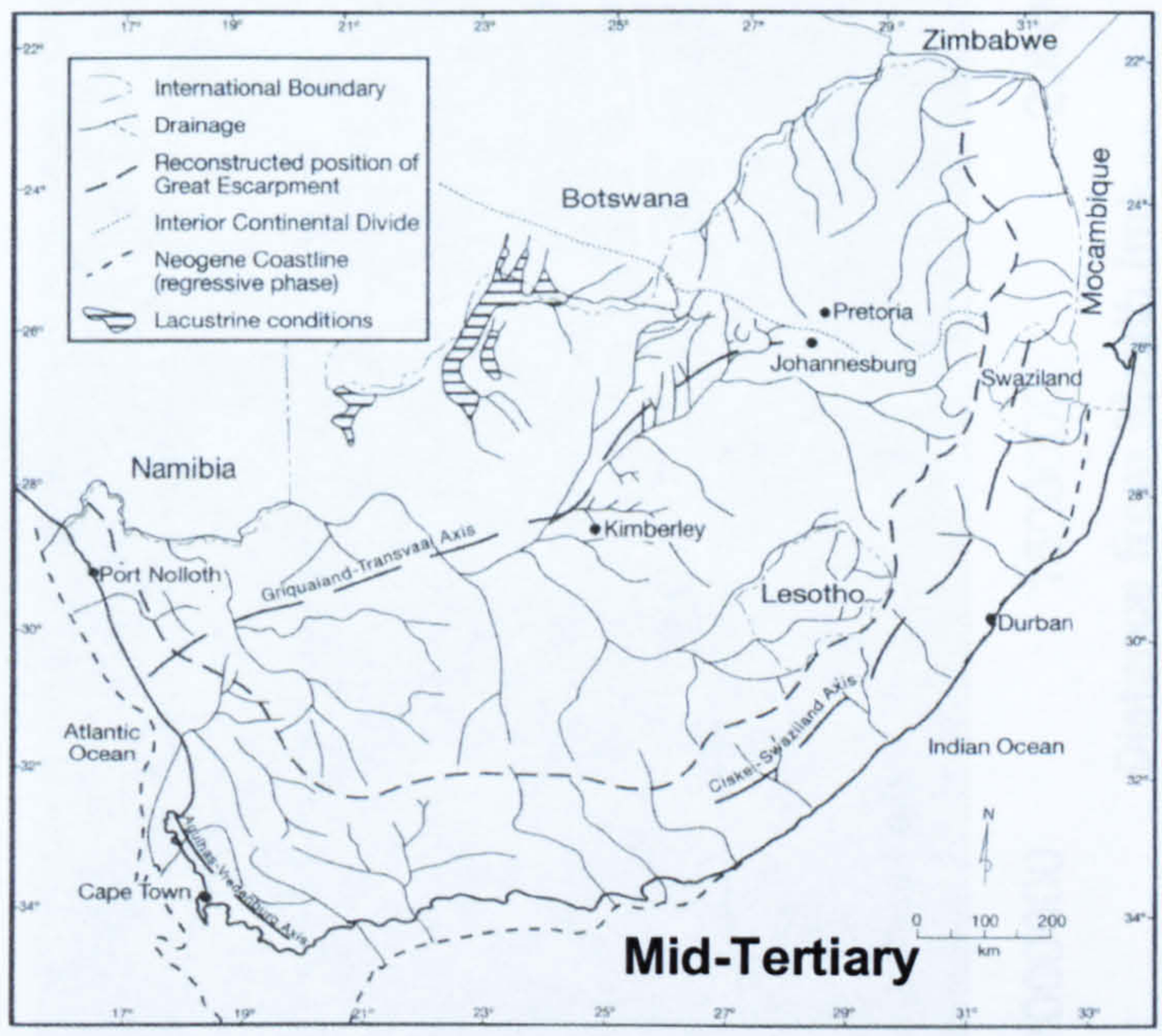

c)

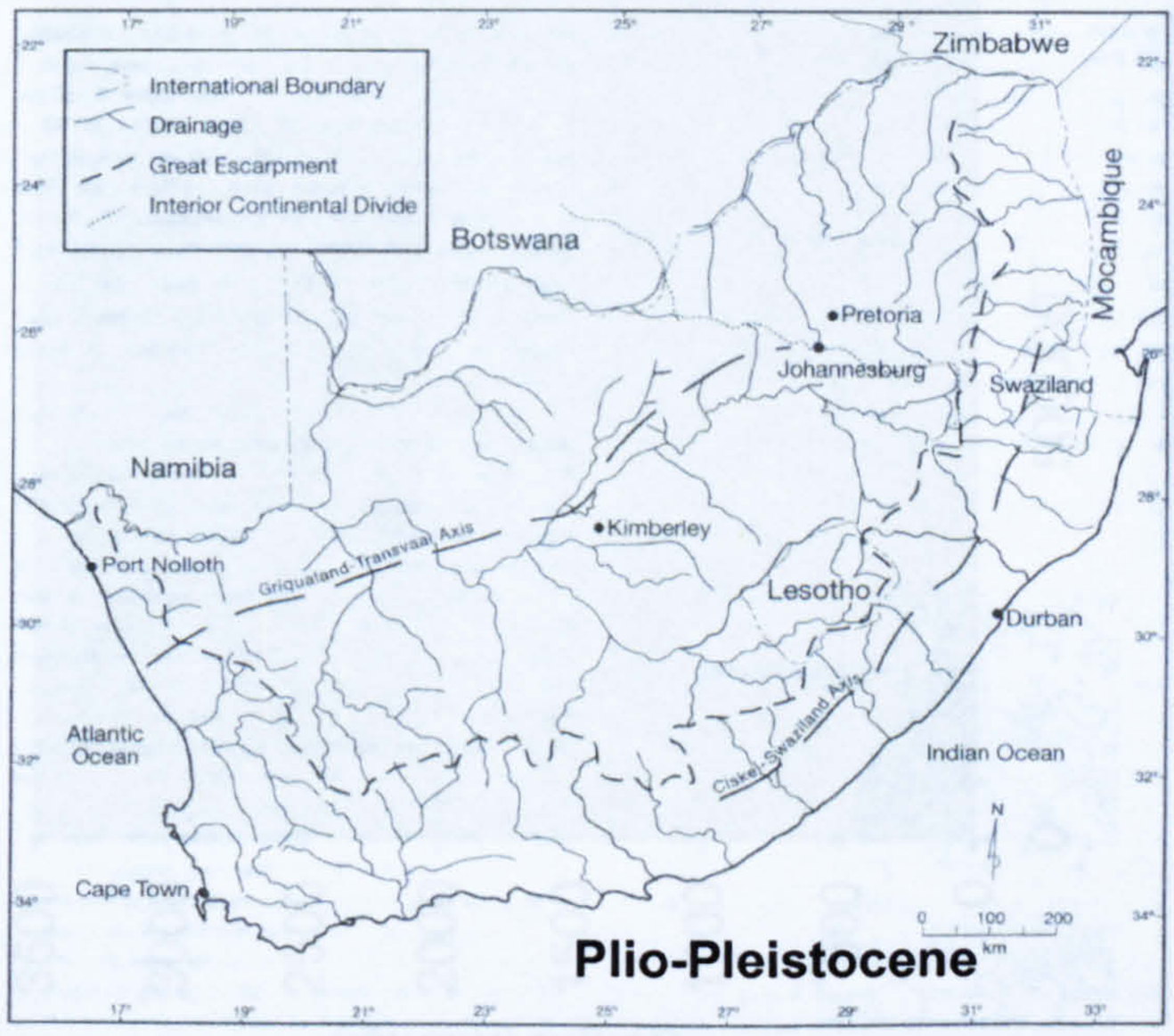

Figure 2.10 Summary of post-1990 work on southwestern African drainage evolution in Post-Gondwana times (after de Wit *et al.* 2000).

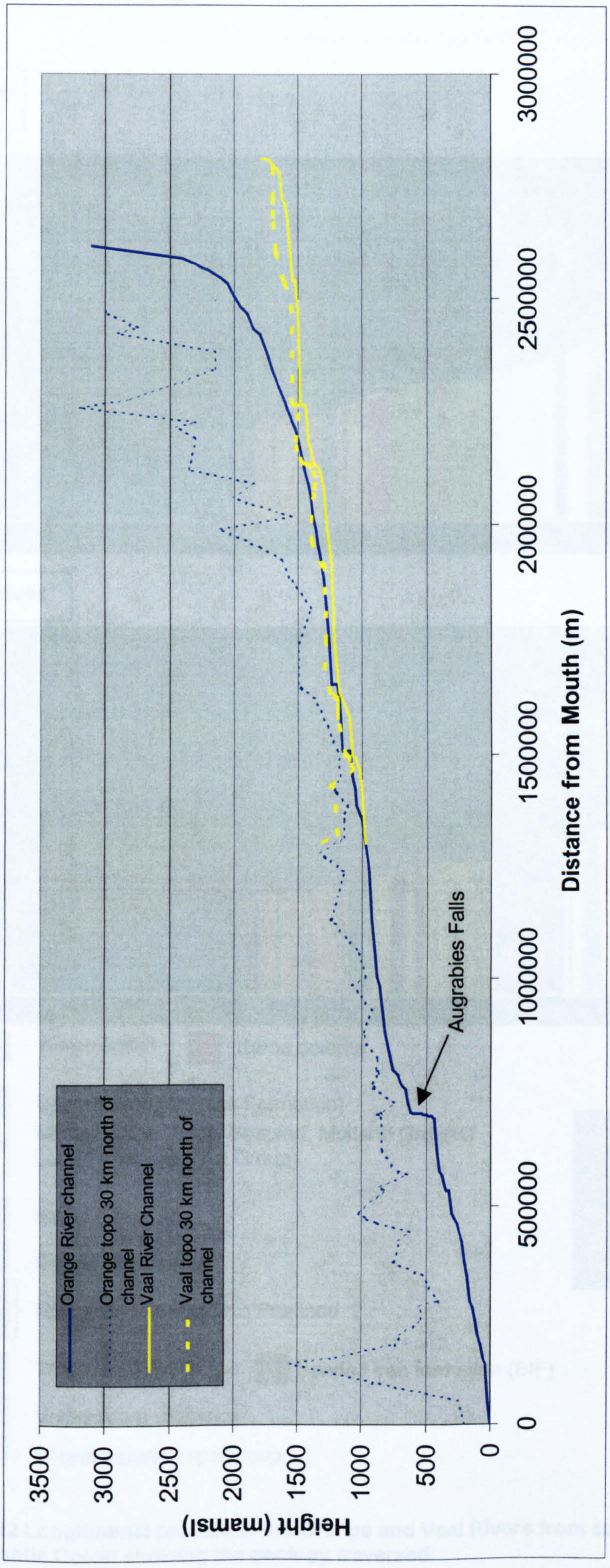

Figure 2.11 Longitudinal profiles of the Orange and Vaal River channels and topographic profiles for landscape 30 km north of the channels.

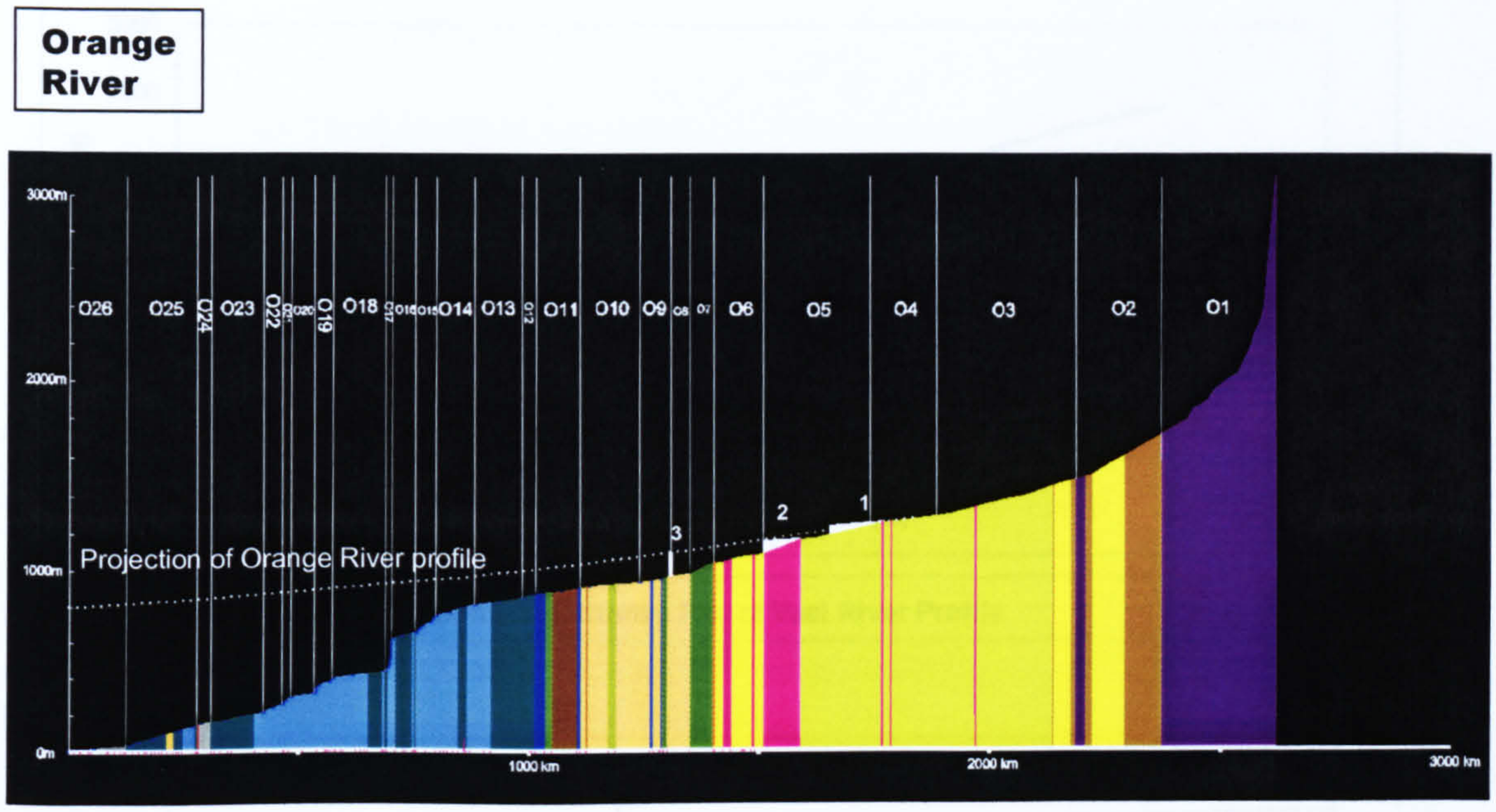

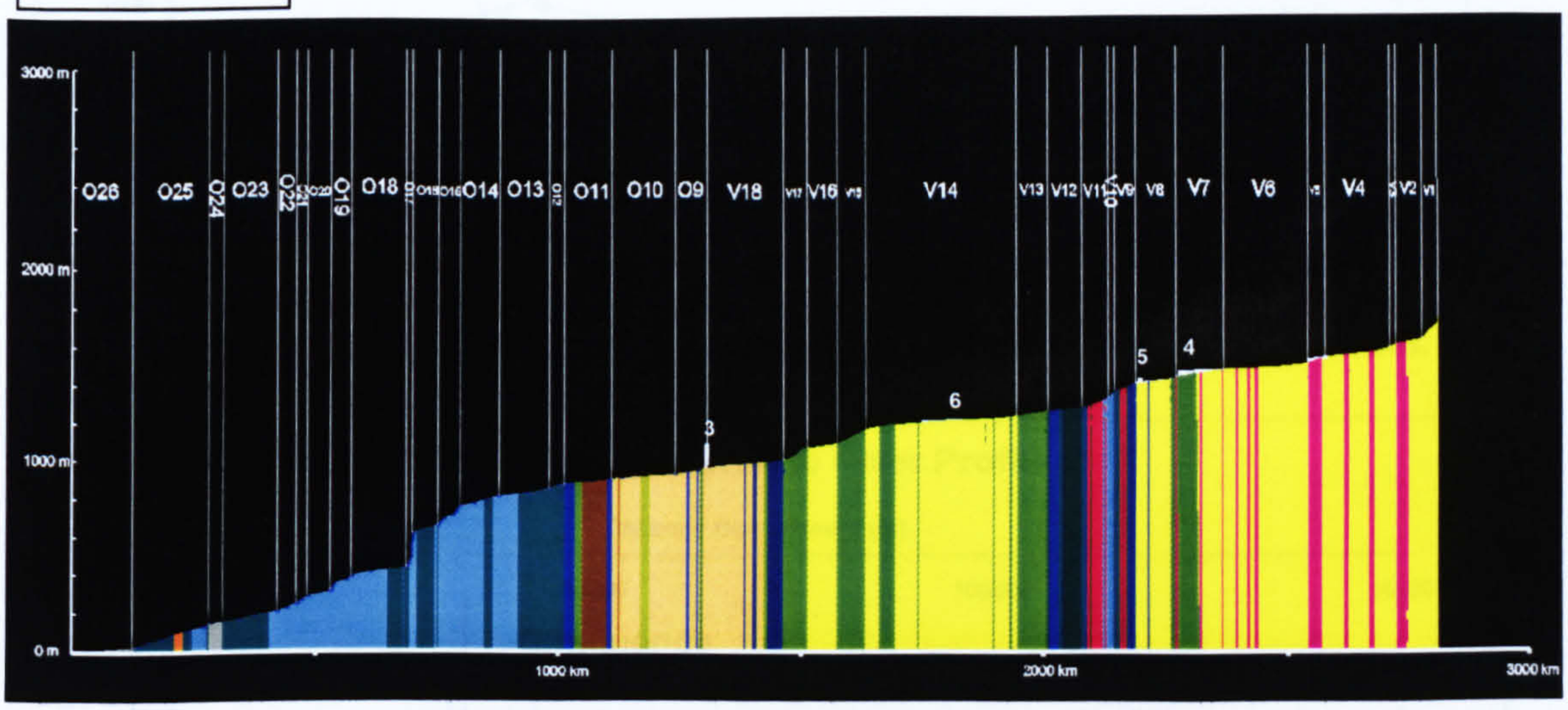

Figure 2.12 Longitudinal profiles of the Orange and Vaal Rivers from source to the Atlantic Ocean showing the geology traversed.

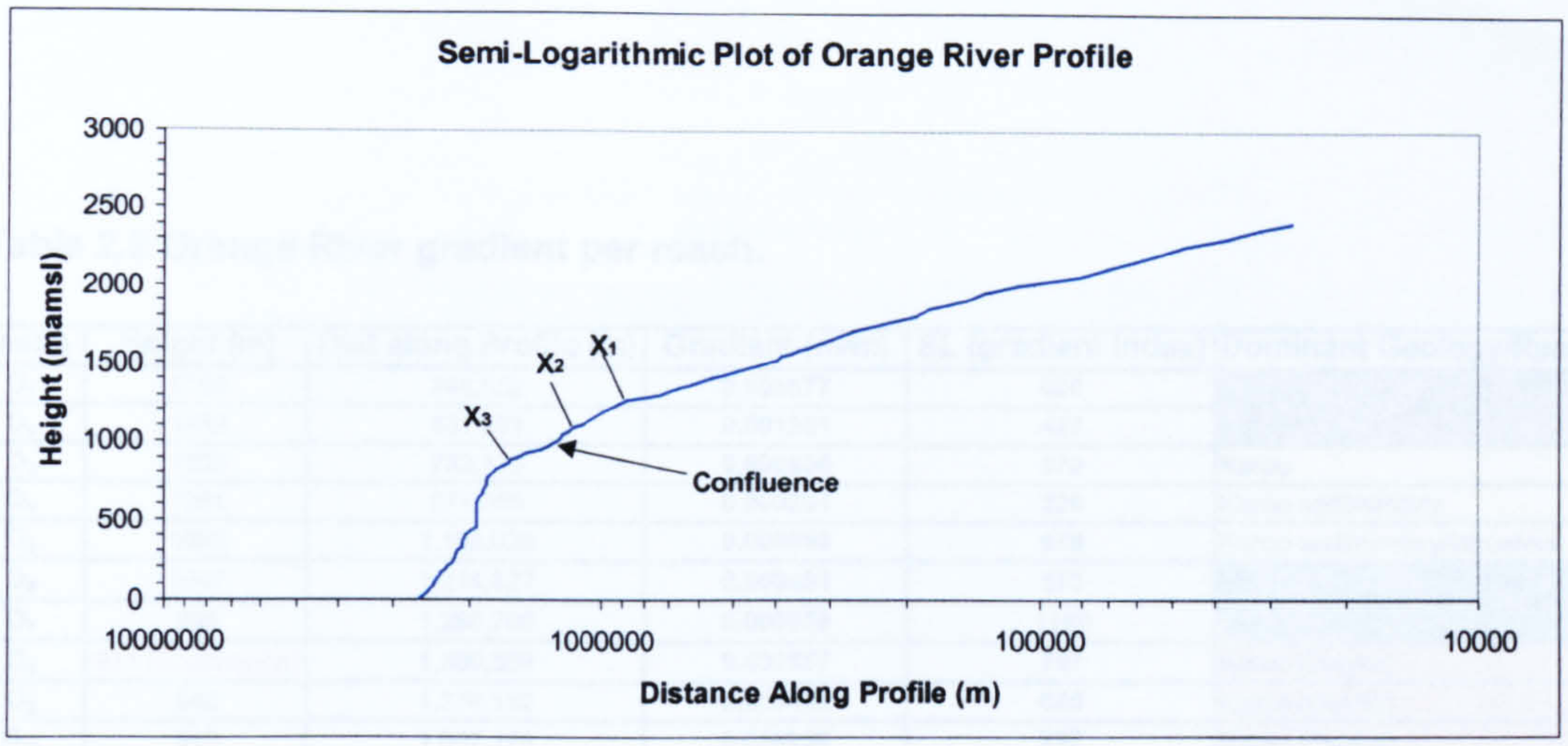

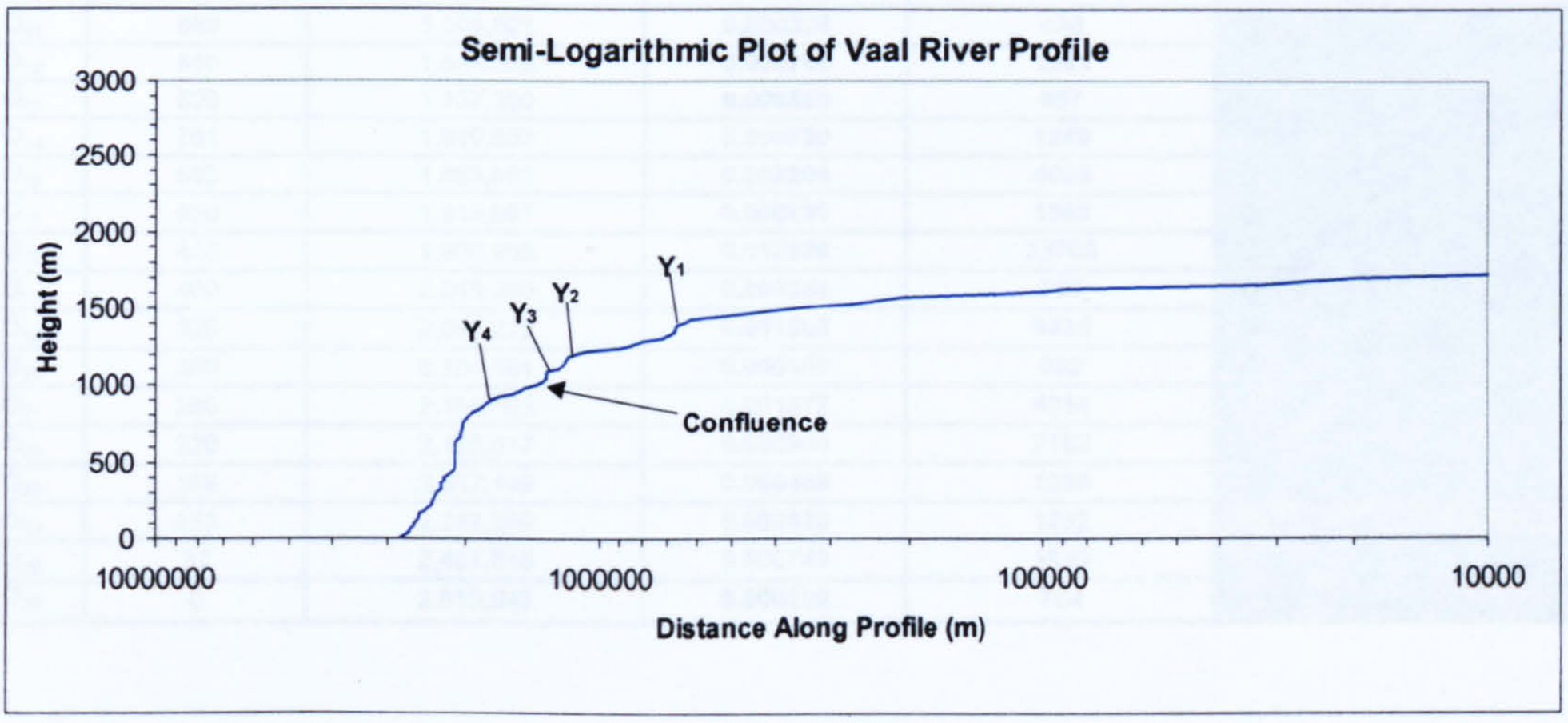

Figure 2.13 Semi-logarithmic longitudinal profiles of the Orange and Vaal Rivers.

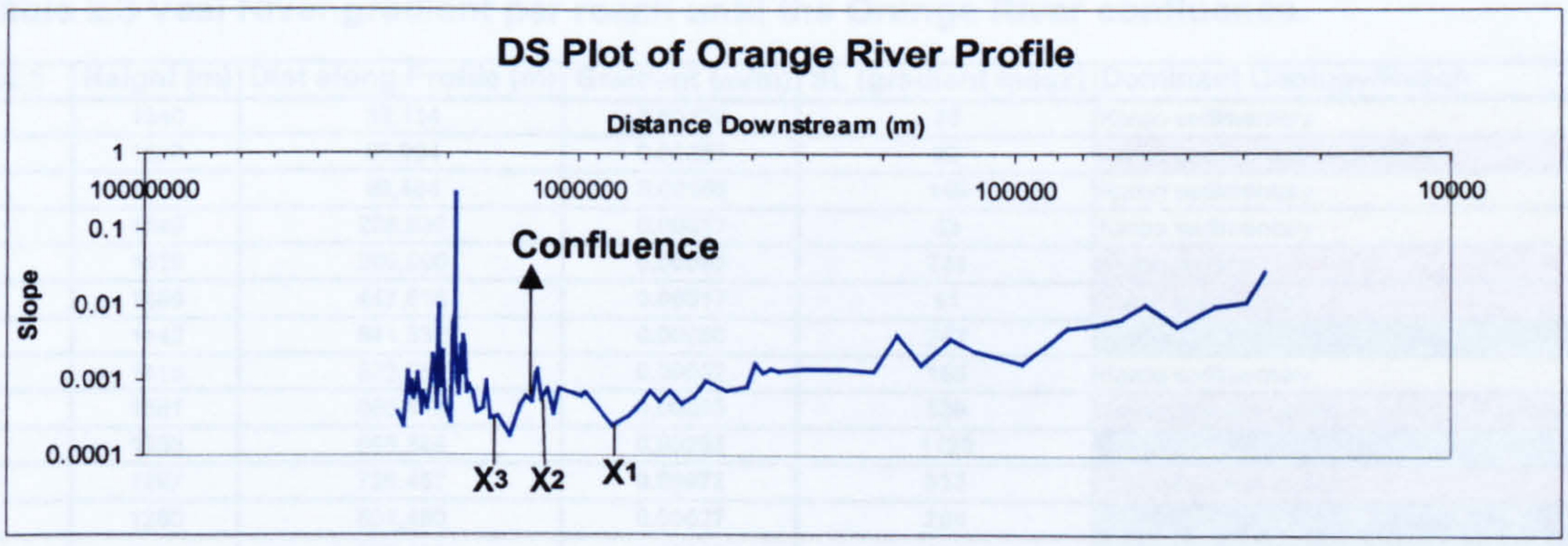

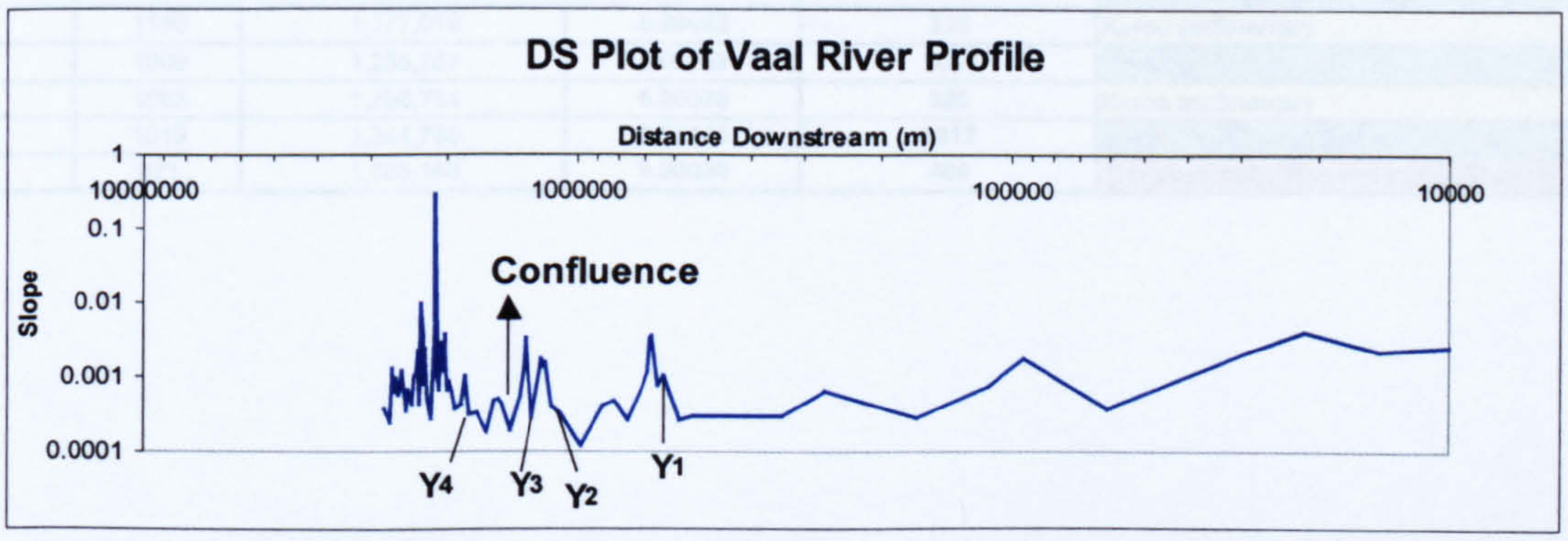

Figure 2.14 DS Plots of Orange and Vaal River longitudinal profiles (note the position of X and Y relative to figure 2.13).

Table 2.2 Orange River gradient per reach.

Reach	Height (m)	Dist along Profile (m)	Gradient (m/m)	SL (gradient index)	Dominant Geology/Reach
O_1	1725	246,552	**0.005577**	**688**	Karoo basalt
O_2	1492	431,291	**0.001261**	**427**	Karoo basalt
O_3	1300	733,175	**0.000636**	**370**	Karoo
O_4	1261	871,955	**0.000281**	**226**	Karoo sedimentary
O_5	1099	1,108,029	**0.000686**	**679**	Karoo sedimentary/Intrusives
O_6	1047	1,214,827	**0.000491**	**570**	Transvaal
O_7	995	1,268,706	**0.000958**	**1189**	Ventersorp
O_8	971 (Confluence)	1,309,569	**0.000587**	**757**	Karoo (Dwyka)
O_9	940	1,376,152	**0.000466**	**625**	Karoo (Dwyka)
O_{10}	913	1,507,179	**0.000206**	**297**	Karoo (Dwyka)
O_{11}	883	1,604,521	**0.000308**	**480**	Transvaal
O_{12}	860	1,634,532	**0.000766**	**1241**	NMP
O_{13}	820	1,737,250	**0.000389**	**657**	NMP
O_{14}	761	1,819,633	**0.000720**	**1280**	NMP
O_{15}	663	1,863,885	**0.002208**	**4066**	NMP
O_{16}	620	1,915,667	**0.000830**	**1569**	NMP
O_{17}	440	1,930,268	**0.012328**	**23706**	NMP
O_{18}	400	2,043,260	**0.000354**	**703**	NMP
O_{19}	320	2,085,222	**0.001906**	**3935**	NMP
O_{20}	300	2,134,191	**0.000408**	**862**	NMP
O_{21}	260	2,155,563	**0.001872**	**4014**	NMP
O_{22}	220	2,195,817	**0.000994**	**2162**	NMP
O_{23}	169	2,307,149	**0.000460**	**1035**	NMP
O_{24}	153	2,337,509	**0.000530**	**1232**	Nama limestone
O_{25}	37	2,491,615	**0.000749**	**1810**	NMP
O_{26}	0	2,615,949	**0.000299**	**764**	Gariep Supergroup

Table 2.3 Vaal River gradient per reach until the Orange River confluence.

Reach	Height (m)	Dist along Profile (m)	Gradient (m/m)	SL (gradient index)	Dominant Geology/Reach
V_1	1640	33,114	**0.00423**	**70**	Karoo sedimentary
V_2	1620	86,994	**0.00037**	**22**	Karoo sedimentary and dolerite
V_3	1600	99,484	**0.00160**	**149**	Karoo sedimentary
V_4	1549	238,636	**0.00037**	**62**	Karoo sedimentary
V_5	1519	269,990	**0.00095**	**241**	Karoo dolerite
V_6	1489	447,616	**0.00017**	**61**	Karoo sedimentary
V_7	1442	541,332	**0.00050**	**247**	Karoo and Ventersdorp andesite
V_8	1416	623,055	**0.00032**	**185**	Karoo sedimentary
V_9	1381	665,413	**0.00083**	**536**	Witwatersrand qtzites & Transvaal dolomite
V_{10}	1335	683,344	**0.00255**	**1720**	Parys Granite
V_{11}	1297	735,457	**0.00072**	**513**	Witwatersrand qtzites
V_{12}	1280	801,480	**0.00027**	**204**	Transvaal dolomites
V_{13}	1251	868,020	**0.00043**	**359**	Ventersdorp andesite
V_{14}	1180	1,177,019	**0.00023**	**236**	Karoo sedimentary
V_{15}	1099	1,235,757	**0.00138**	**1664**	Ventersdorp andesite
V_{16}	1083	1,298,734	**0.00026**	**328**	Karoo sedimentary
V_{17}	1016	1,344,785	**0.00145**	**1912**	Ventersdorp andesite
V_{18}	971	1,503,188	**0.00028**	**405**	Transvaal dolomites and Karoo (Dwyka)

a)

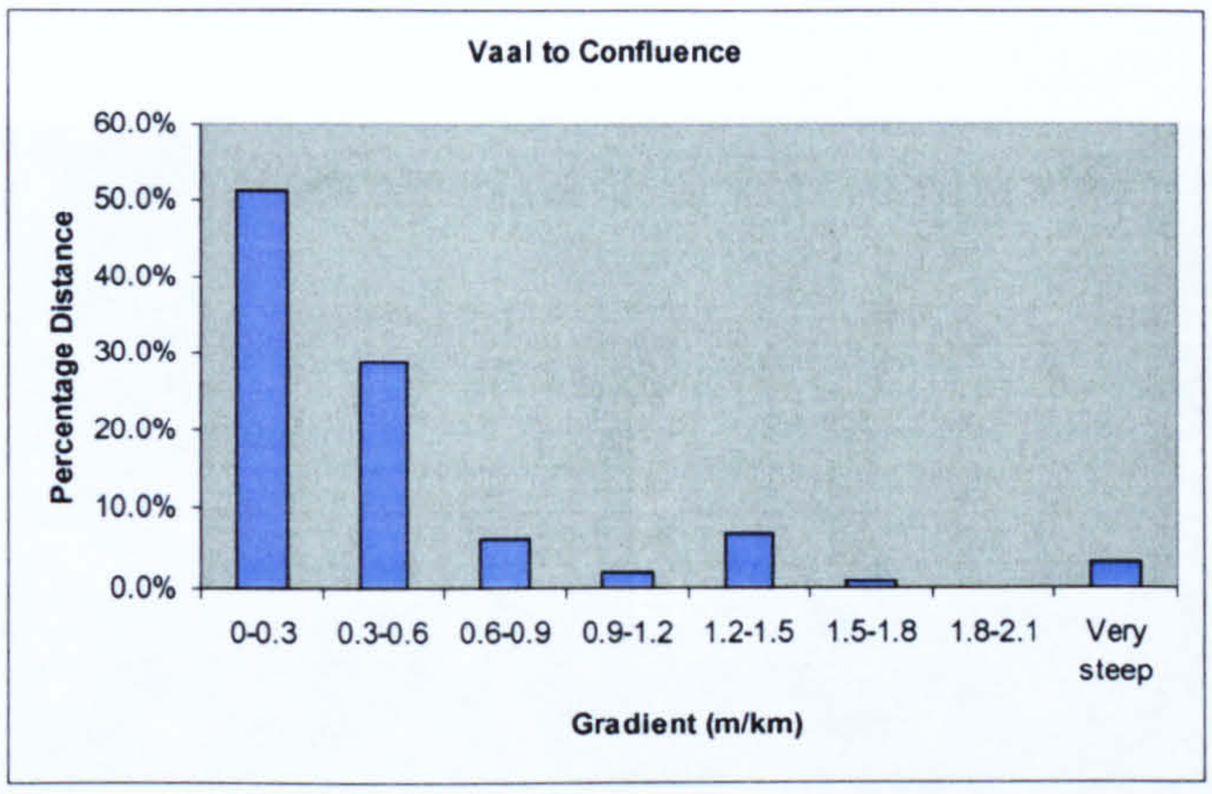

b)

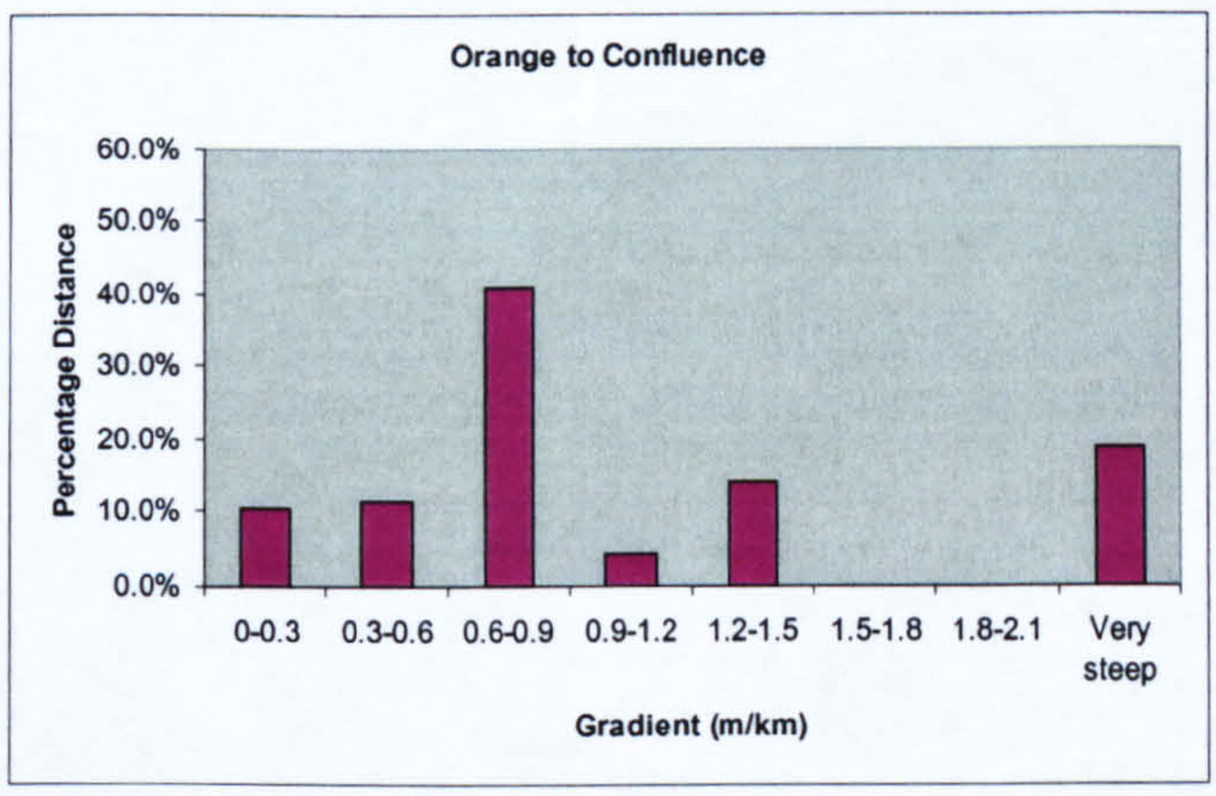

c)

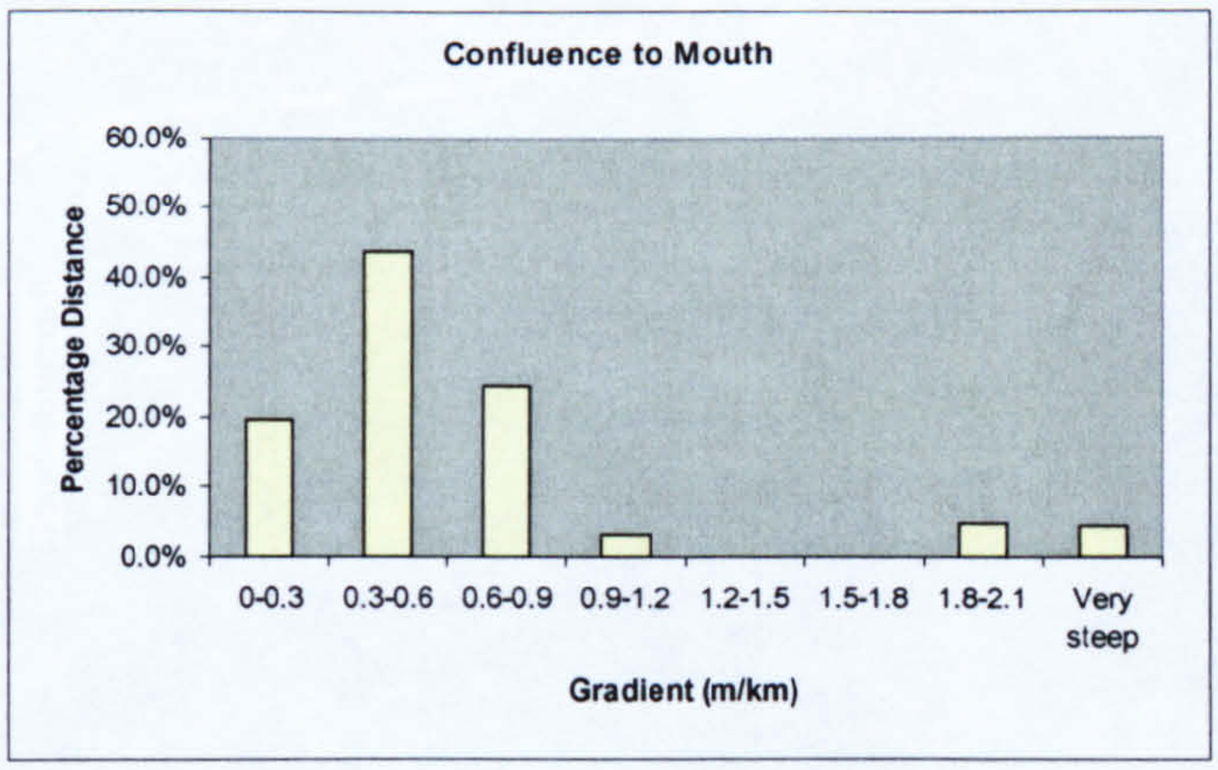

Figure 2.15 Gradient analysis of Reaches defined in figure 2.12.

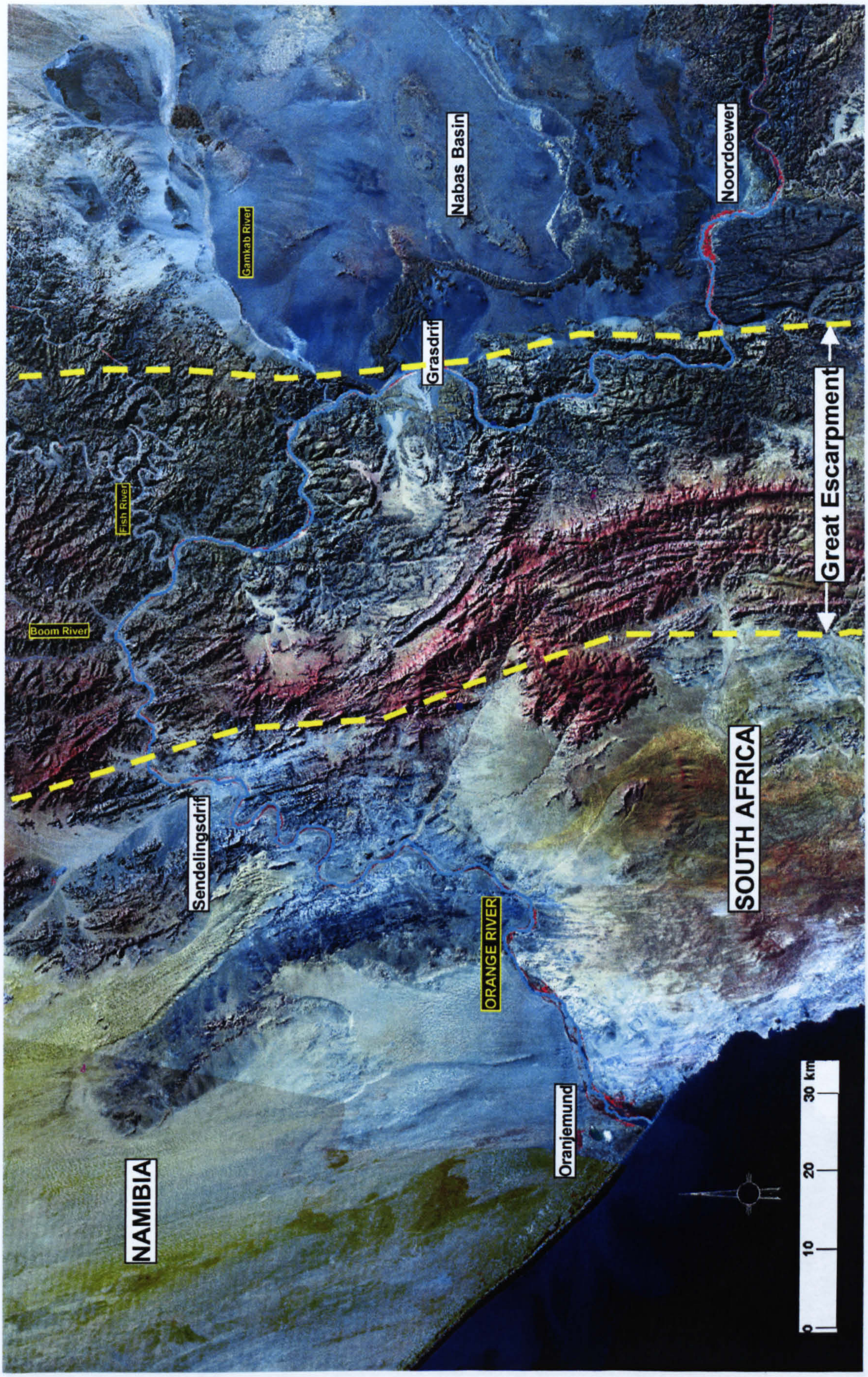

Figure 3. 1 Satellite image of study area (Landsat false colour image - 1995).

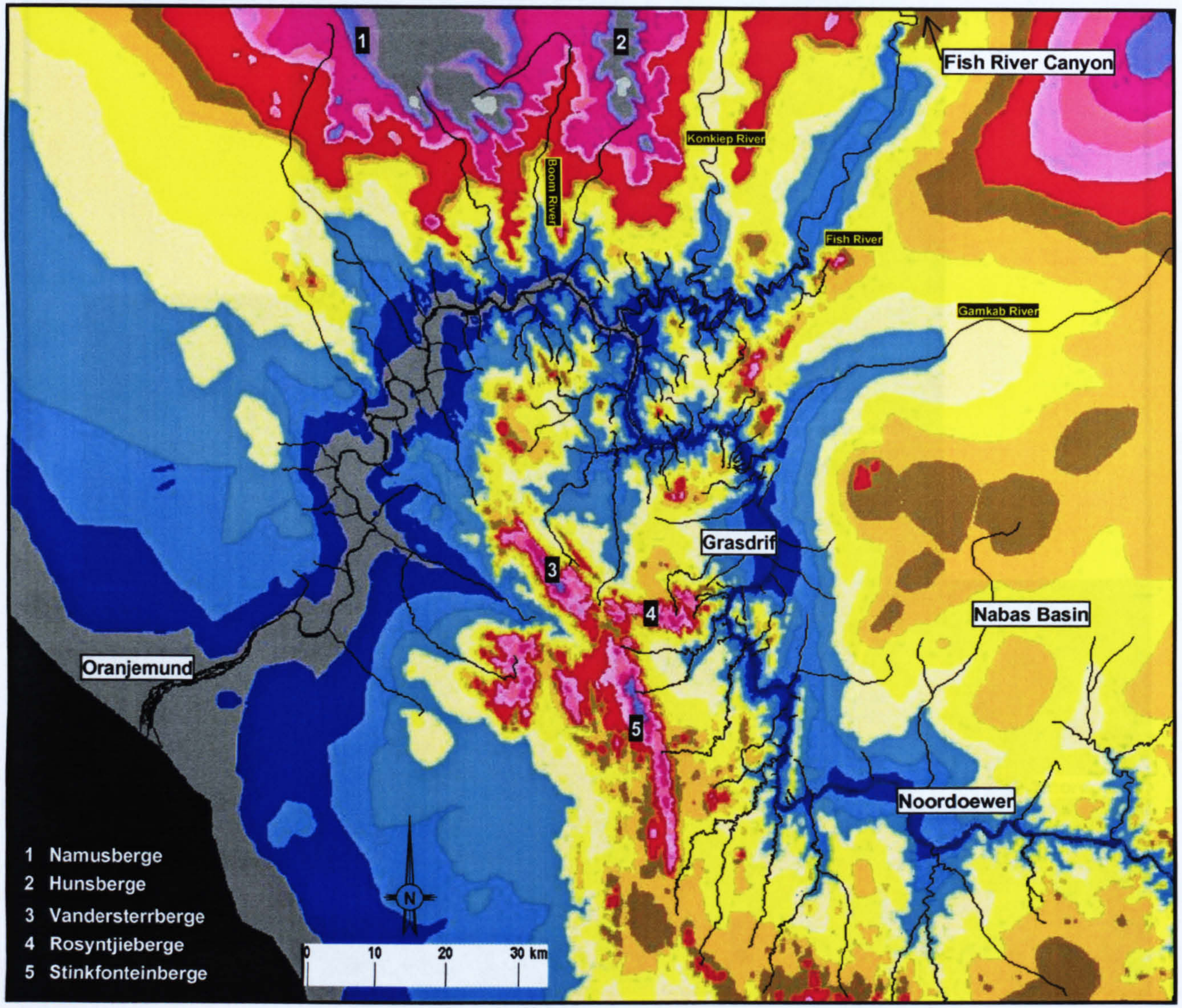

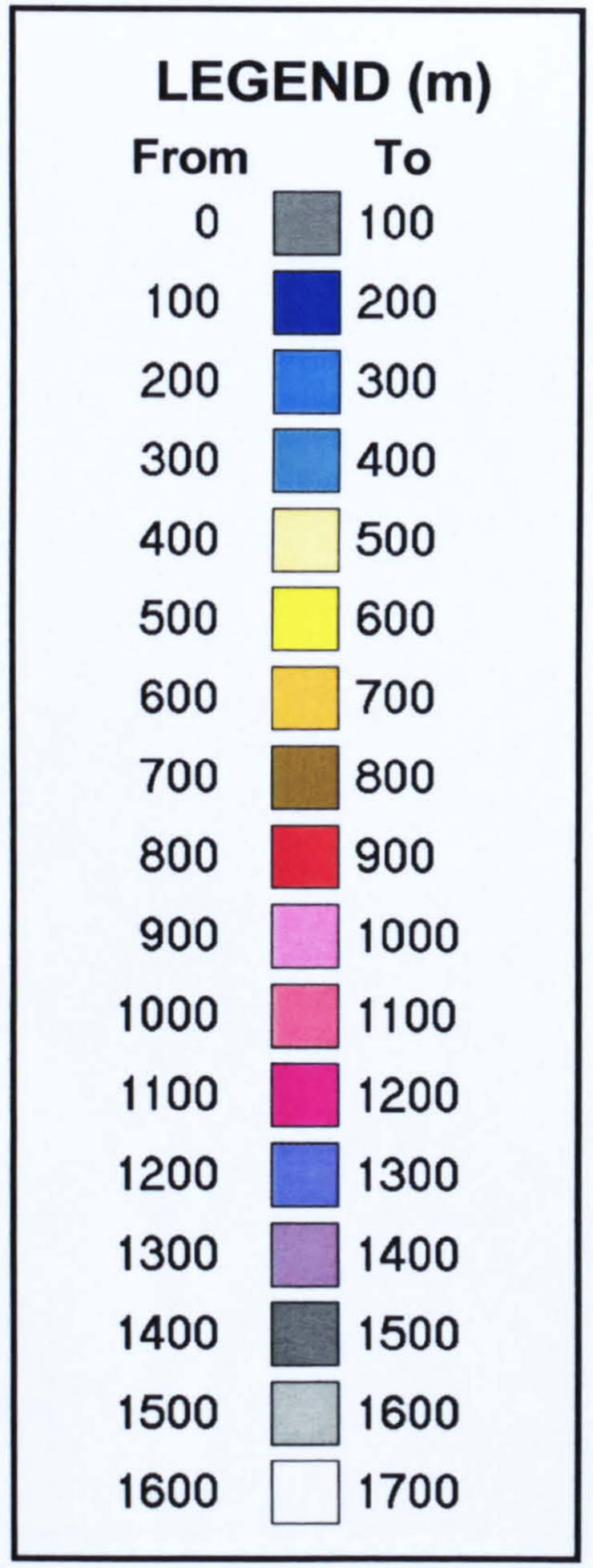

Figure 3. 2a Colour-coded DTM of study area (100 m intervals) showing topography and drainage .

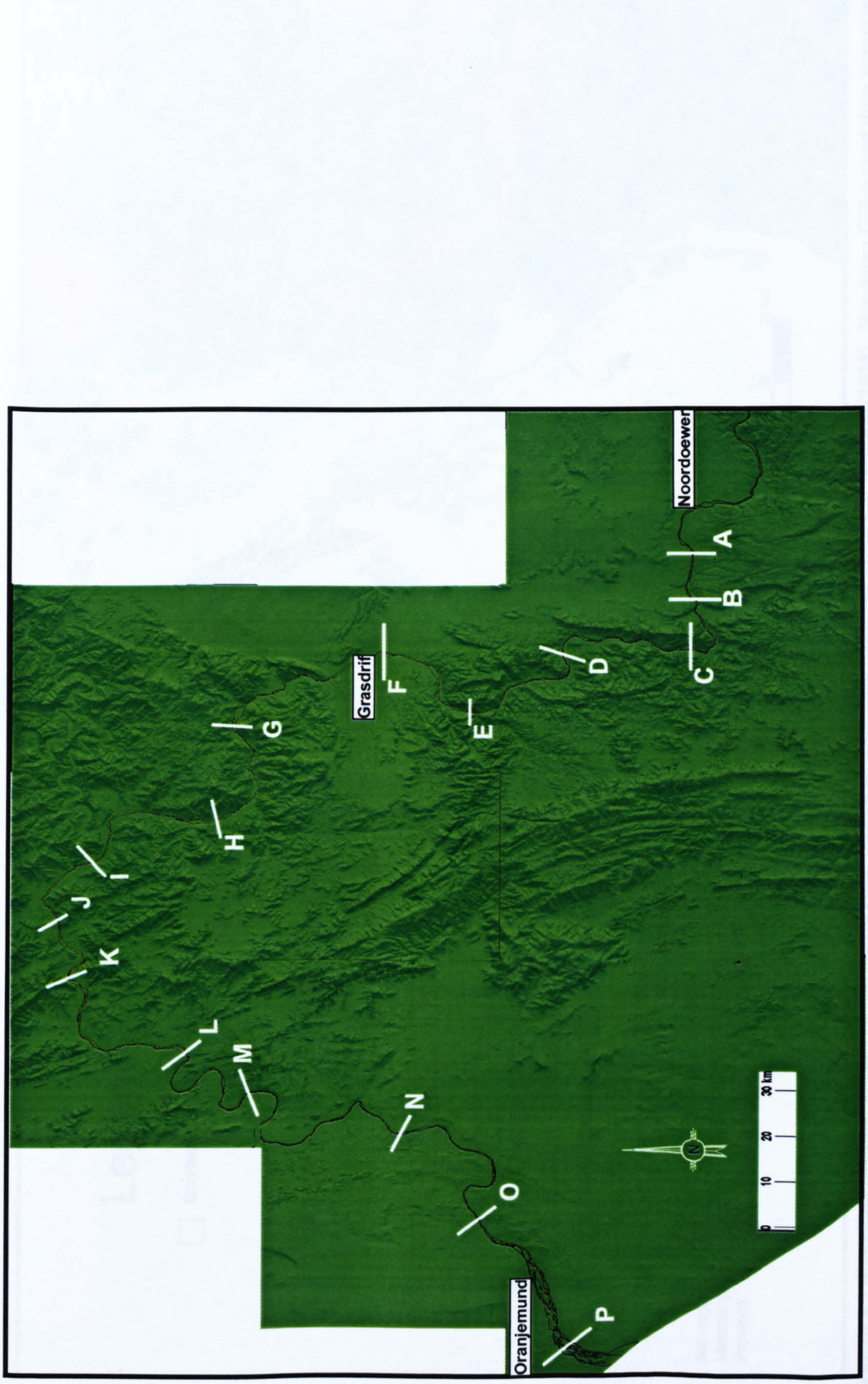

Figure 3. 2b Solid-shaded DTM of study area highlighting the topographic relief. Letters refer to section lines in Fig.3.9 A-P.

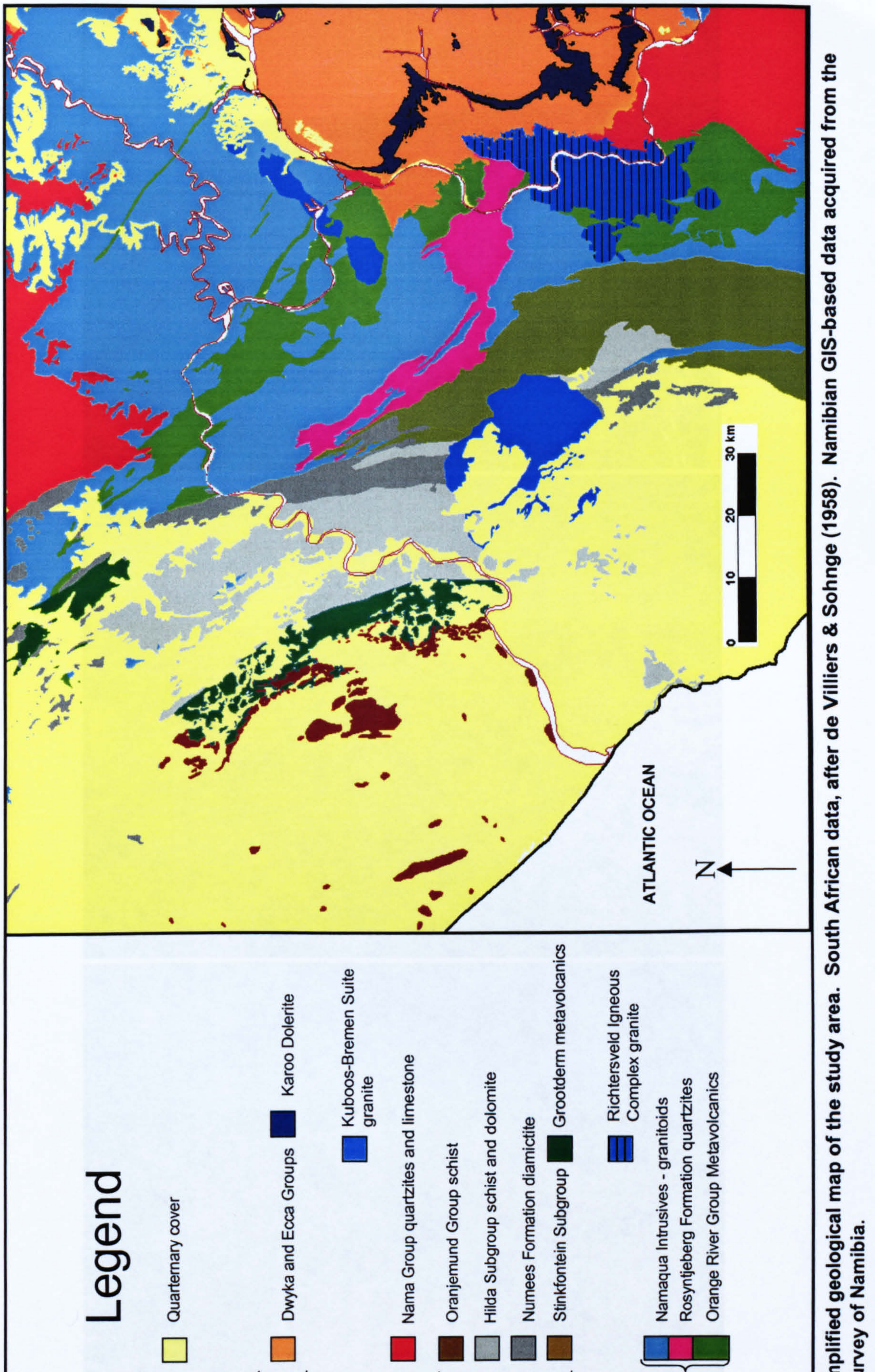

Figure 3.3 Simplified geological map of the study area. South African data, after de Villiers & Sohnge (1958). Namibian GIS-based data acquired from the Geological Survey of Namibia.

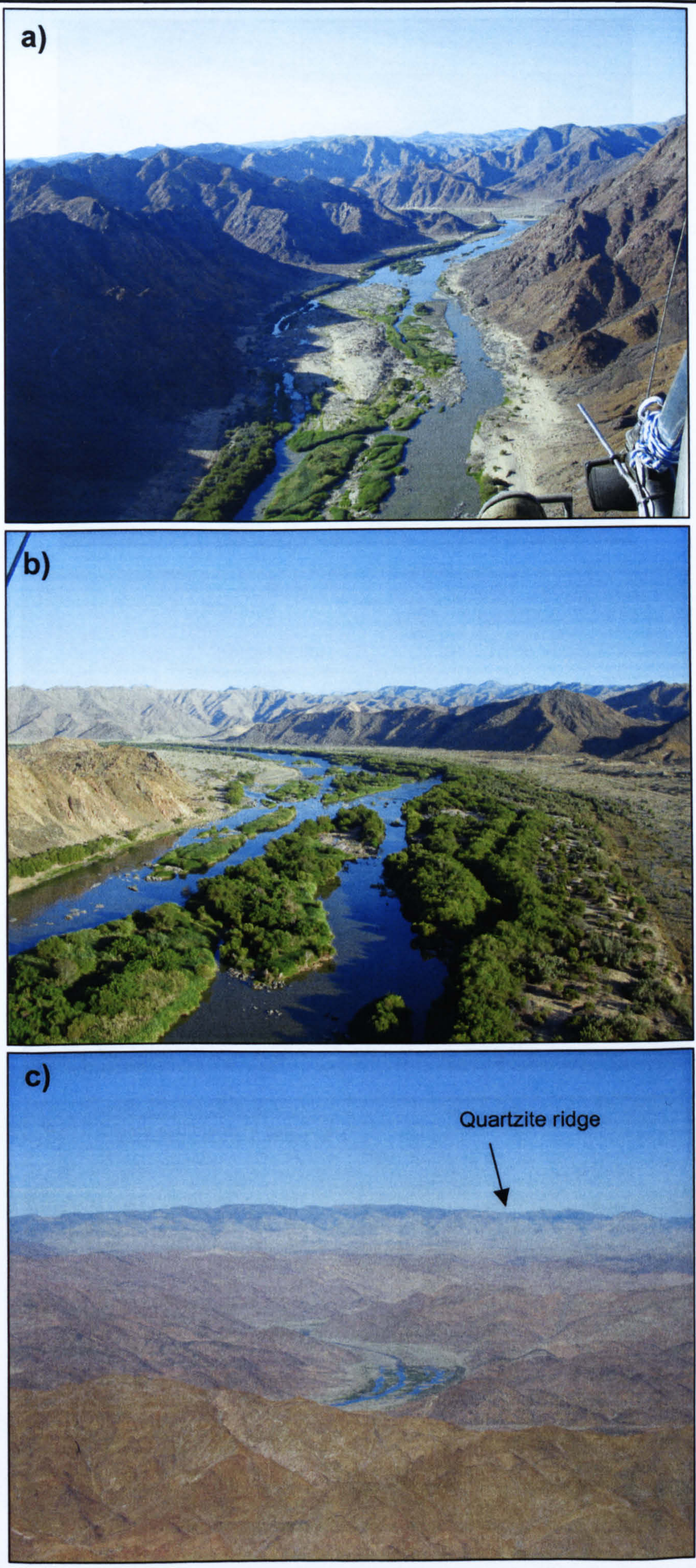

Figure 3.4 a-c Oblique aerial photos illustrating the incision of the Orange River into a landscape with a consistent summit level (500-600m) of the NMC basement rocks. Note the pre-Nama quartzite ridge in c).

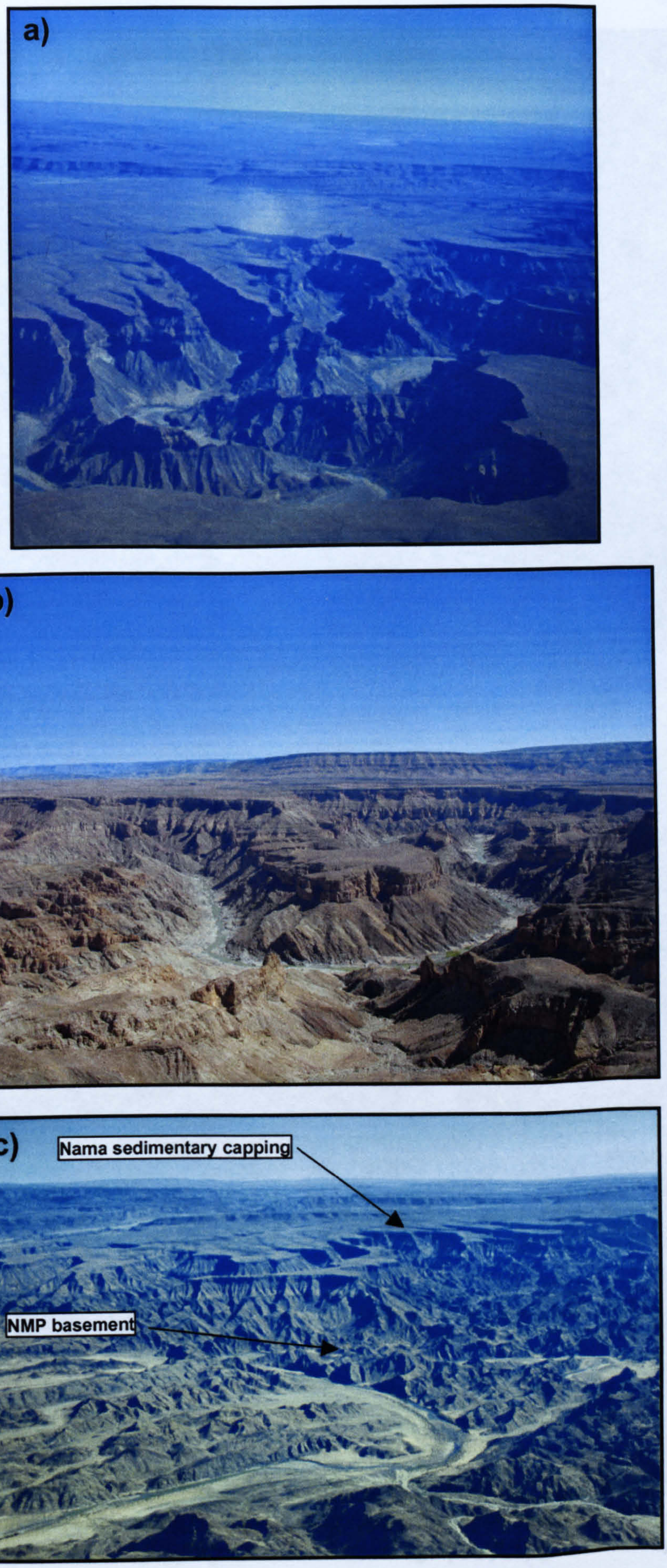

Figure 3.5 The Fish River canyon to the northeast of the study area. a) Upstream canyon reach b) Mid-canyon reach c) Downstream canyon reach with Nama Group sedimentary cover removed from the underlying NMC basement.

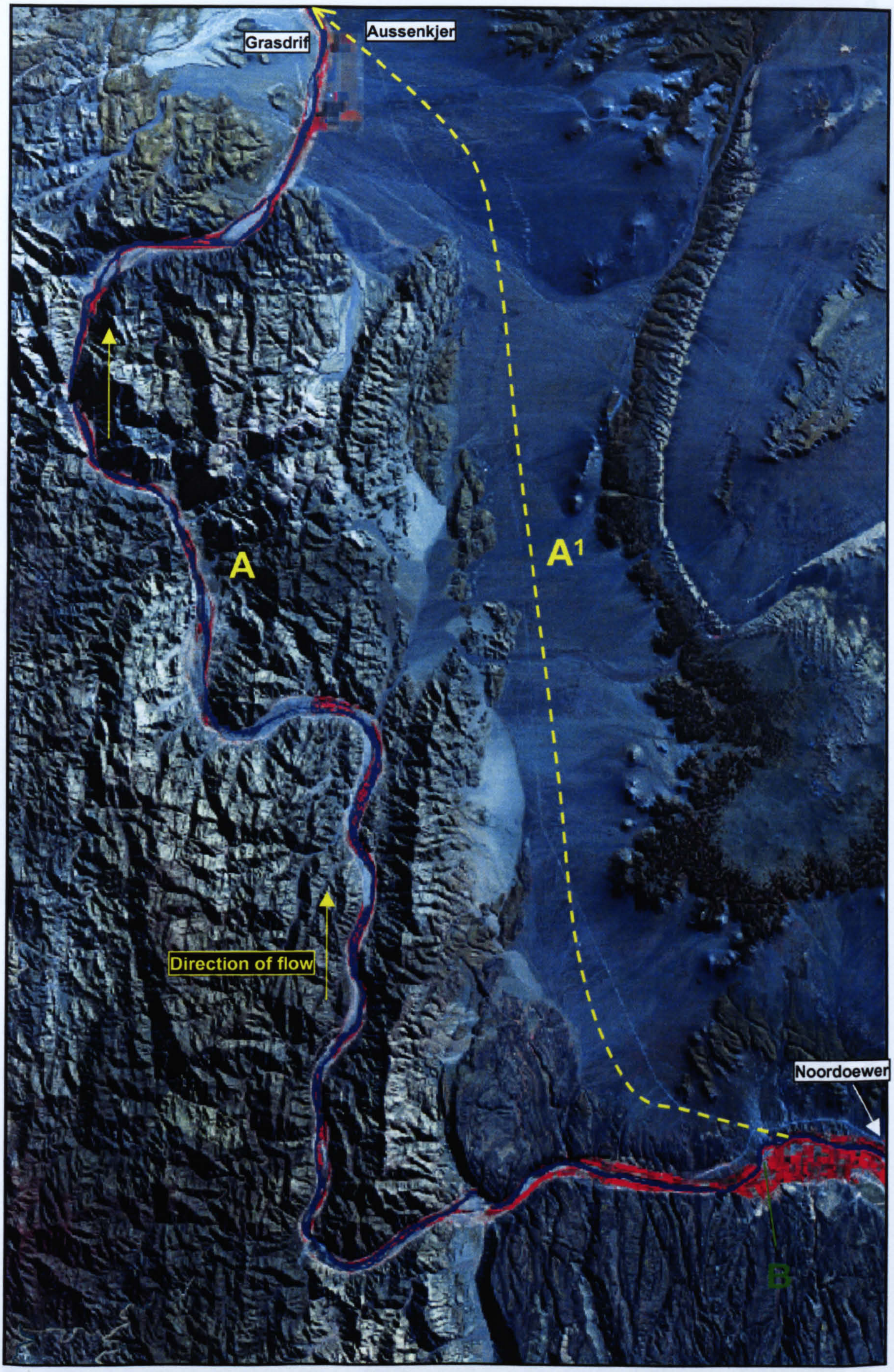

Figure 3.6 Satellite image showing superimposed route A as opposed to easier route A^1 and the short reach B occupying a Carboniferous age (Dwyka) glacial valley.

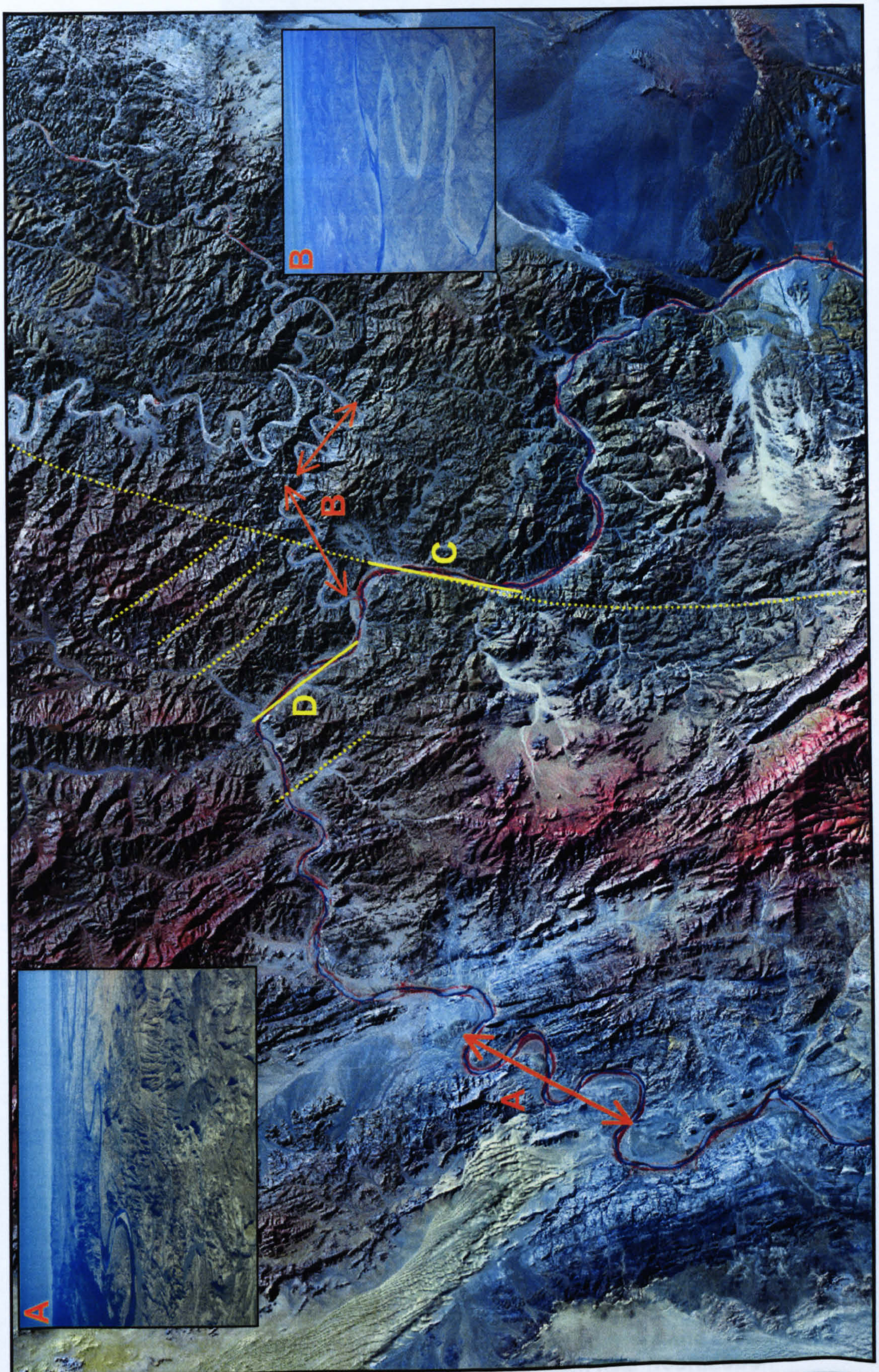

Figure 3.7 Superimposed meanders (A and B) and reaches influenced by basement structures (C exploits path followed by dyke and D exploits regional foliation).

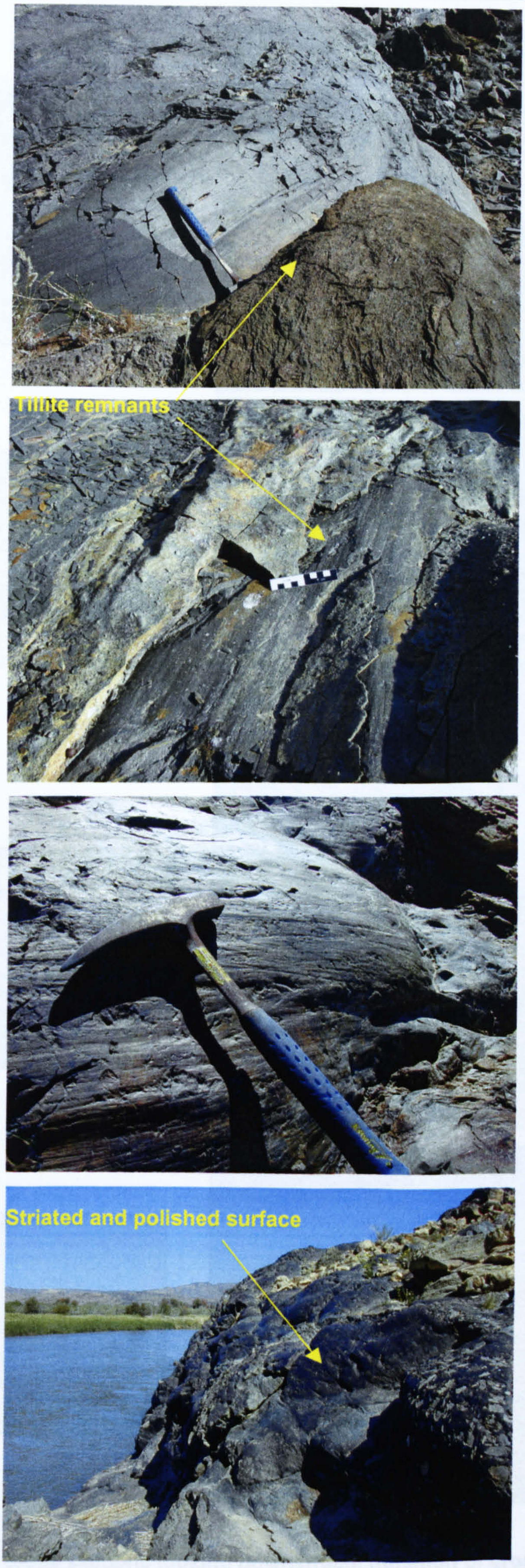

Figure 3.8 Photos illustrating the striated and polished surfaces and Dwyka tillite remnants present in the valley sidewalls of a short reach near Noordoewer.

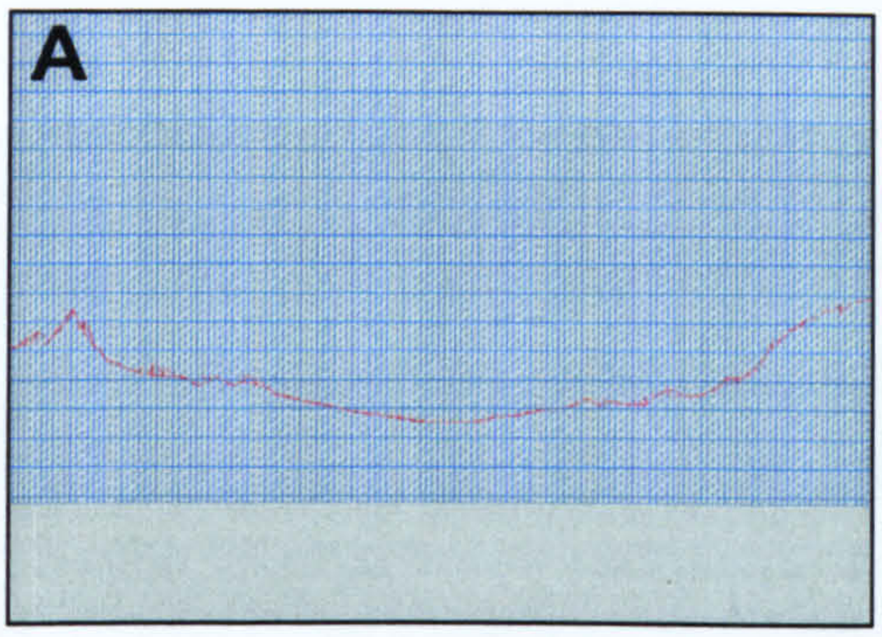

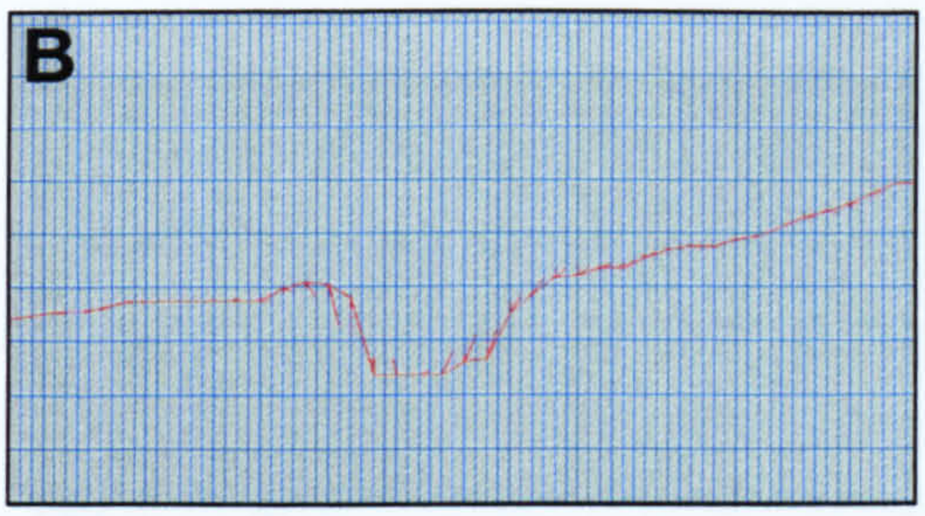

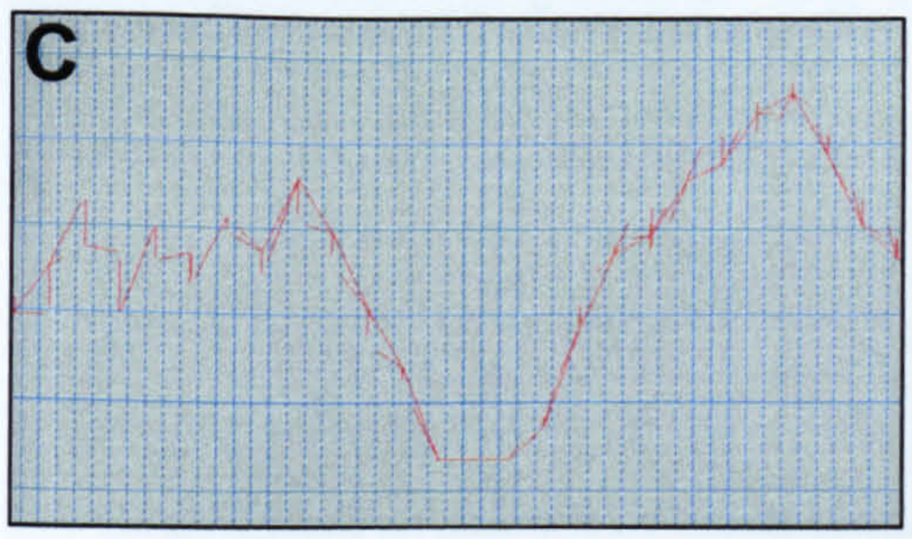

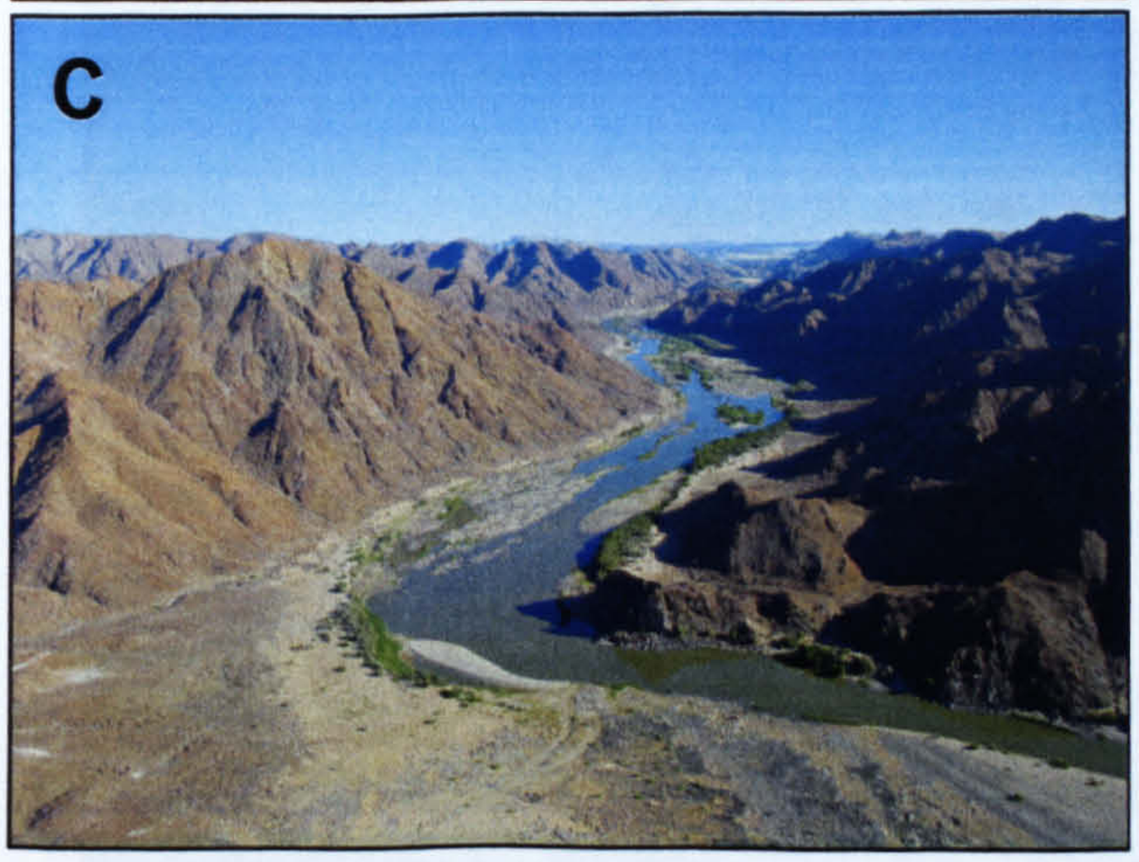

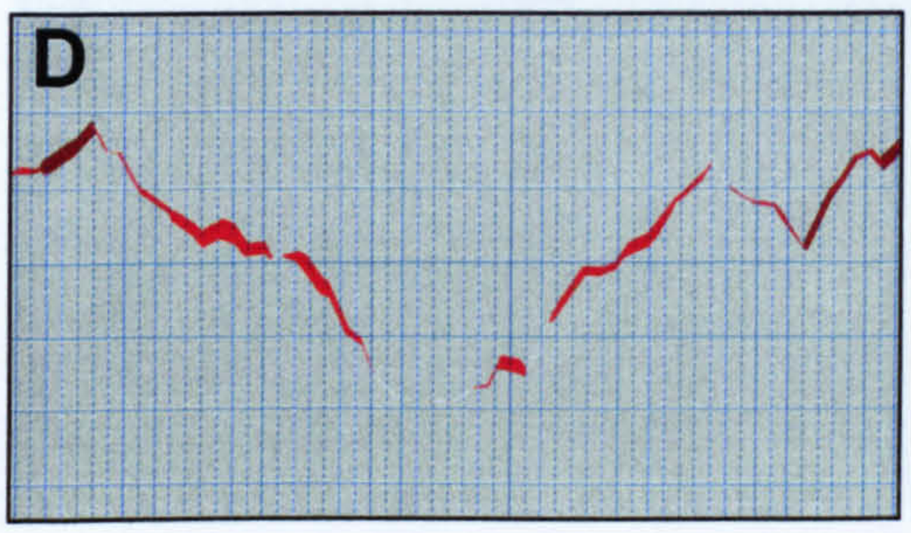

Figure 3.9 A-D Valley cross sections looking downstream (location of cross sections in figure 3.3). Grid dimensions on cross sections are 100x100 m.

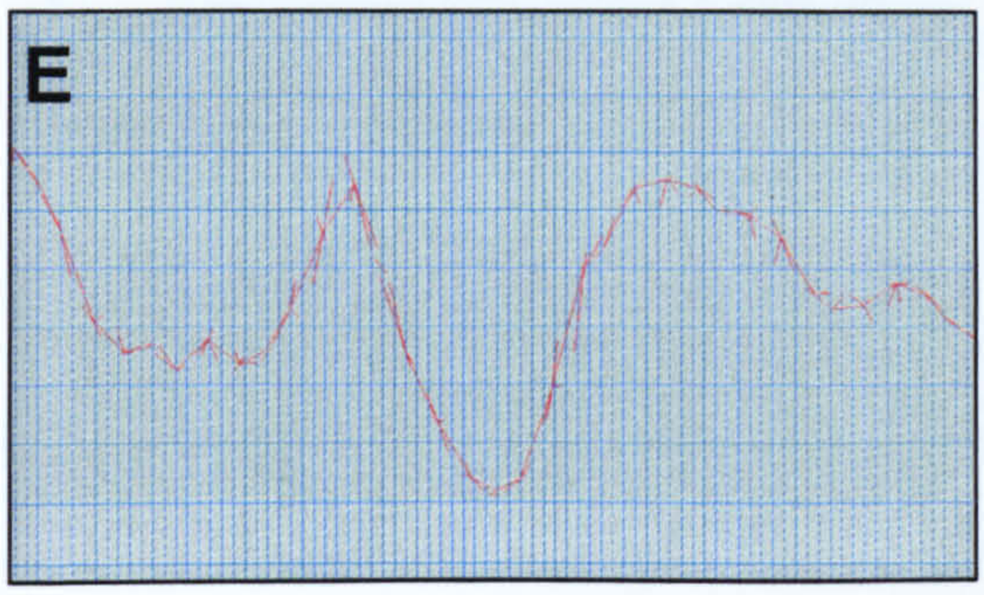

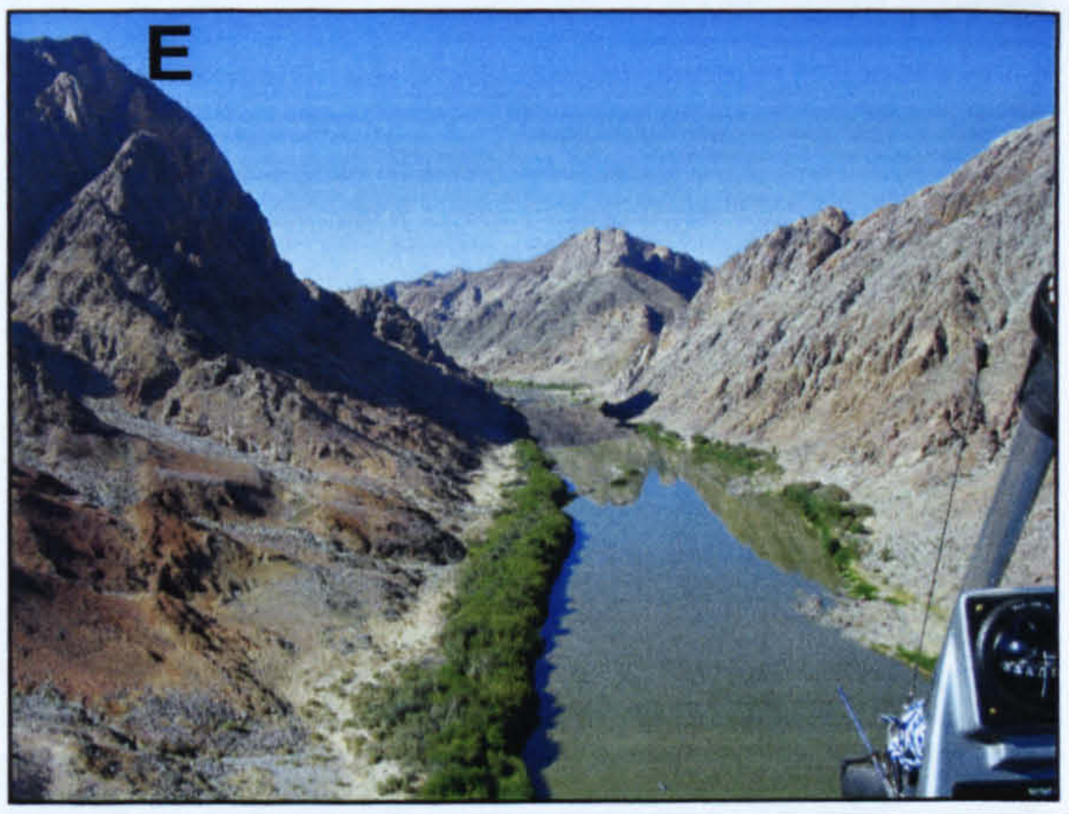

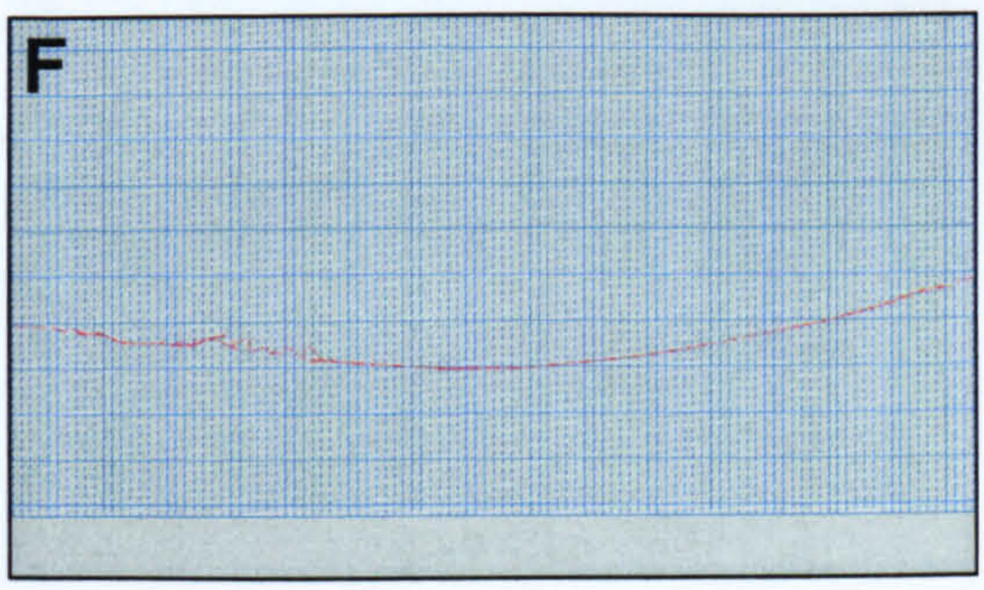

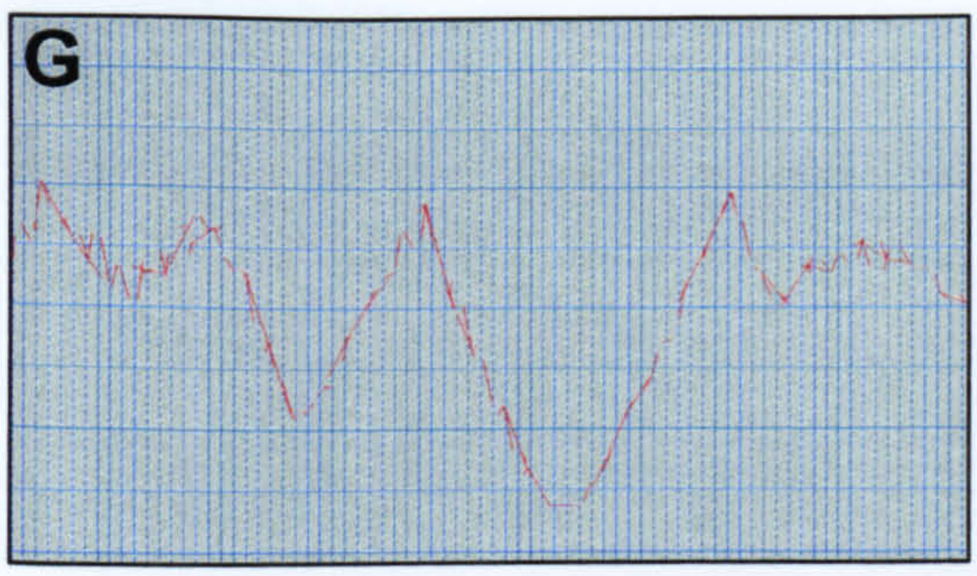

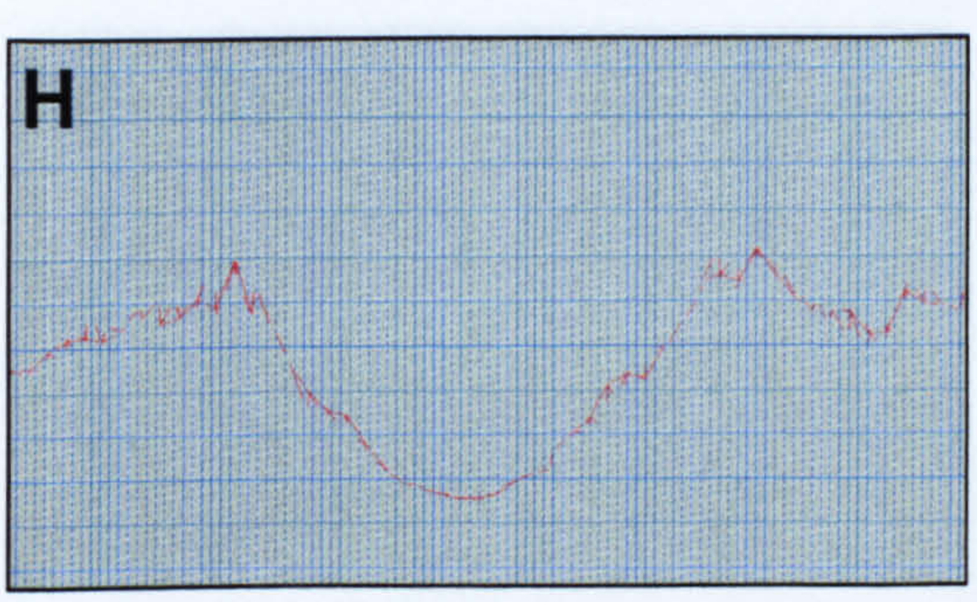

Figure 3.9 E-H Valley cross sections looking downstream (location of cross sections in figure 3.3). Grid dimensions on cross sections are 100x100 m.

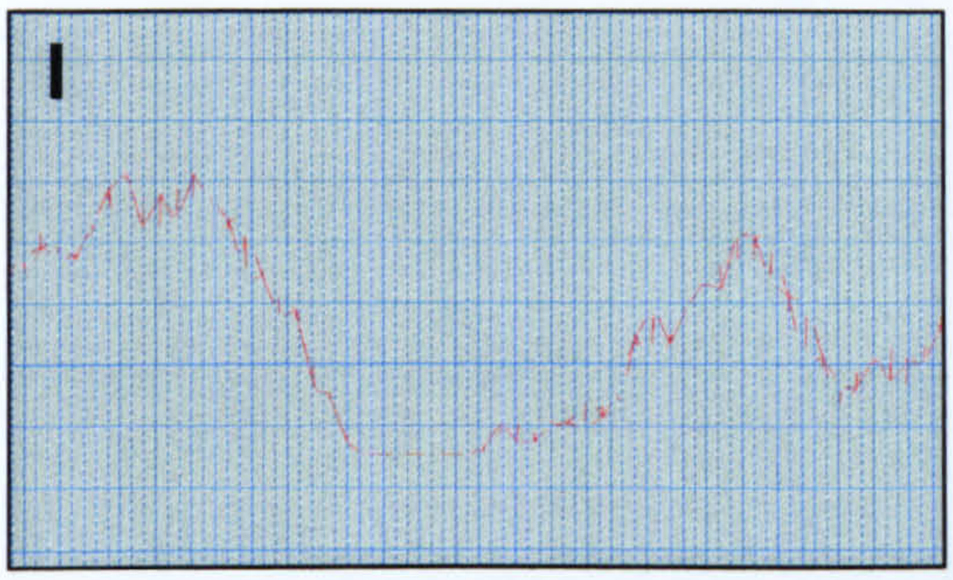

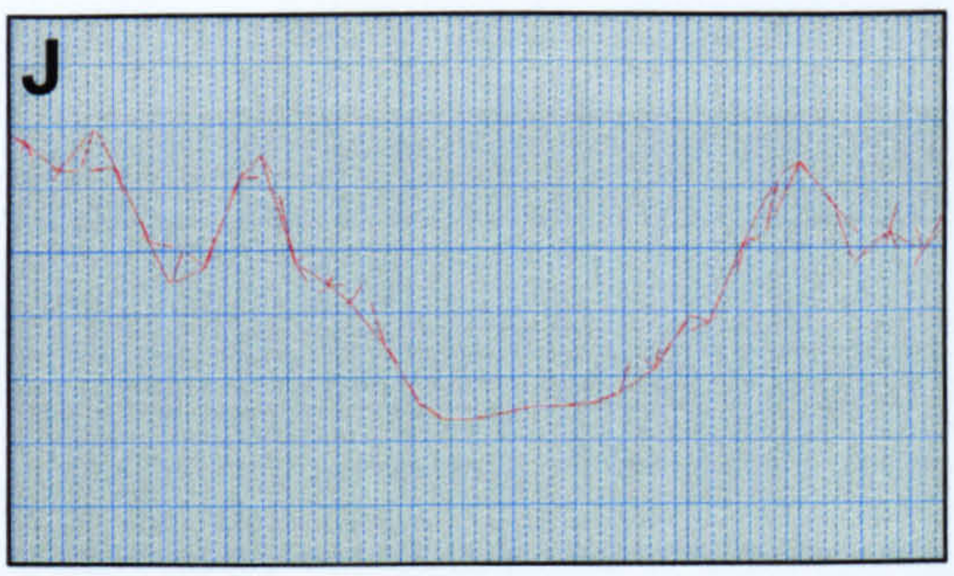

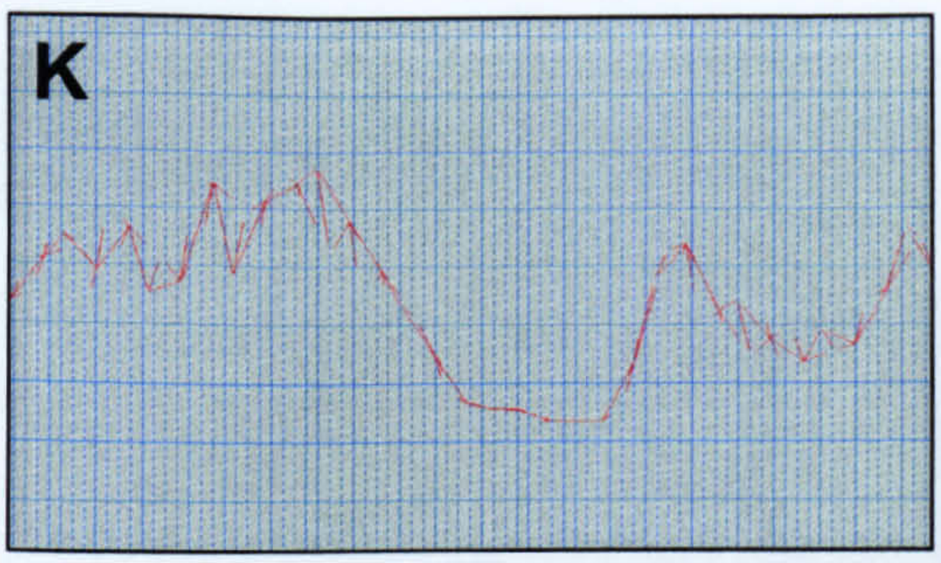

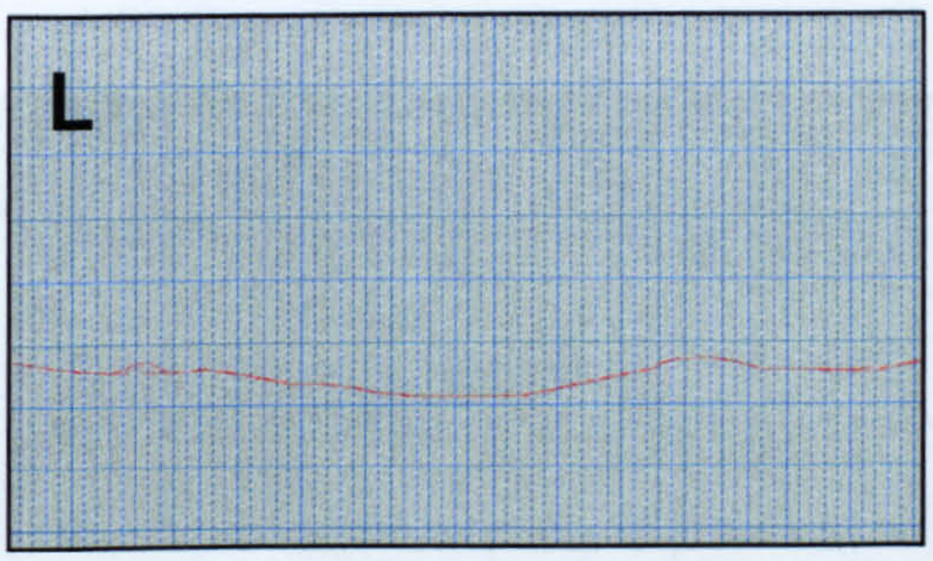

Figure 3.9 I-L Valley cross sections looking downstream (location of cross sections in figure 3.3). Grid dimensions on cross sections are 100x100 m.

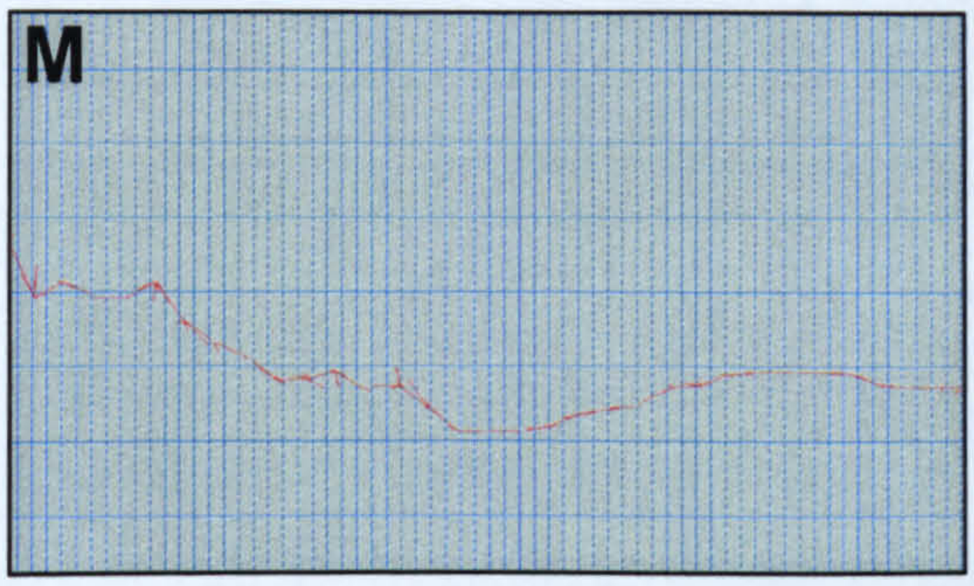

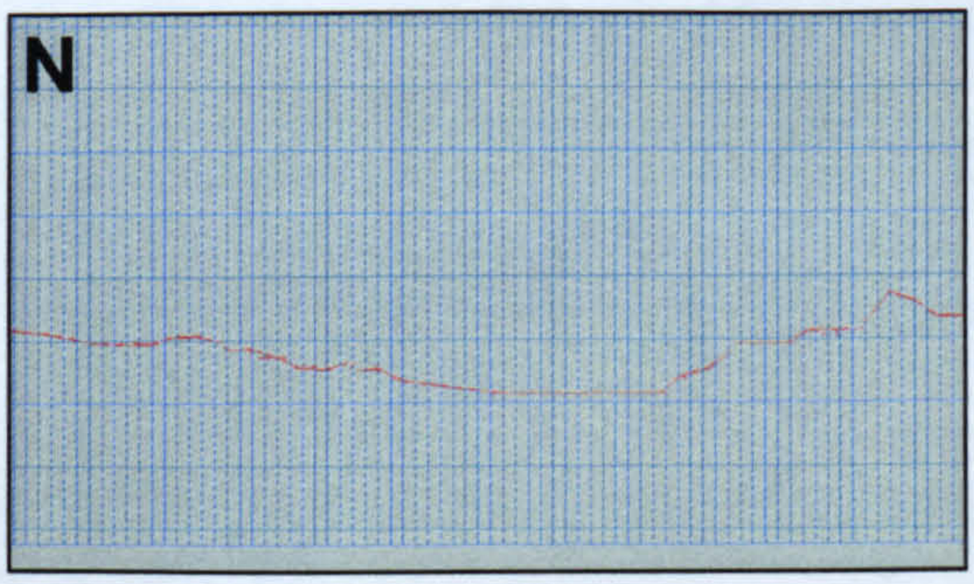

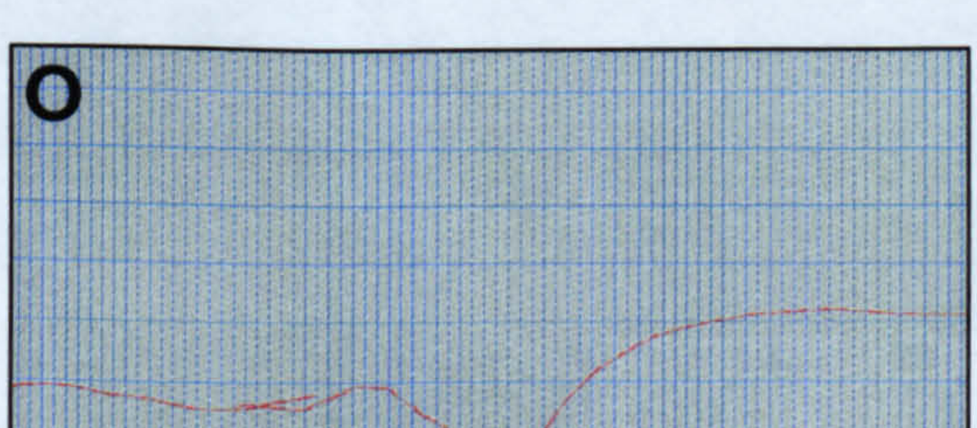

Figure 3.9 M-P Valley cross sections looking downstream (location of cross sections in figure 3.3). Grid dimensions on cross sections are 100x100 m.

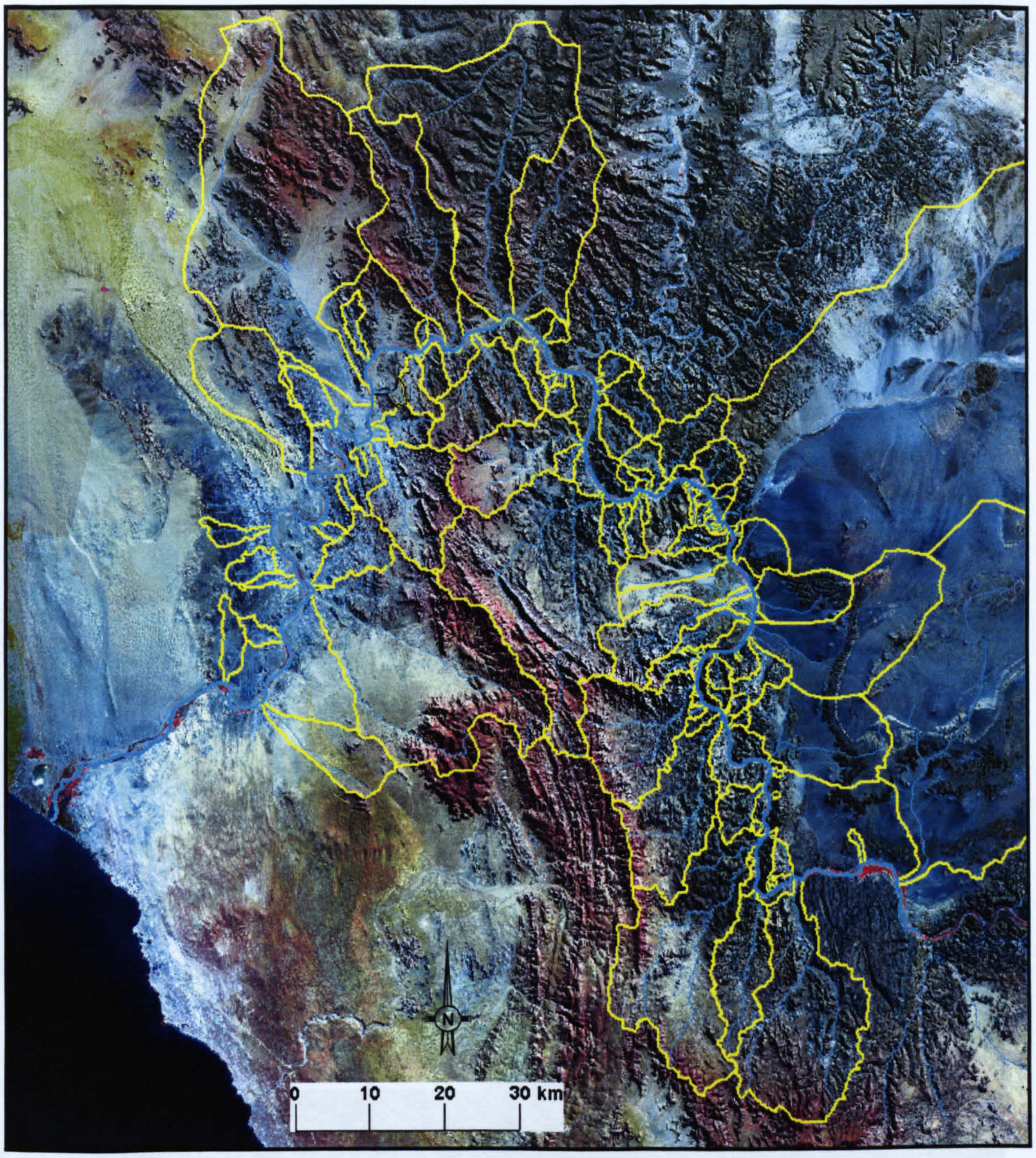

Figure 3.10 Satellite image showing tributary network and their drainage basins.

Figure 3.11 Oblique aerial photograph showing Orange River (bottom right) and different sized tributaries. Large meandering tributary is the Fish River.

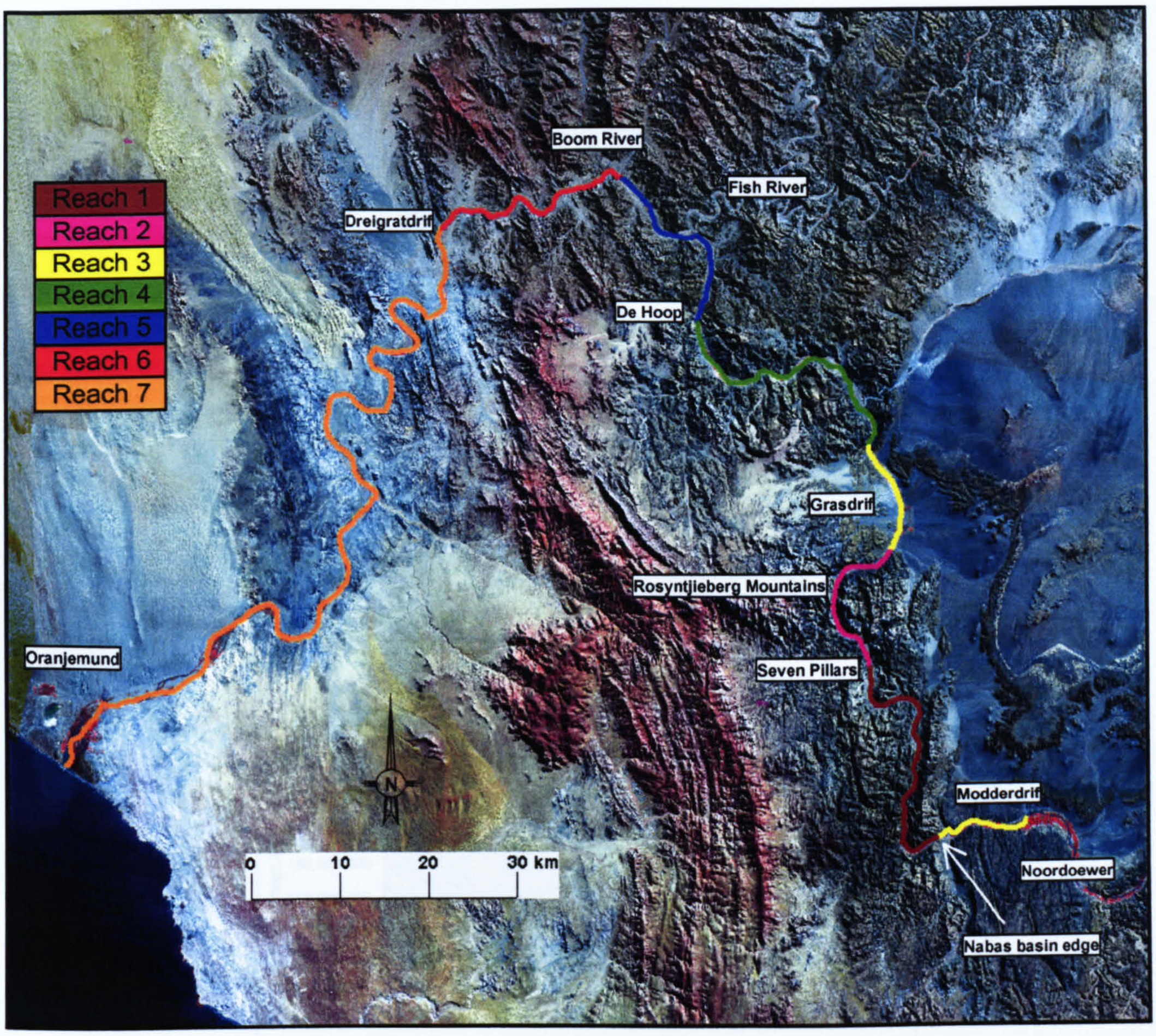

Figure 3.12 Satellite image of study area showing Reaches 1-7.

a)

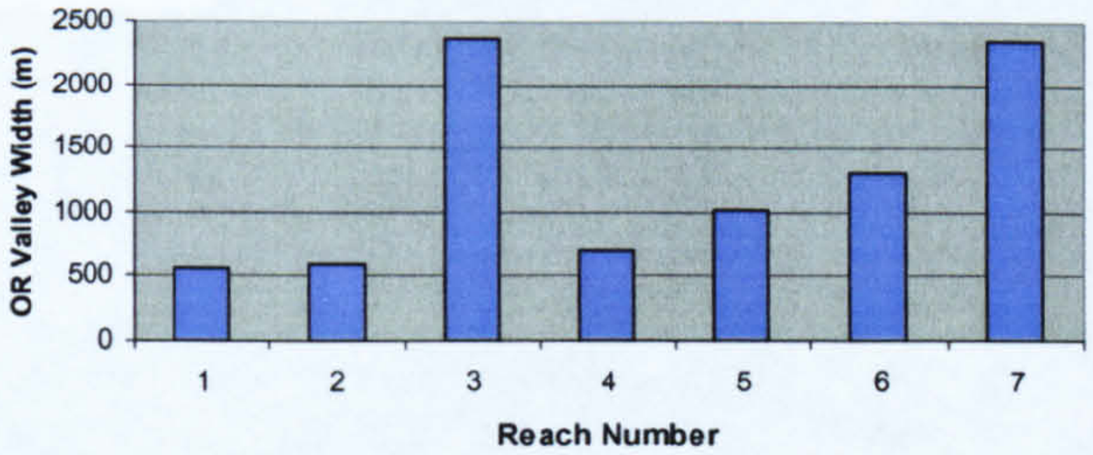

b)

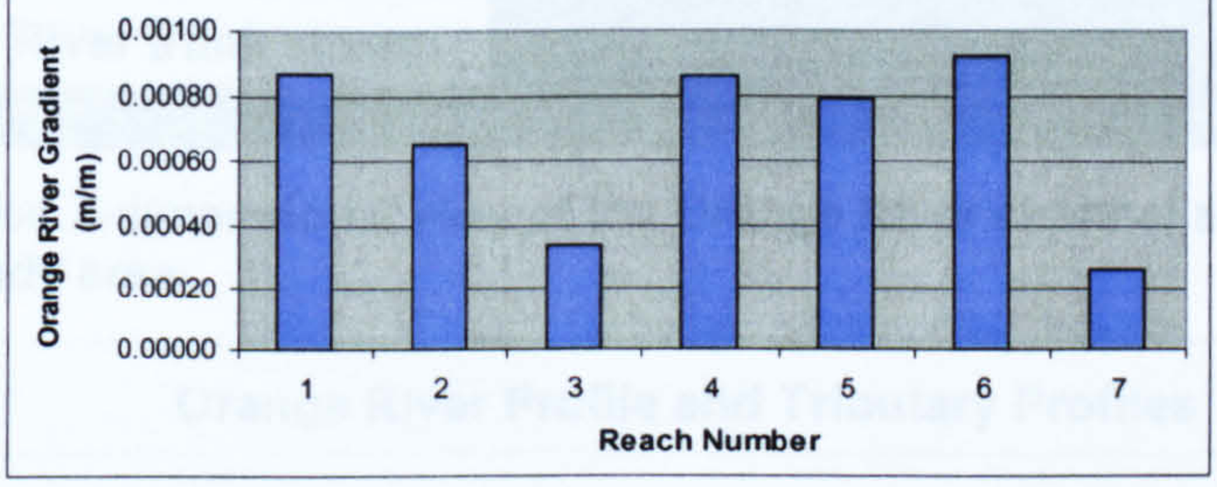

c)

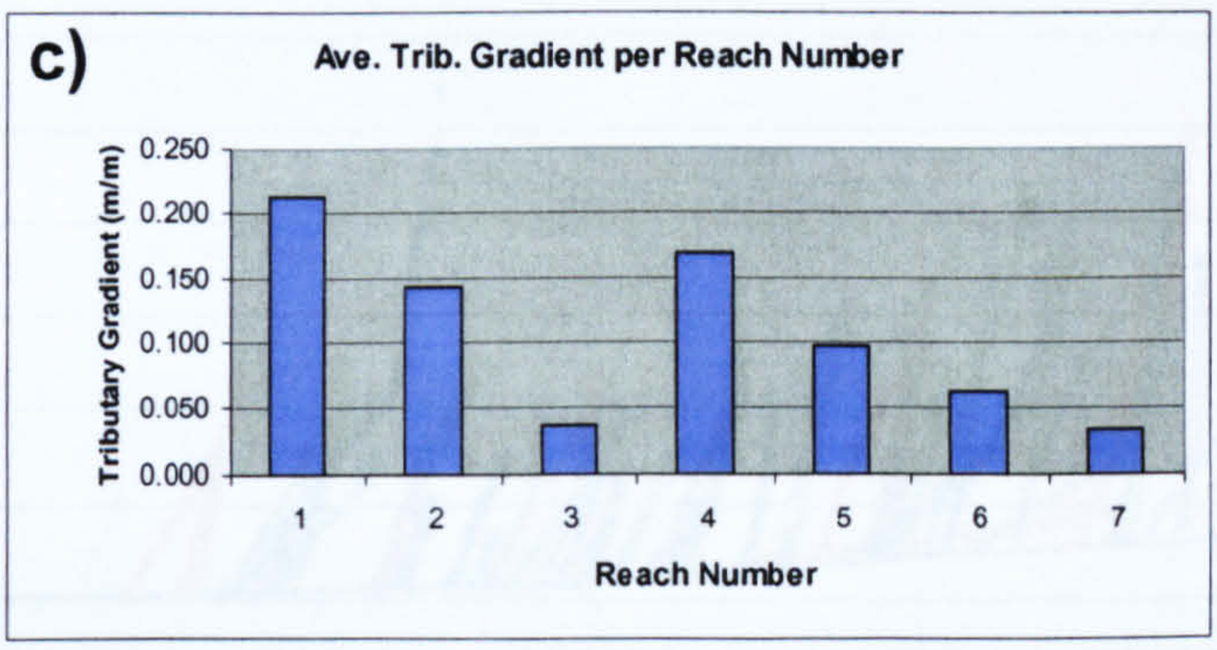

d)

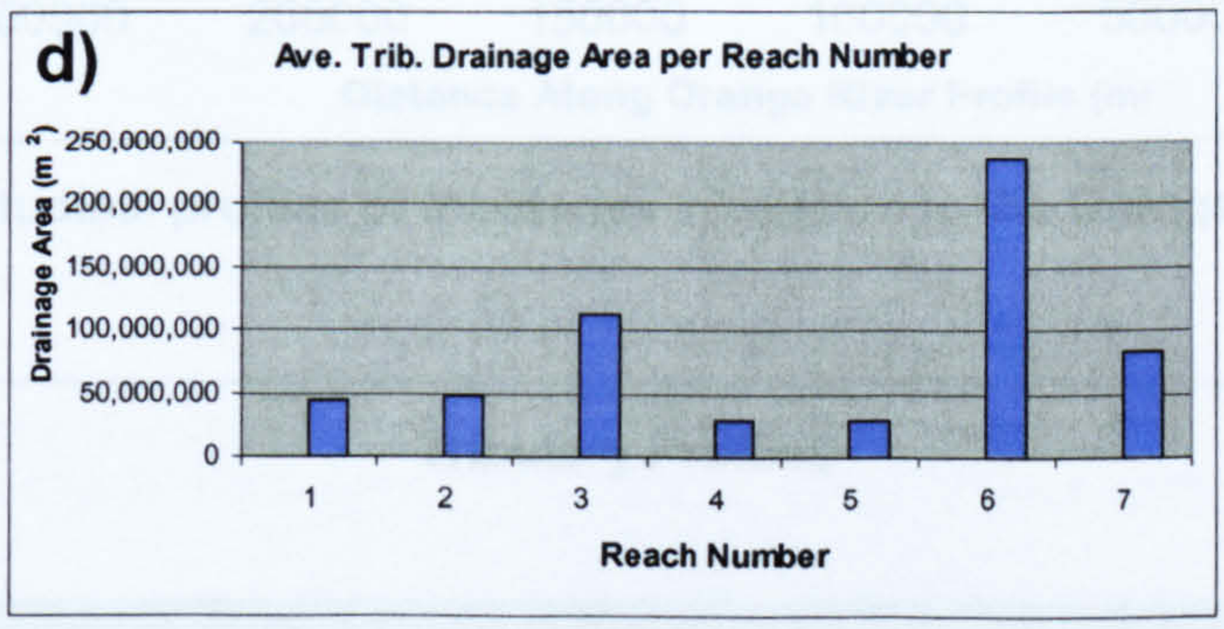

e)

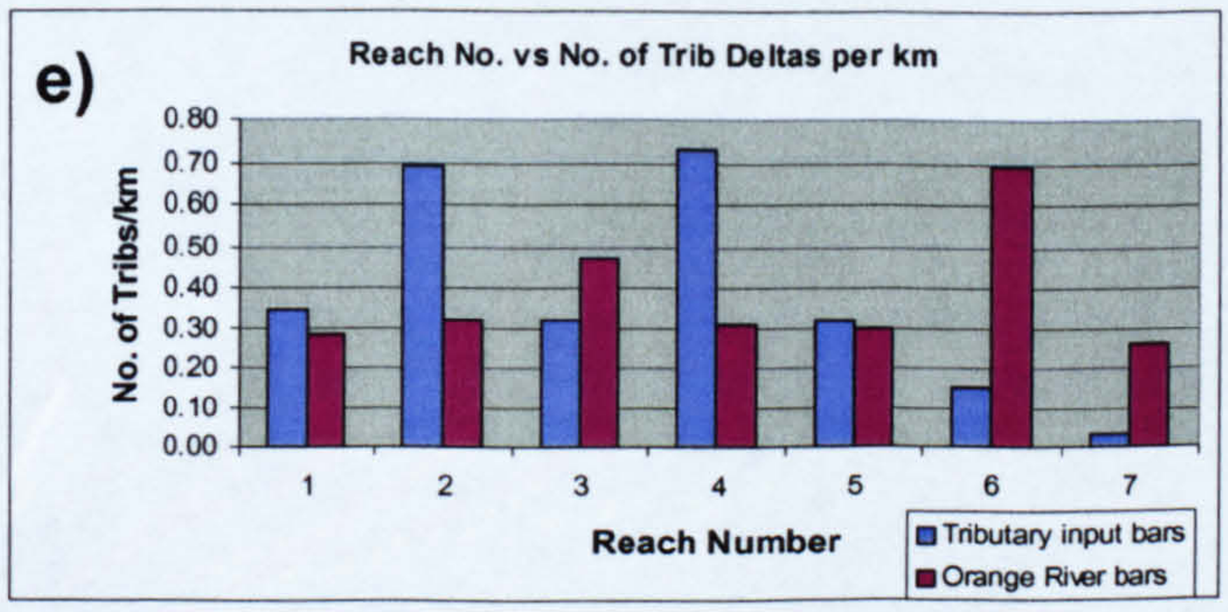

f)

Reach	OR Valley Width (m)	OR Length (km)	Strath %	OR Gradient (m/m)	Av.Trib Gradient (m/m)	Av.Trib DB Area (m^2)	Av.Trib Length (m)	Tributary Bars per km	Normal Bars per km
1	554	32	49%	0.00087	0.212	44,075,229	8,497	0.34	0.28
2	597	19	9%	0.00066	0.143	47,134,766	8,632	0.69	0.32
3	2371	26	3%	0.00034	0.035	112,075,591.67	16,796	0.32	0.47
4	690	34	37%	0.00086	0.168	29,167,649	6,234	0.73	0.31
5	1012	24	8%	0.00080	0.097	28,673,298	7,104	0.32	0.30
6	1302	26	0%	0.00093	0.061	236,172,994	34,524	0.15	0.69
7	2347	115	0%	0.00026	0.033	83,557,934	14,092	0.03	0.26

Figure 3.13 Comparison of overall characteristics per geomorphic reach.

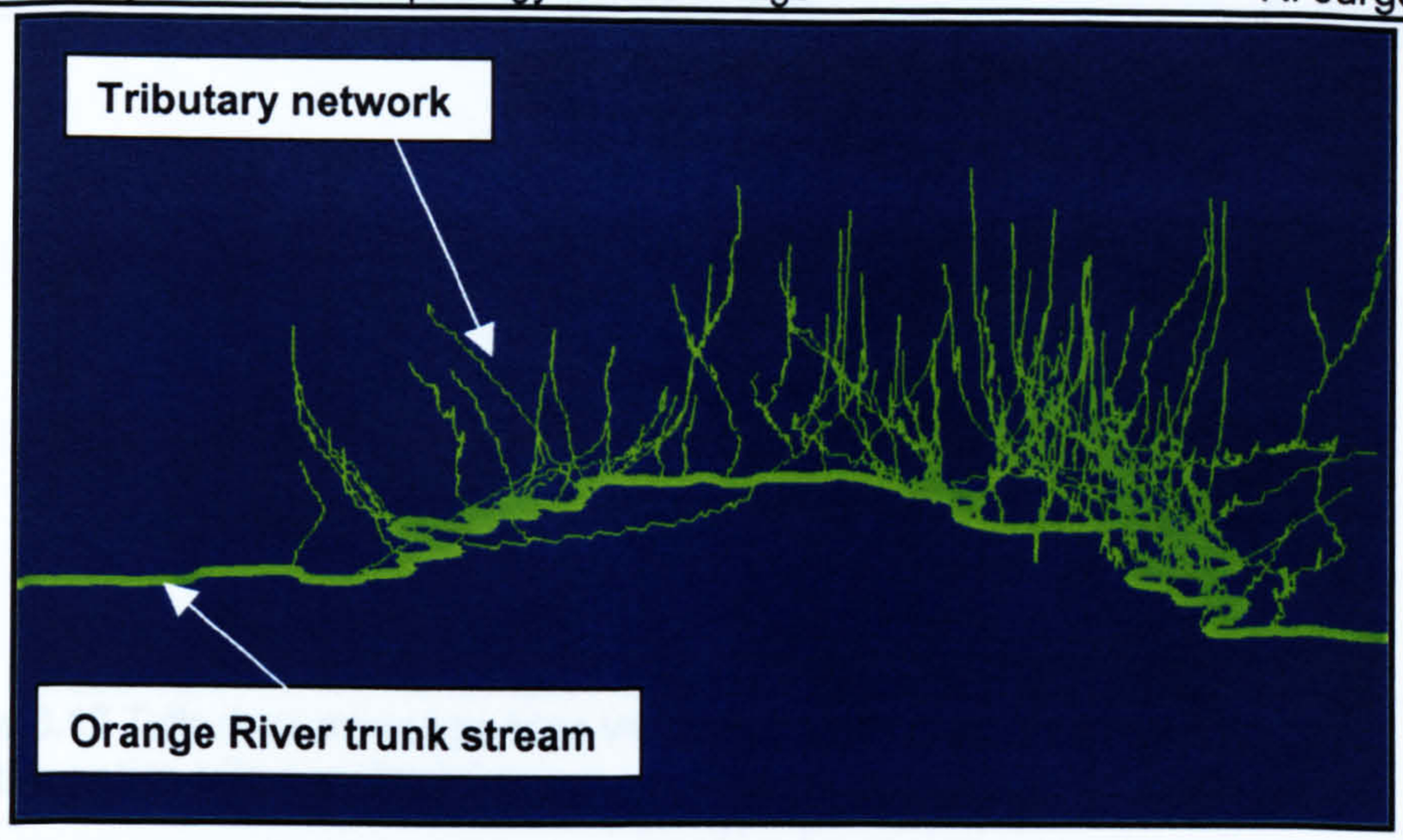

Figure 3.14 Rotated 3-dimensional view of the Orange River channel and its tributary network in the study area.

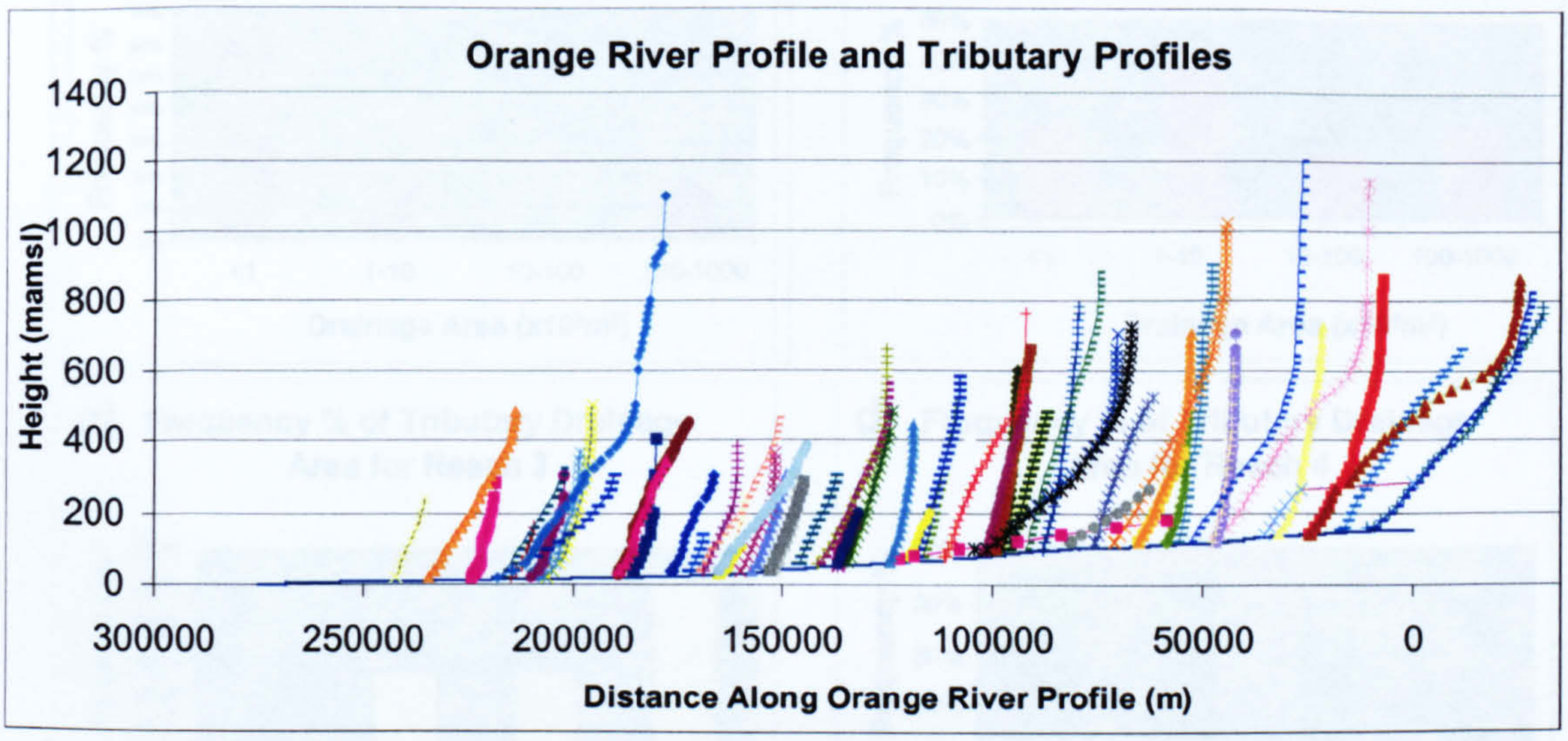

Figure 3.15 Longitudinal profiles of tributaries in relation to the Orange River profile.

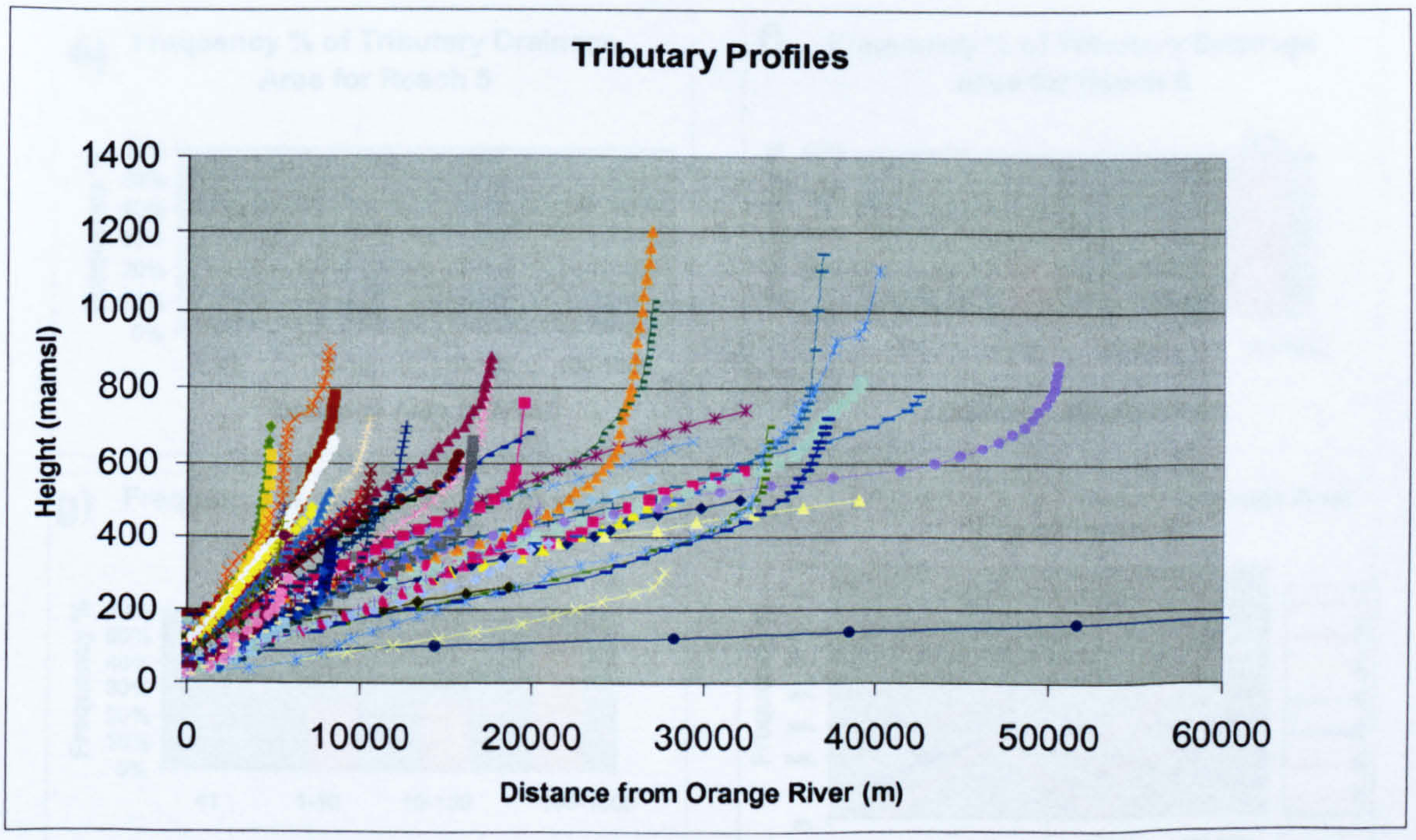

Figure 3.16 All tributary profiles in the study area. Low gradient tributary is the Fish River.

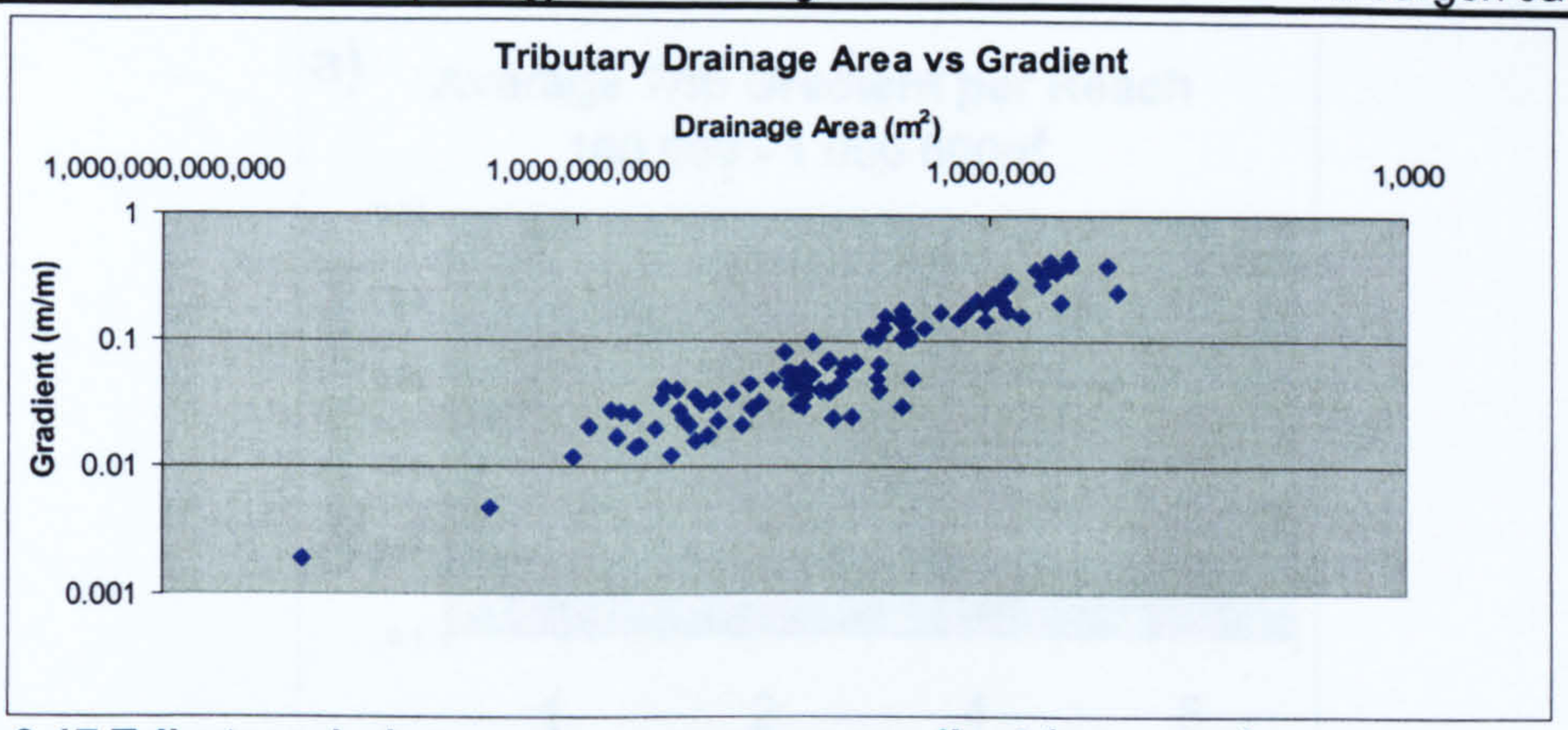

Figure 3.17 Tributary drainage area vs average gradient (averaged over the entire tributary length).

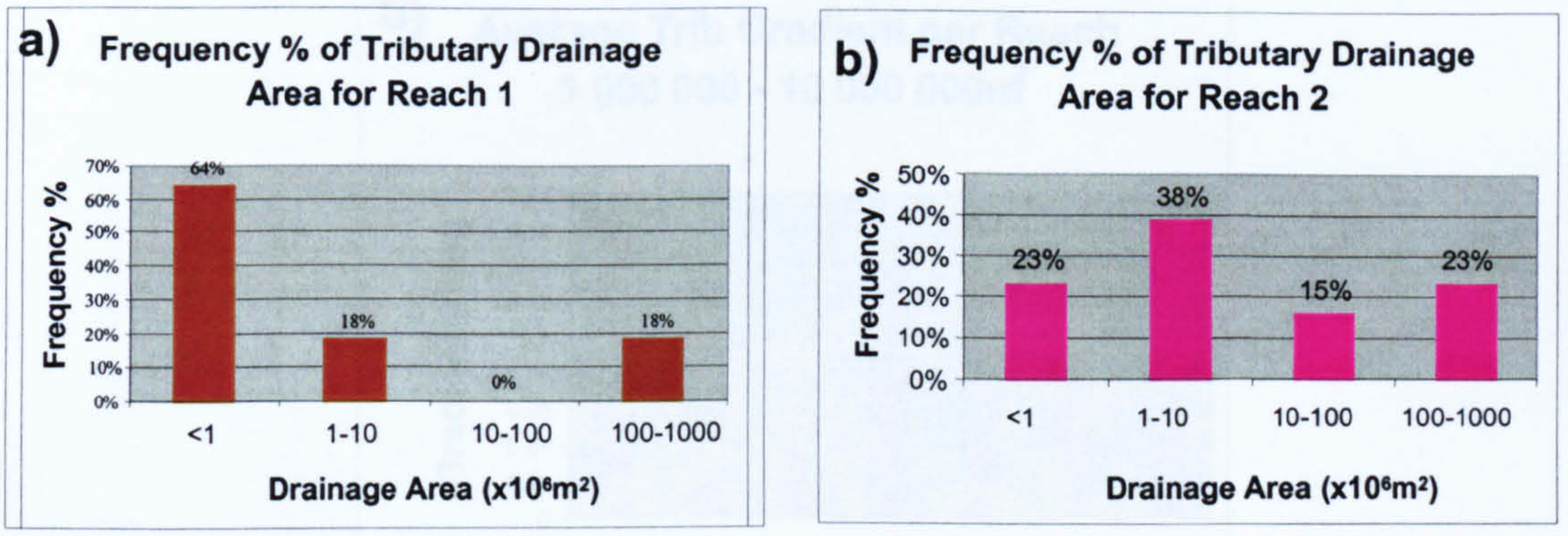

Figure 3.18 Drainage area analysis of the tributary catchments for Reaches 1-7.

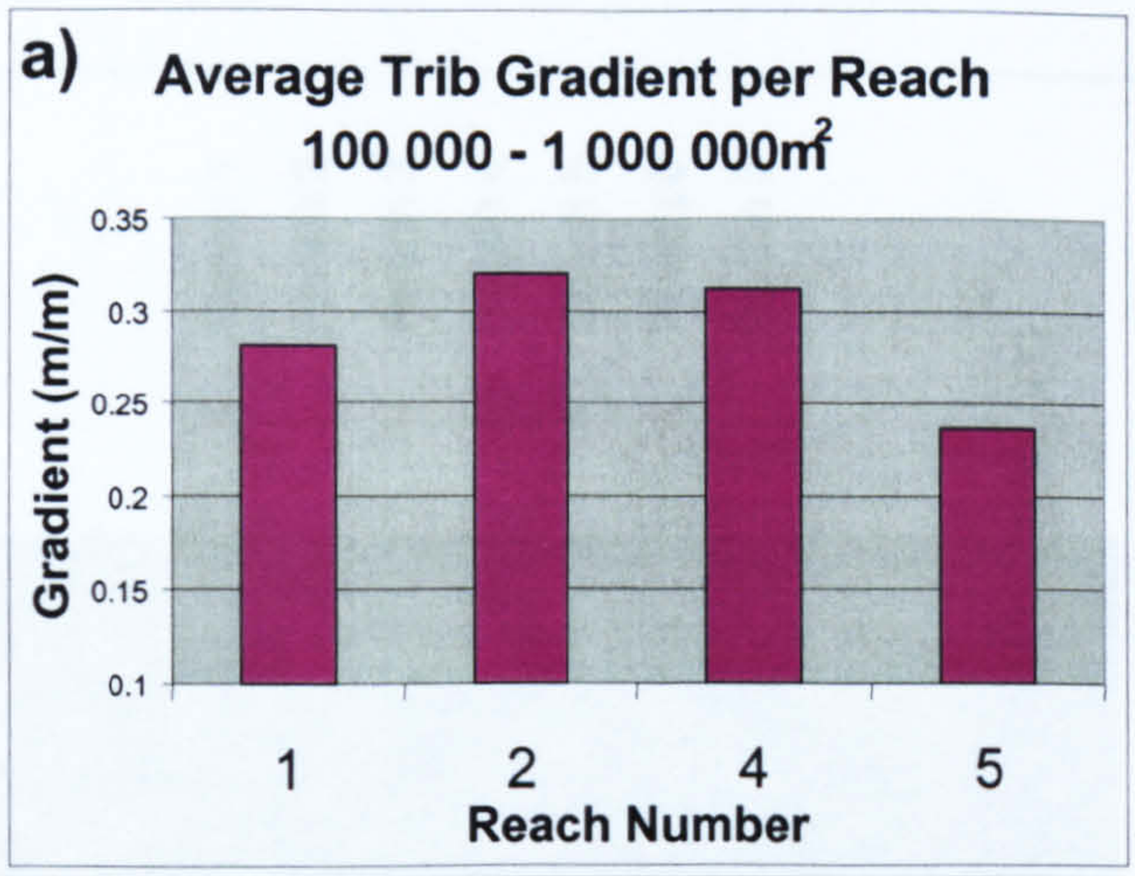

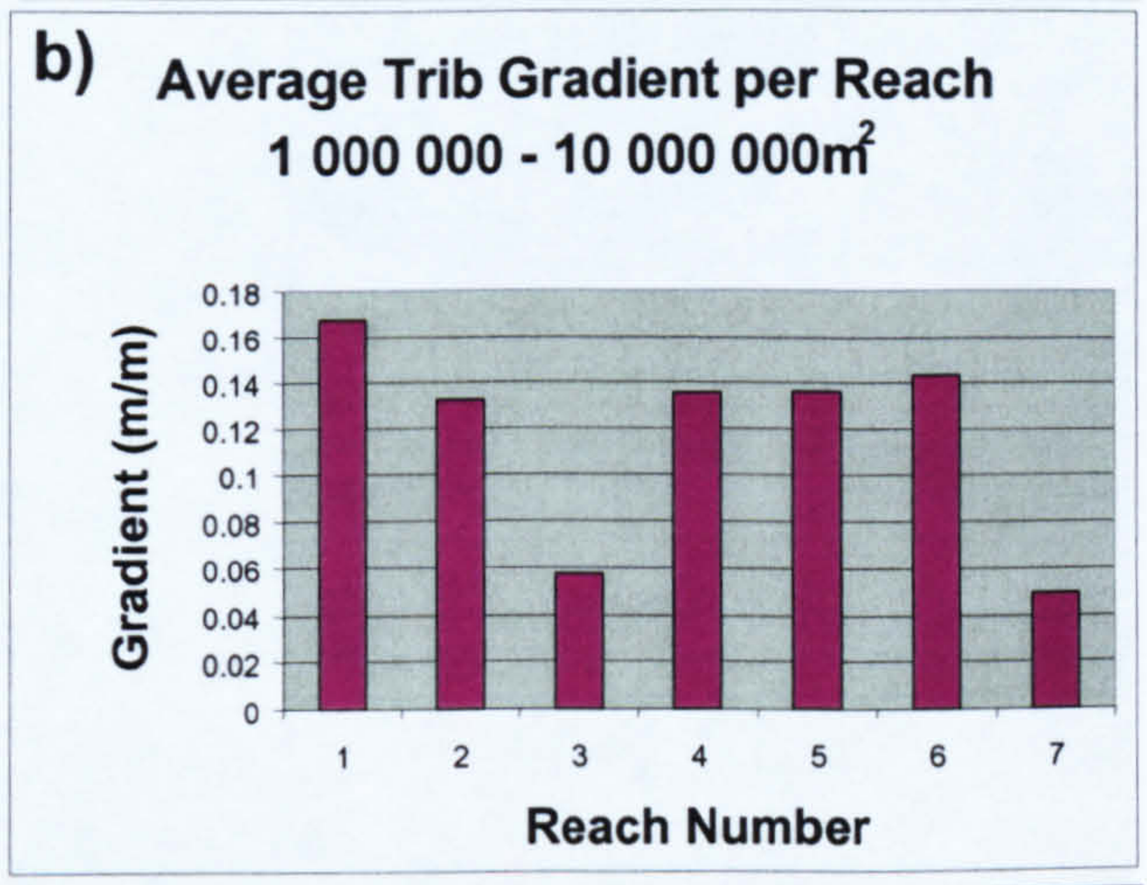

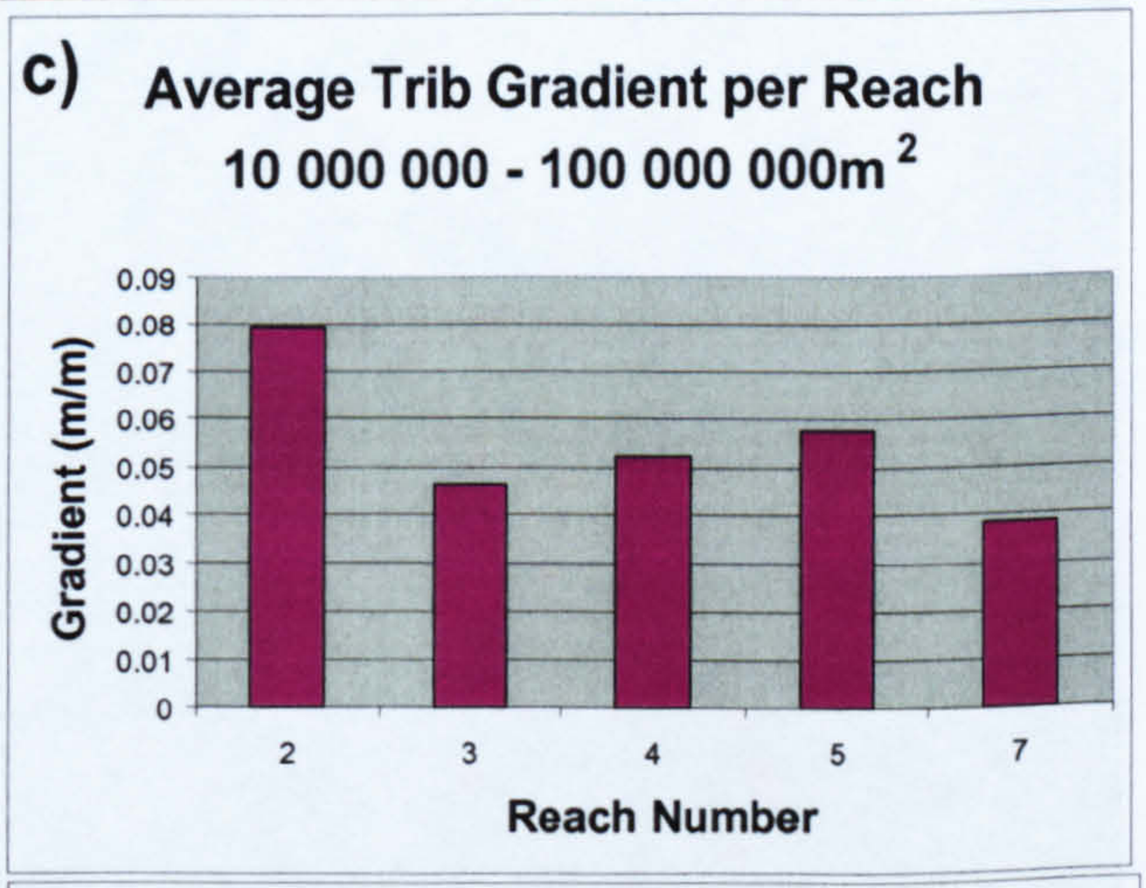

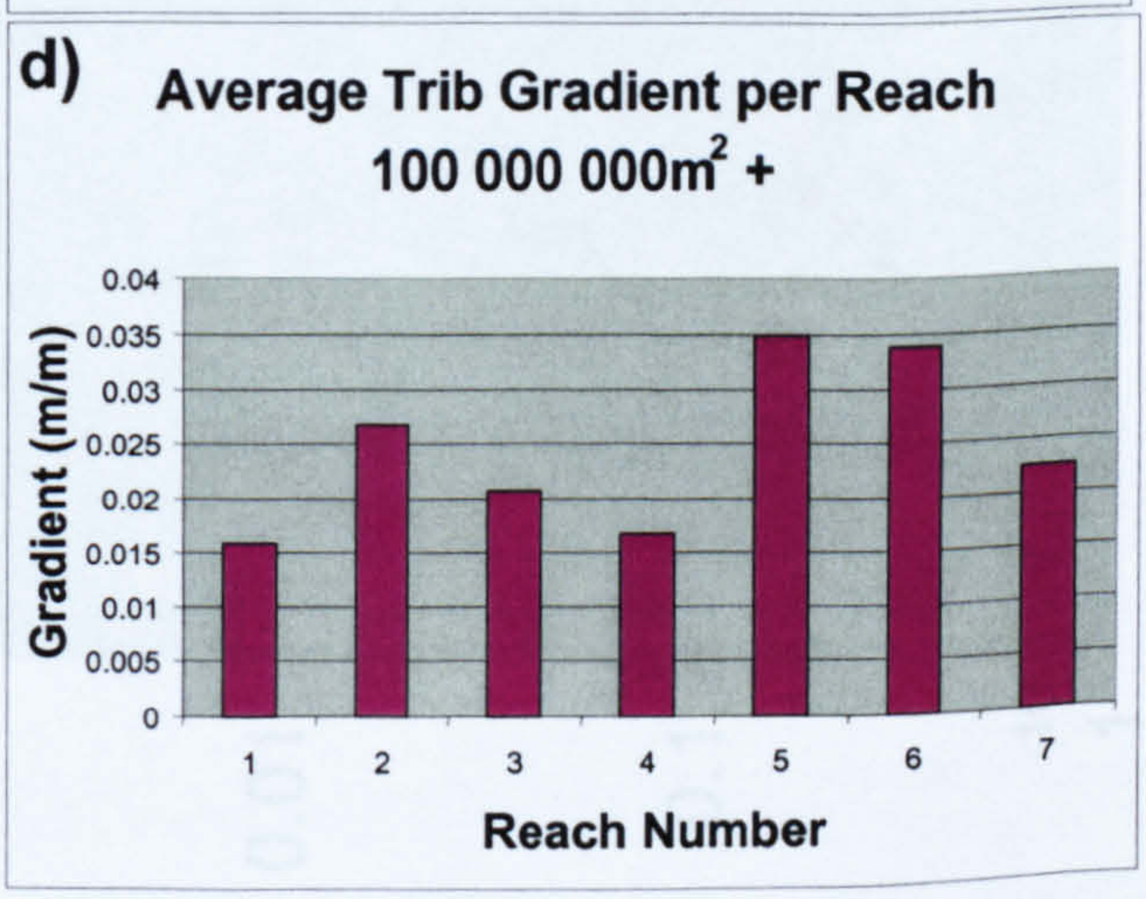

Figure 3.19 Tributary gradient analysis per reach for equivalent drainage basin areas.

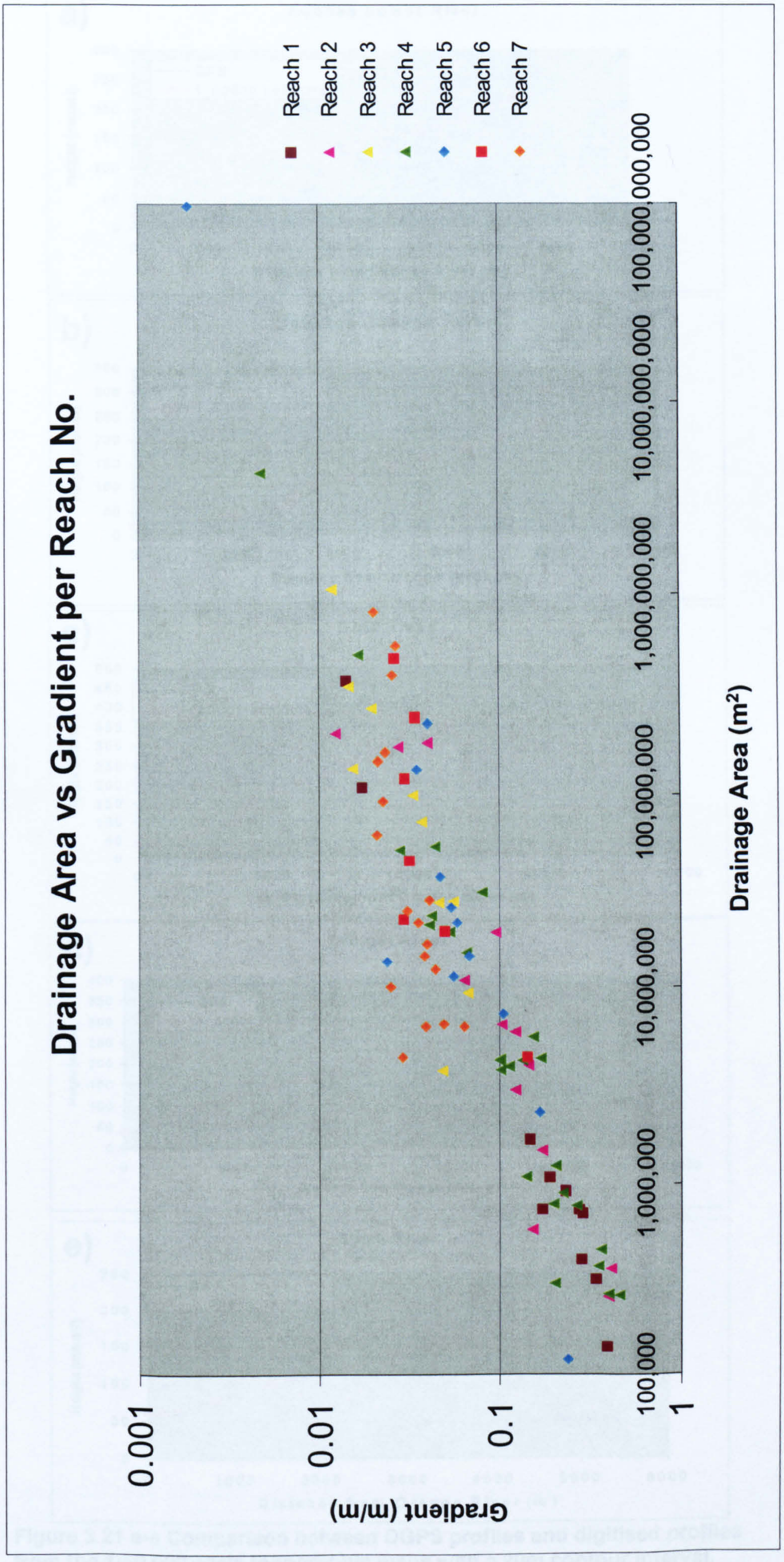

Figure 3.20 Drainage area vs tributary gradient per Geomorphic Reach.

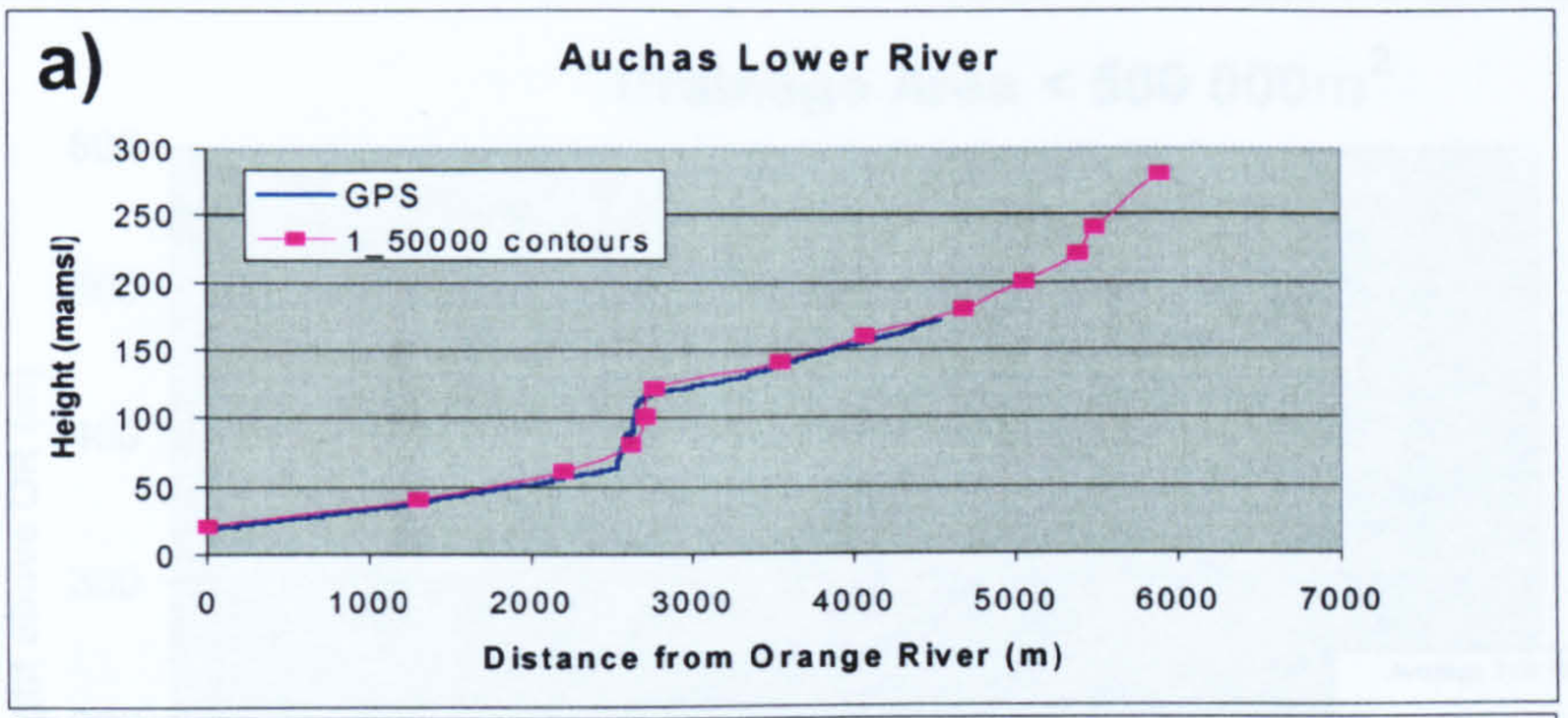

Figure 3.21 a-e Comparison between DGPS profiles and digitised profiles from the 1:50 000 scale topographic maps with a 20m contour interval.

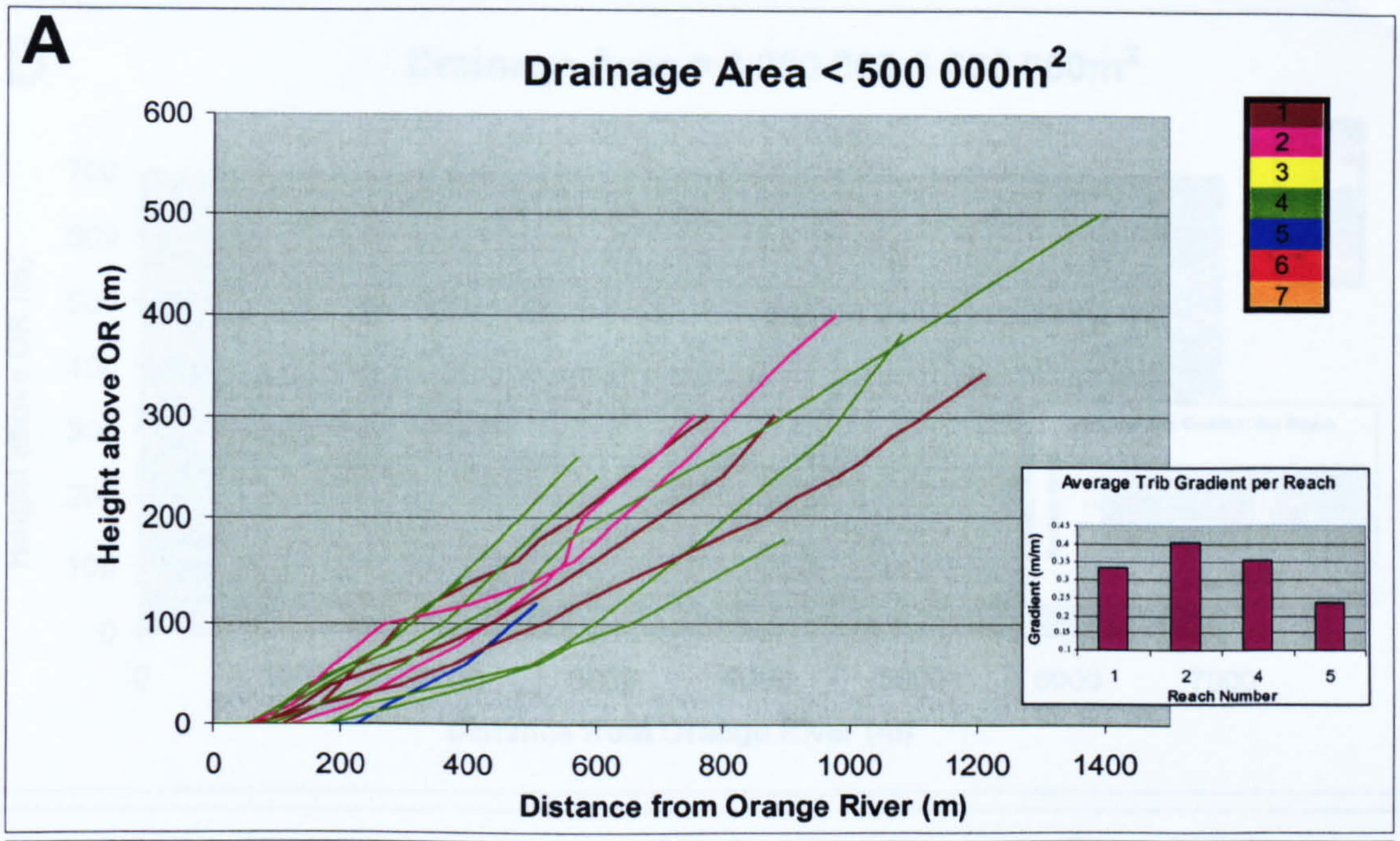

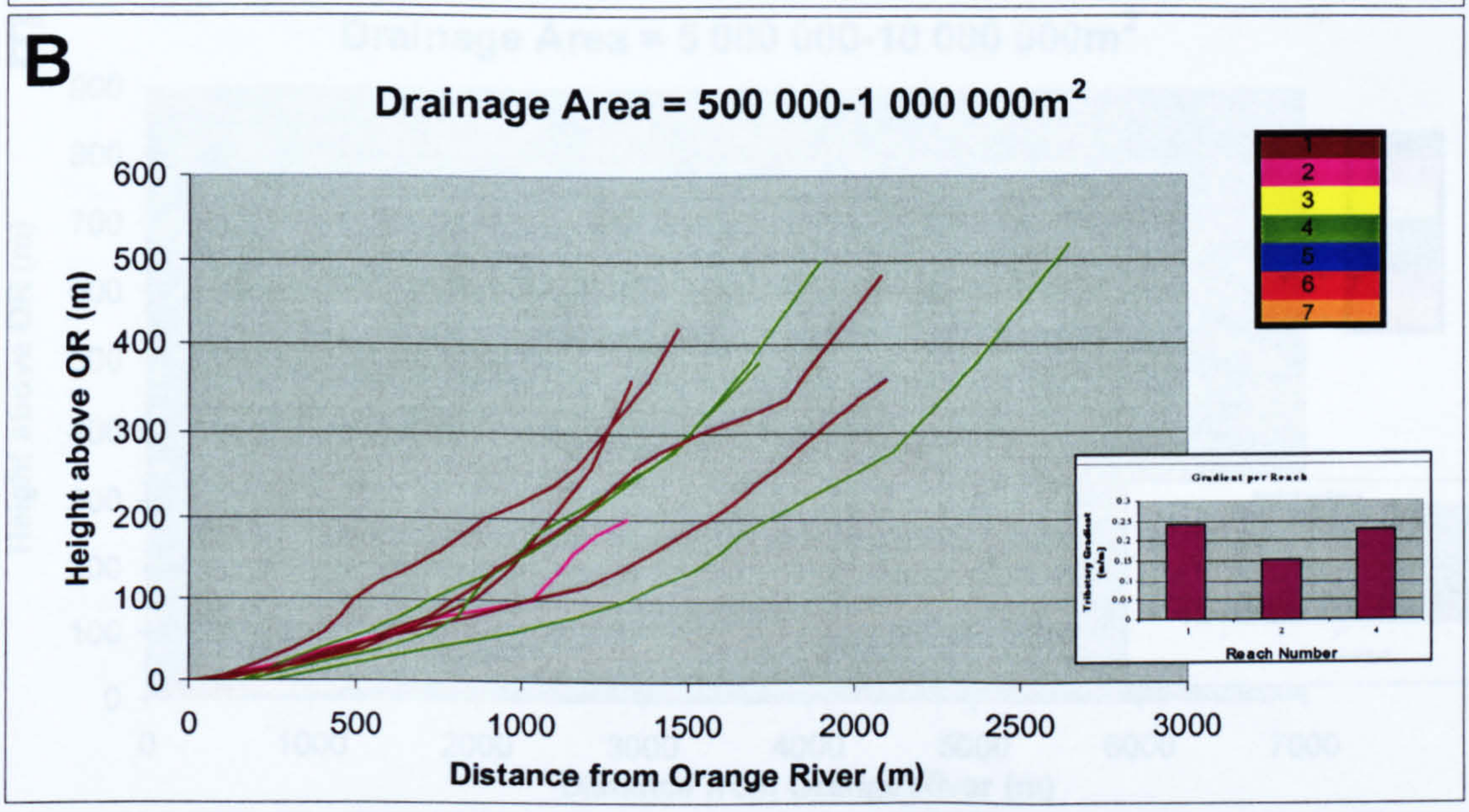

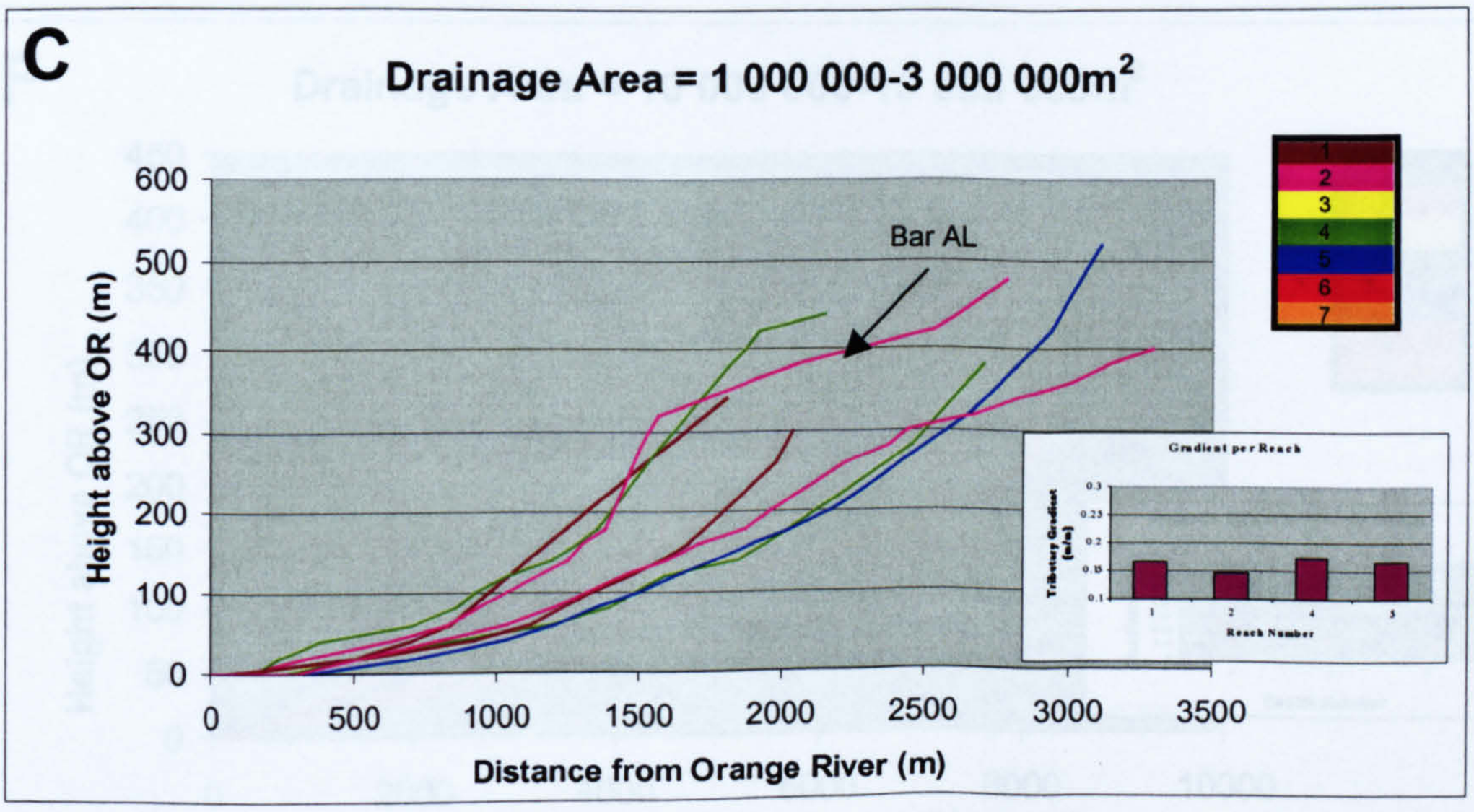

Figure 3.22 A-C Tributary profiles colour-coded per reach.

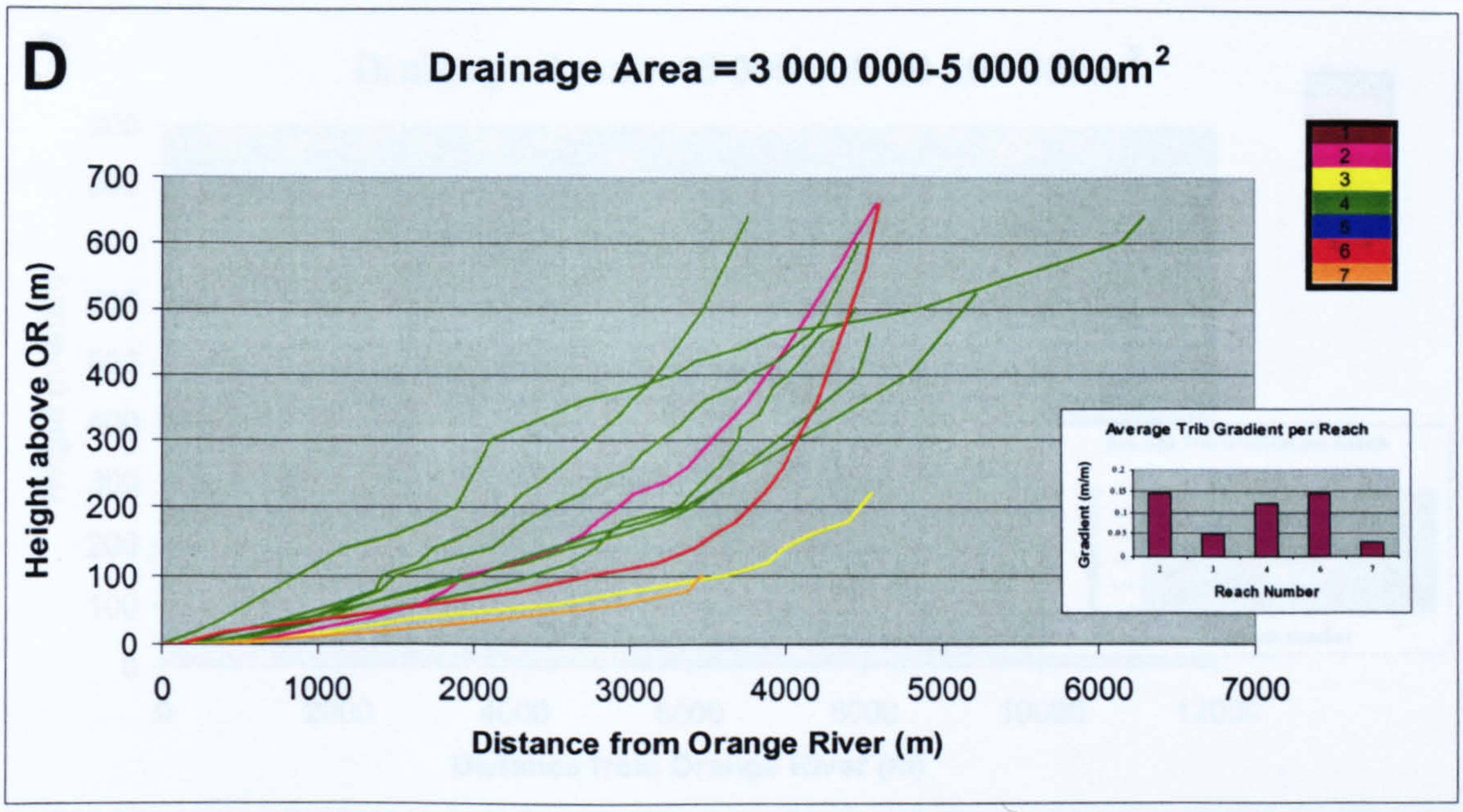

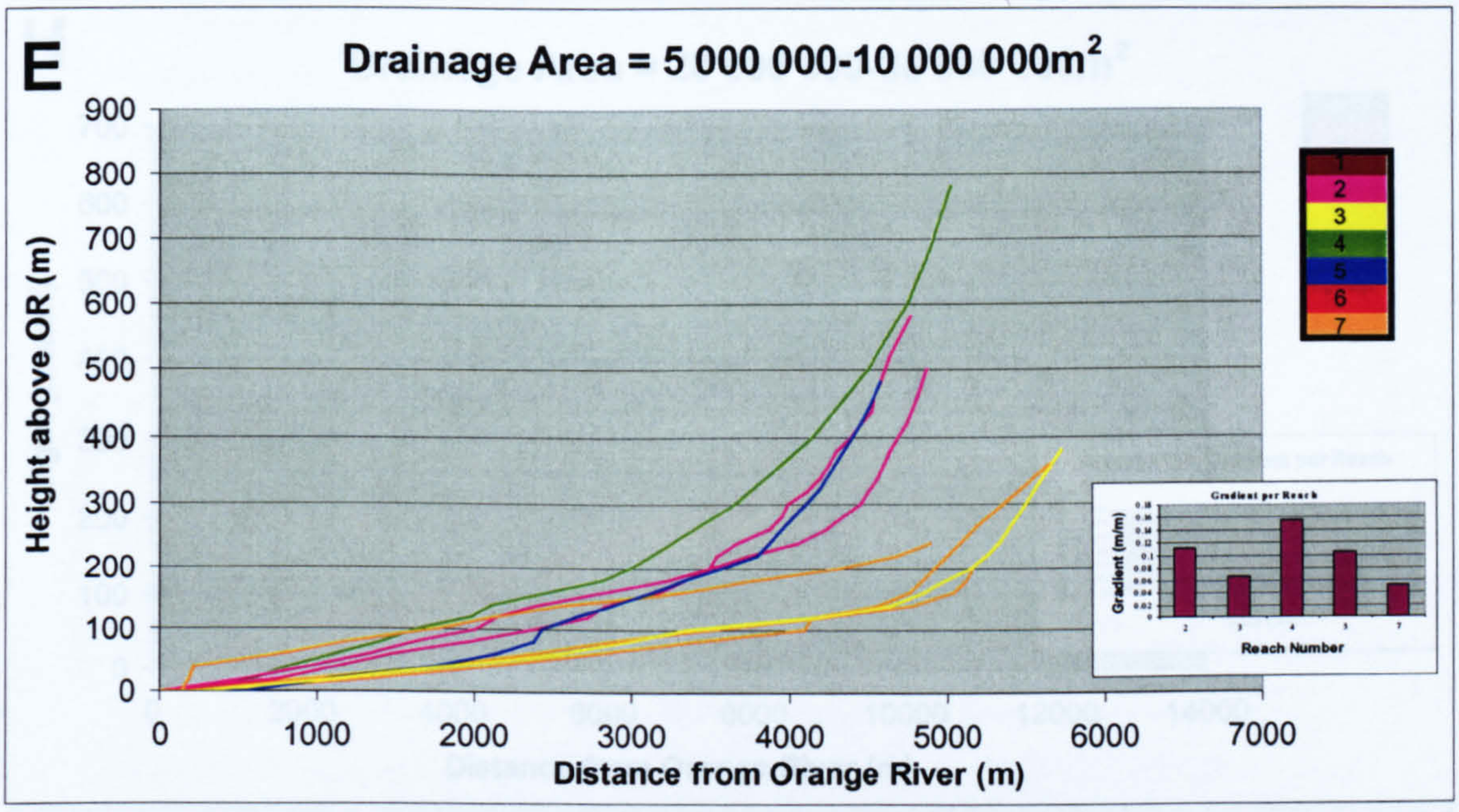

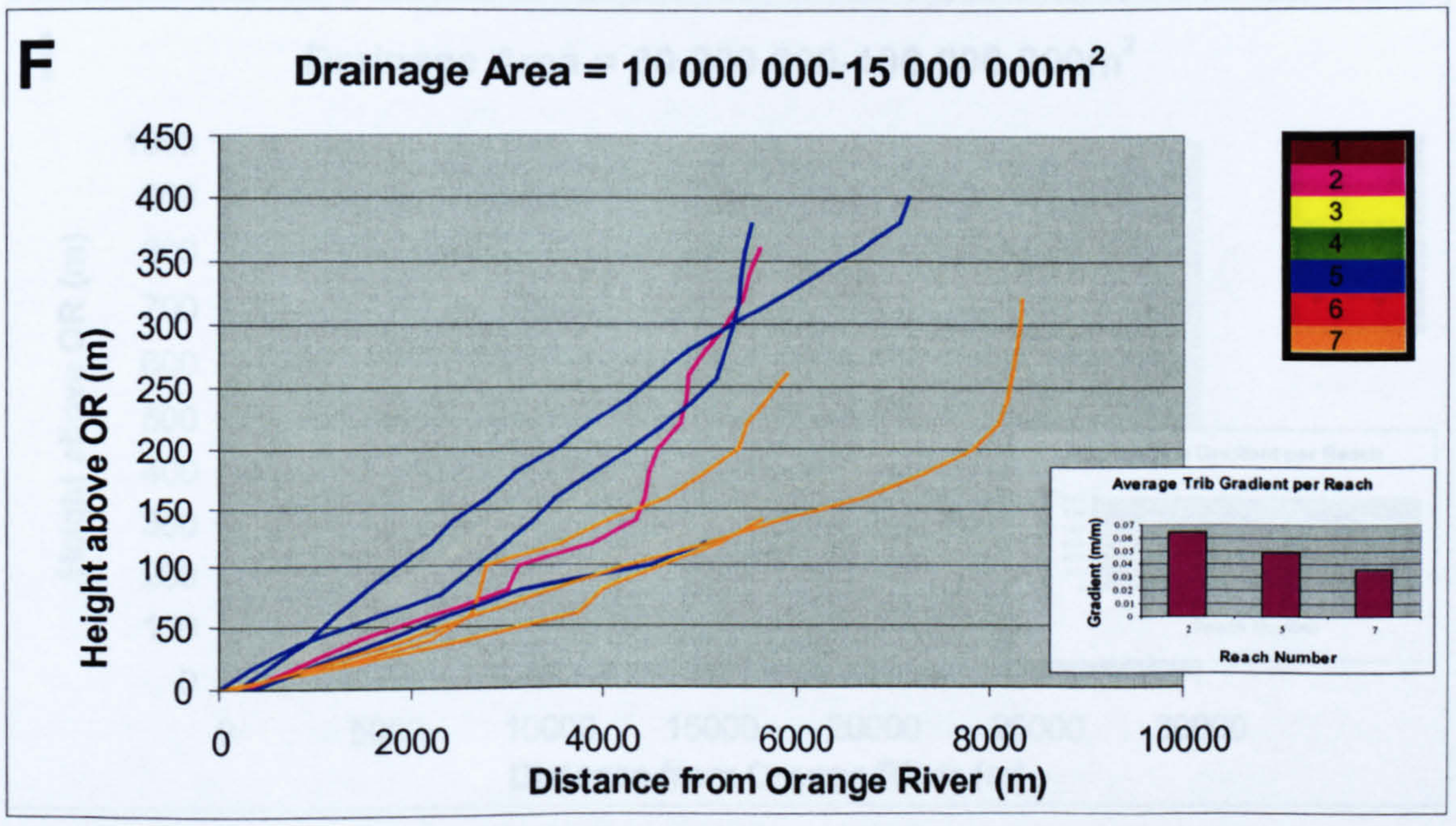

Figure 3.22 D-F Tributary profiles colour-coded per reach.

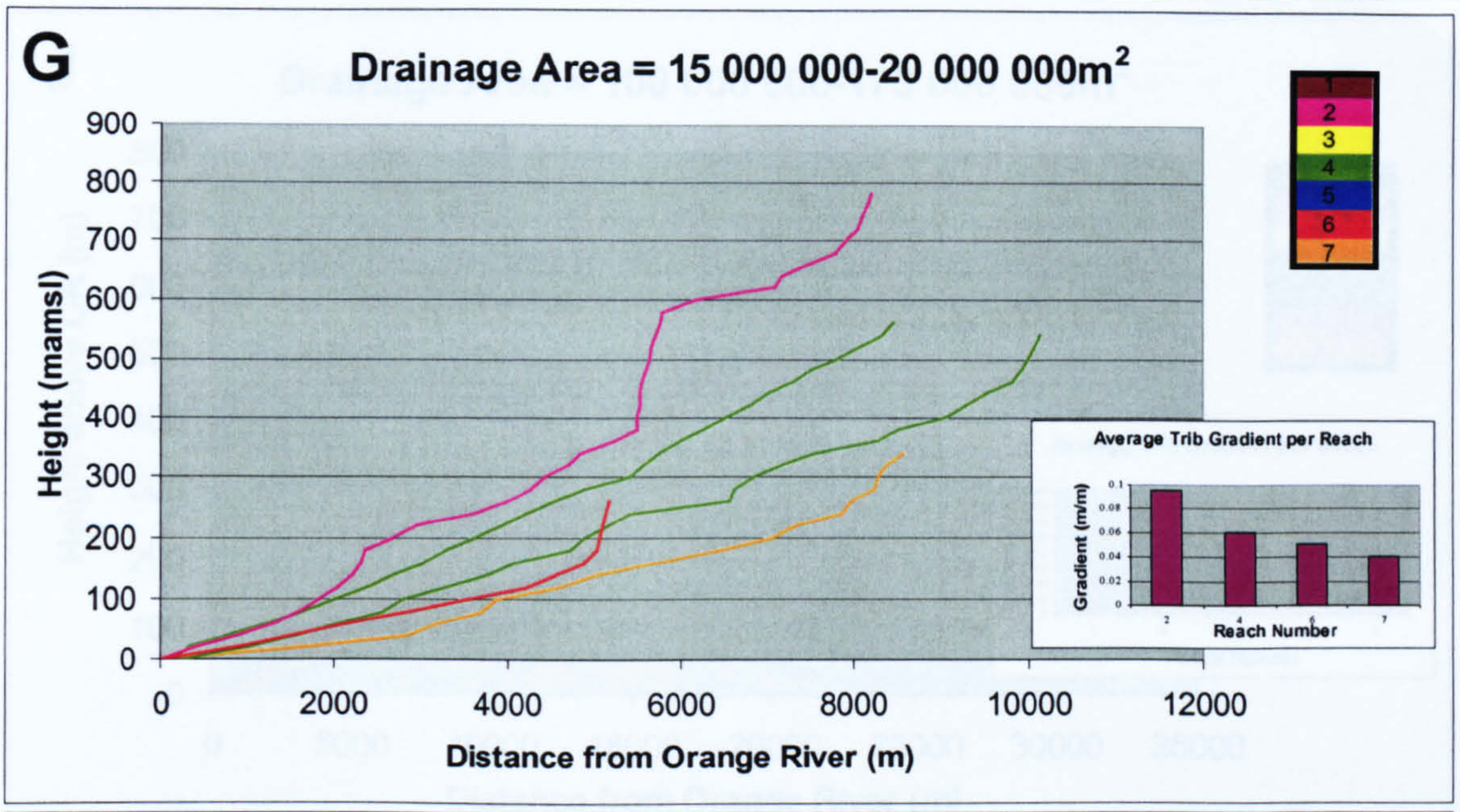

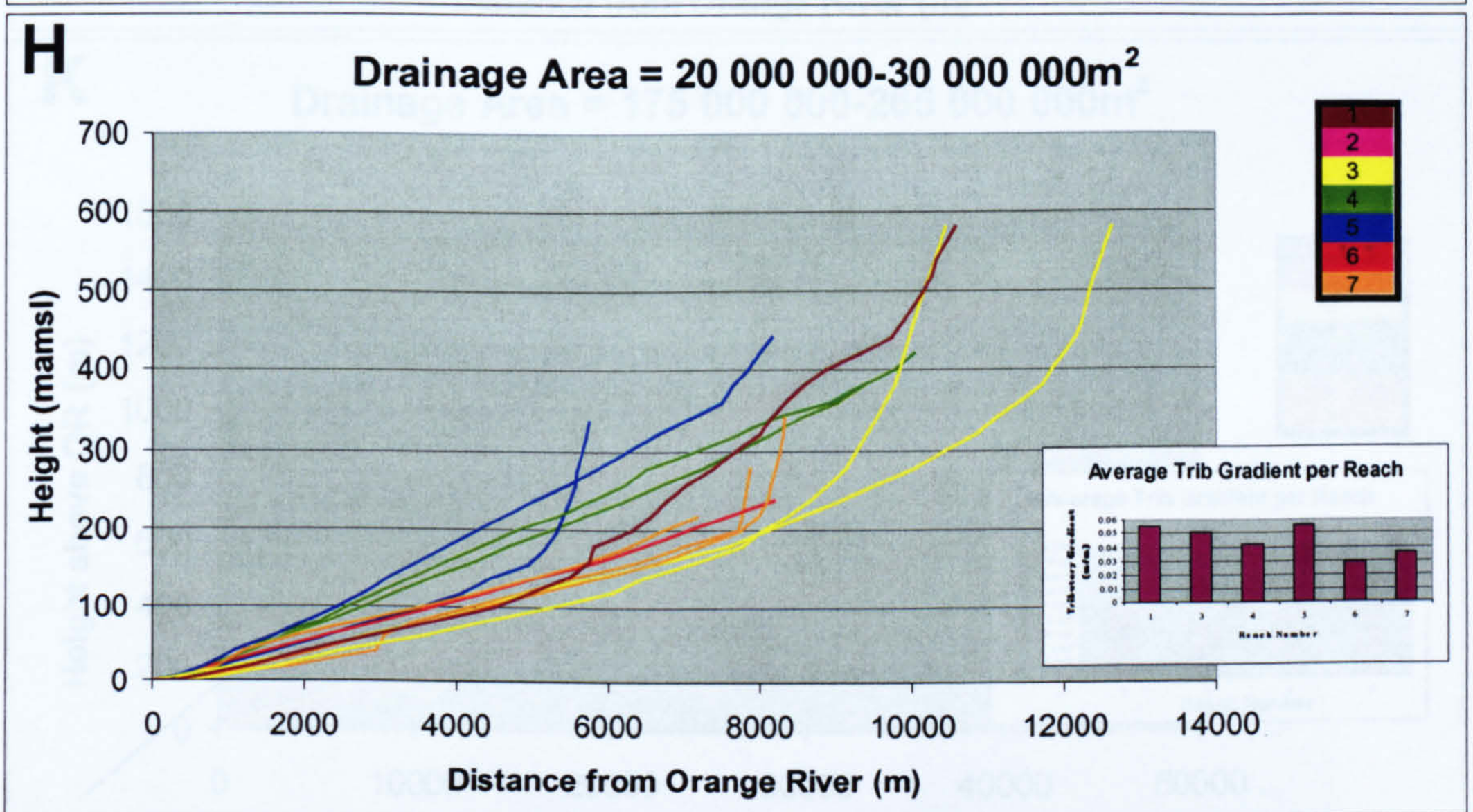

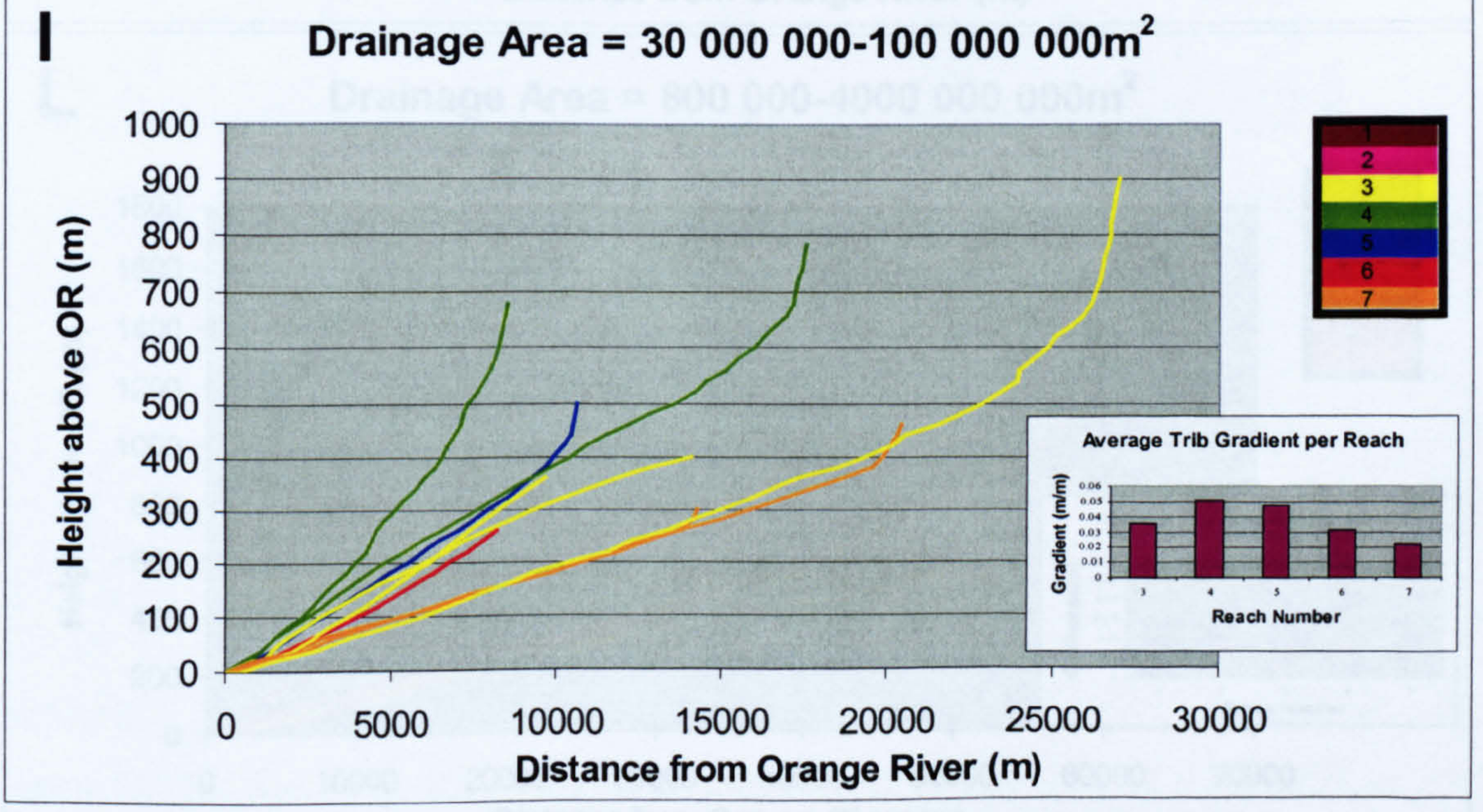

Figure 3.22 G-I Tributary profiles colour-coded per reach.

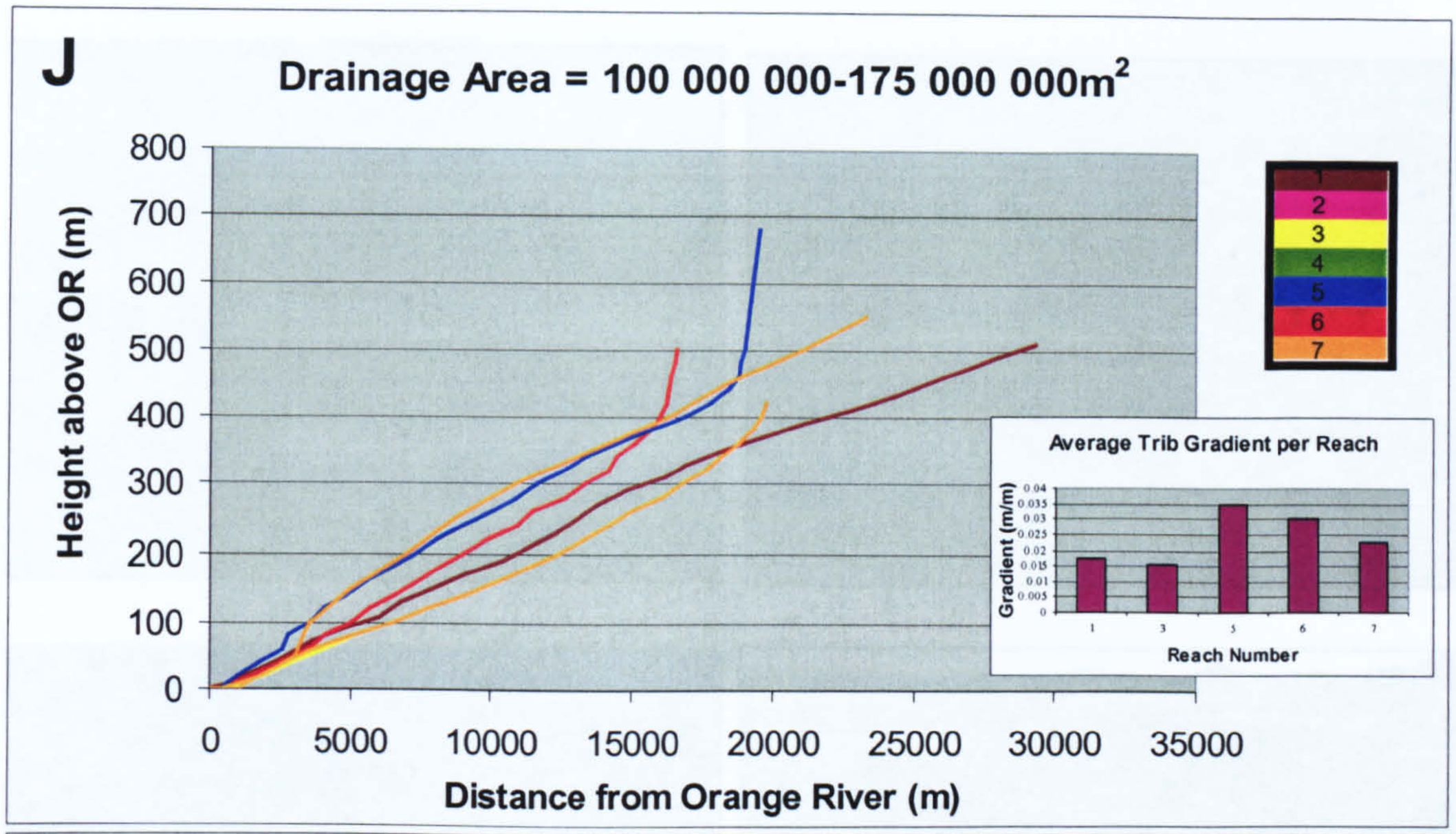

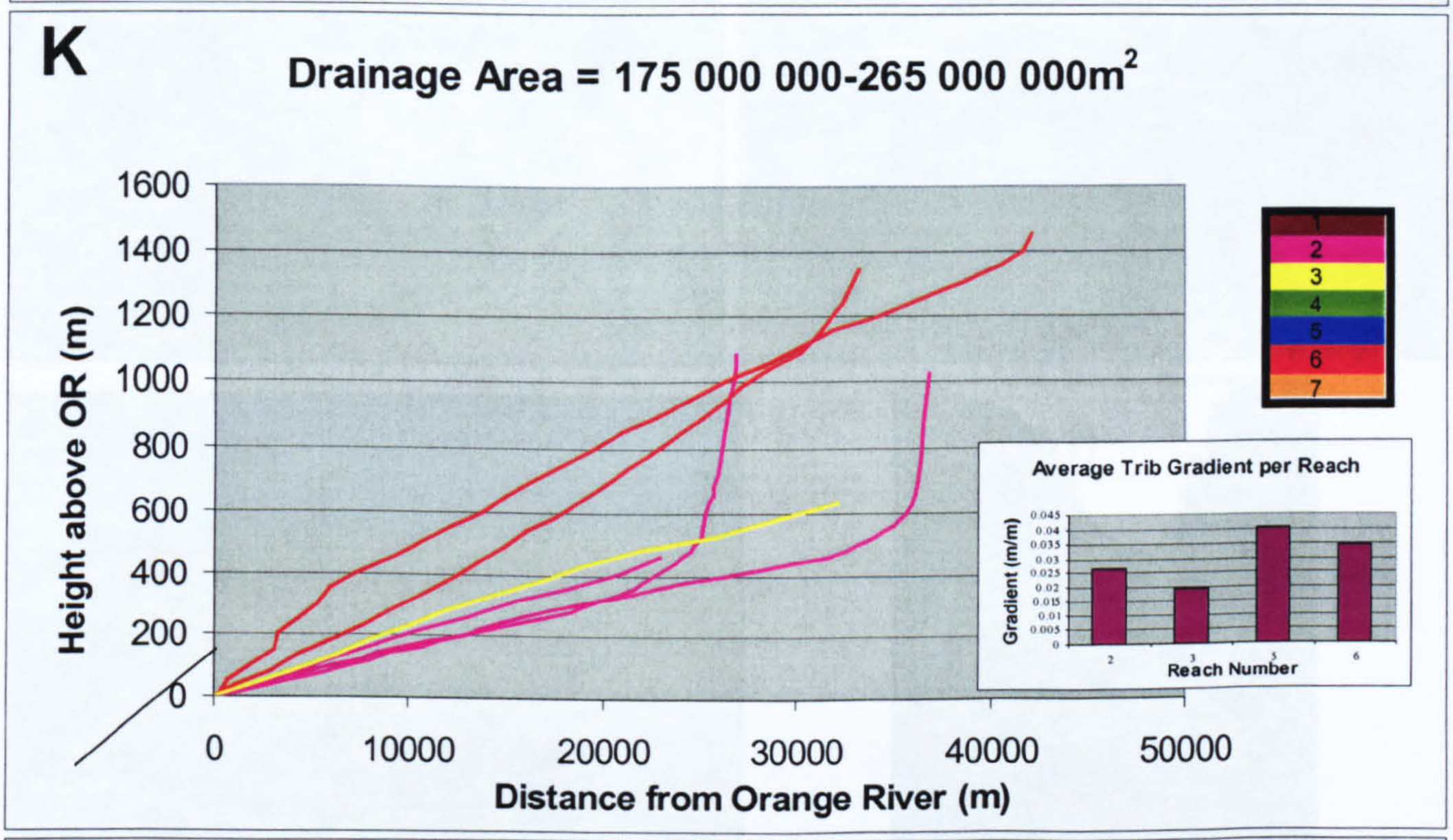

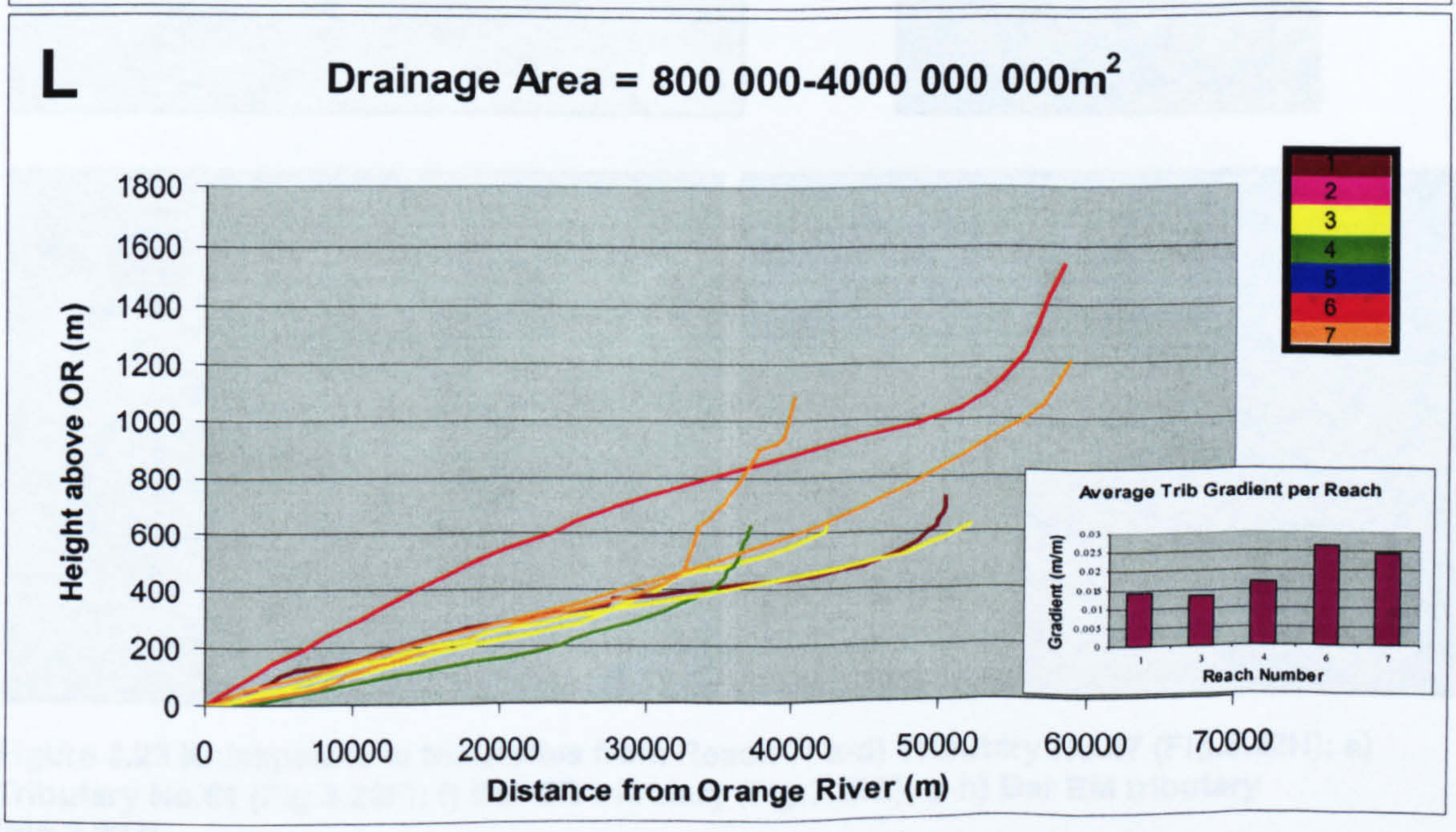

Figure 3.22 J-L Tributary profiles colour-coded per reach.

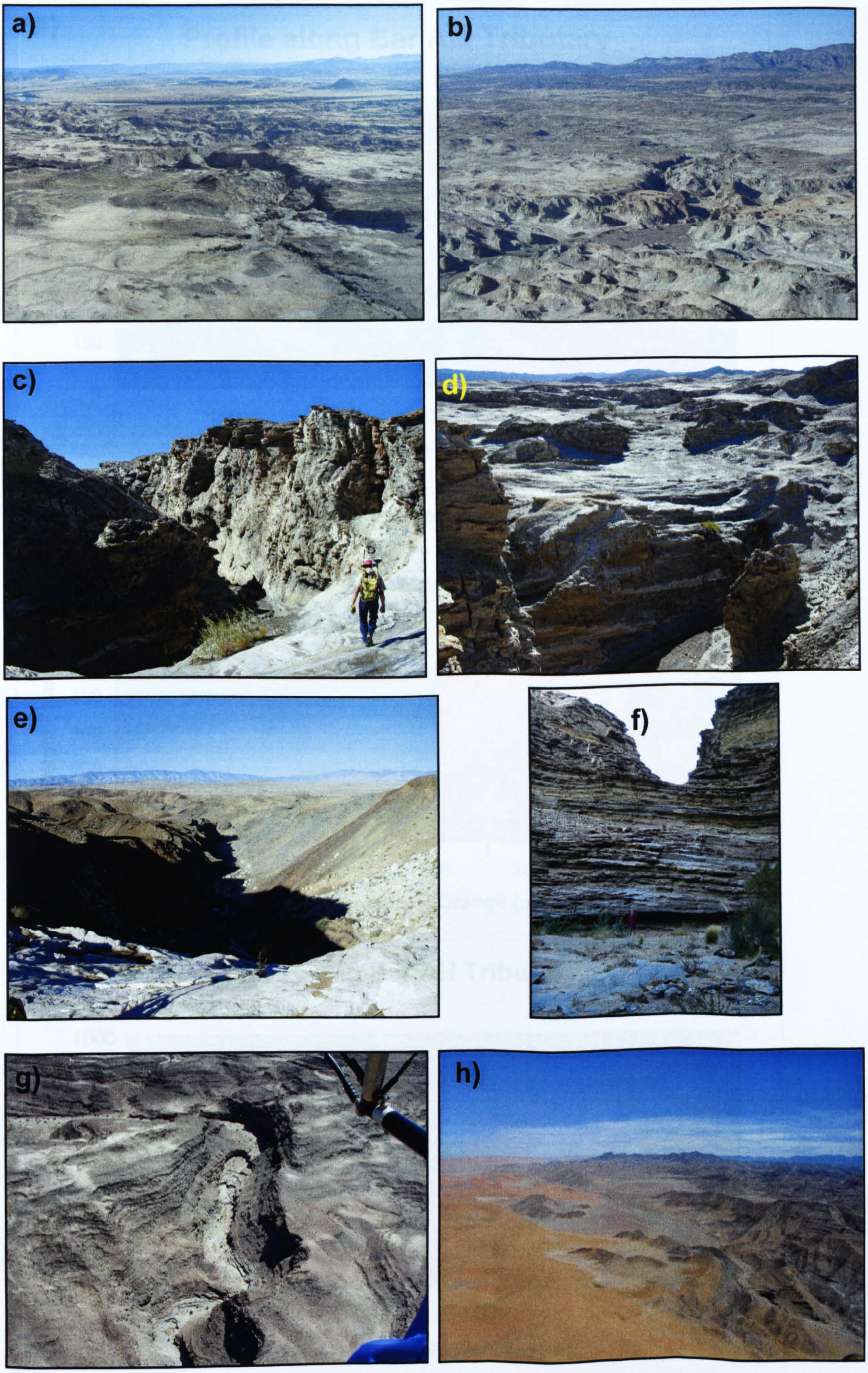

Figure 3.23 Knickpoints in tributaries from Reach 7; a-d) Tributary No.57 (Fig.3.22H); e) Tributary No.61 (Fig.3.22F); f) Bar EQ tributary (Fig.3.22E); g-h) Bar EM tributary (Fig.3.22J).

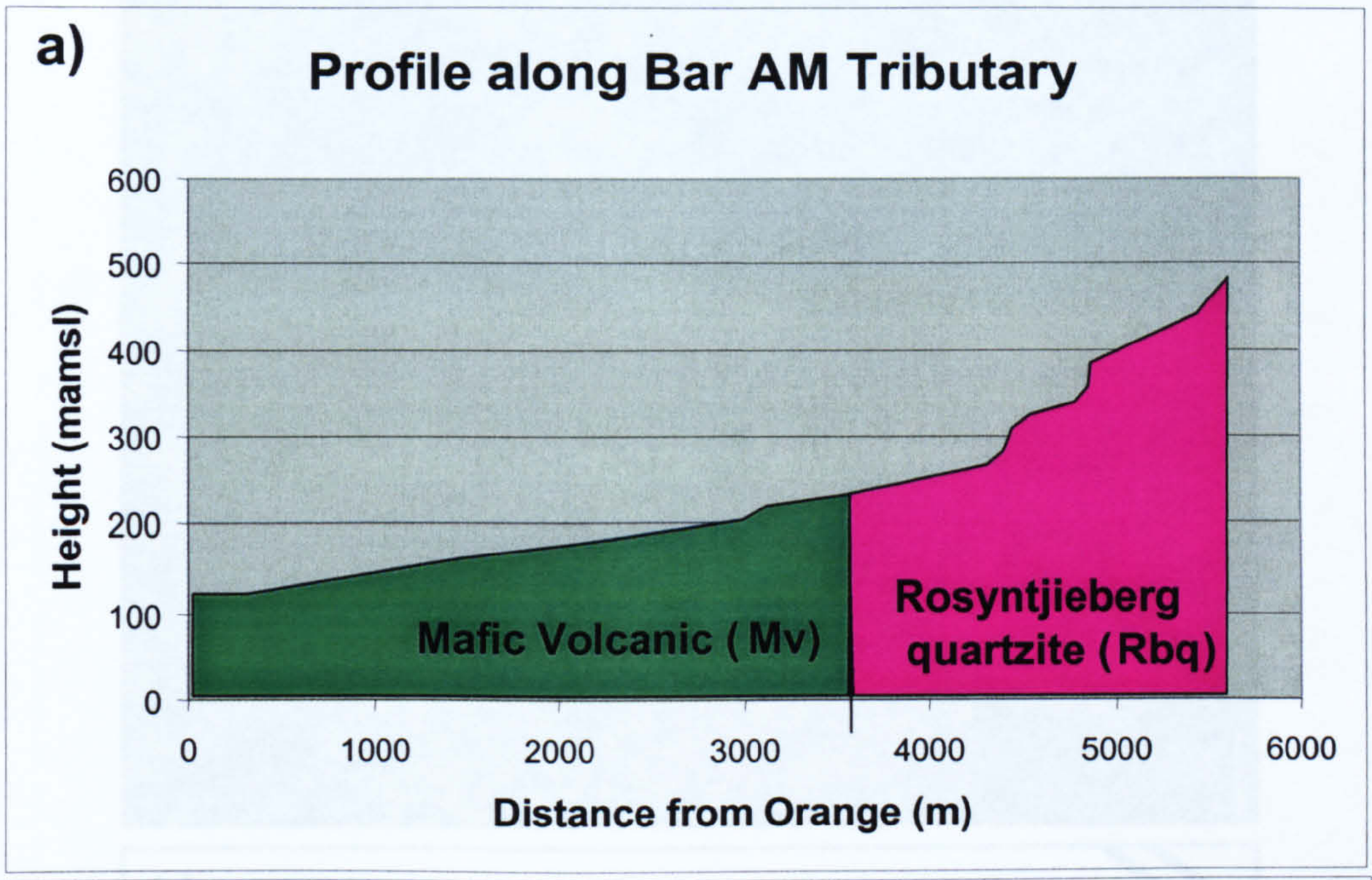

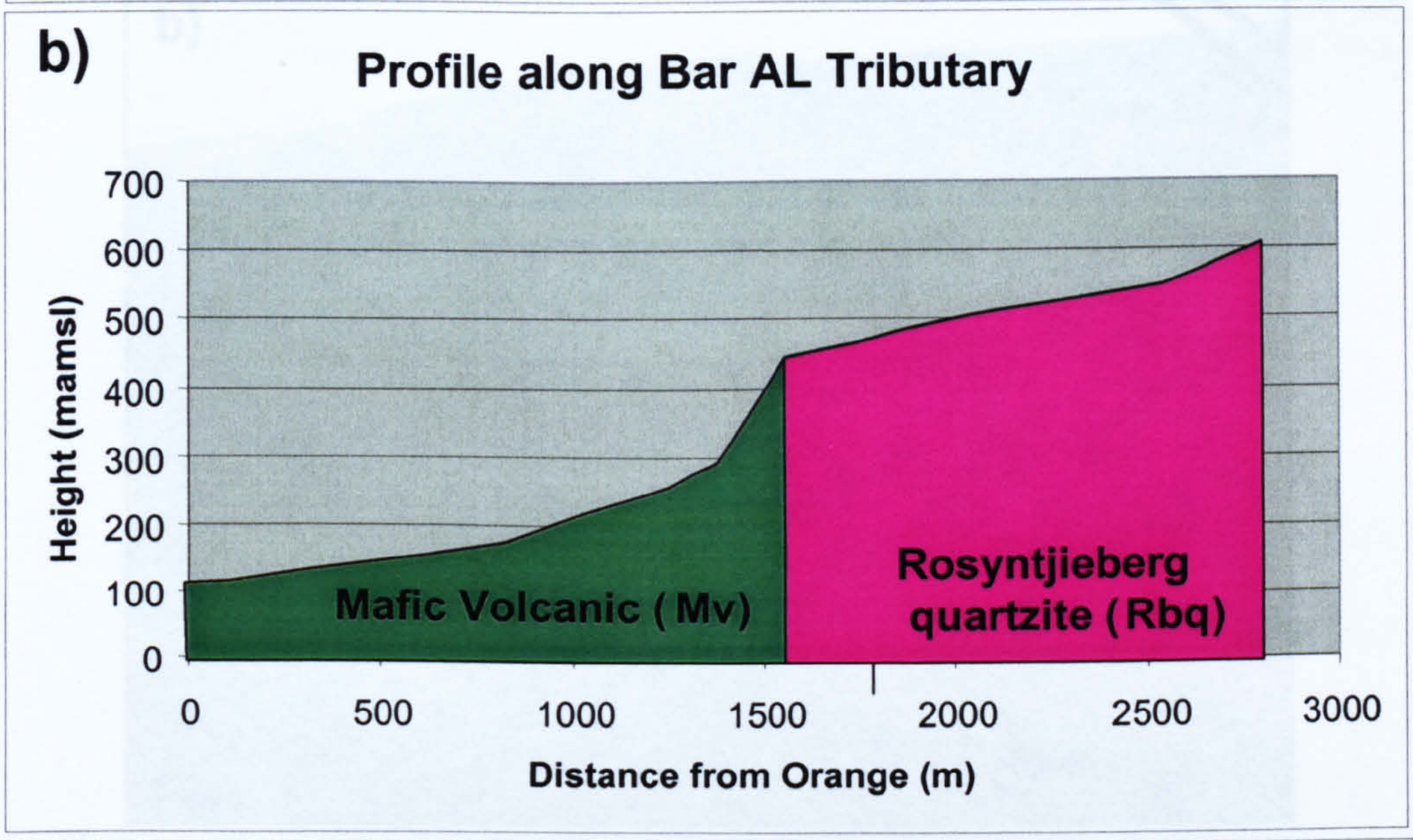

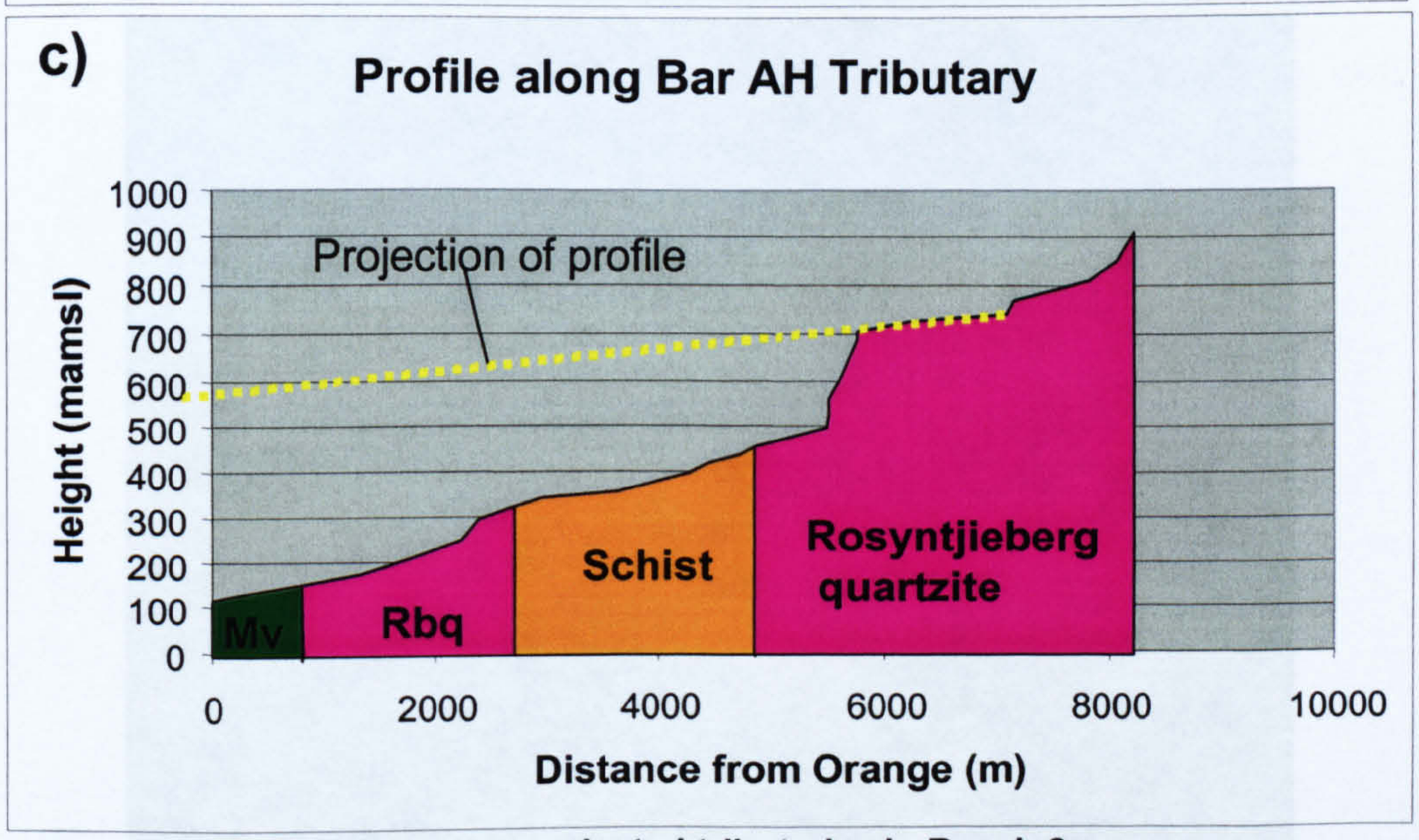

Figure 3.24 a-c Profiles along selected tributaries in Reach 2.

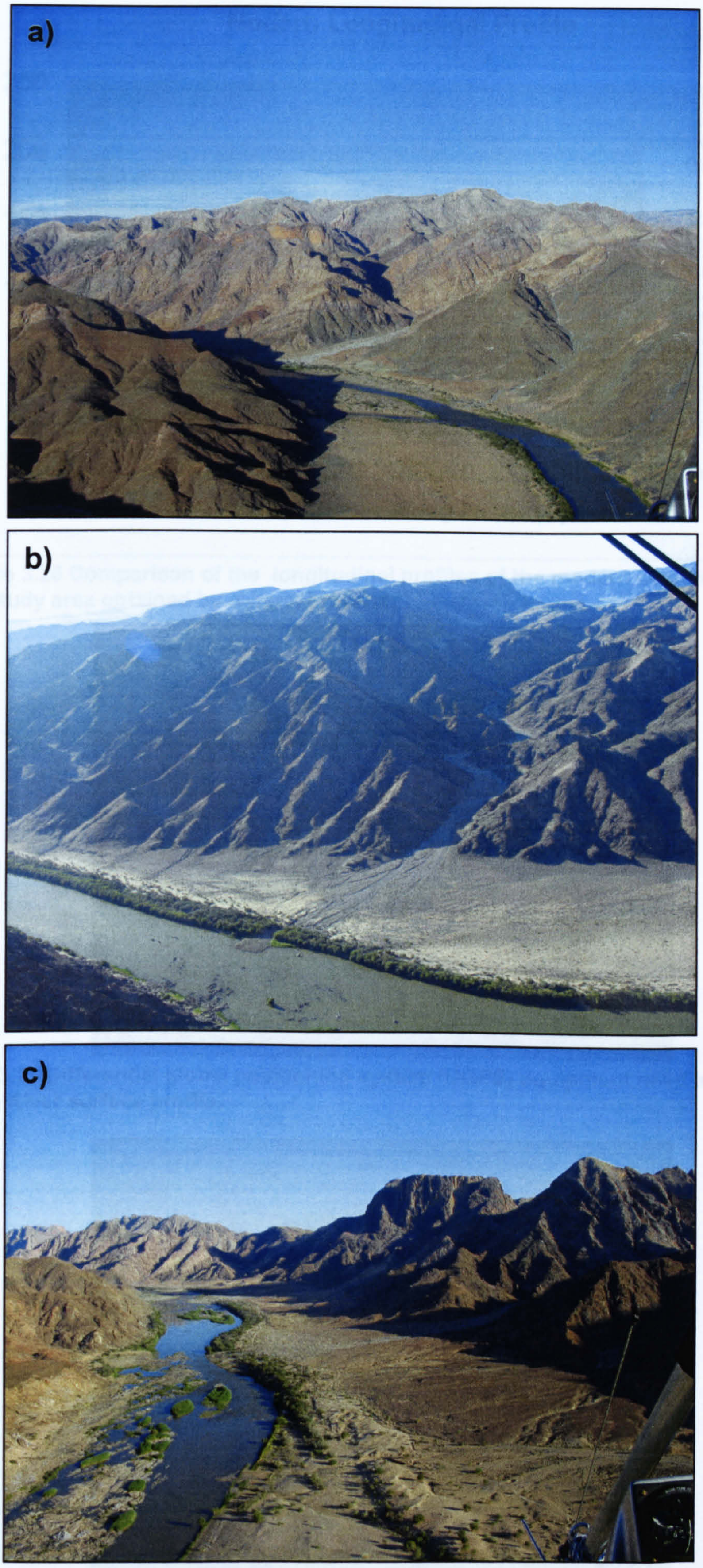

Figure 3.25 a-c) Photos illustrating the flat-topped nature of the Rosyntjieberg mountains. Deeply incised tributary in a) is the Bar AH tributary in (Fig.3.24c).

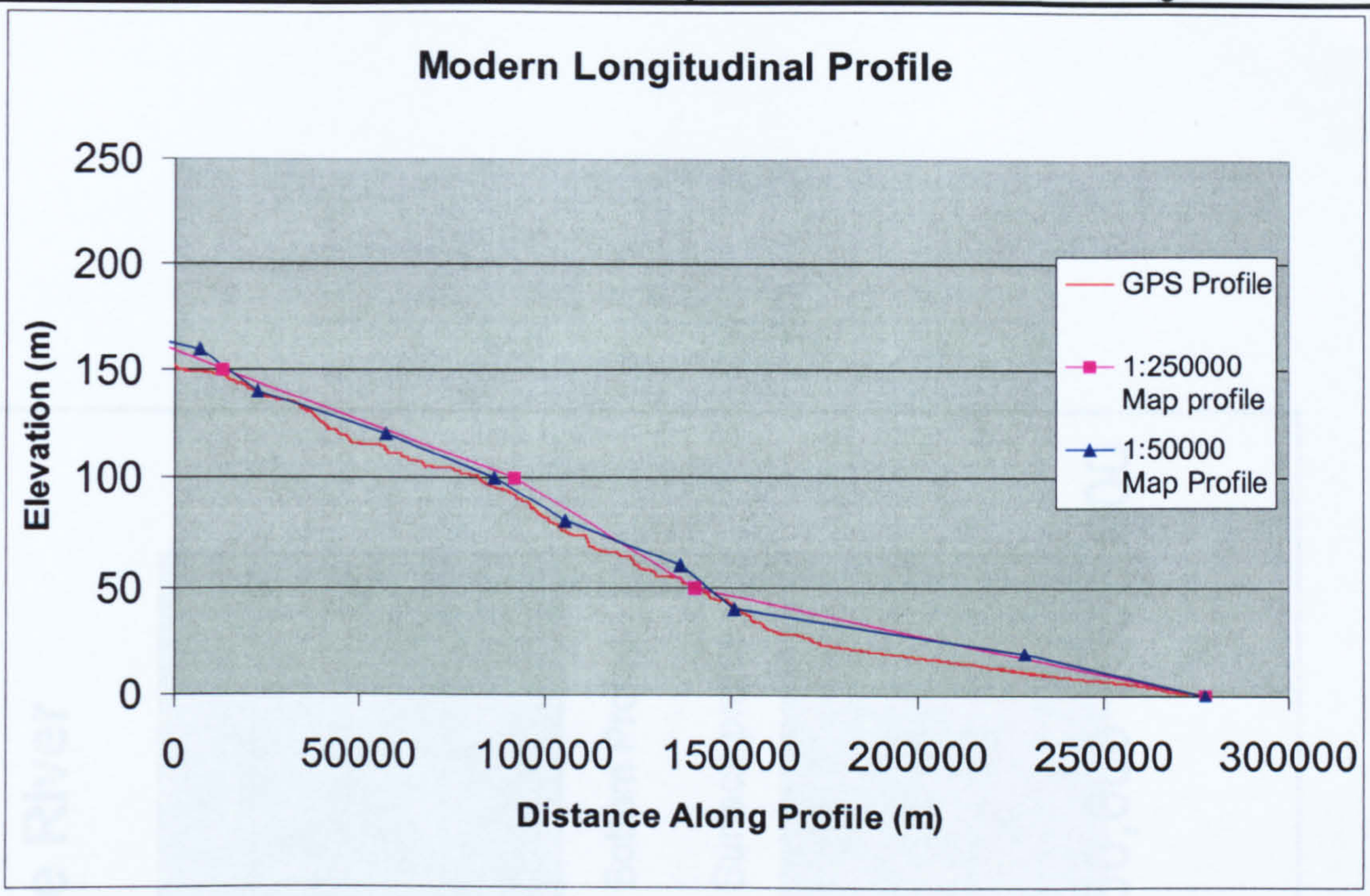

Figure 3.26 Comparison of the longitudinal profiles of the modern Orange River in the study area obtained by different means.

Figure 3.27 Differential global positioning system (DGPS) equipment used in measuring Orange River surface profile.

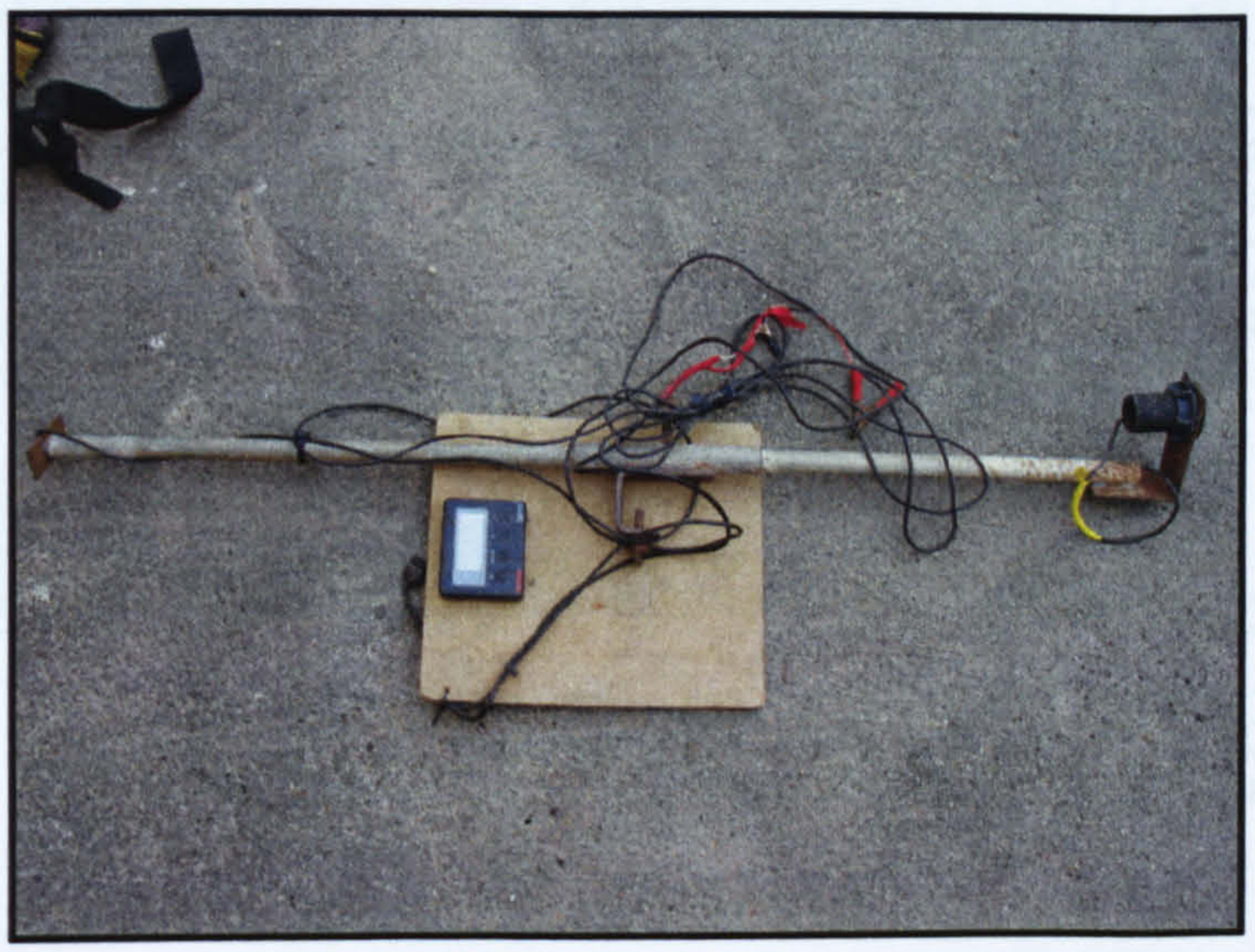

Figure 3.28 Echo sounding equipment used in measuring Orange River bottom profile.

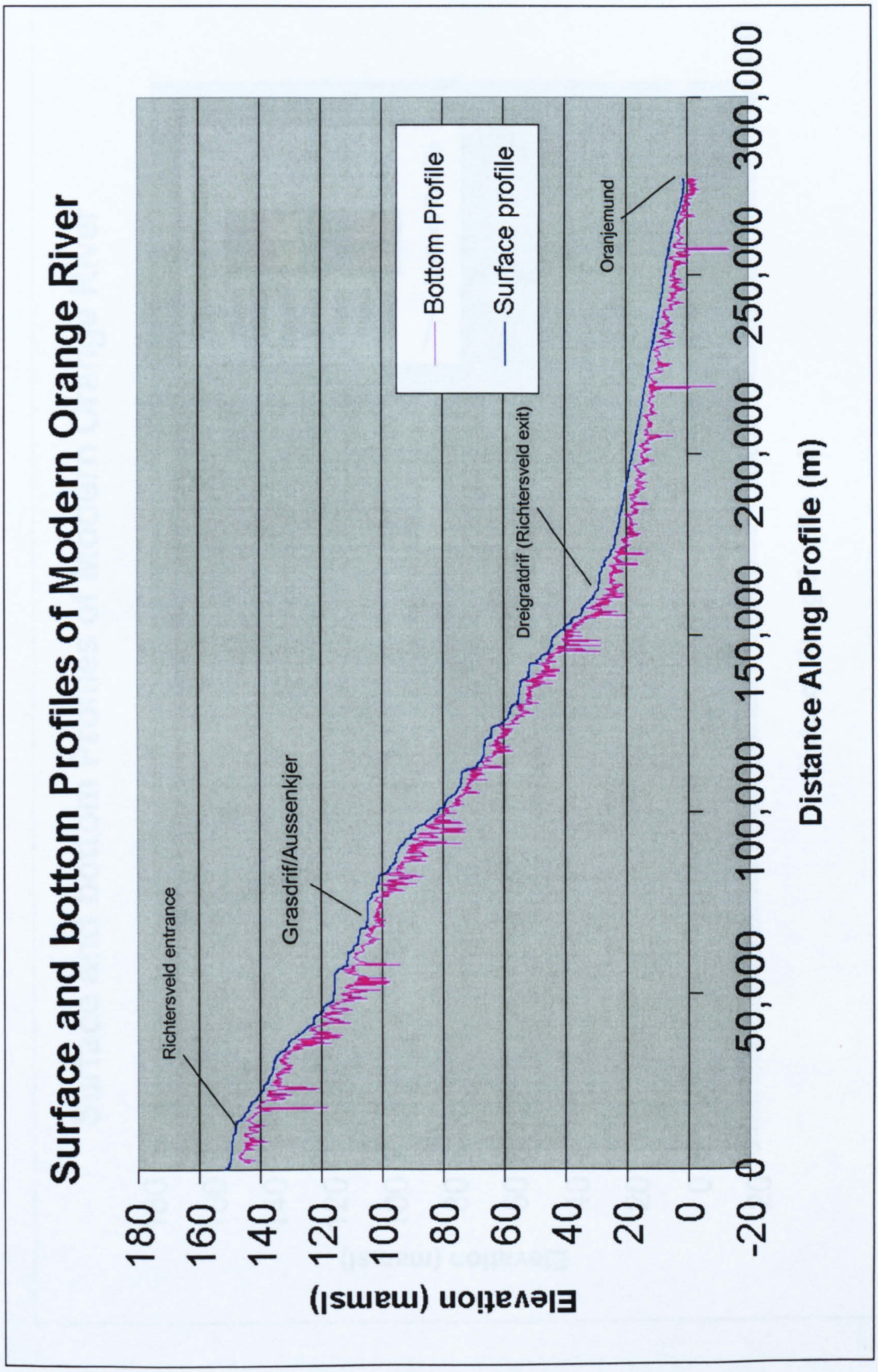

Figure 3.29 Surface and bottom profiles of the modern Orange River in the study area.

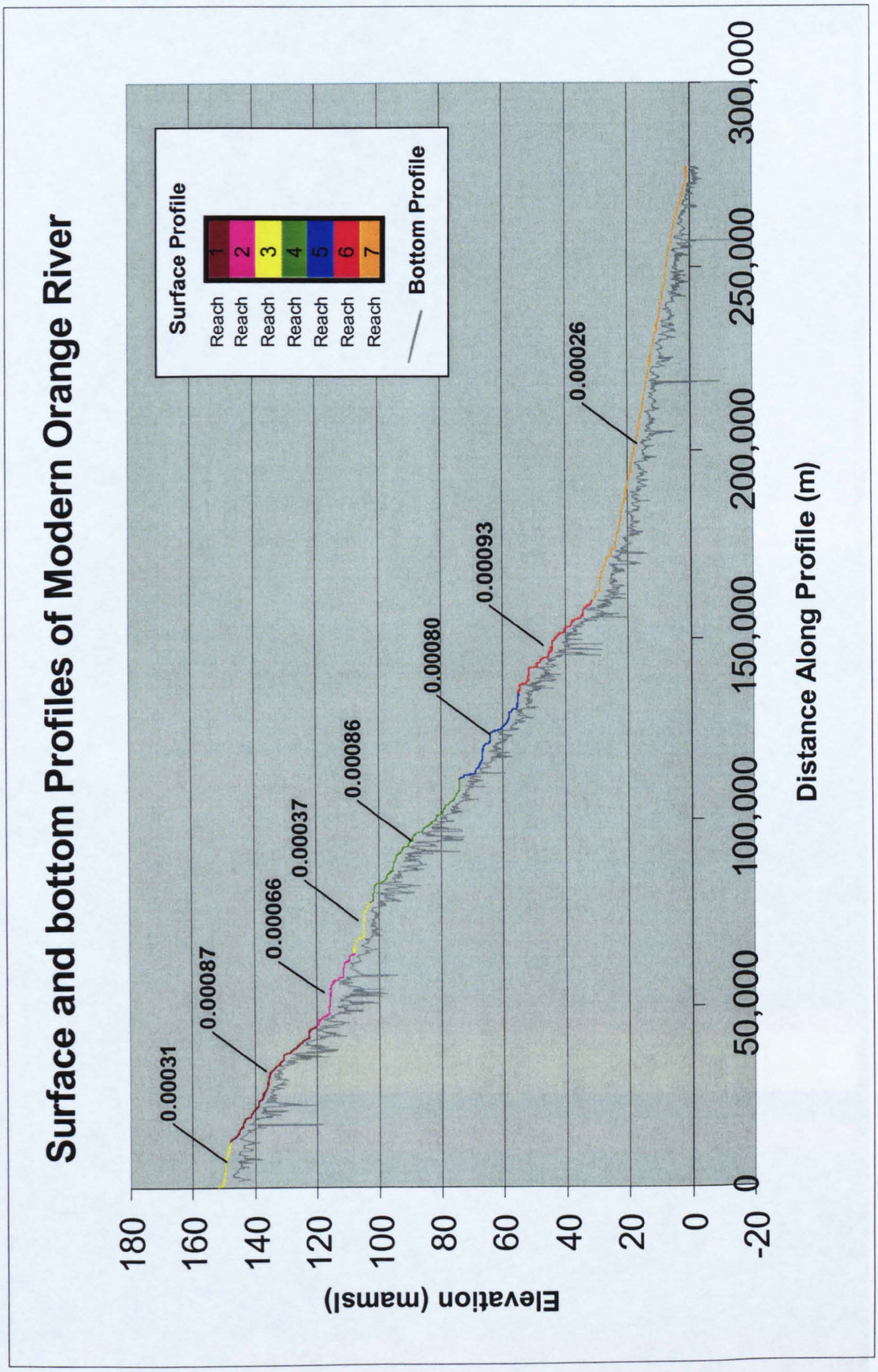

Figure 3.30 Surface and bottom profiles of the modern Orange River colour-coded per Geomorphic Reach.

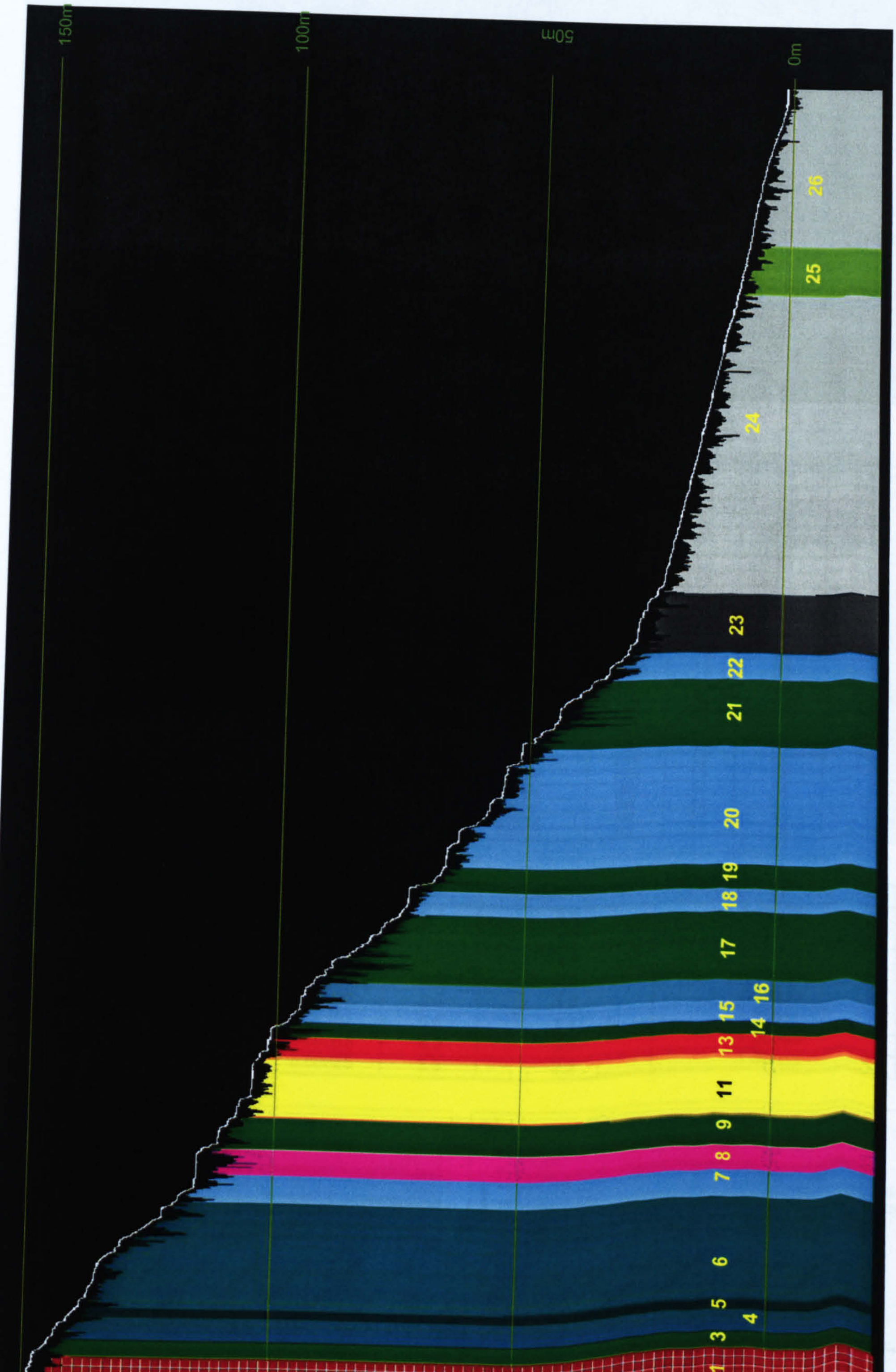

Figure 3.31 Surface and bottom profiles with underlying geological reaches (Geological units identified in figure 3.32).

a)

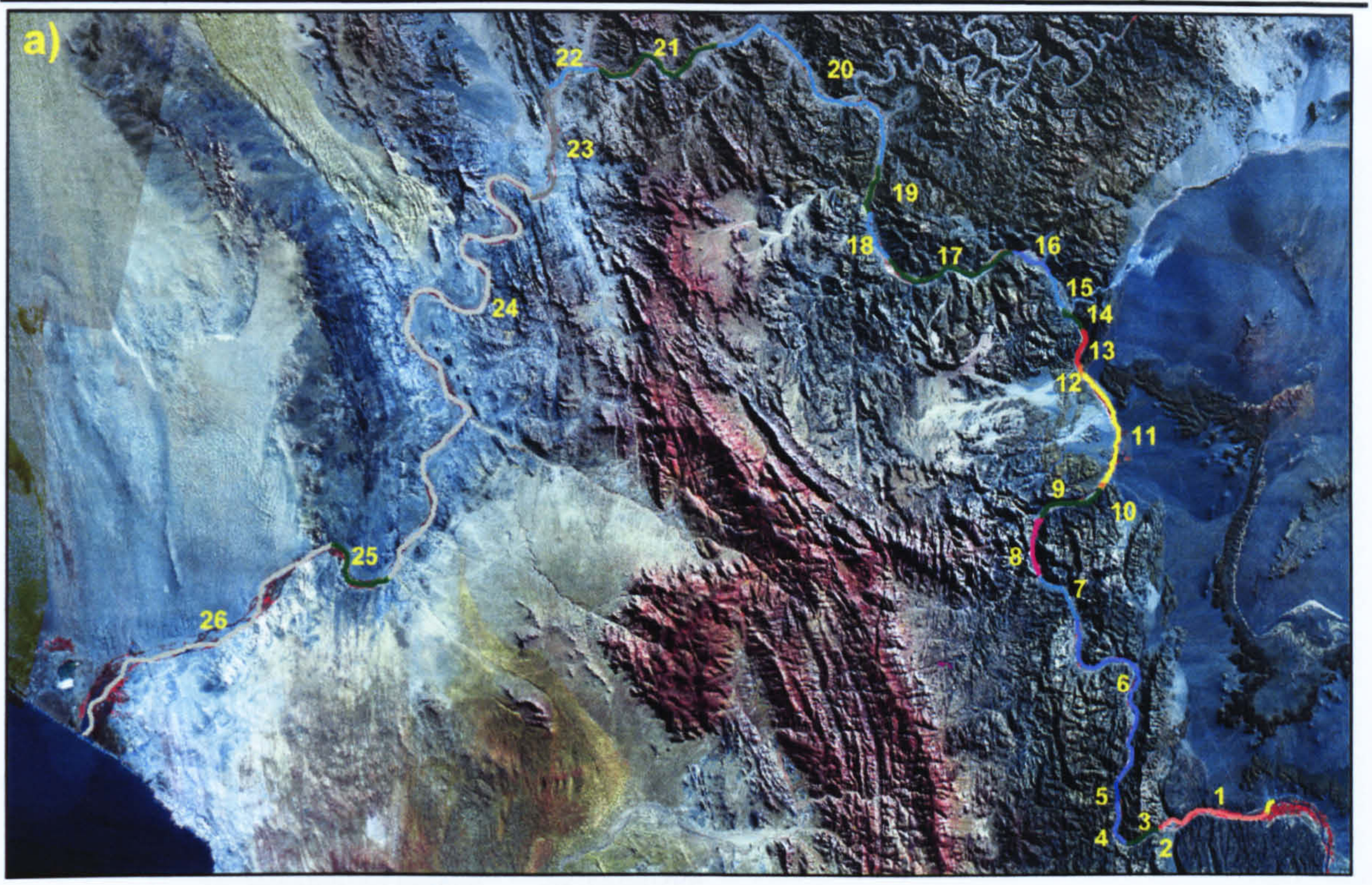

b)

Lithology	Dist along profile	Surf.elev.	Hor. diff.	Vert.diff.	SurfaceGradient (m/m)	SL Grad IDX	Ave. Depth	Depth Std.dev	Bottom:Surface dist.
1Nama limestone	12165.9249	148.1	10189.9	2.0	**0.00019**	**448**	5.4	1.8	1.000086
2Nama quartzite	12499.89068	148.0	334.0	0.1	**0.00022**	**518**	7.3	1.2	1.000122
3Mafic metavolcanic	15724.67065	145.1	3224.8	3.0	**0.00092**	**2145**	4.2	2.3	1.000008
4RIC granite	20293.86478	141.4	4569.2	3.7	**0.00081**	**1889**	7.3	5.7	1.001036
5RIC syenite	22392.01783	139.6	2098.2	1.8	**0.00084**	**1976**	4.8	2.9	1.000355
6RIC granite	44672.93839	120.3	22280.9	19.4	**0.00087**	**2054**	6.1	3.8	1.000299
7Vioolsdrif Suite	50644.80567	115.7	5971.9	4.5	**0.00075**	**1791**	5.9	2.9	1.000237
8Rosyntjieberg quartzite	55964.16966	114.6	5319.4	1.2	**0.00022**	**515**	9.6	4.0	1.000879
9Mafic metavolcanic	62841.6097	108.8	6877.4	5.8	**0.00084**	**1999**	4.4	3.3	1.000192
10Dwyka	63391.60472	108.0	550.0	0.8	**0.00153**	**3658**	3.6	0.8	1.000017
11Karoo sandstones and shales	74981.98033	104.0	11590.4	4.0	**0.00035**	**829**	3.7	1.0	1.000046
12Dwyka	75862.12809	103.4	880.1	0.6	**0.00068**	**1643**	2.3	1.1	1.000010
13Nama quartzite and limestone	79562.27861	101.3	3700.2	2.1	**0.00057**	**1362**	5.8	2.4	1.000673
14Mafic & Felsic metavolcanics	82569.9587	98.4	3007.7	2.8	**0.00094**	**2273**	7.3	3.6	1.000353
15Vioolsdrif Suite	86474.49576	95.3	3904.5	3.1	**0.00080**	**1923**	4.5	2.3	1.000092
16Kuboos-Bremen granite	90855.16445	92.8	4380.7	2.5	**0.00058**	**1405**	6.9	3.5	1.000936
17Mafic & Felsic metavolcanics	104893.9989	75.6	14038.8	17.2	**0.00122**	**2964**	5.9	3.7	1.000294
18Vioolsdrif Suite	109944.1454	73.9	5050.1	1.7	**0.00034**	**825**	3.6	1.3	1.000120
19Mafic & Felsic metavolcanics	114769.966	67.0	4825.8	6.9	**0.00142**	**3468**	3.7	2.4	1.000301
20Vioolsdrif Suite	140119.7604	51.7	25349.8	15.3	**0.00060**	**1484**	4.6	1.8	1.000141
21Mafic & Felsic metavolcanics	154666.6044	37.6	14546.8	14.1	**0.00097**	**2392**	5.2	3.2	1.000441
22Vioolsdrif Suite	160276.5893	30.7	5610.0	6.9	**0.00123**	**3052**	5.6	2.5	1.000623
23Numees diamictite	172773.8808	25.2	12497.3	5.5	**0.00044**	**1099**	5.5	2.1	1.000159
24Gariep greywacke/schist	237102.964	9.7	64329.1	15.5	**0.00024**	**610**	4.2	2.1	1.000106
25Gariep mafic volc	245472.2747	8.1	8369.3	1.7	**0.00020**	**507**	3.4	1.3	1.000044
26Gariep greywacke/schist	277766.0871	1.0	32293.8	7.0	**0.00022**	**564**	3.0	1.9	1.000172

c)

Summary

Lithology	Ave.Gradient	Ave.Depth	Ave Depth Std.Dev.	Ave Bottom:Surface Ratio
Nama	0.00029	5.7	2.1	1.00024
Karoo	0.00042	3.7	1.0	1.00004
RIC	0.00086	6.2	4.0	1.00041
Vioolsdrif Suite	0.00069	4.8	2.2	1.00020
Rosyntjeberg quartzite	0.00022	9.6	4.0	1.00088
de Hoop Metavolcanics	0.00107	5.5	3.5	1.00031
Kuboos-Bremen granite	0.00058	6.9	3.5	1.00094
Gariep Supergroup	0.00025	3.9	2.2	1.00013

d)

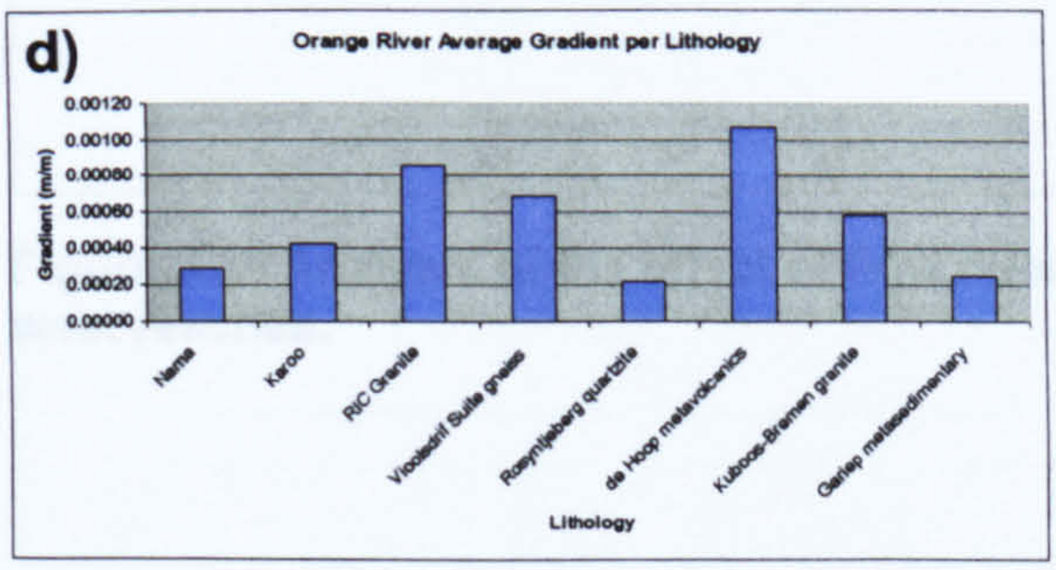

e)

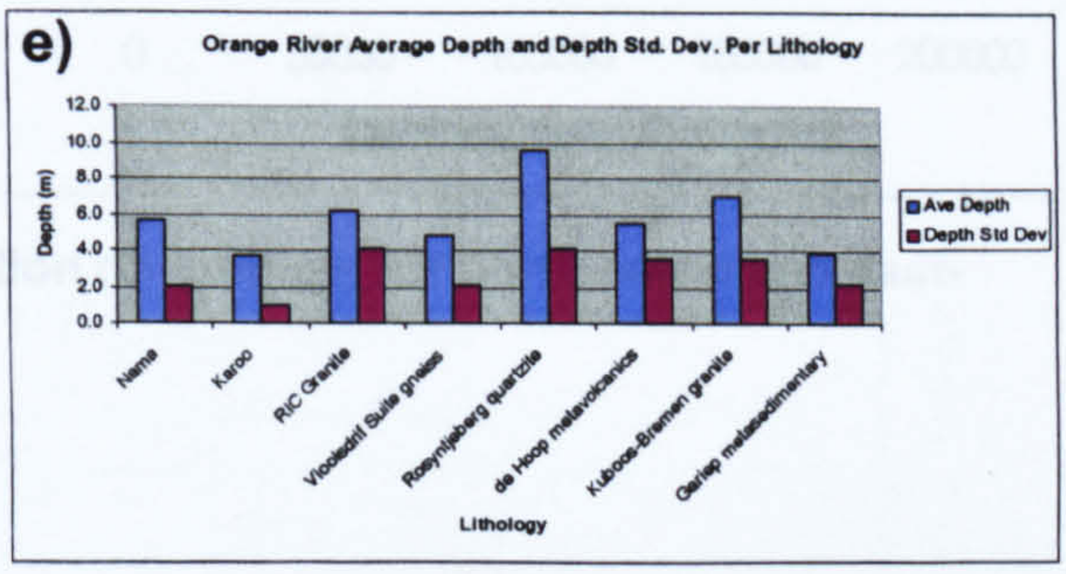

Figure 3.32 a) Location and b) data from the geological reaches of the profile presented in figure 3.31.

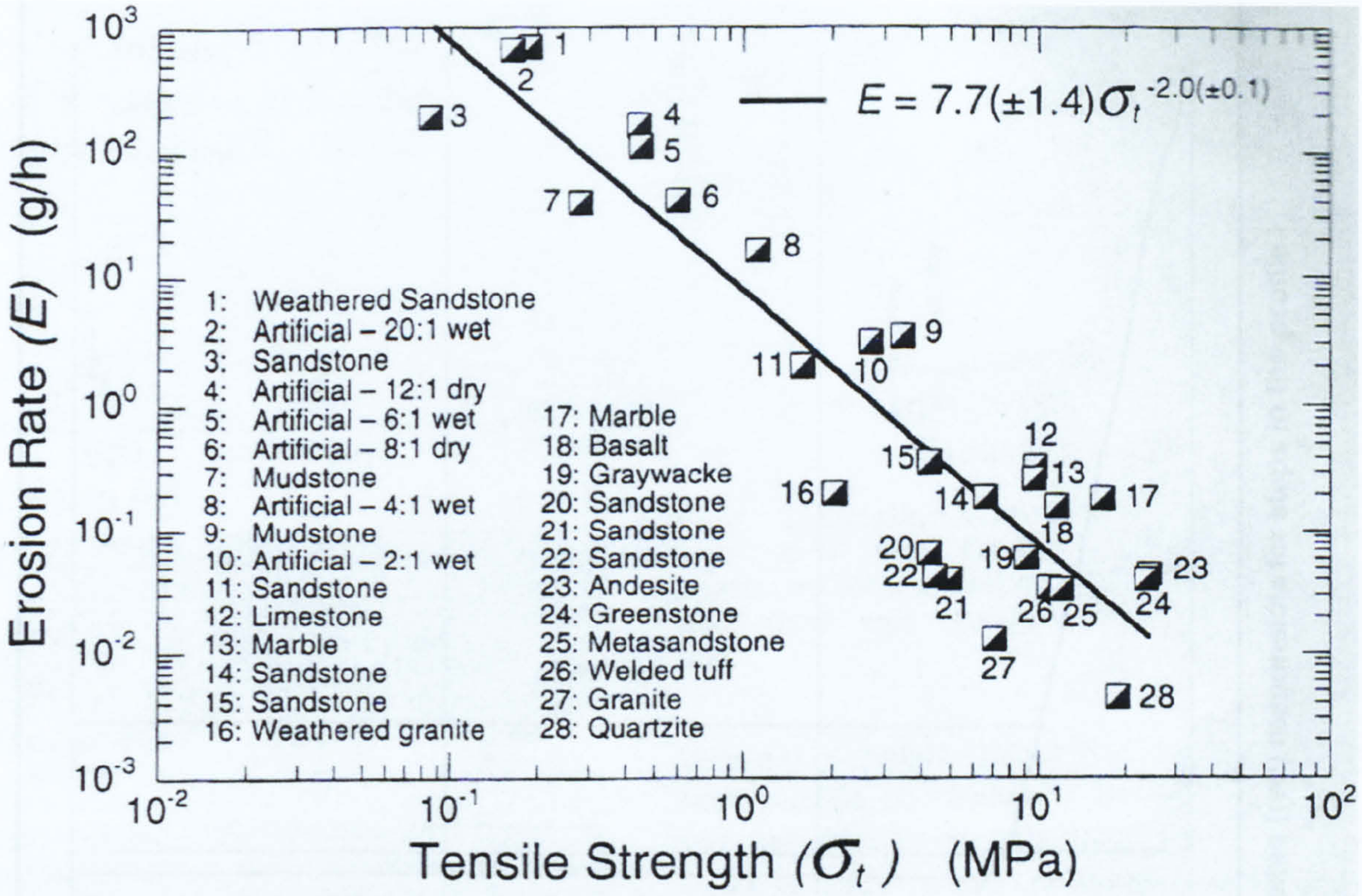

Figure 3.33 Plot of tensile strength vs rock erodability for various lithologies (after Sklar & Dietrich 2001).

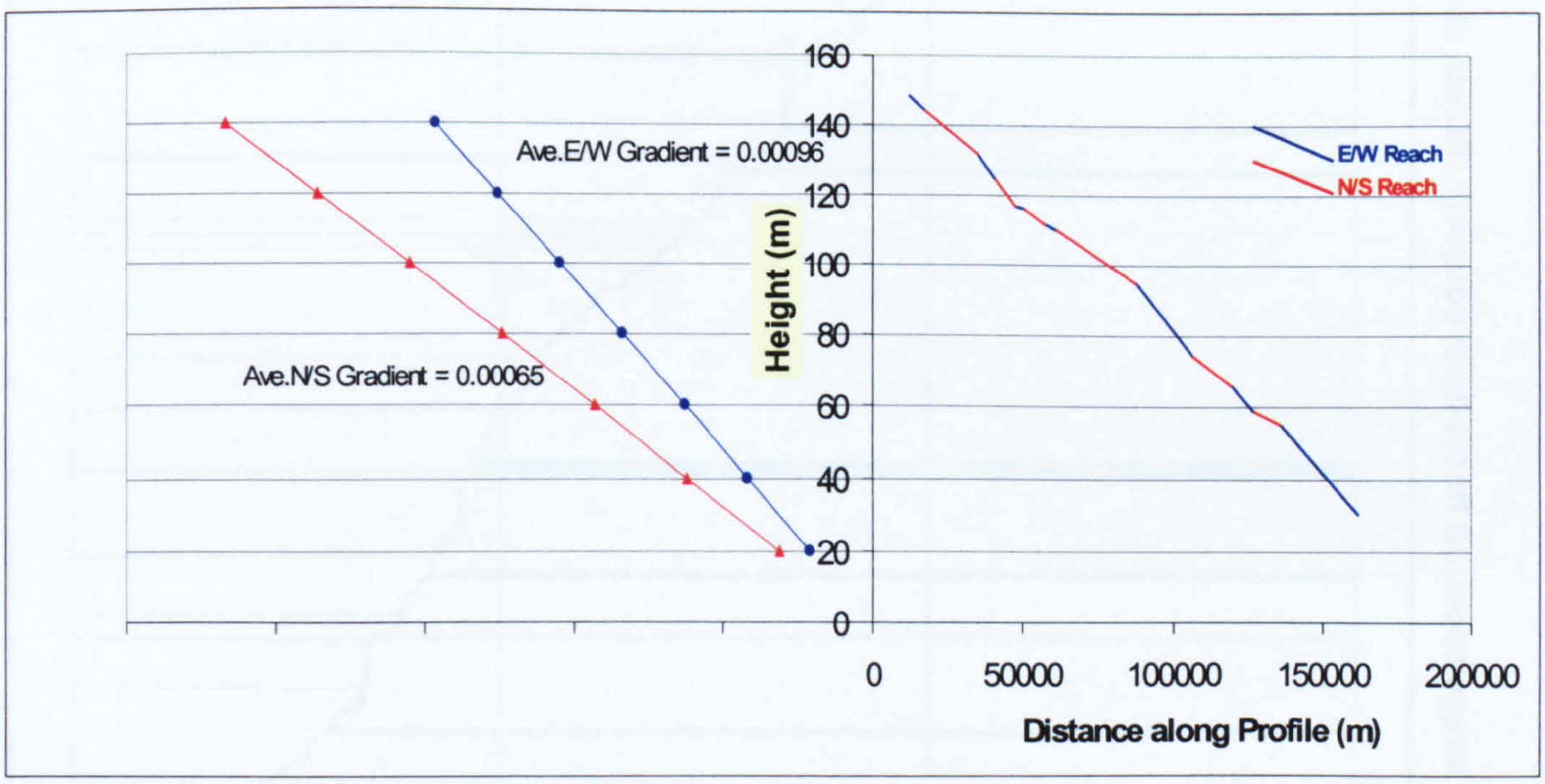

Figure 3.34 Analysis of the effect of flow direction on gradient for north-south and east-west reaches.

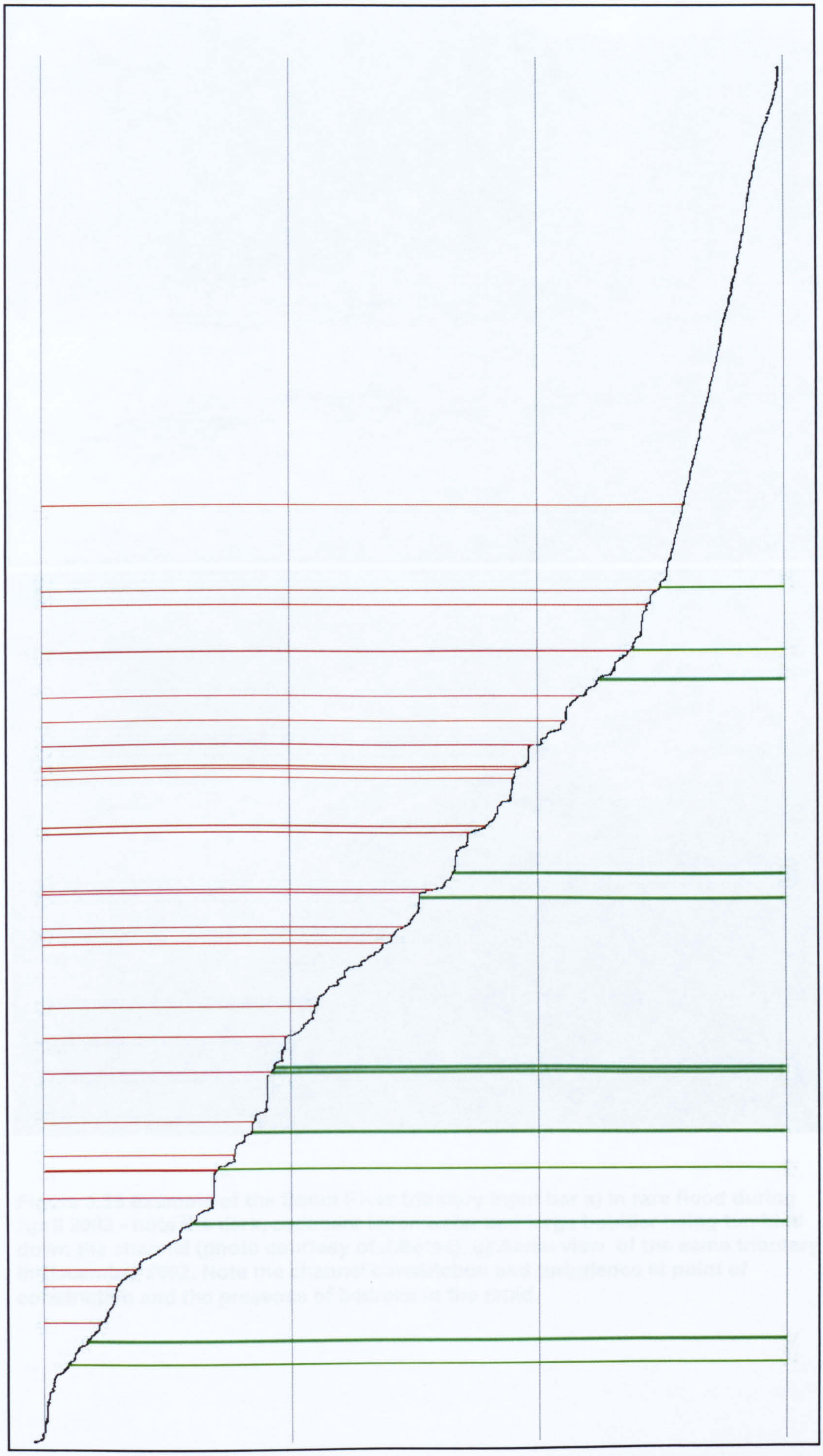

Figure 3.35 Surface profile showing geological contacts (green) and tributary input deltas (red) responsible for steps in the profile.

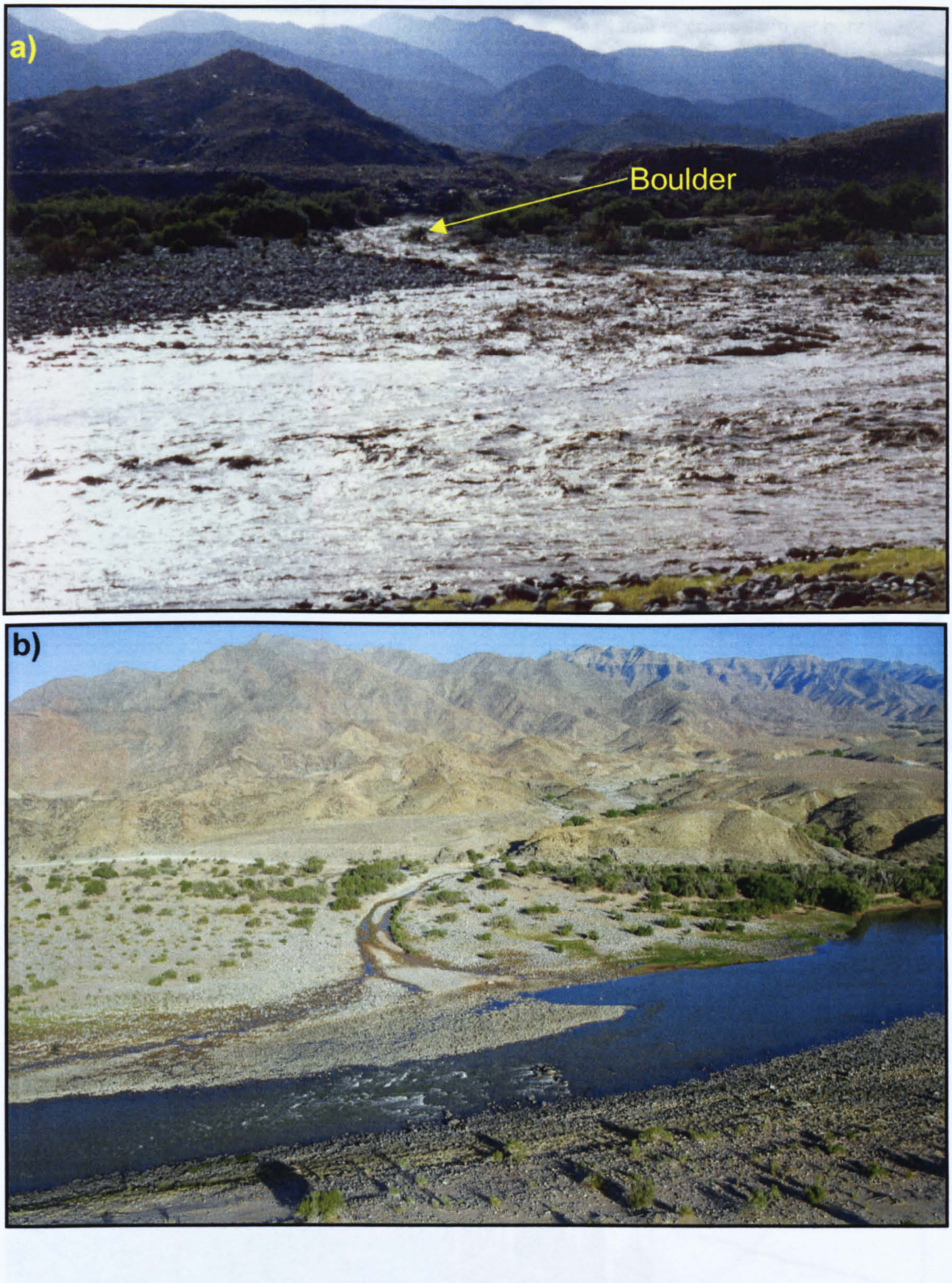

Figure 3.36 Example of the Boom River tributary input bar a) In rare flood during April 2002 - note the dark, sediment laden water and large boulder being tumbled down the channel (photo courtesy of J.Botes). b) Aerial view of the same tributary in December 2002. Note the channel constriction and turbulence at point of constriction and the presence of bedrock in the rapid.

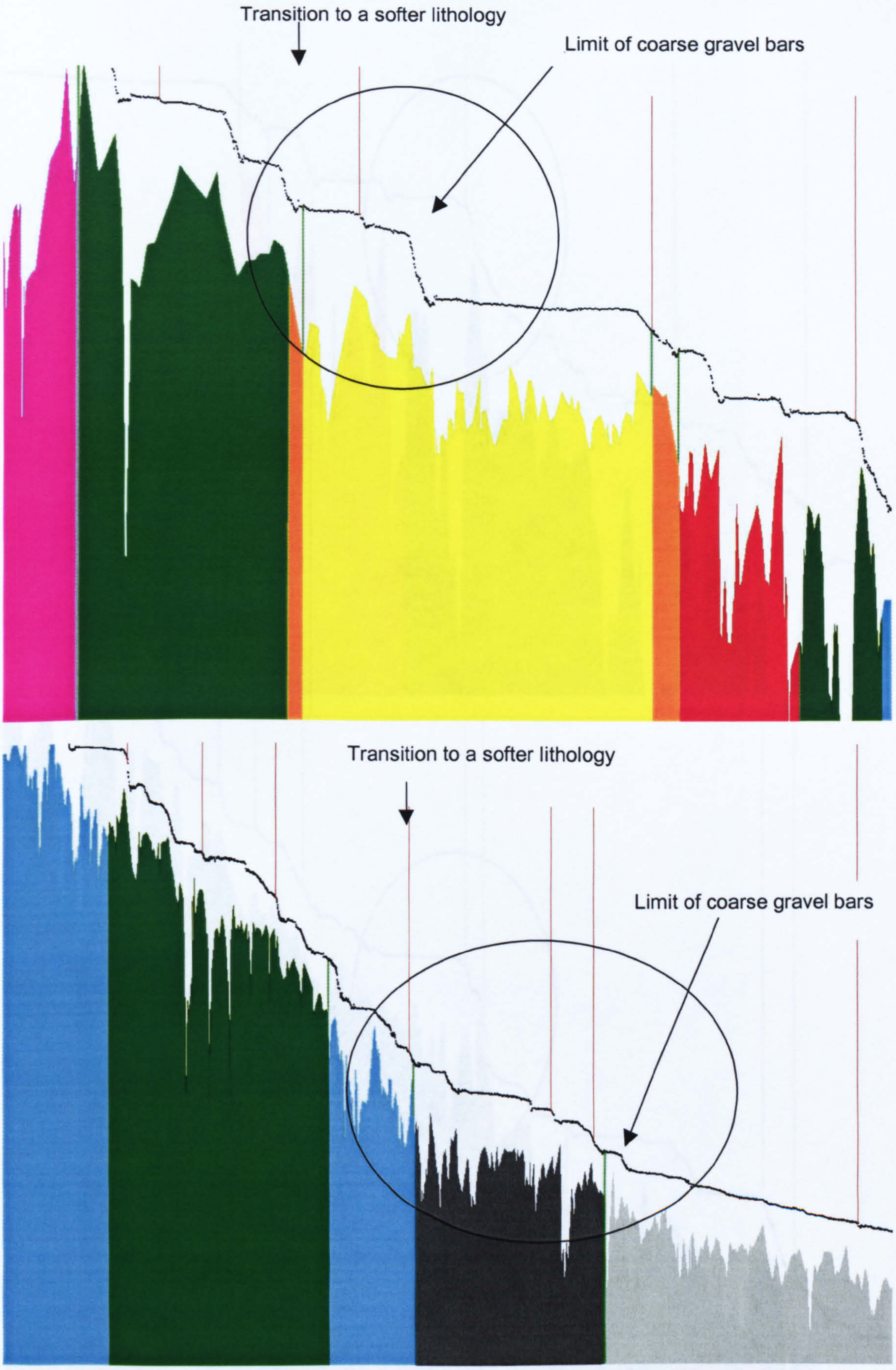

Figure 3.37 Surface and bottom profile showing the effect of coarse gravel bars on the profile (areas of interest are within oval shapes). Red lines above the profile are tributary input deltas.

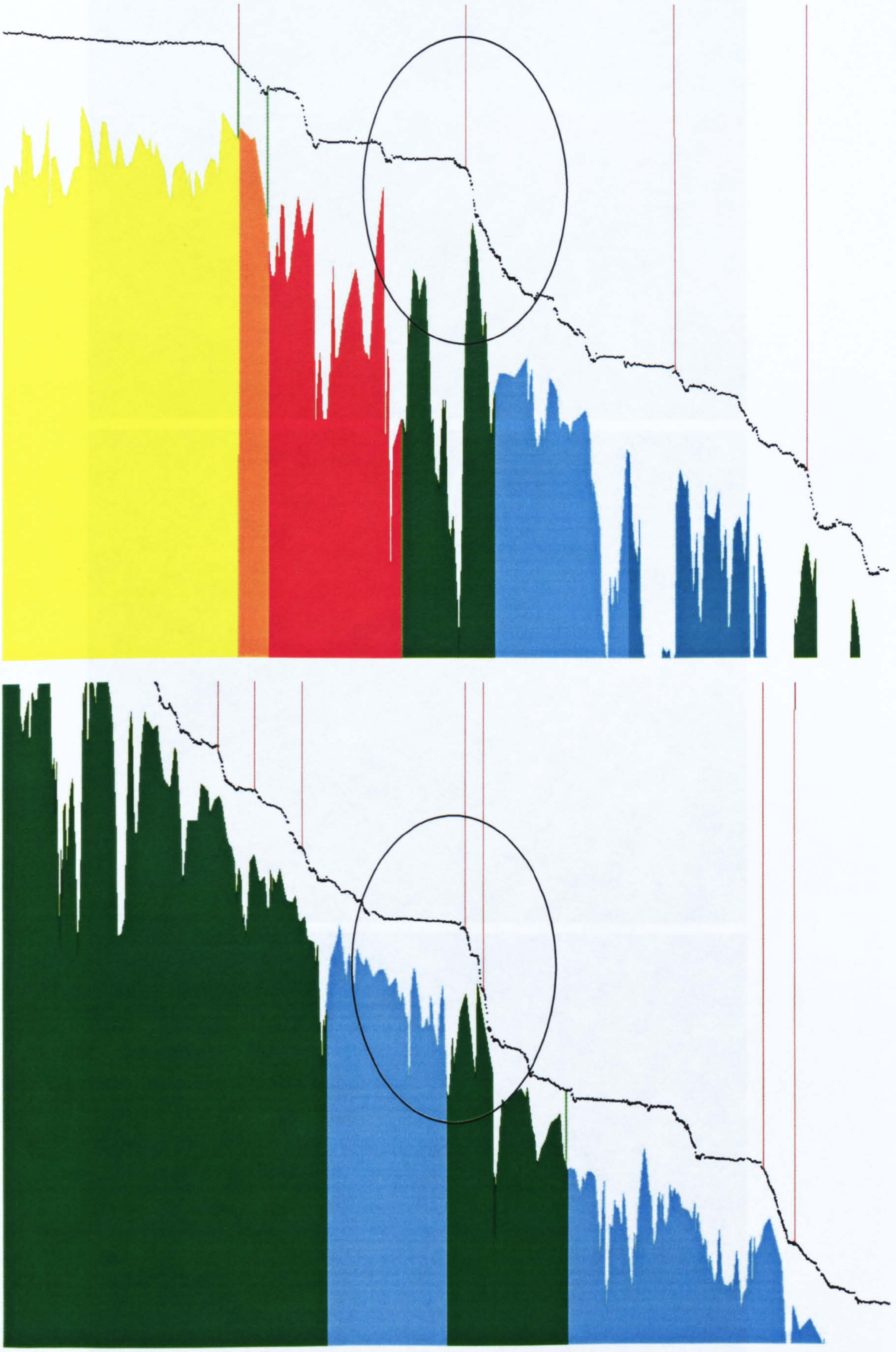

Figure 3.38 Surface and bottom profile showing the effect of tributary fans on the profile (areas of interest are within oval shapes). Red lines above the profile are tributary input deltas.

Figure 3.39 Inner channels with flanking straths in the study reach (flow direction indicated).

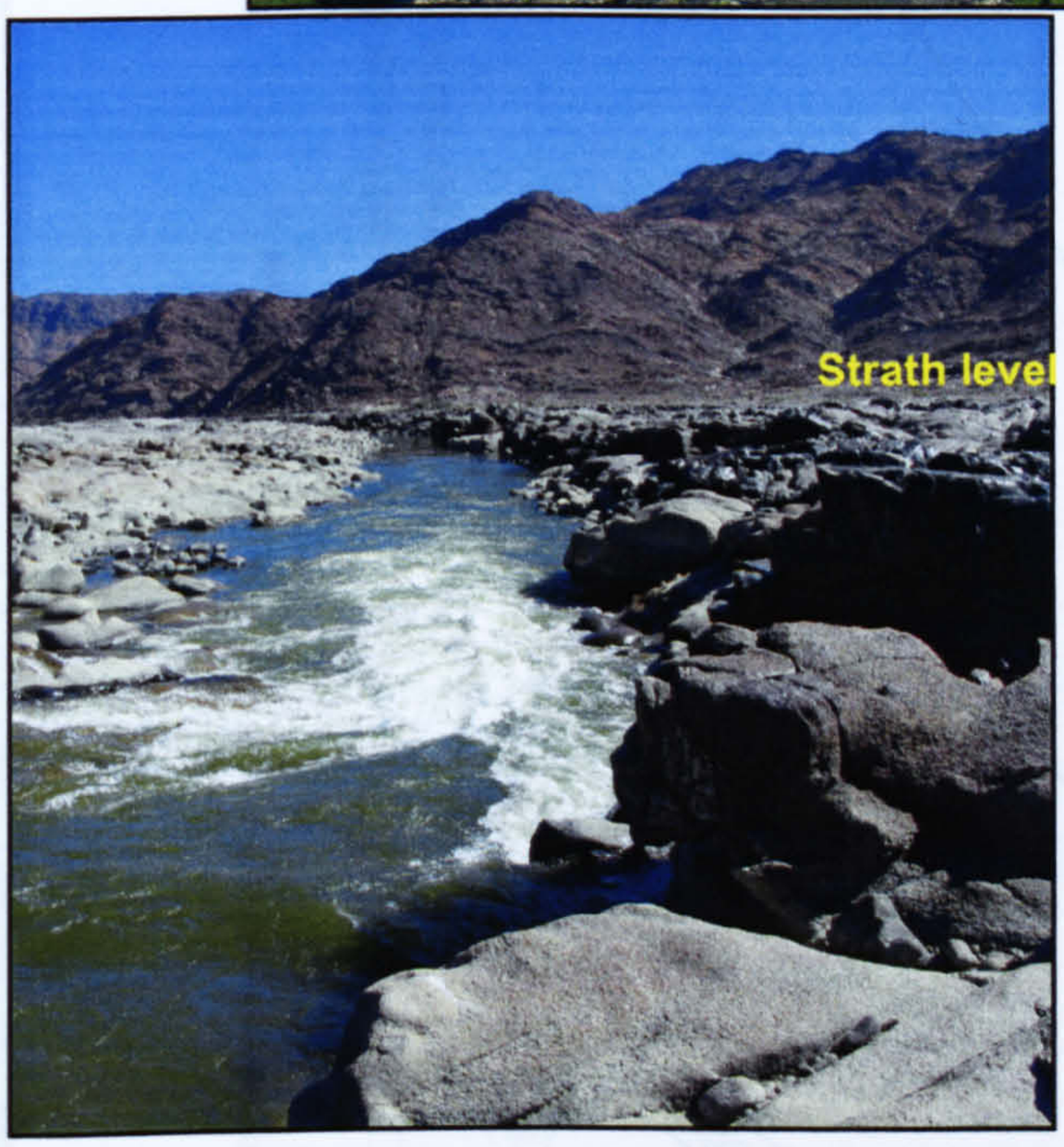

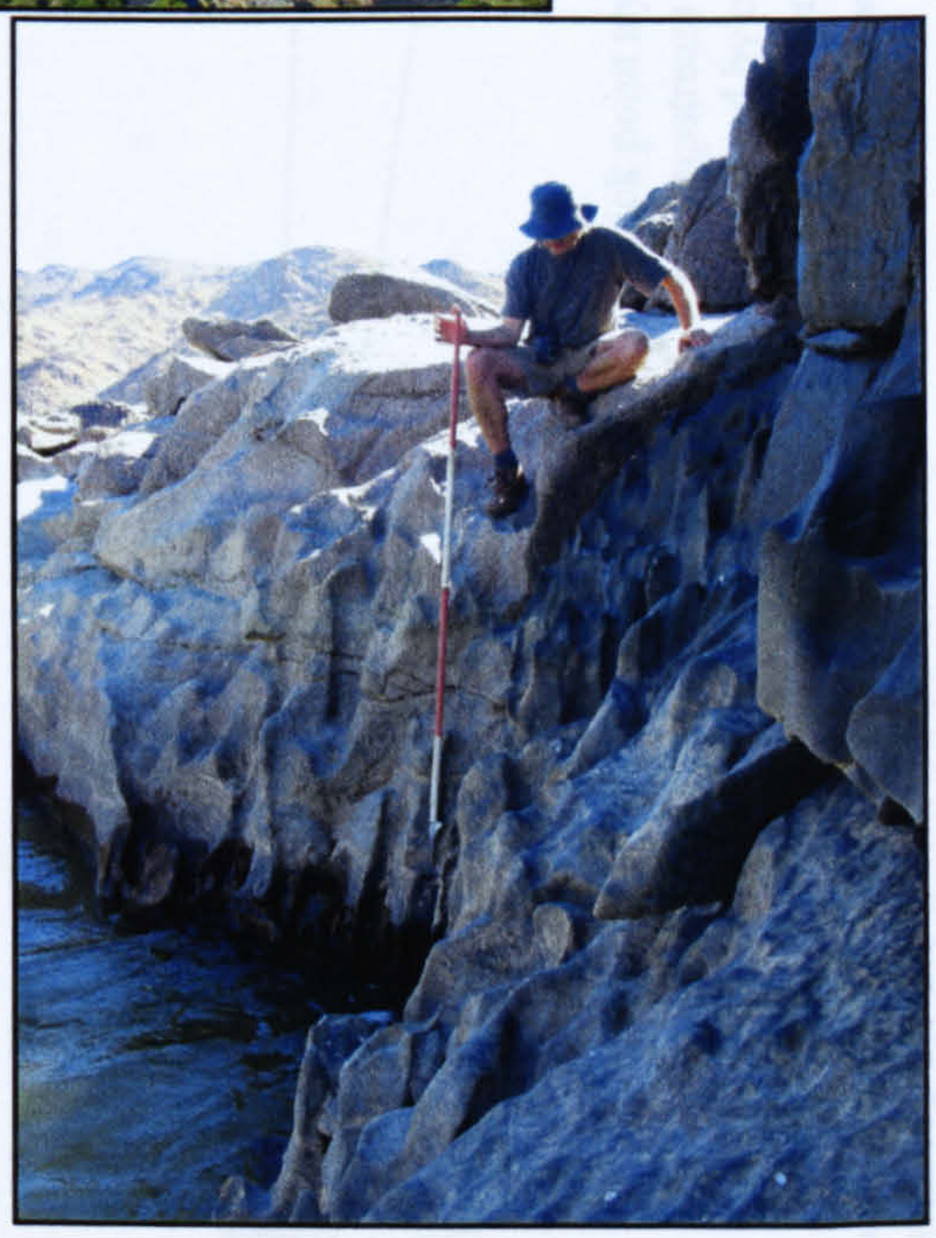

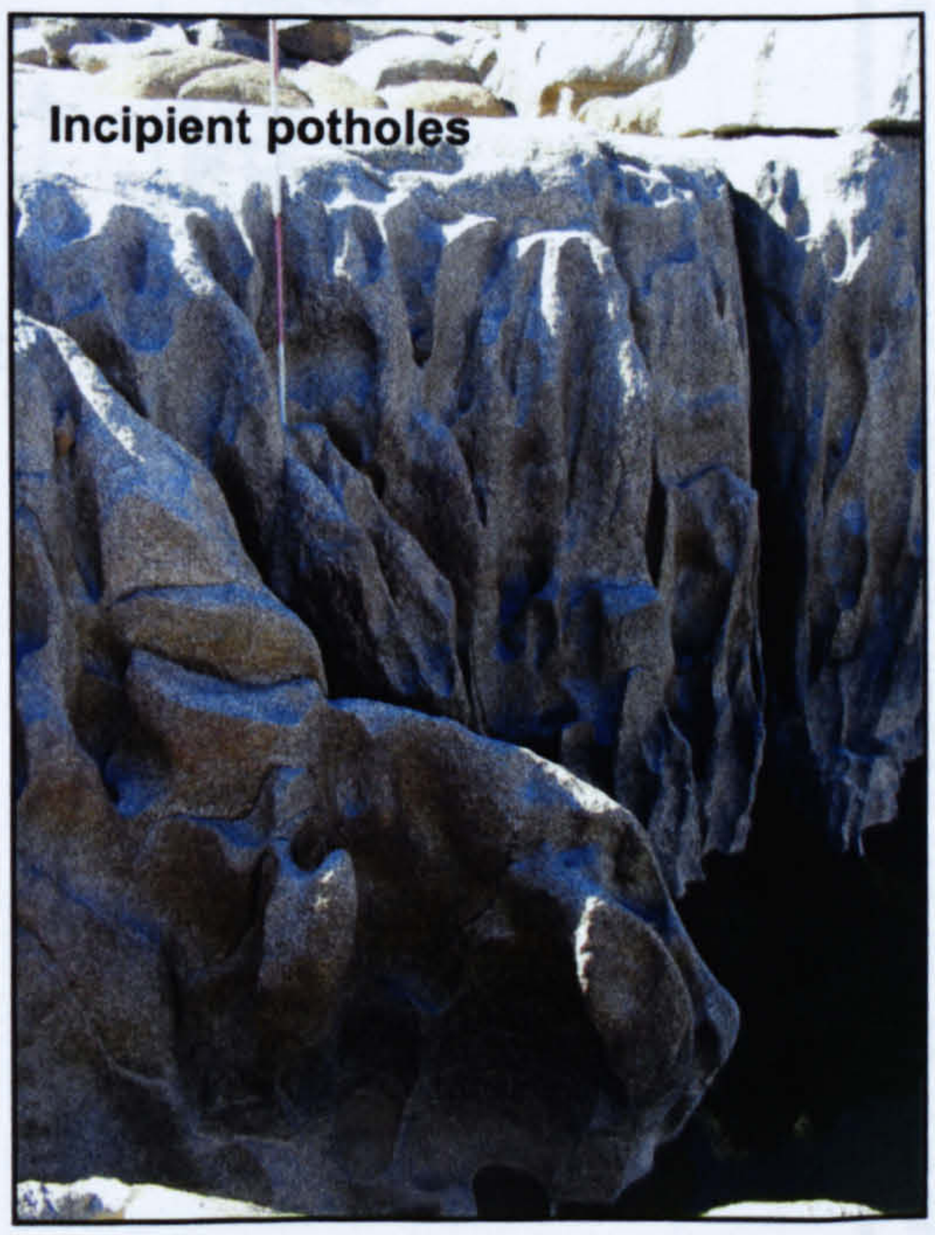

Figure 3.40 Inner channel in the Sambok area displaying abundant features indicating recent incision.

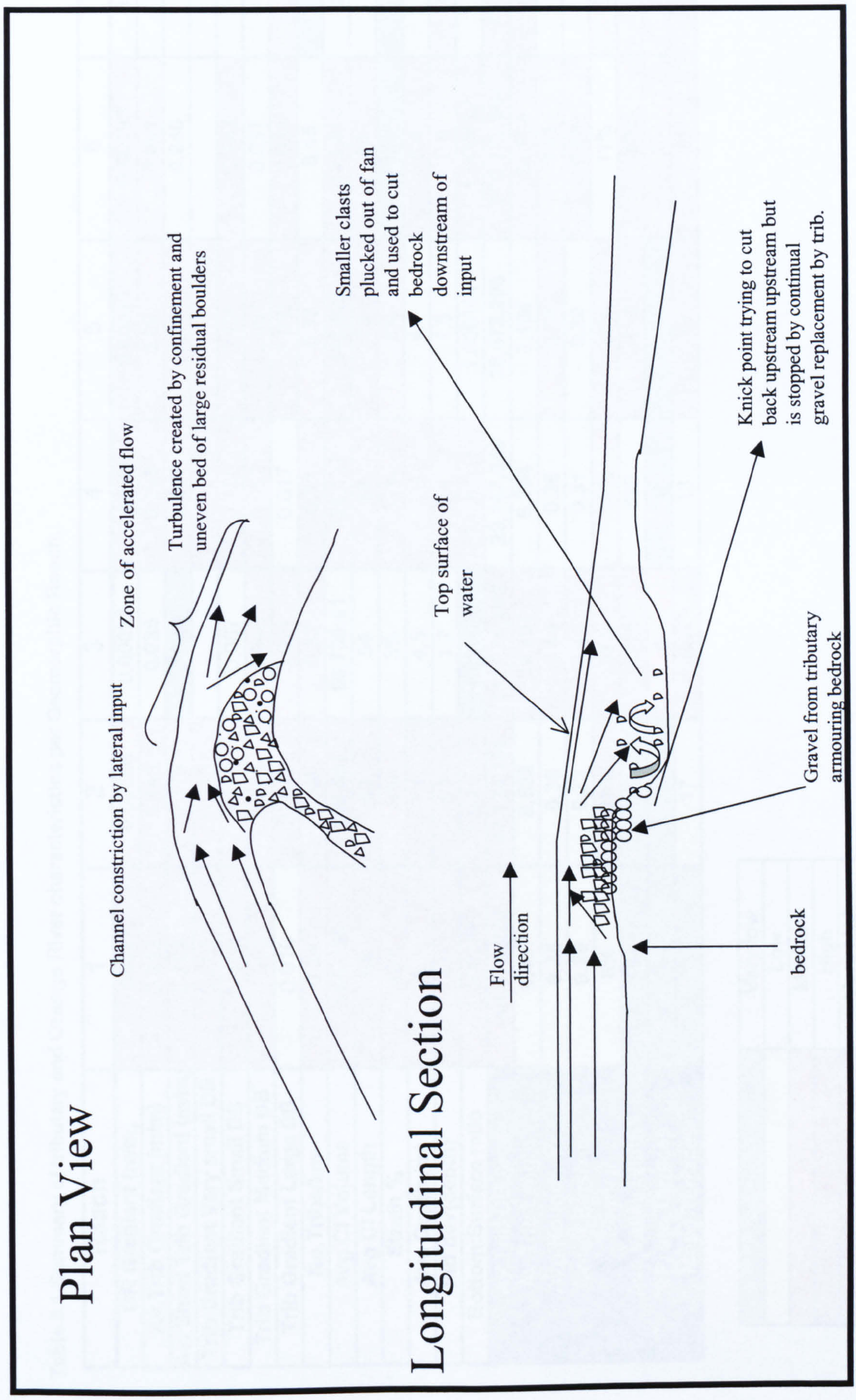

Figure 3.41 Schematic diagram illustrating the effect of tributaries on the trunk stream.

Table 3.1 Summary of tributary and Orange River characteristics per Geomorphic Reach.

Reach	1	2	3	4	5	6	7
OR Gradient (m/m)	0.00087	0.00066	0.00034	0.00086	0.00080	0.00093	0.00026
Av.Trib Gradient (m/m)	0.212	0.143	0.035	0.168	0.097	0.061	0.033
Av. Short Trib Gradient (m/m)	0.203	0.119	0.020	0.147	0.064	0.040	0.030
Trib Gradient Very small DB	0.281	0.319		0.312	0.237		
Trib Gradient Small DB	0.168	0.132	0.057	0.135	0.136	0.143	0.049
Trib Gradient Medium DB	0.055	0.080	0.046	0.052	0.057	0.037	0.038
Trib Gradient Large DB	0.016	0.027	0.021	0.017	0.035	0.034	0.022
No.Tribs/km	0.34	0.69	0.32	0.73	0.32	0.15	0.03
Avg CI Volume	166,026	109,681	66,730.41	126,127	145,925	113,617	50,350
Avg CI Length	68	63	54	69	73	65	49
Strath %	49%	9%	3%	37%	8%	0%	0%
Ave Depth (m)	6.1	7.1	4.5	5.8	4.1	5.4	3.8
Std dev(depth)	4.0	4.1	1.7	3.4	1.5	2.8	2.2
Bottom:Surface ratio	1.000357	1.000386	1.000067	1.000381	1.000144	1.000432	1.000126
Av.Trib DB Area	44,075,229	47,134,766	112,075,592	29,167,649	28,673,298	236,172,994	83,557,934
Av.Trib Length	8,497	8,632	16,796	6,234	7,104	34,524	14,092
Avg Roundness	0.35	0.35	0.44	0.36	0.38	0.41	0.34
Oriver Bars/km	0.28	0.32	0.47	0.31	0.30	0.69	0.26
% Graded	8%	23%	36%	15%	25%	11%	17%
Ave Valley Width	554	597	2371	690	1012	1302	2347
% Proto Terraces	0	0	8	0	0	16	35
% Meso Terraces	0	17	49	13	39	39	74

	Very low
	Low
	Medium
	High
	Very high

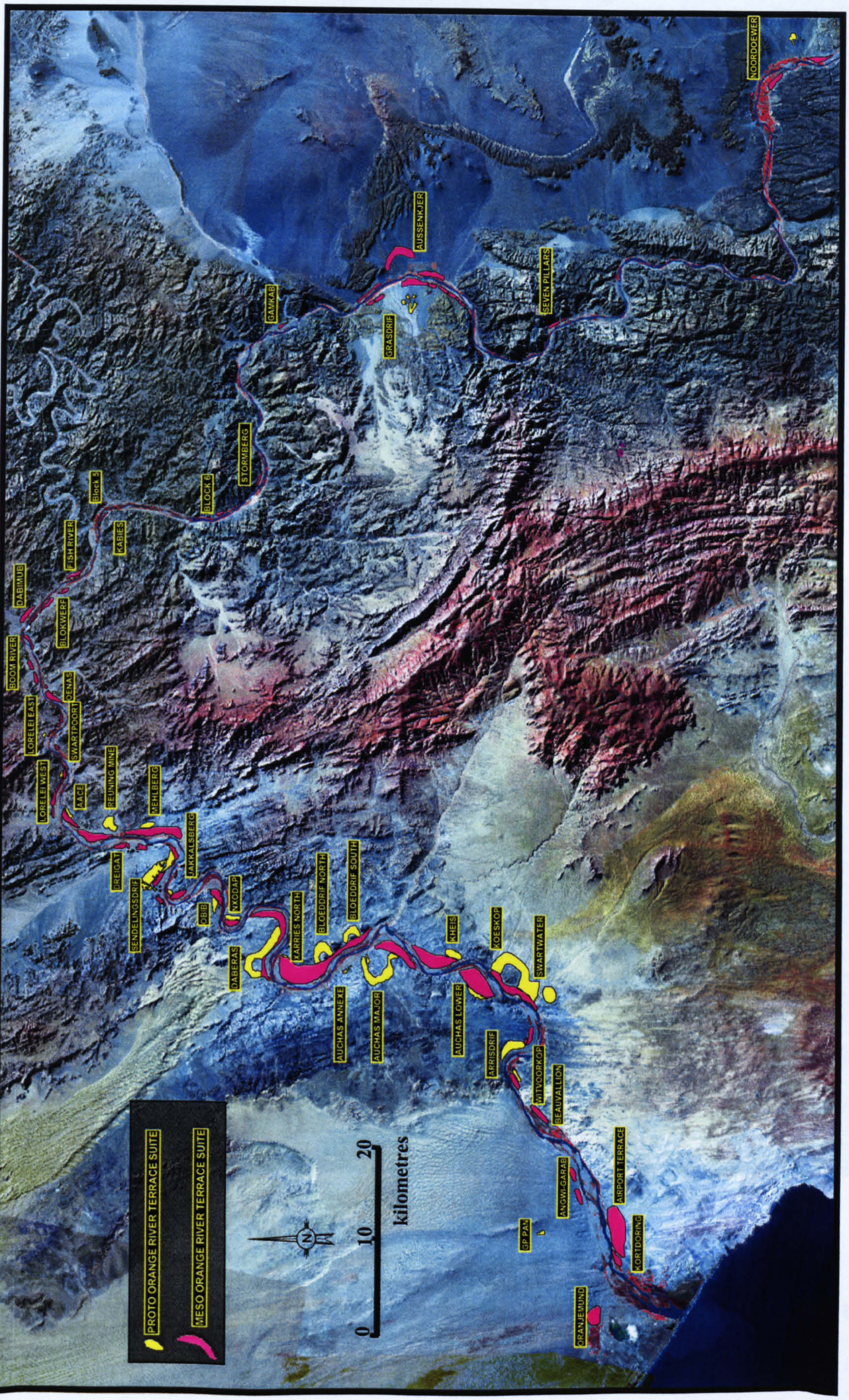

Figure 4.1 Satellite image of study area showing the distribution of Proto and Meso Orange River terrace suites.

Figure 4.2 a) Oblique aerial view showing Proto and Meso Terraces at Daberas b) Oblique aerial view showing Pre-Proto1, Proto and Meso terraces at Sendelingsdrif. Note that terrace labelled as P2 is a lower terrace than P1, however they are underlain by the same bedrock strath, hence both are classified as Proto terraces.

PROTO SUITE
POST EOCENE TO EARLY MIDDLE MIOCENE (10-37Ma)
- 1C - PROTO AGGRADATIONAL SEQUENCE (17.5-19Ma)
- 1B - PRE-PROTO 2 DEGRADATIONAL DEPOSITS
- 1A - PRE-PROTO 1 DEPOSITS

MESO SUITE
POST EARLY MIDDLE MIOCENE TO PLIO-PLEISTOCENE (2-10Ma)
- 2D - LOWER MESO AGGRADATIONAL SEQUENCE
- 2C - UPPER MESO AGGRADATIONAL SEQUENCE
- 2B - MESO DEGRADATIONAL DEPOSITS
- 2A - INTERMEDIATE DEPOSITS

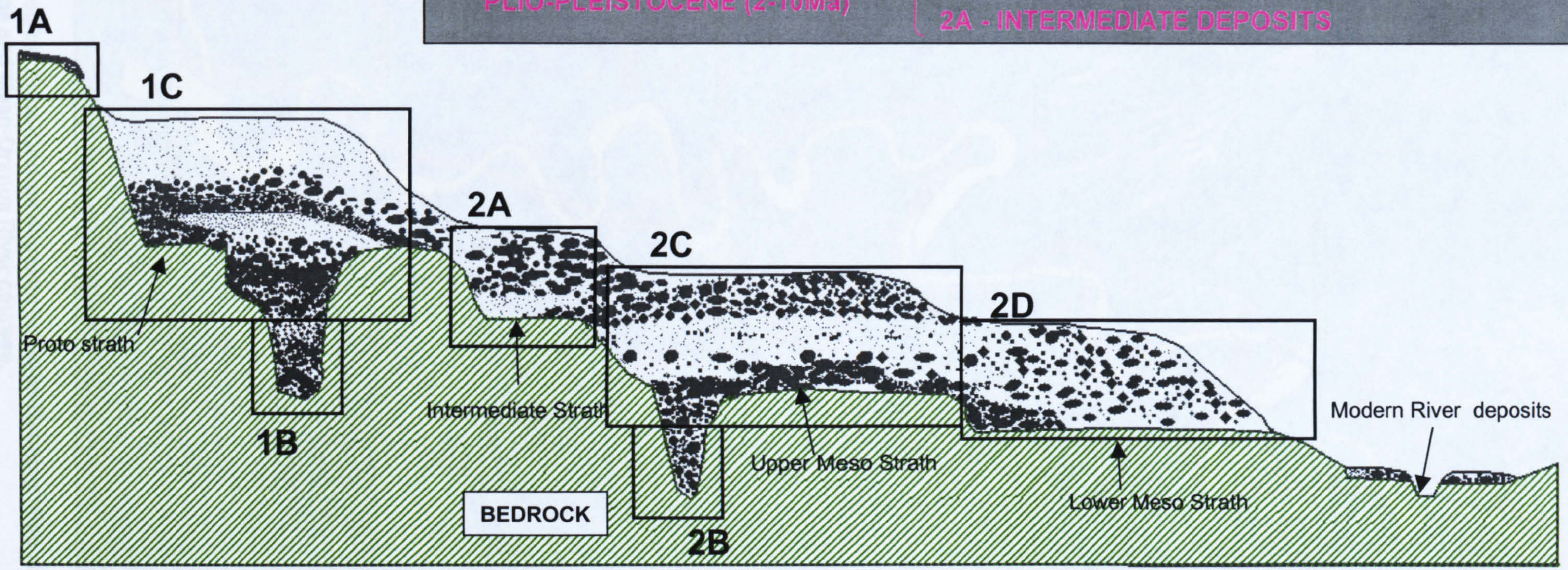

Figure 4.3 Sequence of Orange River deposits at one locality.

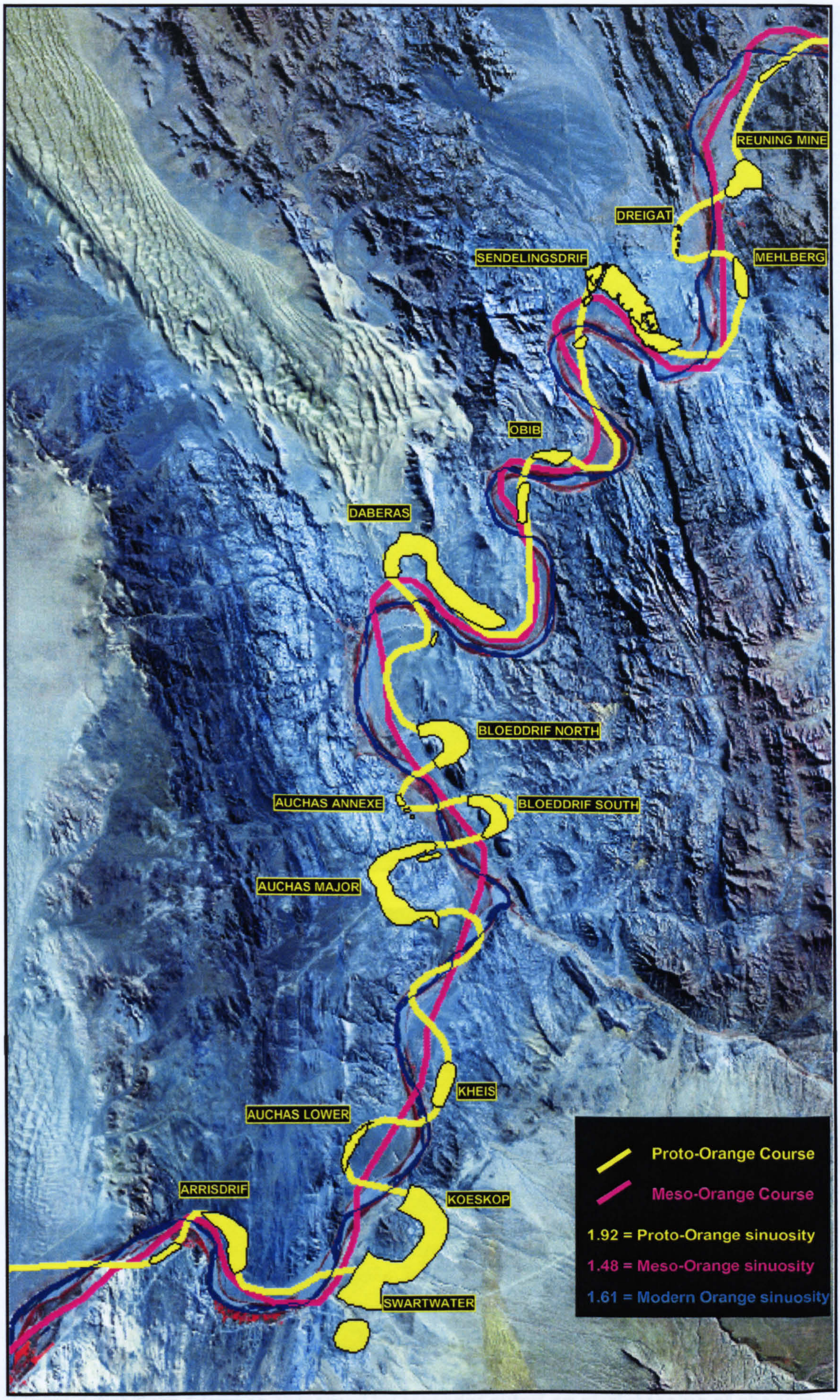

Figure 4.4 Satellite image showing Proto-Orange deposits between Reuning Mine and Arrisdrif and the Proto-Orange and Meso-Orange River courses.

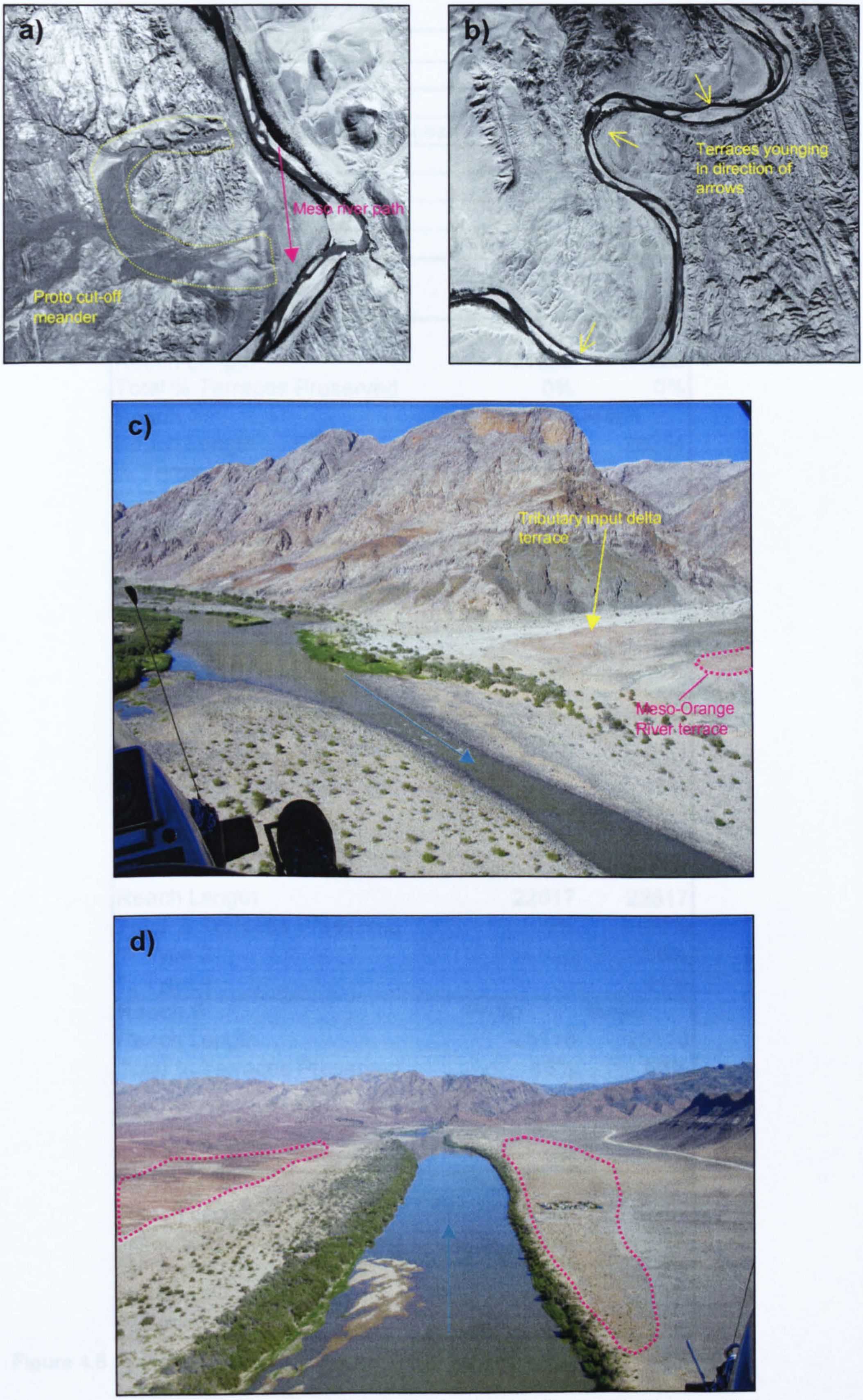

Figure 4.5 a) Type 1 terrace preserved by meander cutoff on straightening of channel. b) Type 2 terraces preserved by lateral erosion of meander prior to incision. c) Type 3 terraces preserved downstream of tributary input delta. d) Type 4 terrace formed by dissection of modern channel, leaving paired terraces.

Overall Terrace Data	Proto	Meso
Total Length (m)	302867	277160
Terrace Length (m)	54789	135905
% Length Preserved as Terraces	**18%**	**49%**
% Type 1	58%	0%
% Type 2	39%	59%
% Type 3	3%	5%
% Type 4	0%	36%

Reach 1	**Proto**	**Meso**
Reach Length	21286	21286
Total % Terraces Preserved	**0%**	**0%**
Reach 2	**Proto**	**Meso**
Reach Length	28264	28264
% Terraces Preserved	**0%**	**17%**
% Type 2		47%
% Type 3		53%
Reach 3	**Proto**	**Meso**
Reach Length	36967	36967
Total % Terraces Preserved	**49%**	**8%**
% Type 2	100%	26%
% Type 3	0%	19%
% Type 4	0%	55%
Reach 4	**Proto**	**Meso**
Reach Length	32007	32007
Total % Terraces Preserved	**0%**	**13%**
% Type 2		71%
% Type 4		29%
Reach 5	**Proto**	**Meso**
Reach Length	22617	22617
Total % Terraces Preserved	**0%**	**39%**
% Type 2		56%
% Type 4		44%
Reach 6	**Proto**	**Meso**
Reach Length	25118	25118
Total % Terraces Preserved	**16%**	**69%**
% Type 2	62%	92%
% Type 3	38%	0%
% Type 4	0%	8%
Reach 7	**Proto**	**Meso**
Reach Length	136608	110901
Total % Terraces Preserved	**35%**	**74%**
% Type 1	67%	0%
% Type 2	33%	59%
% Type 4	0%	41%

Figure 4.6 Analysis of terrace types per reach for Proto and Meso terraces.

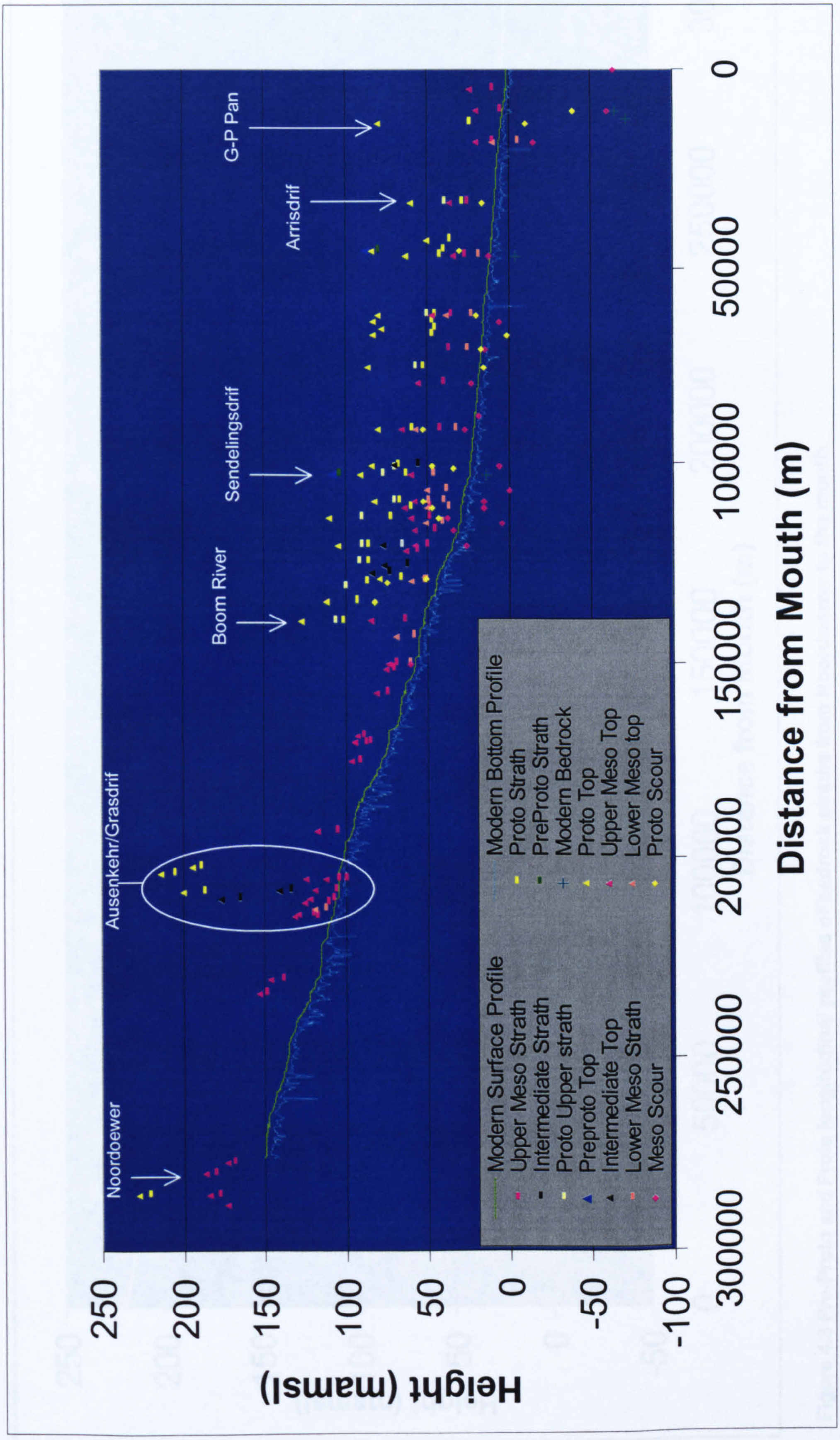

Figure 4.7 Survey data from Noordoewer to the river mouth used to construct longitudinal profiles.

Figure 4.8 Pre-Proto and Proto longitudinal profiles of bedrock straths from Noordoewer to the mouth.

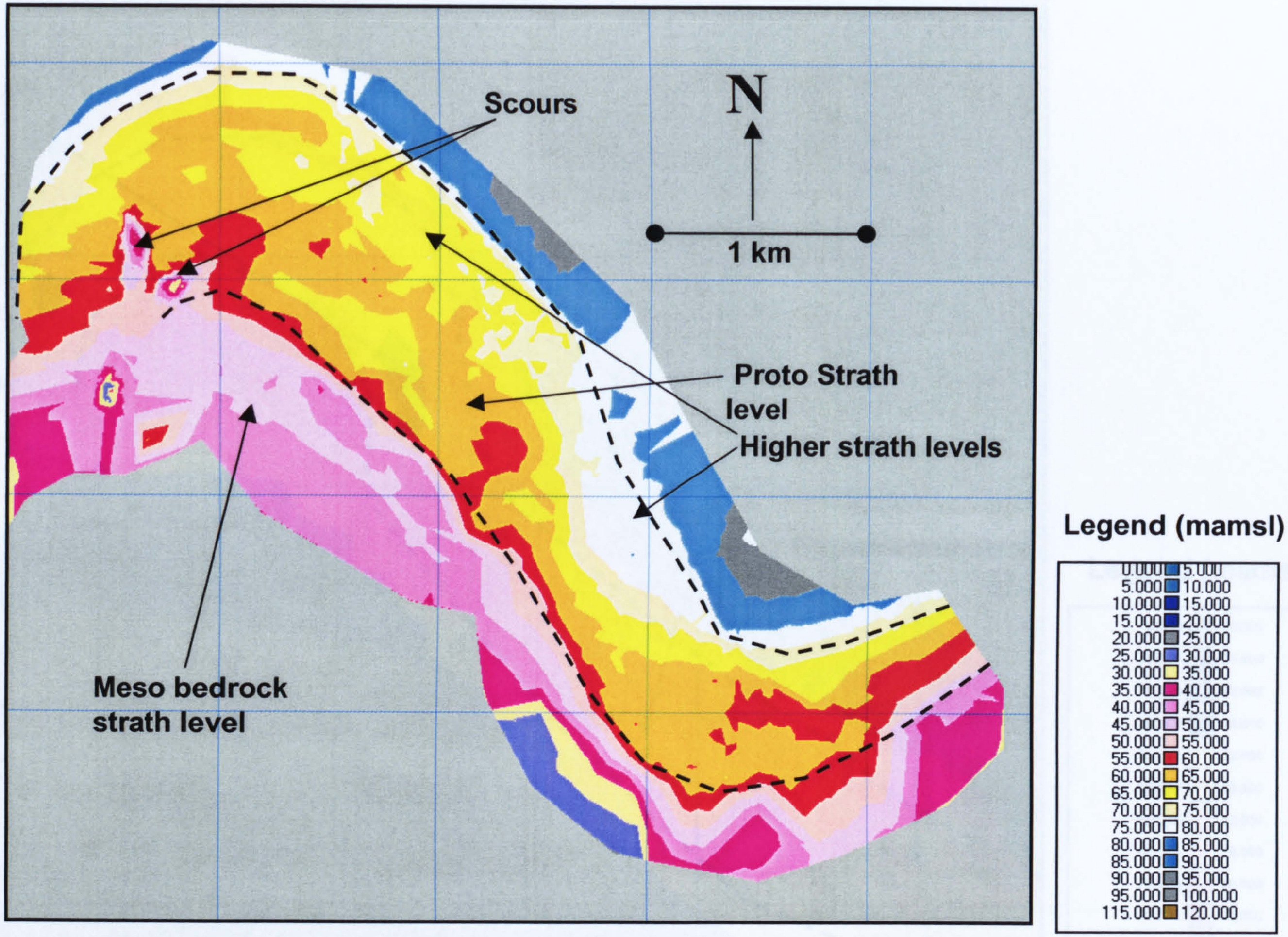

Figure 4.9a Bedrock surface of the Sendelingsdrif deposit obtained from percussion drilling data.

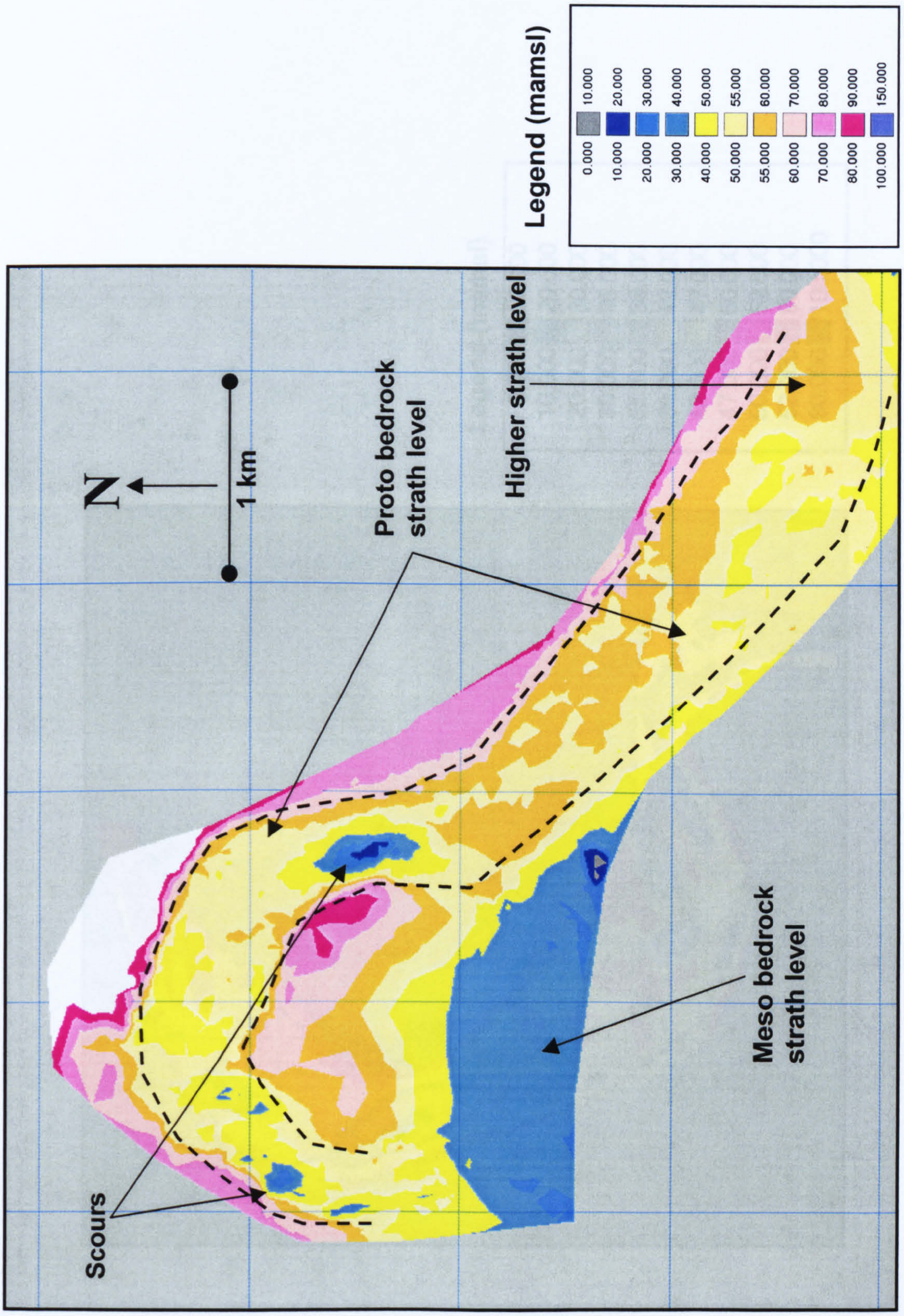

Figure 4.9b Bedrock surface of the Daberas Proto deposit obtained from percussion drilling data.

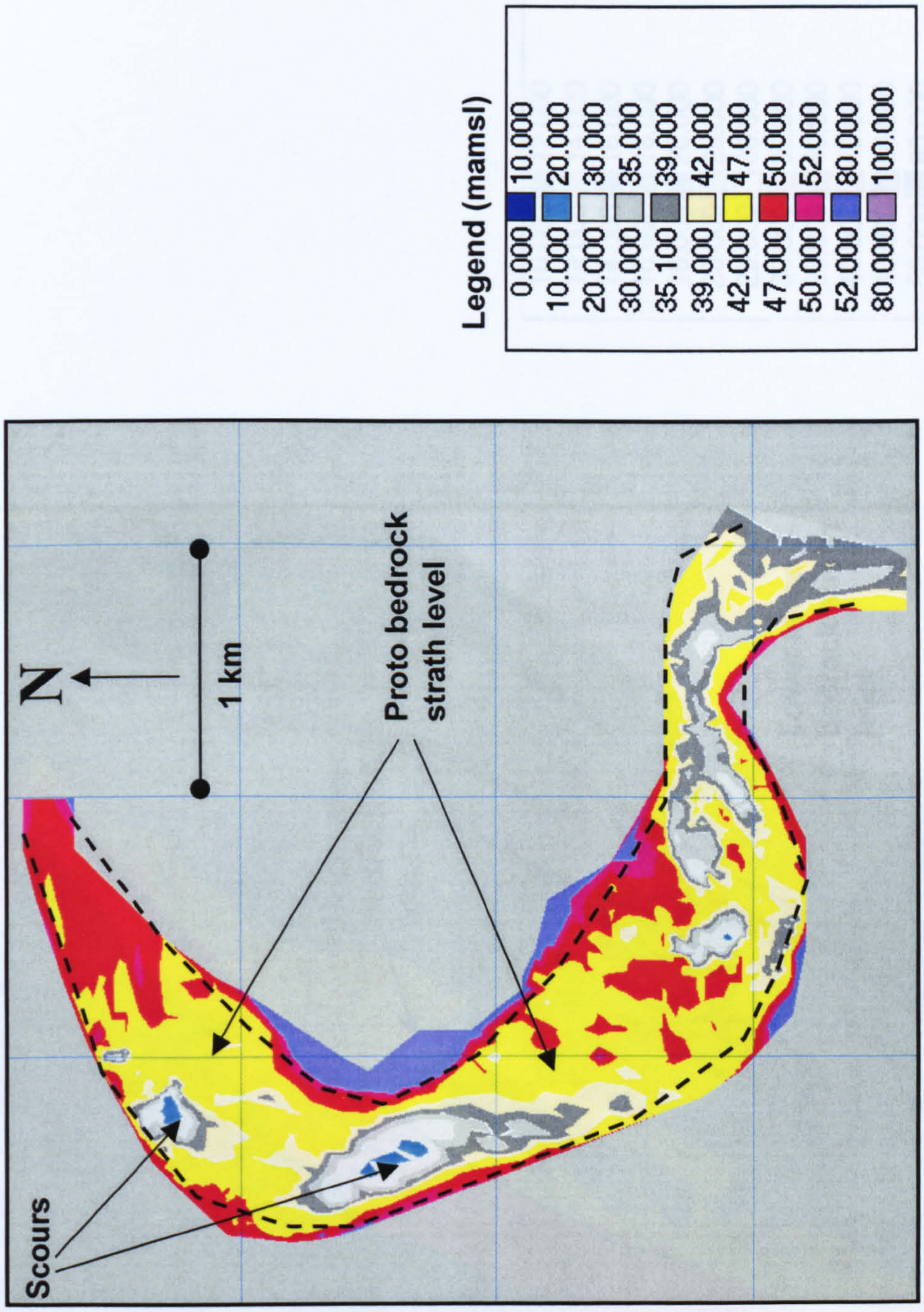

Figure 4.9c Bedrock surface of the Auchas Major Proto deposit obtained from percussion drilling data.

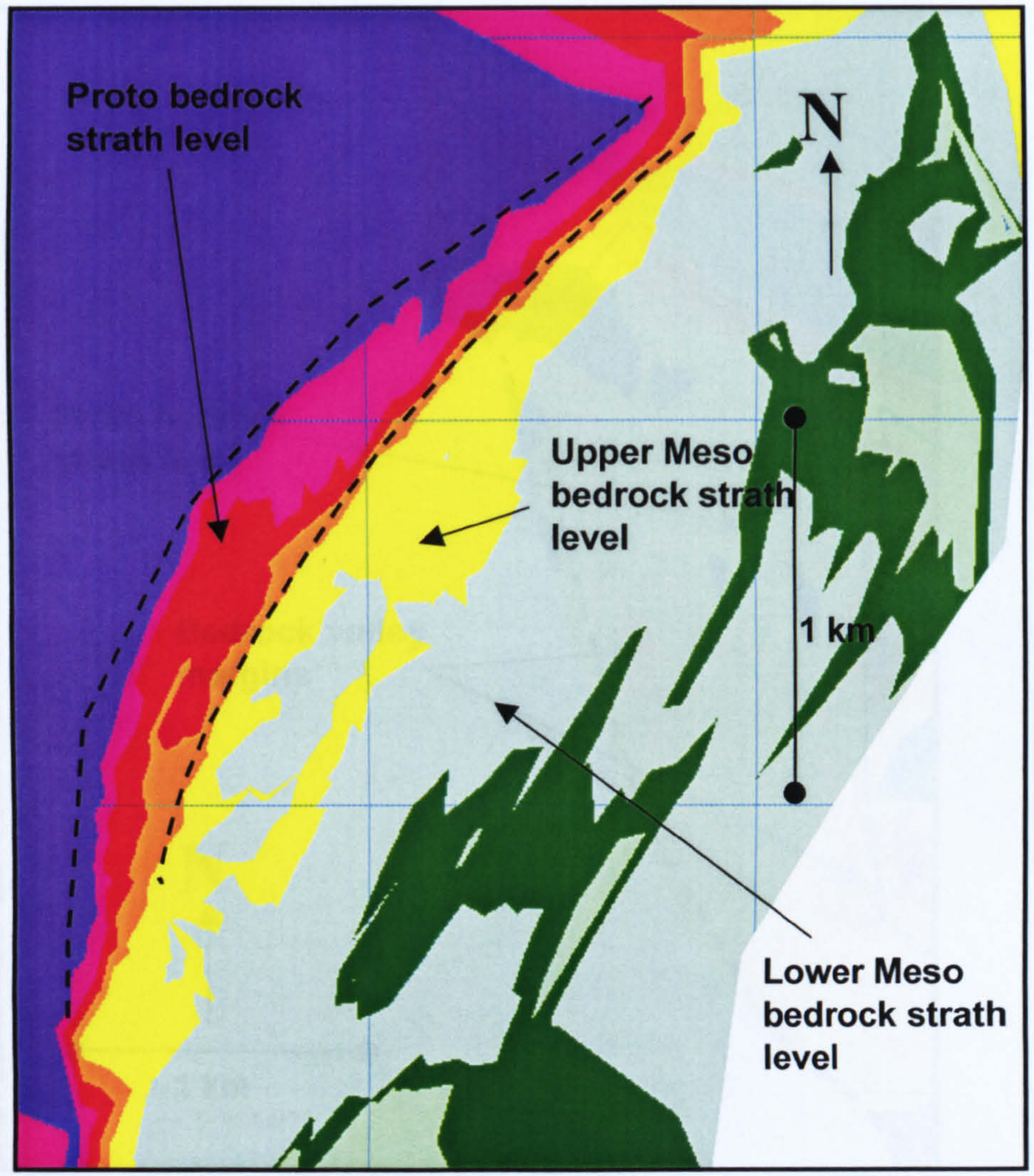

Figure 4.9d Bedrock surface of the Auchas Lower deposit obtained from percussion drilling data.

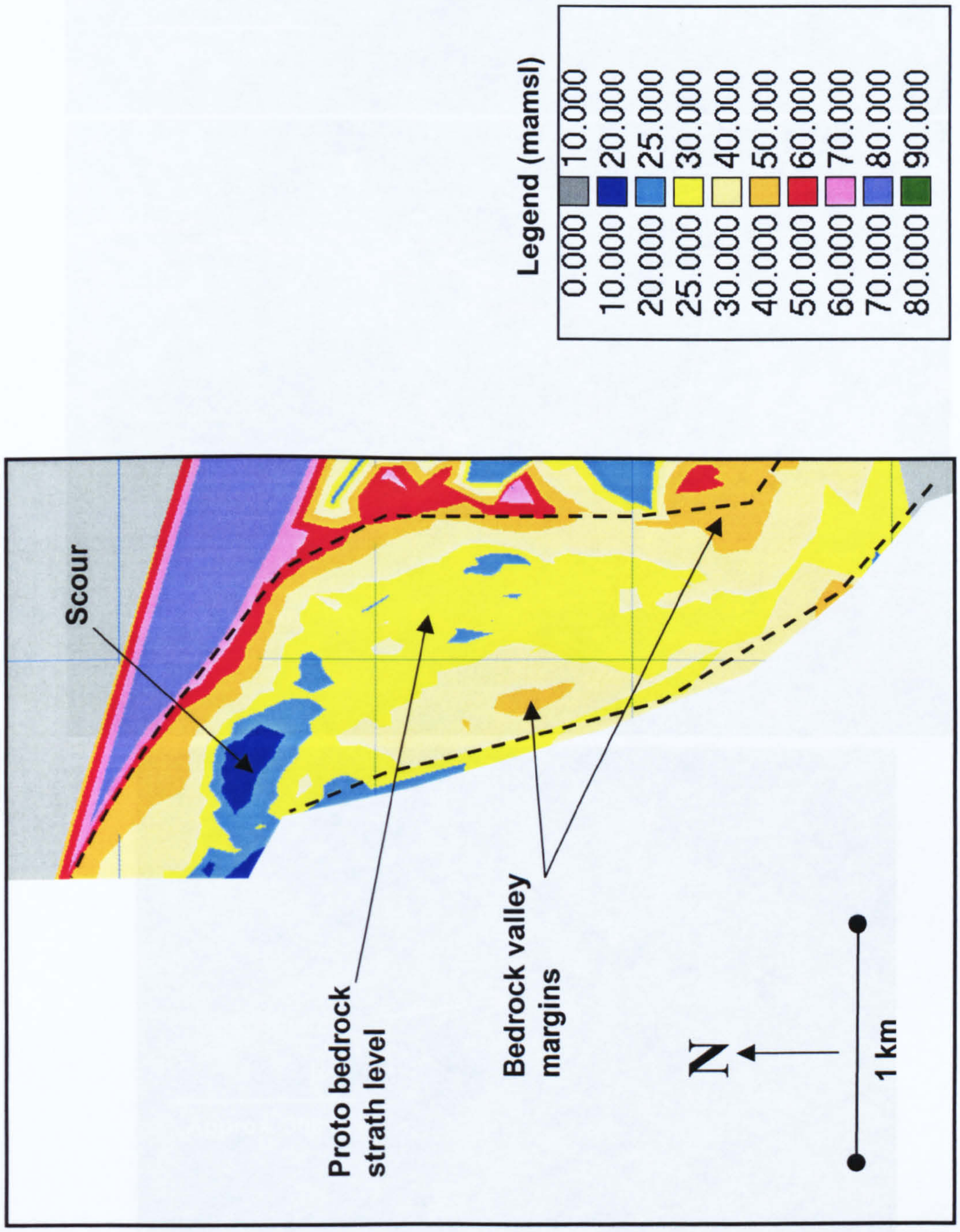

Figure 4.9e Bedrock surface of the Arrisdrif Proto deposit obtained from percussion drilling data.

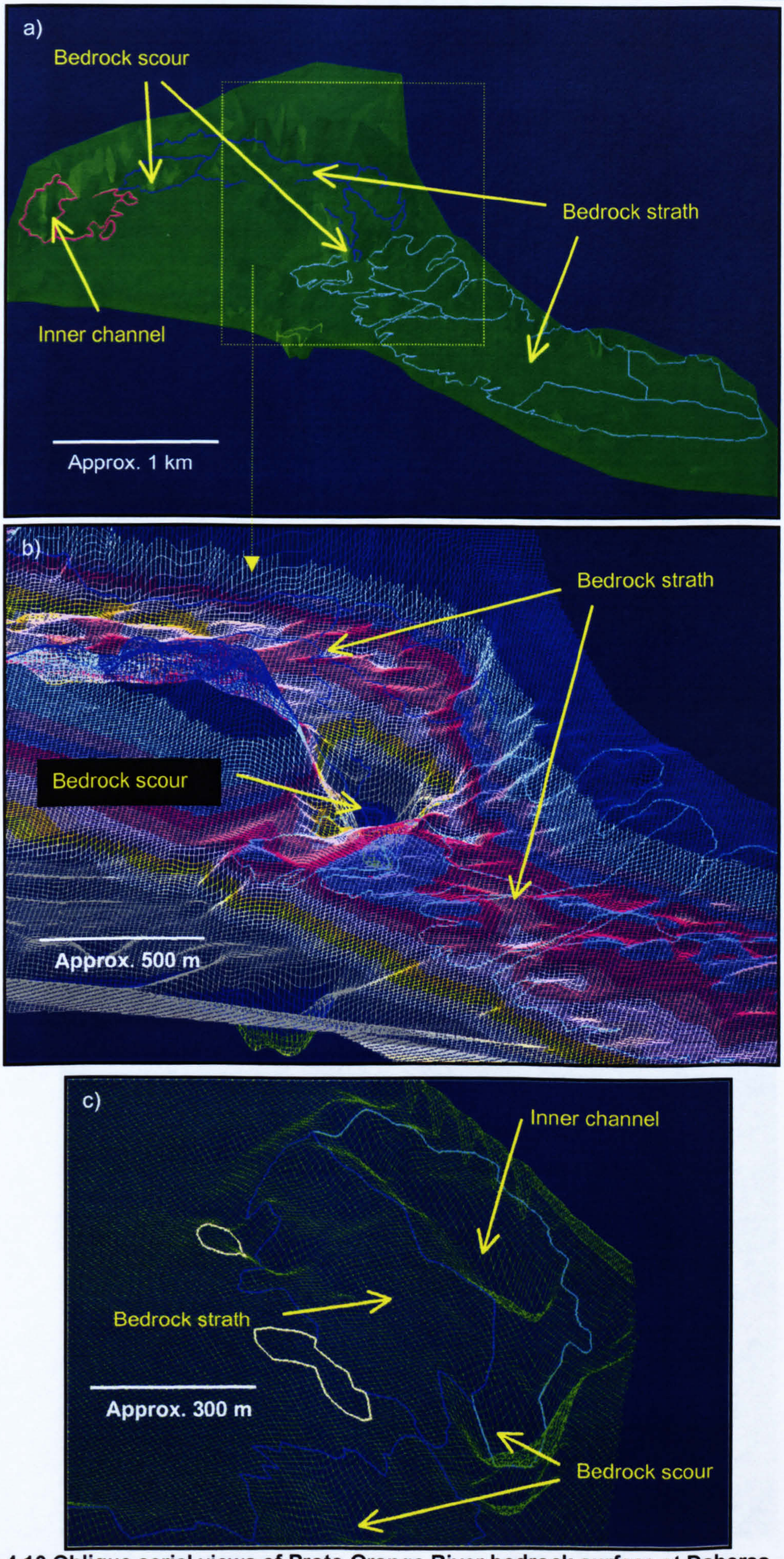

Figure 4.10 Oblique aerial views of Proto Orange River bedrock surface at Daberas showing straths, scours and inner channels. Surface was based on drilling data, created using Vulcan modelling software.

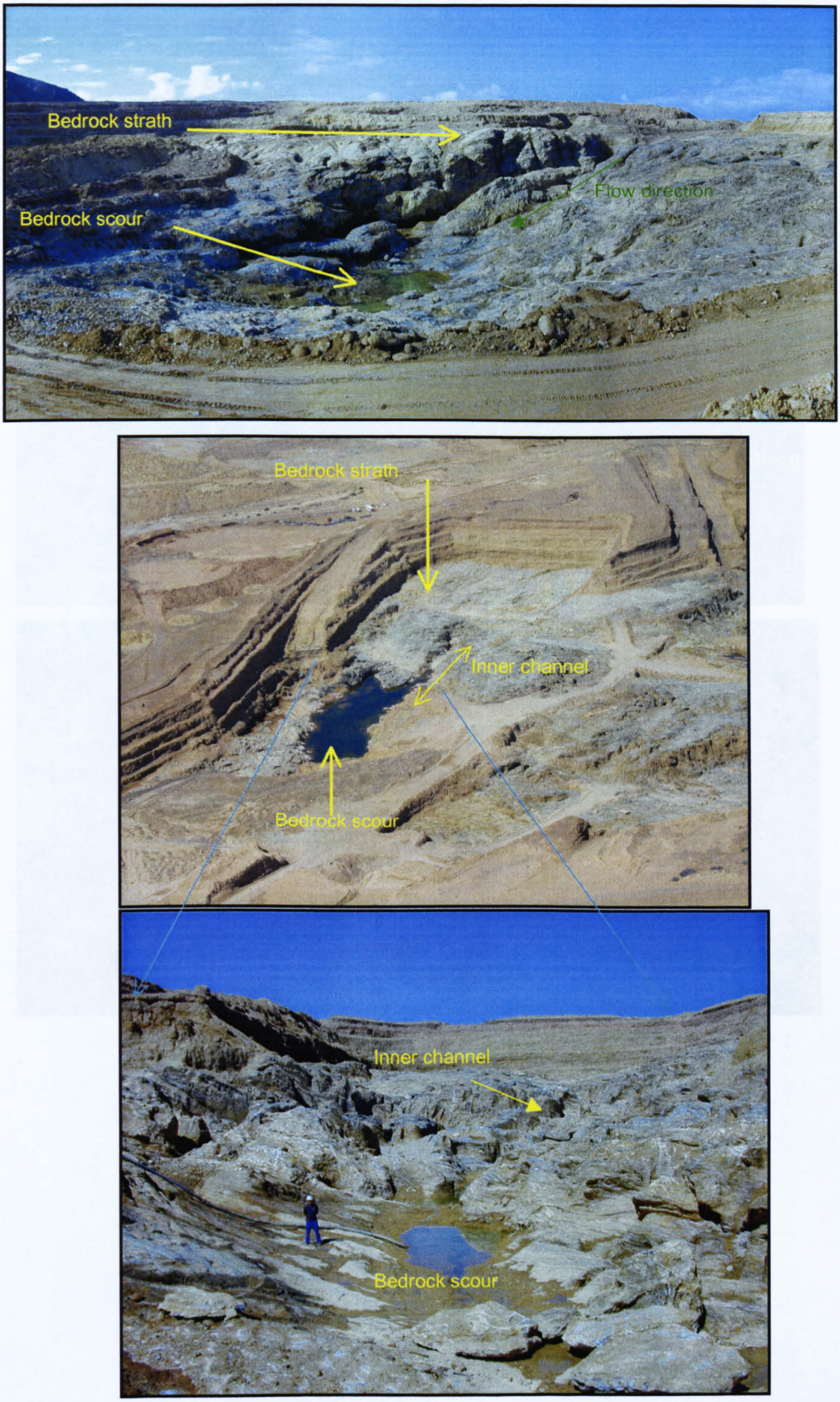

Figure 4.11 Various features of the bedrock surface at Auchas Major, exposed by mining operations.

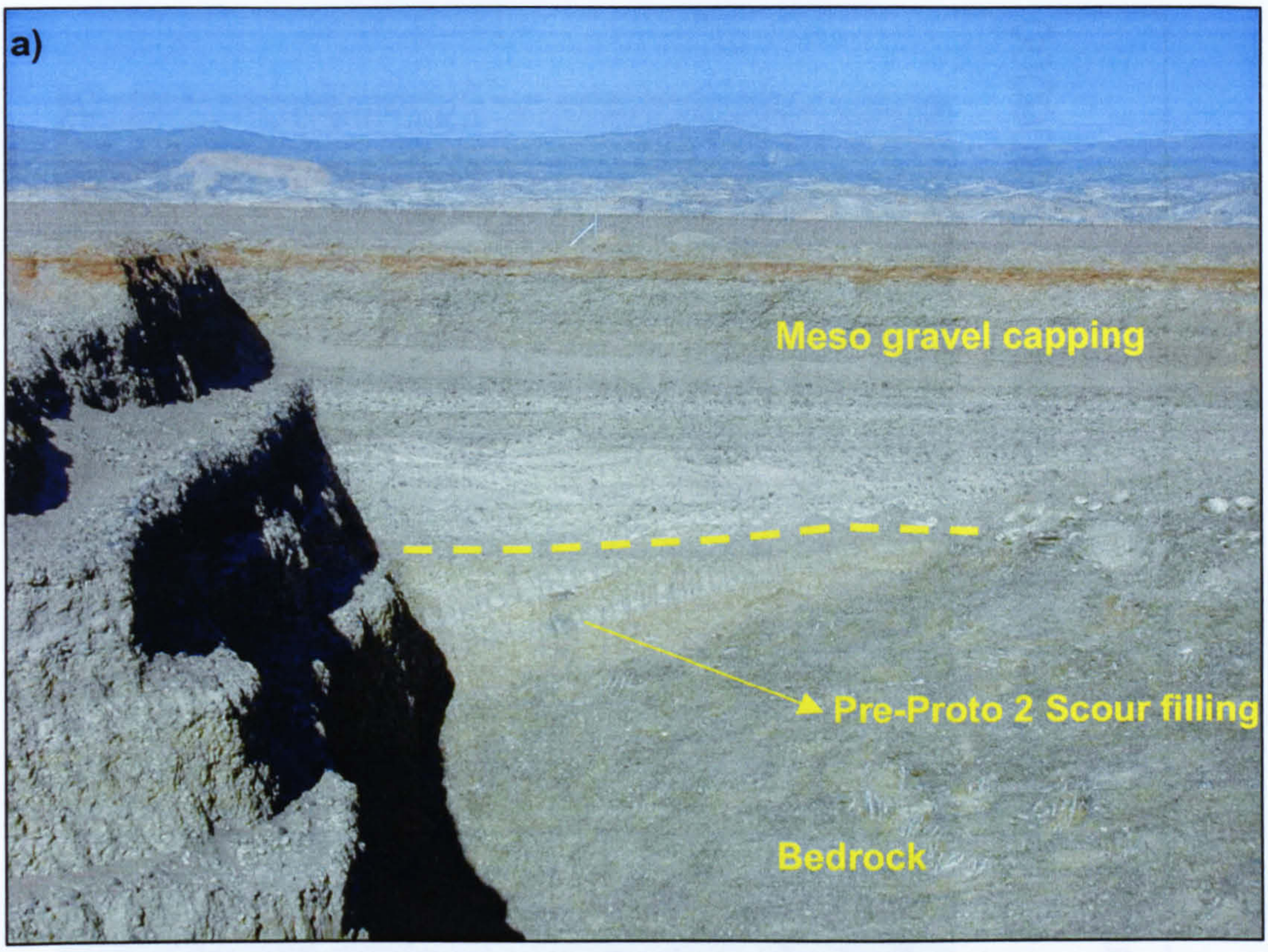

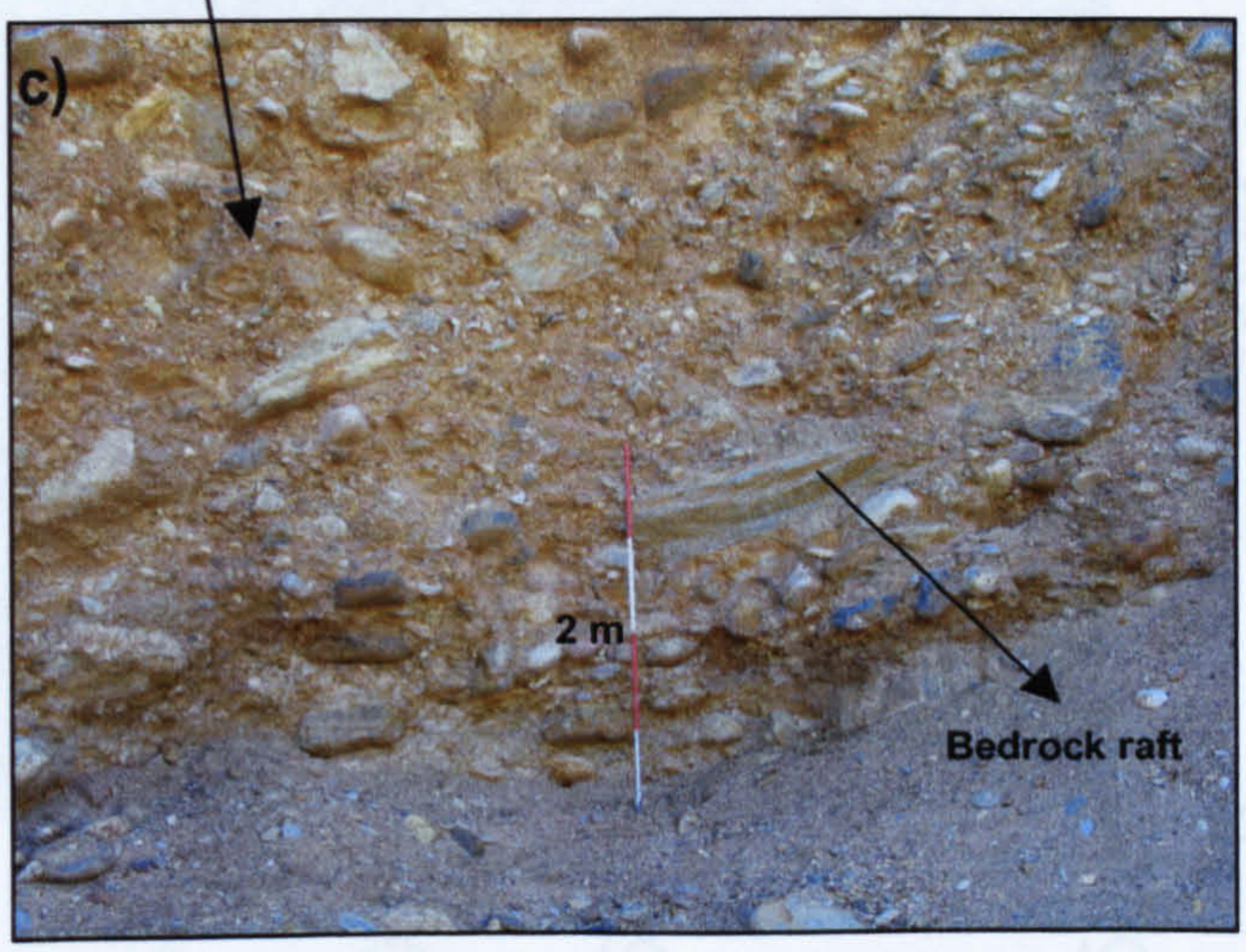

Figure 4.12 Scour filling of Pre-Proto 2 scours a) Xarries North, where Meso gravel overlies scour filled by Pre-Proto 2 gravel b) Lorelei East Pre-Proto c) Close-up of Lorelei East gravel face - note the large bedrock rafts.

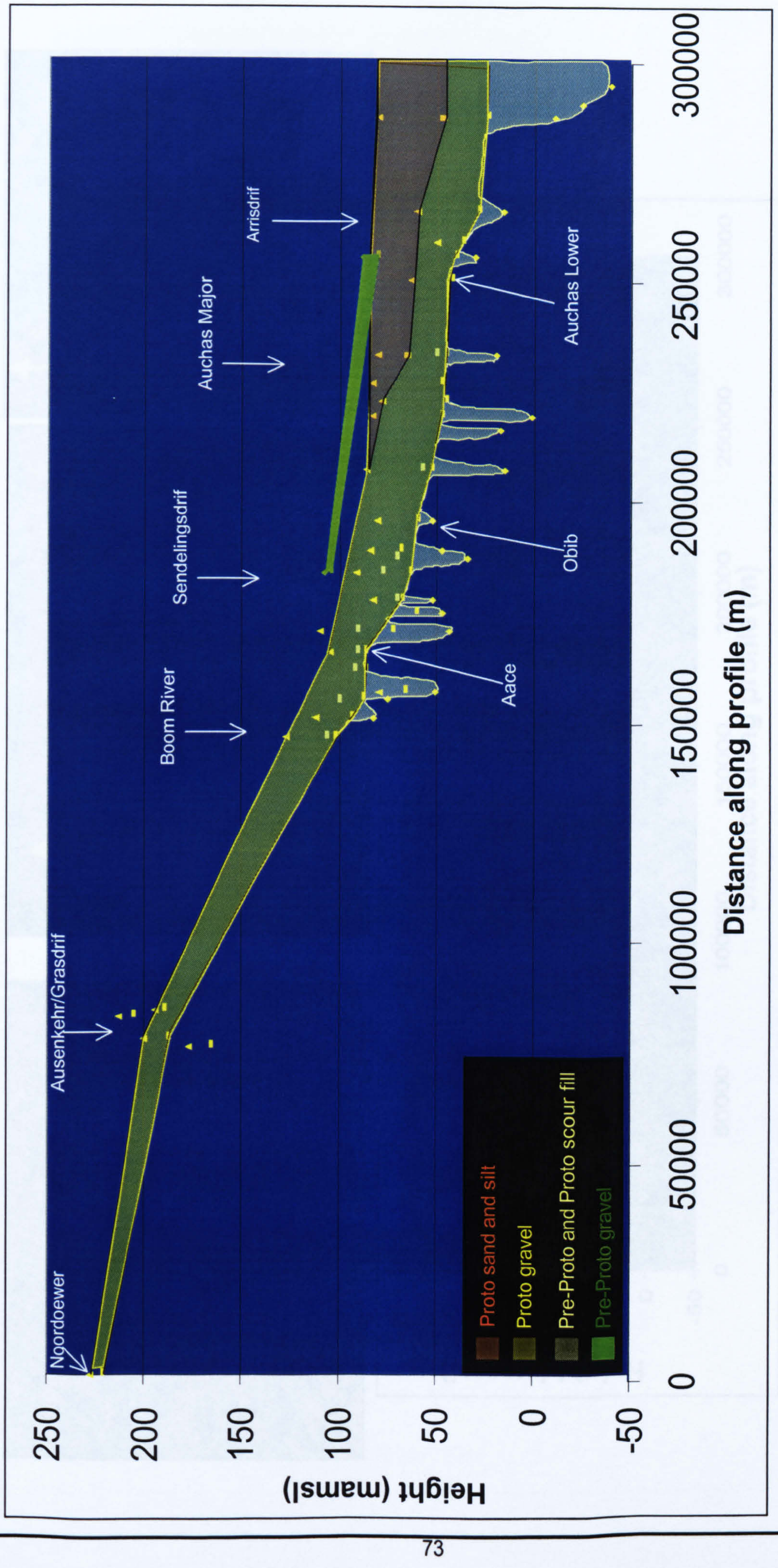

Figure 4.13 Pre-Proto and Proto longitudinal profiles from Noordoewer to the mouth.

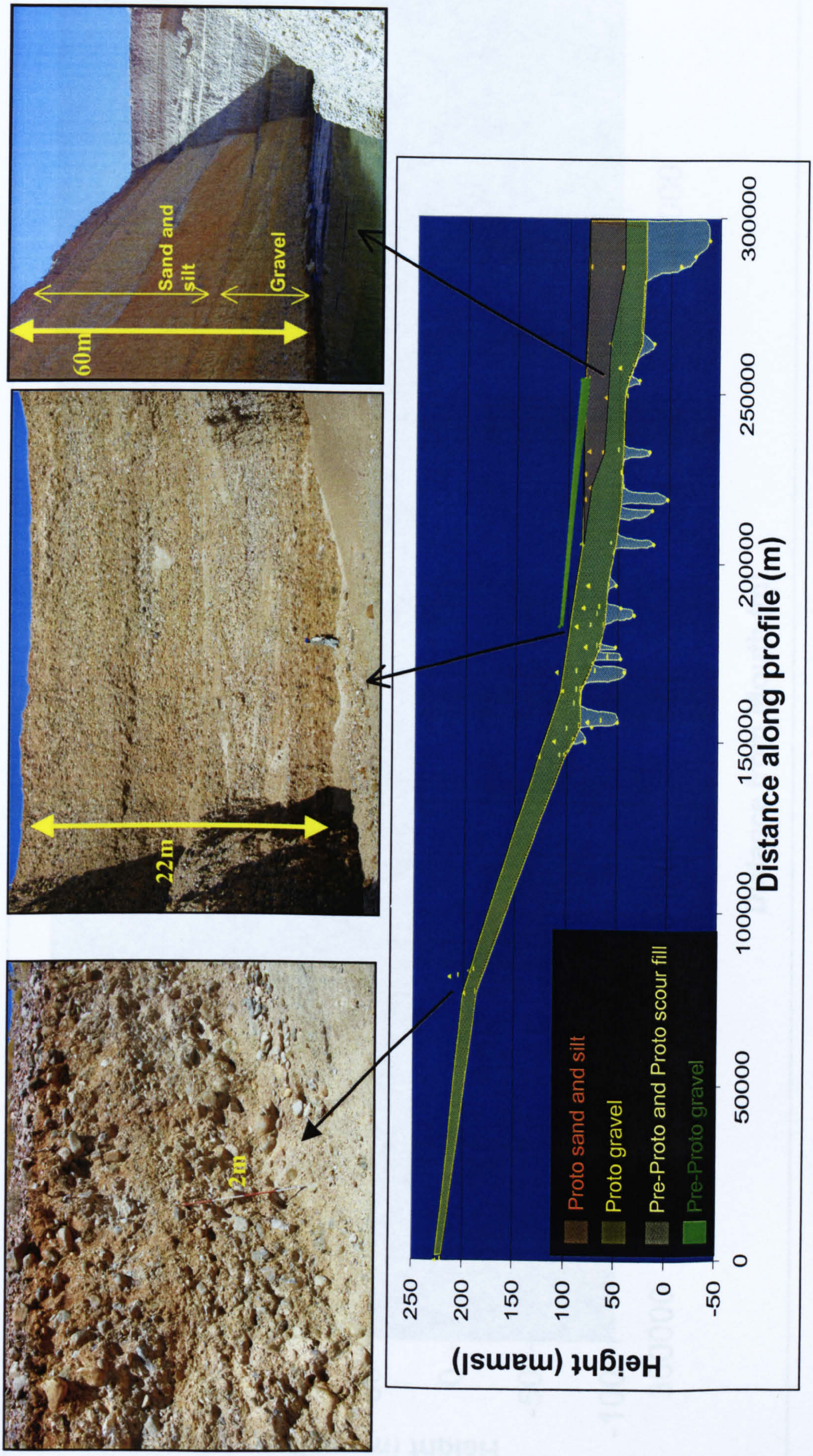

Figure 4.14 Pre-Proto and Proto longitudinal profiles from Noordoewer to the mouth showing sections through some deposits along the profile

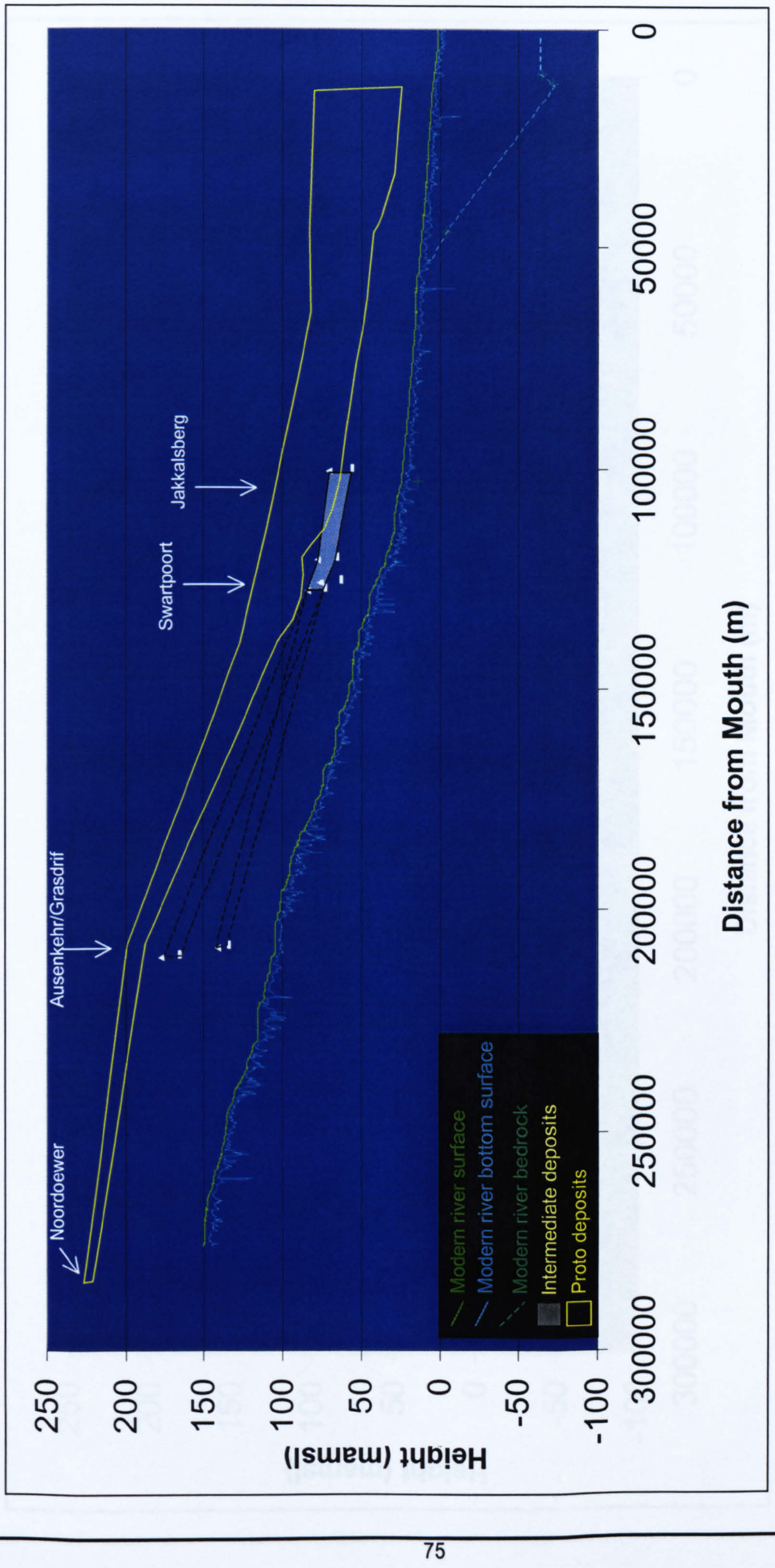

Figure 4.15 Intermediate terrace longitudinal profile. Note the restricted longitudinal occurrence of this group of terraces.

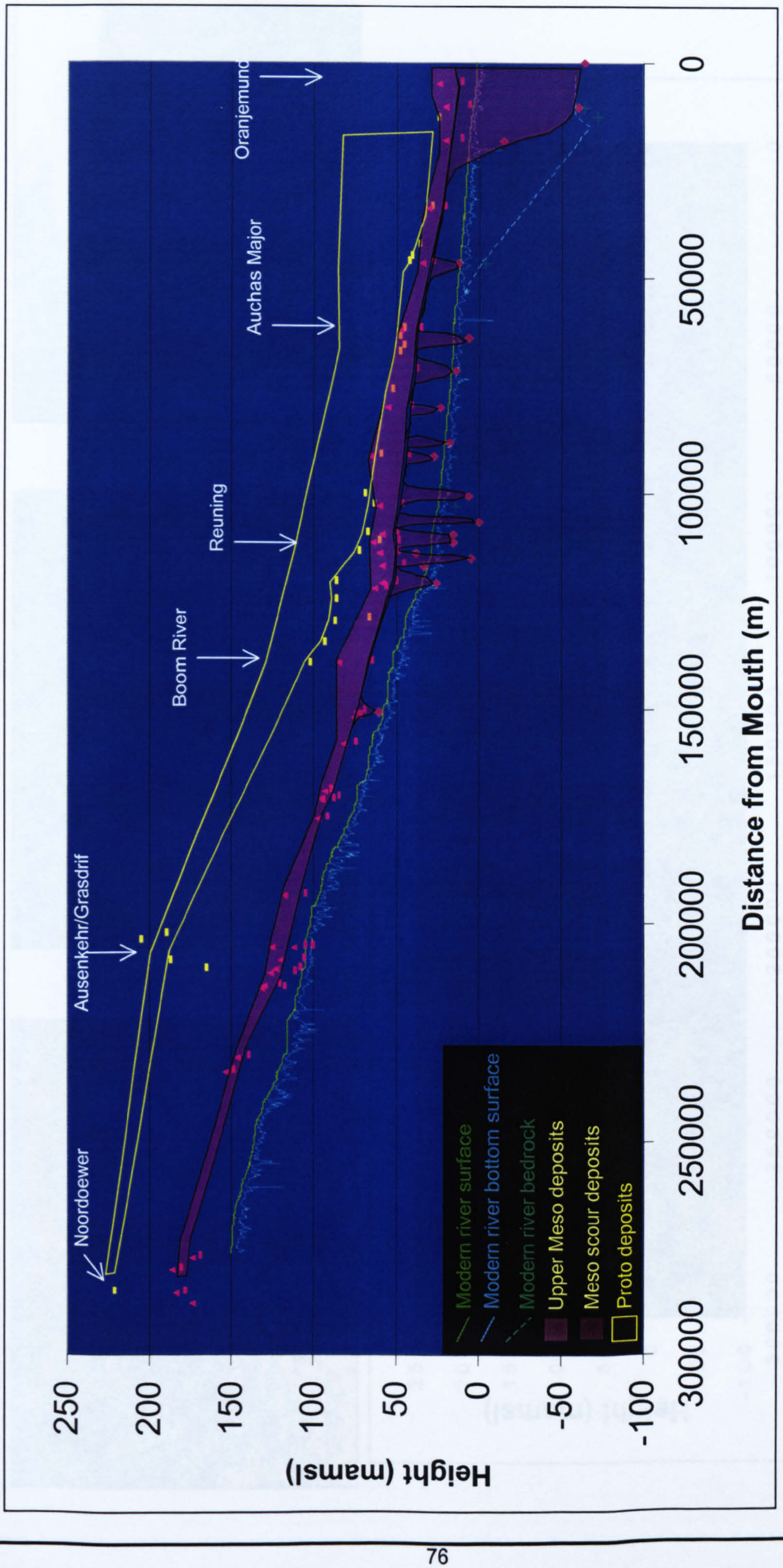

Figure 4.16 Upper Meso terrace longitudinal profile from Noordoewer to the river mouth.

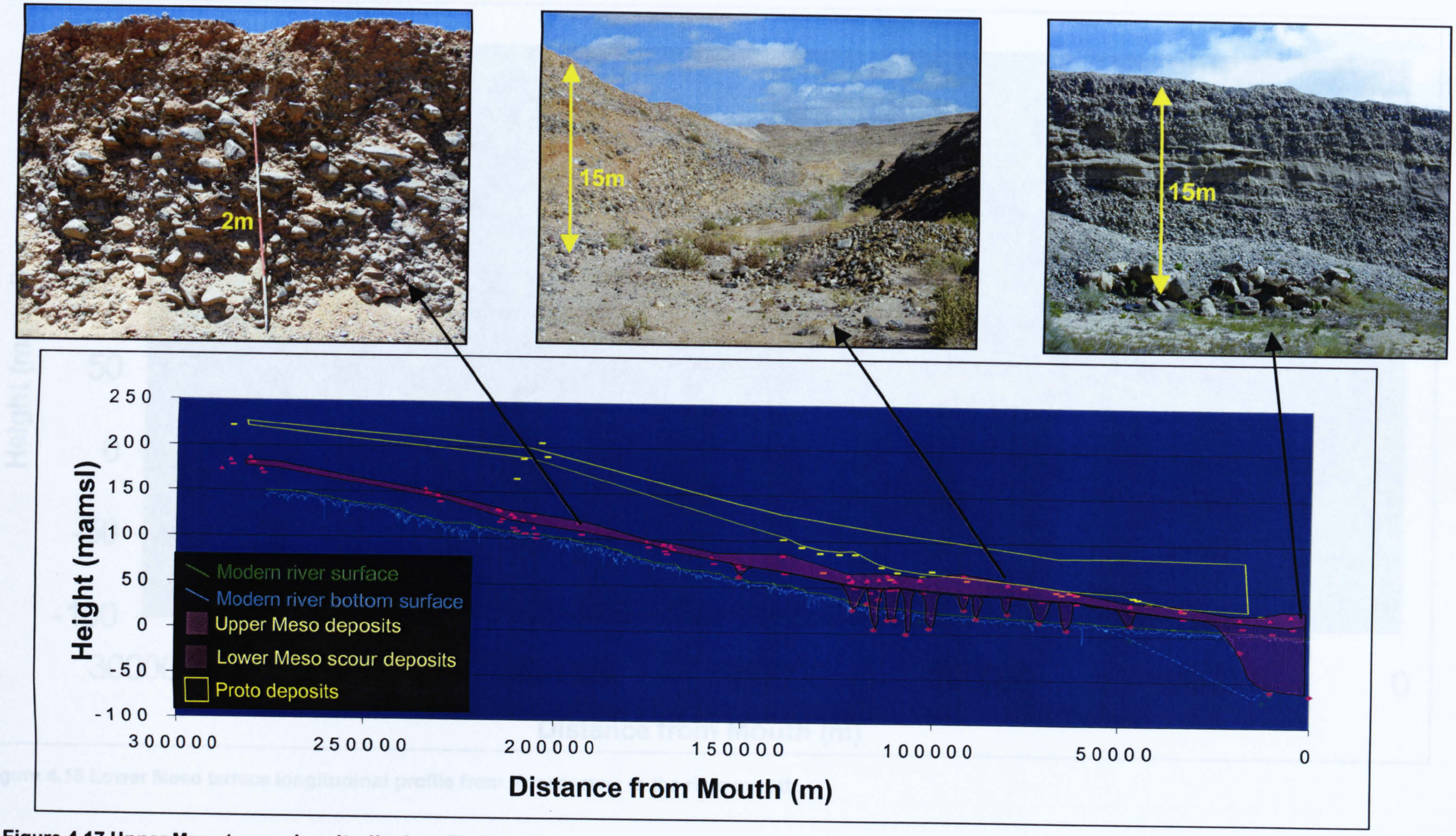

Figure 4.17 Upper Meso terrace longitudinal profile from Noordoewer to the river mouth showing sections through some deposits along the profile.

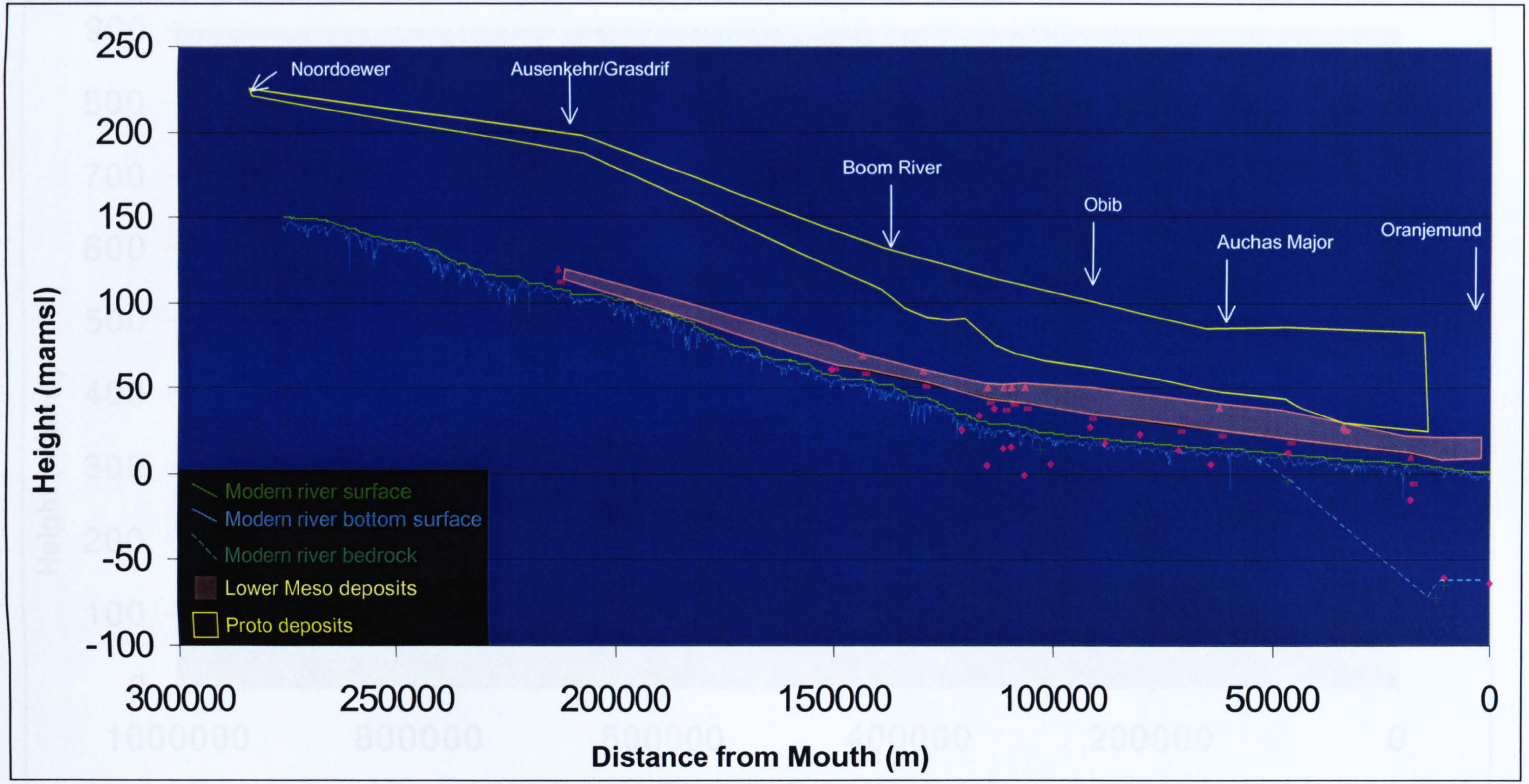

Figure 4.18 Lower Meso terrace longitudinal profile from Noordoewer to the river mouth.

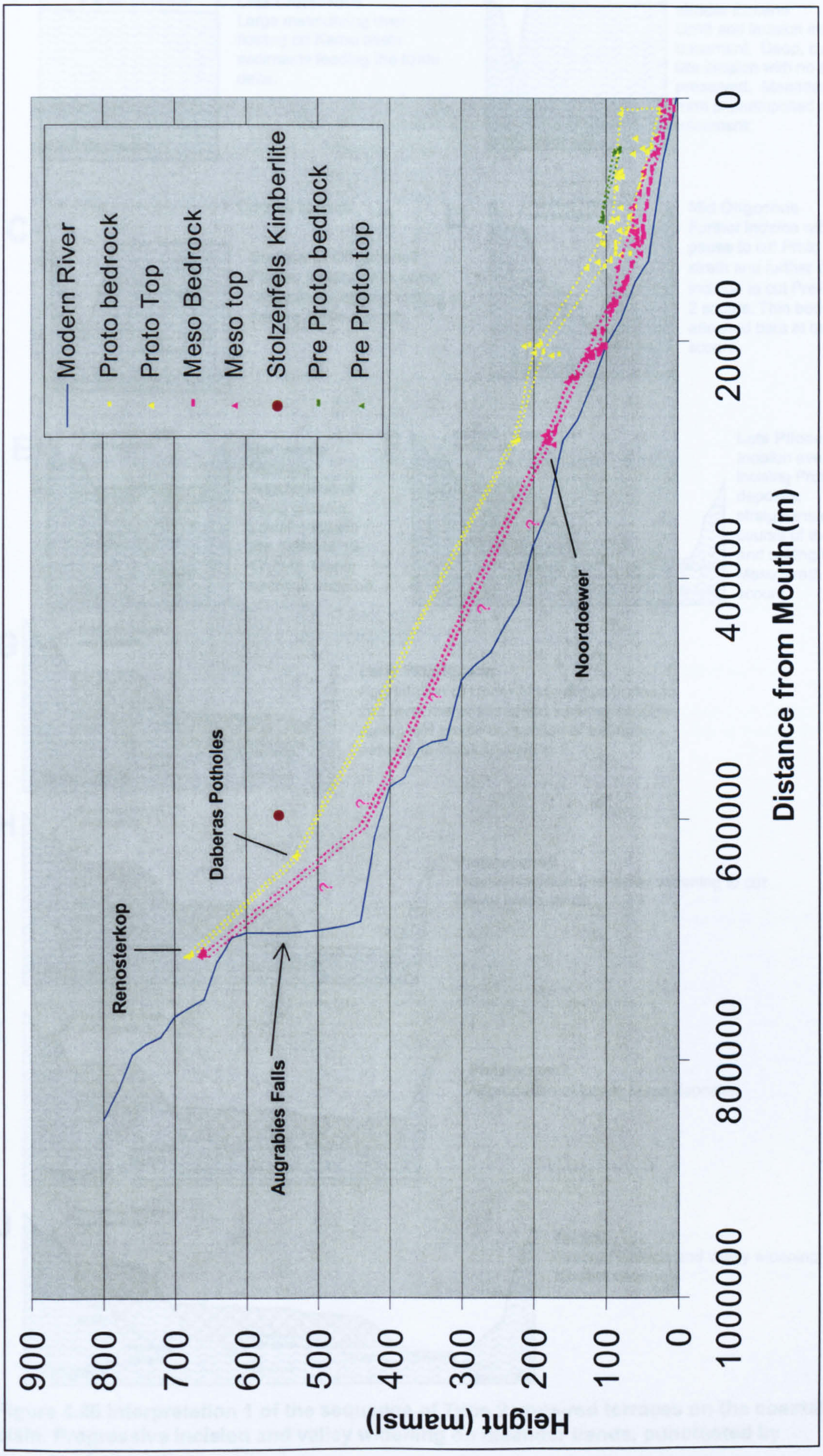

Figure 4.19 Longitudinal profiles of the terraces from Renosterkop (near Augrabies Falls) to the river mouth.

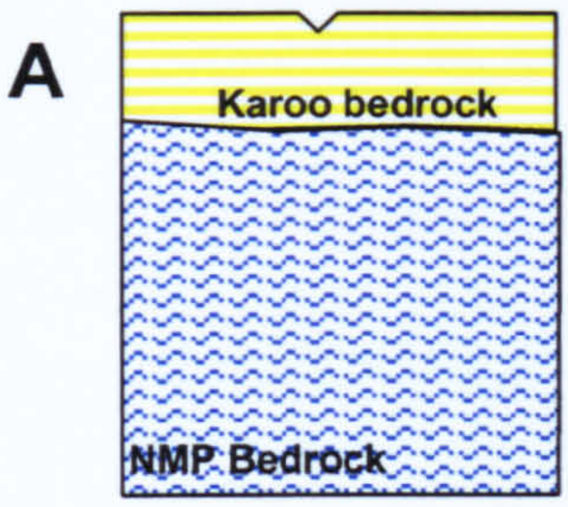

Late Cretaceous
Large meandering river flowing on Karoo basin sediments feeding the Kudu delta.

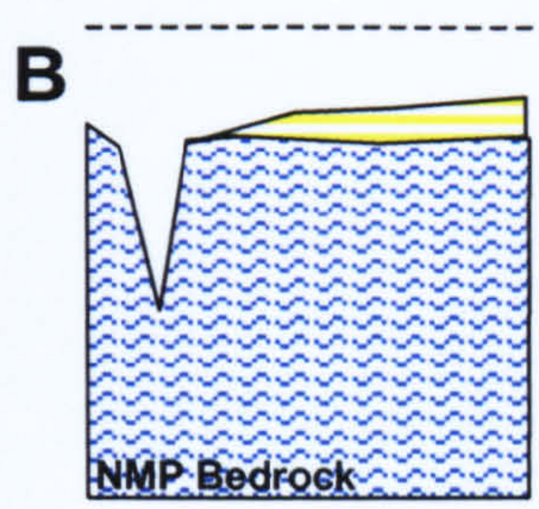

Middle Eocene
Uplift and incision into NMP basement. Deep, canyon-like incision with no straths preserved. Meandering form superimposed onto basement.

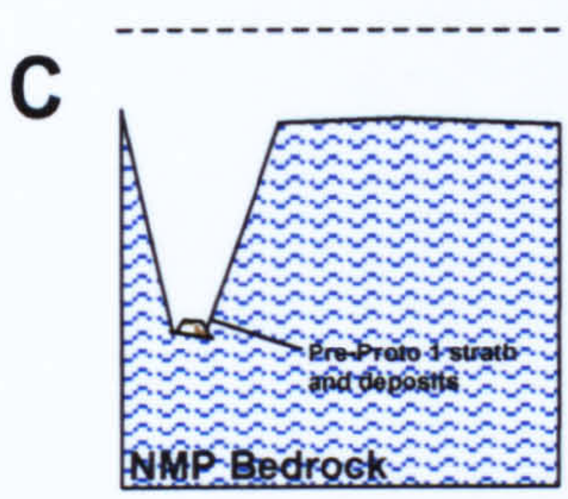

Eocene to Oligocene?
Further incision with some valley widening and cutting of the Pre-Proto 1 strath.

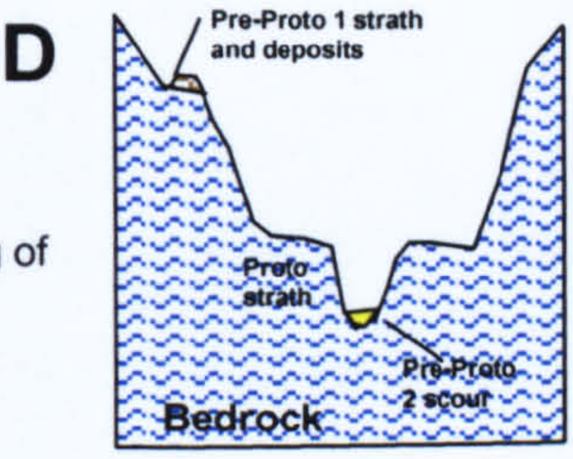

Mid Oligocene
Further incision with pause to cut Proto strath and further deep incision to cut Pre-Proto 2 scours. Thin bedrock-attached bars at base of scours.

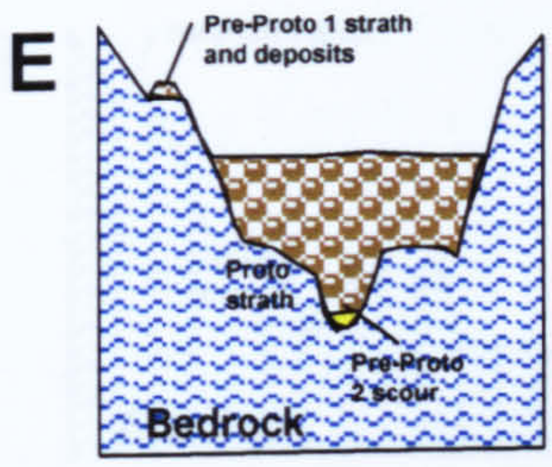

Early-Late Miocene
Aggradation of Proto gravels. Lower sections are dated to 19-17.5Ma. Upper sections undated.

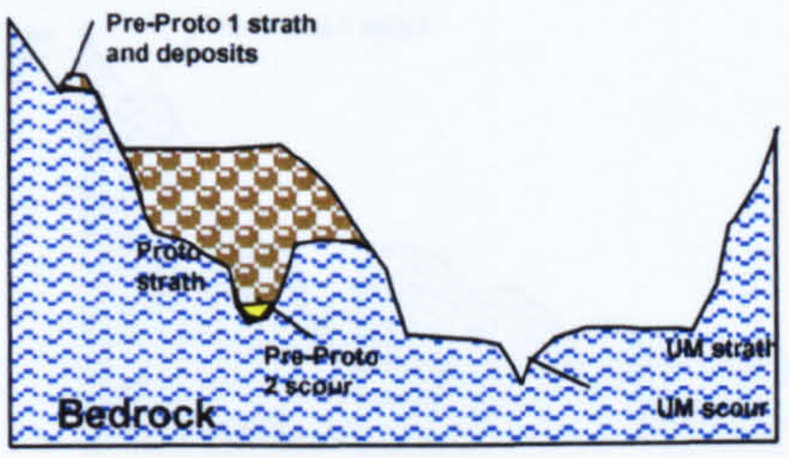

Late Pliocene
Incision event incising Proto deposits, straightening the course of the river and cutting Upper Meso strath and scours.

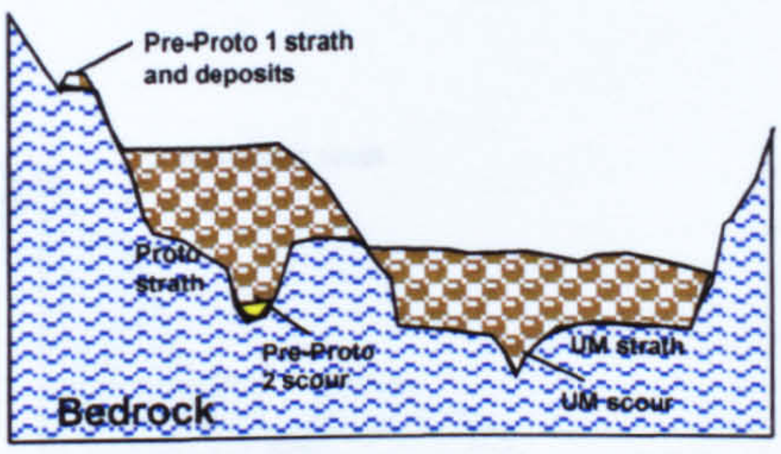

Early Pleistocene
Aggradation of Upper Meso deposits due to sea level rise or increased sediment supply during wet phase or reaction of tributary network to incision event in F.

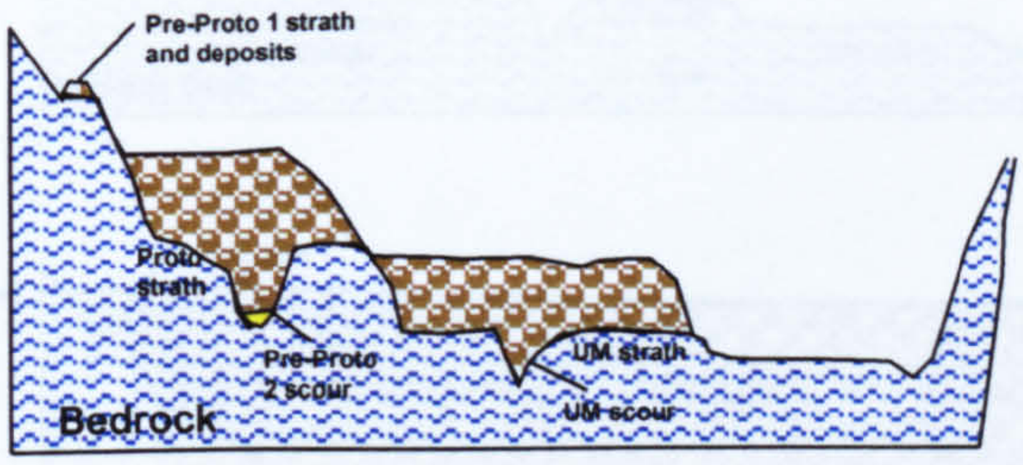

Pleistocene?
Gradual incision and valley widening to cut Lower Meso strath.

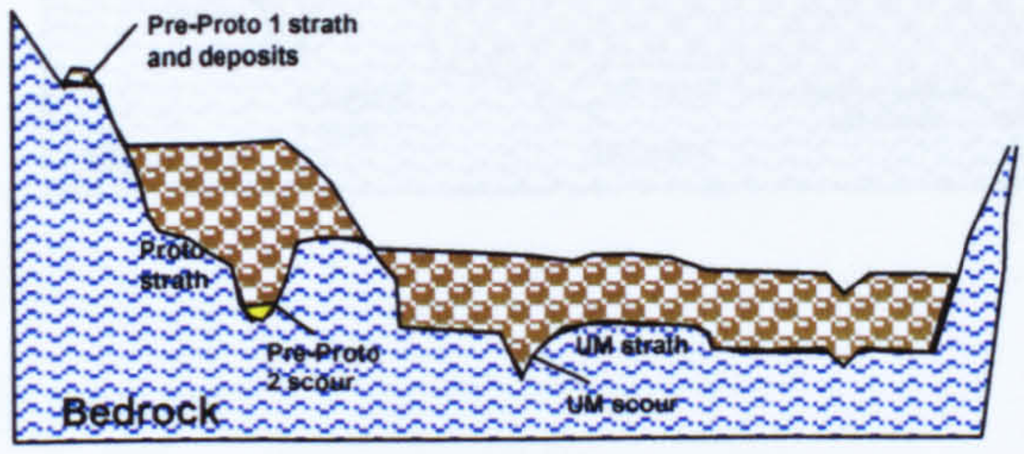

Pleistocene?
Aggradation of Lower Meso deposits.

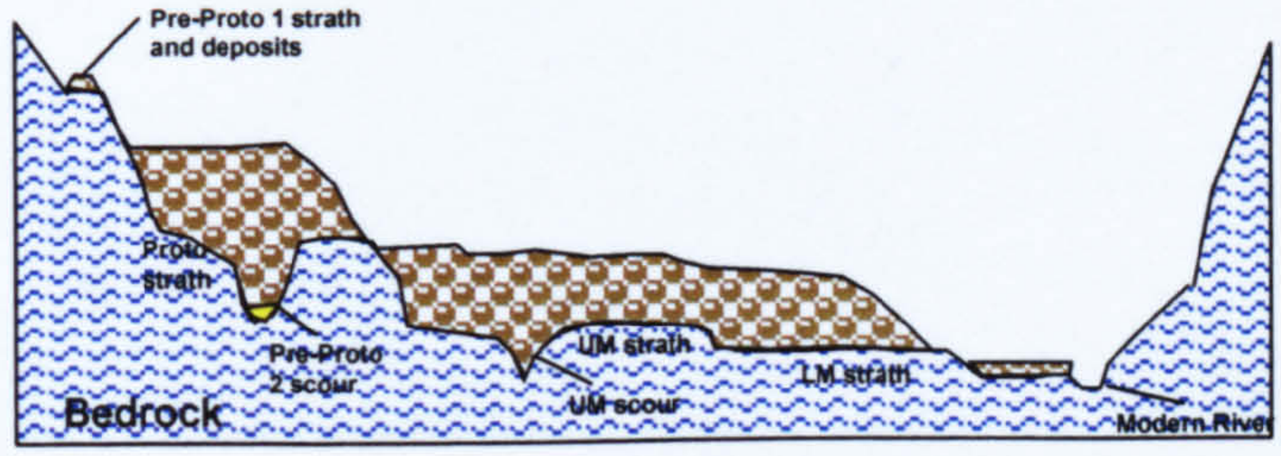

Recent
Gradual incision and valley widening to cut modern channel.

Figure 4.20 Interpretation 1 of the sequence of Type 2 unpaired terraces on the coastal plain. Progressive incision and valley widening on meander bends, punctuated by periods of alluviation.

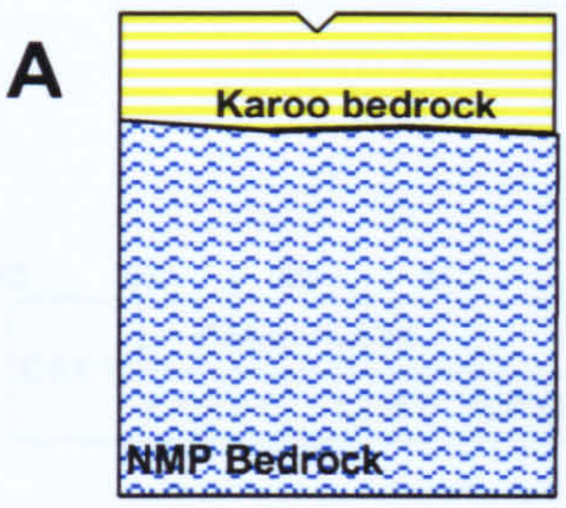

Late Cretaceous
Large meandering river flowing on Karoo basin sediments feeding the Kudu delta.

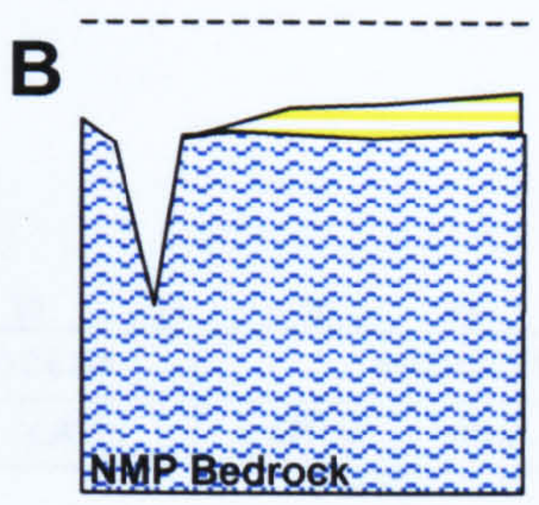

Middle Eocene
Uplift and incision into NMP basement. Deep, canyon-like incision with no straths preserved. Meandering form superimposed onto basement.

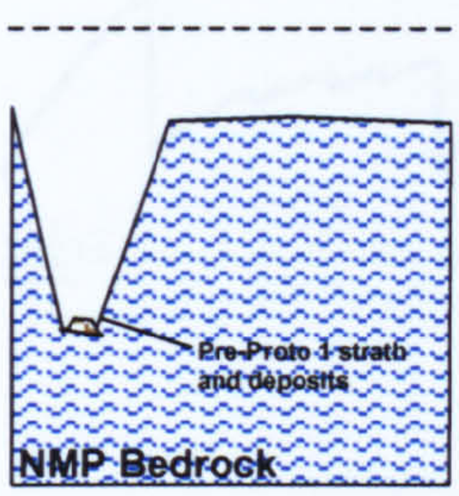

Eocene to Oligocene?
Further incision with some valley widening and cutting of the Pre-Proto 1 strath.

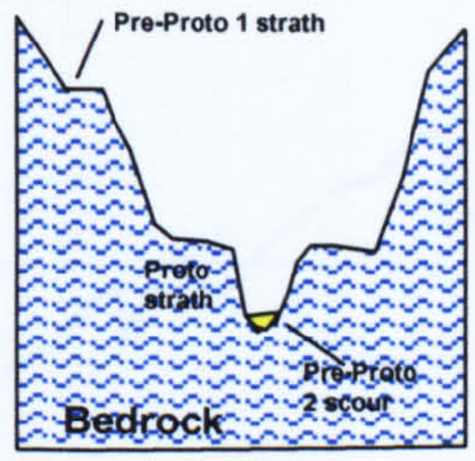

Mid Oligocene
Further incision with pause to cut Proto strath and further deep incision to cut Pre-Proto 2 scours. Thin bedrock-attached bars at base of scours.

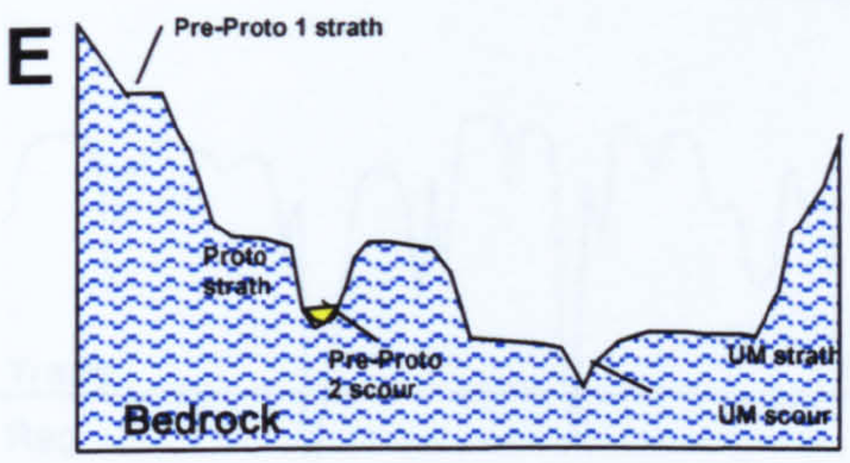

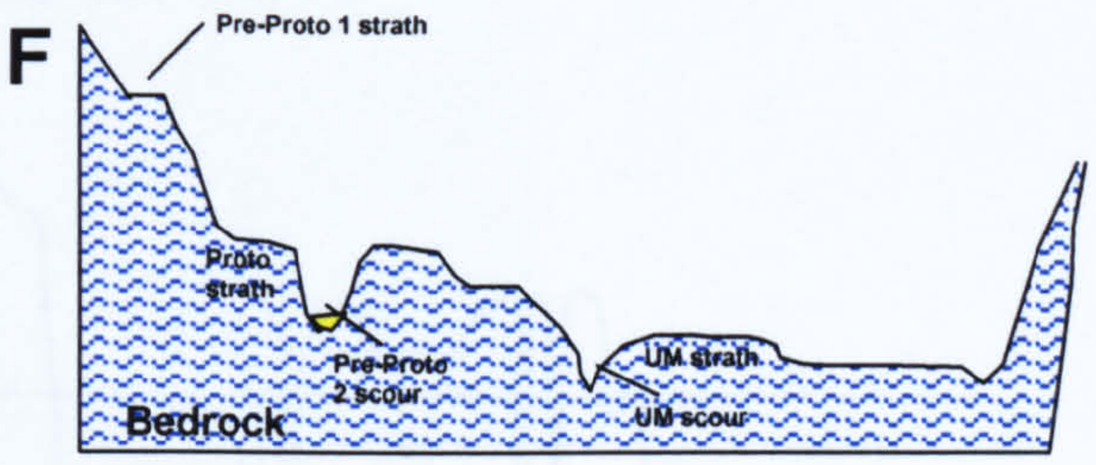

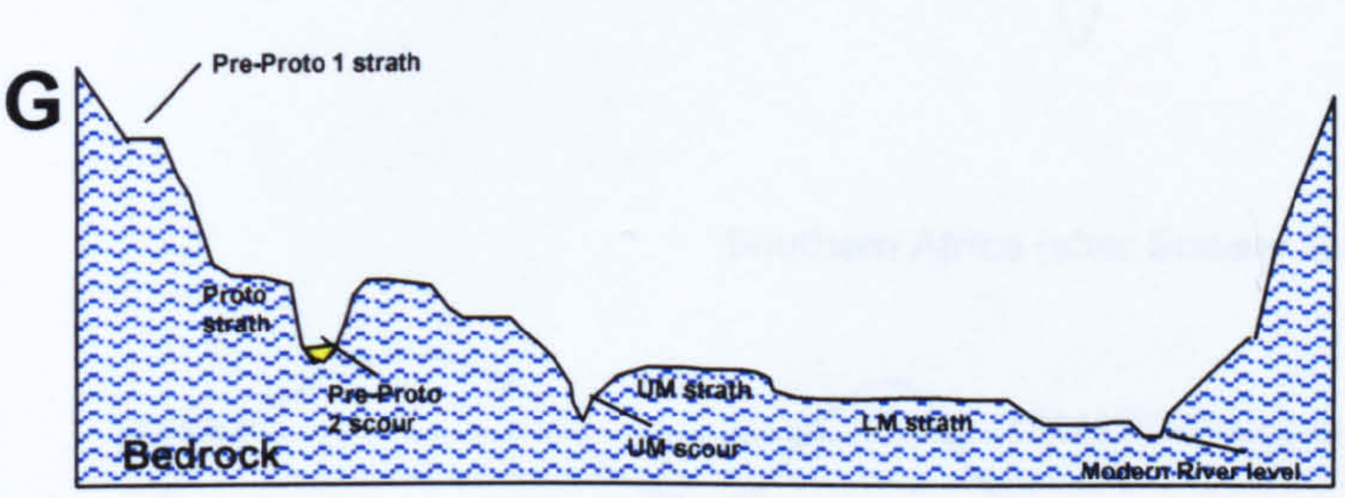

D-G Mid Oligocene to Early Miocene
Progressive incision and pauses to cut straths down to present river level.

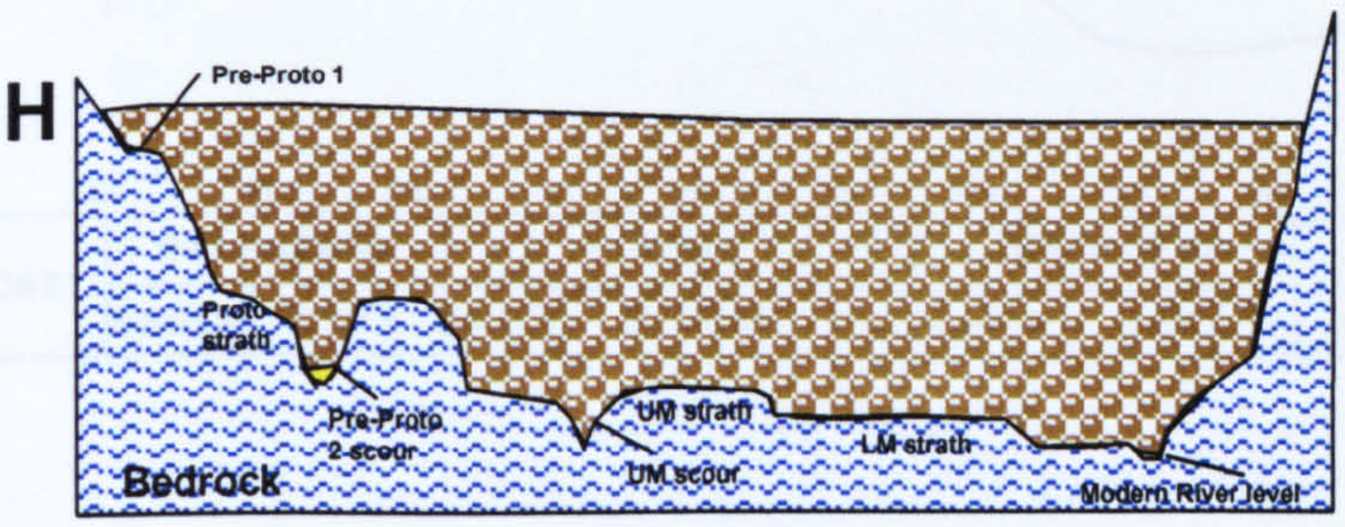

Early -Late Miocene
Major aggradational event filling entire valley.

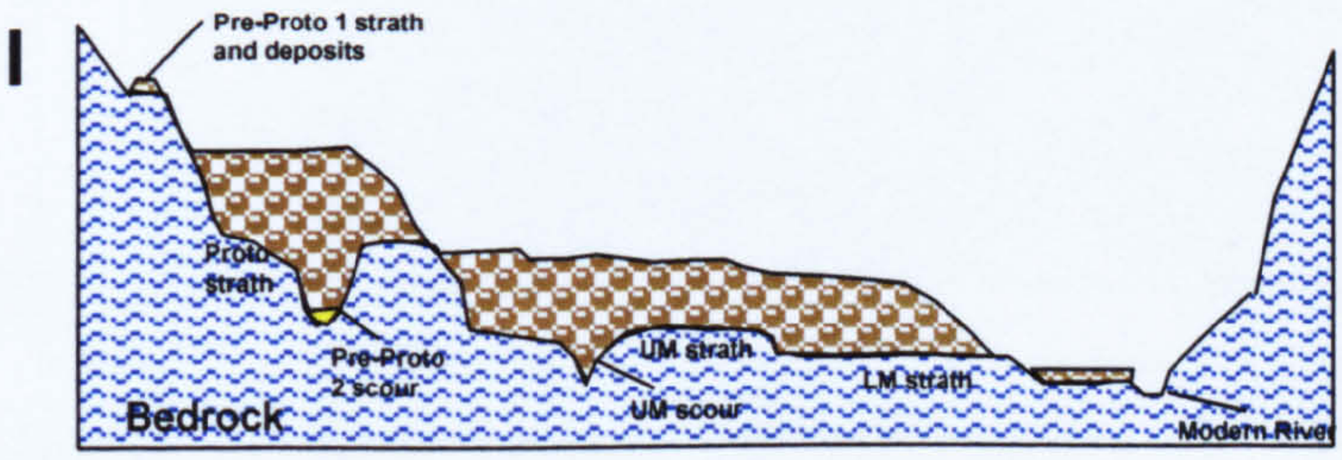

Late Miocene to Present
Gradual incision of valley fill to leave terraces. River re-enters old straths.

Figure 4.21 Interpretation 2 of the sequence of type 2 unpaired terraces on the coastal plain. Initial incision and valley widening, followed by long period of alluviation and gradual incision into valley fill.

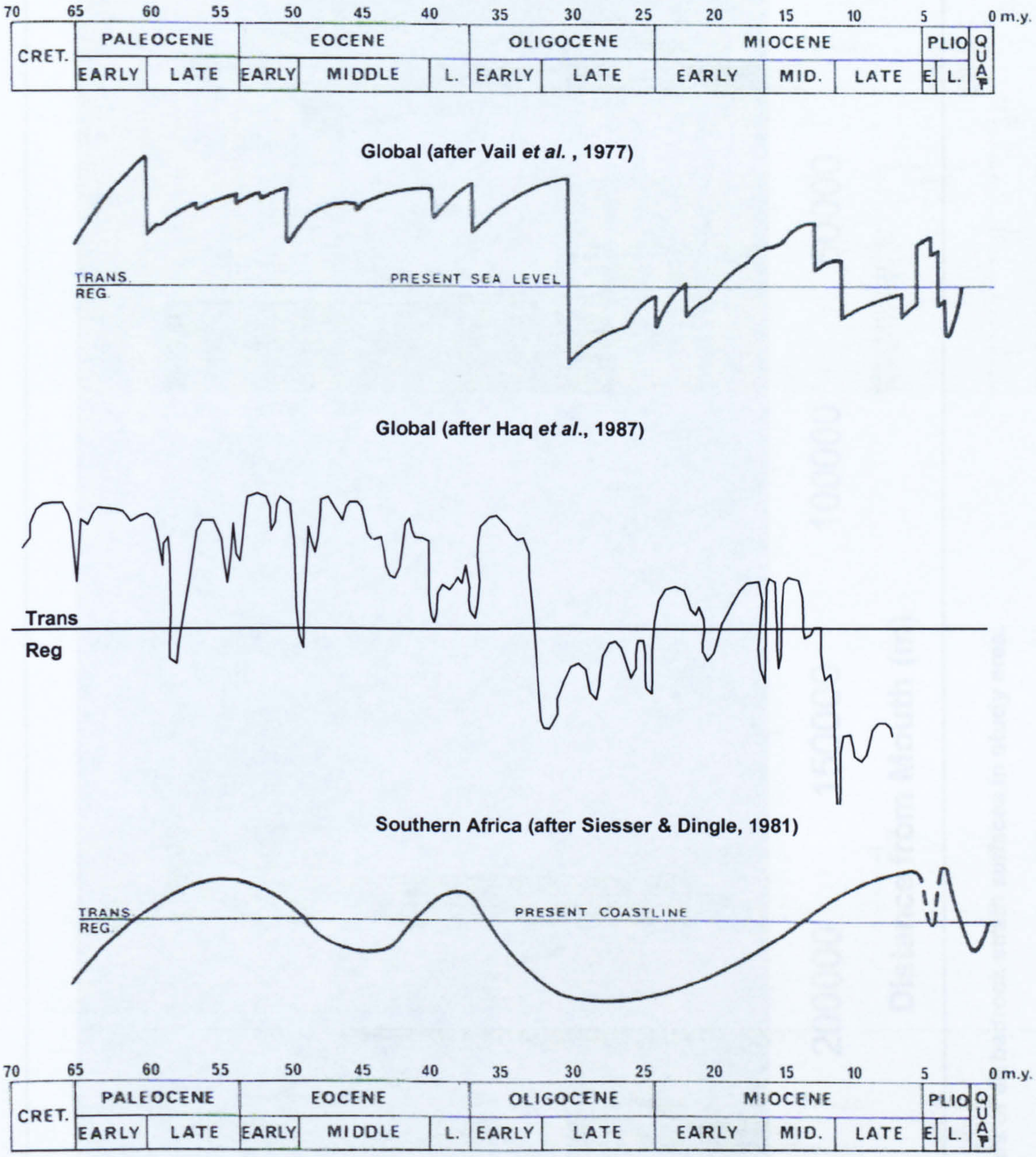

Figure 4.22 Cainozoic sea level curves (modified after Siesser & Dingle 1981).

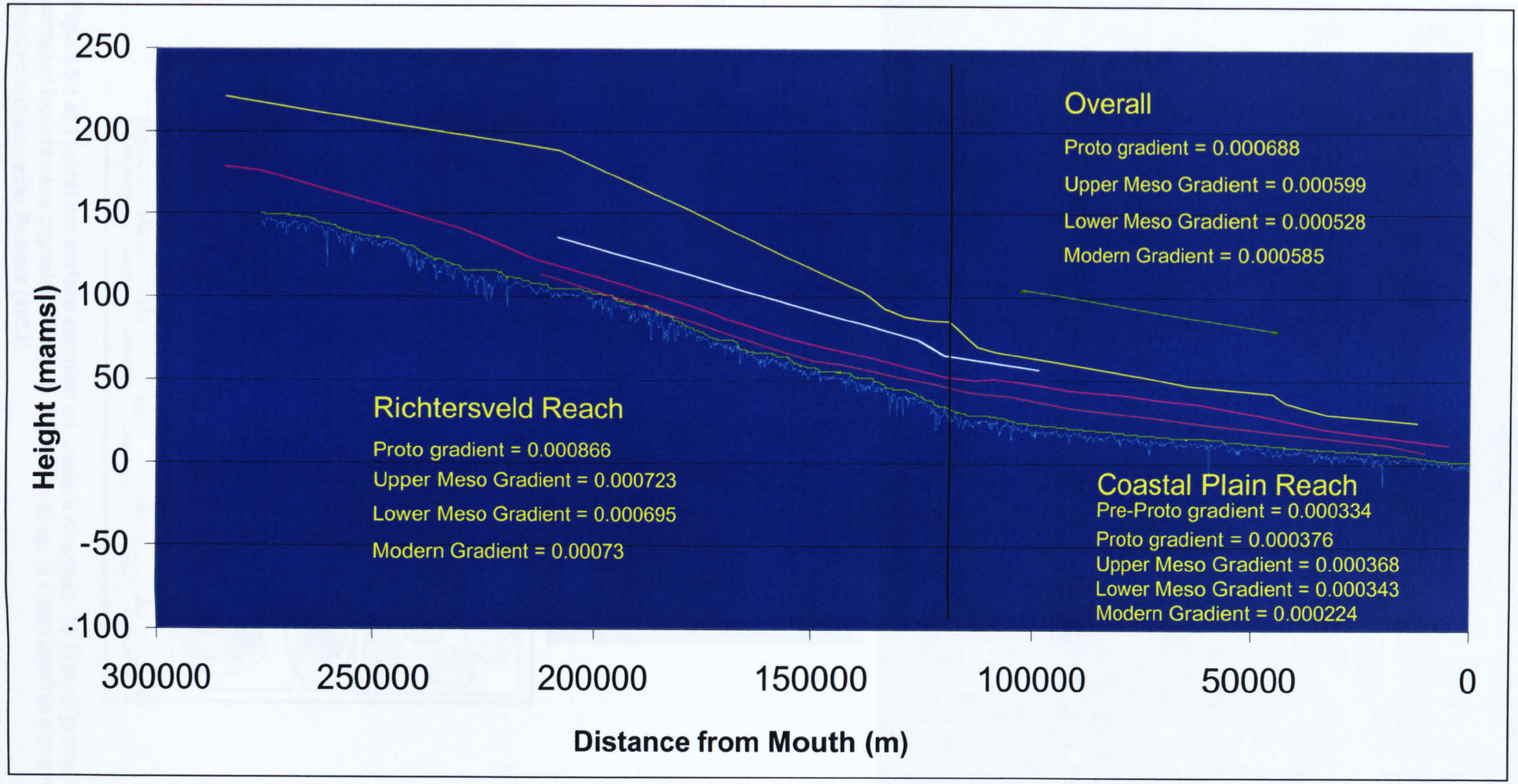

Figure 4.23 Longitudinal profiles and gradients of all bedrock strath surfaces in study area.

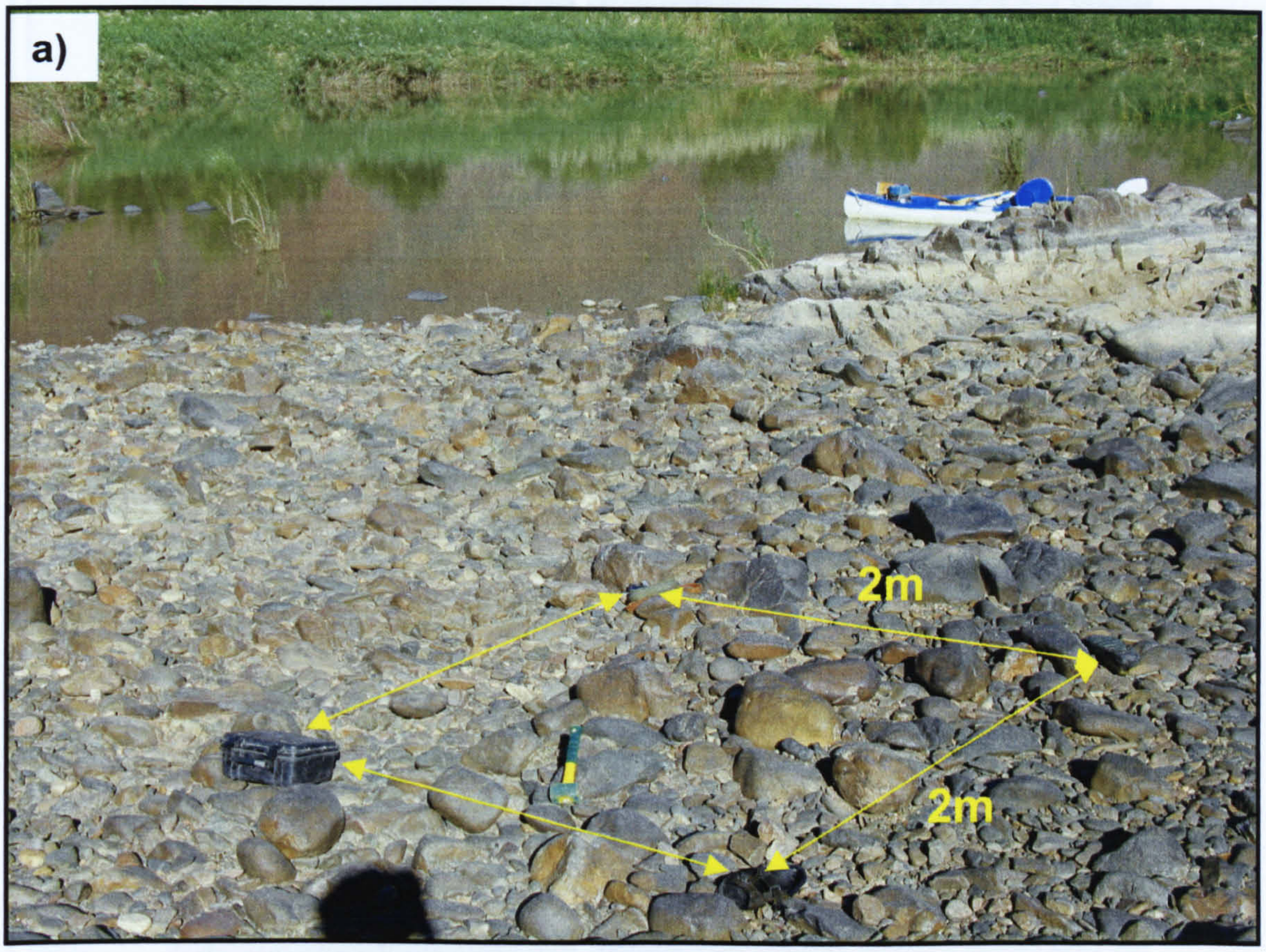

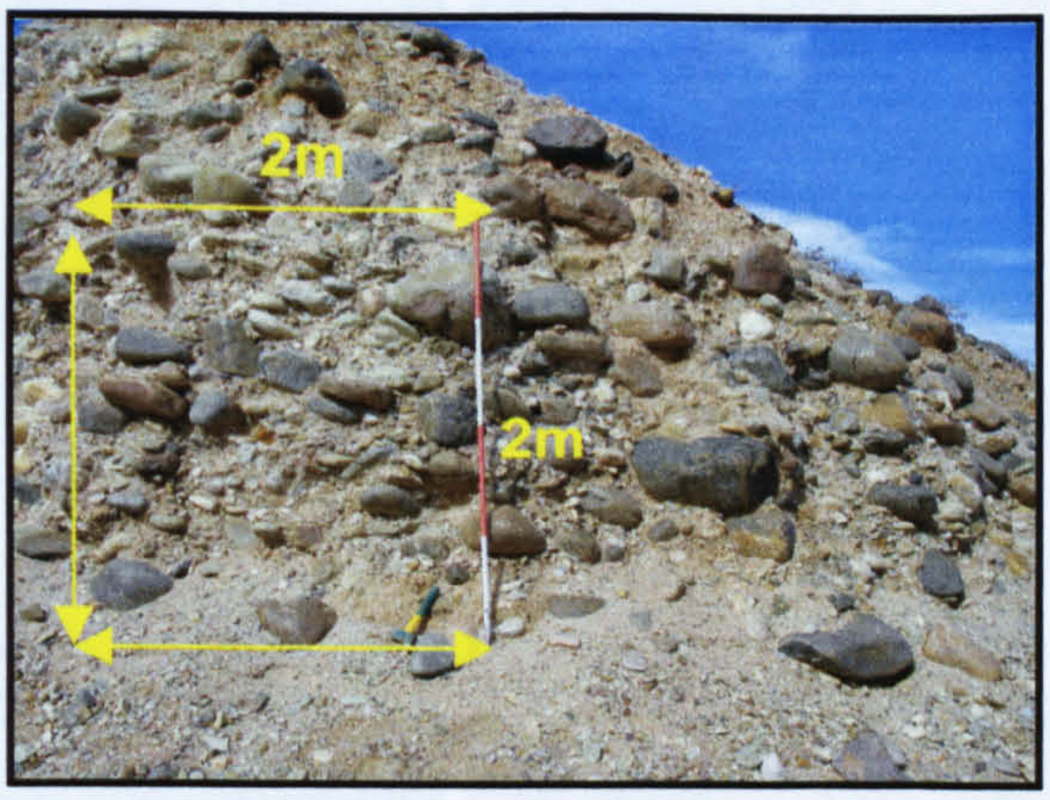

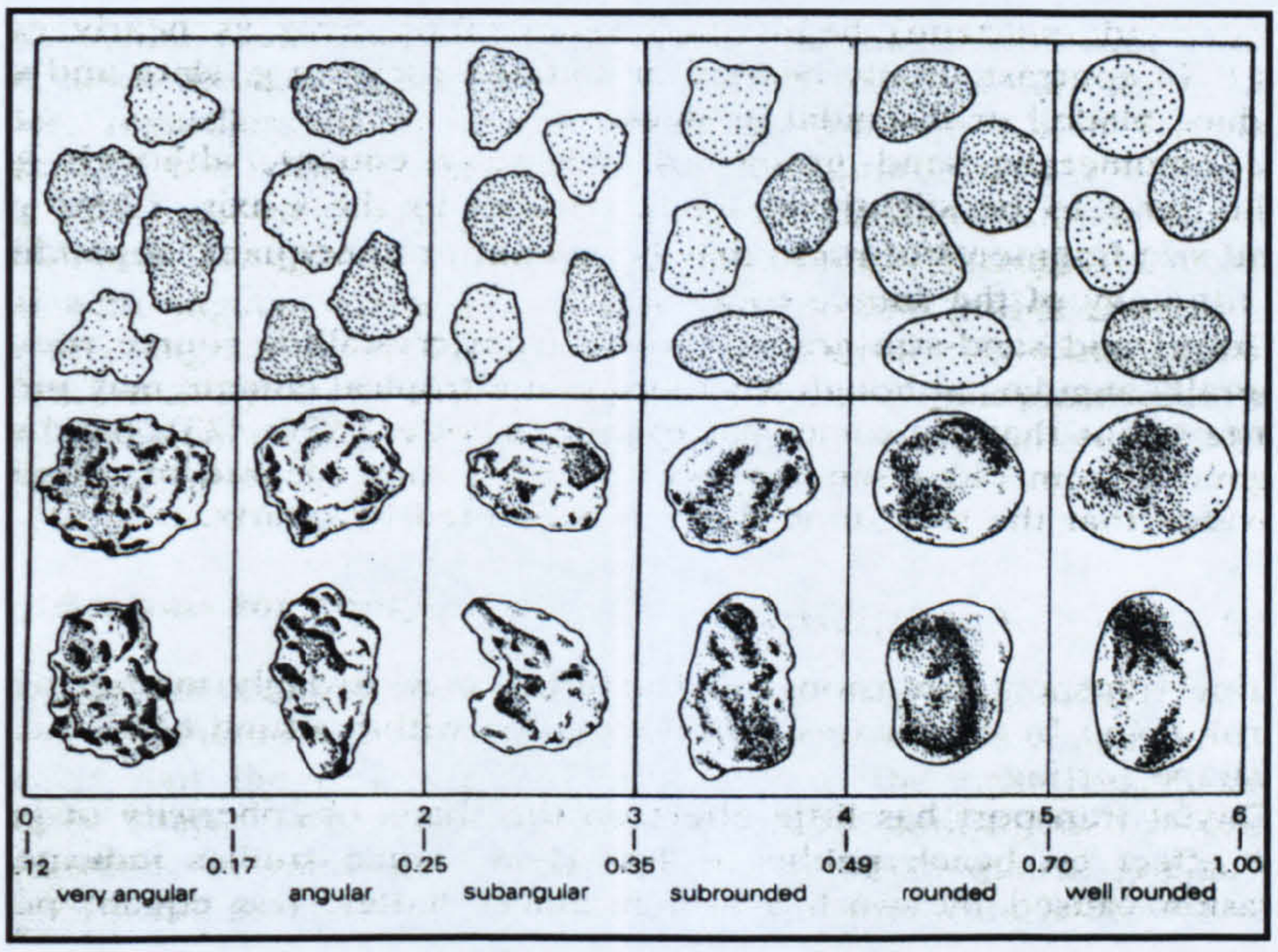

Figure 5.1 a) Typical bar surface sampled on modern riverbars. b) Typical gravel face sampled from terrace deposits. Ranging rod is 2 m long. c) Chart used to visually estimate clast roundness after Powers (1953).

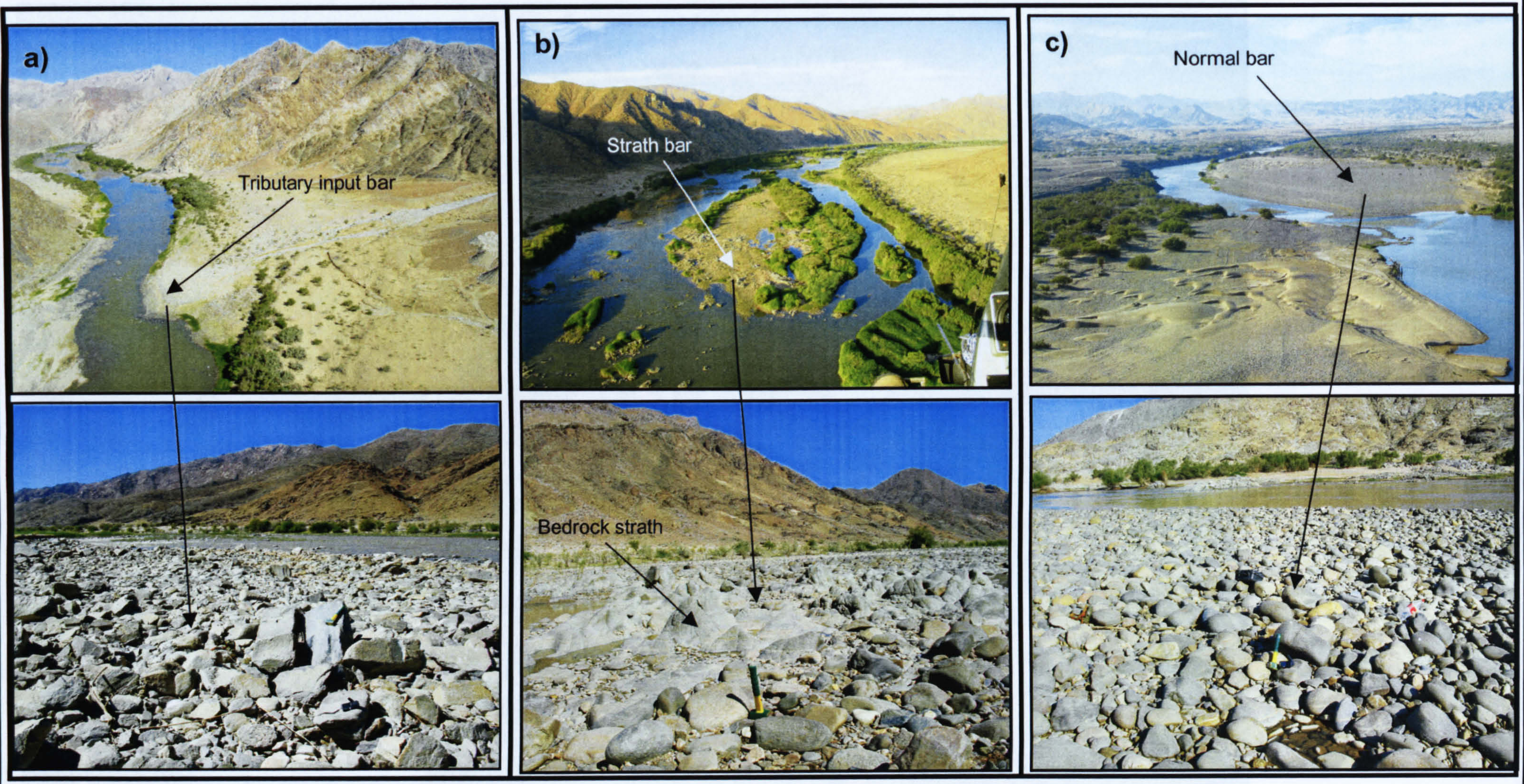

Figure 5.2 Bar categories a) Tributary input bar b) Strath bar c) Normal bar.

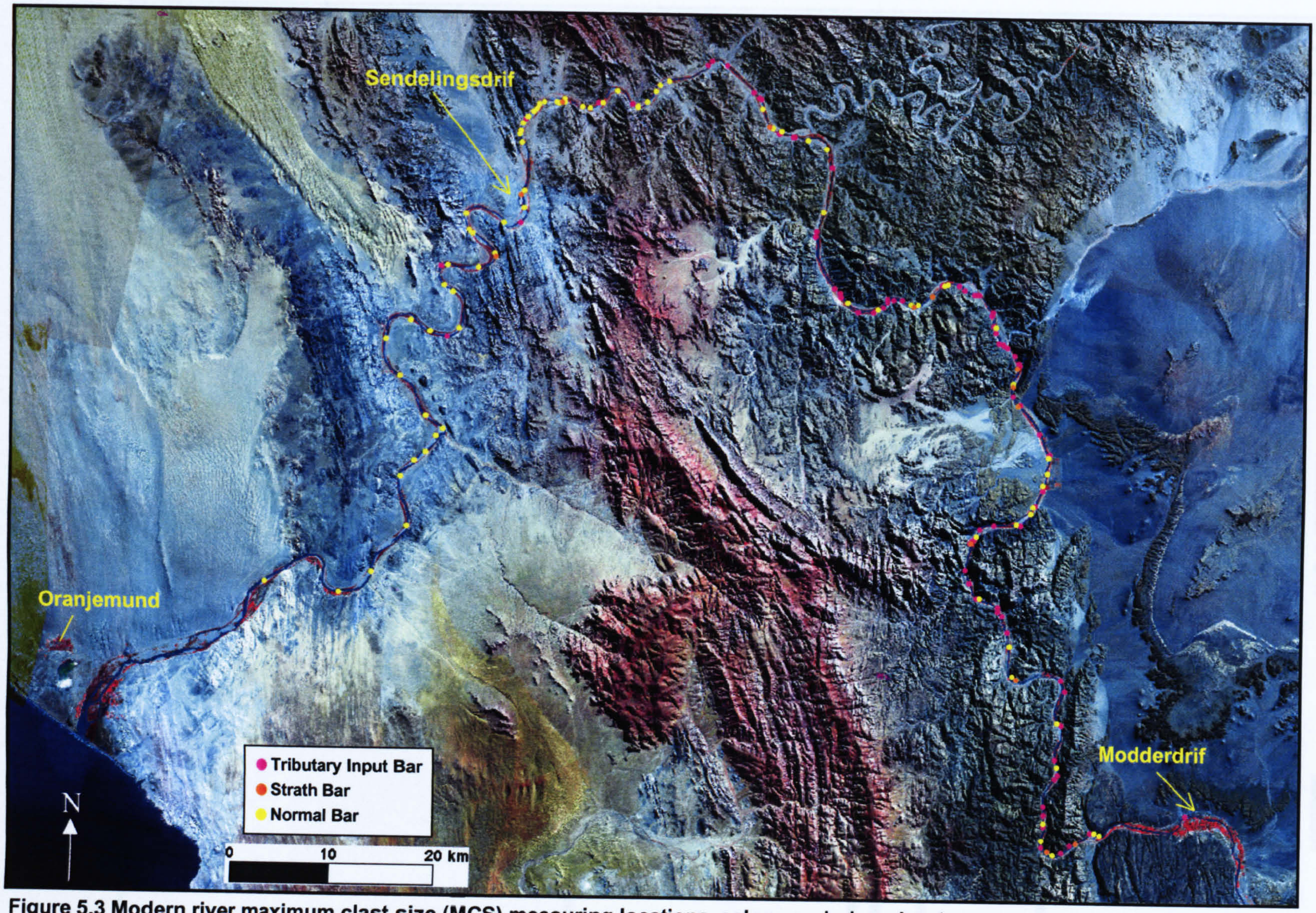

Figure 5.3 Modern river maximum clast size (MCS) measuring locations, colour-coded per bar type.

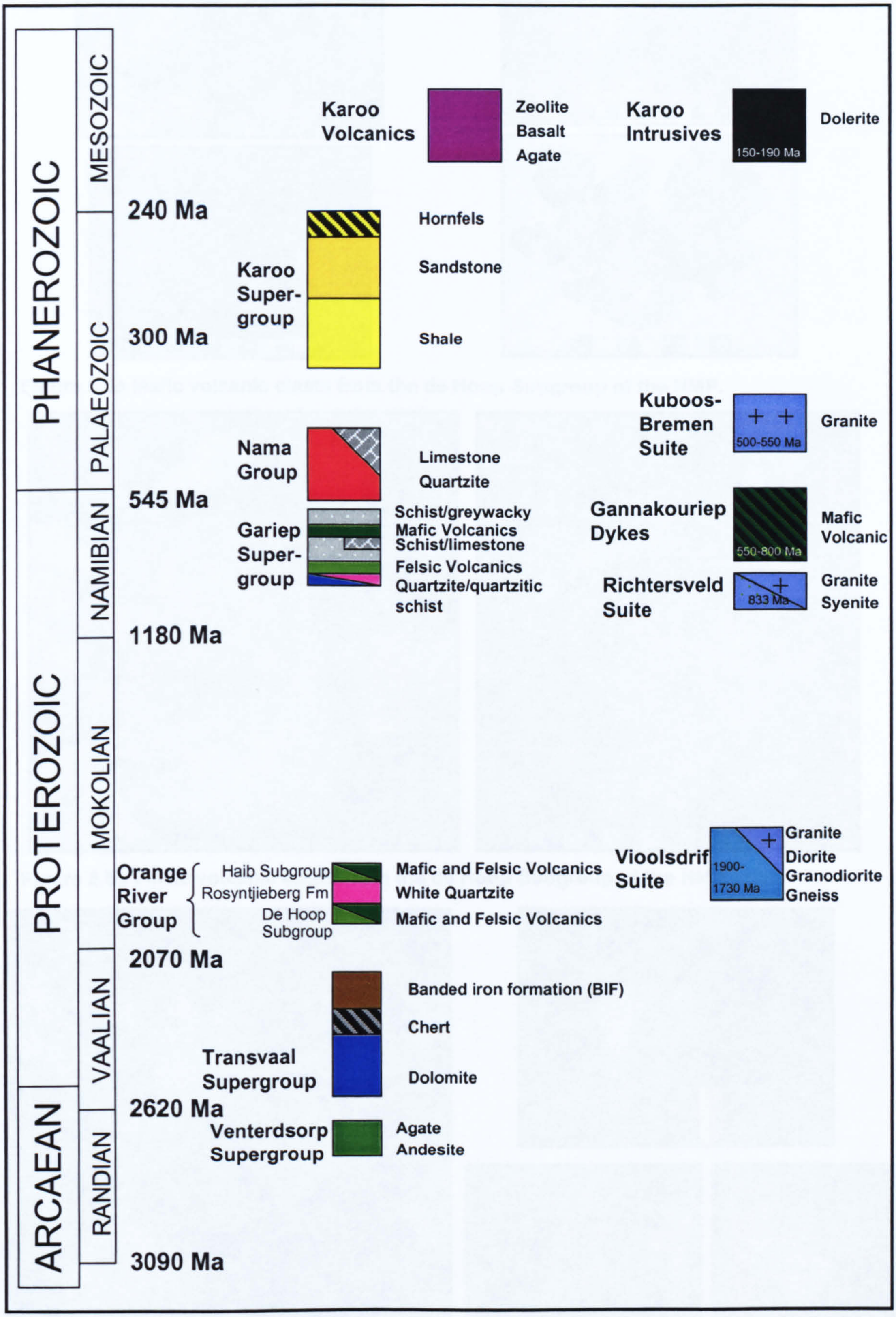

Figure 5.4 Simplified stratigraphic table illustrating clast types found in the Orange River deposits and clast provenance, adapted from (SACS, 1980).

Figure 5.5a Mafic volcanic clasts from the de Hoop Subgroup of the NMP.

Figure 5.5b Felsic volcanic clasts from the de Hoop Subgroup of the NMP.

Figure 5.5c Rosyntjieberg Formation quartzites from the Orange River Group of the NMP.

Figure 5.5d Namaqua metamorphic province "basement" clasts.

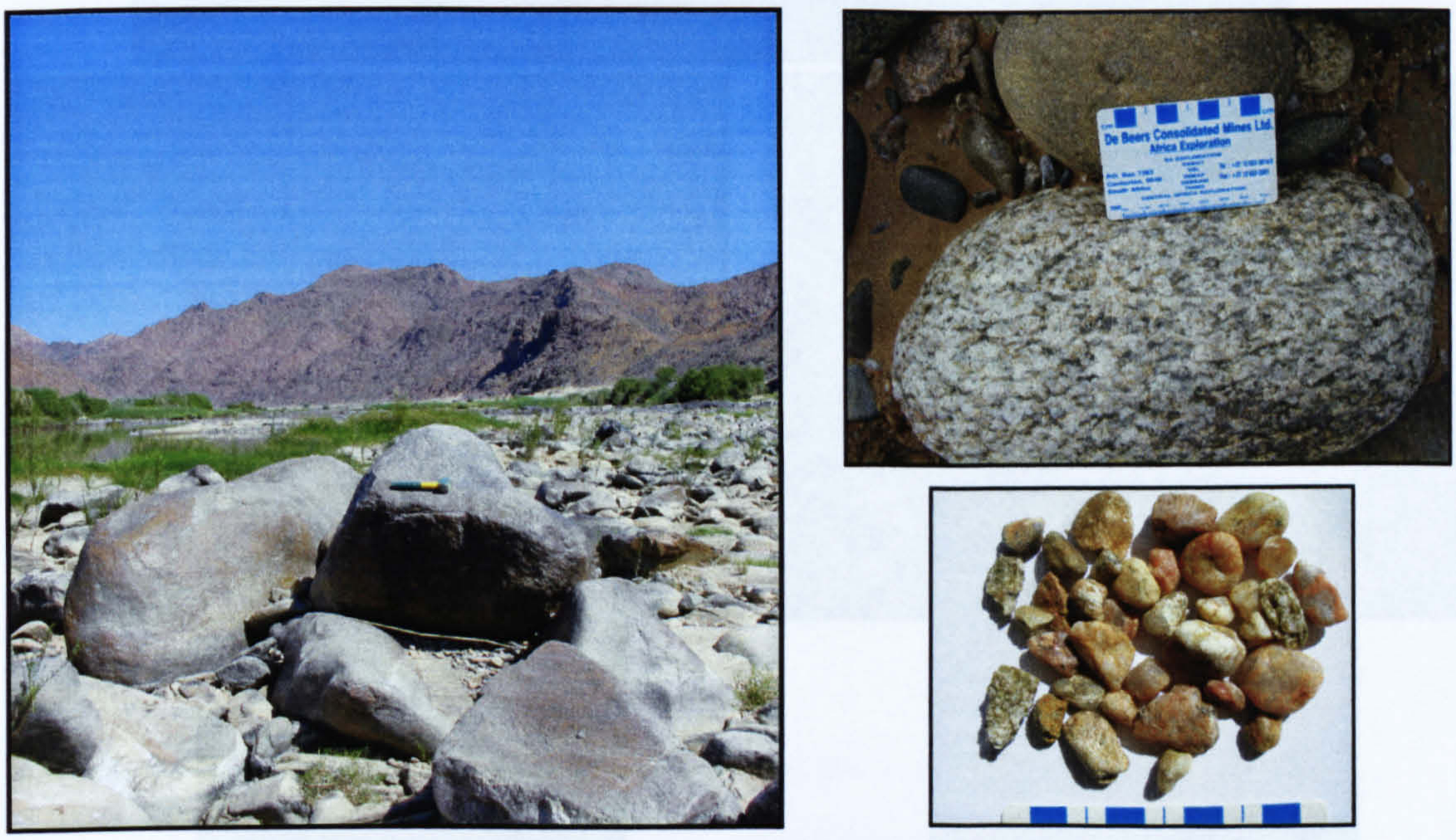

Figure 5.5e Various granite clasts from the Richtersveld igneous complex, Kuboos-Bremen Suite and NMP.

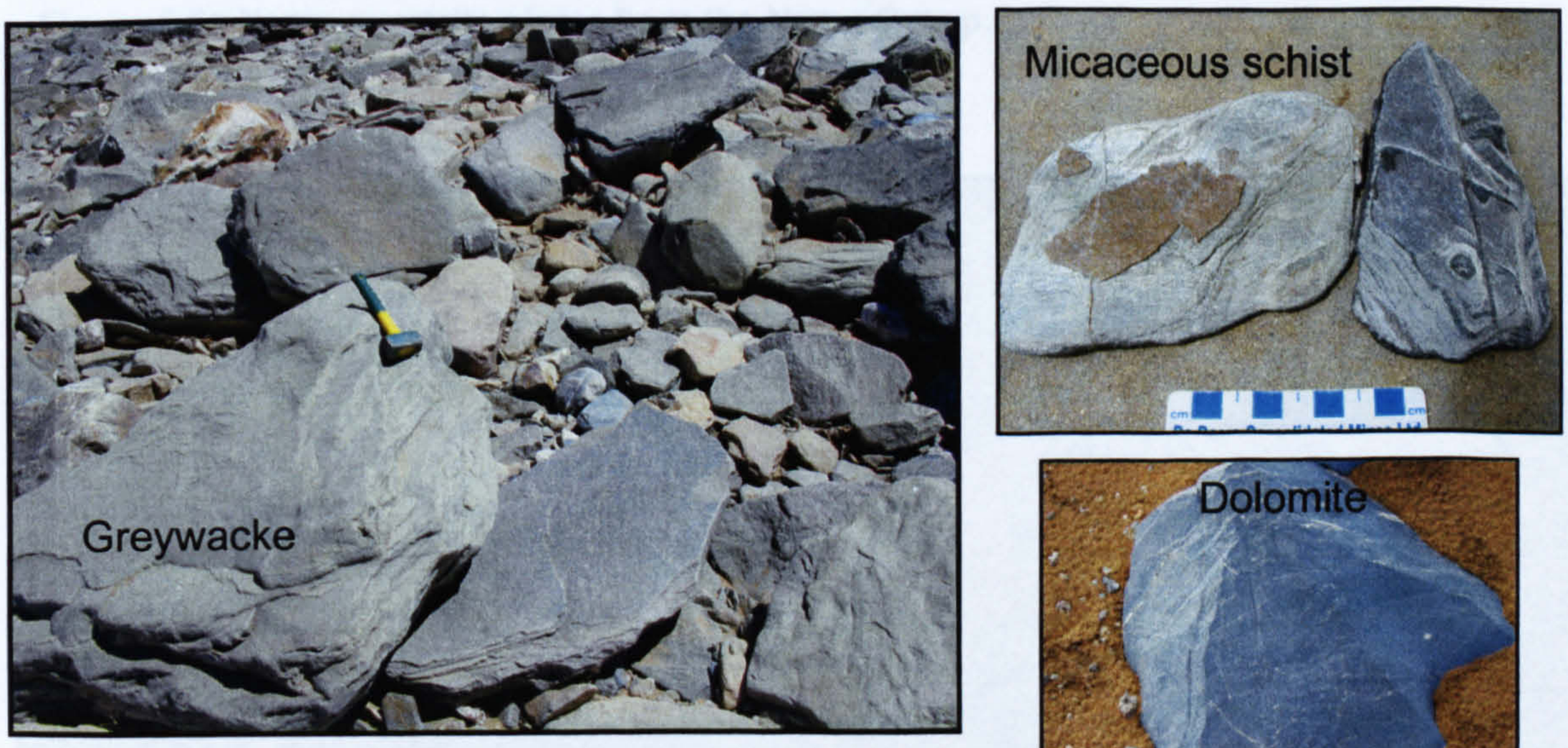

Figure 5.5f Metasedimentary clasts from the Gariep Supergroup.

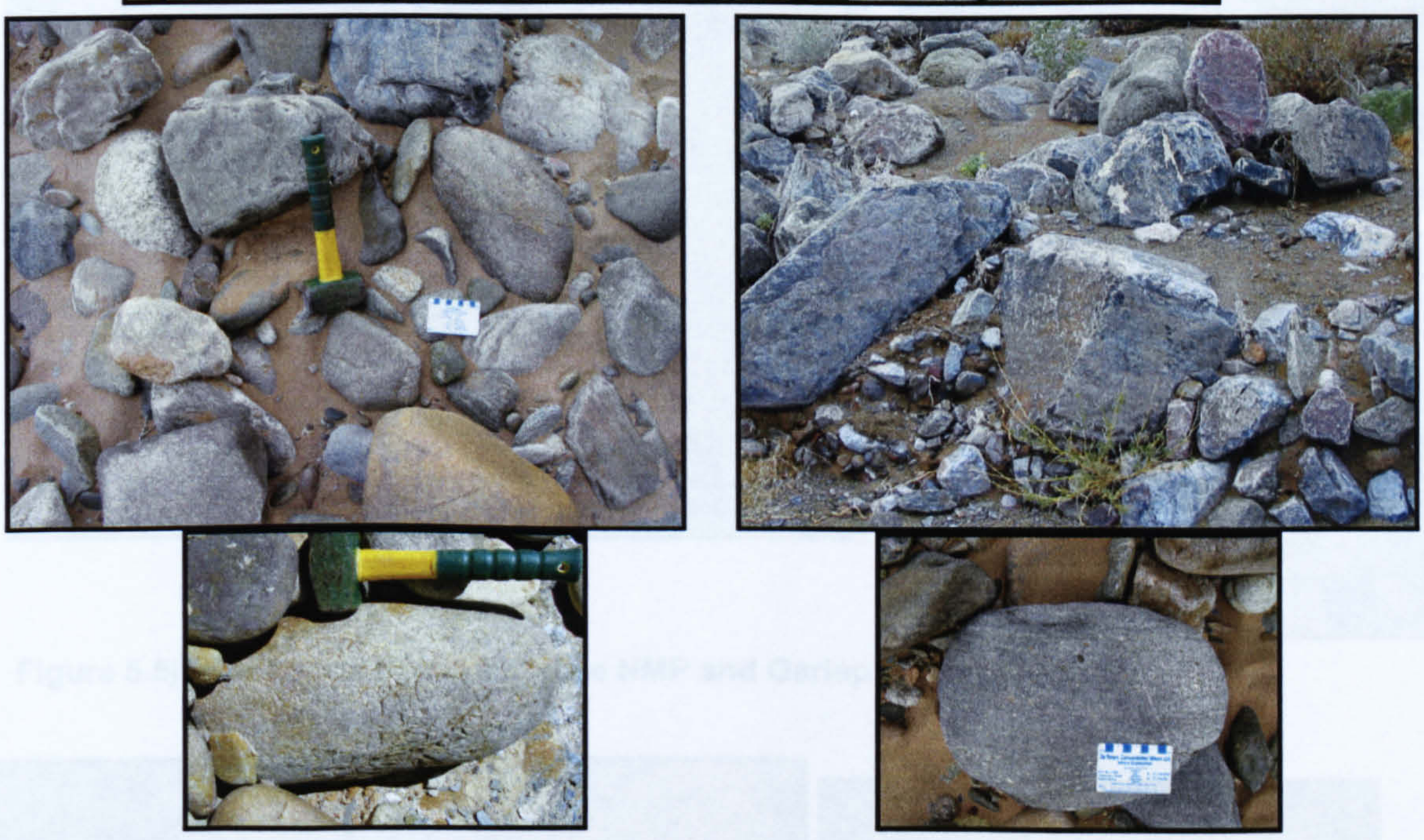

Figure 5.5g Nama quartzite clasts from the Nama Group.

Figure 5.5h Nama limestone clasts from the Nama Group.

Figure 5.5i Karoo sandstones

Figure 5.5j Vein quartz clasts from the NMP and Gariep Supergroup.

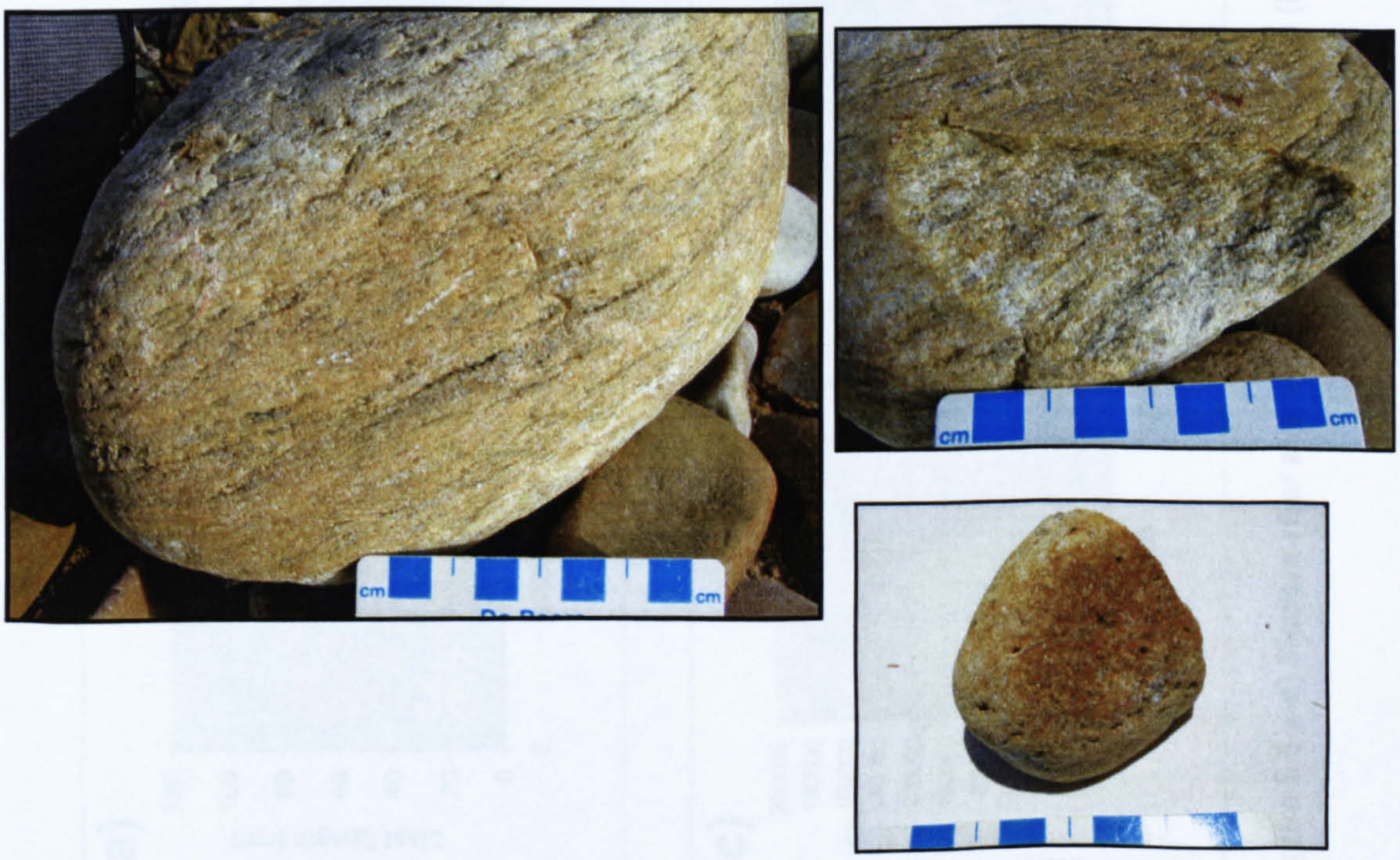

Figure 5.5k Basement quartzite clasts (quartz schist) from the NMP and Stinkfontein Subgroup of the Gariep Supergroup.

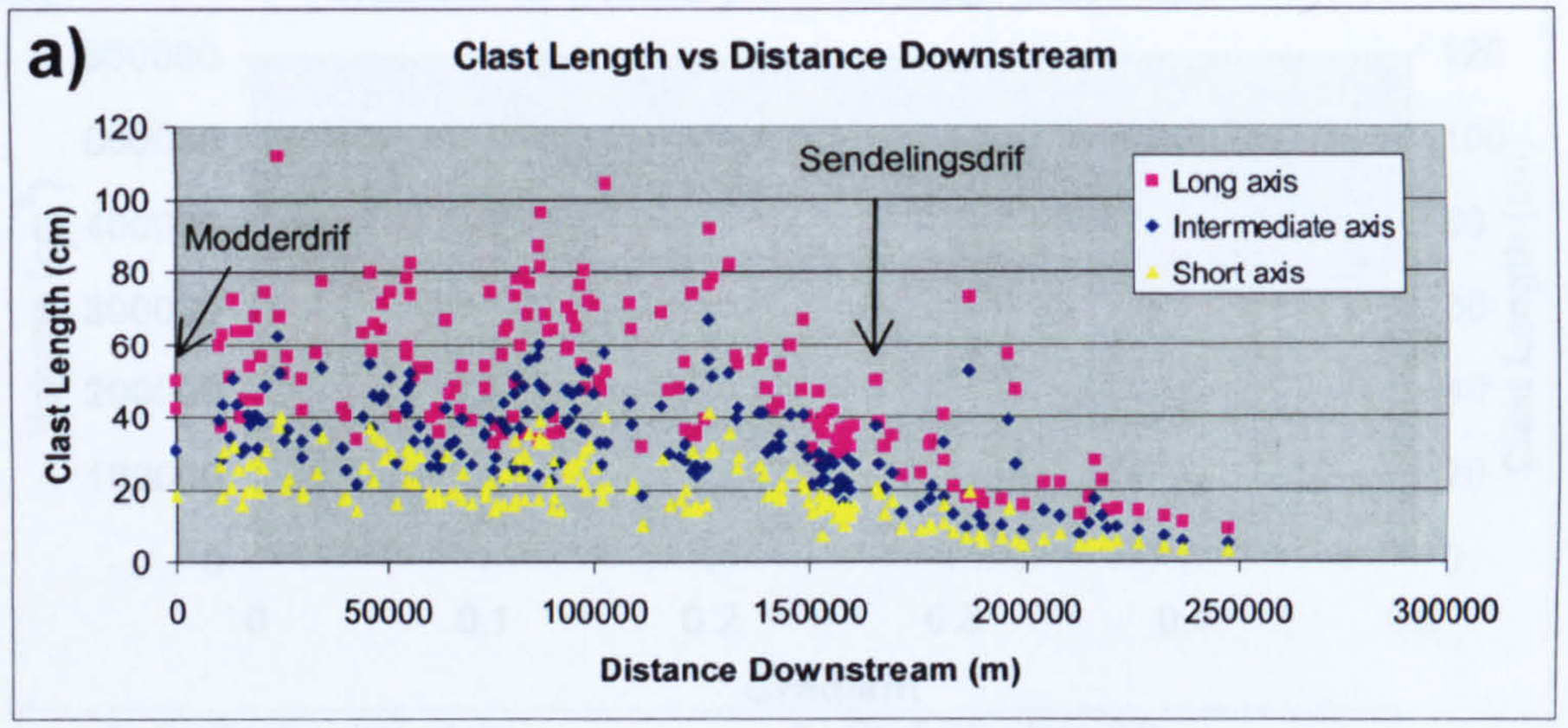

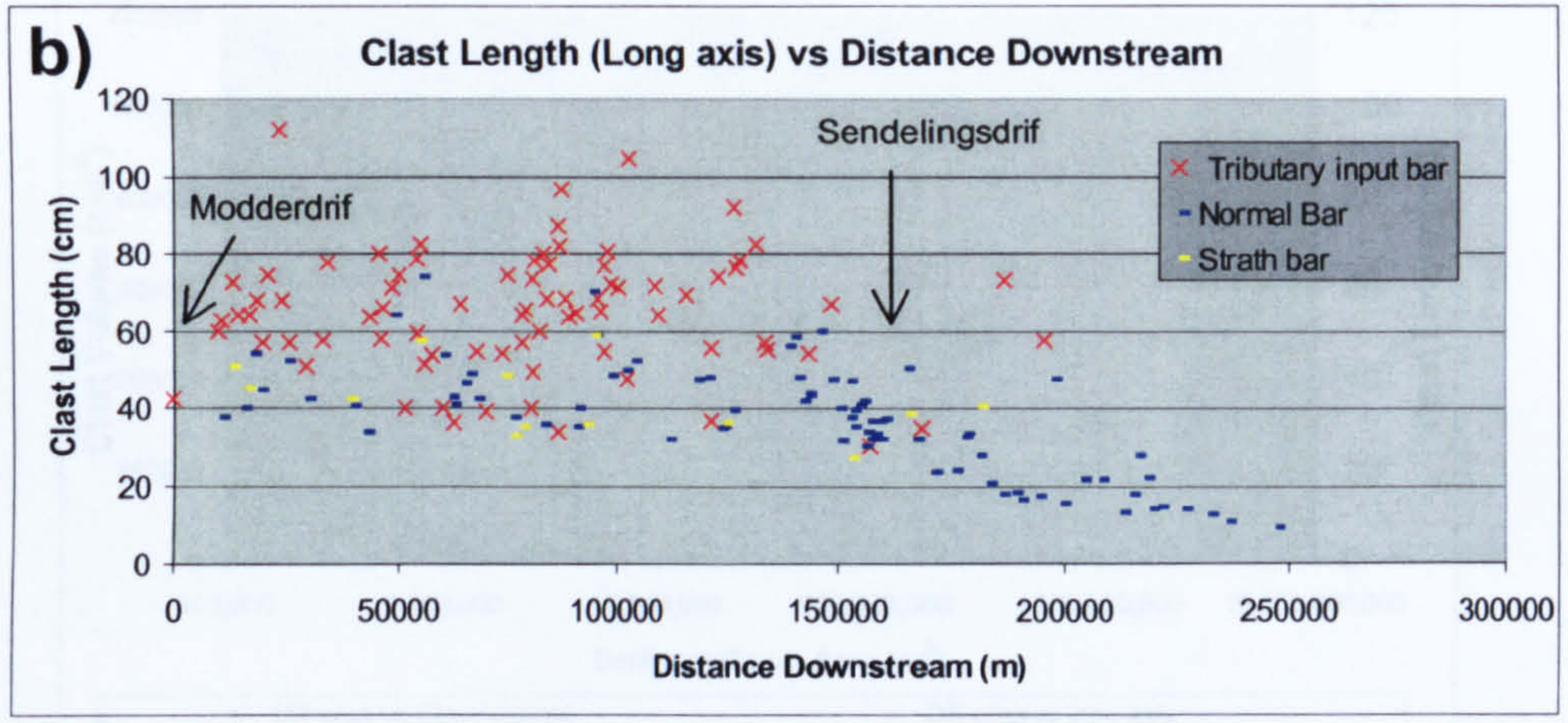

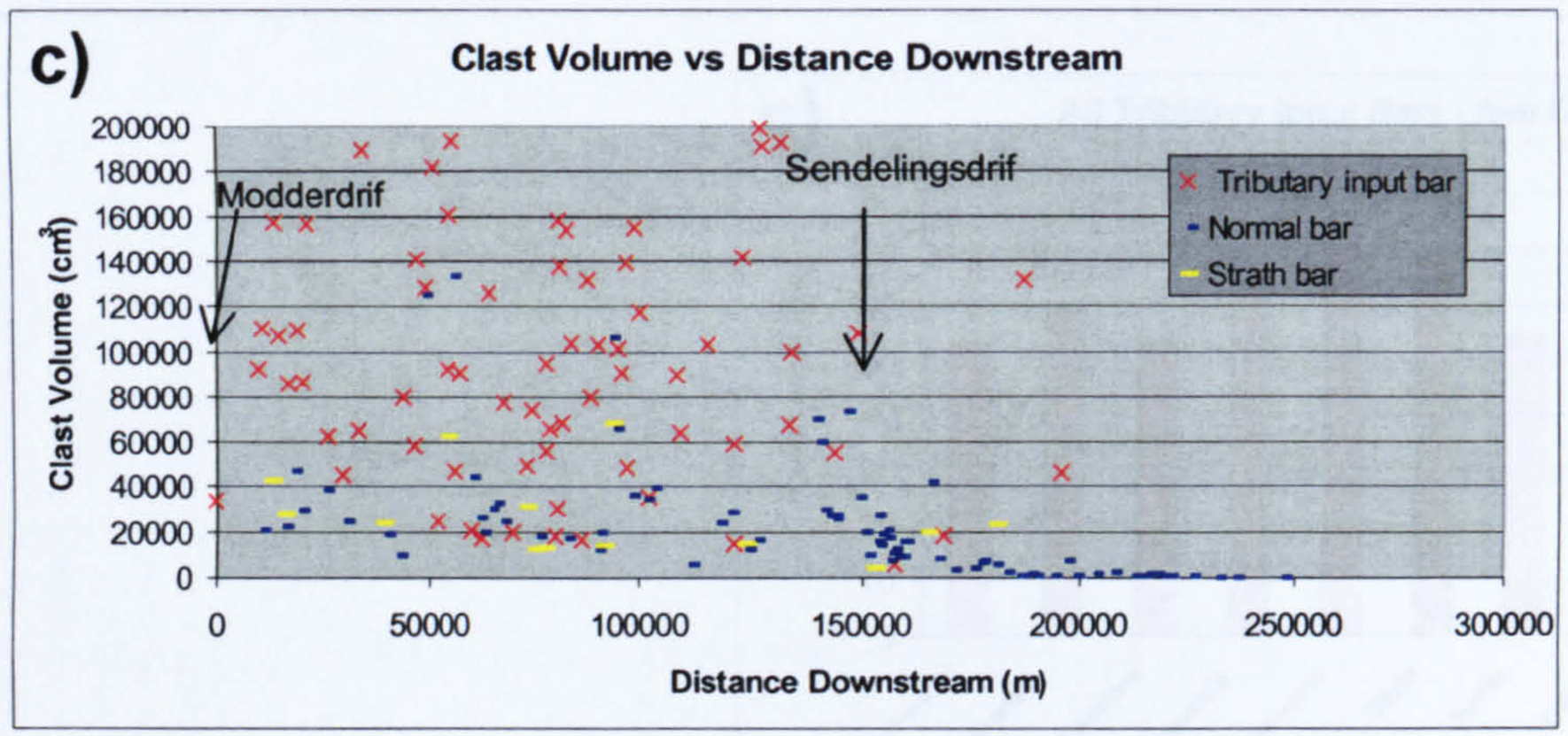

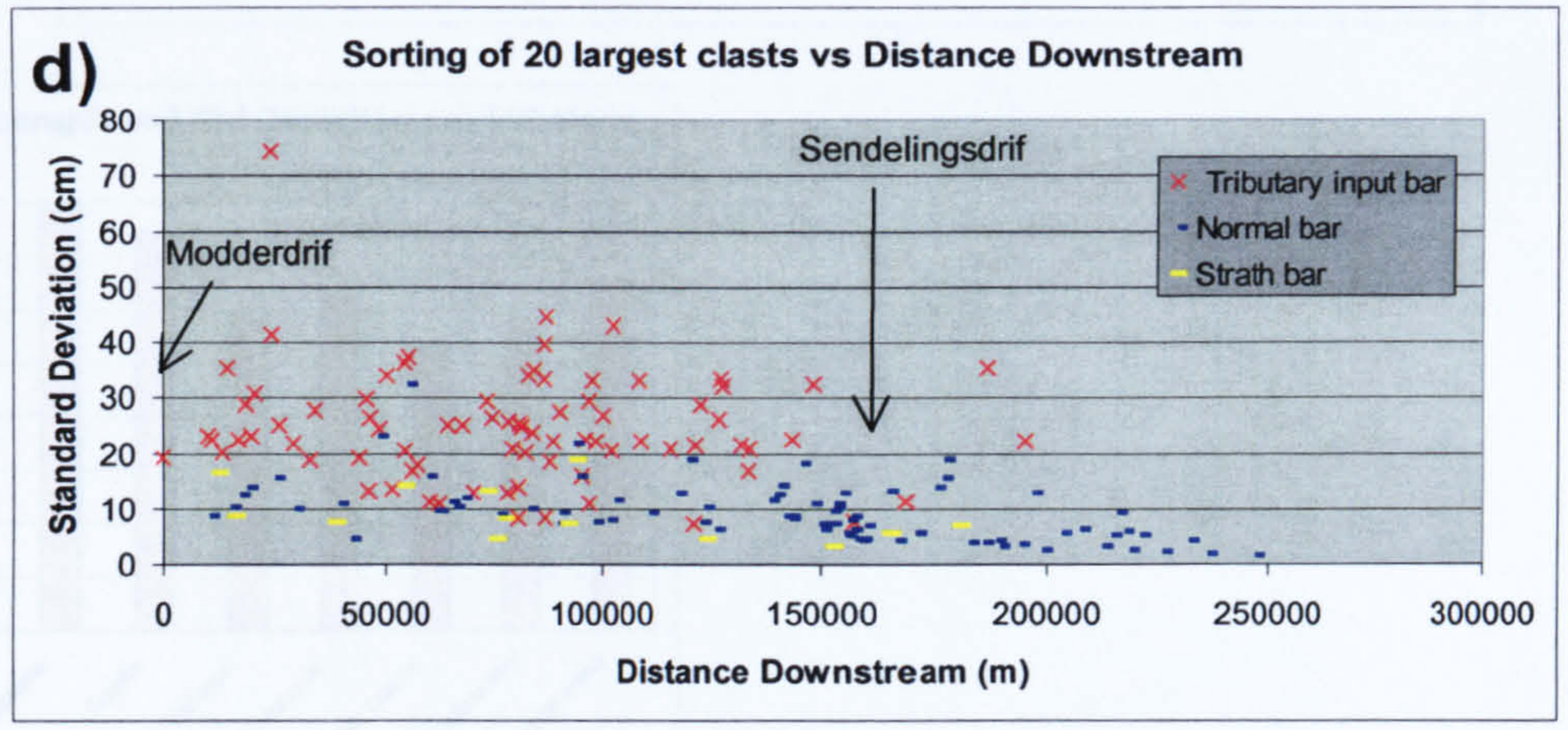

Figure 5.6 a-c) Modern river average maximum clast size (MCS) and d) Clast length standard deviation per bar from Modderdrif to Hohenfels.

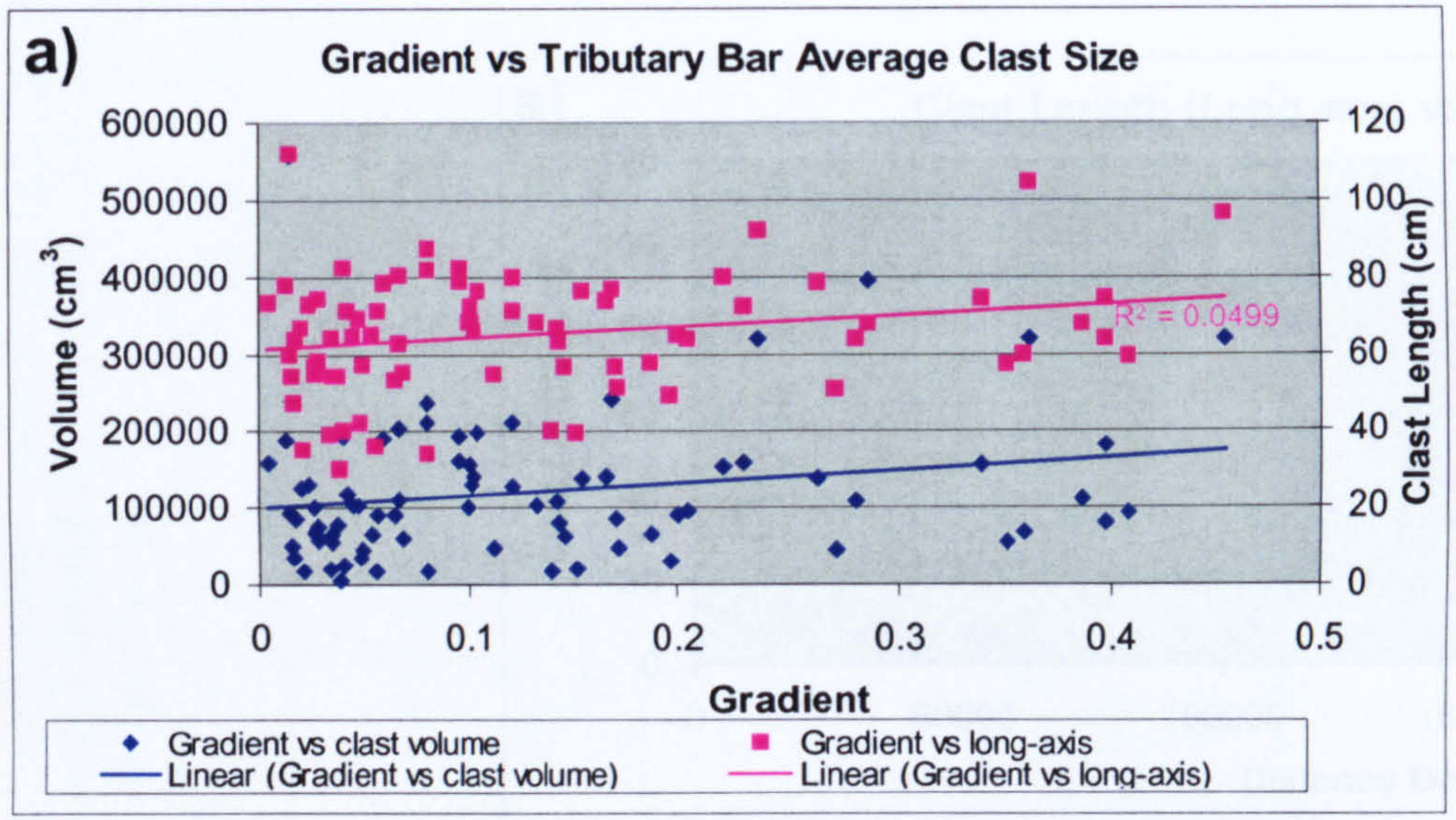

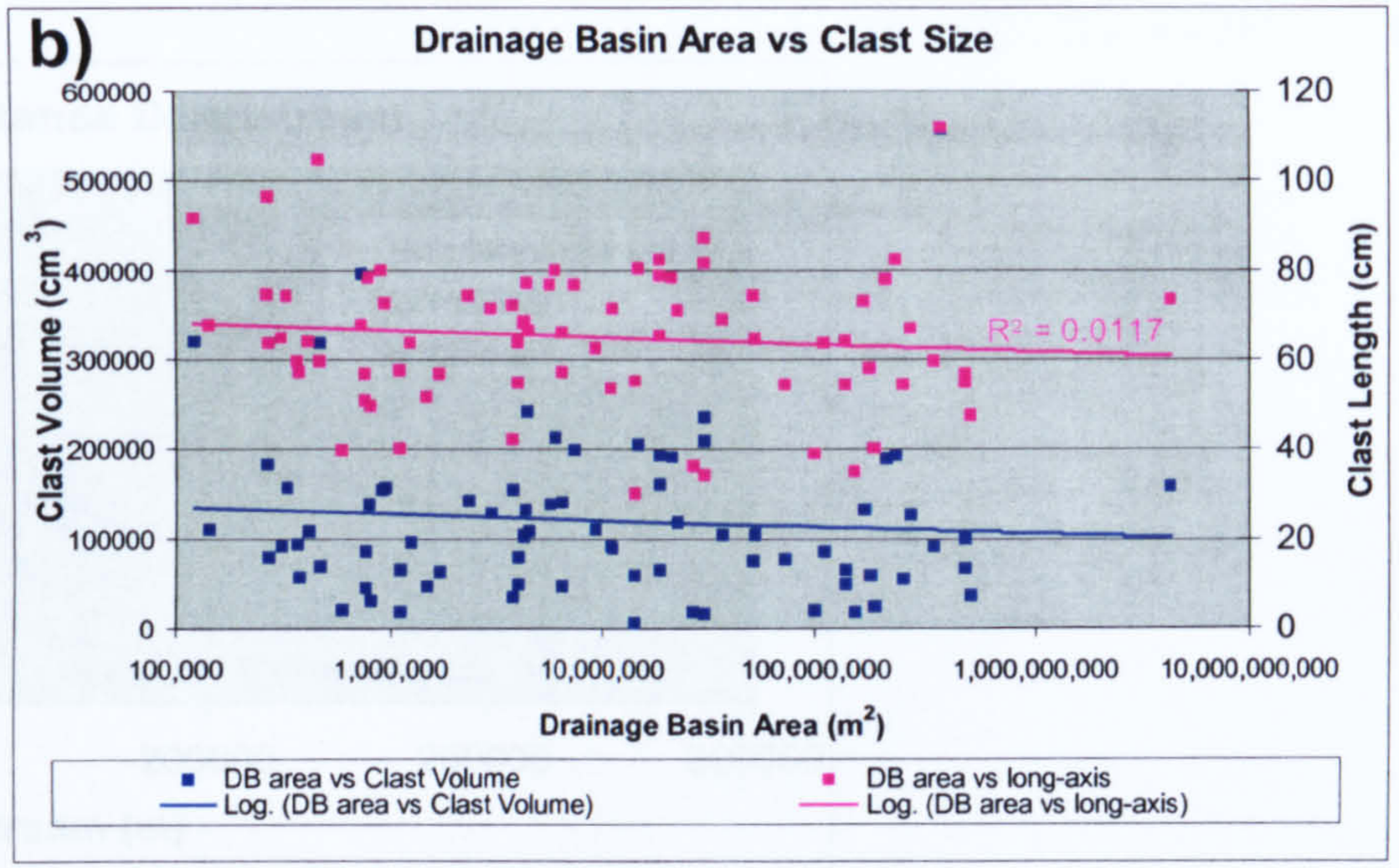

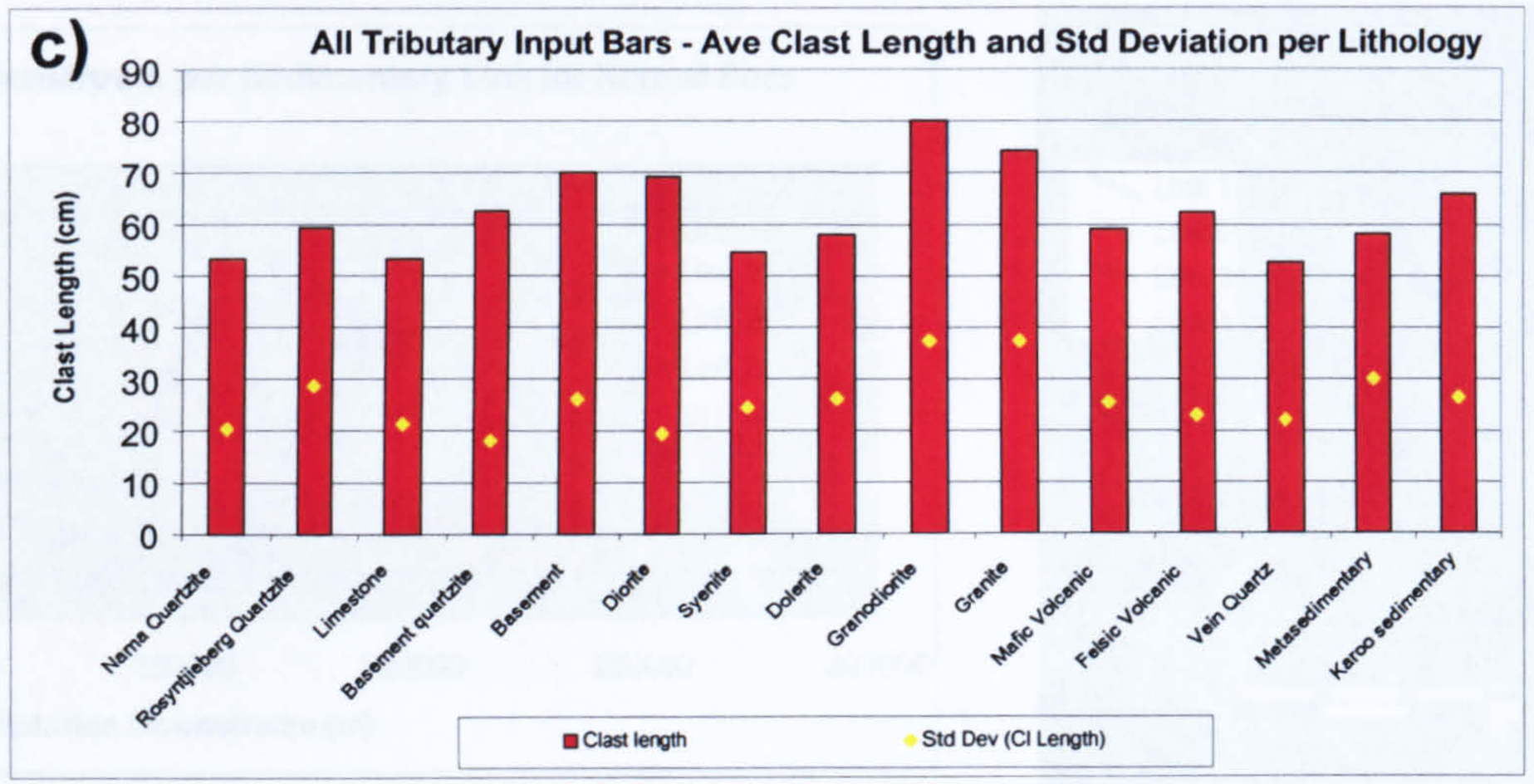

Figure 5.7 Controls on tributary input bar clast size a) Tributary gradient b) Tributary drainage basin area c) Clast lithology.

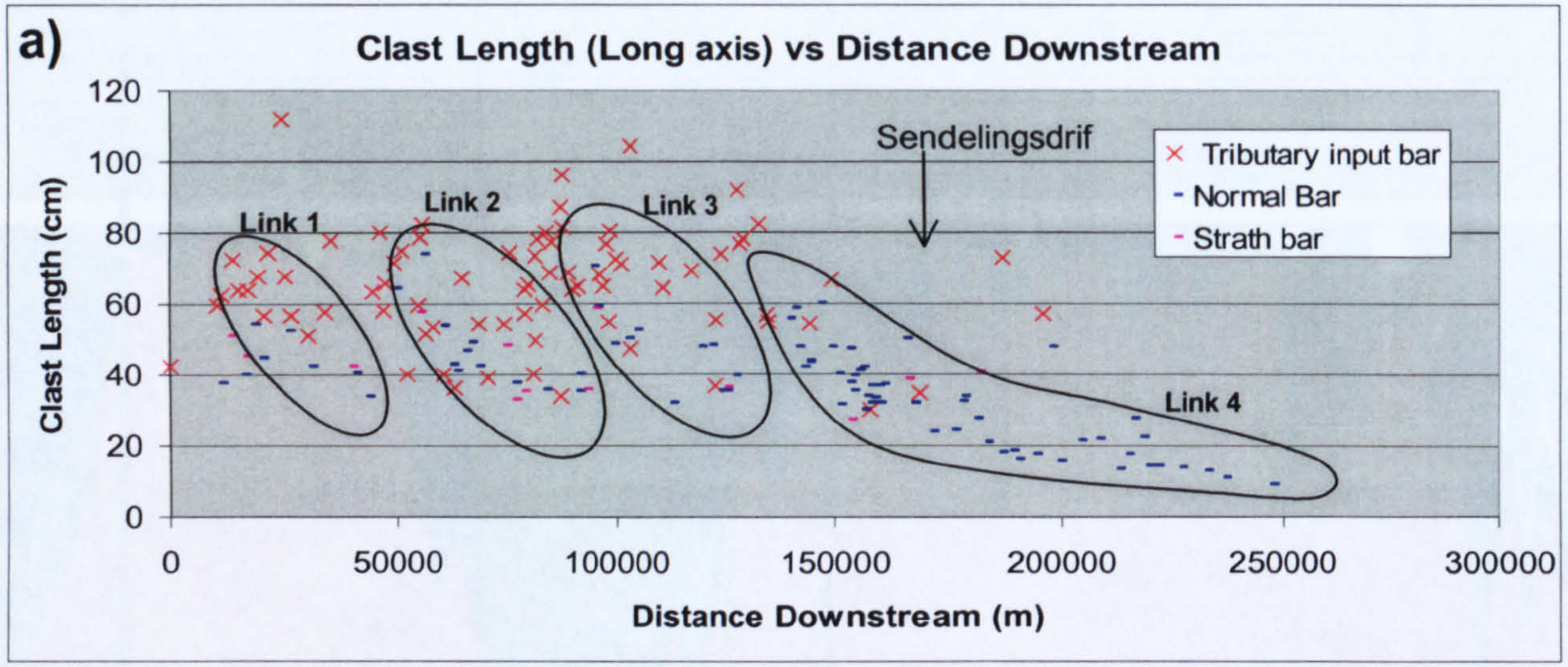

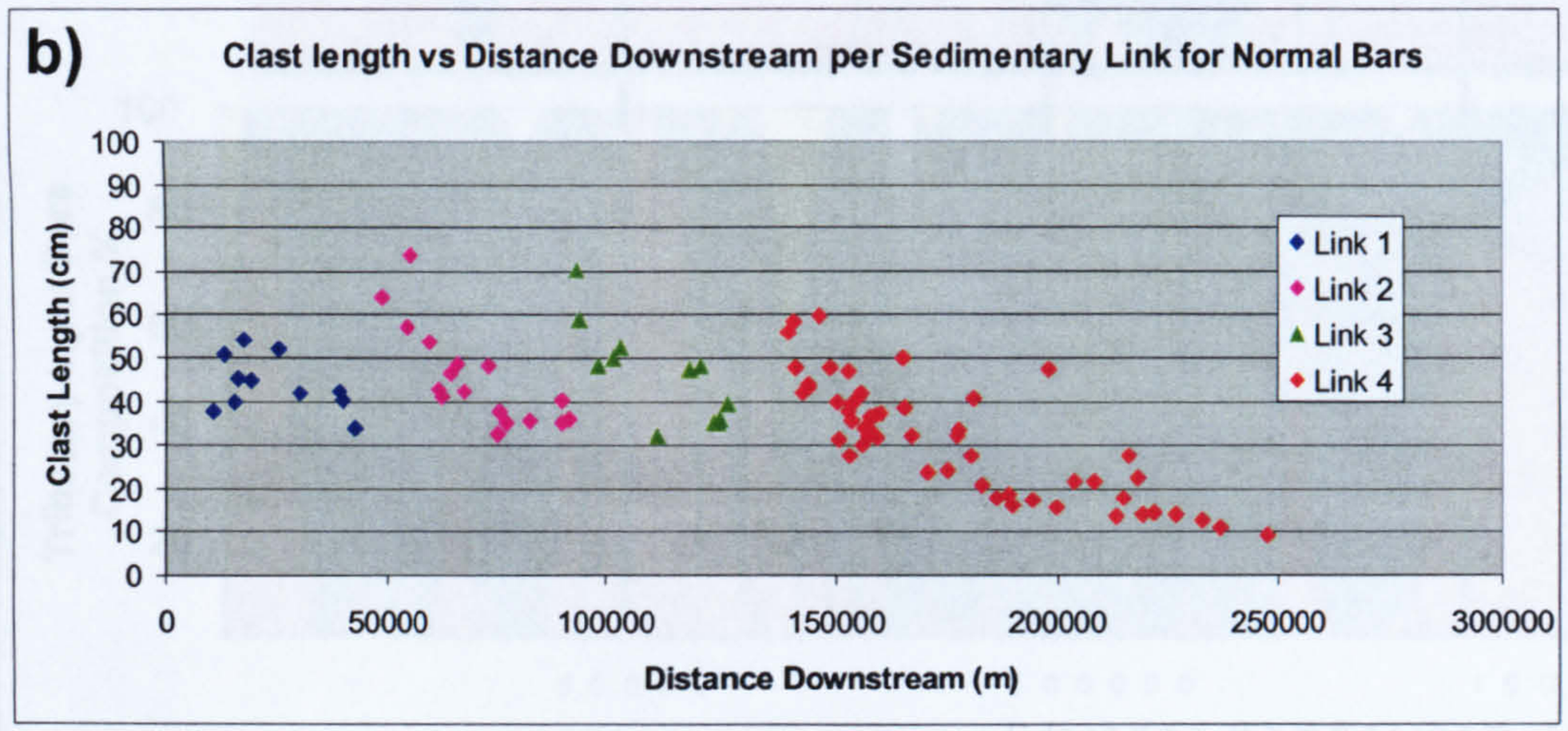

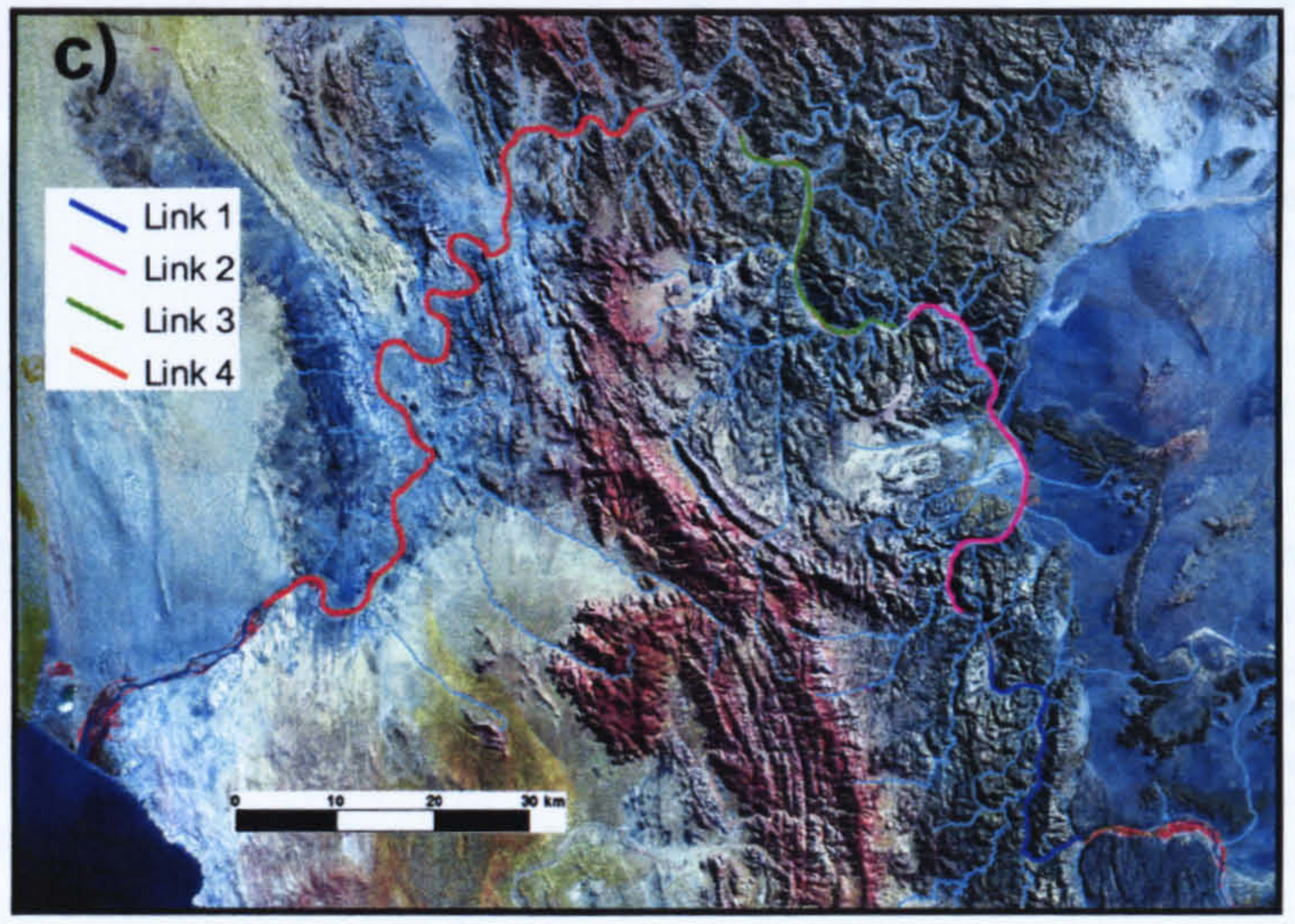

Figure 5.8 a-b Position of the 4 major downstream fining sedimentary links as defined in dataset c) Position of Links 1-4 within the study reach.

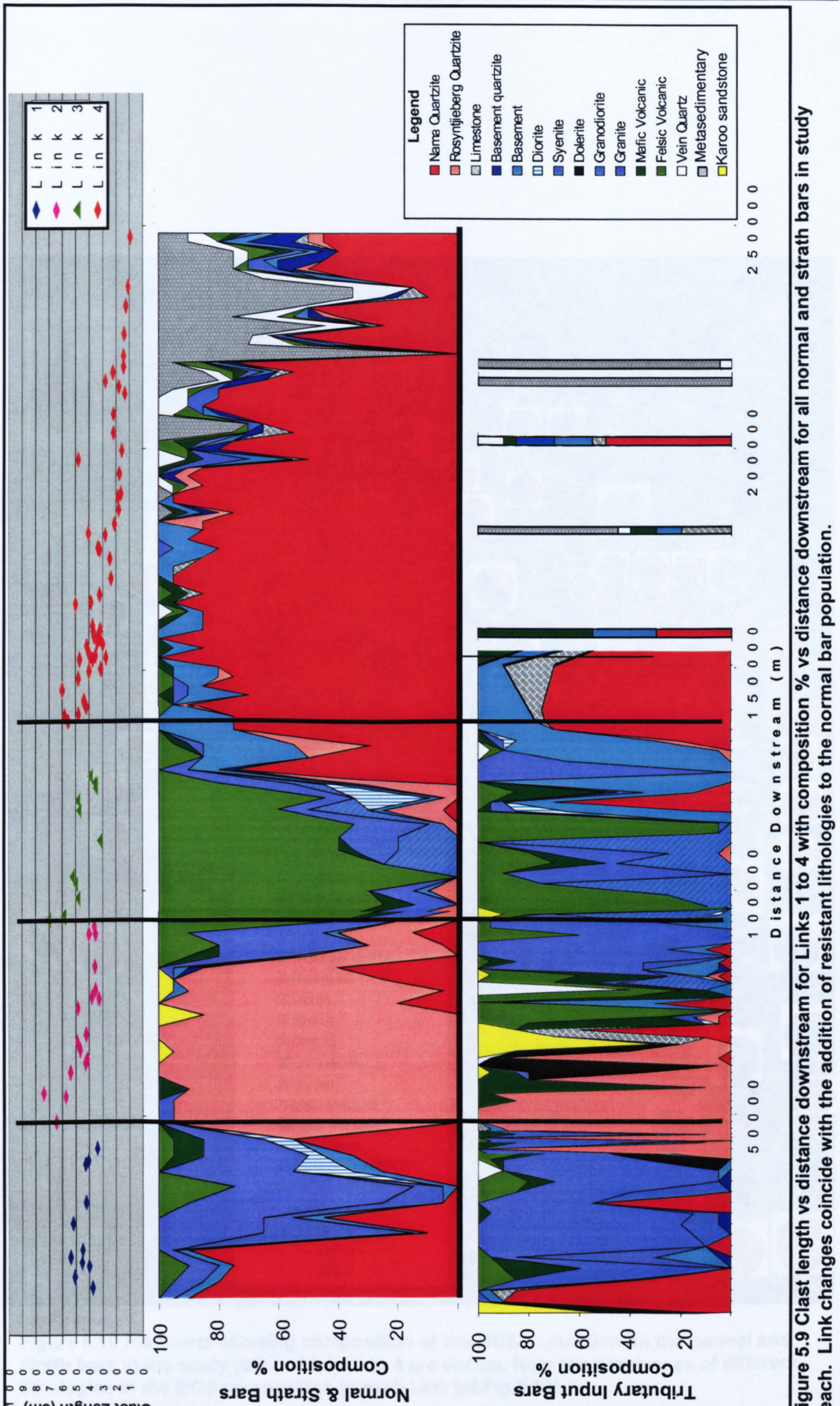

Figure 5.9 Clast length vs distance downstream for Links 1 to 4 with composition % vs distance downstream for all normal and strath bars in study reach. Link changes coincide with the addition of resistant lithologies to the normal bar population.

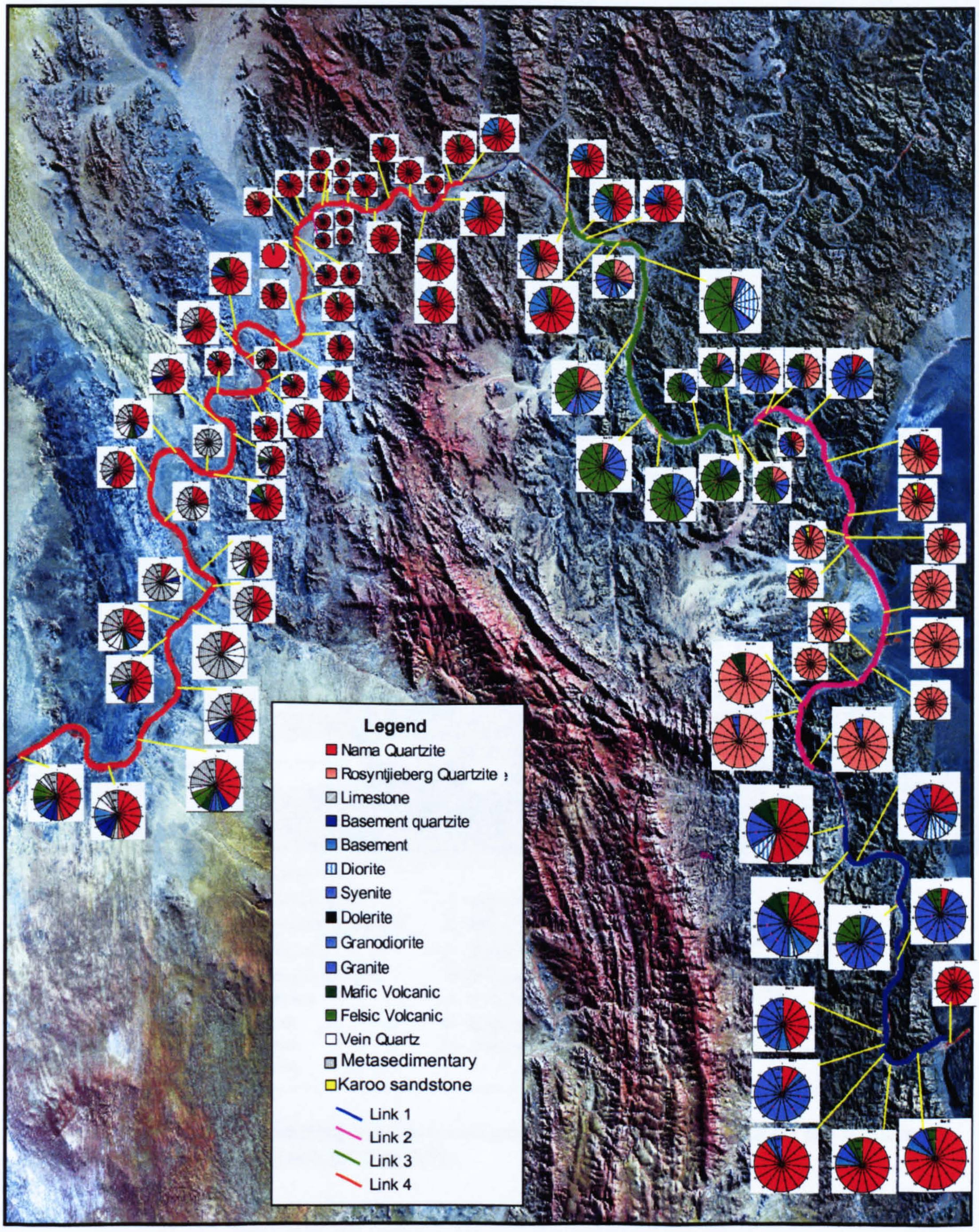

Figure 5.10 Pie charts showing composition of the MCS population on the normal and strath bars in the study reach. Links 1 to 4 are shown. Note the dominance of different lithologies in the MCS composition in each Link (cf.Fig.5.11).

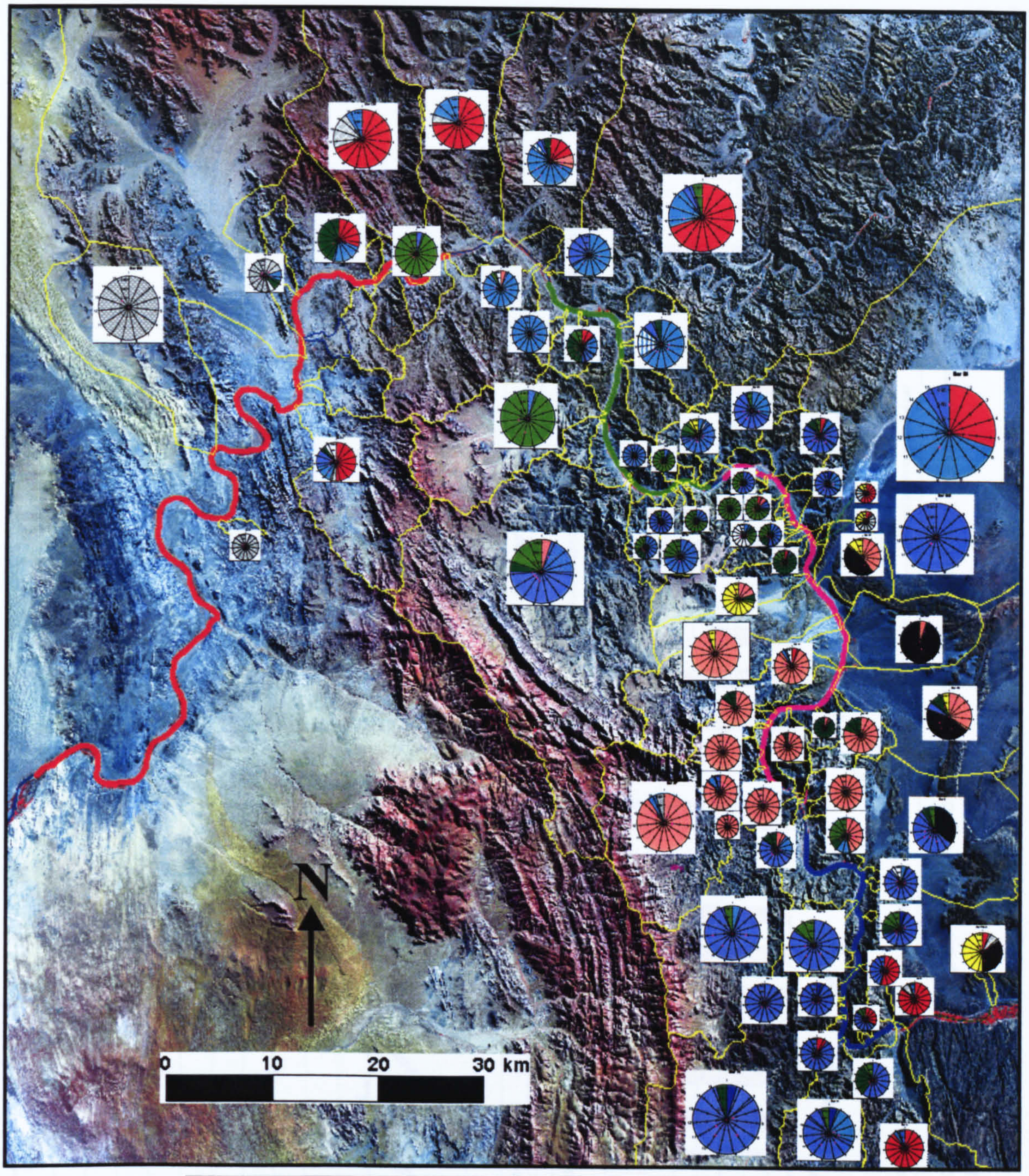

Figure 5.11 Pie charts showing the composition of the MCS population on the tributary input bars in the study reach (cf. Fig.5.10).

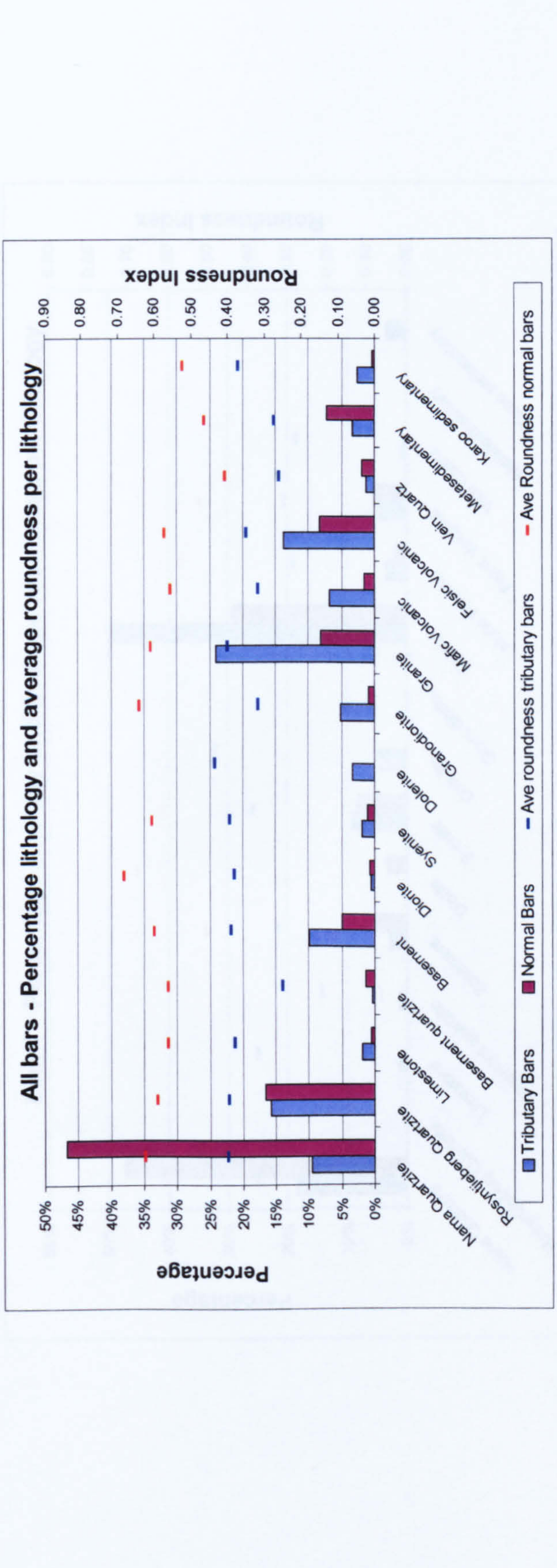

Figure 5.12 Comparison between the maximum clast size (MCS) population composition of tributary input and normal bars (comprising normal and strath bars) for the entire dataset in the study reach.

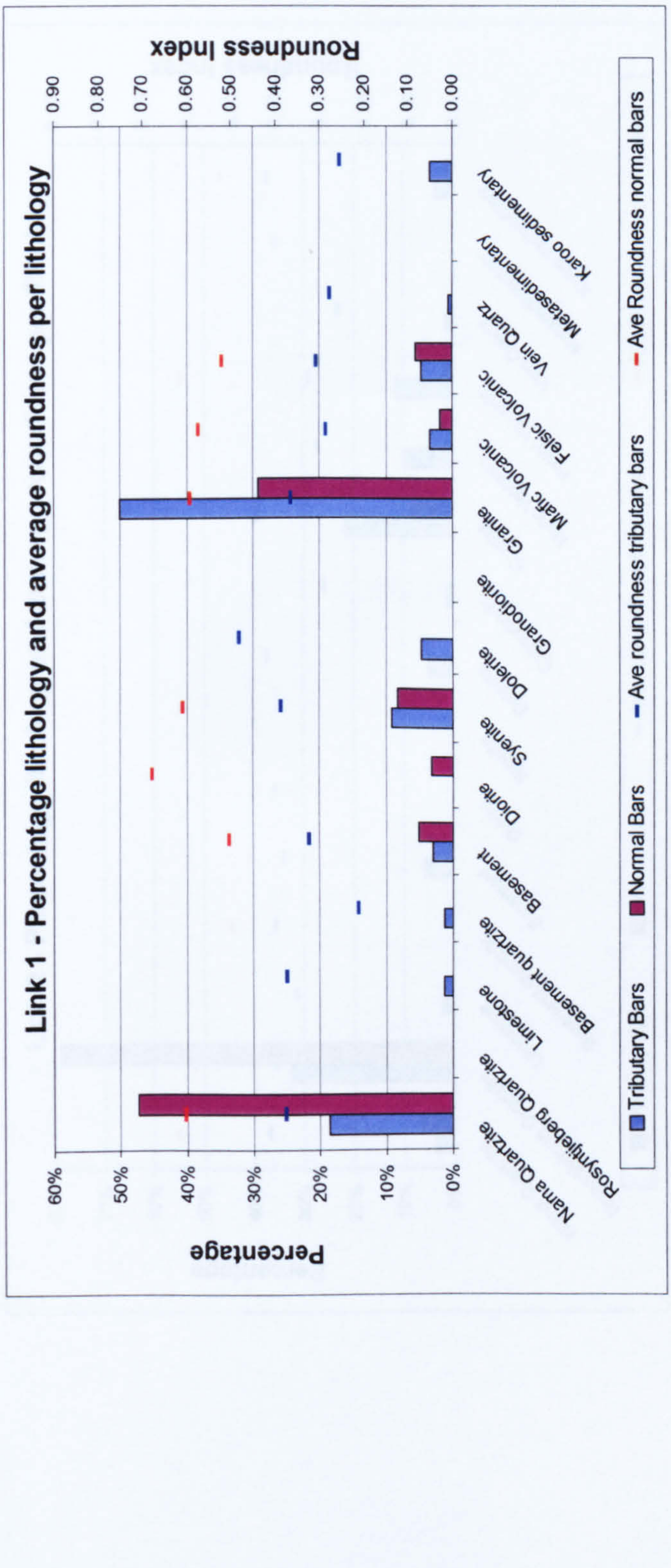

Figure 5.13 Comparison between the MCS population composition of tributary input and normal bars for Link 1.

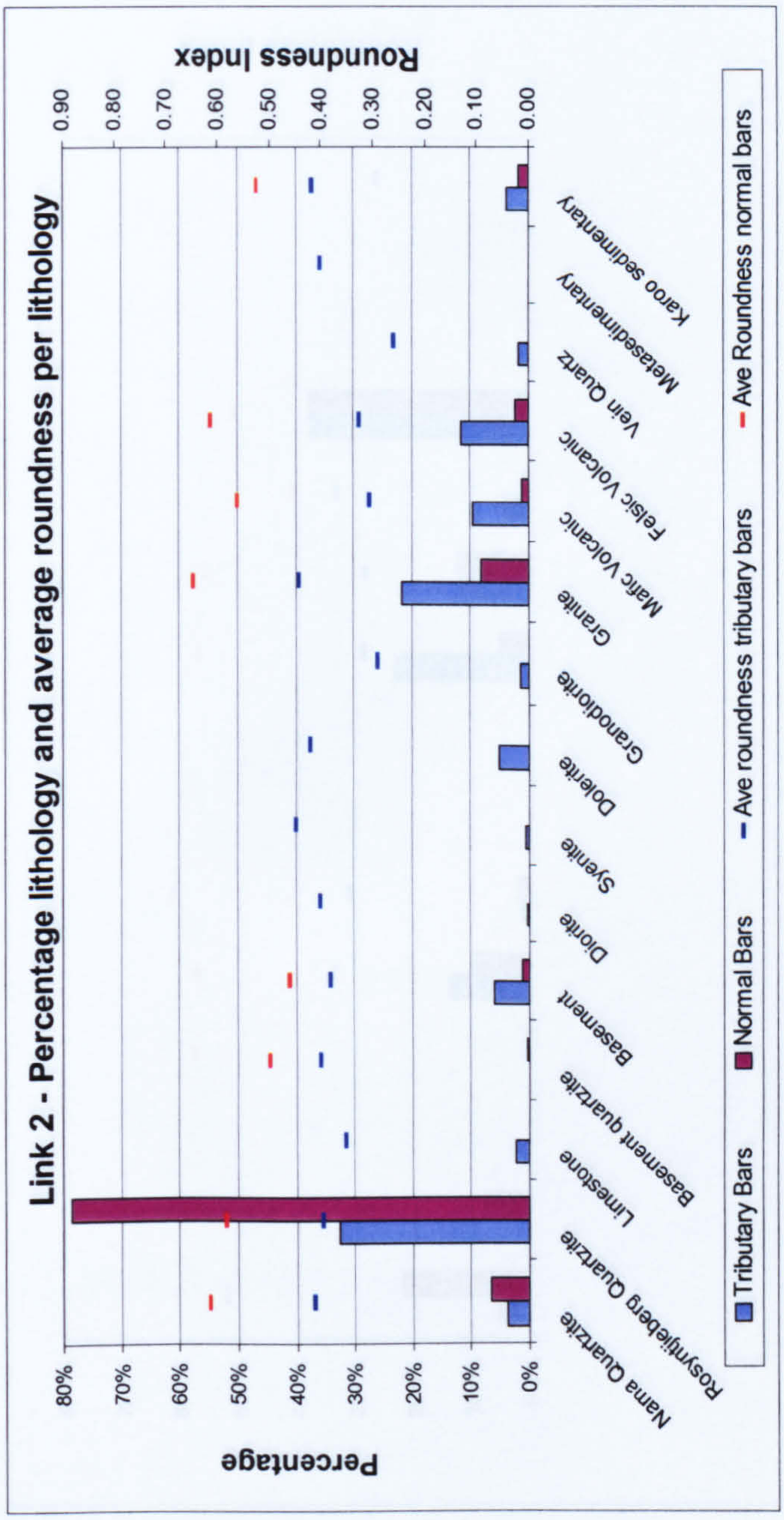

Figure 5.14 Comparison between the MCS population composition of tributary input and normal bars for Link 2.

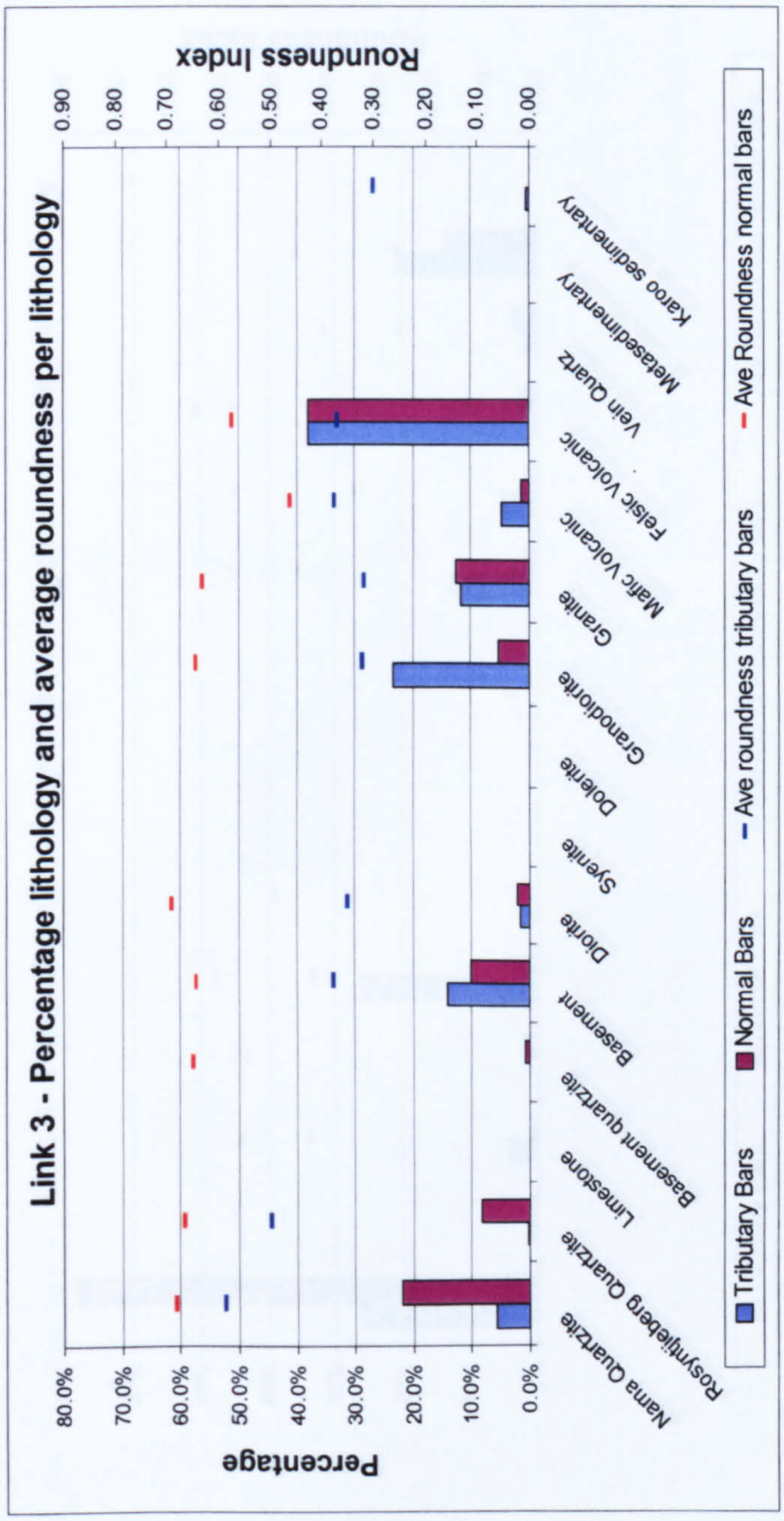

Figure 5.15 Comparison between the MCS population composition of tributary input and normal bars for Link 3.

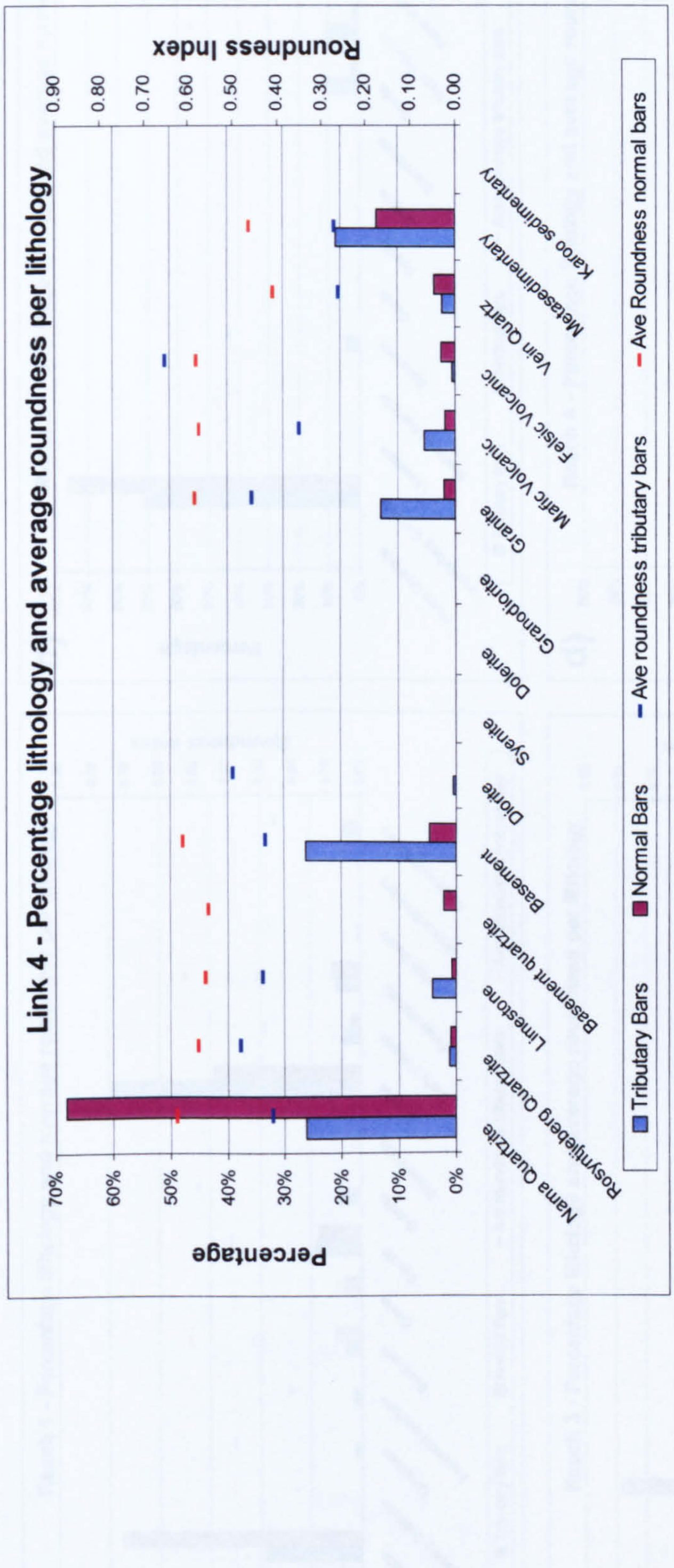

Figure 5.16 Comparison between the MCS population composition of tributary input and normal bars for Link 4.

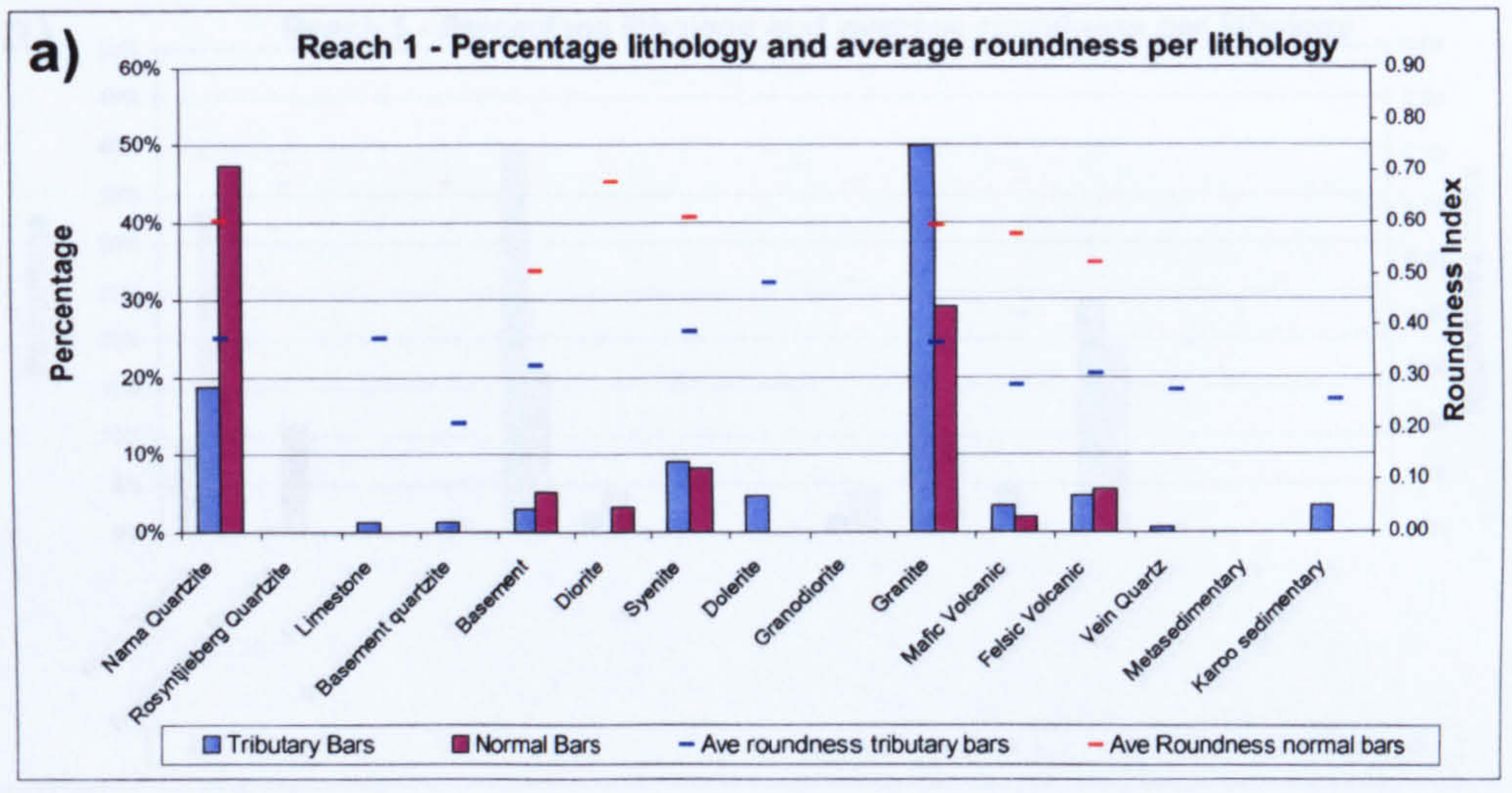

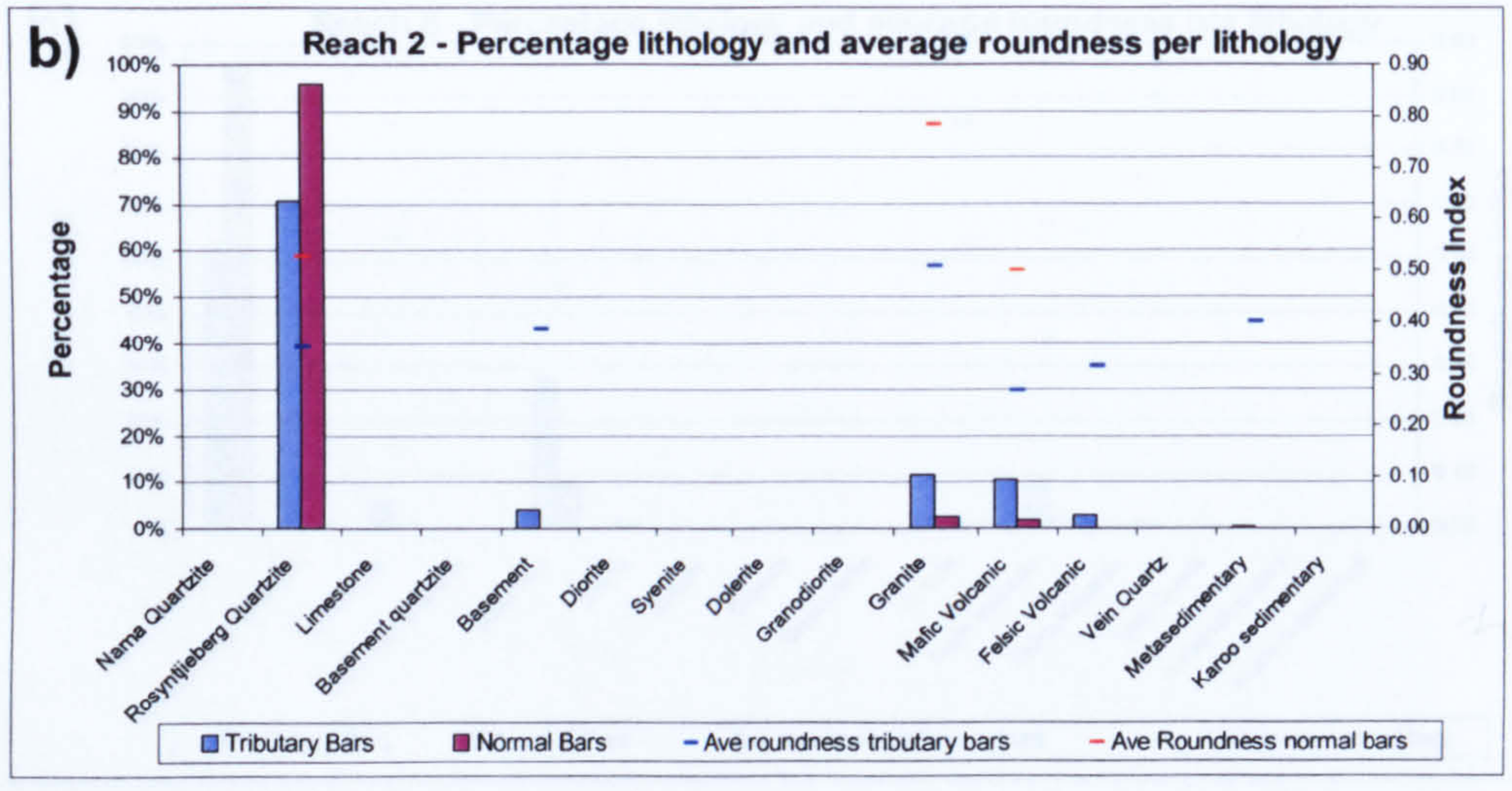

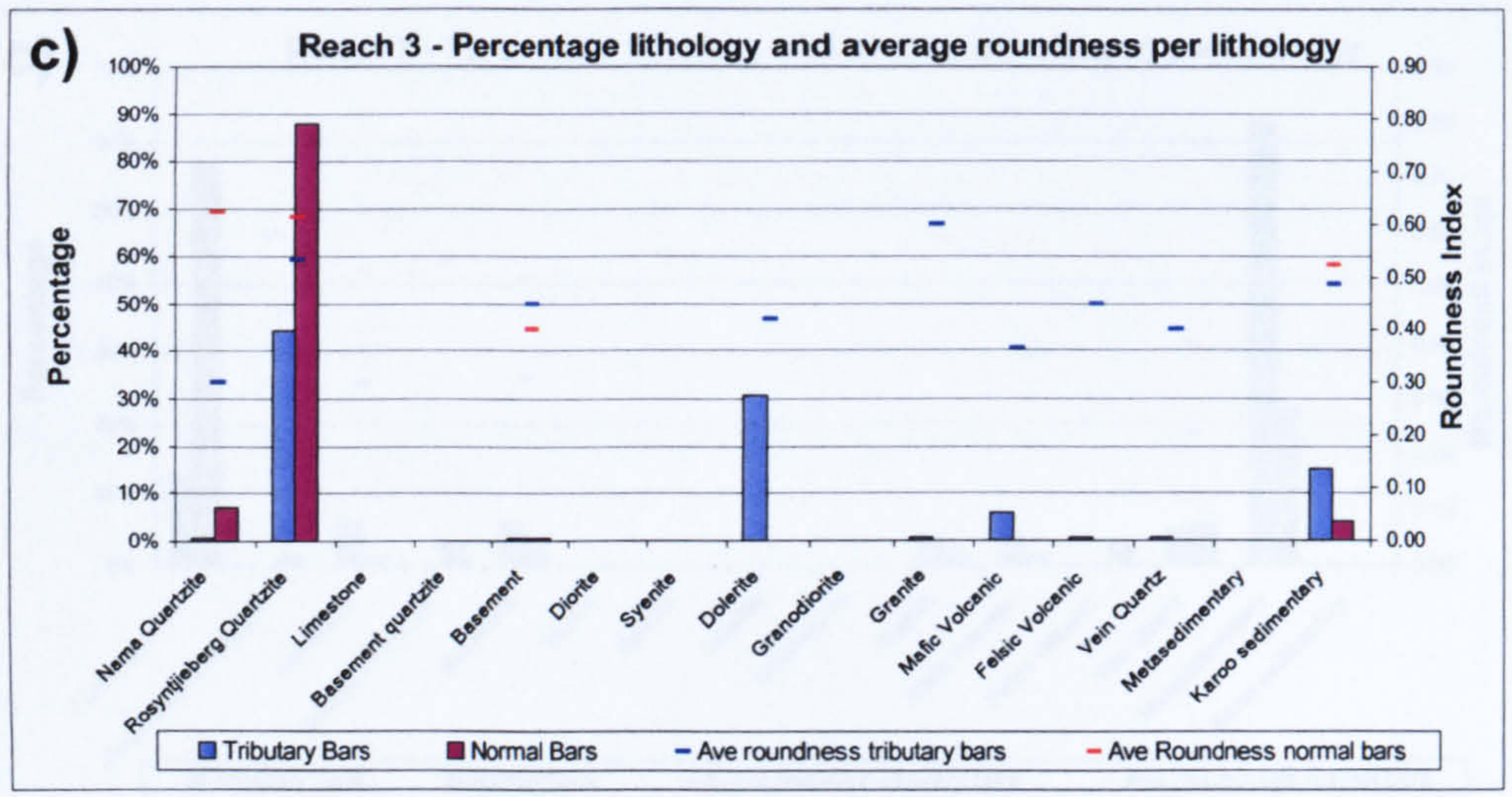

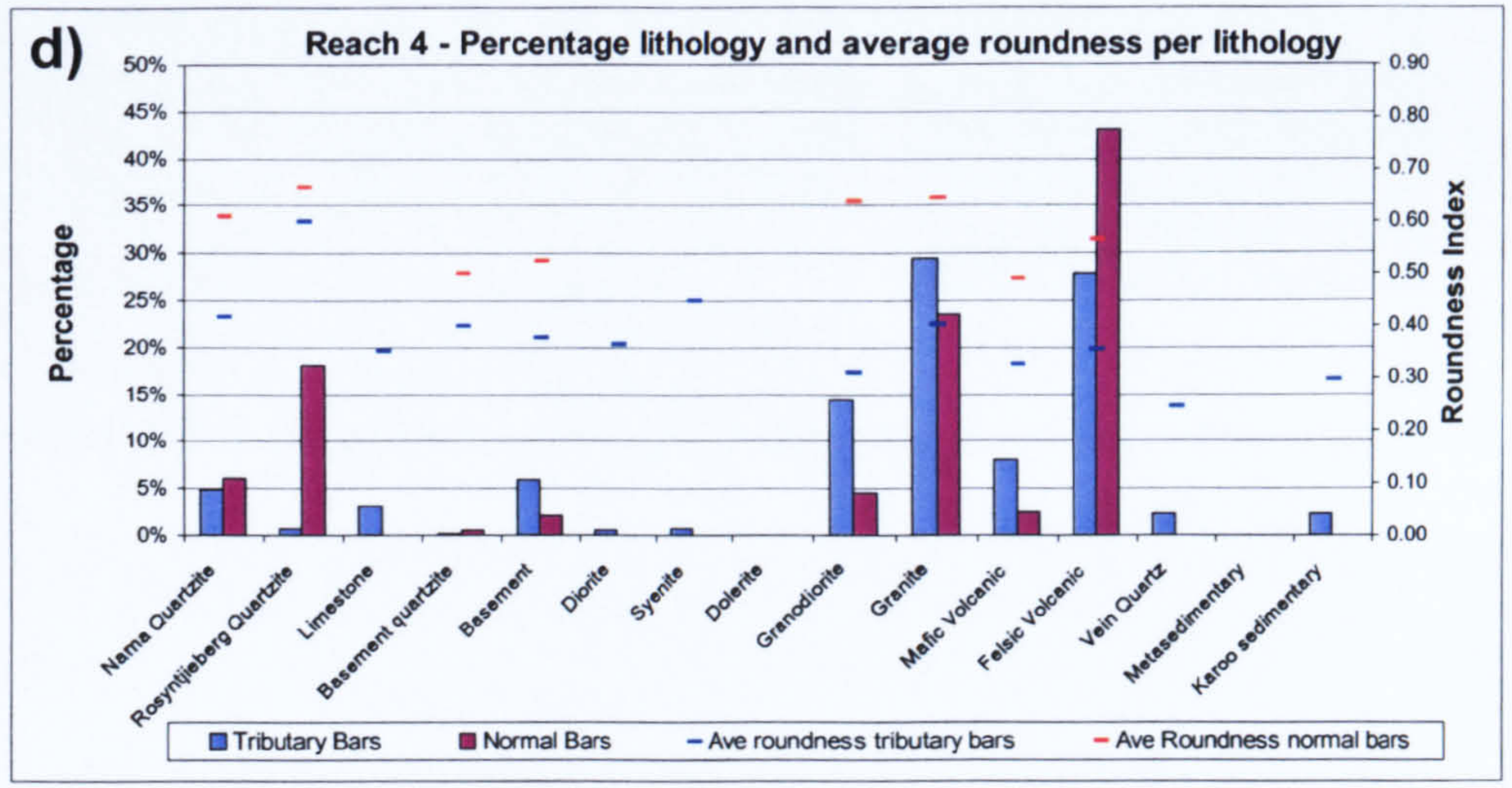

Figure 5.17 a-d Comparison between the MCS population composition of tributary input and normal bars for Reaches 1 to 4.

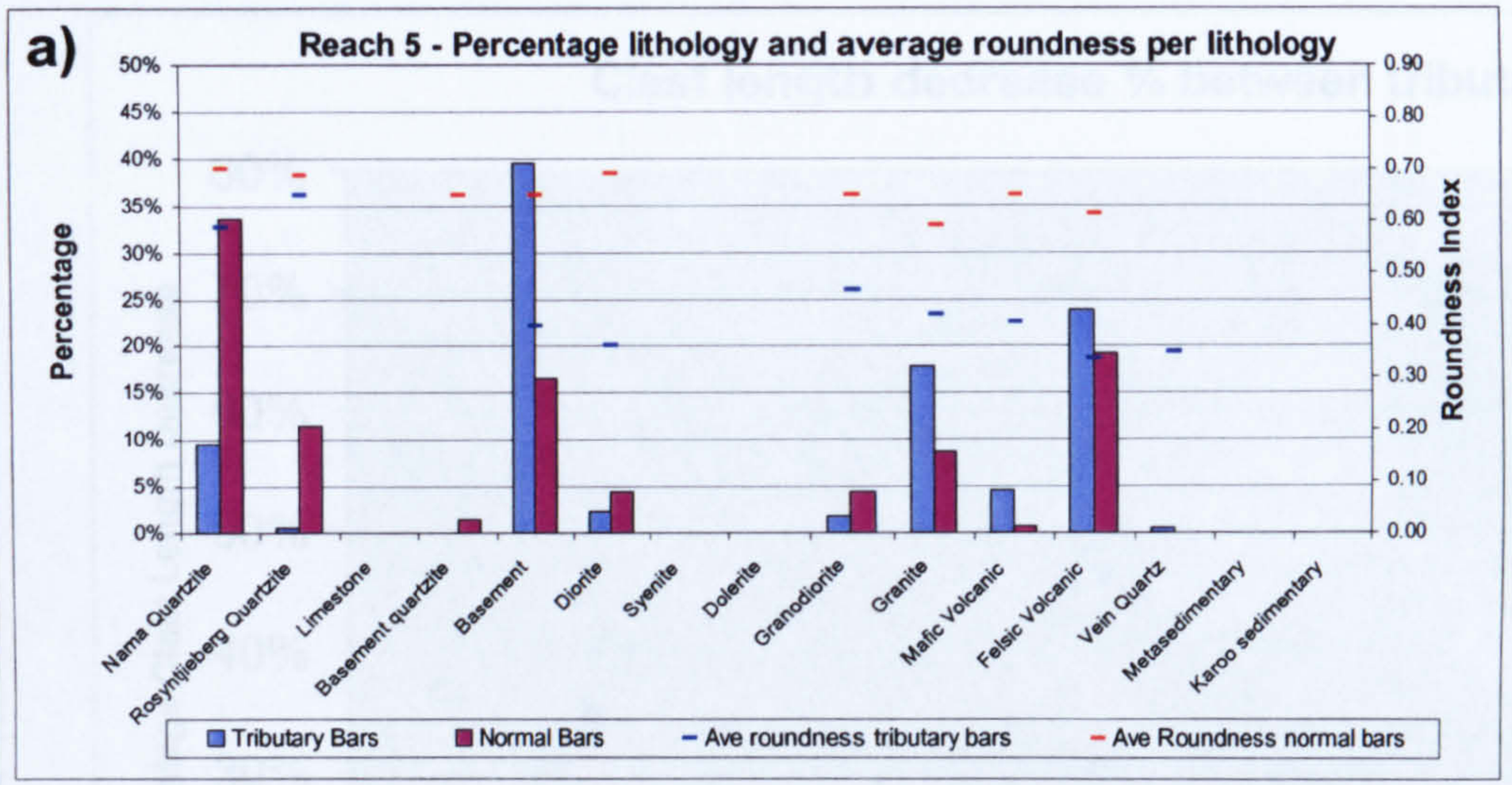

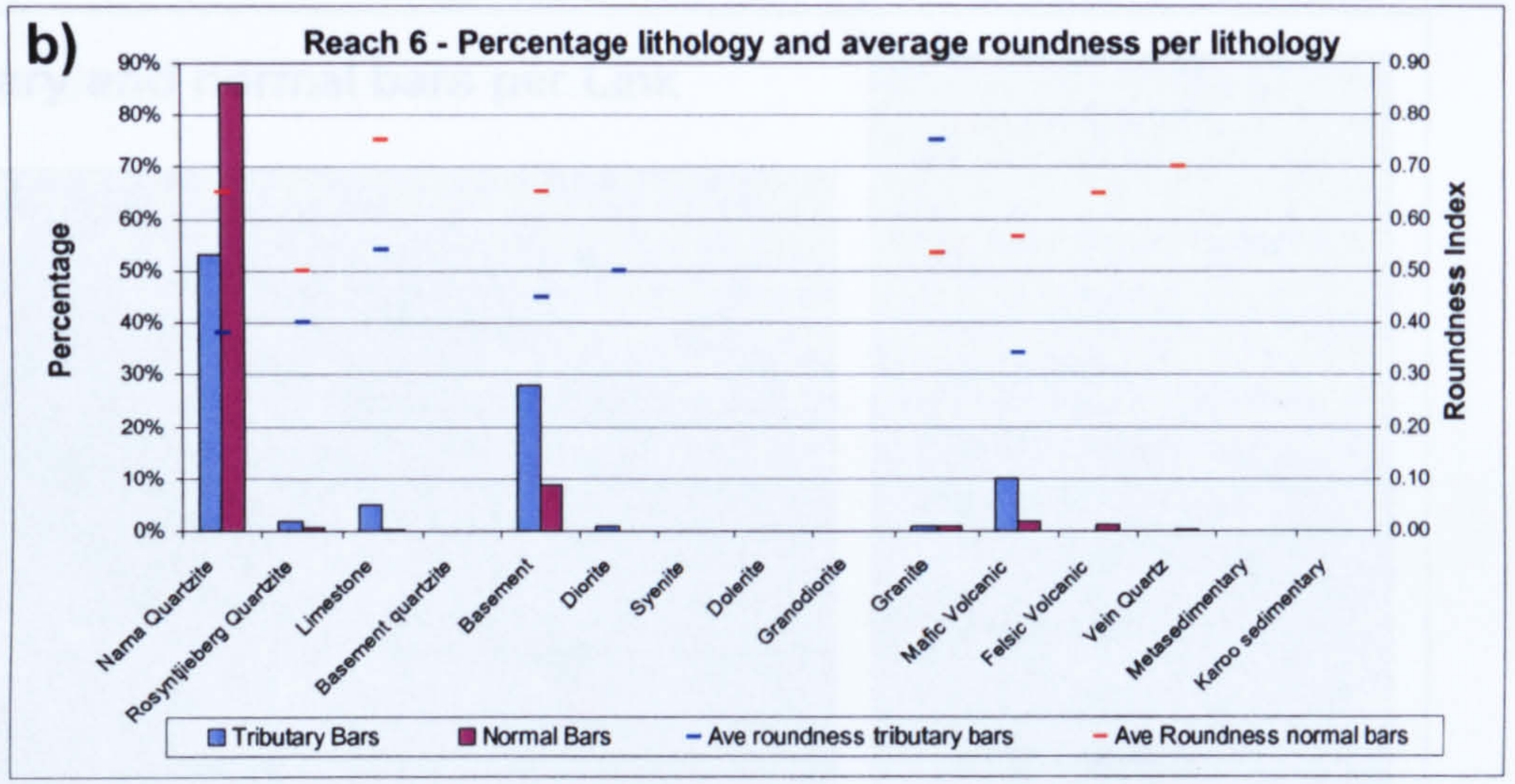

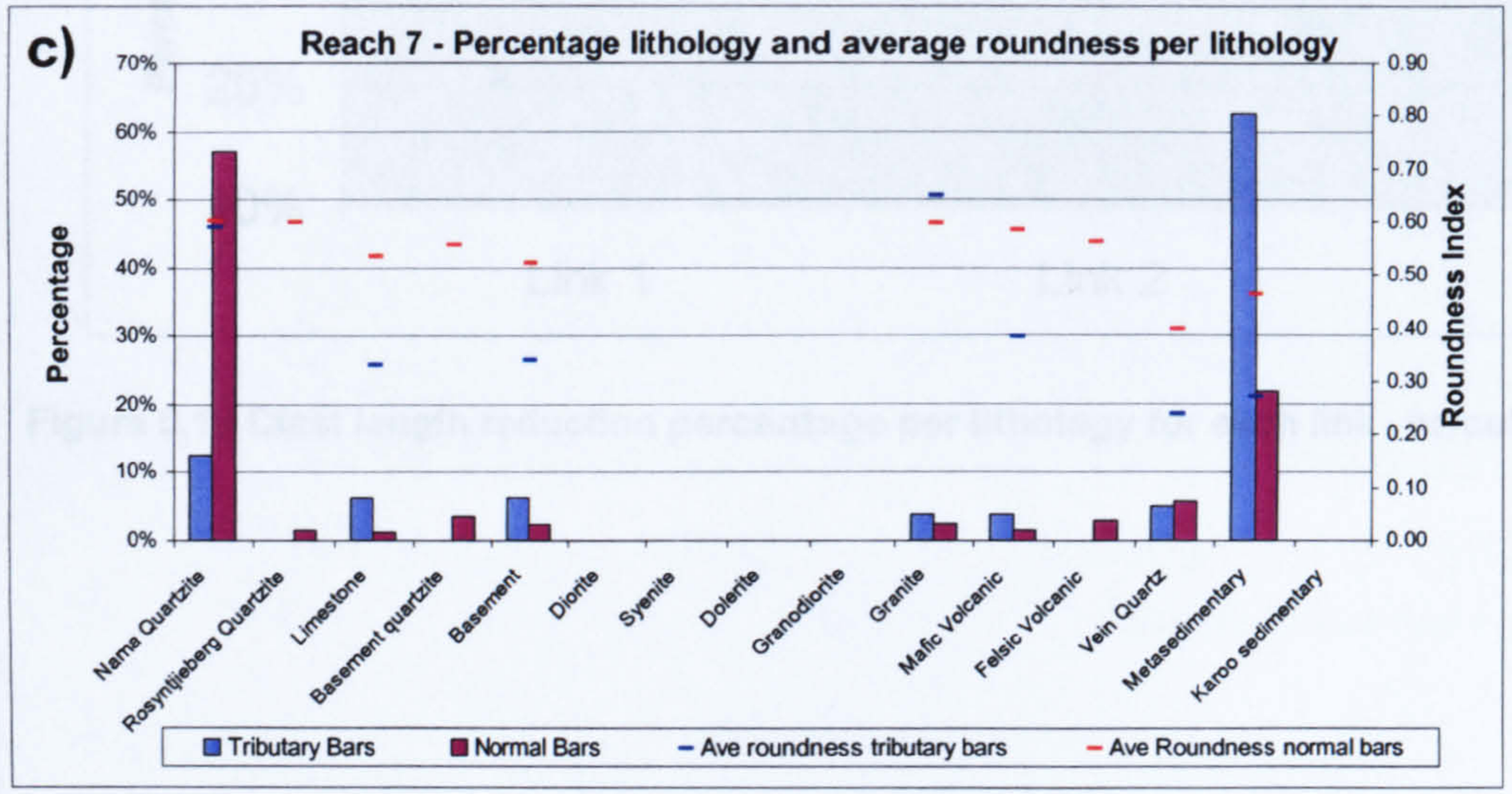

Figure 5.18 a-c Comparison between the MCS population composition of tributary input and normal bars for Reaches 5 to 7.

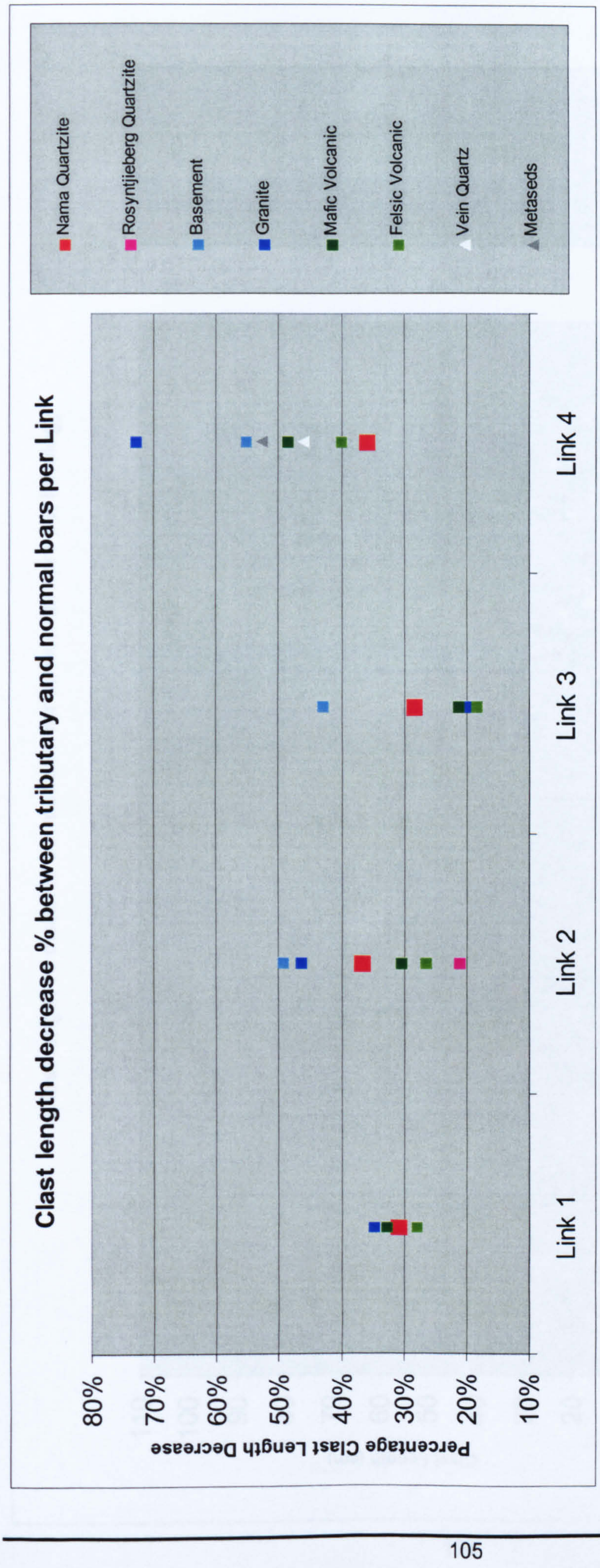

Figure 5.19 Clast length reduction percentage per lithology for each link - calculated by difference between average tributary input and normal bar clast size.

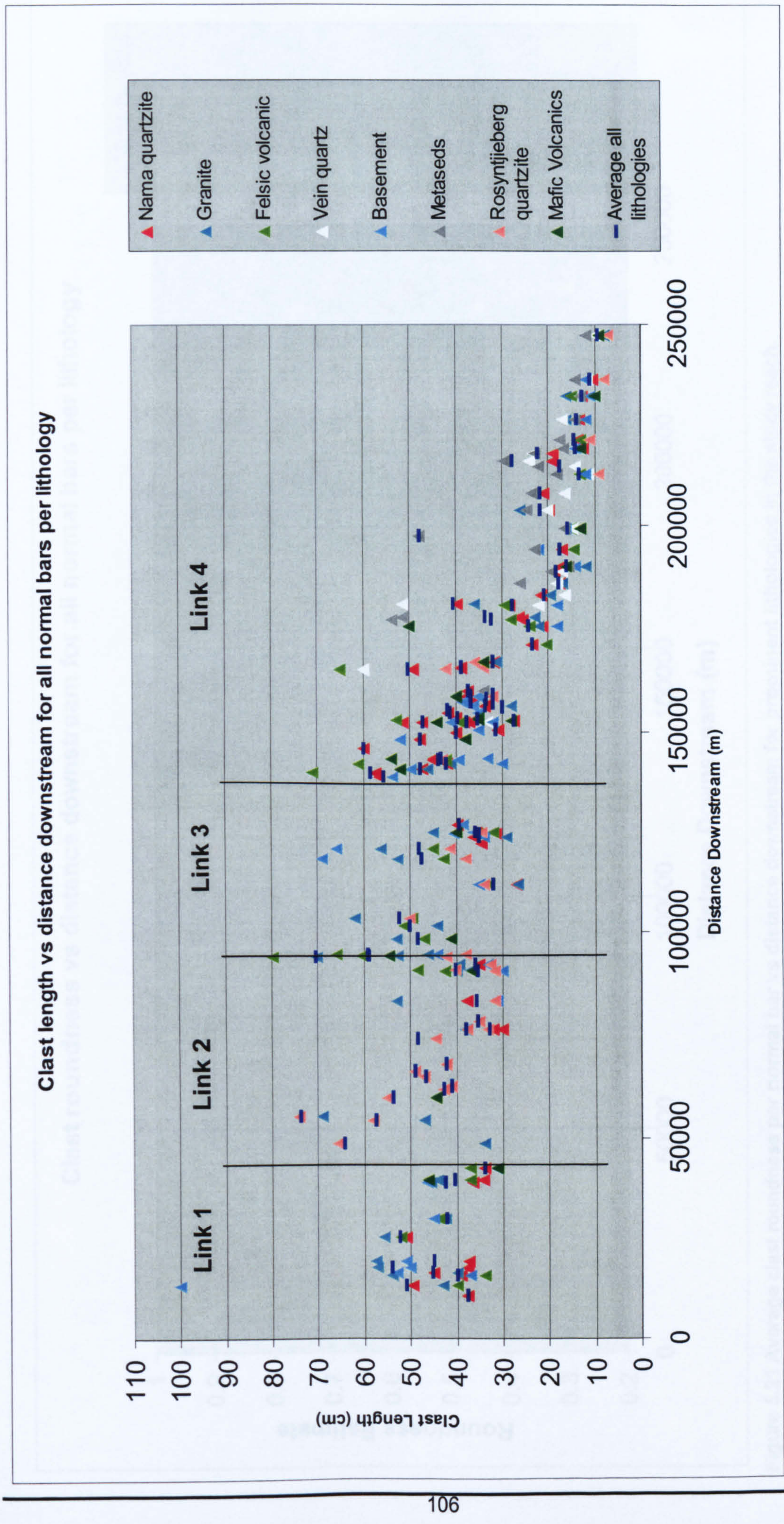

Figure 5.20 Average clast length per normal bar vs distance downstream for prominent lithologies in the study reach.

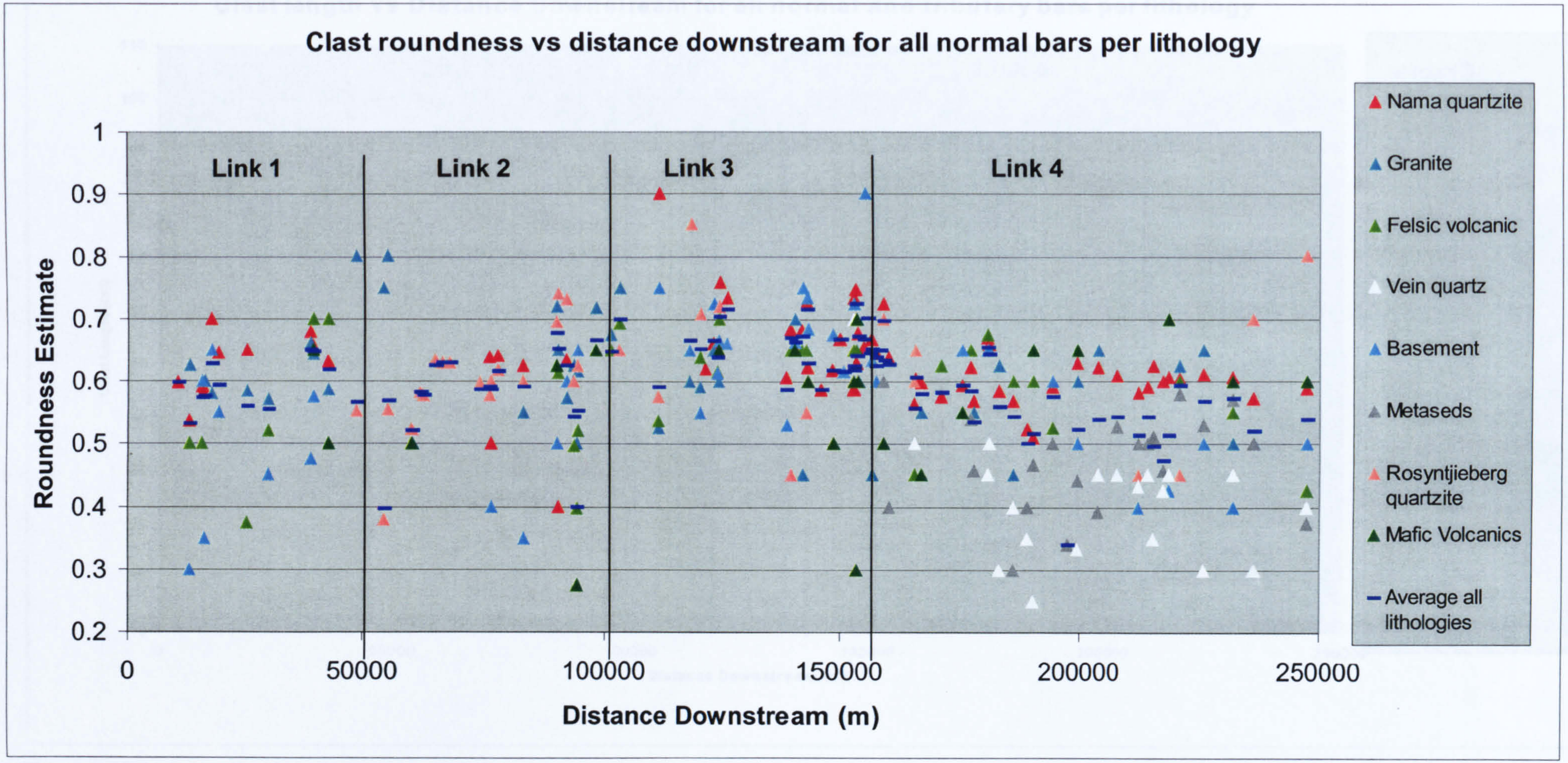

Figure 5.21 Average clast roundness per normal bar vs distance downstream for prominent lithologies in the study reach.

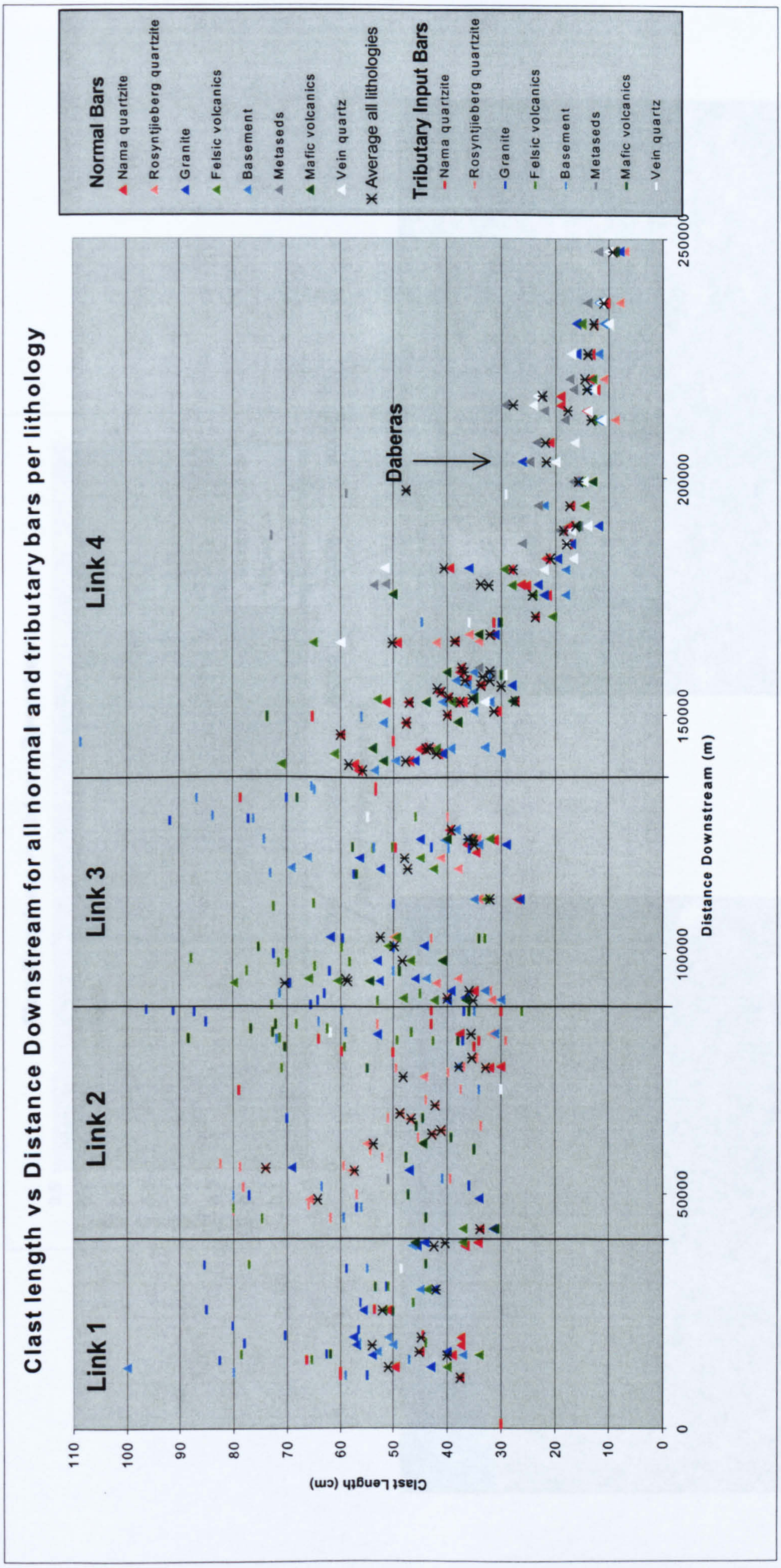

Figure 5.22 Average clast length per bar vs distance downstream for tributary and normal bars for prominent lithologies in the study reach.

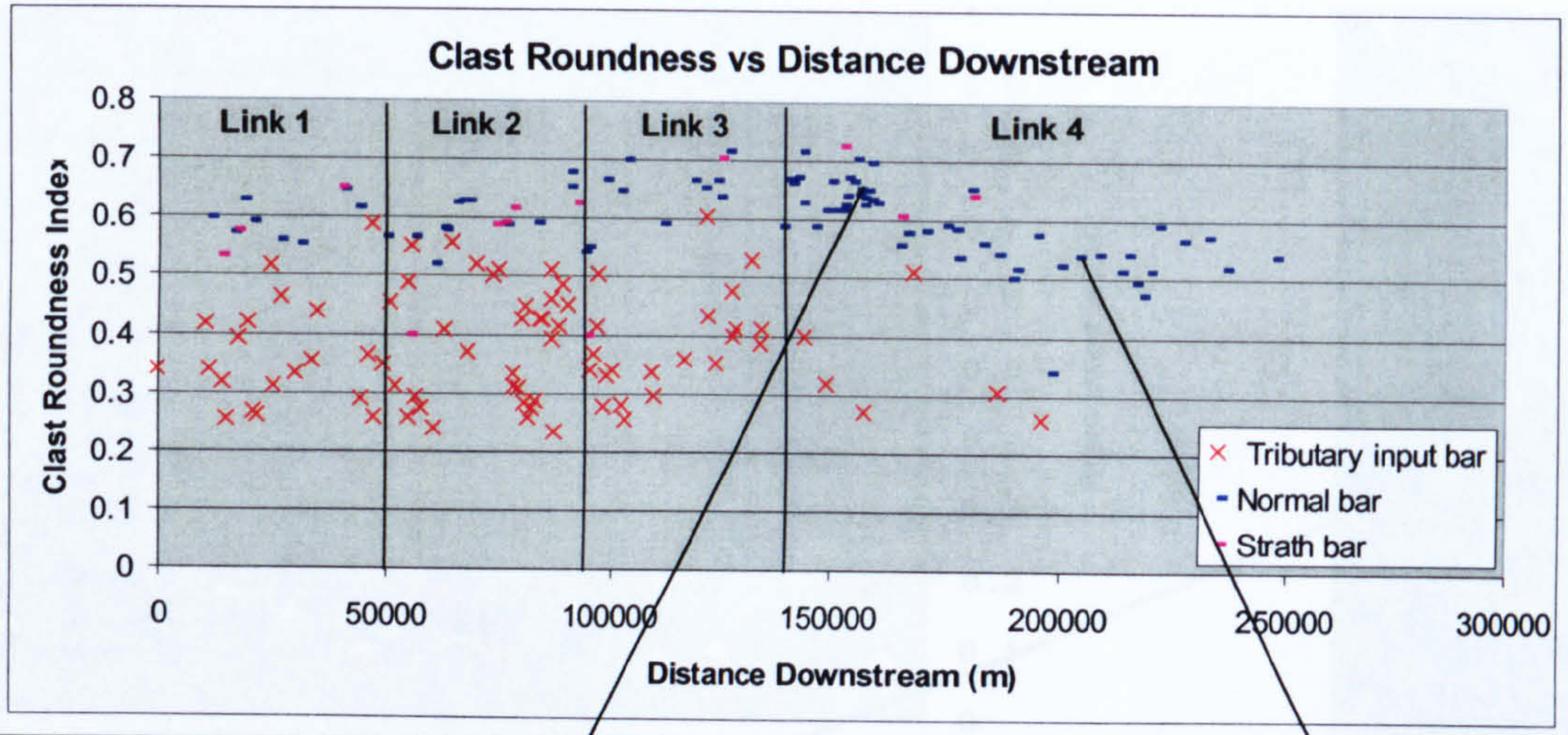

Figure 5.23 Clast roundness differences in proximal and distal normal bars in Link 4, mainly due to the decrease in rounding with decreasing clast size.

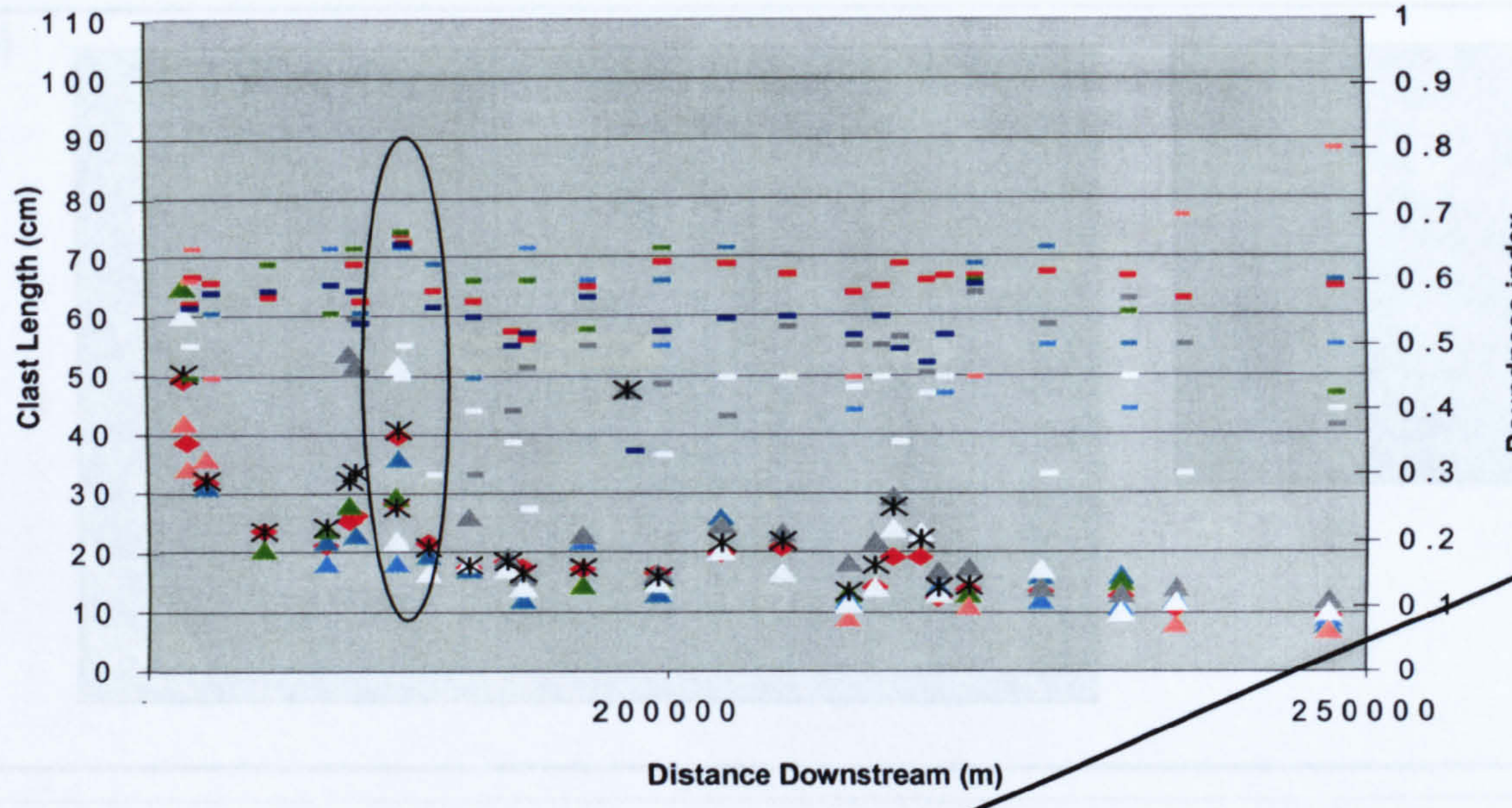

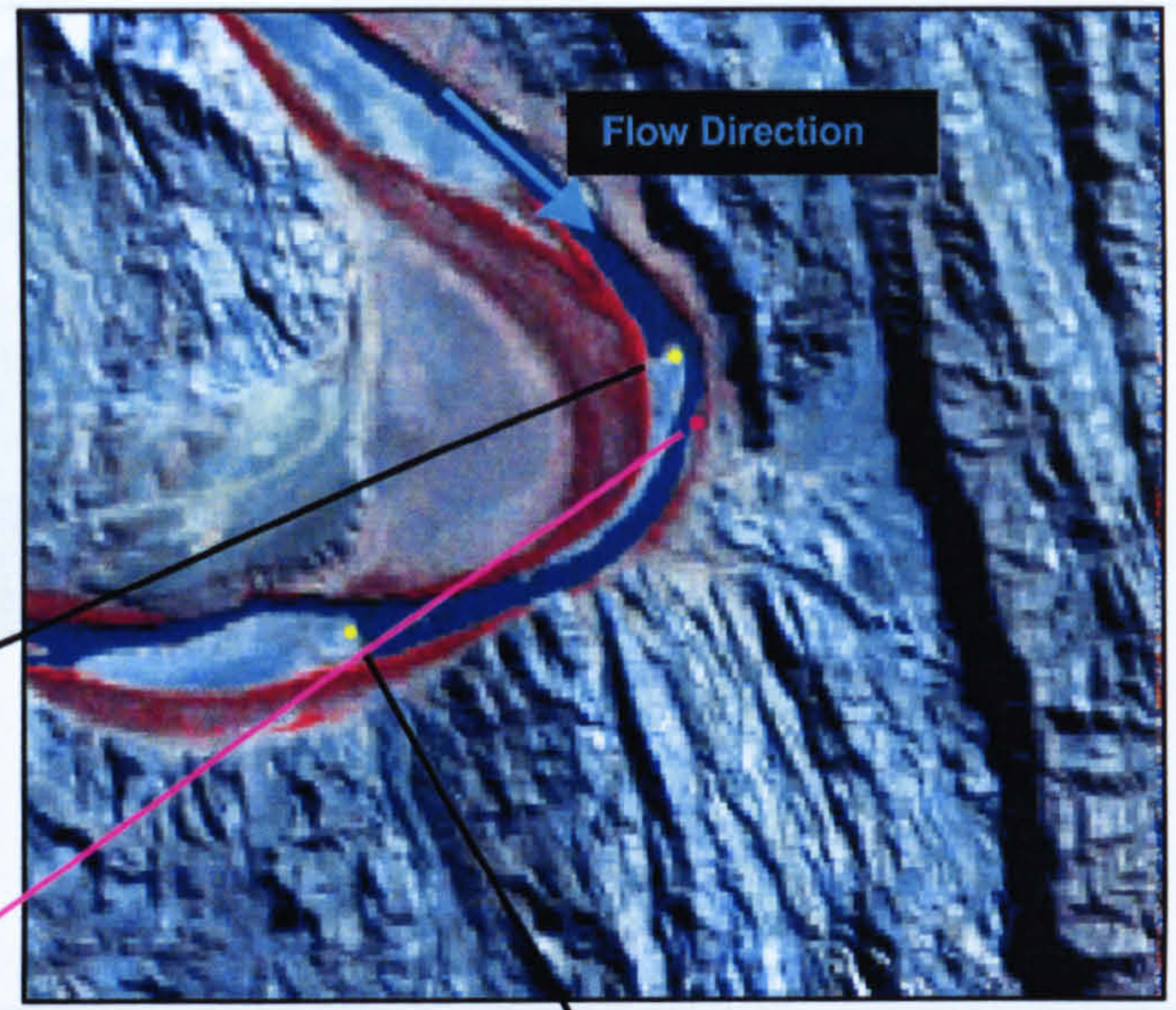

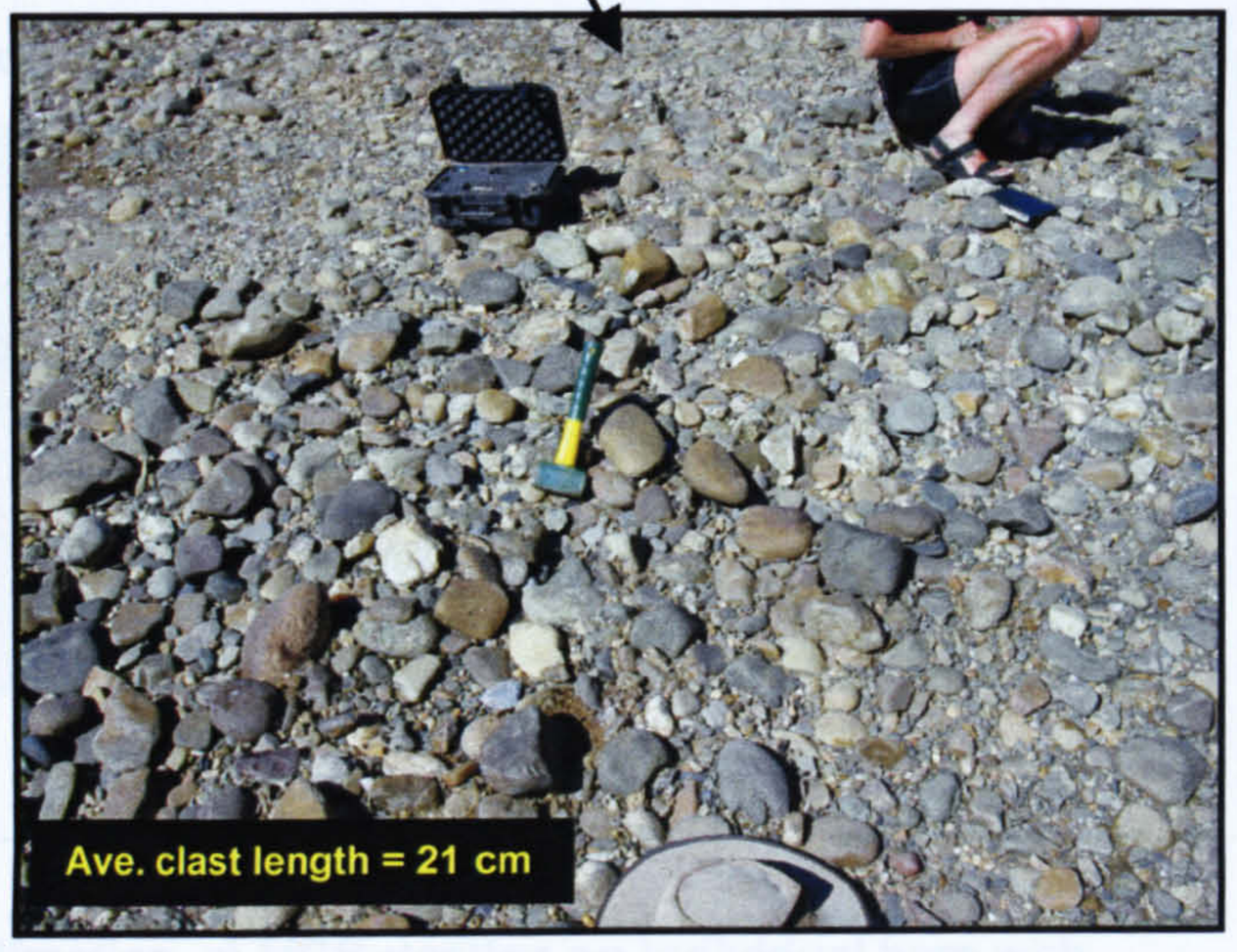

Figure 5.24 Clast size and roundness differences between adjacent point and strath bars.

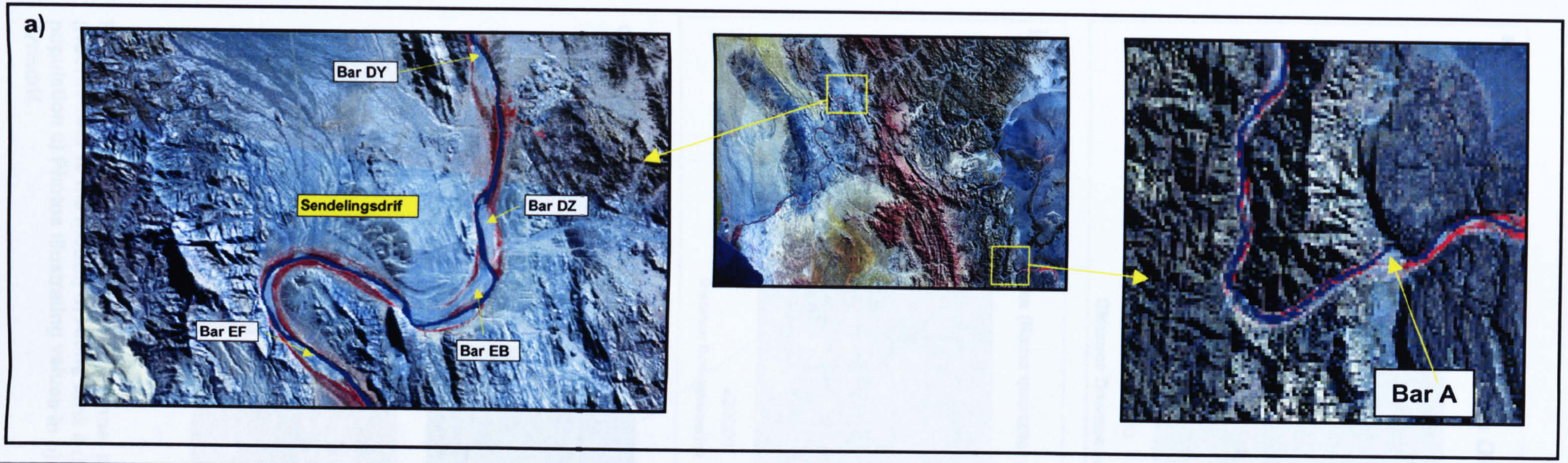

Figure 5.25 a) Location of selected bar measure sites b) MCS decline on individual bars in a downstream direction. c) MCS decline on individual bars with MCS data per bar for the entire study reach.

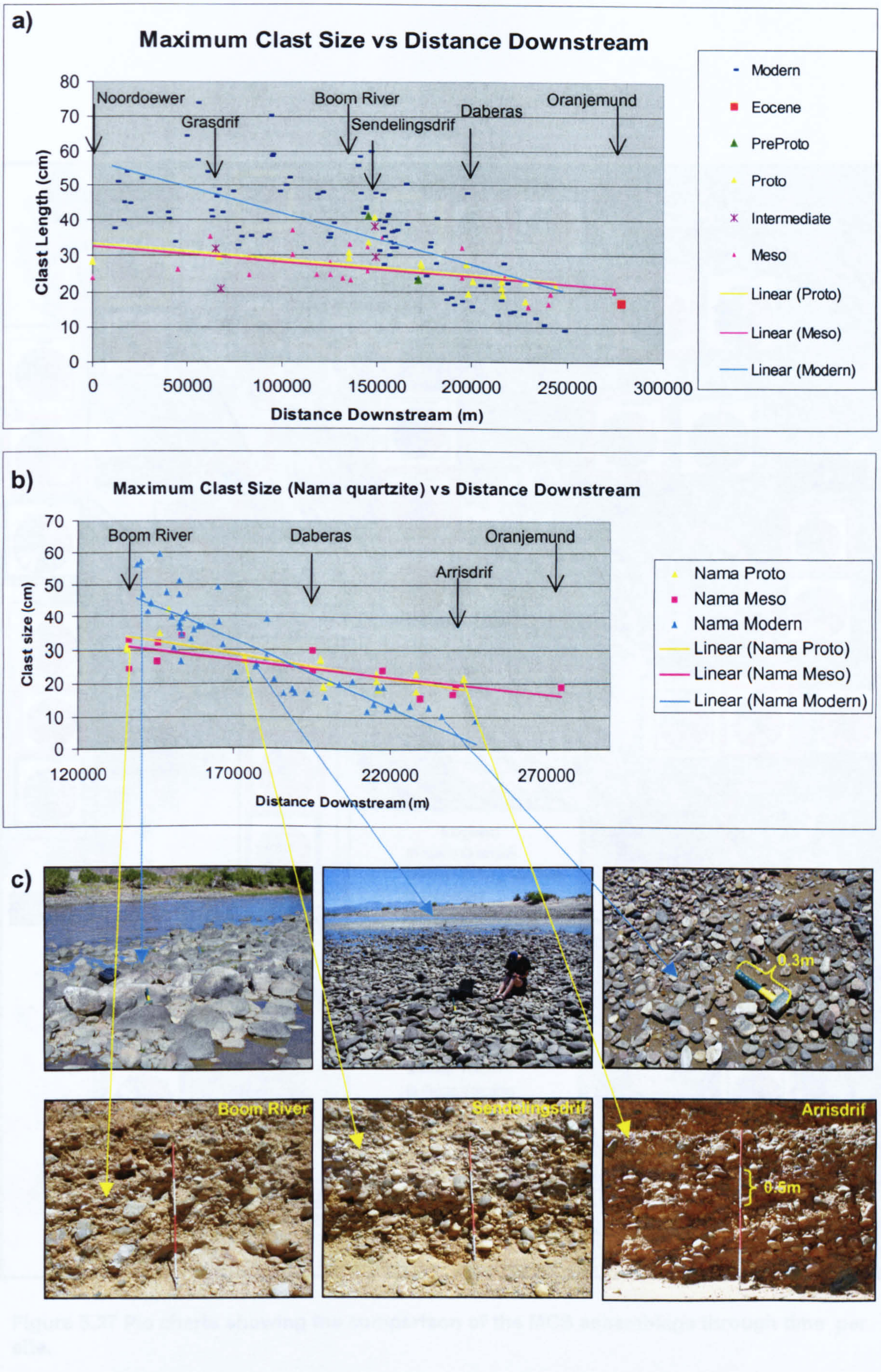

Figure 5.26 MCS vs distance along channel per gravel age. a) Along entire study reach (Noordoewer to the mouth) b) Along Link 4 (Boom River to the mouth) for Nama quartzite population c) Photos illustrating values in b) at the Boom River, Sendelingsdrif and Arrisdrif.

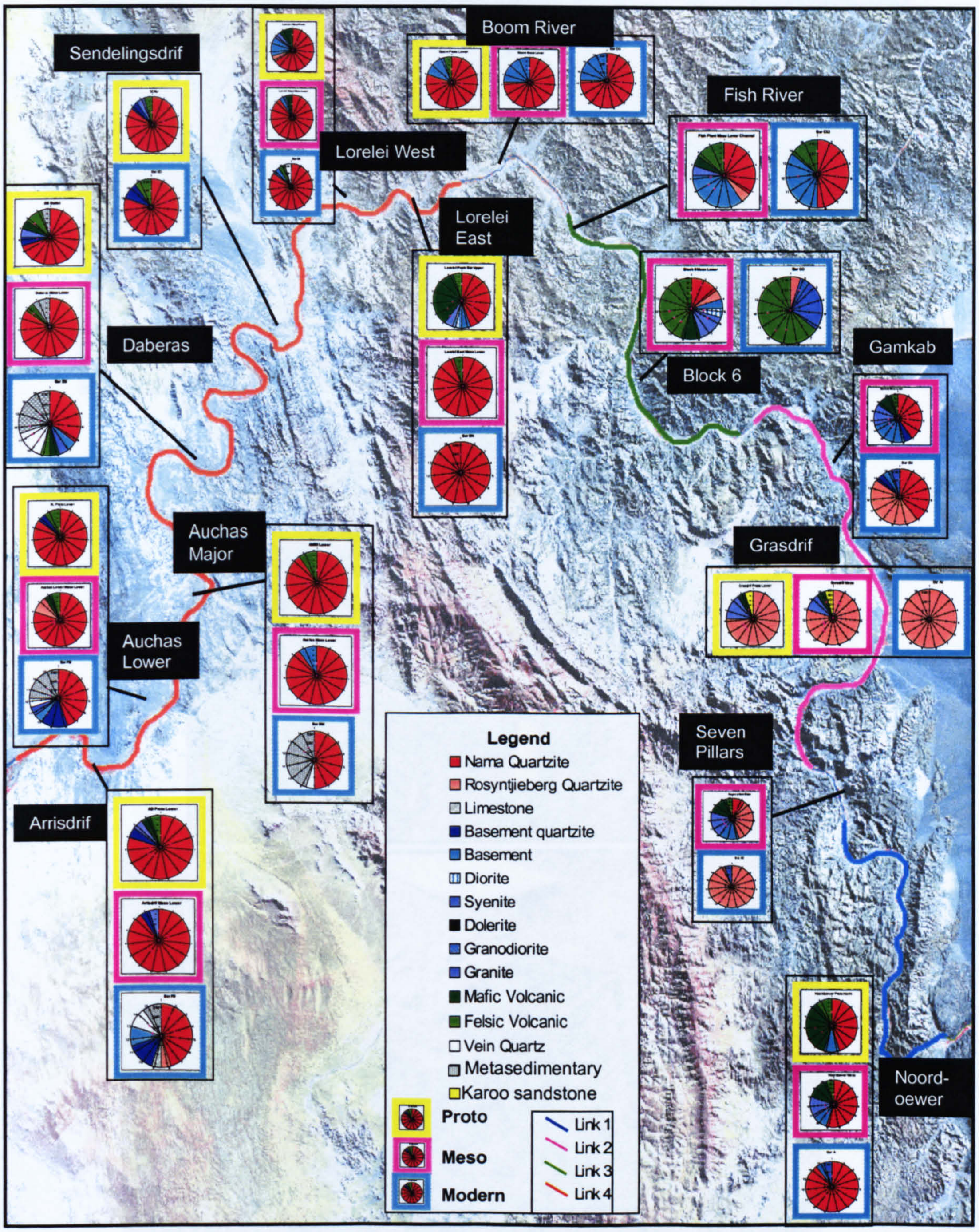

Figure 5.27 Pie charts showing the comparison of the MCS assemblage through time per site.

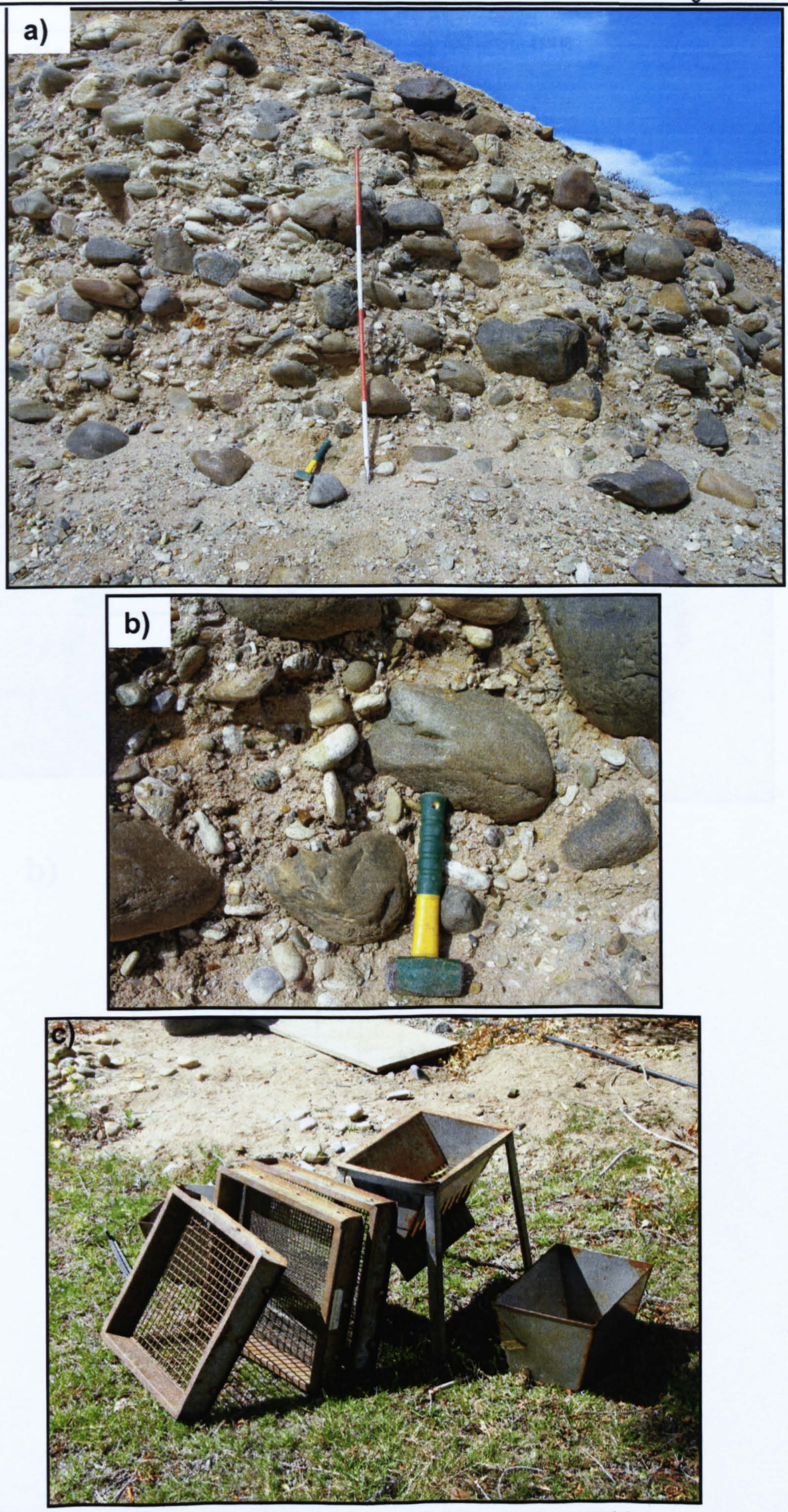

Figure 6.1 a) Typical face of gravel that was sampled for clast assemblage analysis. Ranging rod is 2m long. b) Close-up view of face illustrating area which was excavated and sieved. c) Sampling equipment used.

a)

Size Fraction (mm)	No. of Clasts Sorted	% Error
+300	20-30	14-16
200-300	20-30	14-16
90-200	50	8-14
40-90	50	8-14
25-40	50	8-14
16-25	100	4-10
8-16	100	4-10
3-8	100	4-10

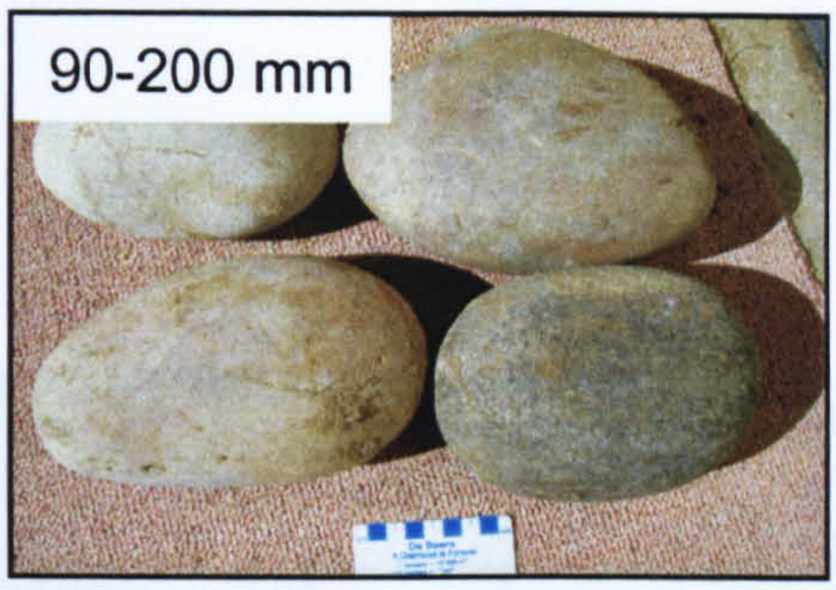

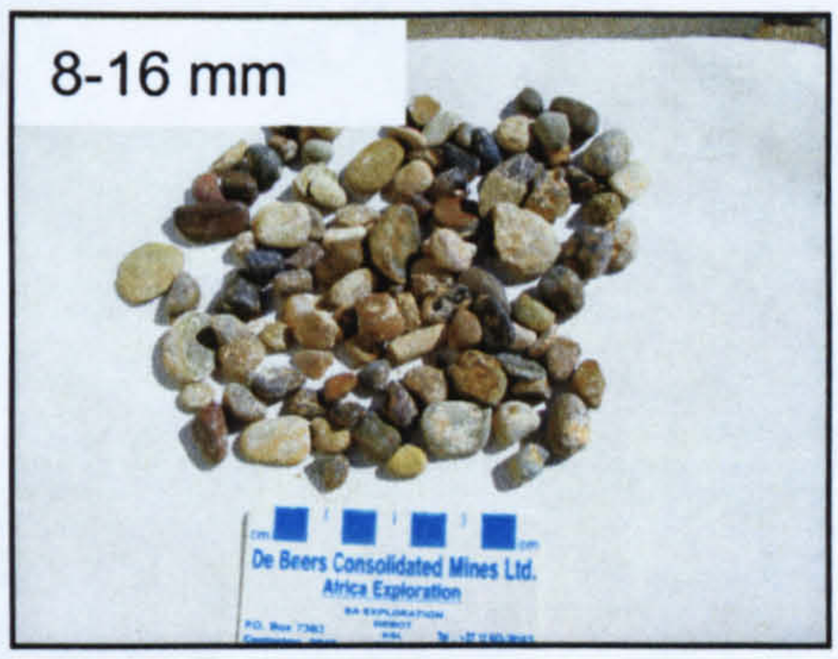

b)

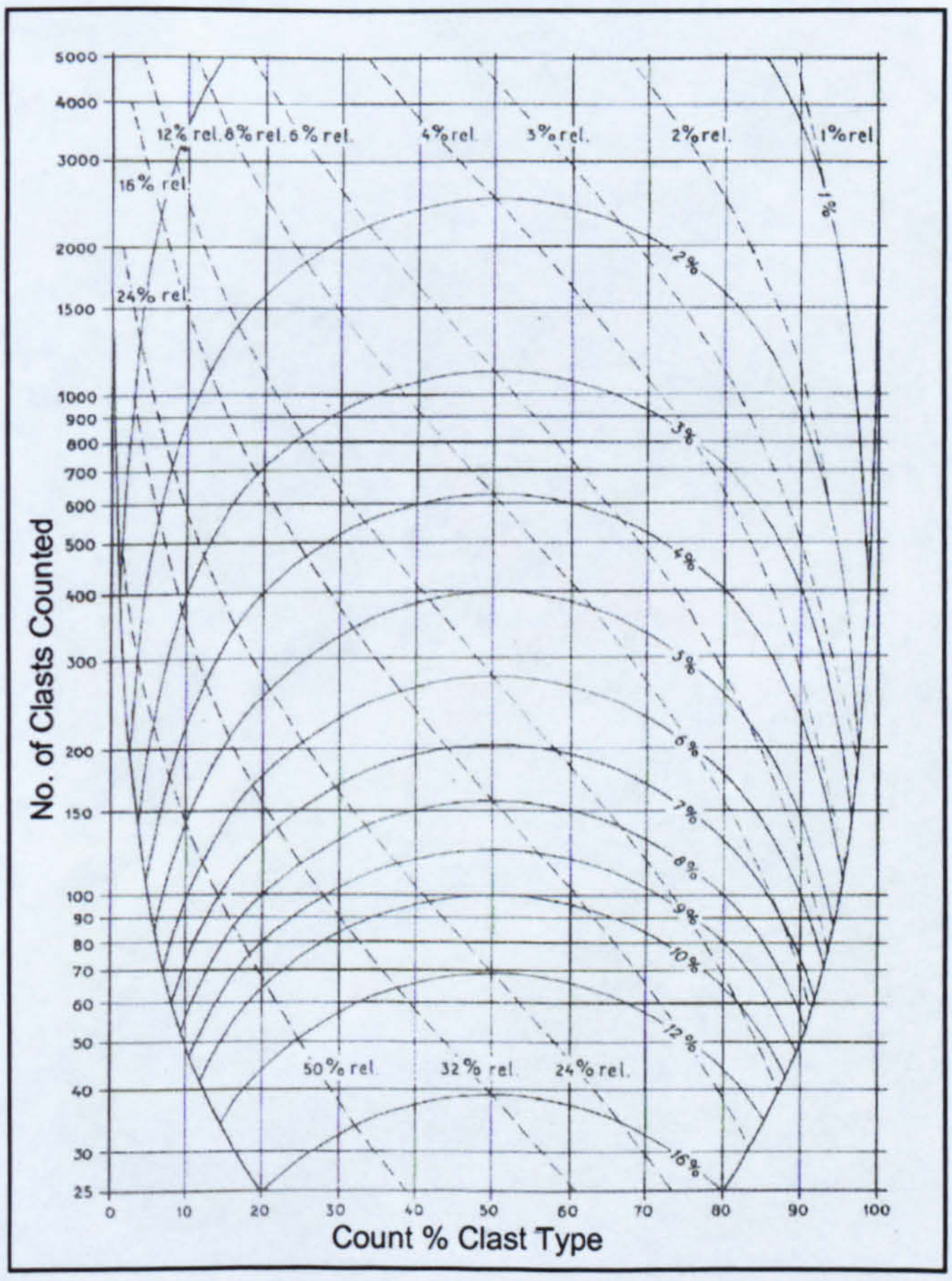

Figure 6.2 a) Clasts assemblage analysis per size fraction: amount of clasts sorted per size fraction and their percentage relative error, based on twice the standard deviation. b) Visual chart for estimating % error (after van der Plas & Tobi, 1965).

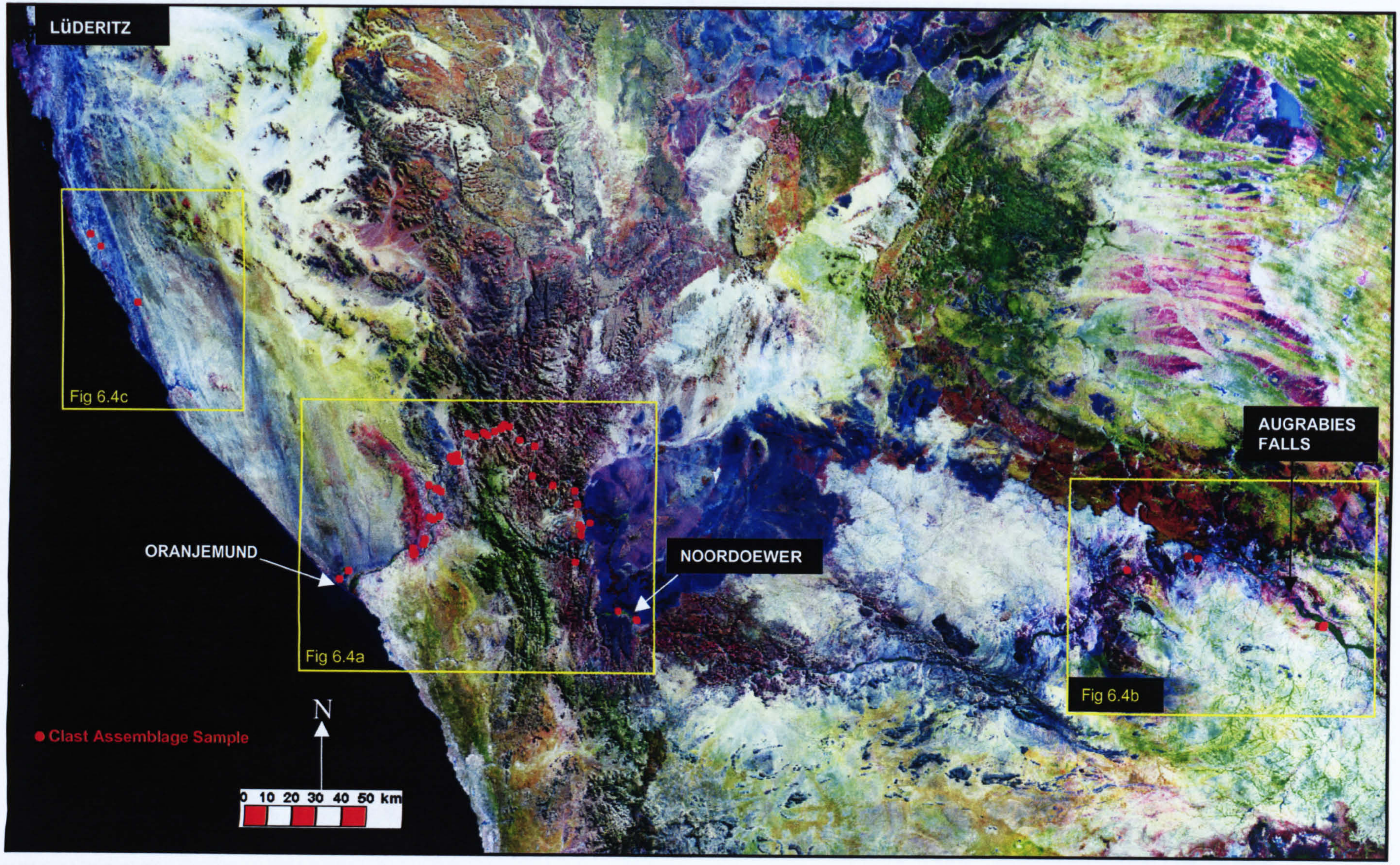

Figure 6.3 Regional satellite image from Augrabies Falls to the mouth showing the location of the clast assemblage samples taken in this study.

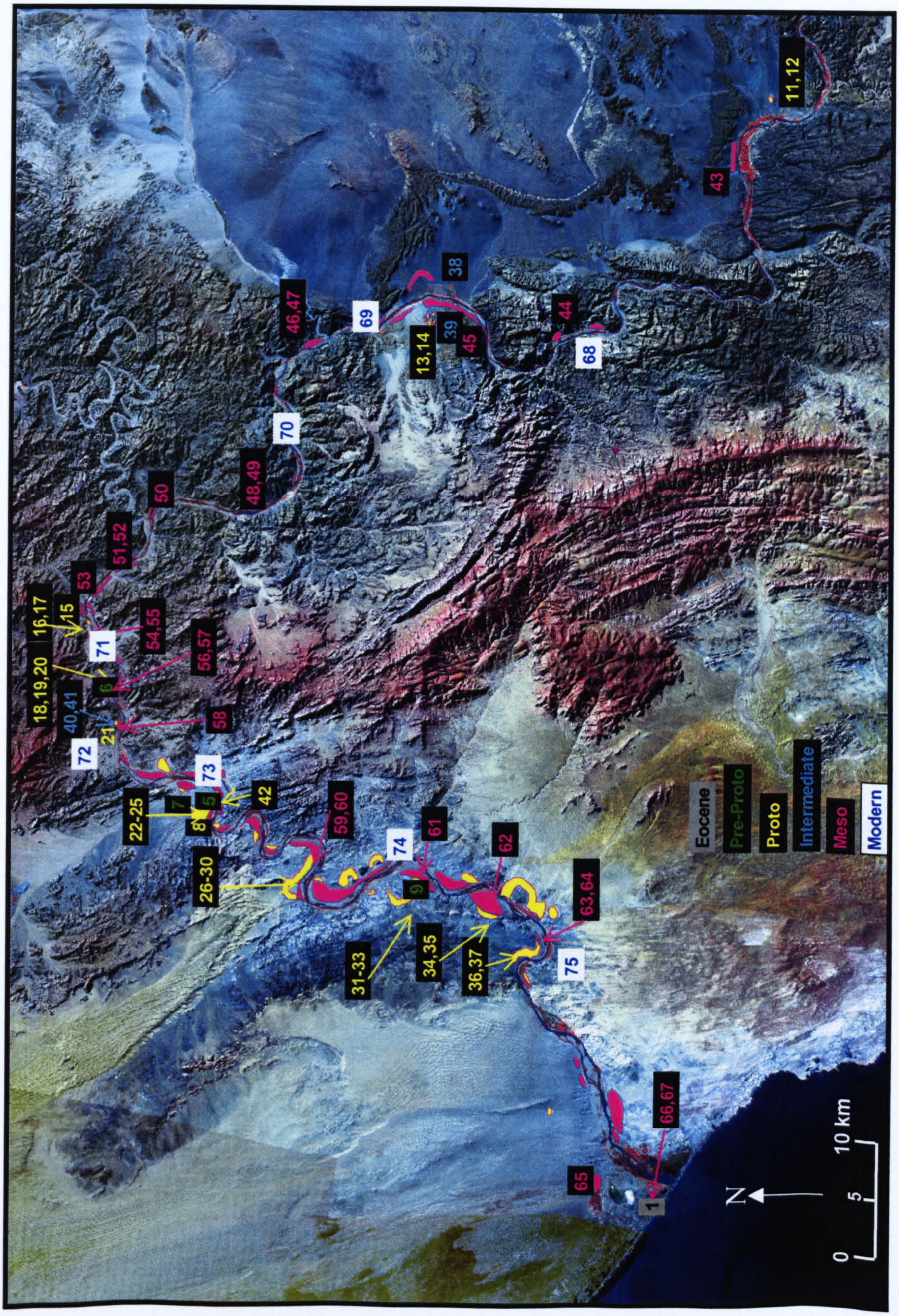

Figure 6.4a) Clast assemblage samples analysed in the study reach between Noordoewer and the mouth.

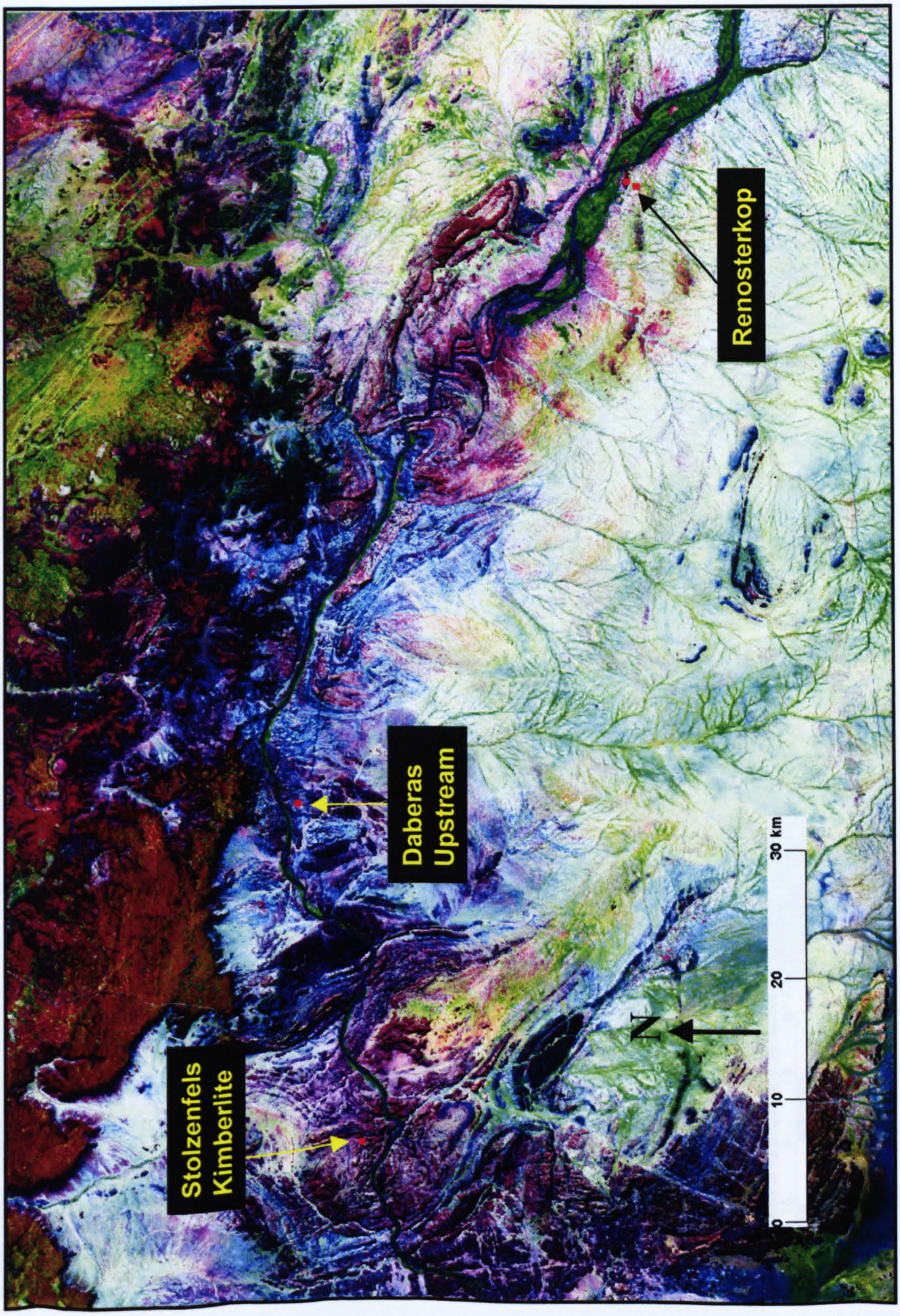

Figure 6.4b) Clast assemblage samples collected in the Augrabies Falls area.

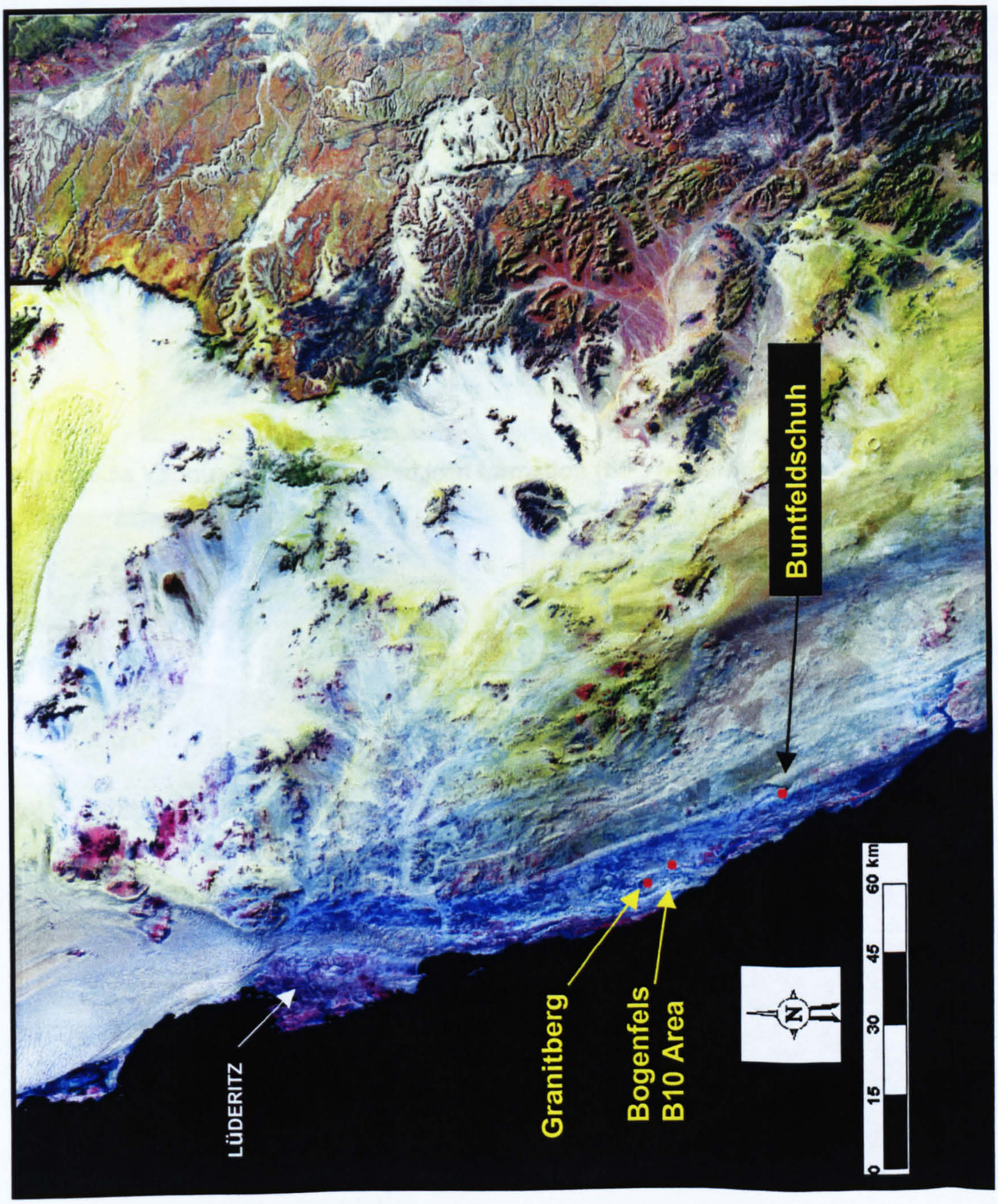

Figure 6.4c) Clast assemblage samples analysed in the Buntfeldschuh/Bogenfels Area.

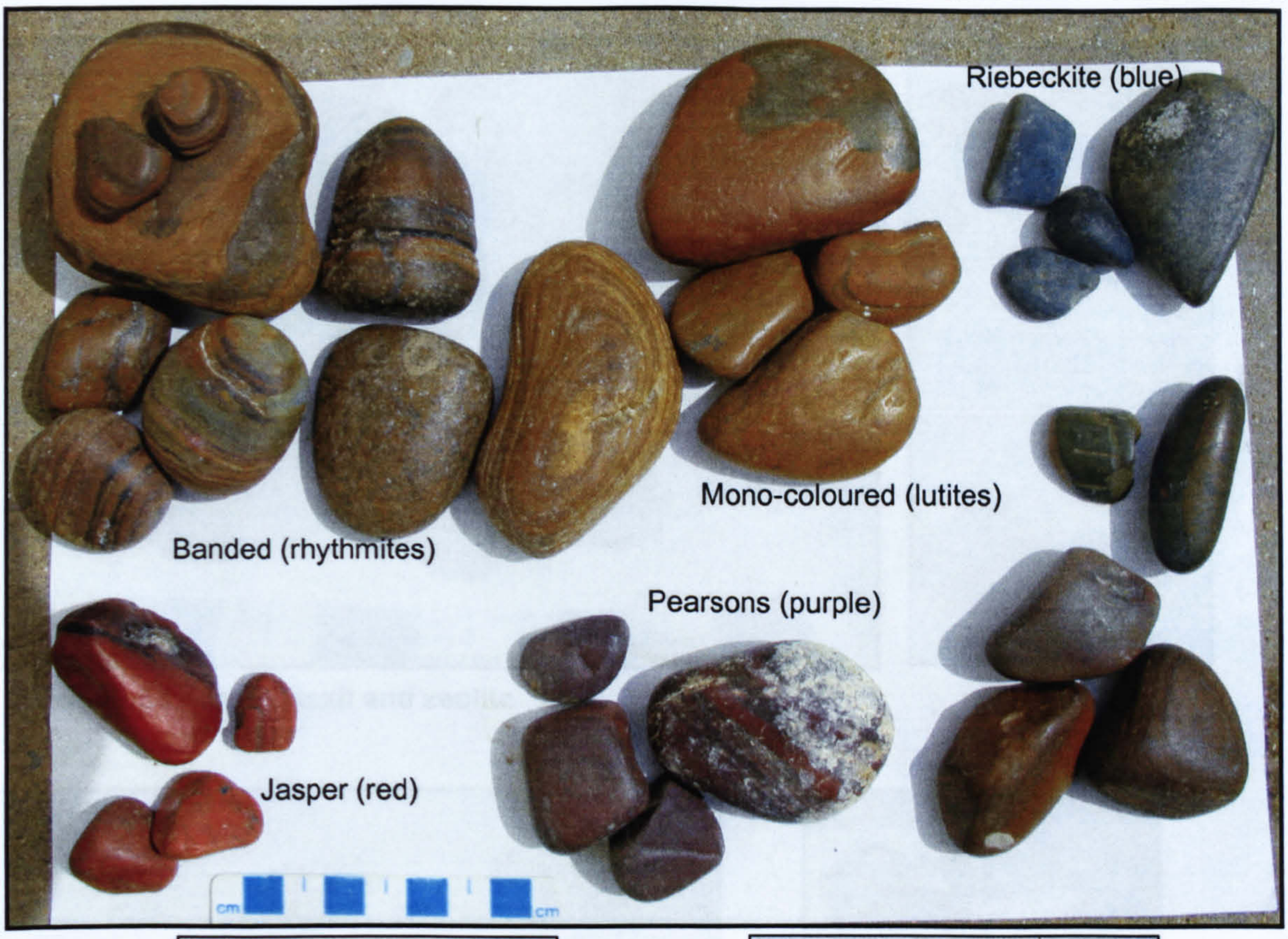

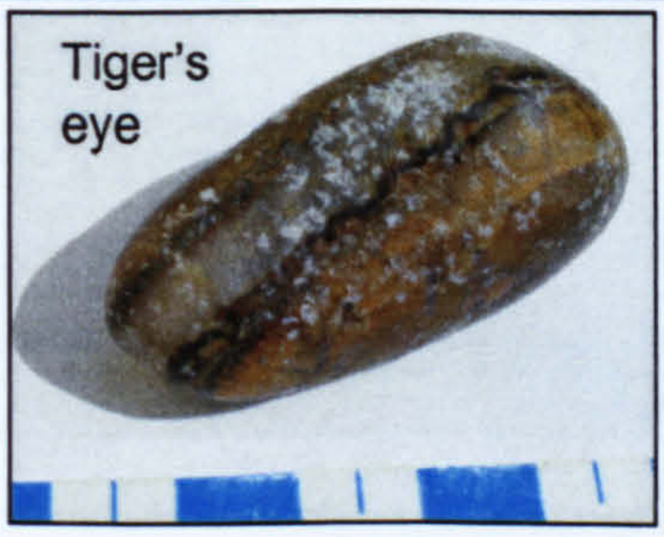

Figure 6.5a Various types of banded iron formation (BIF) from the Transvaal Supergroup.

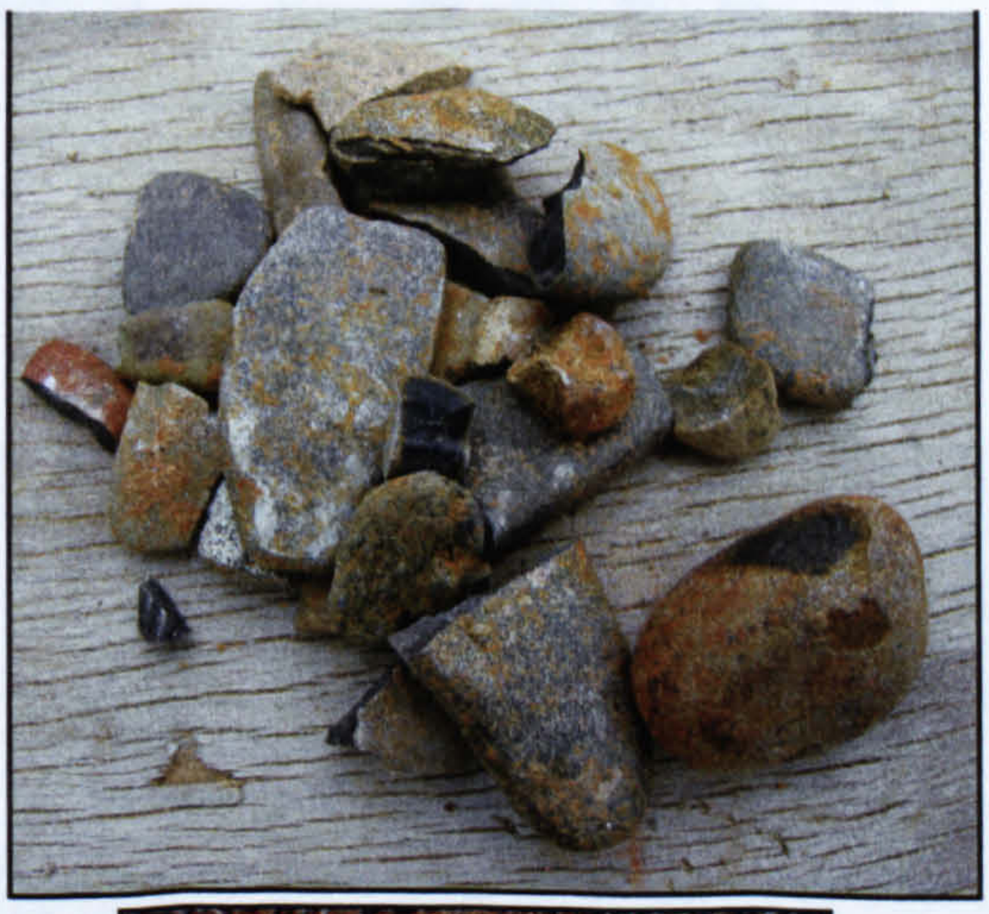

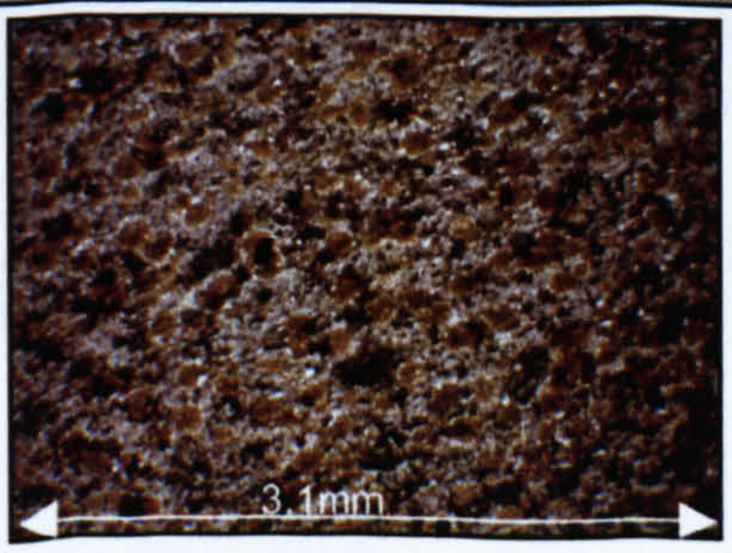

Figure 6.5b Karoo sandstones, shales and hornfels.

Figure 6.5c Karoo basalt and zeolite

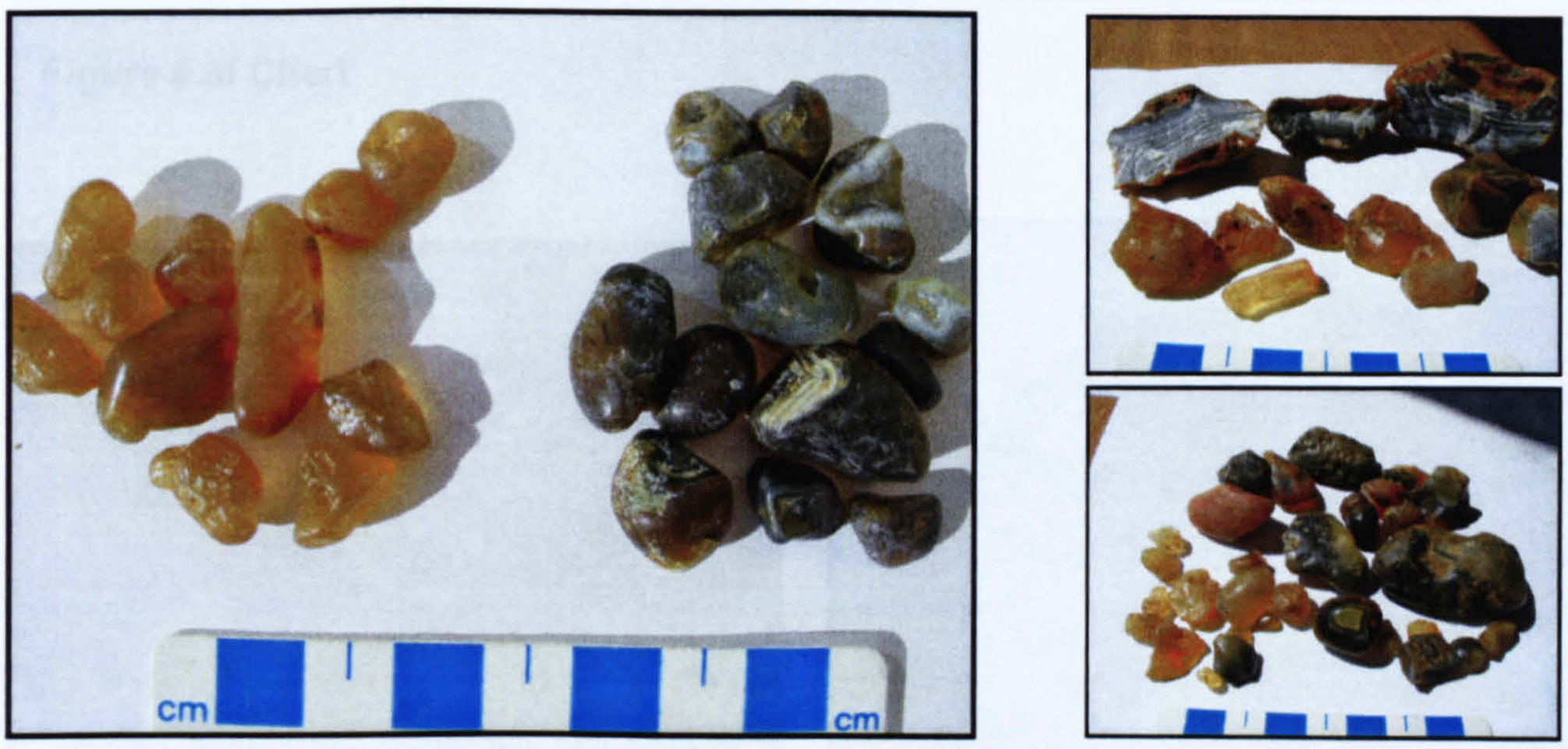

Figure 6.5d Vaal River type agate

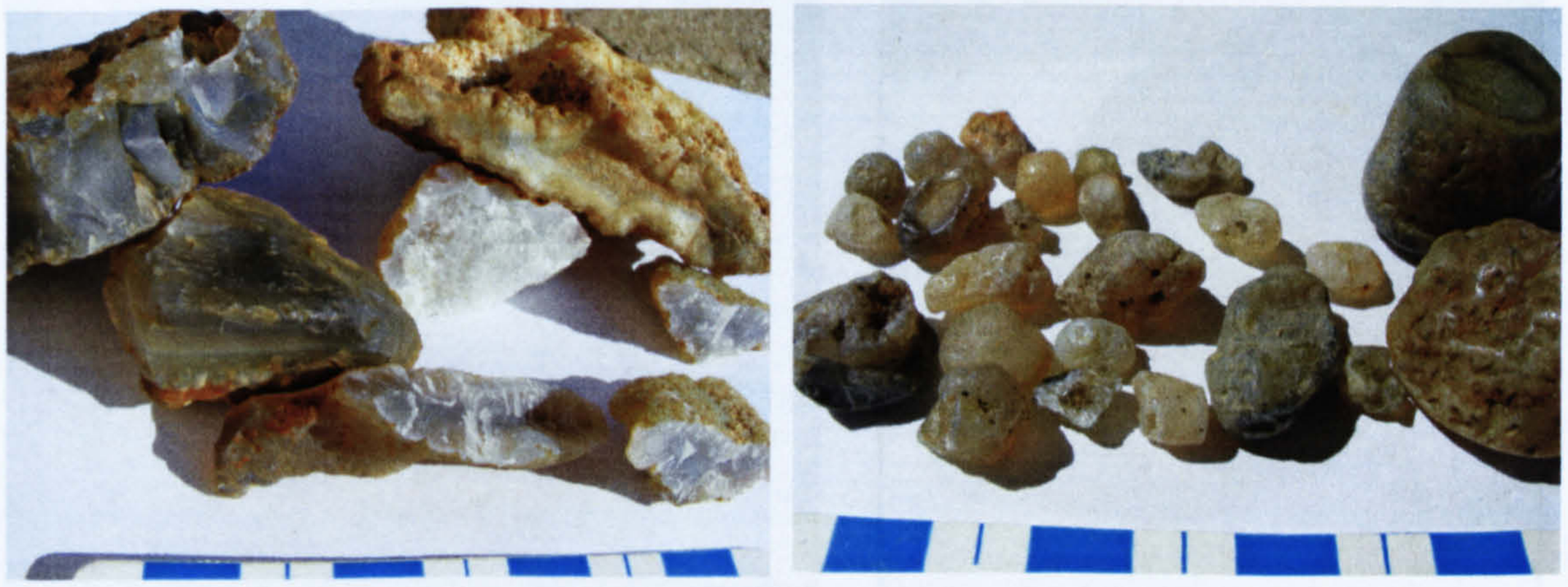

Figure 6.5e Orange River type agate

Figure 6.5f Chert

Figure 6.5g Epidosite

Figure 6.5h Feldspar

Figure 6.5i Makwassie porphyry

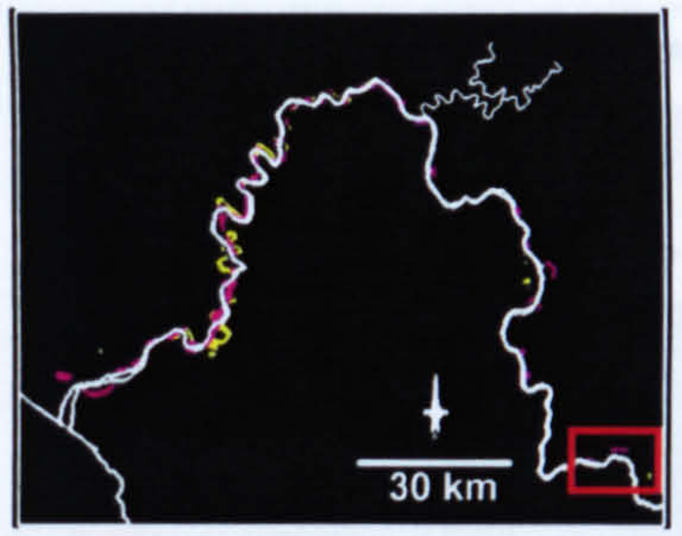

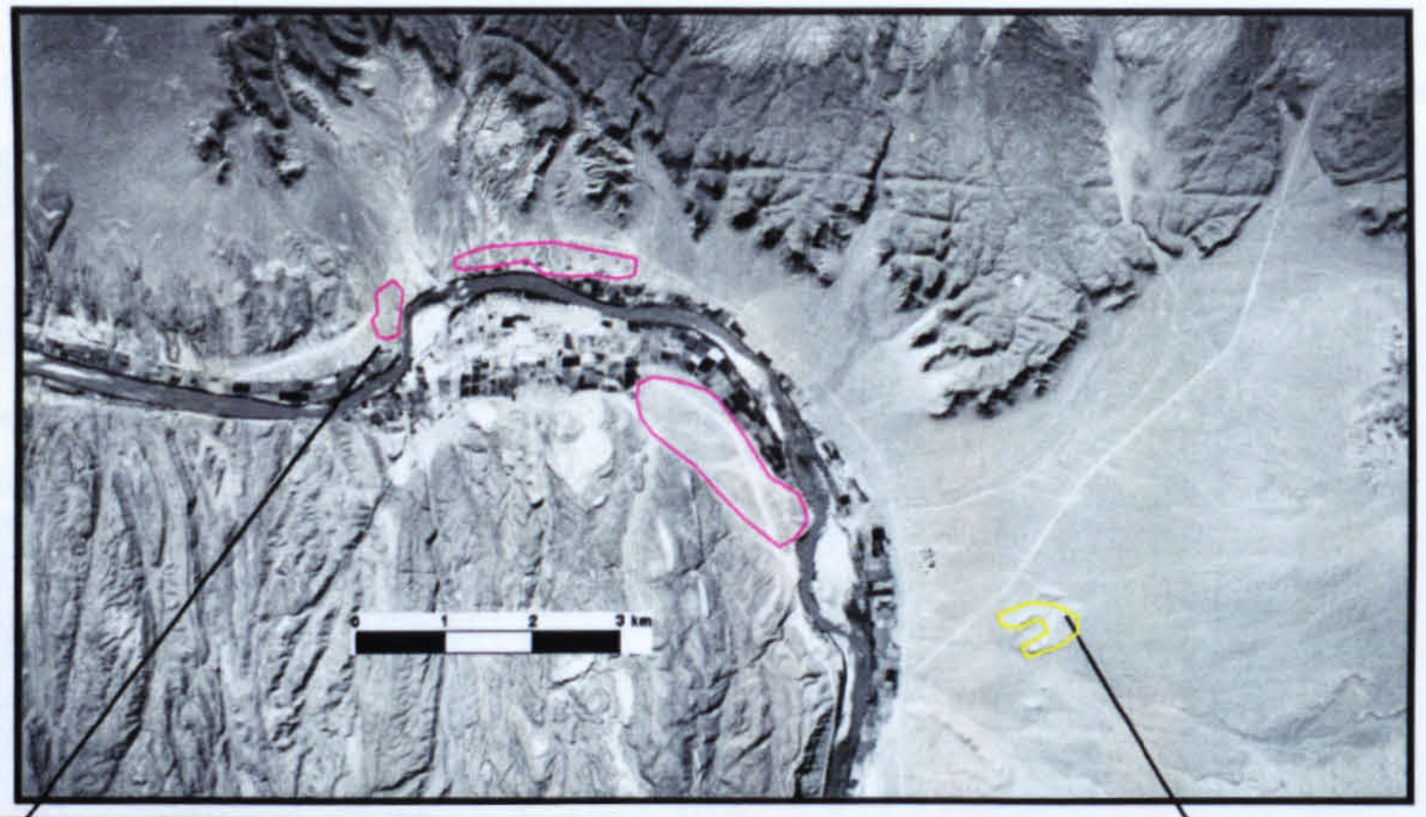

Proto terrace
Intermediate Terrace
Meso terrace

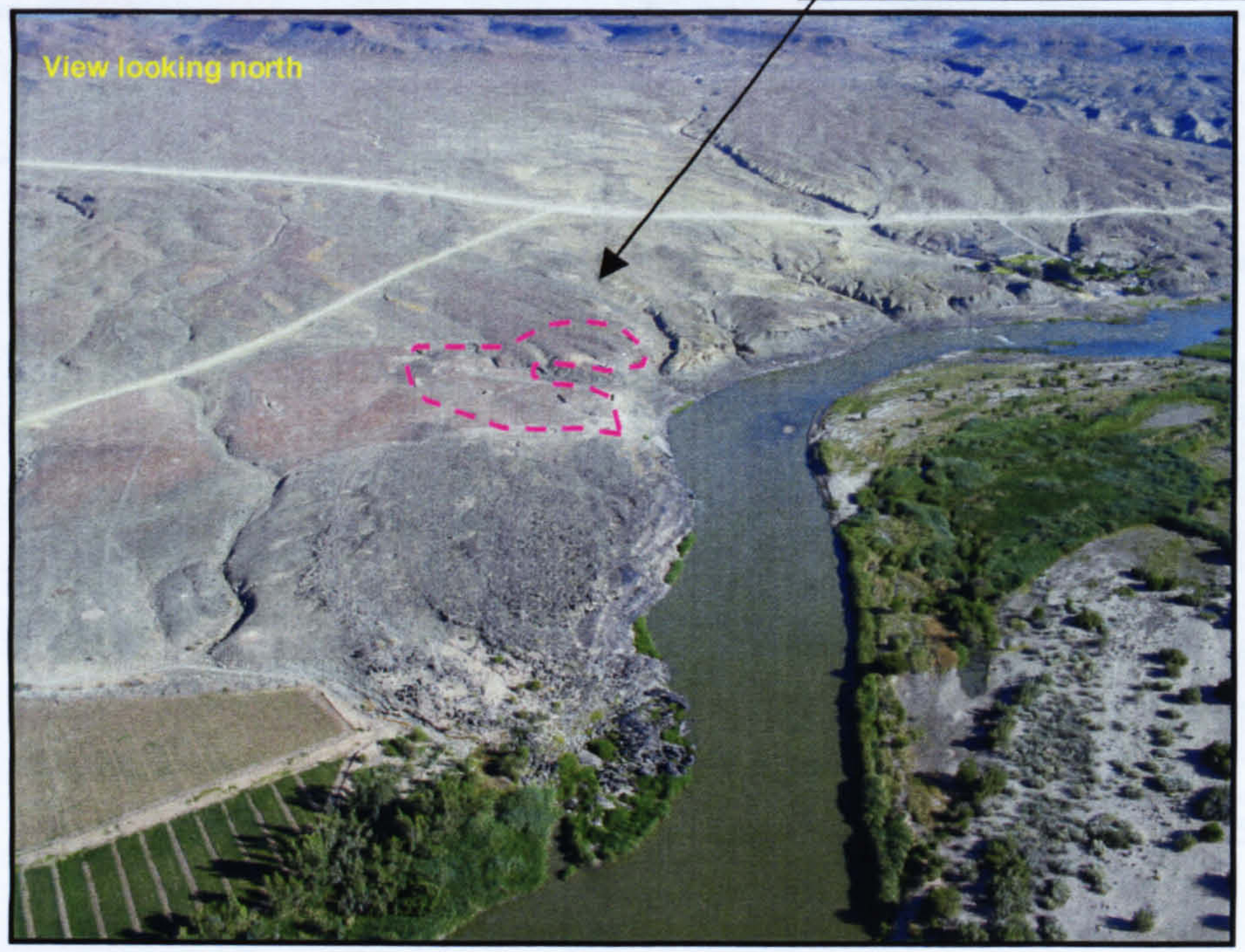

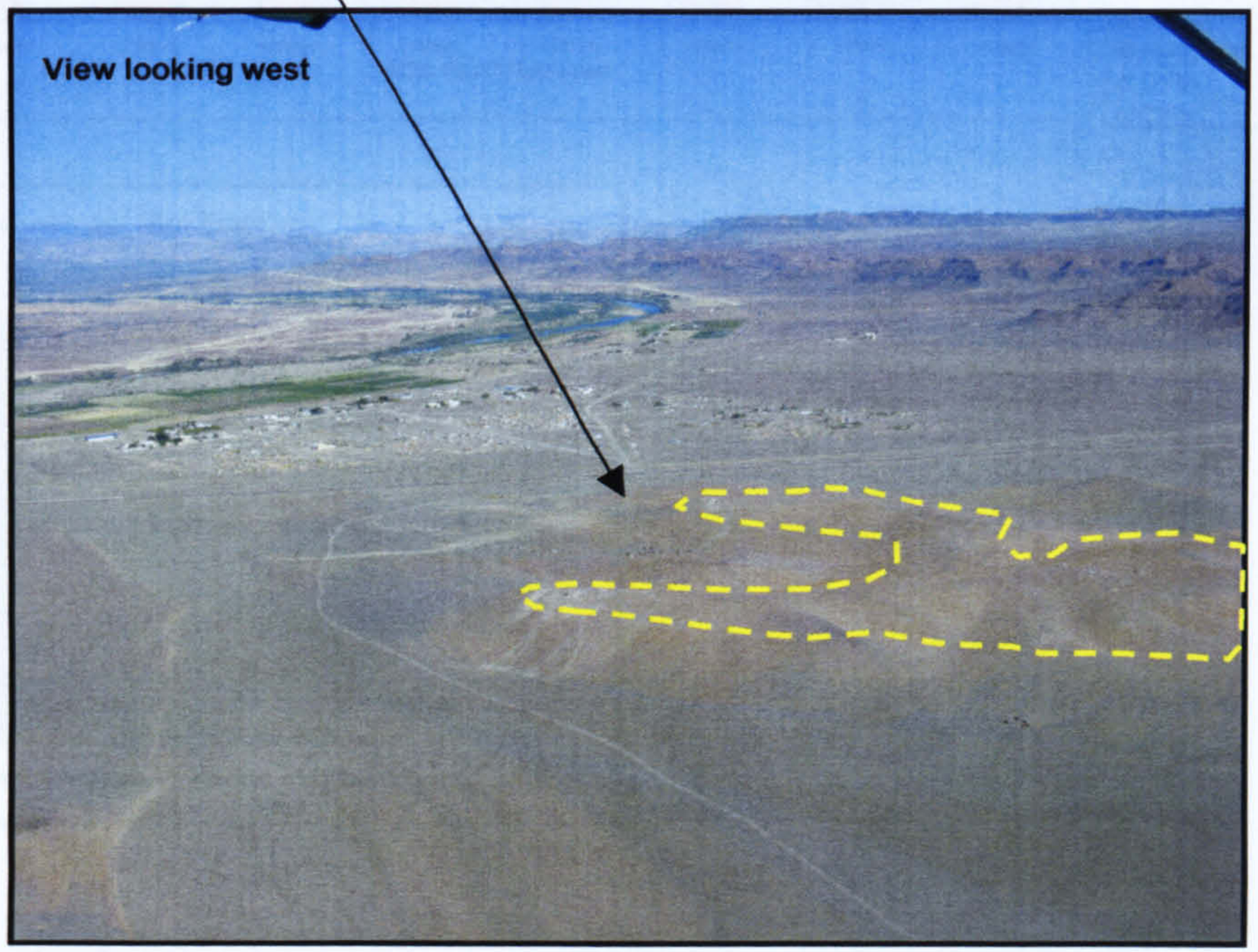

Figure 6.6 Distribution of Proto and Meso terraces in the Noordoewer area.

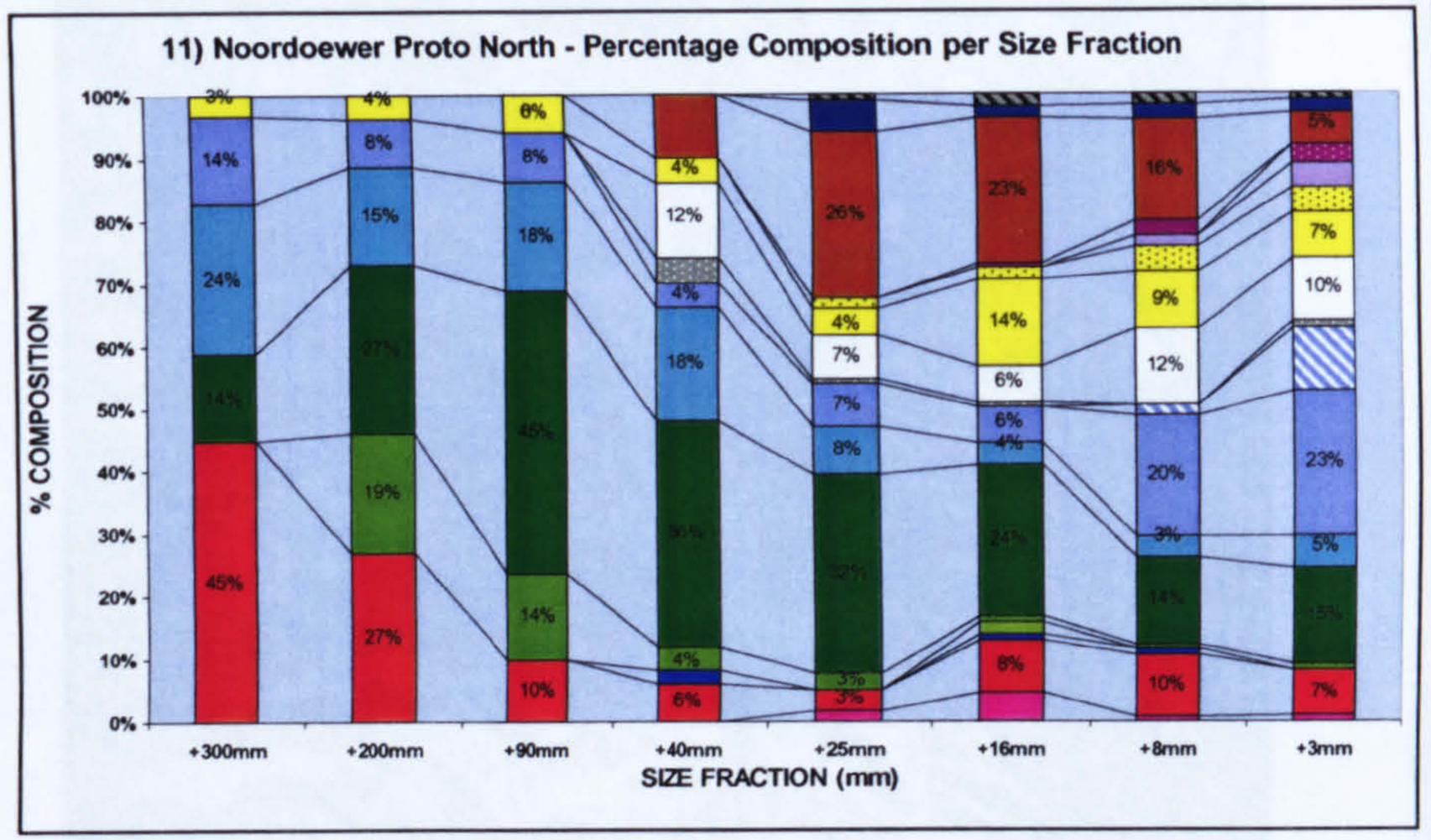

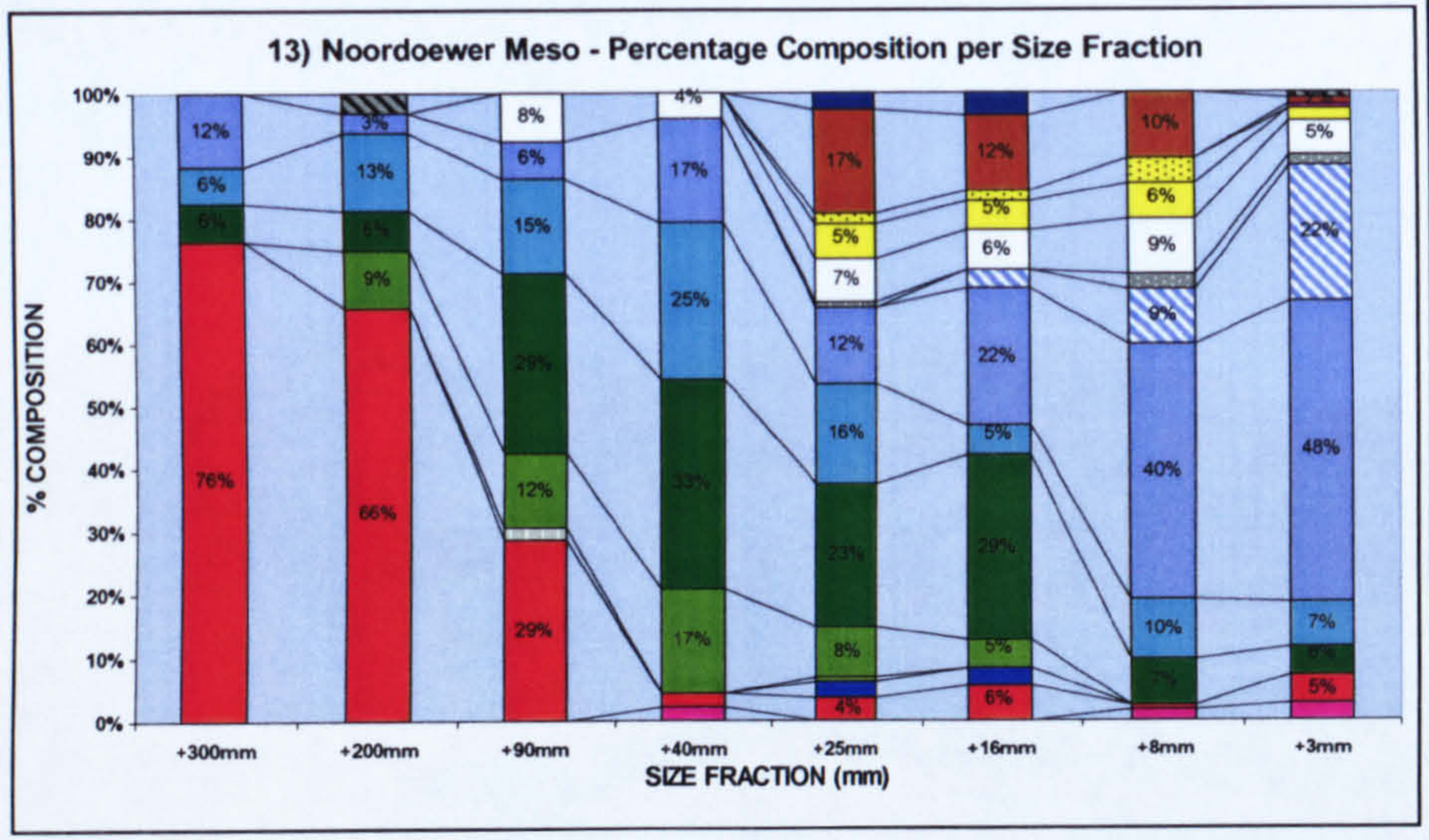

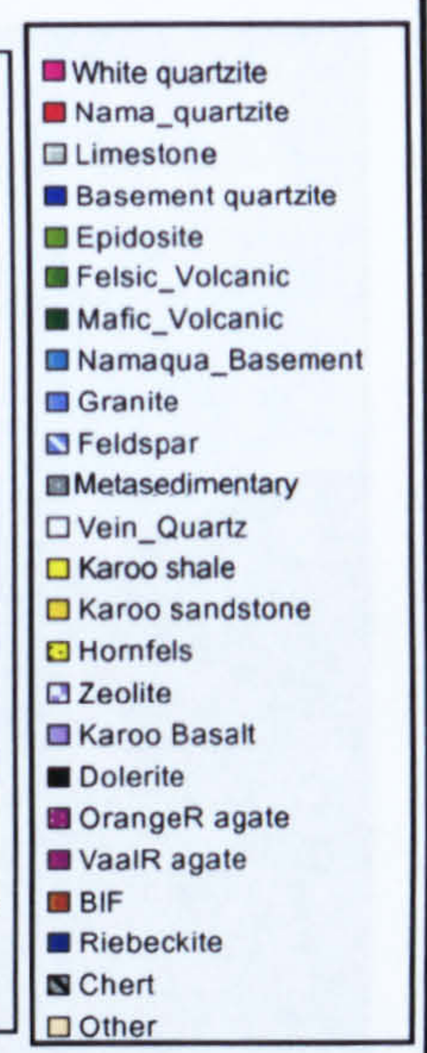

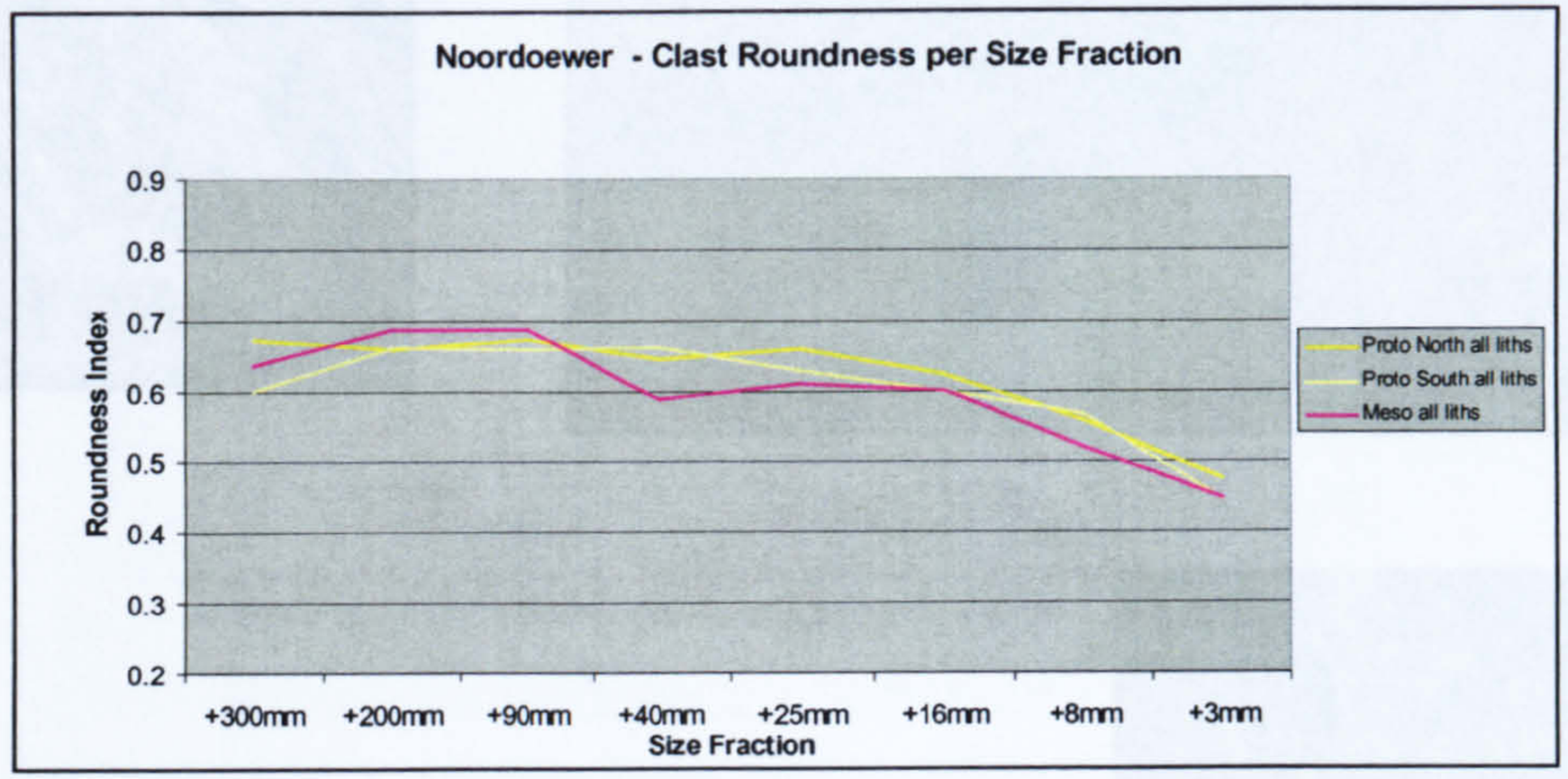

Figure 6.7 Clast type proportions per size fraction and average clast roundness per size fraction for samples in the Noordoewer area.

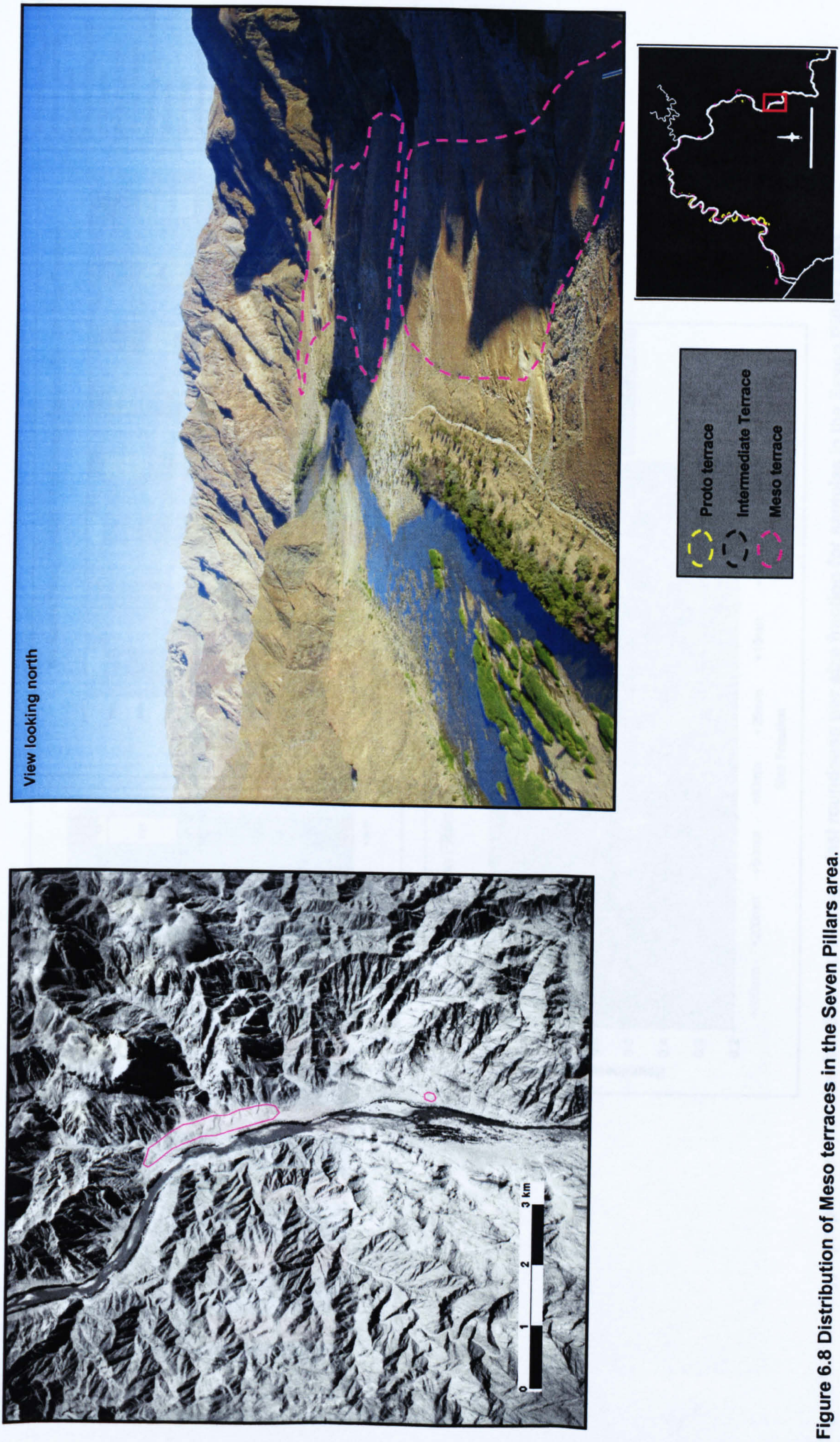

Figure 6.8 Distribution of Meso terraces in the Seven Pillars area.

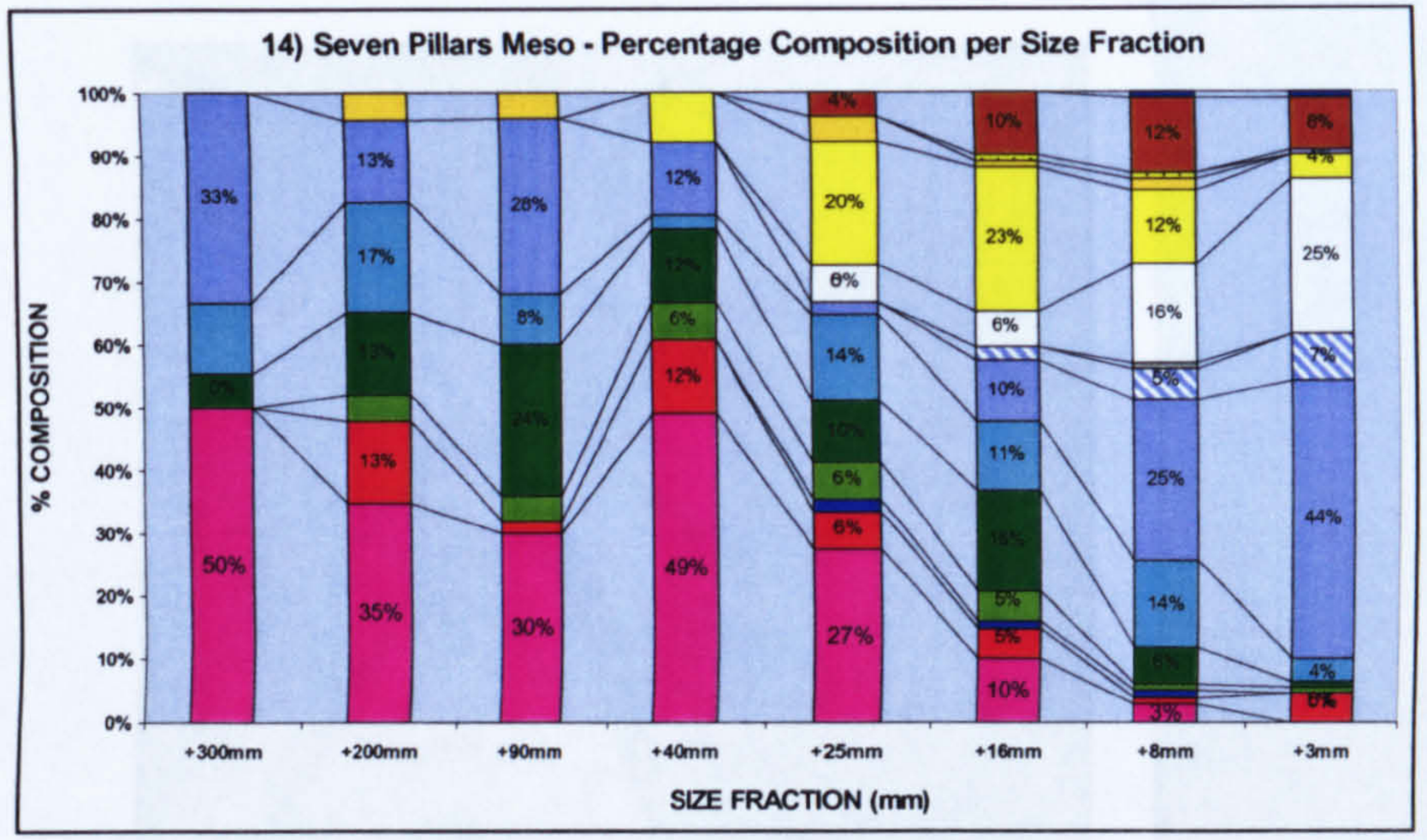

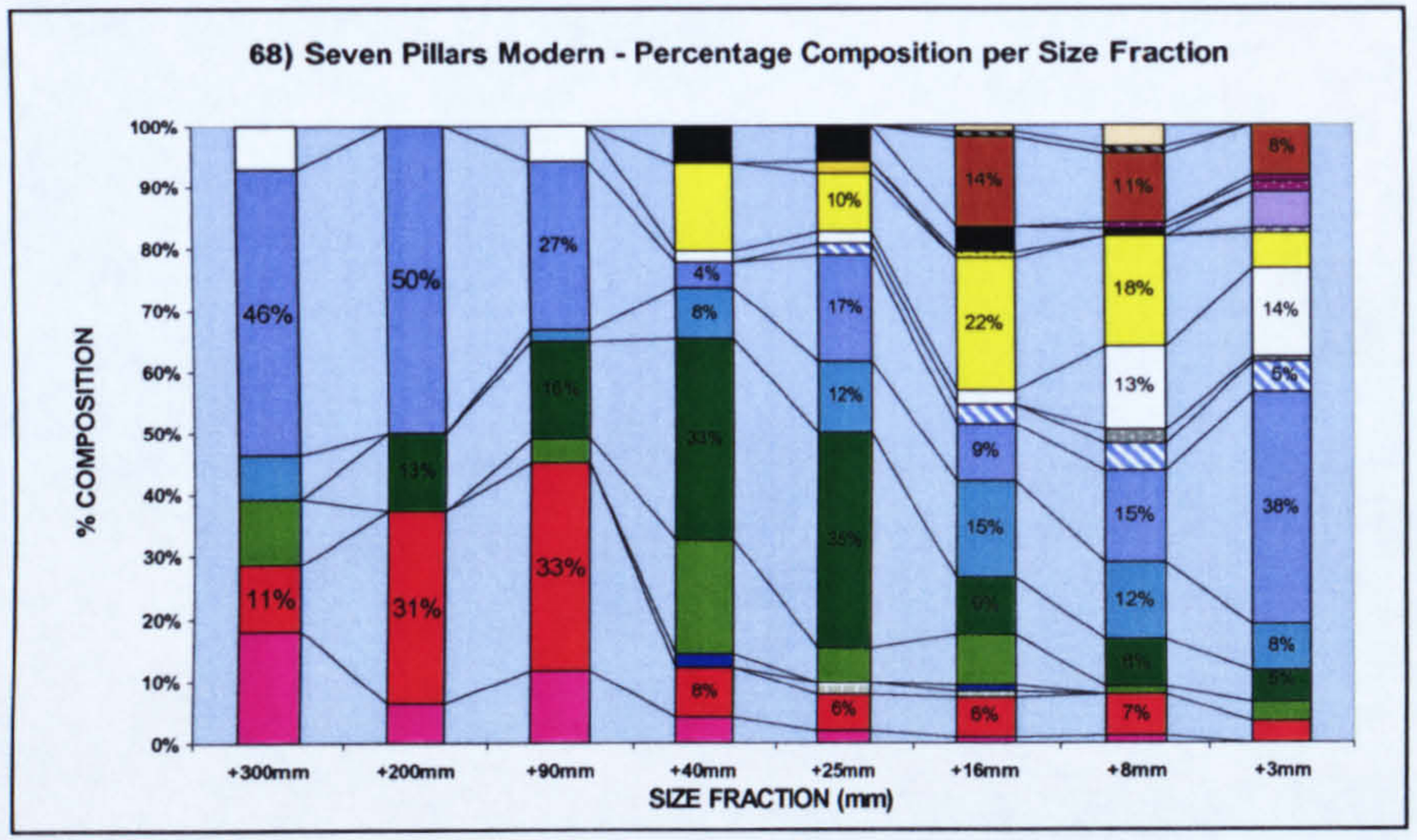

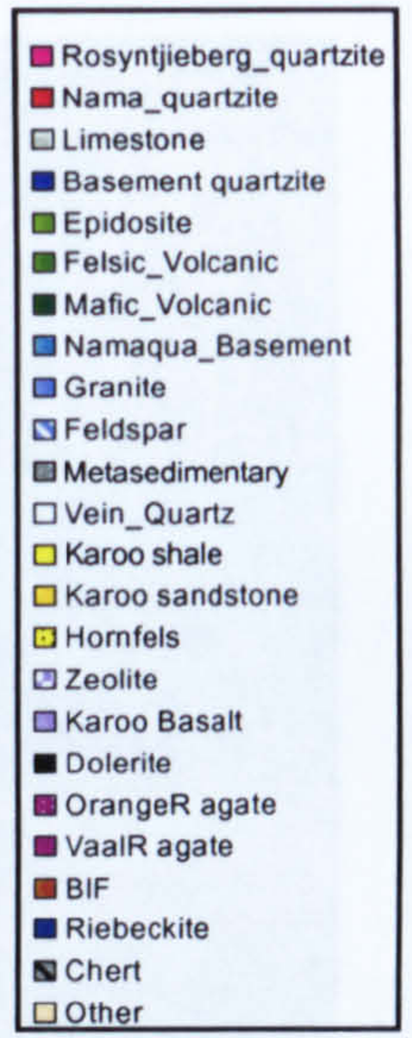

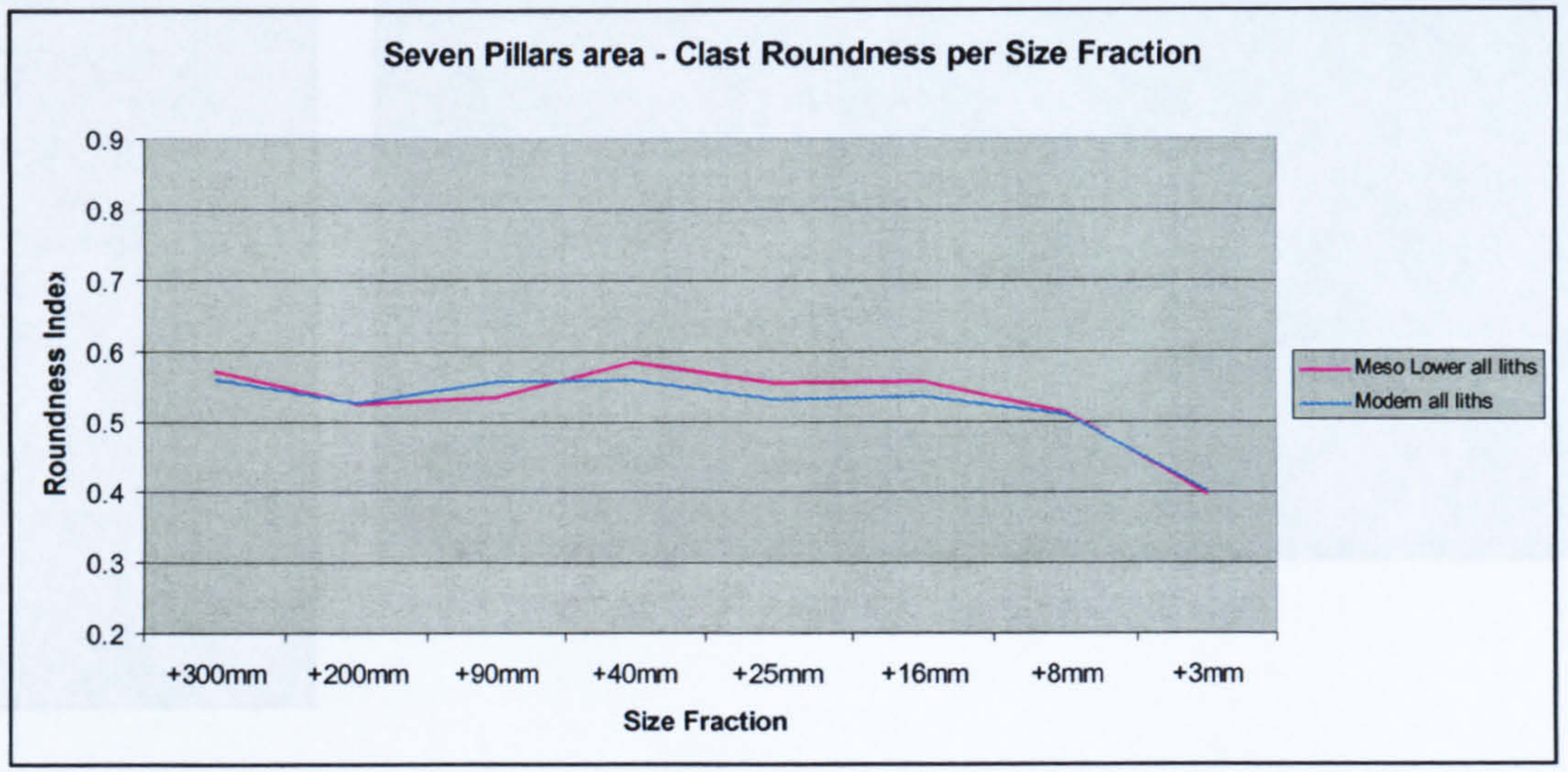

Figure 6.9 Clast type proportions per size fraction and average clast roundness per size fraction for samples in the Seven Pillars area.

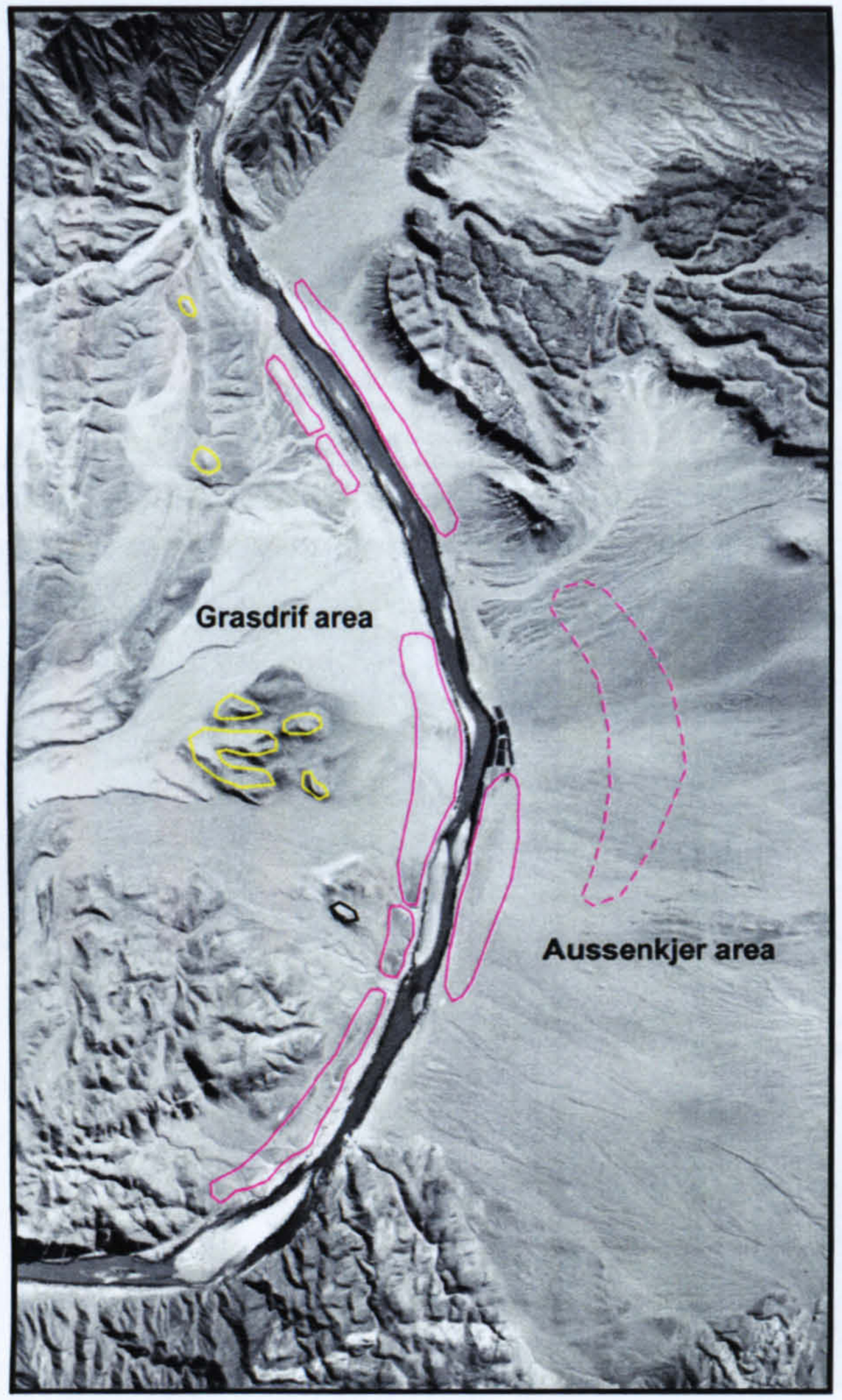

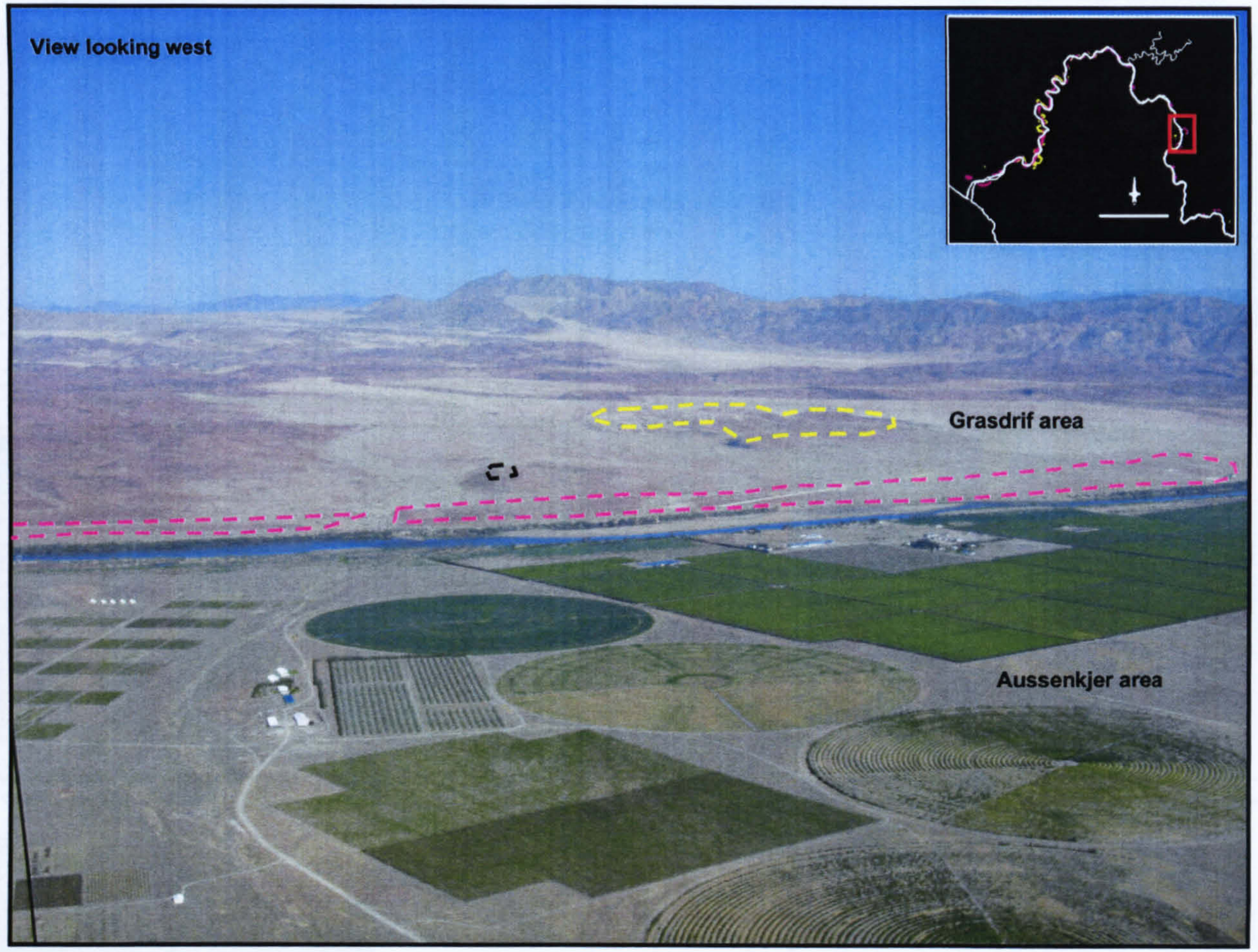

Proto terrace
Intermediate Terrace
Meso terrace

Figure 6.10 Distribution of Proto, Intermediate and Meso terraces in the Grasdrif/Aussenkjer area.

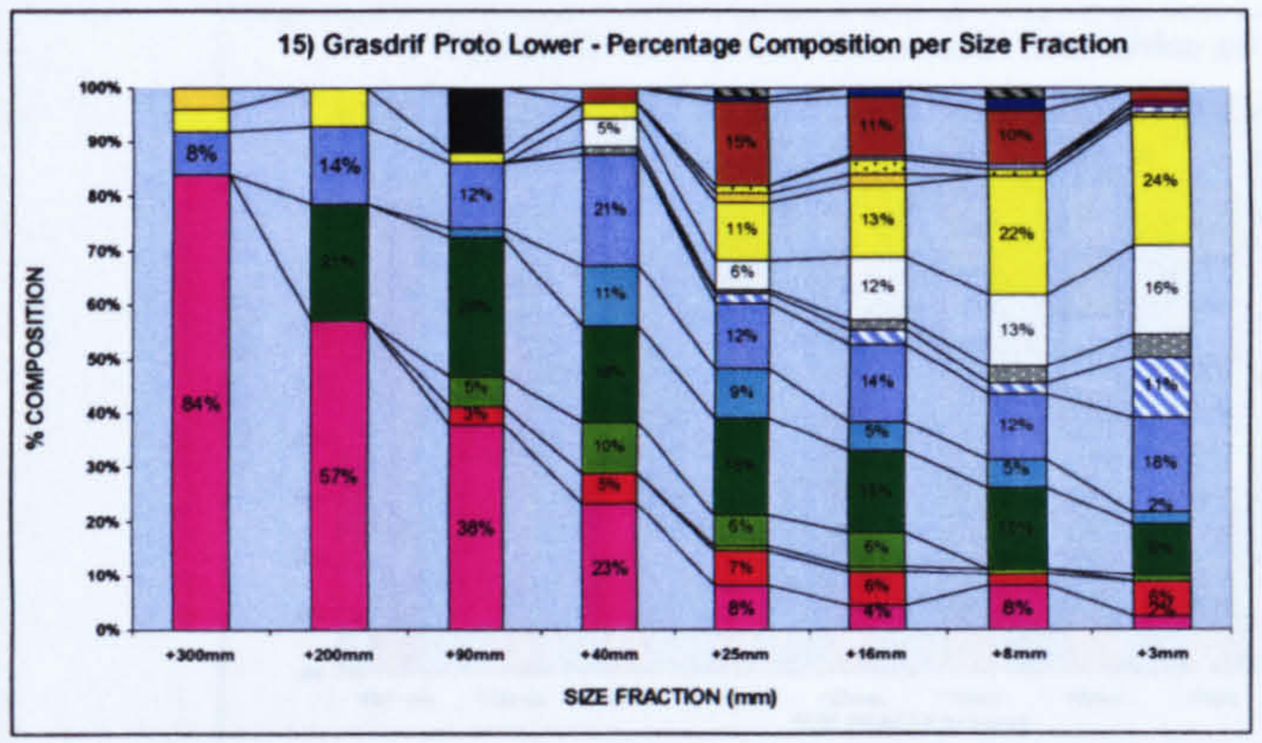

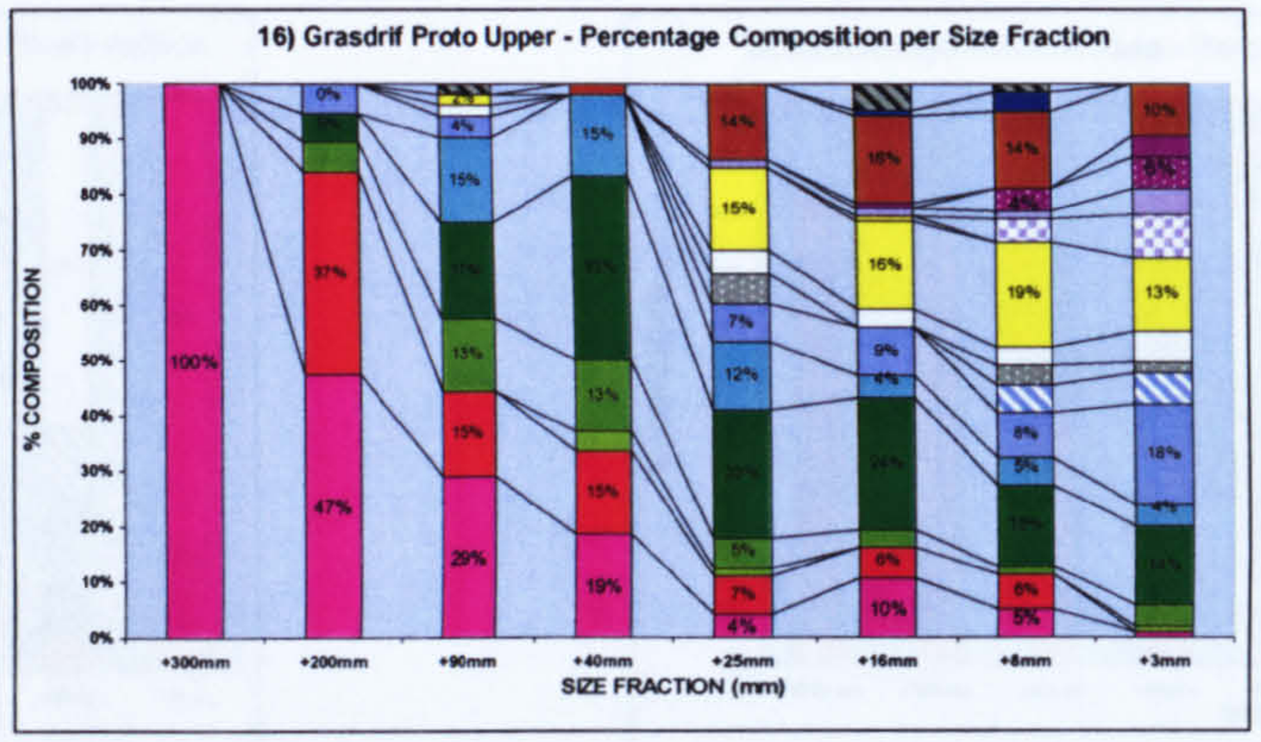

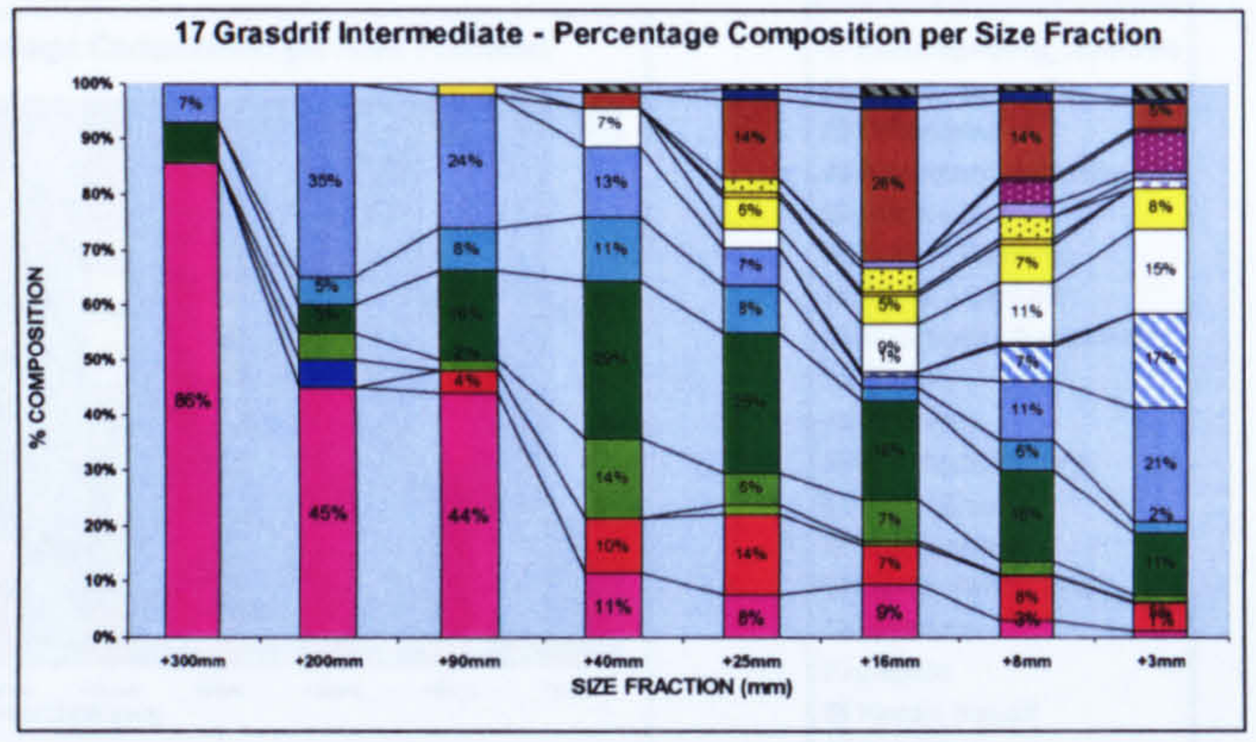

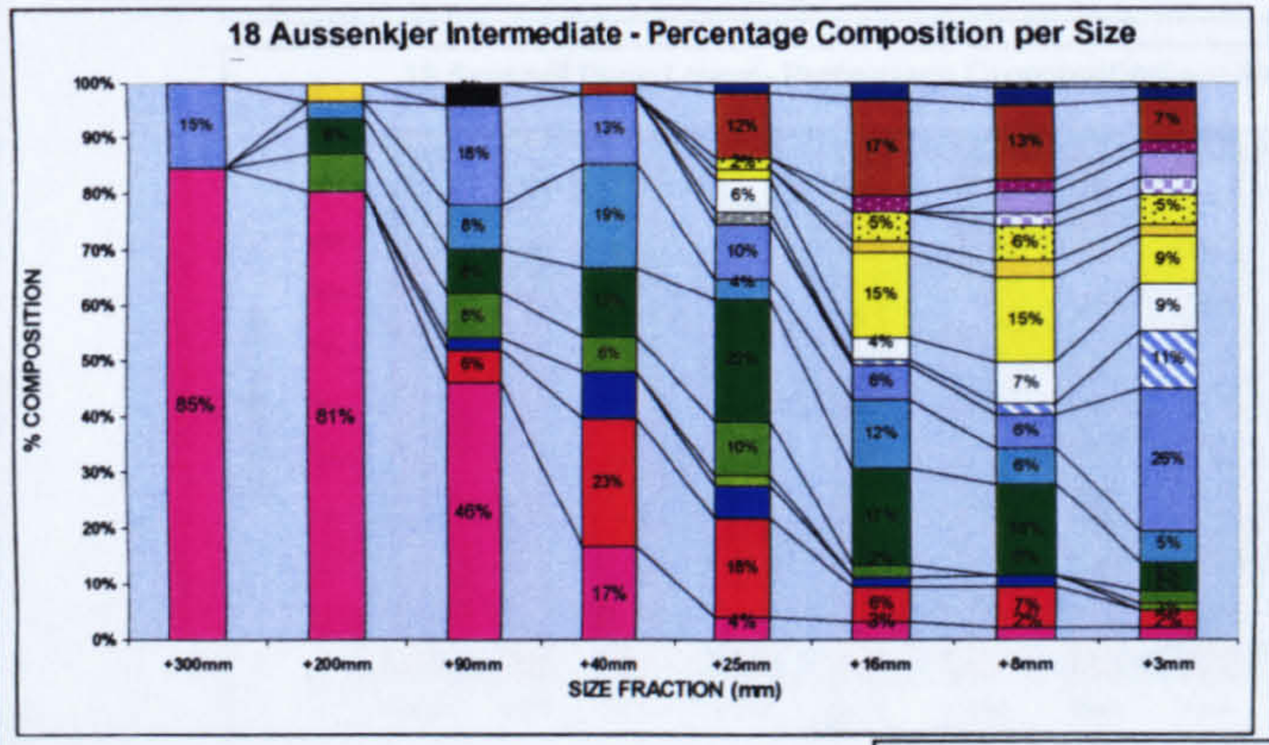

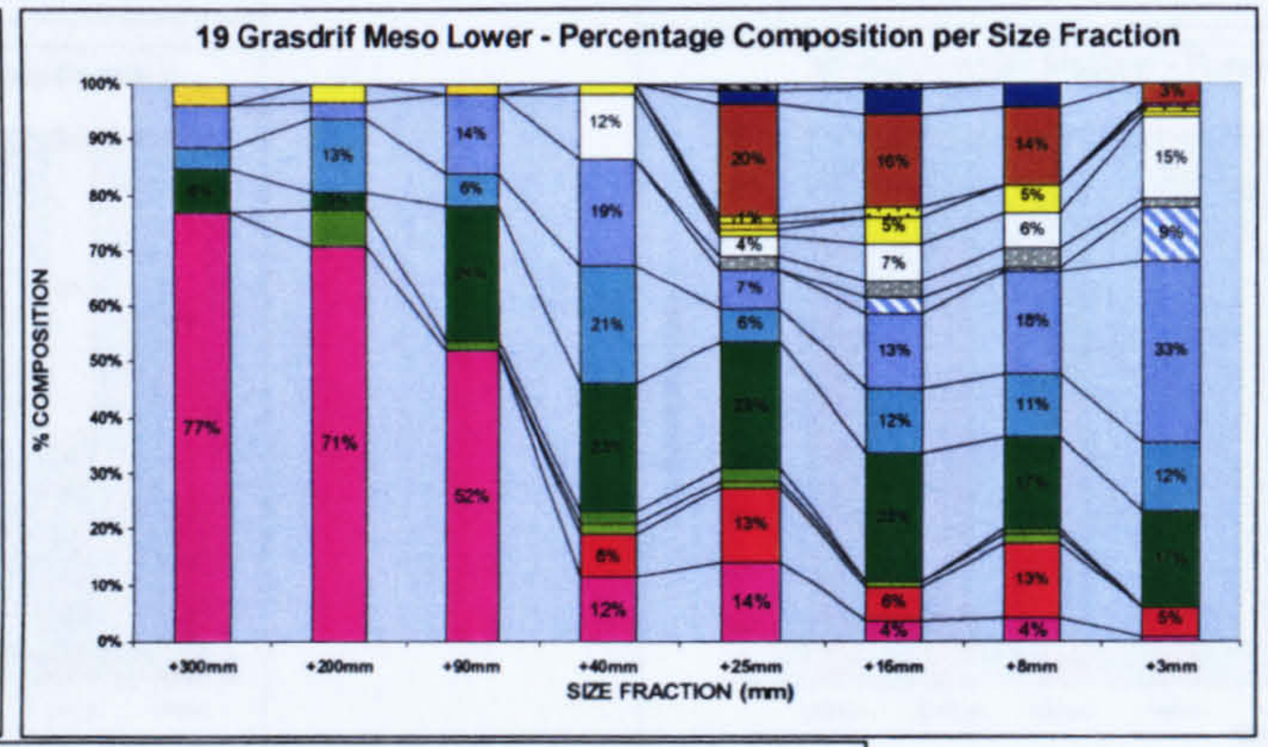

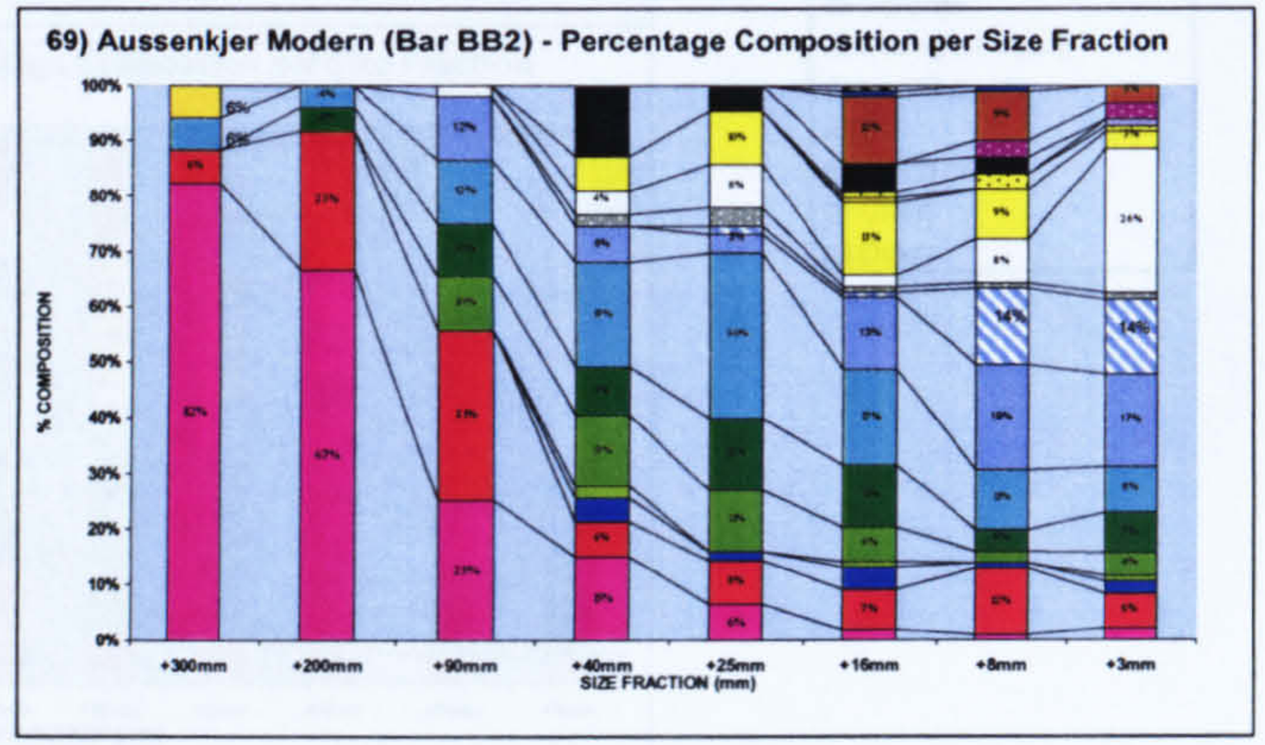

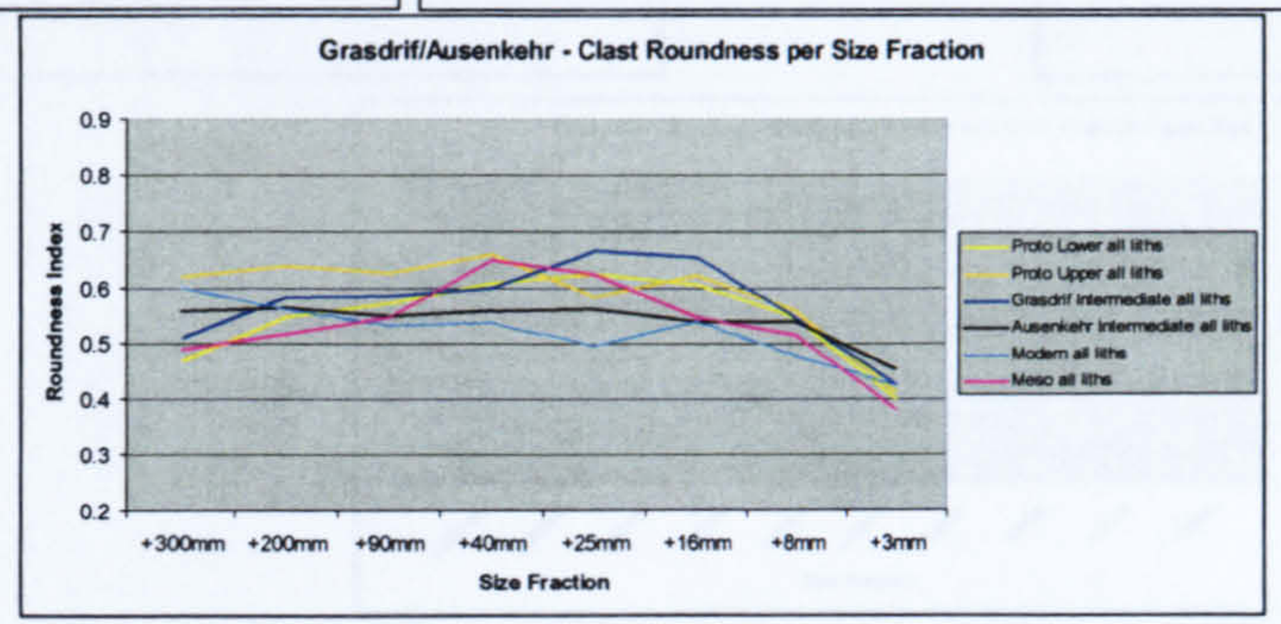

Figure 6.11a Clast type proportions per size fraction and average clast roundness per size fraction for samples in the Grasdrif/Aussenkjer area.

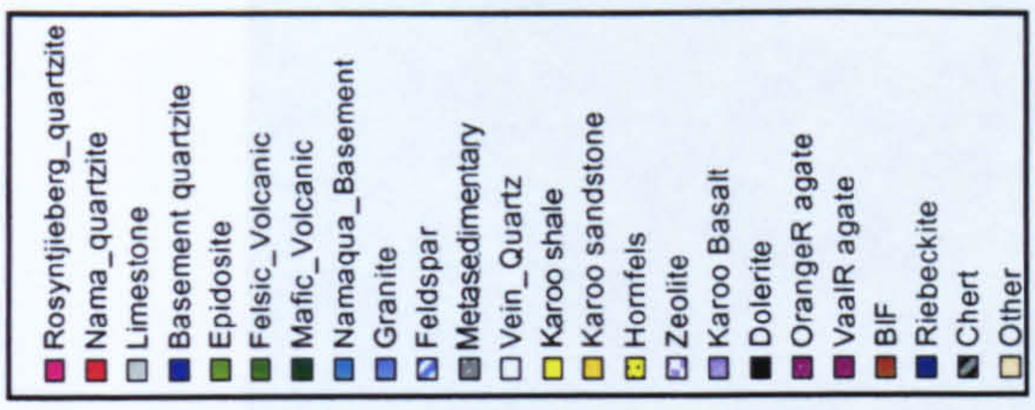

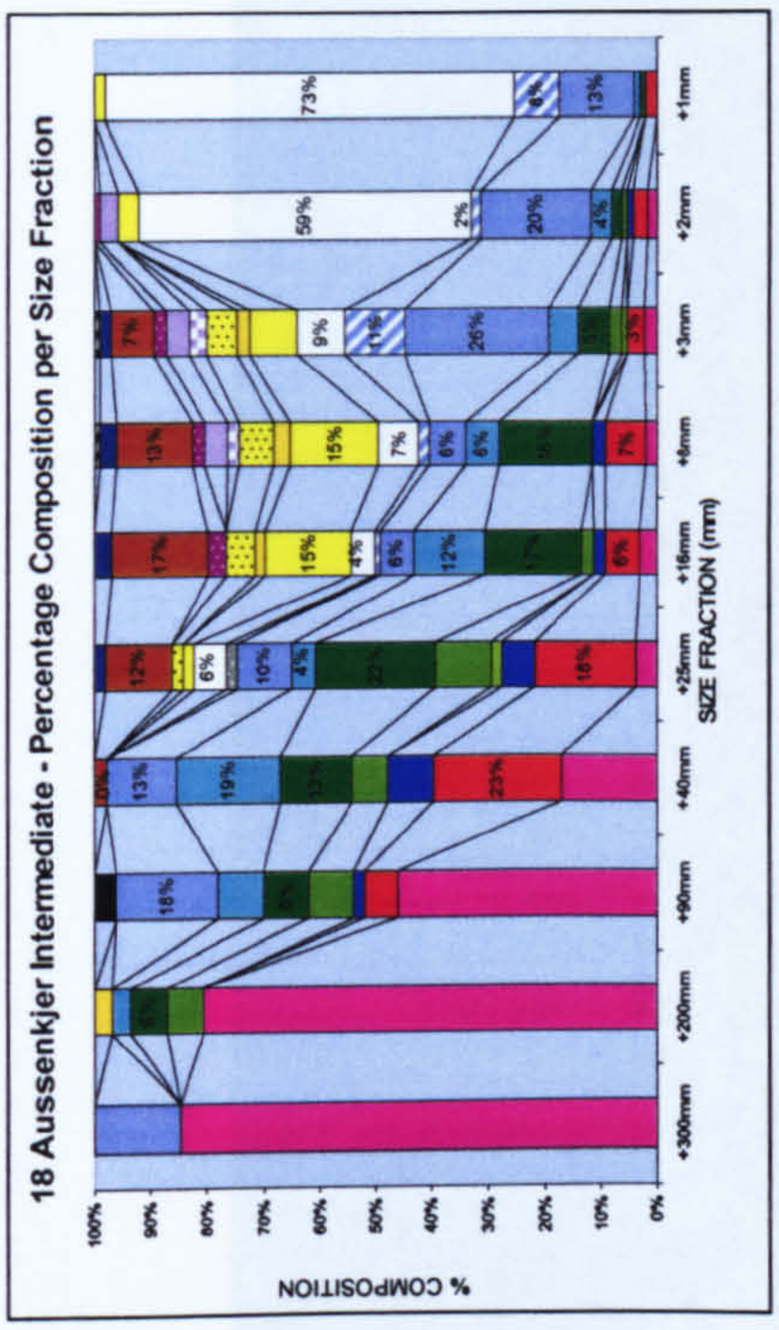

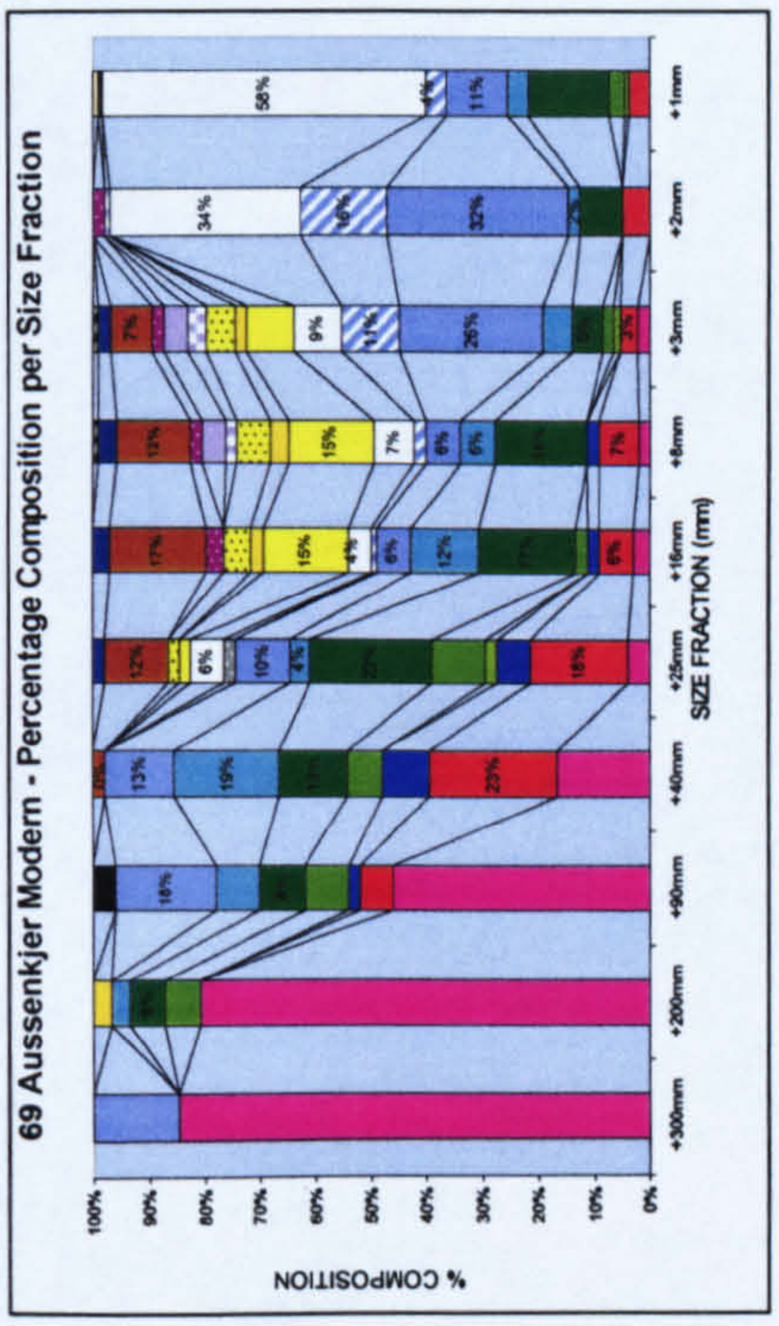

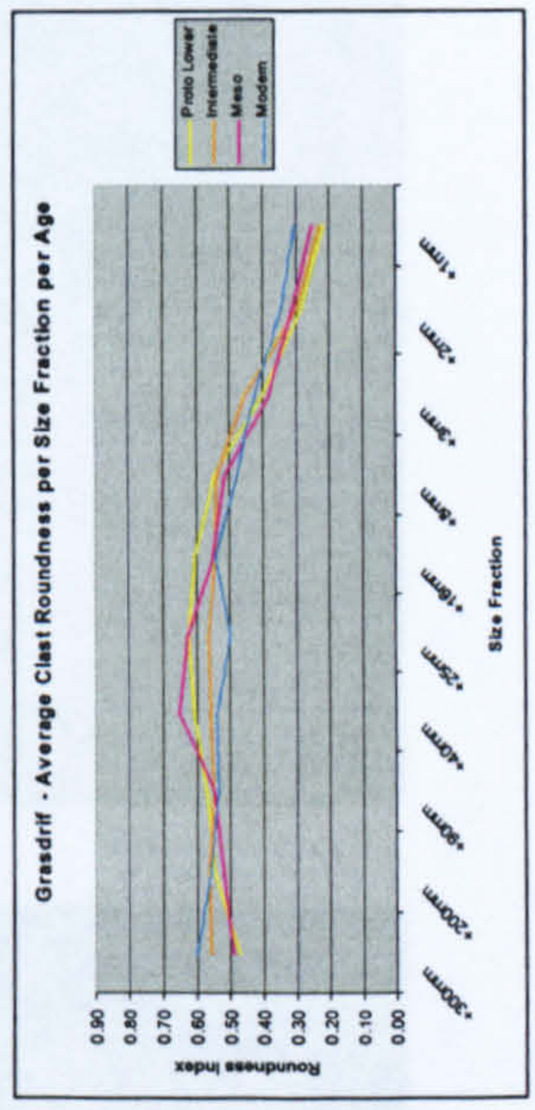

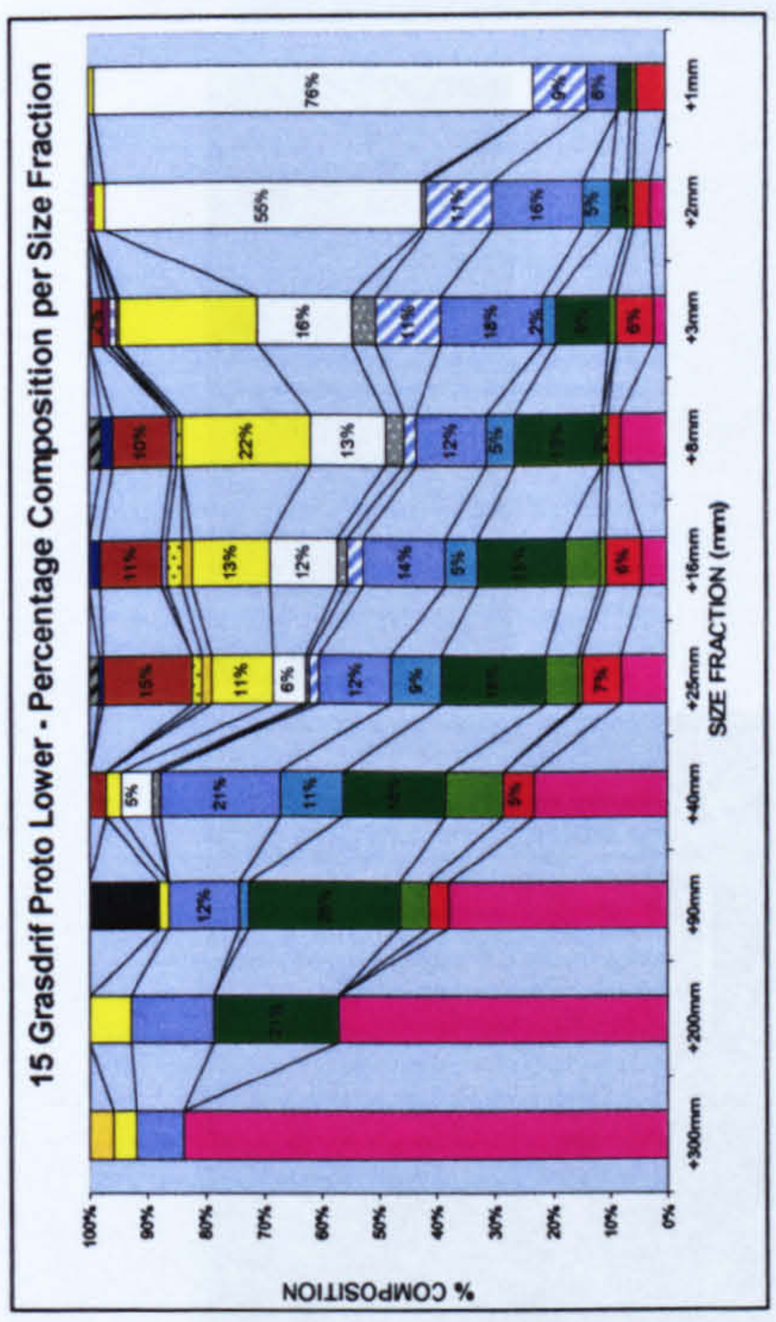

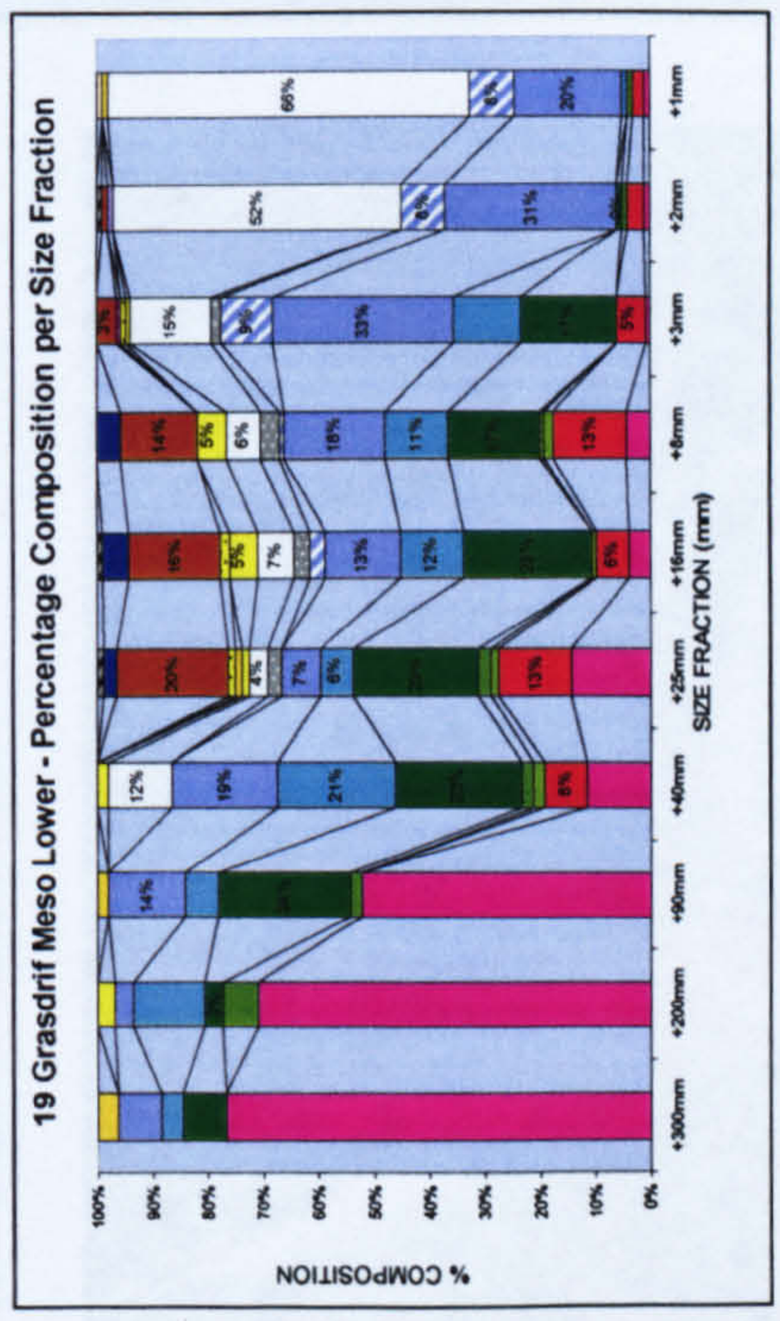

Figure 6.11b Clast type proportions per size fraction for samples in the Grasdrif/Aussenkjer area including the +2 and +1mm sand fractions and average clast roundness per size fraction and average clast roundness per size fraction.

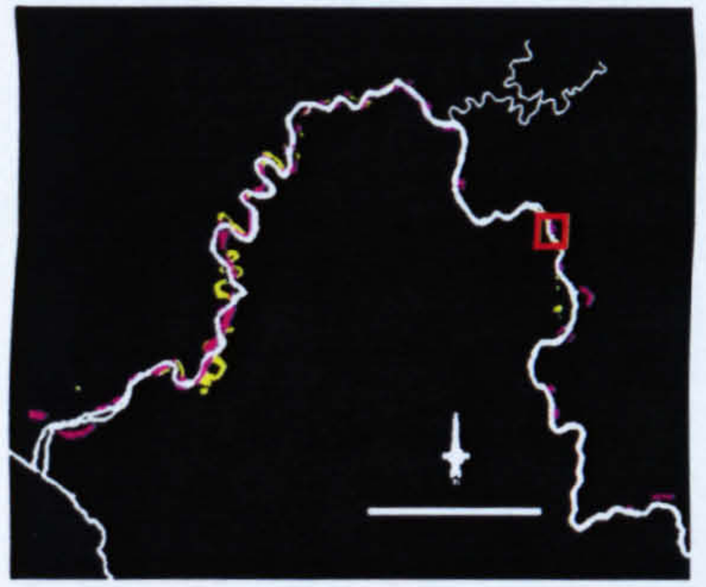

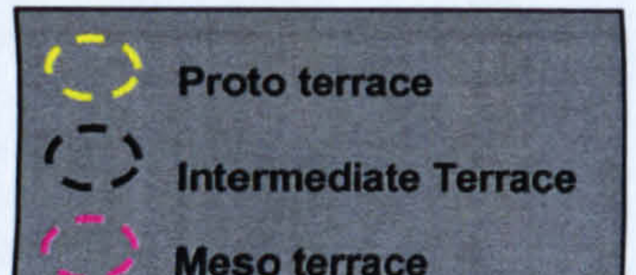

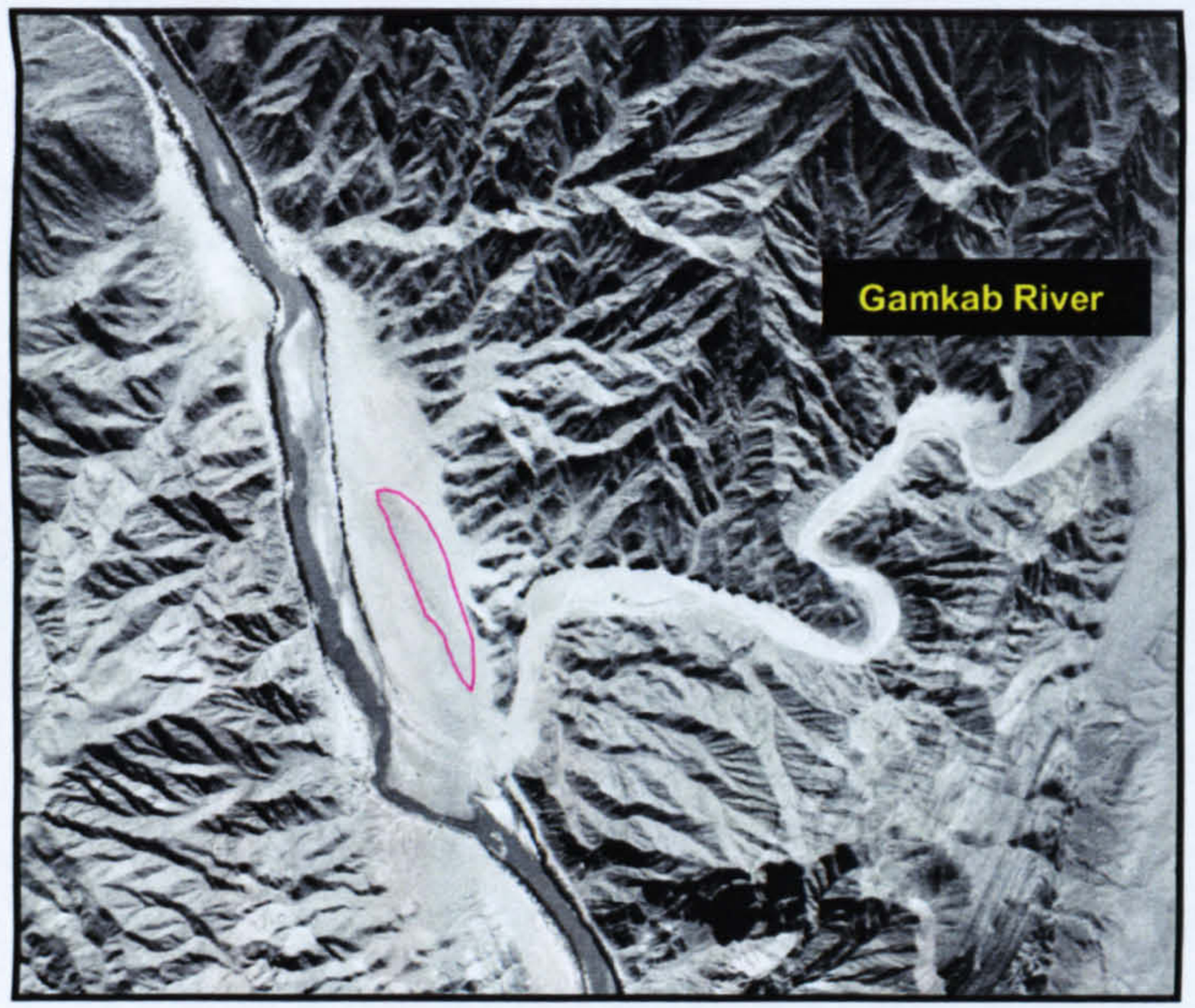

Figure 6.12 Distribution of the Meso terrace in the Gamkab River area.

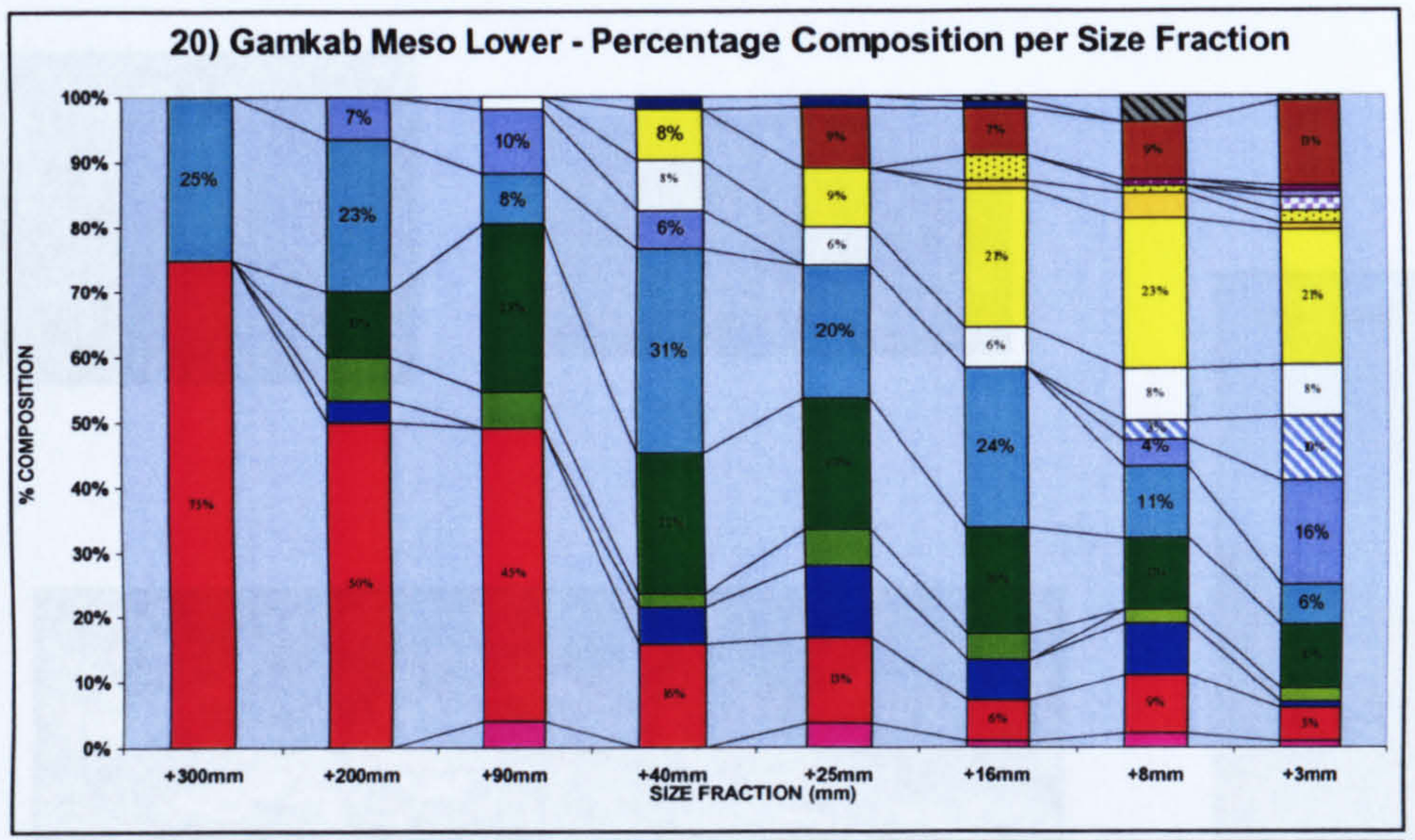

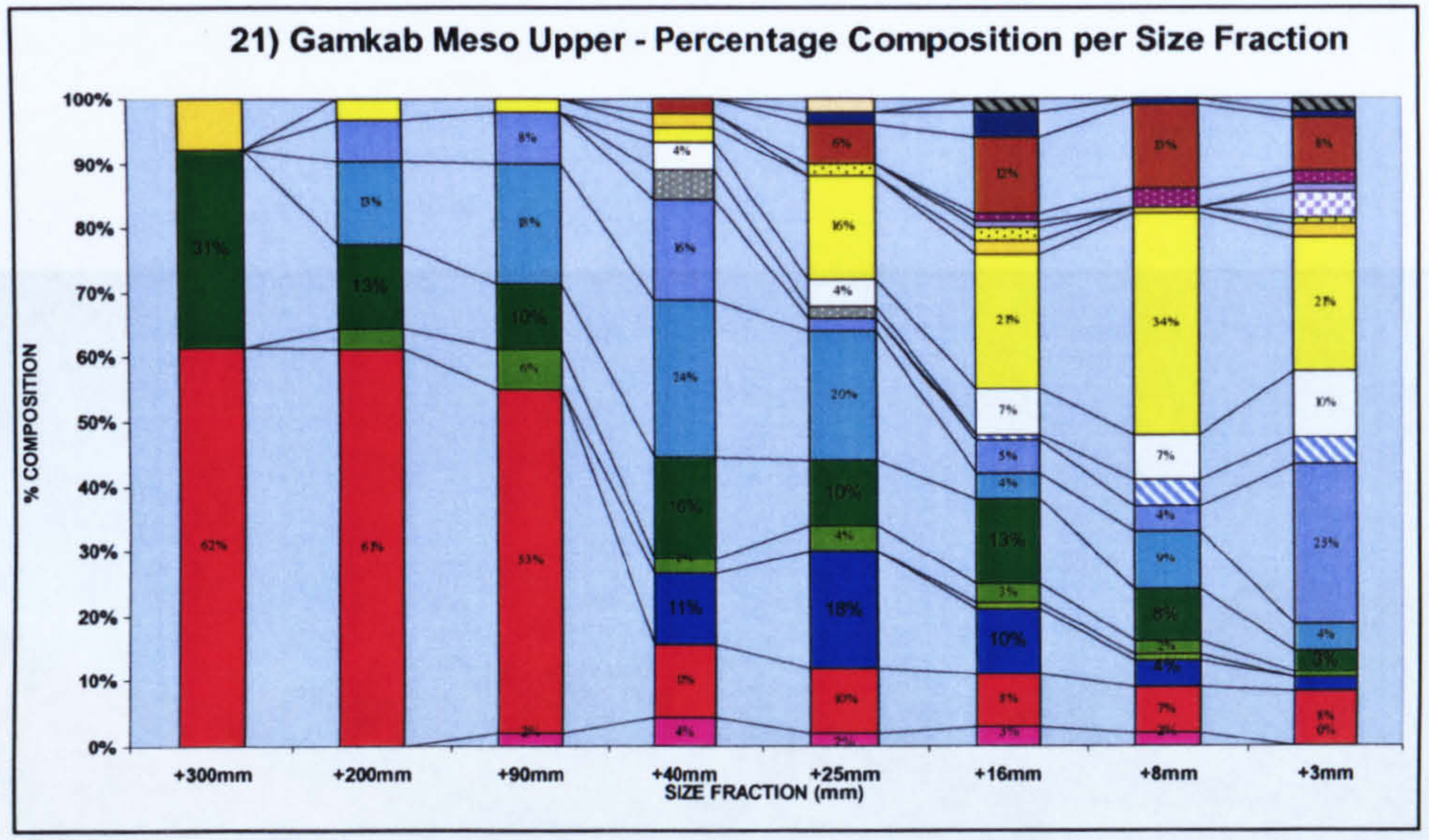

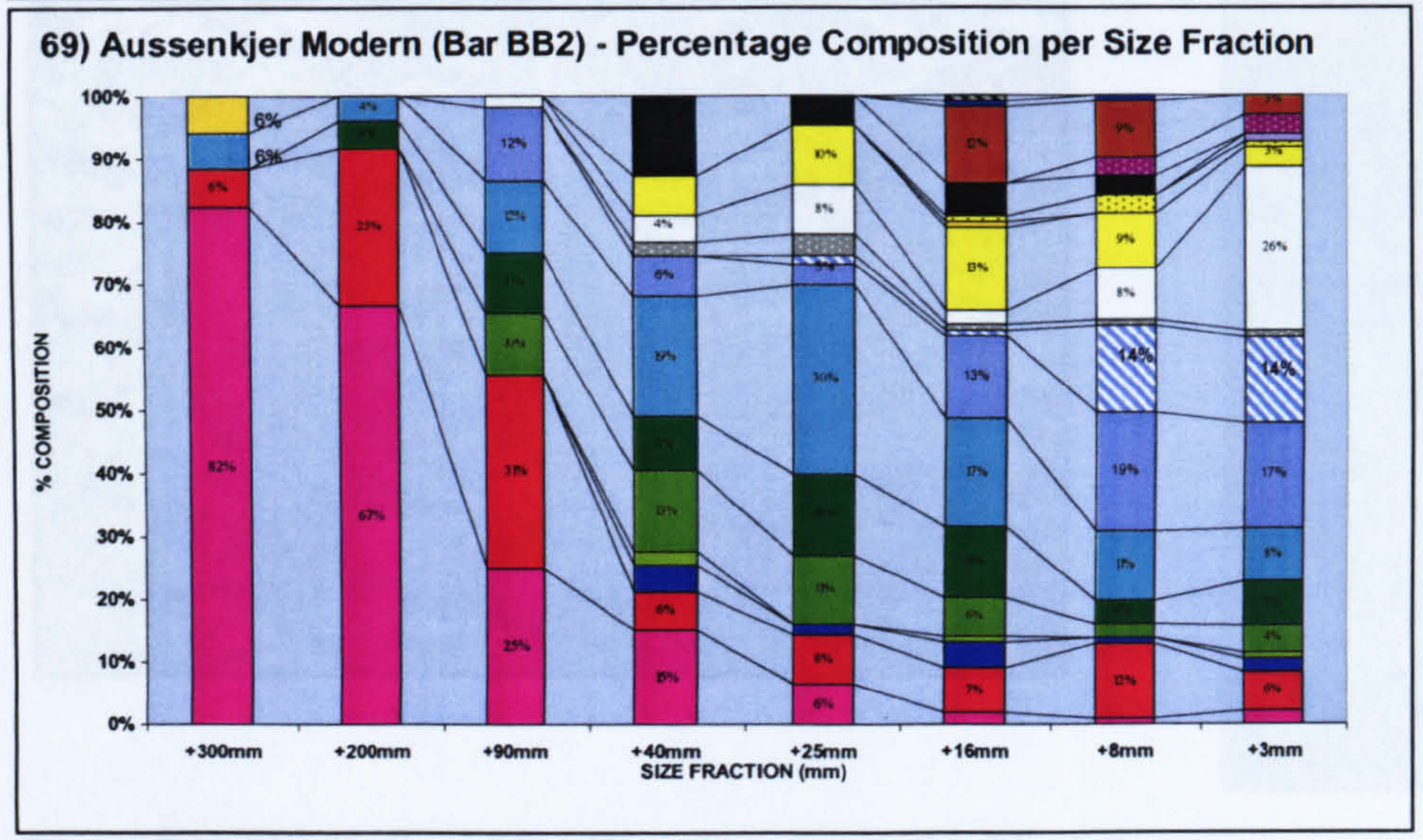

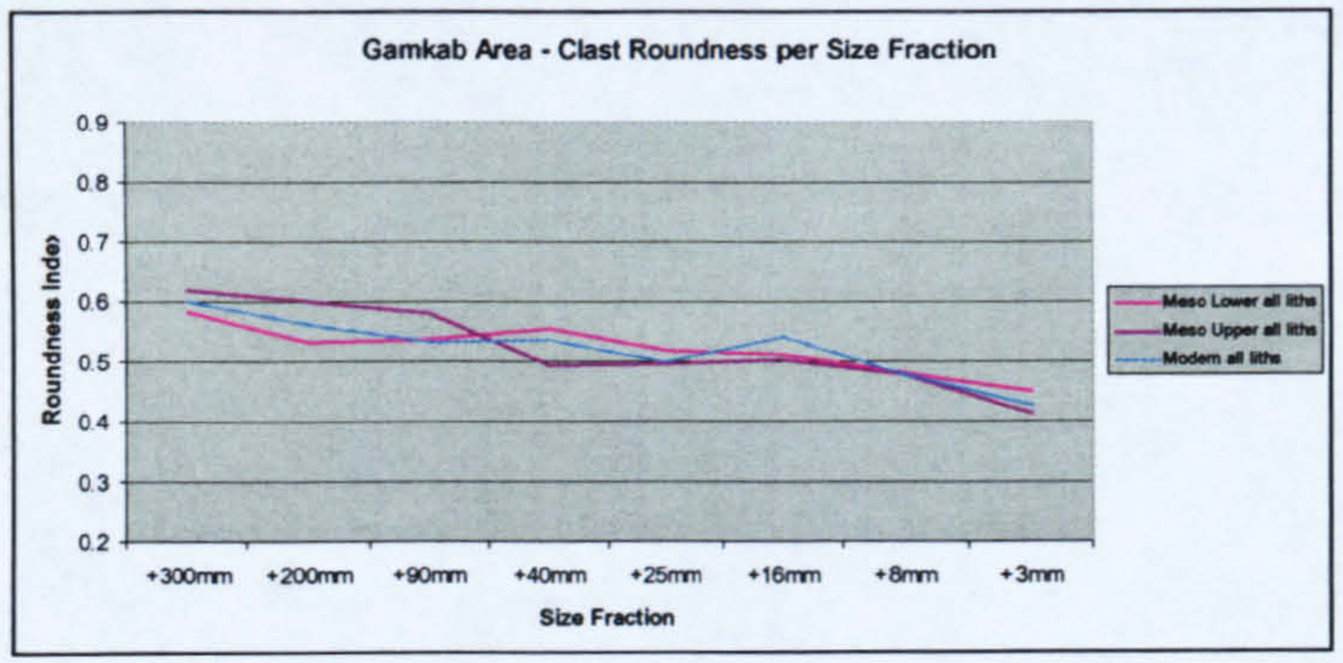

Figure 6.13 Clast type proportions per size fraction and average clast roundness per size fraction for samples in the Gamkab River area.

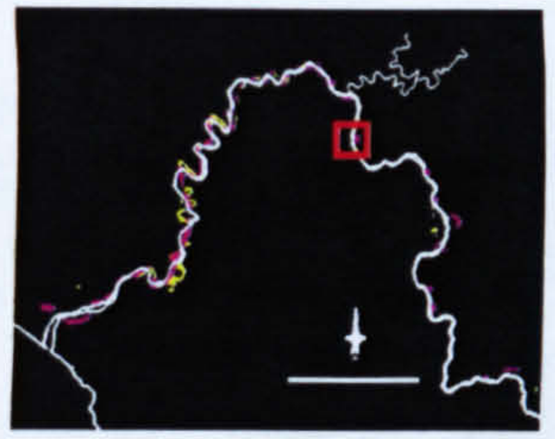

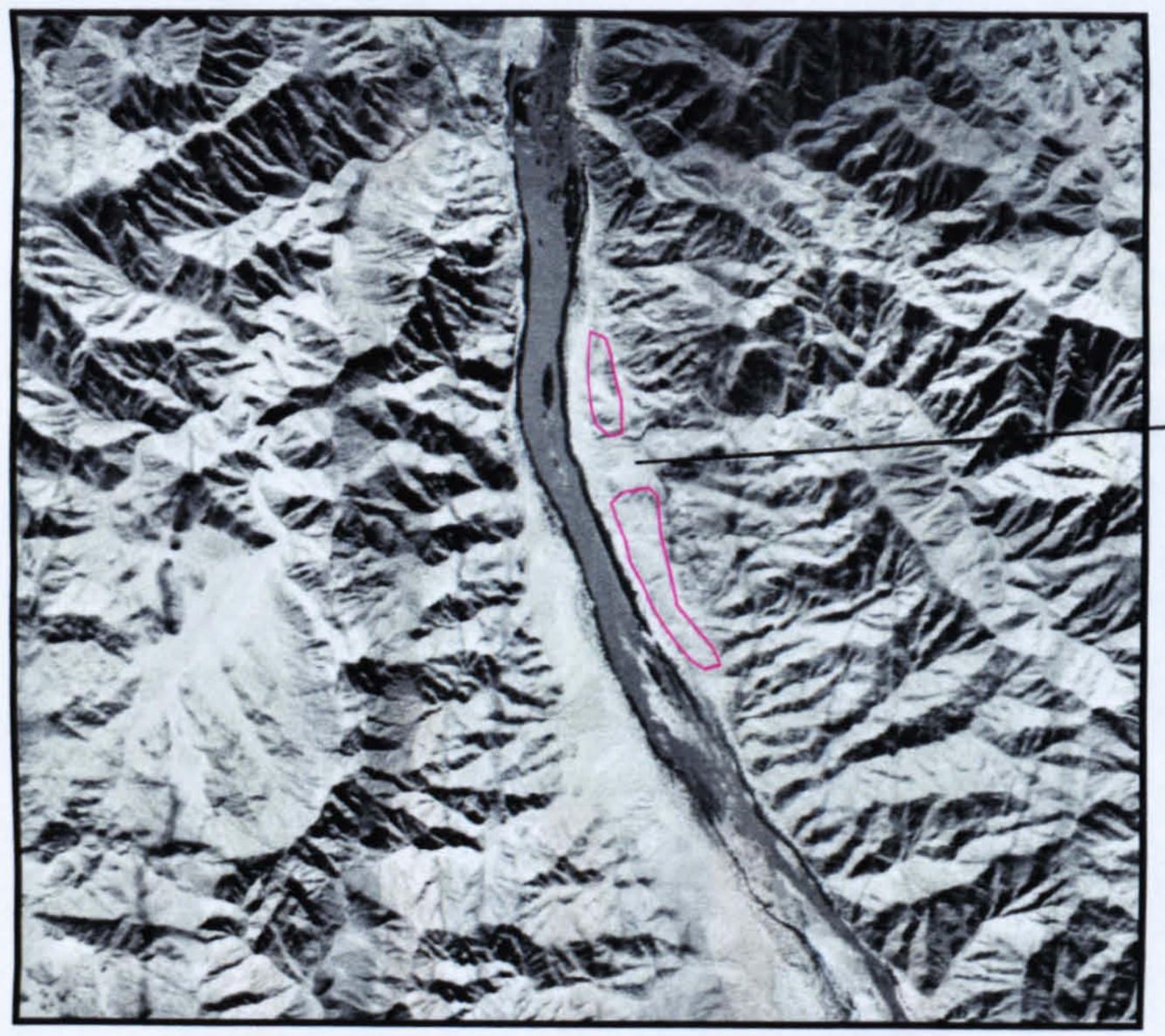

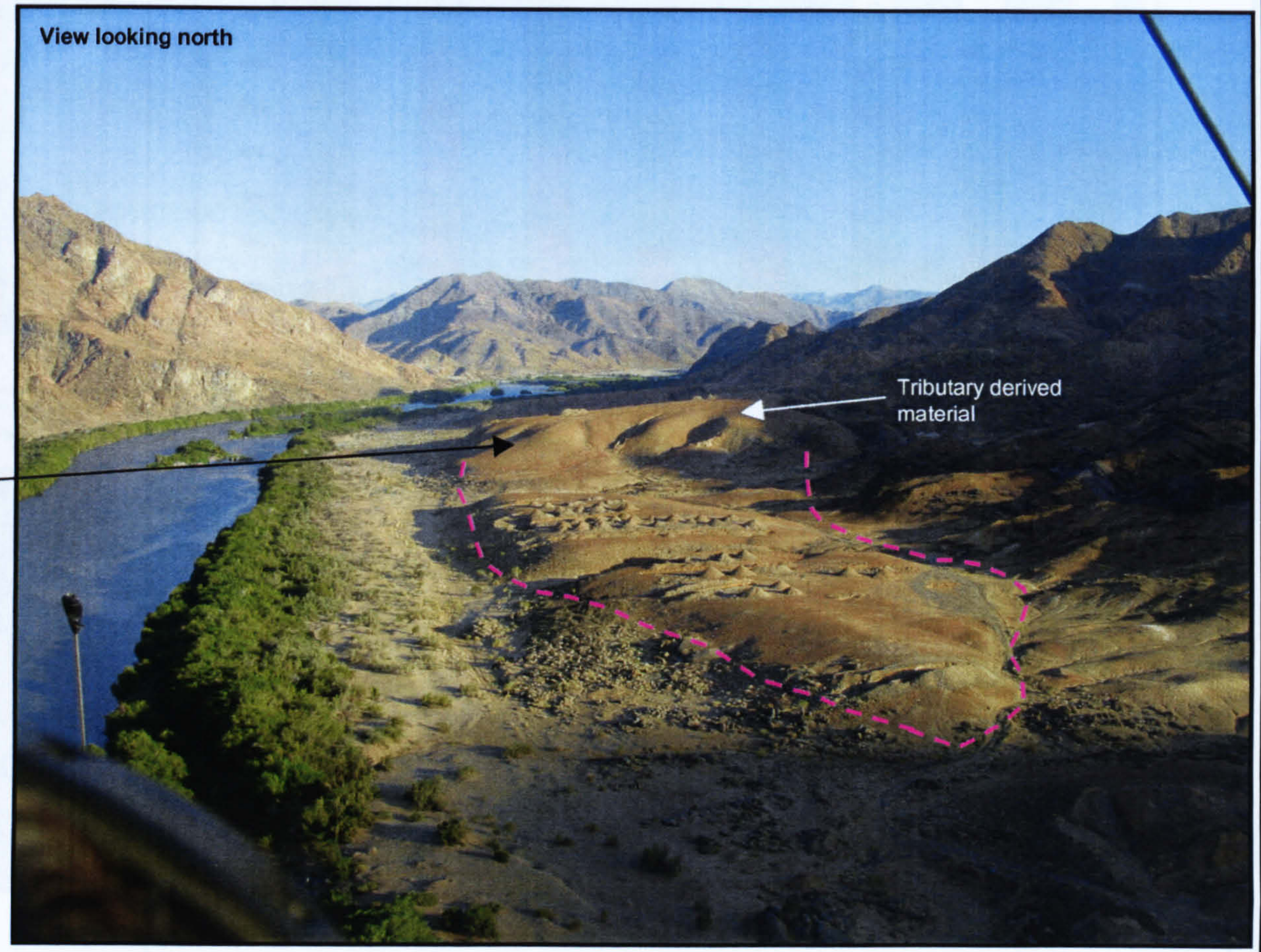

Figure 6.14 Distribution of the Meso terraces in the Block 6 area.

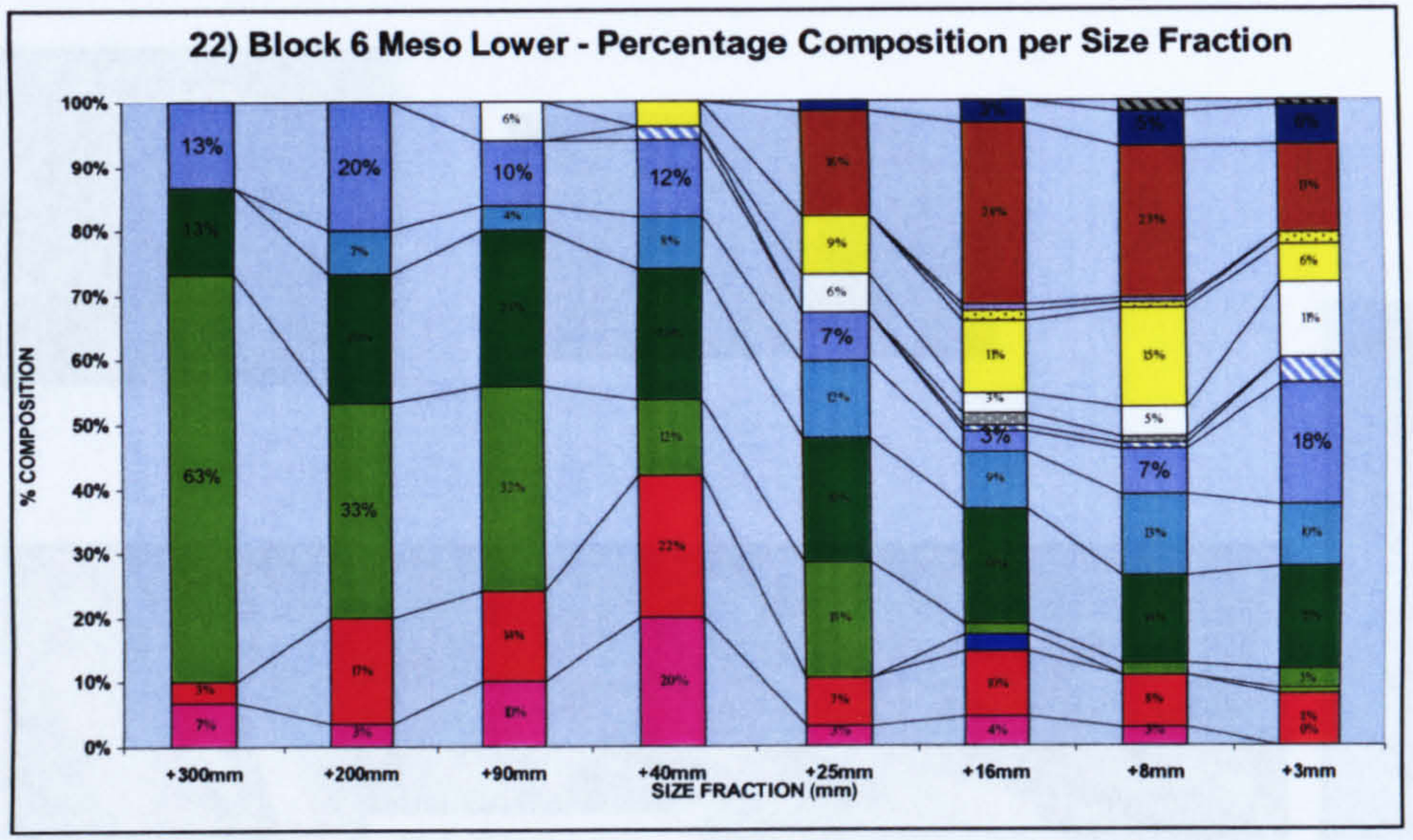

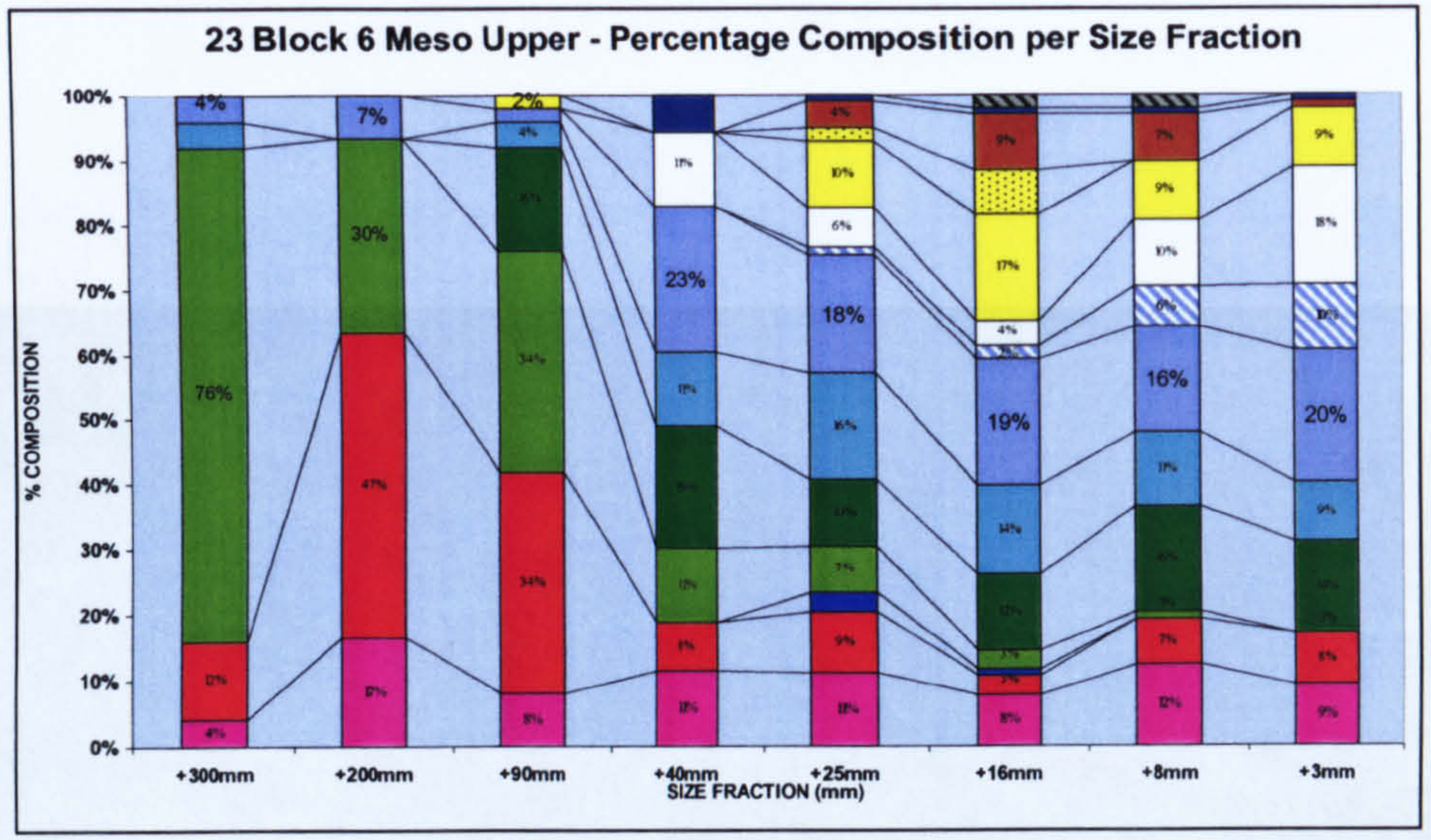

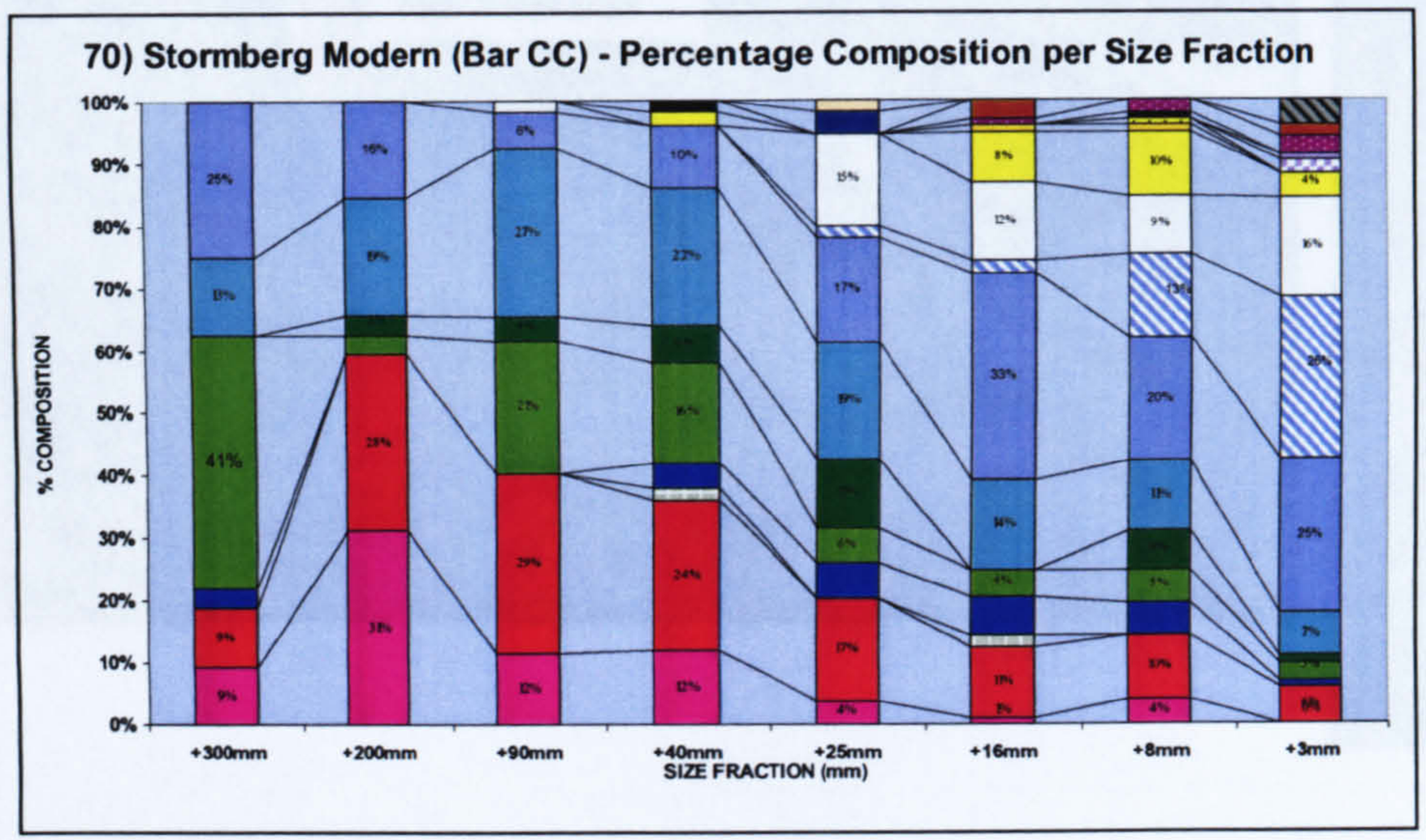

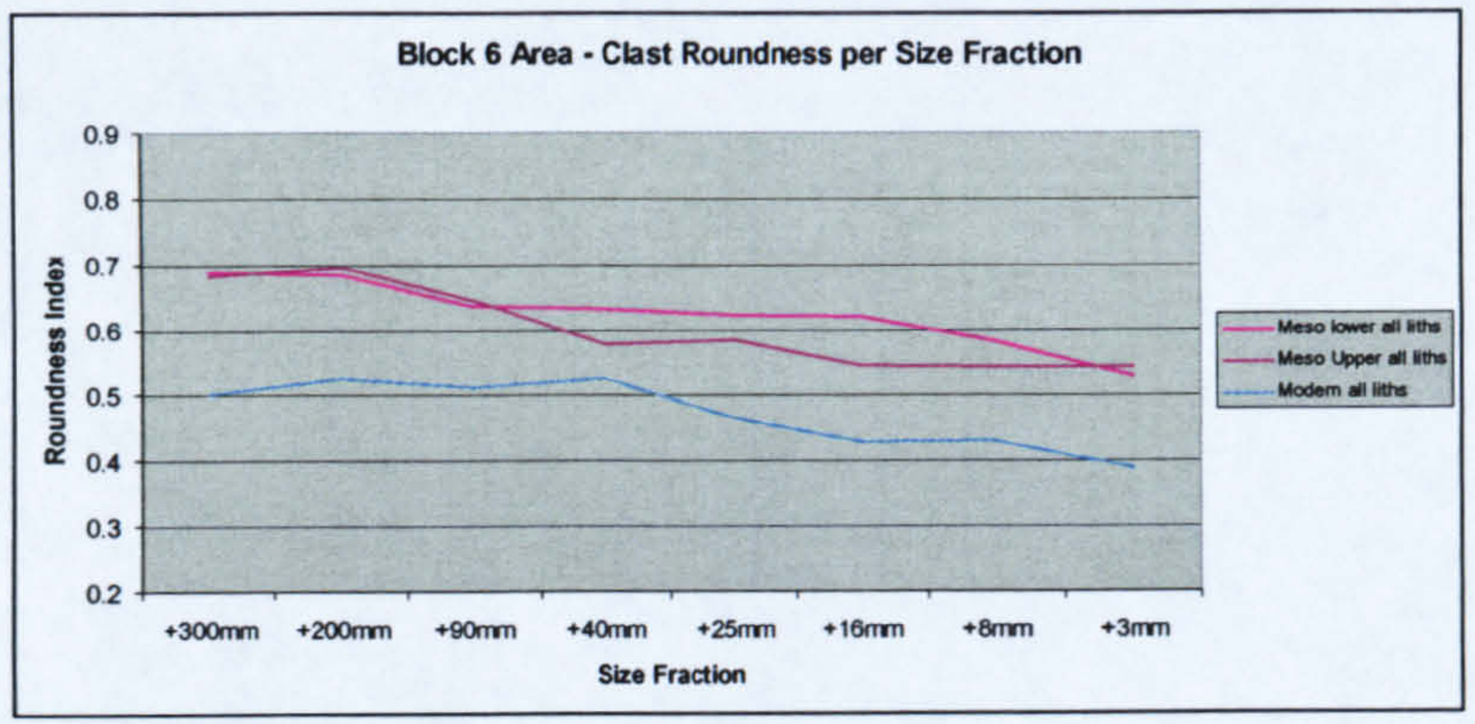

Figure 6.15 Clast type proportions per size fraction and average clast roundness per size fraction for samples in the Block 6 area.

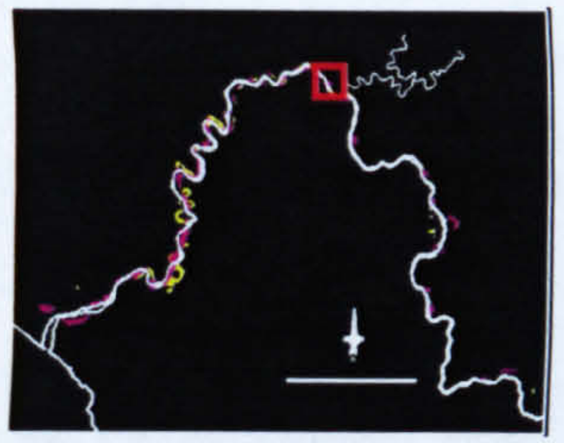

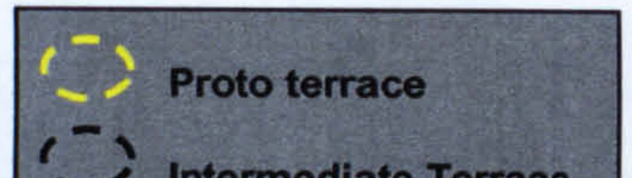

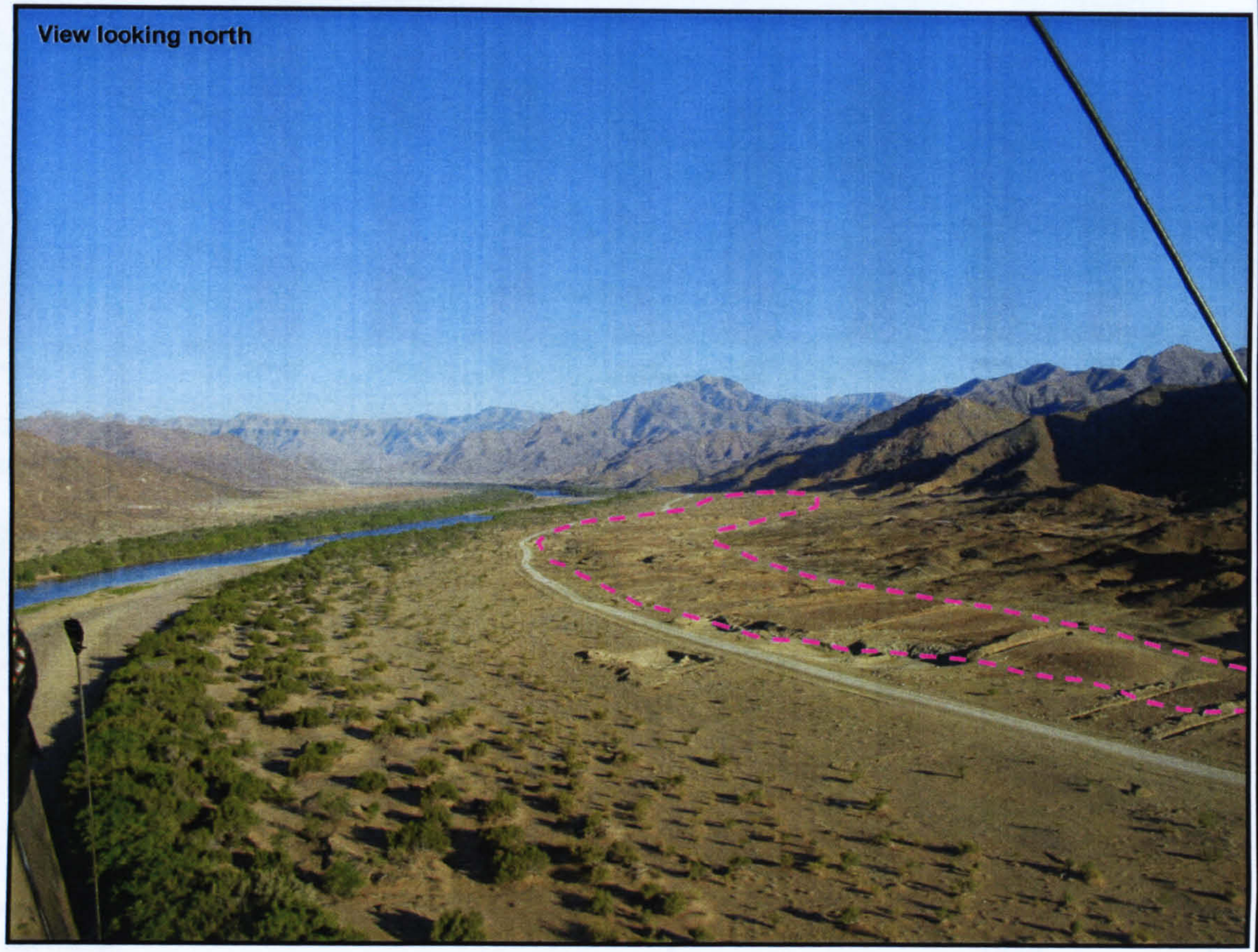

Figure 6.16 Distribution of the Meso terraces in the Fish River area.

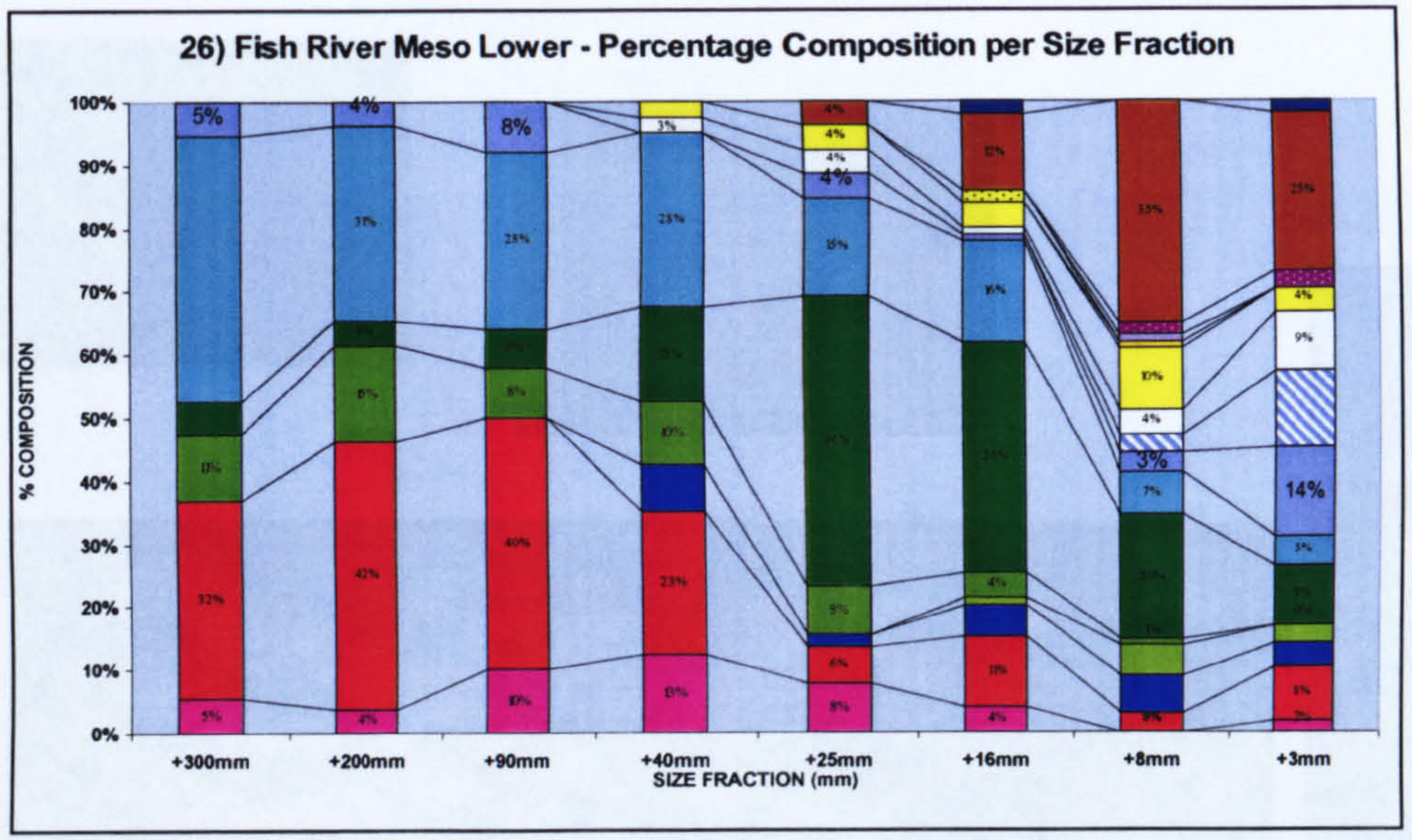

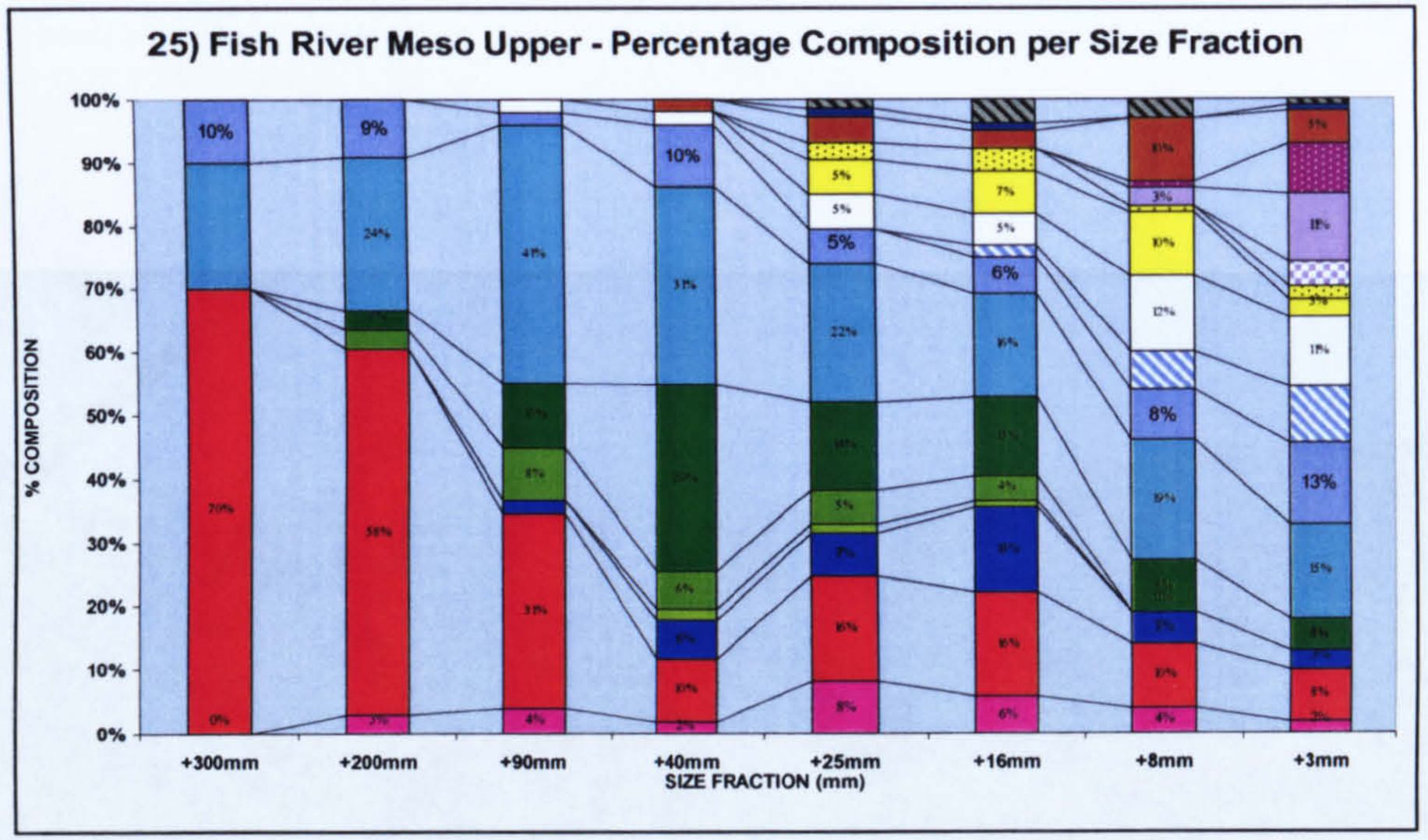

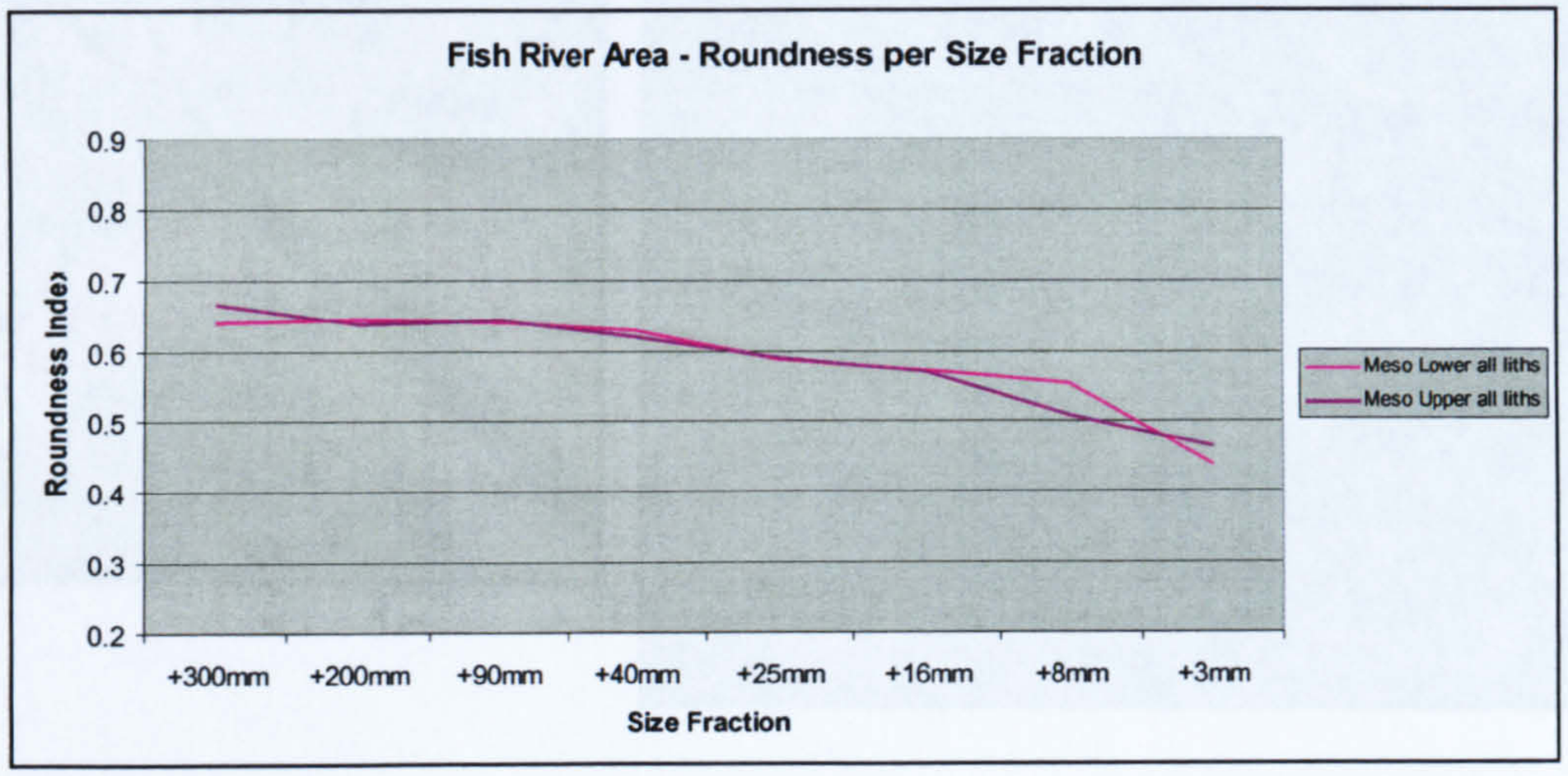

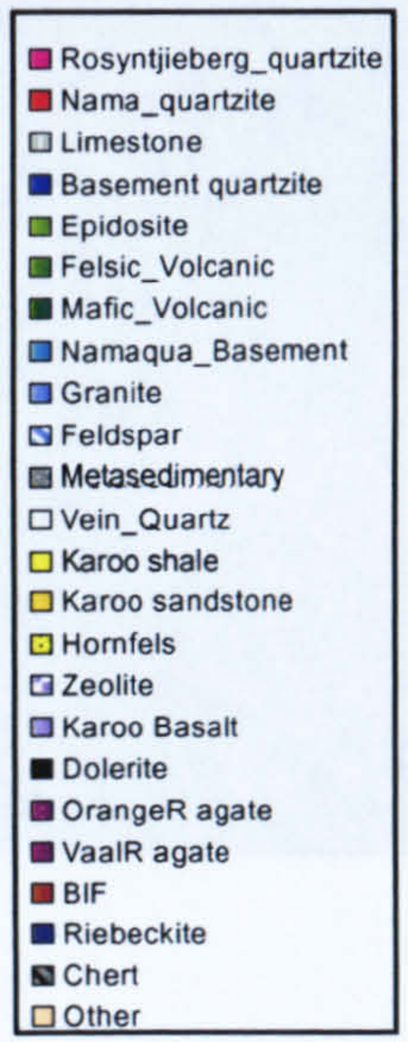

Figure 6.17 Clast type proportions per size fraction and average clast roundness per size fraction for samples in the Fish River area.

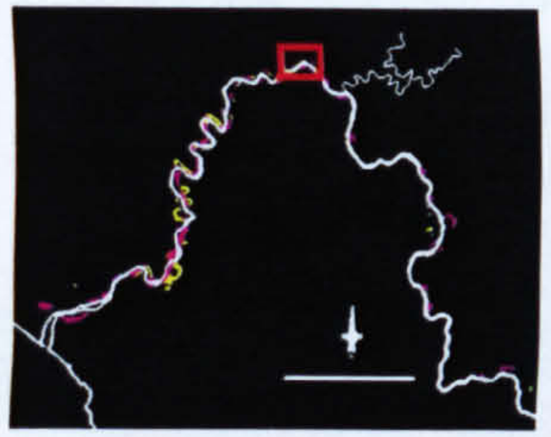

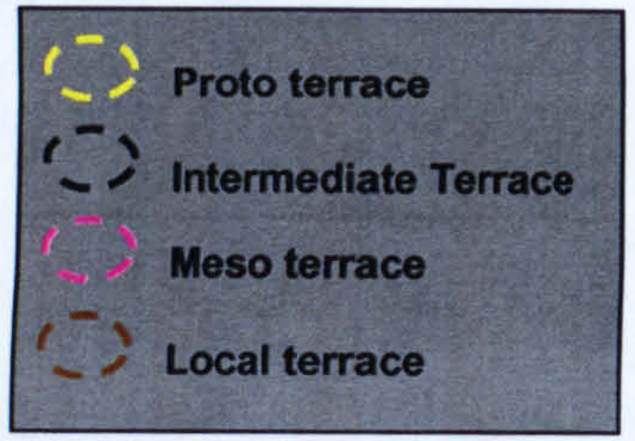

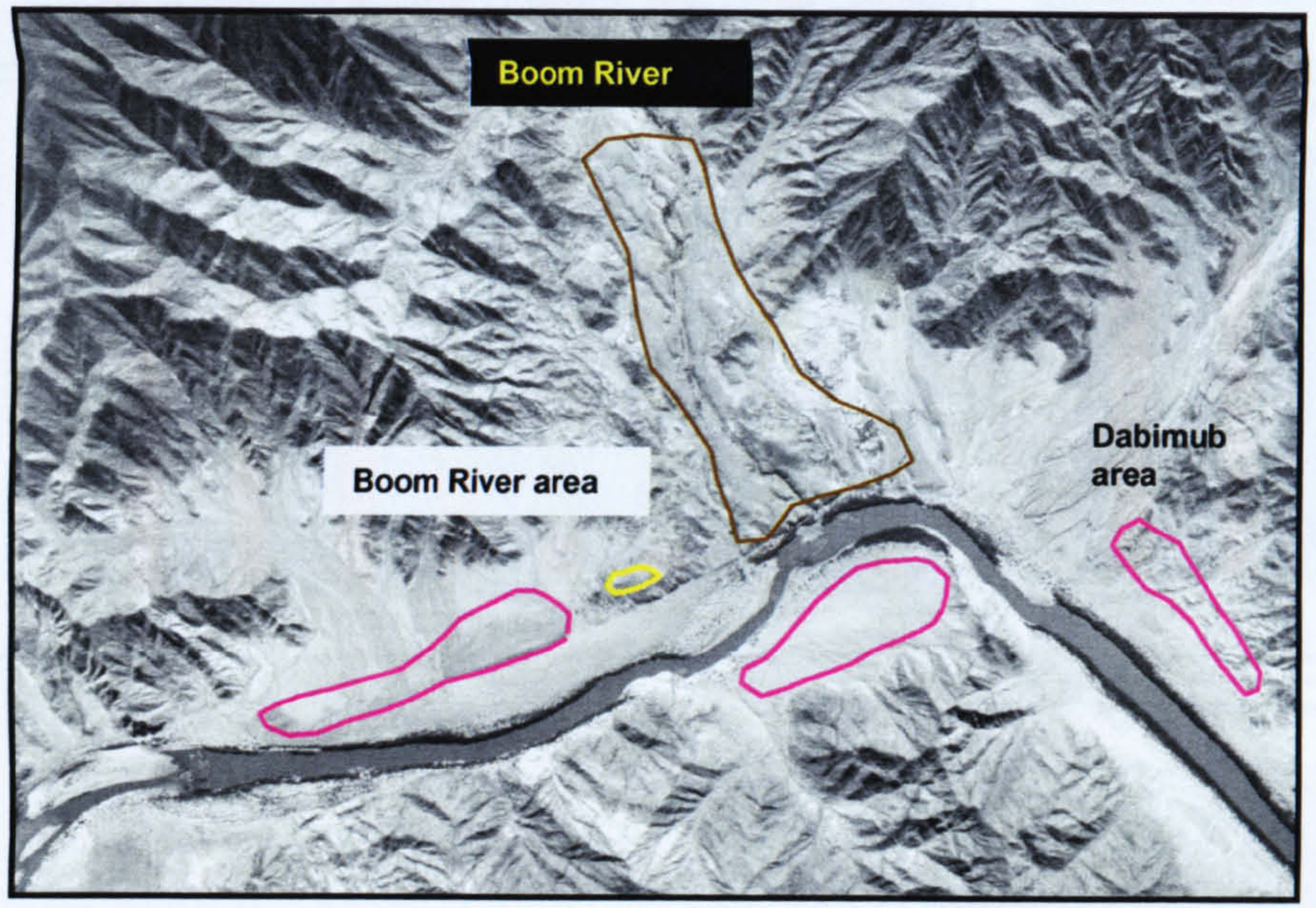

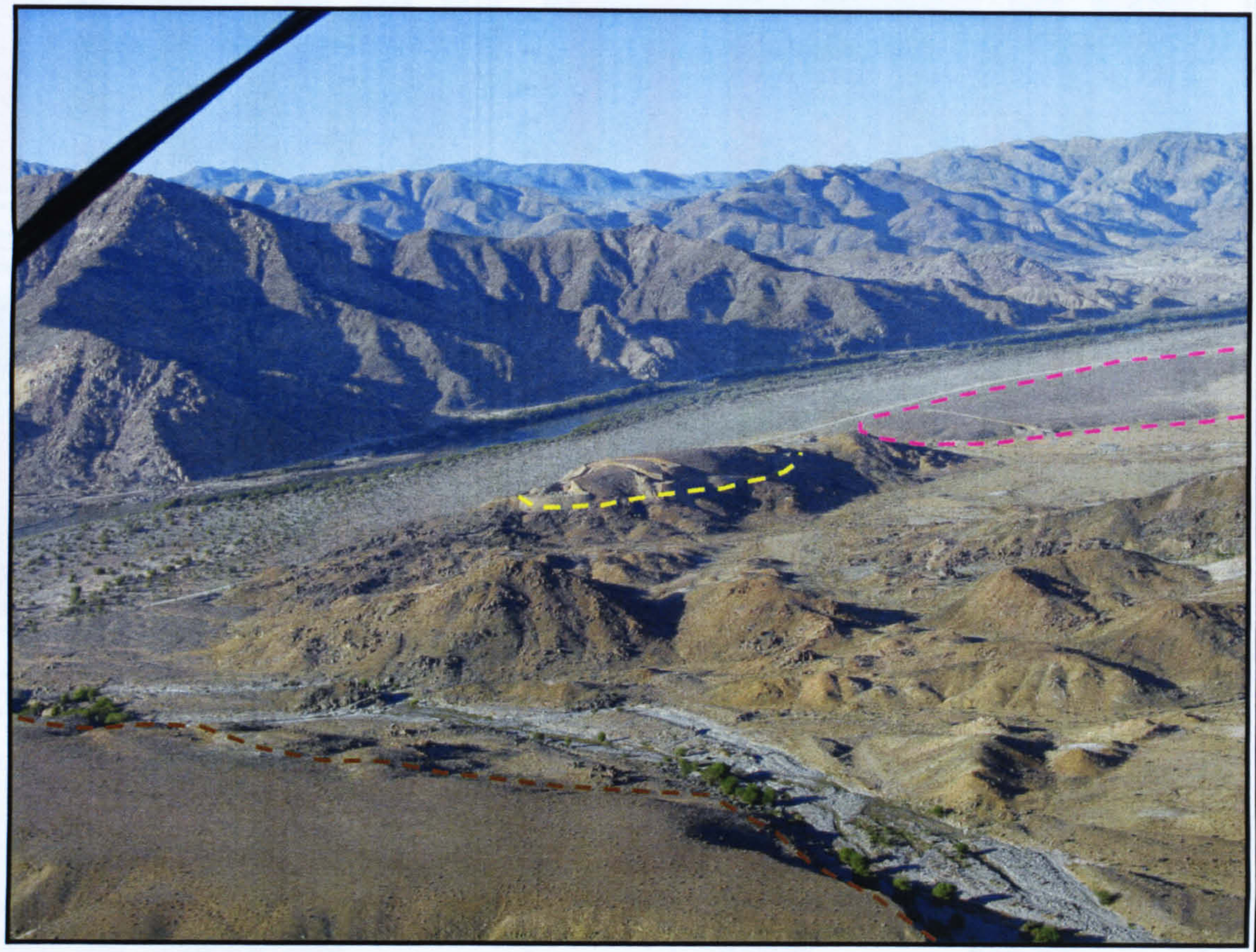

Figure 6.18 Distribution of Proto and Meso terraces in the Boom River and Dabimub areas.

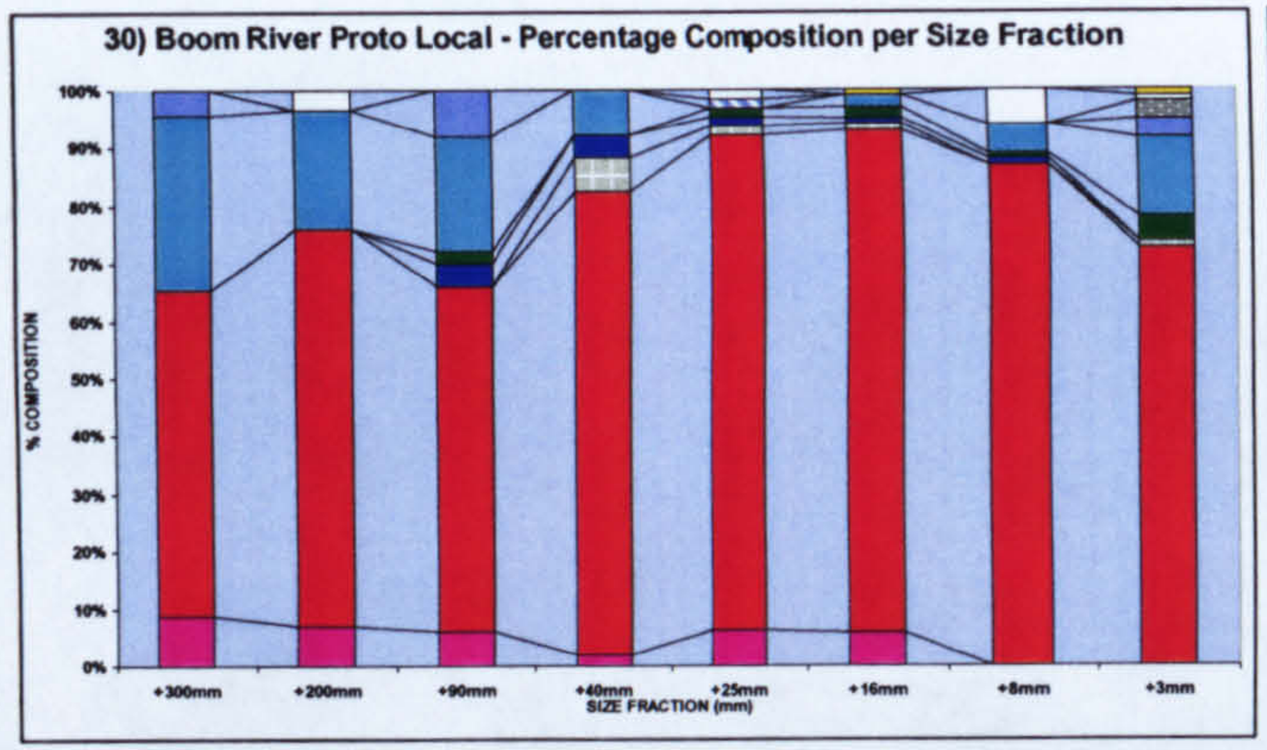

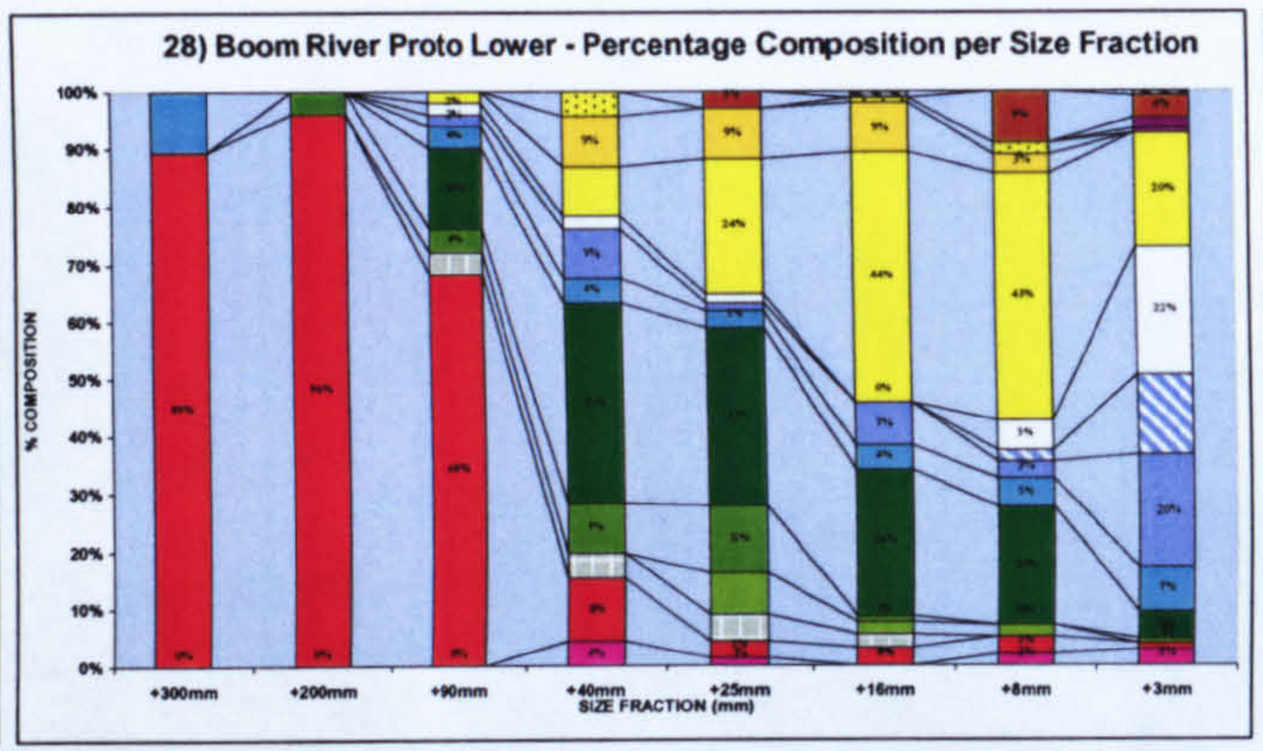

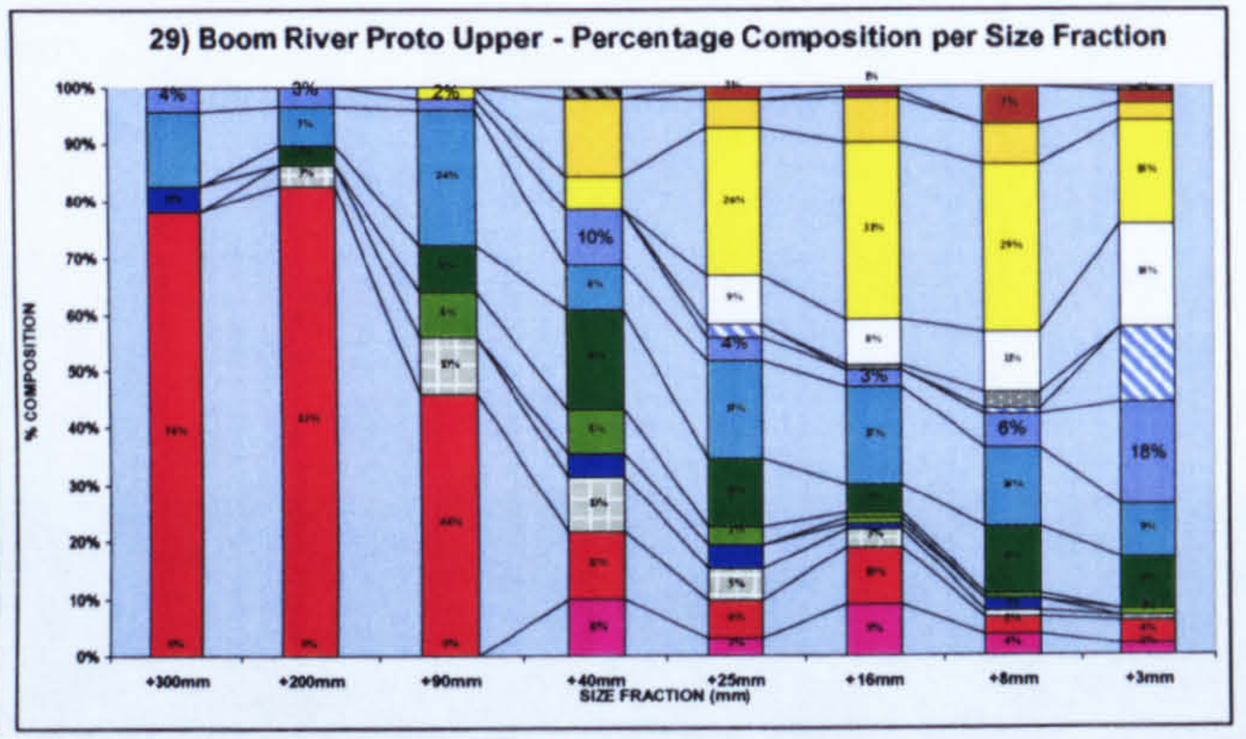

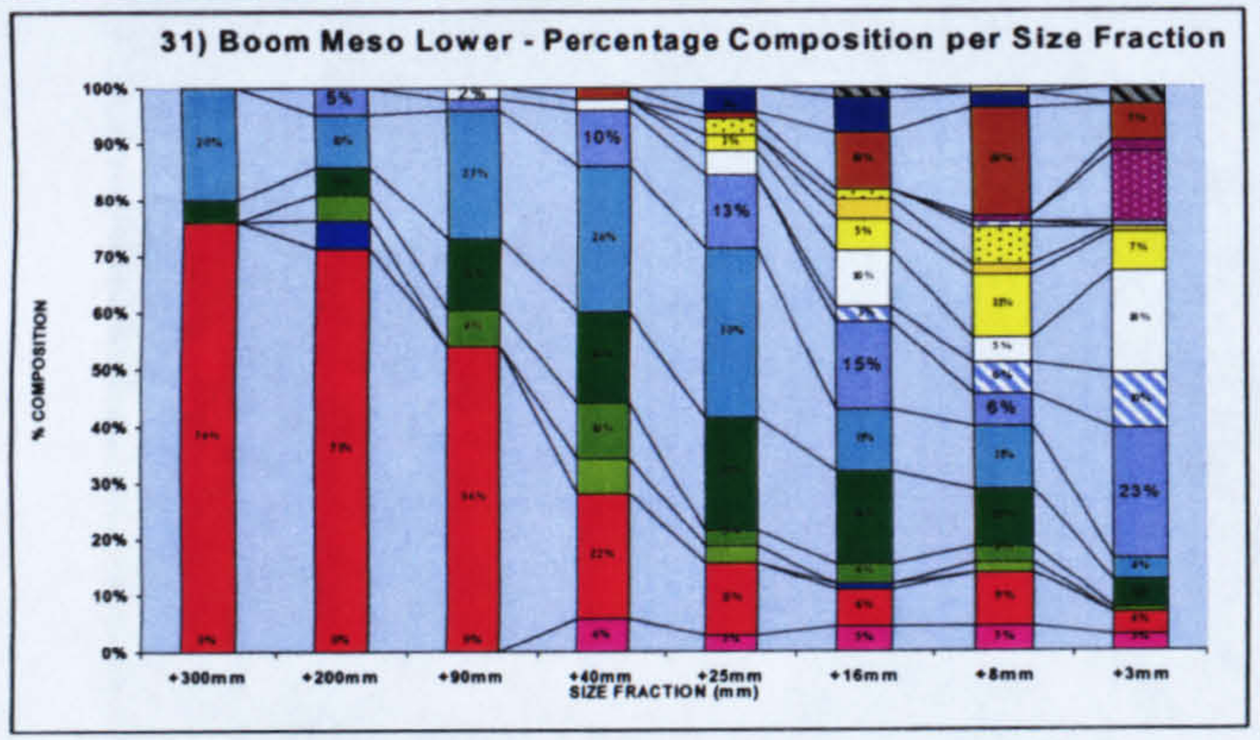

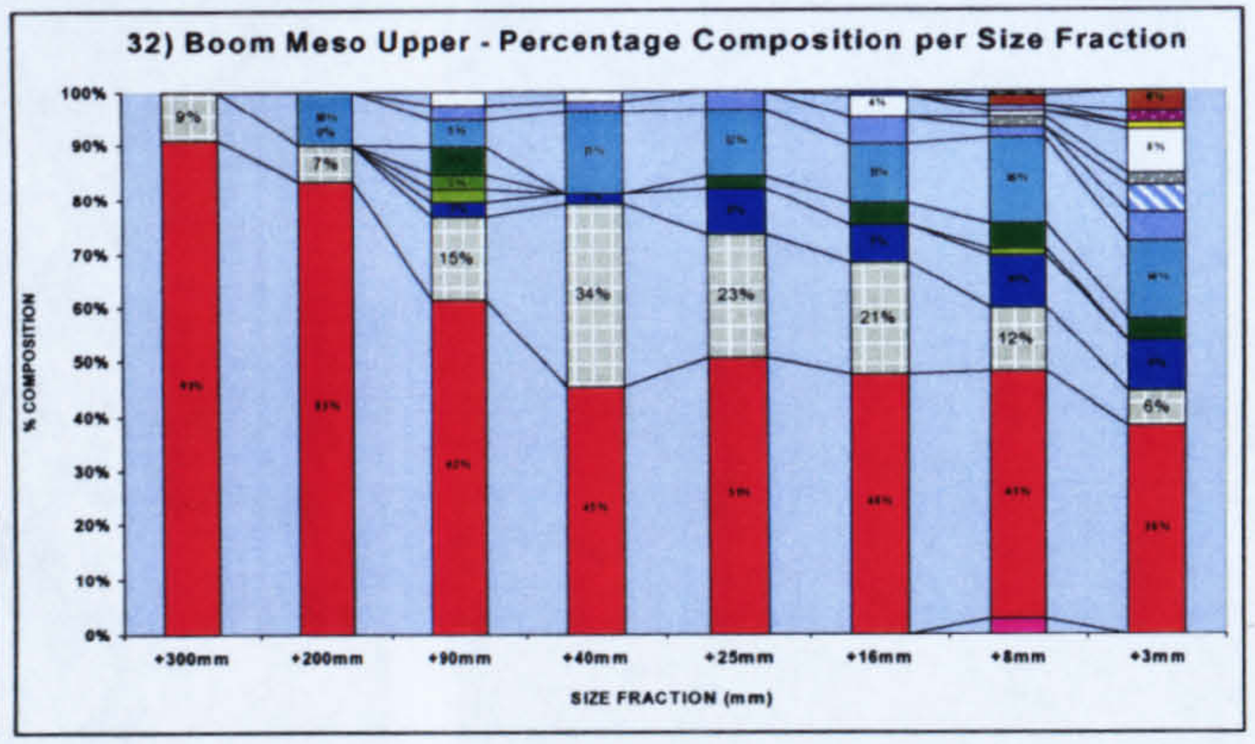

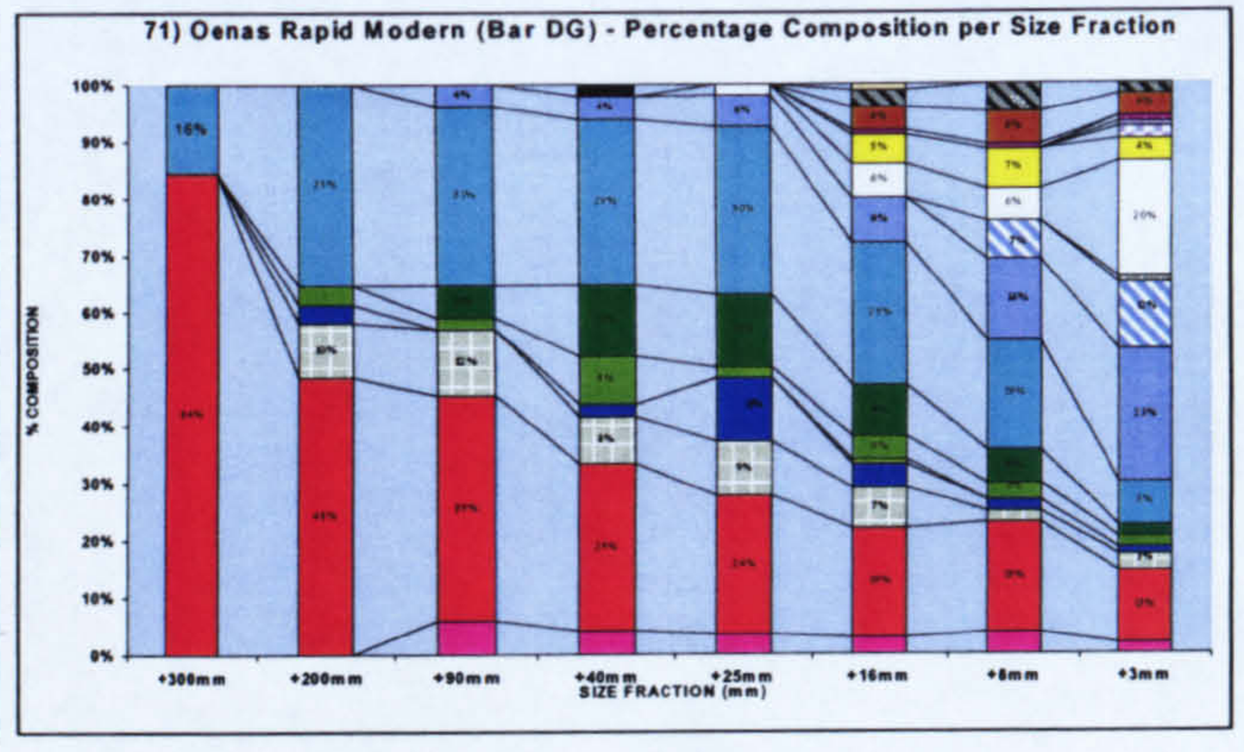

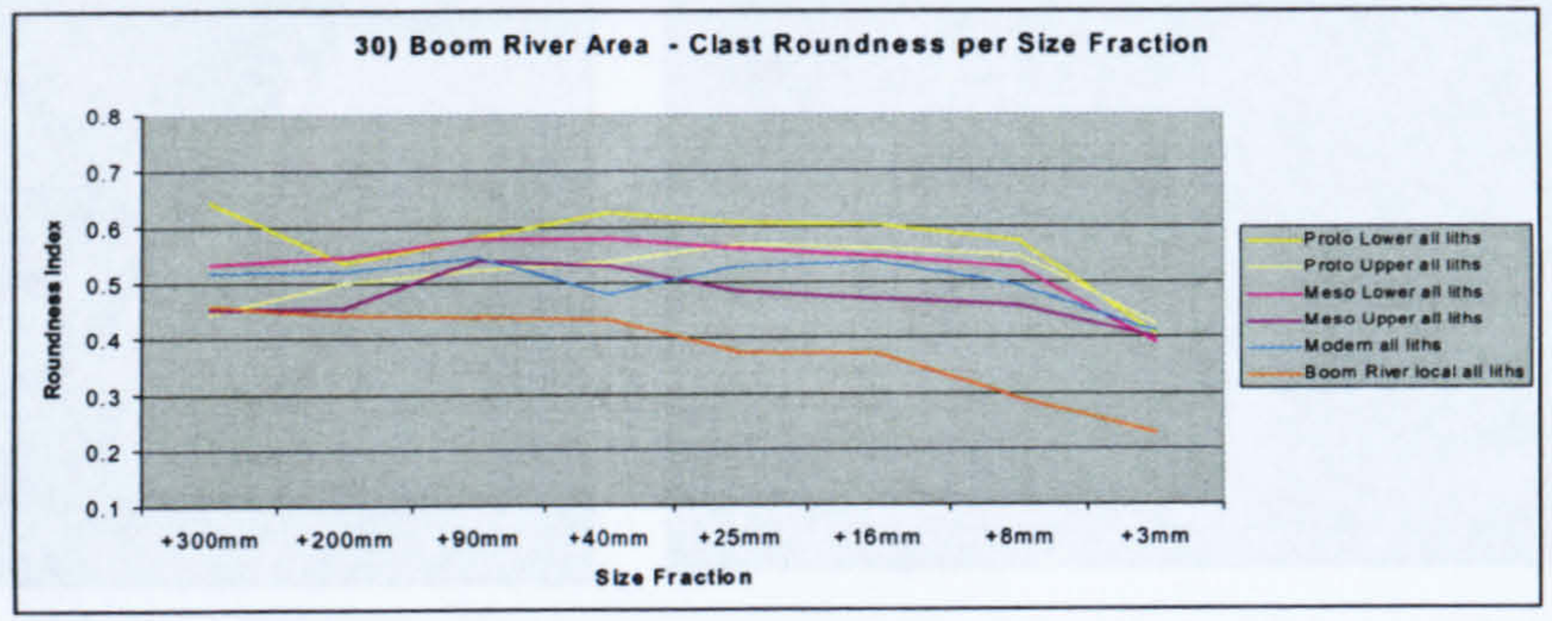

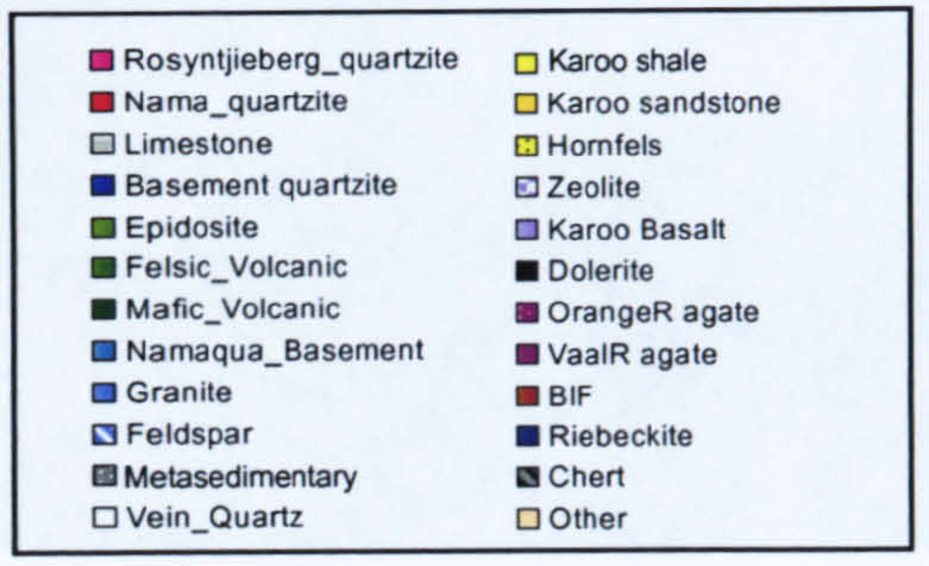

Figure 6.19 Clast type proportions per size fraction and average clast roundness per size fraction for samples in the Boom River area.

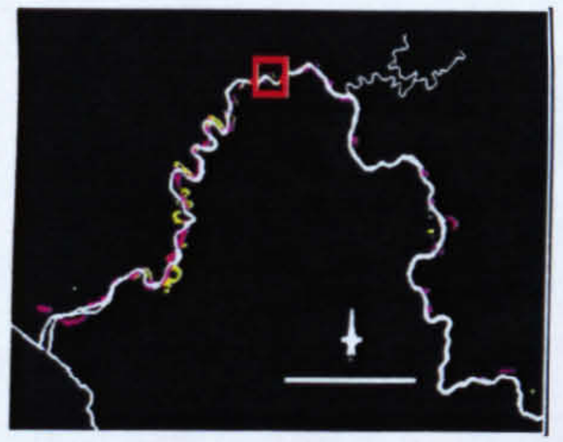

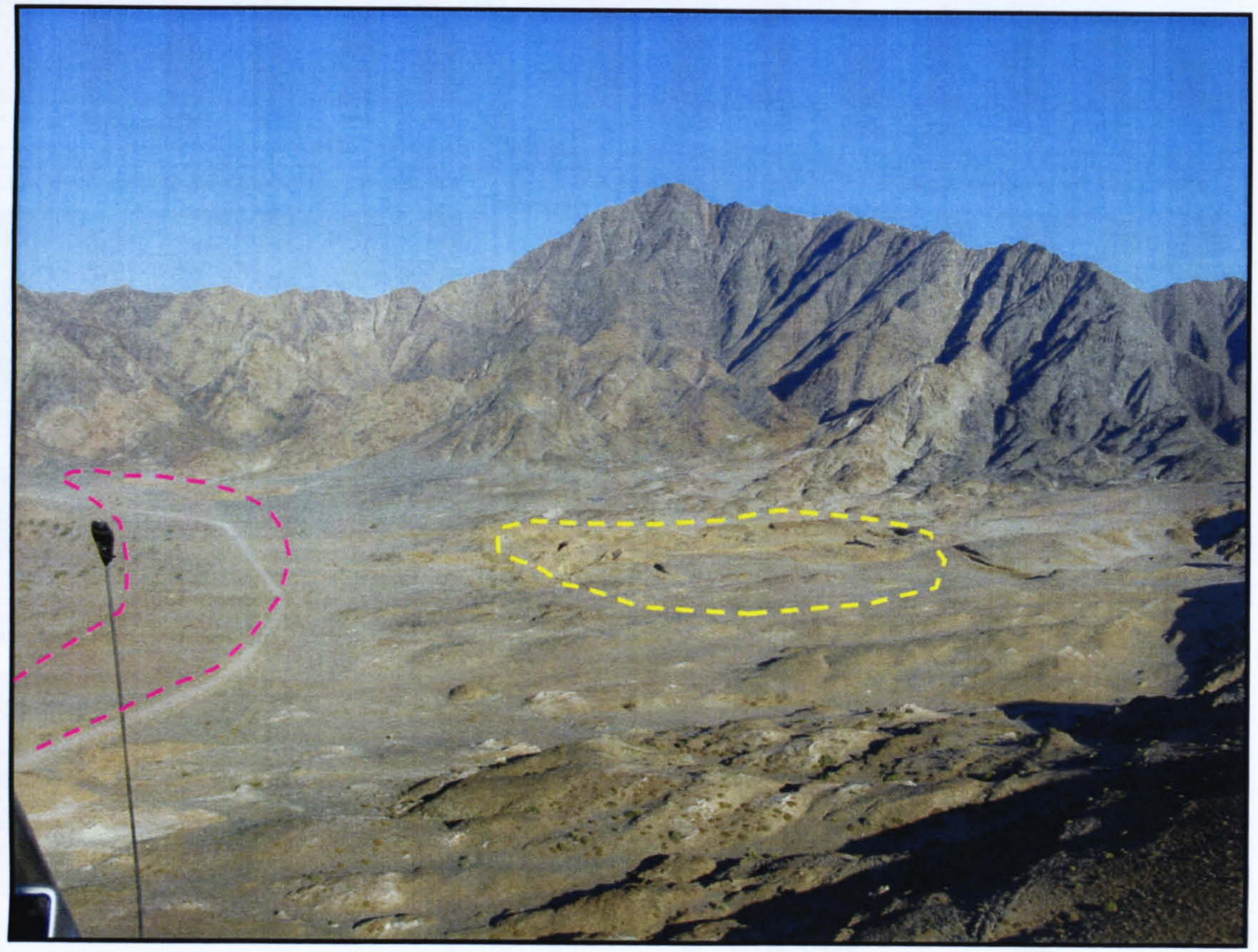

Figure 6.20 Distribution of Proto and Meso terraces in the Lorelei East area.

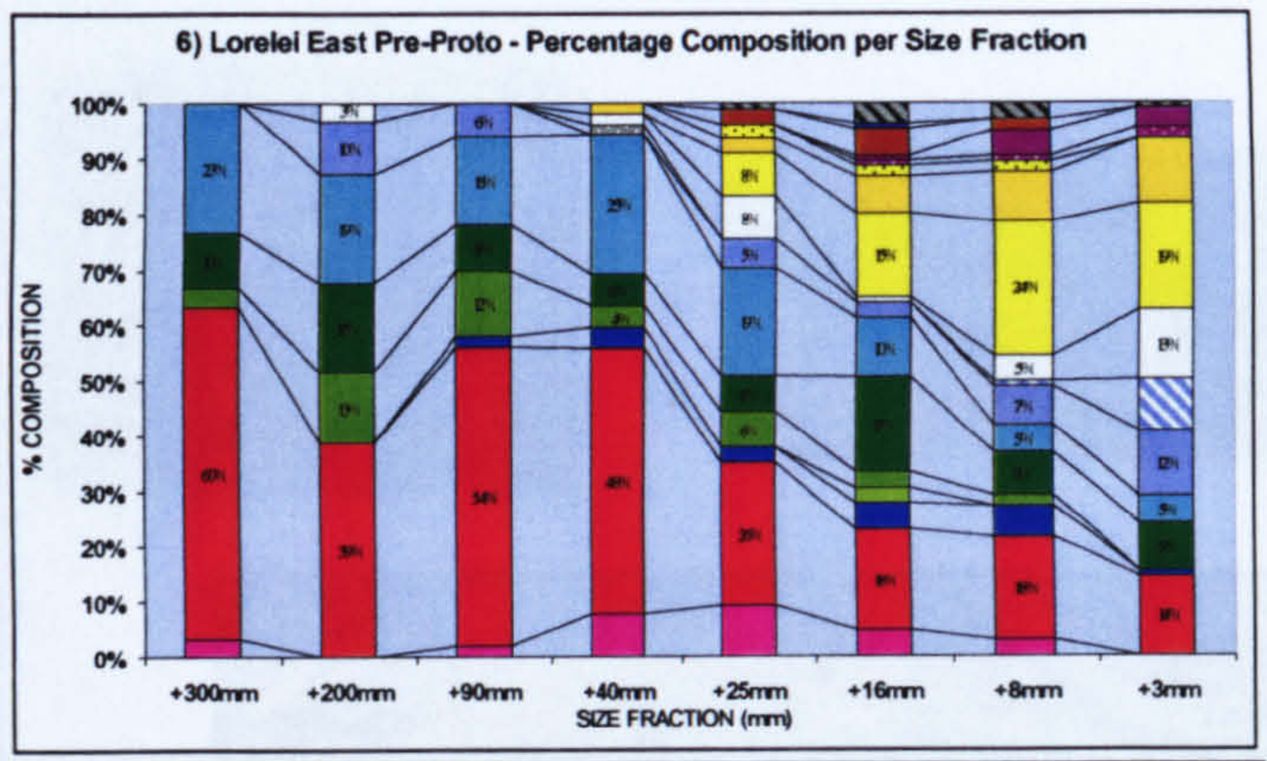

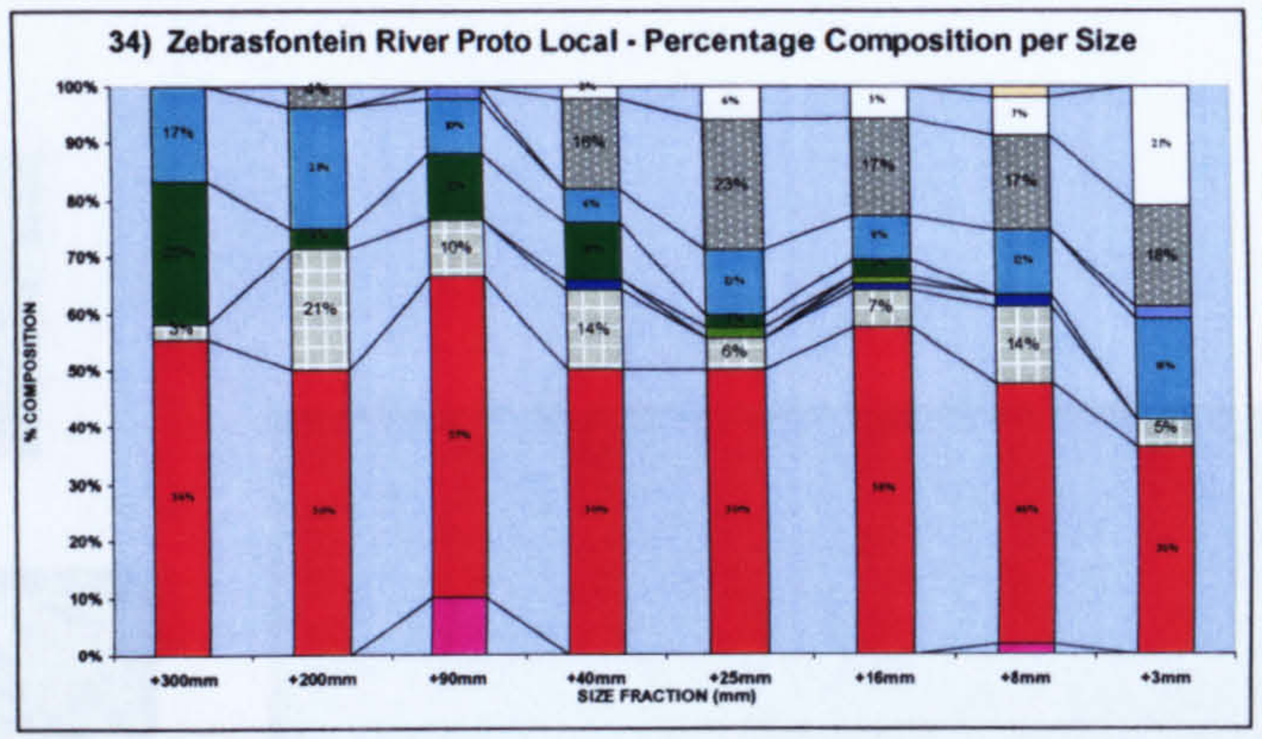

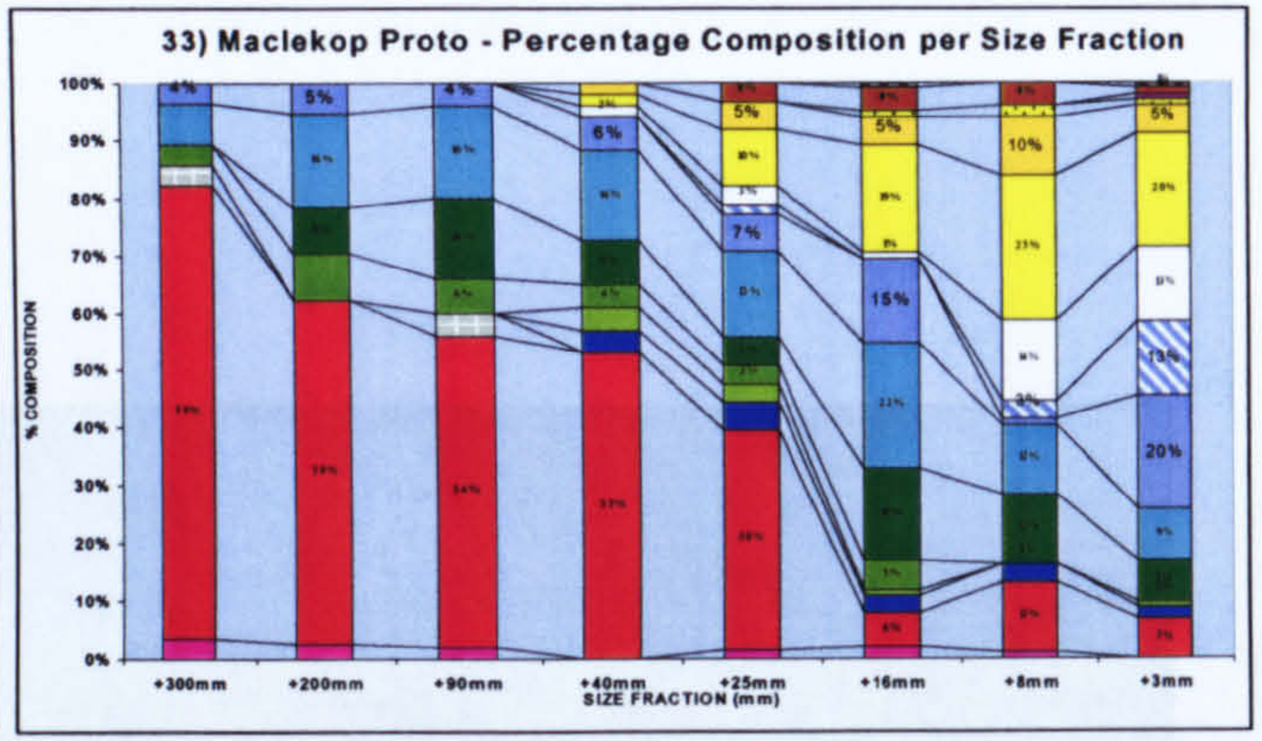

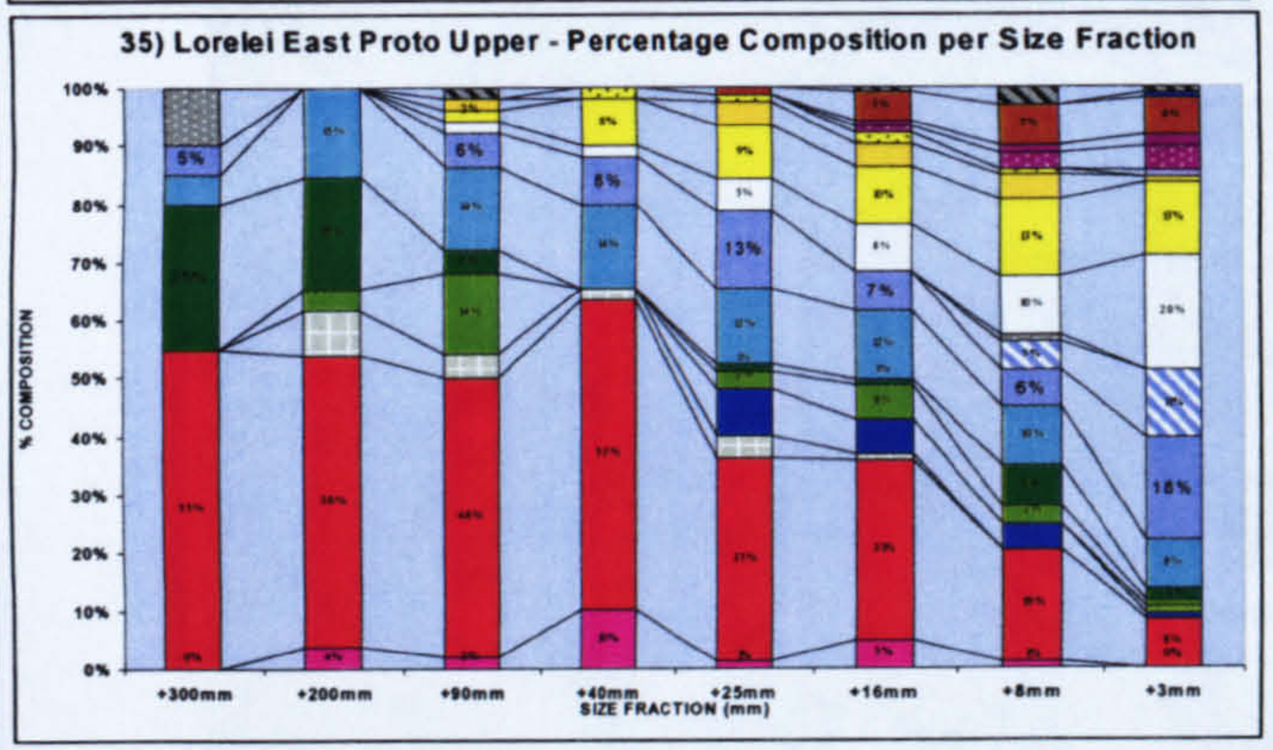

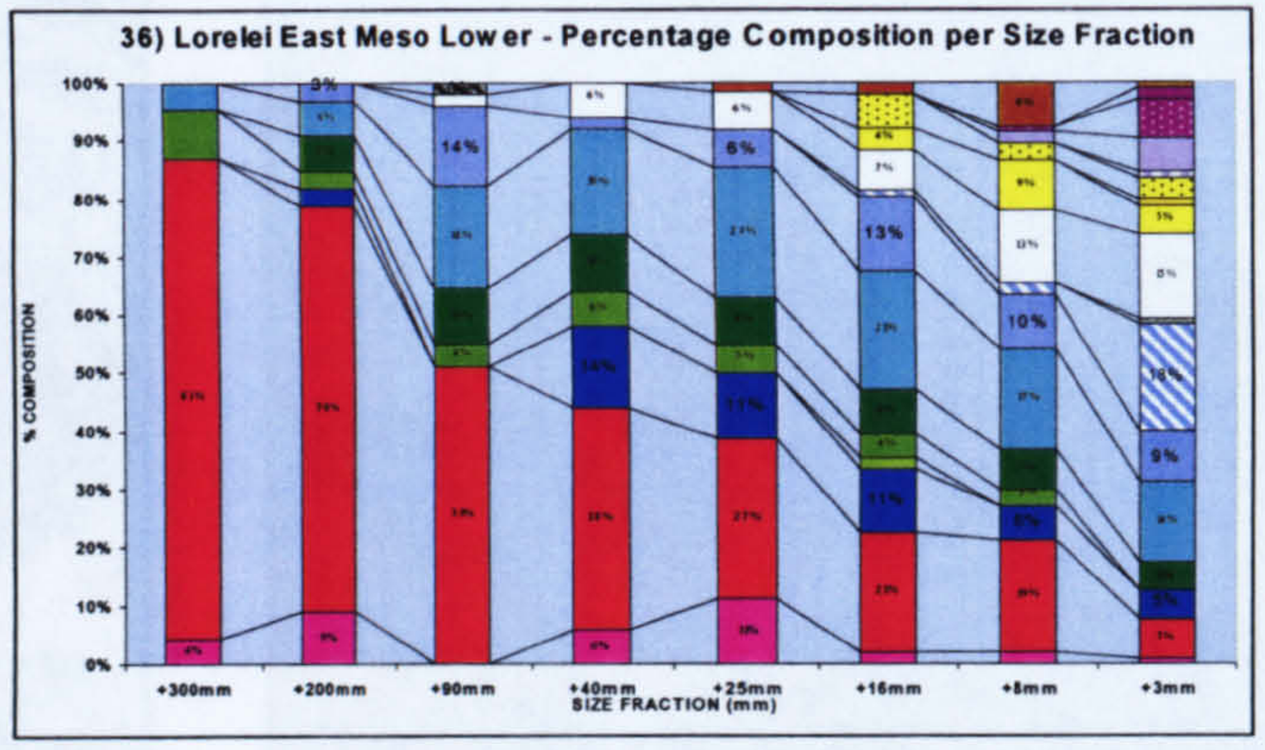

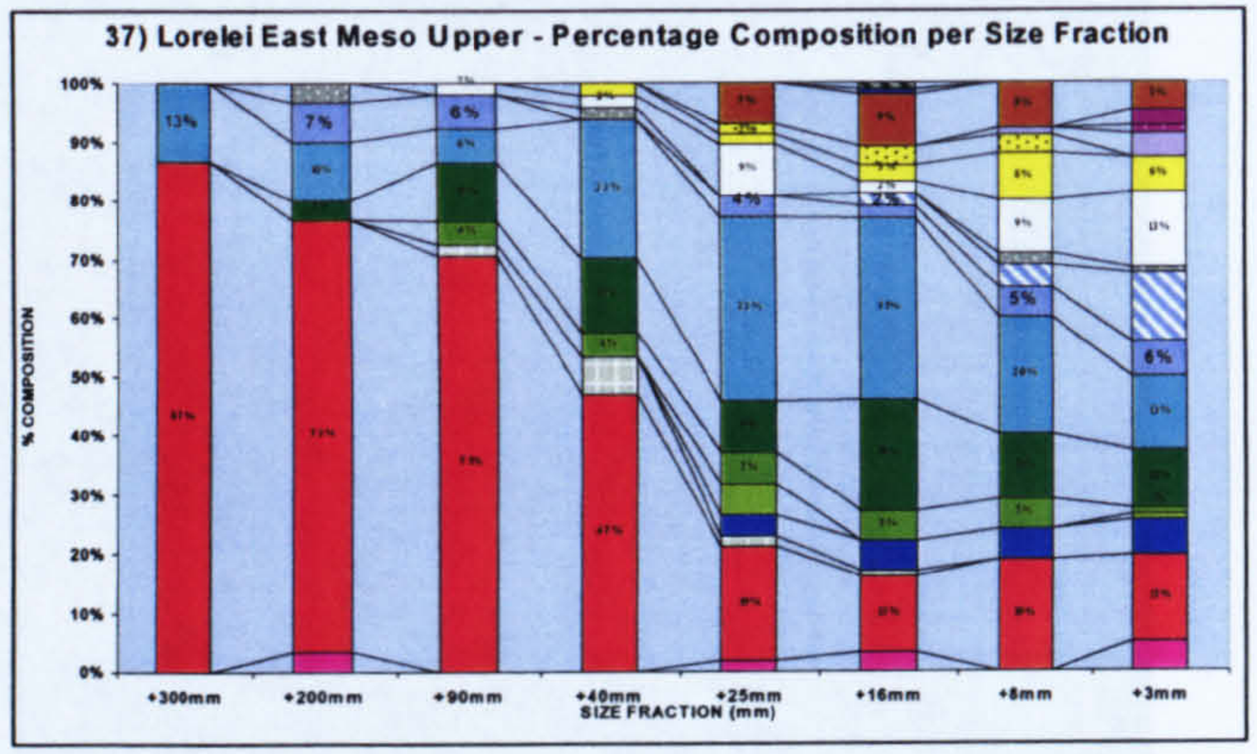

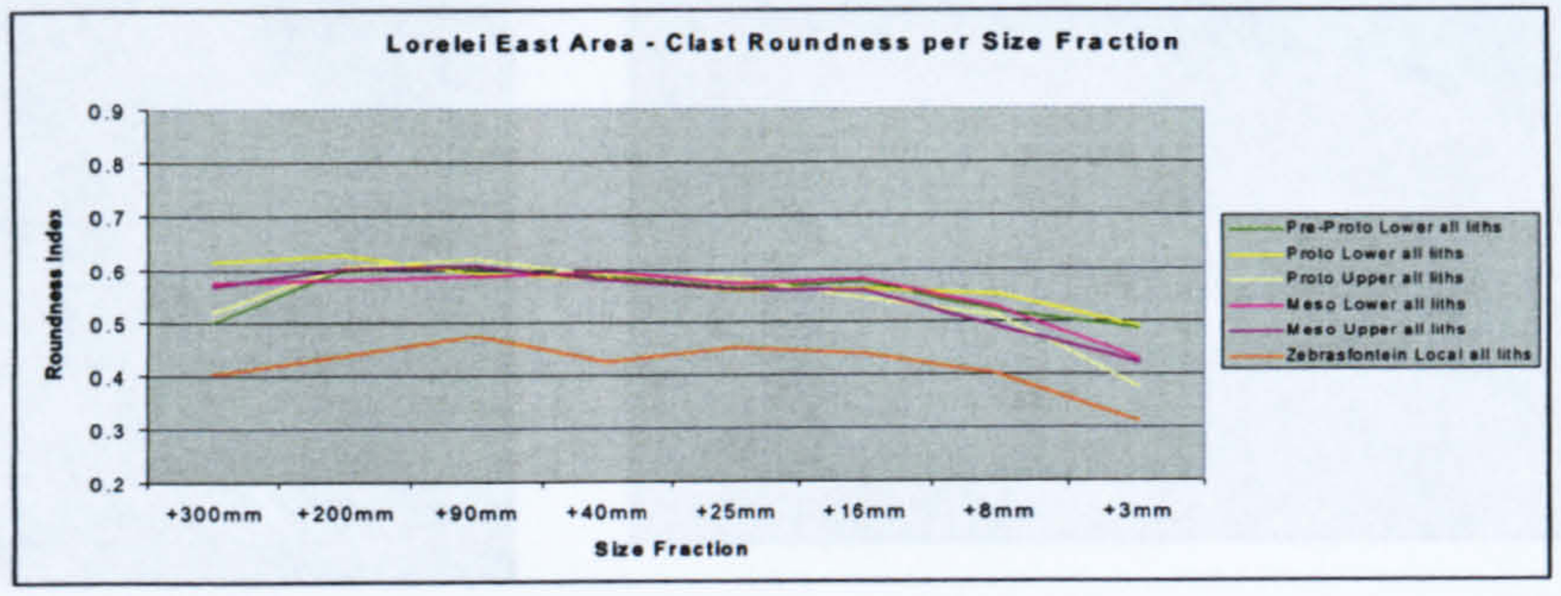

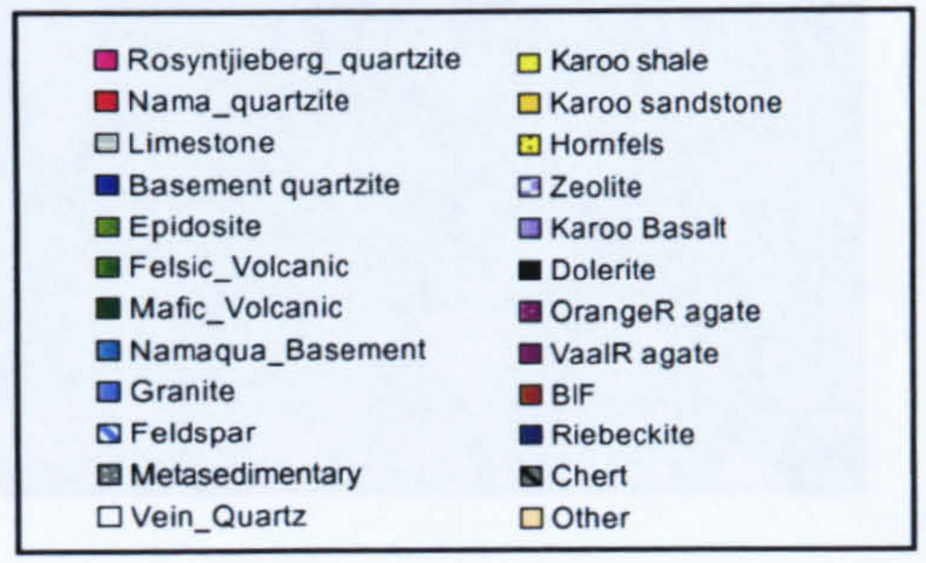

Figure 6.21 Clast type proportions per size fraction and average clast roundness per size fraction for samples in the Lorelei East area.

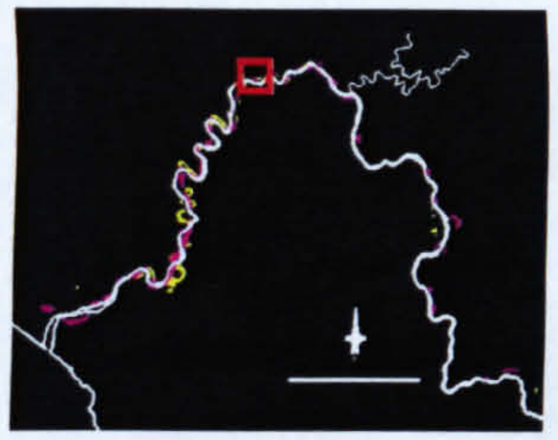

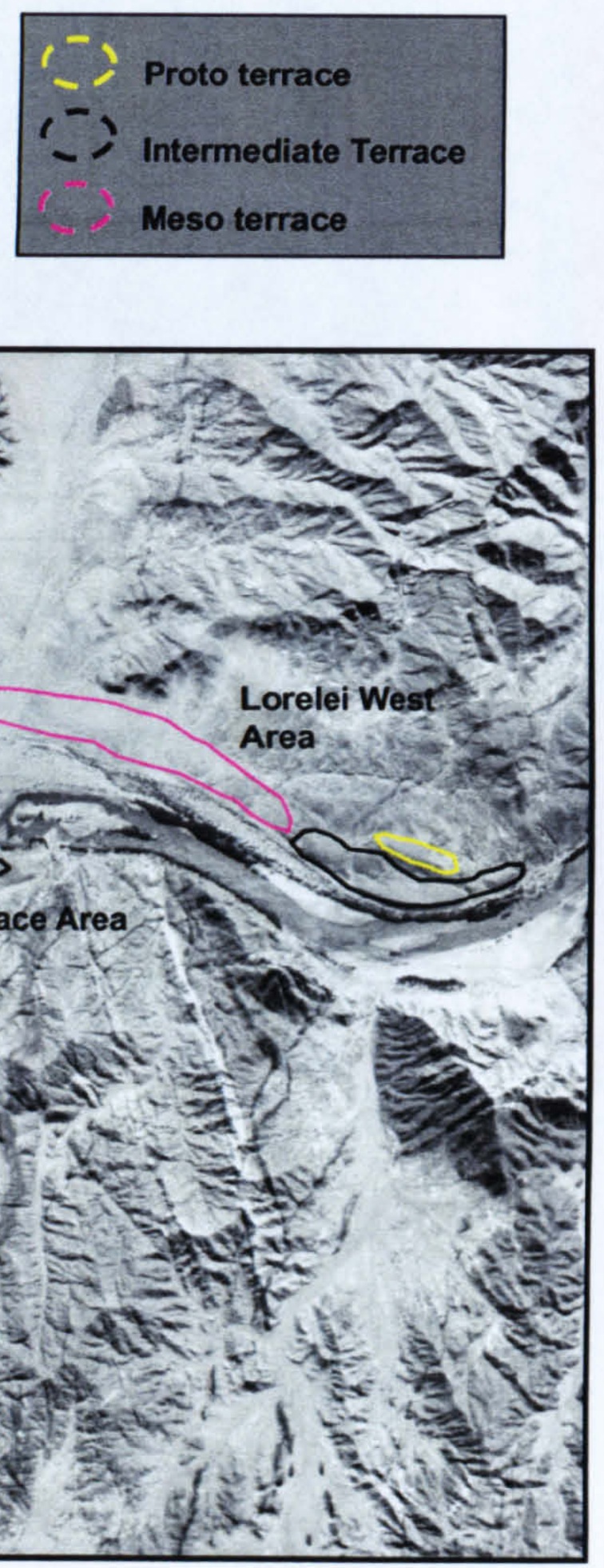

Figure 6.22 Distribution of Proto, Intermediate and Meso terraces in the Lorelei West area.

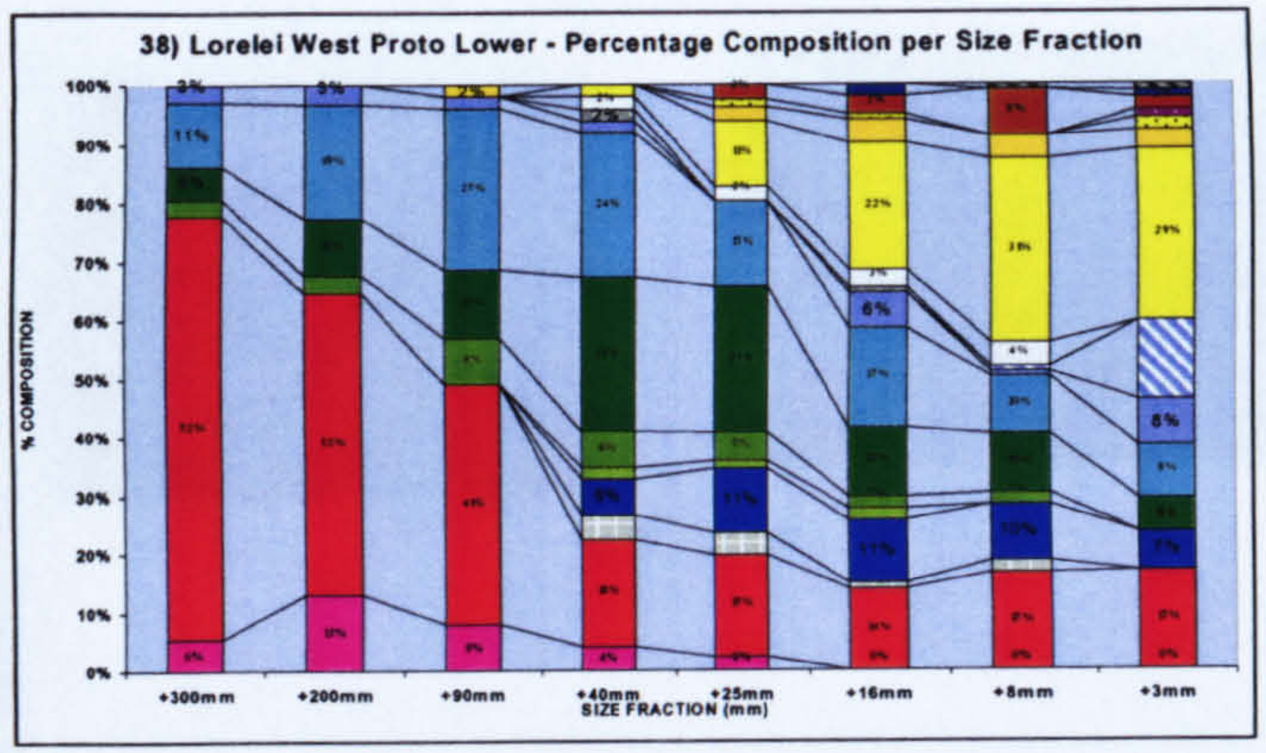

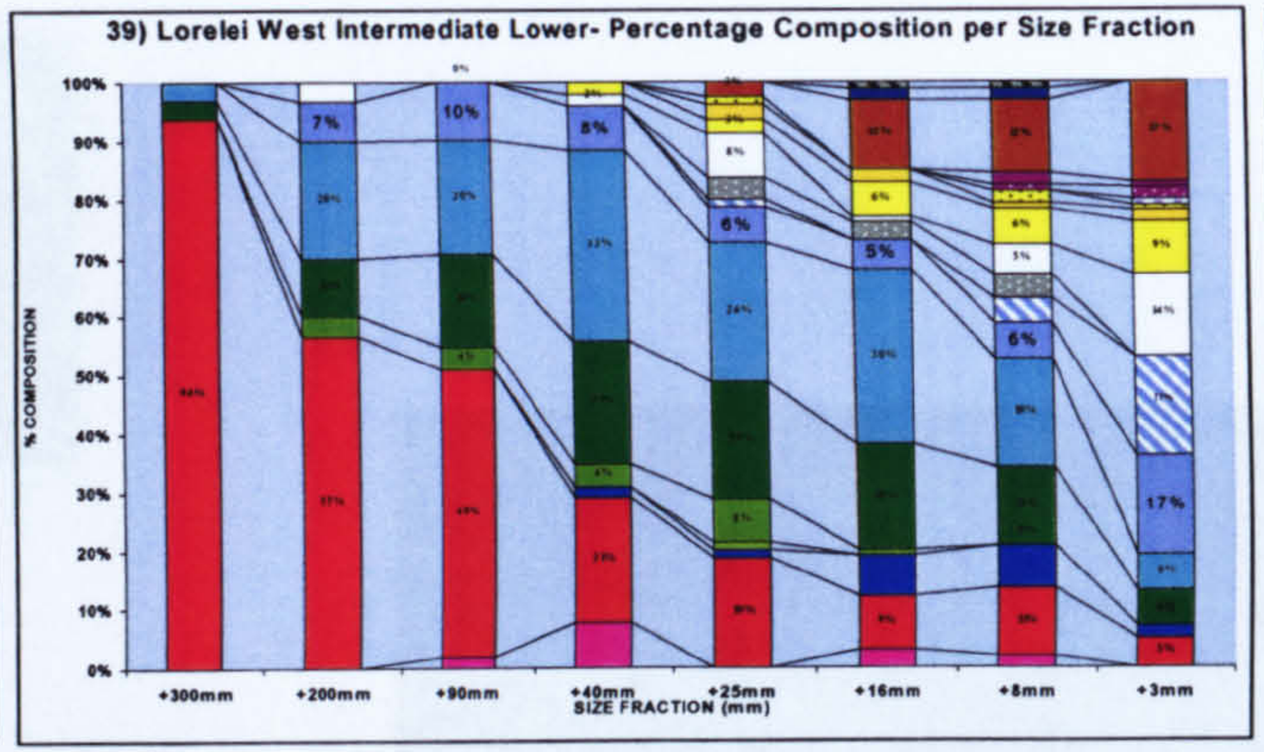

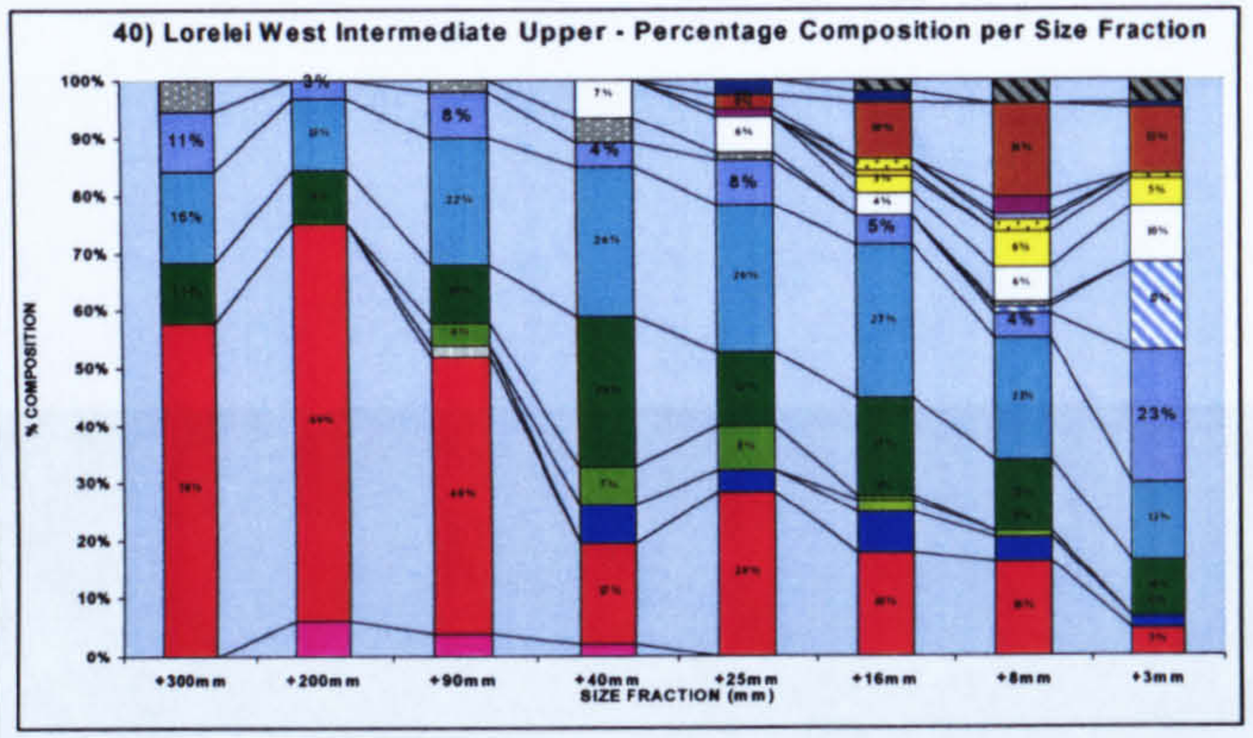

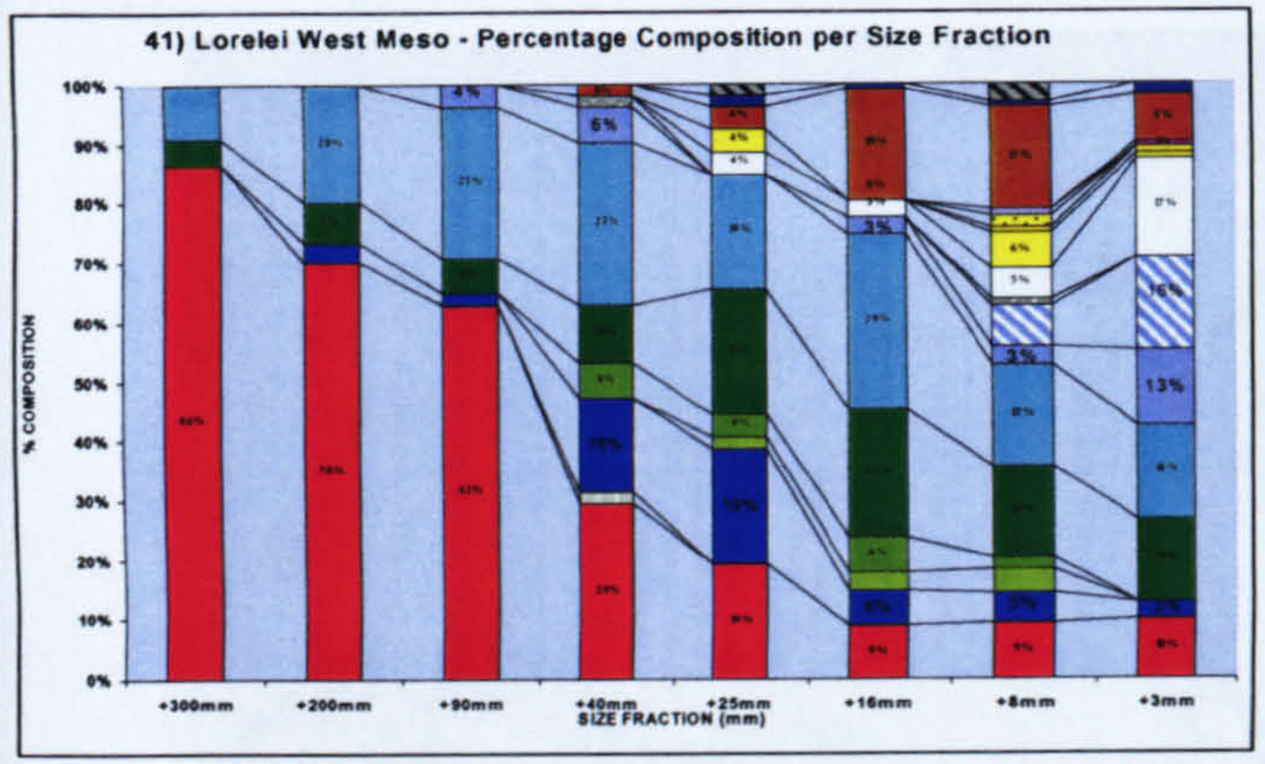

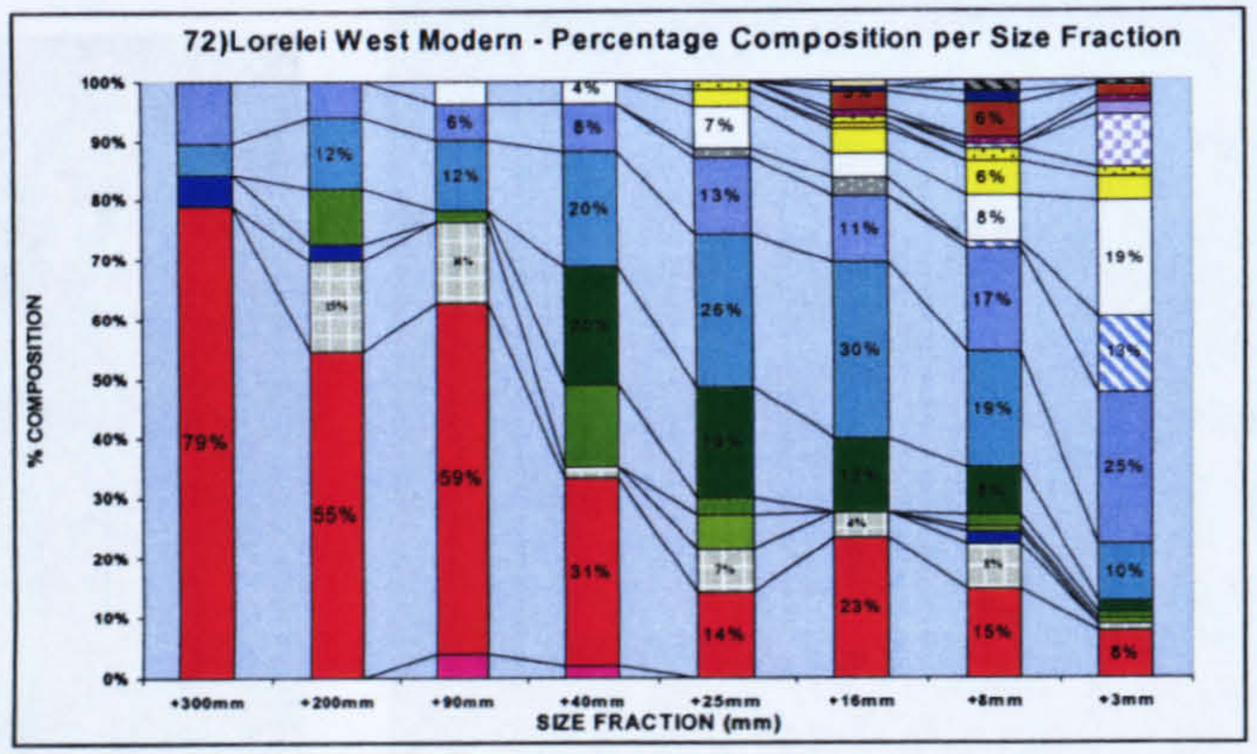

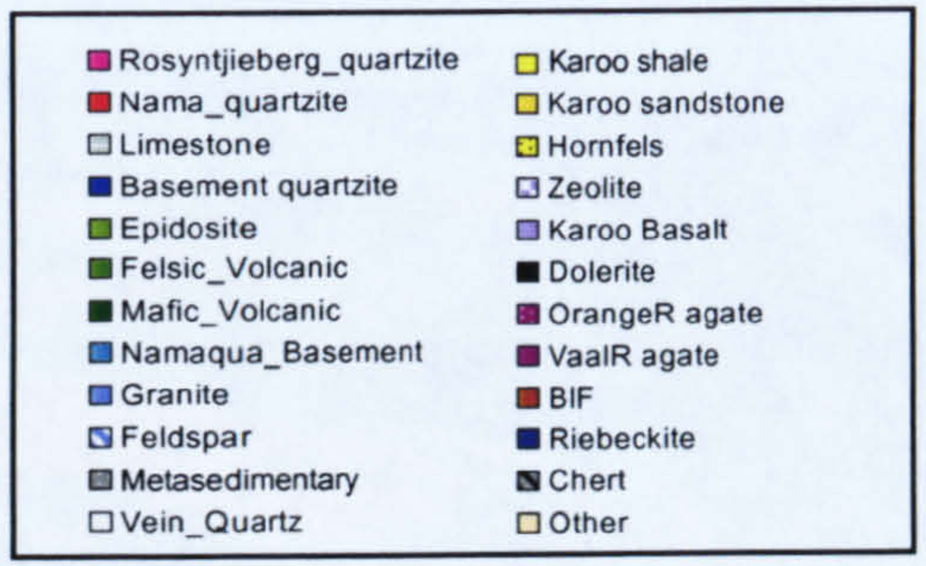

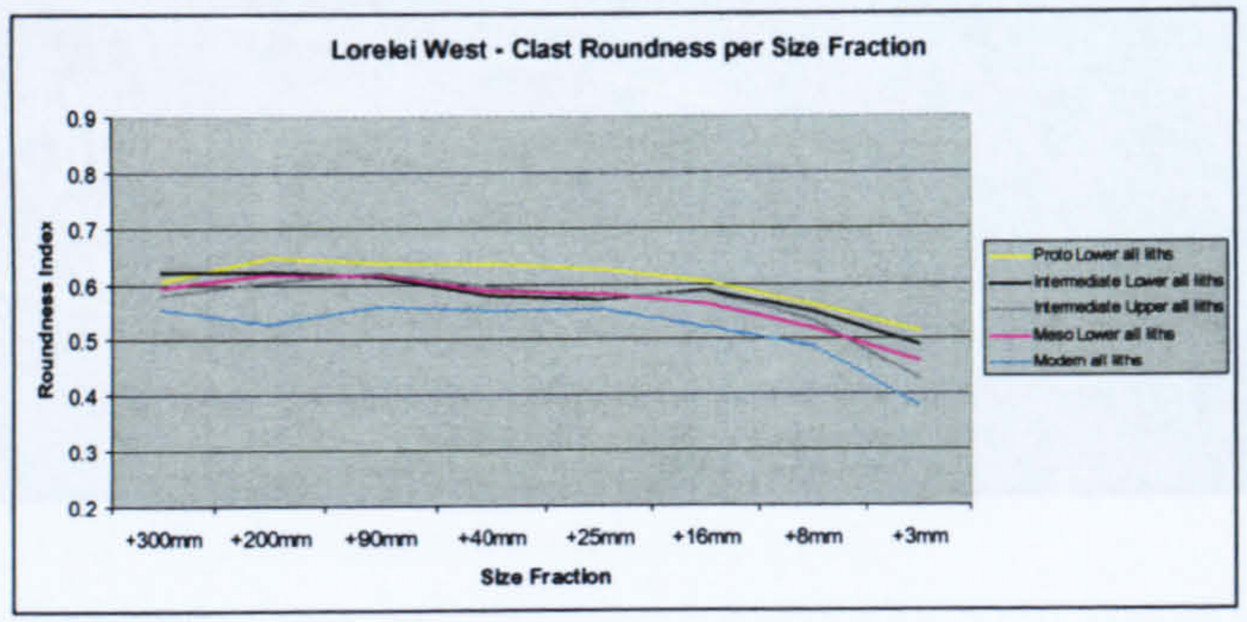

Figure 6.23 Clast type proportions per size fraction and average clast roundness per size fraction for samples in the Lorelei West area.

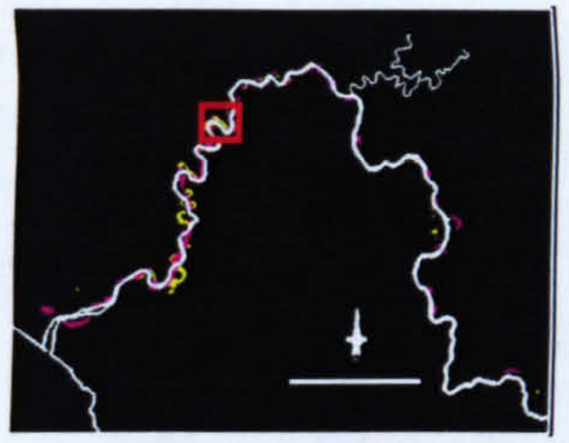

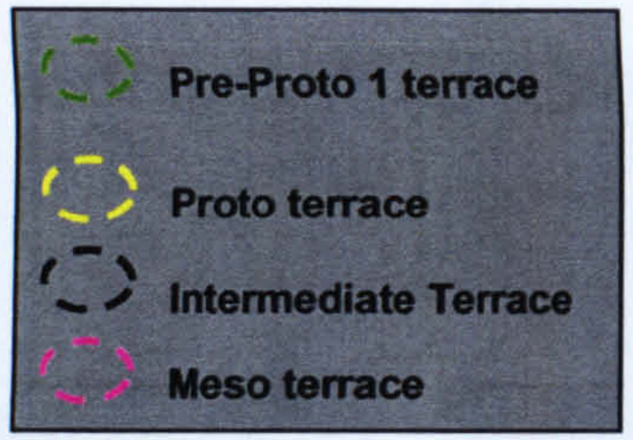

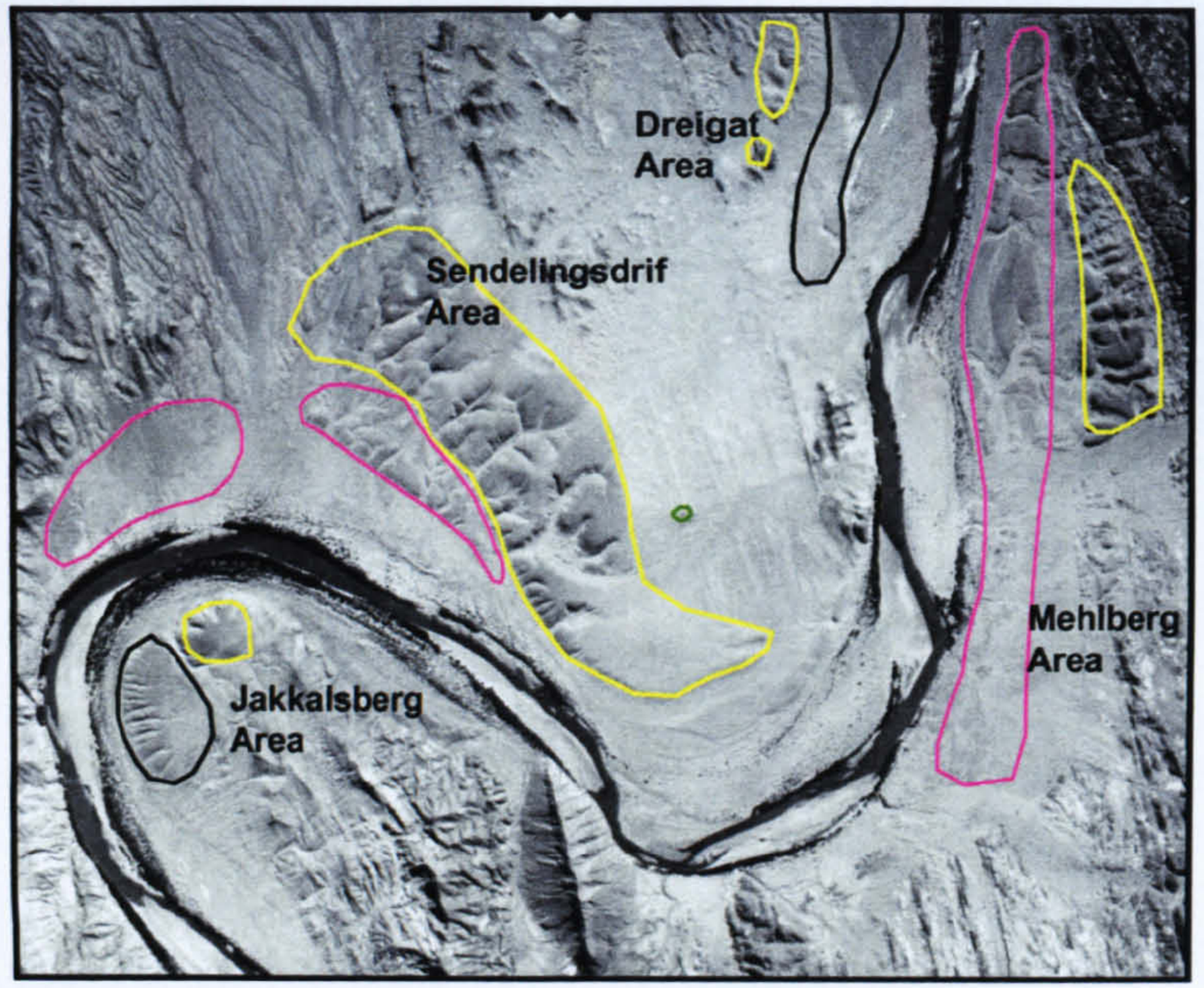

Figure 6.24 Distribution of Pre-Proto 1, Proto and Meso terraces in the Sendelingsdrif area.

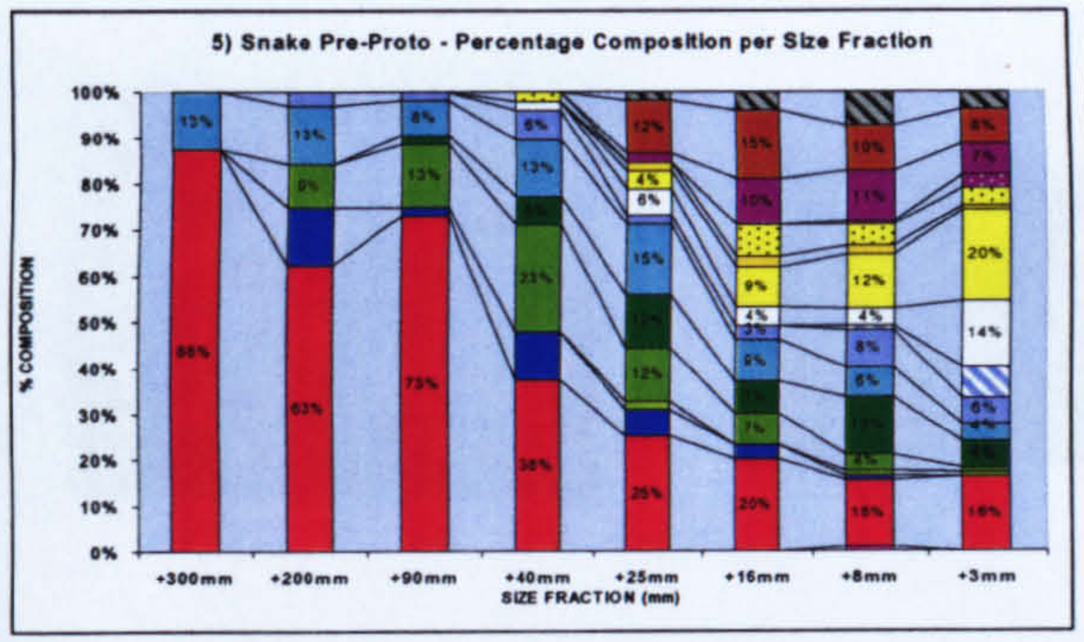

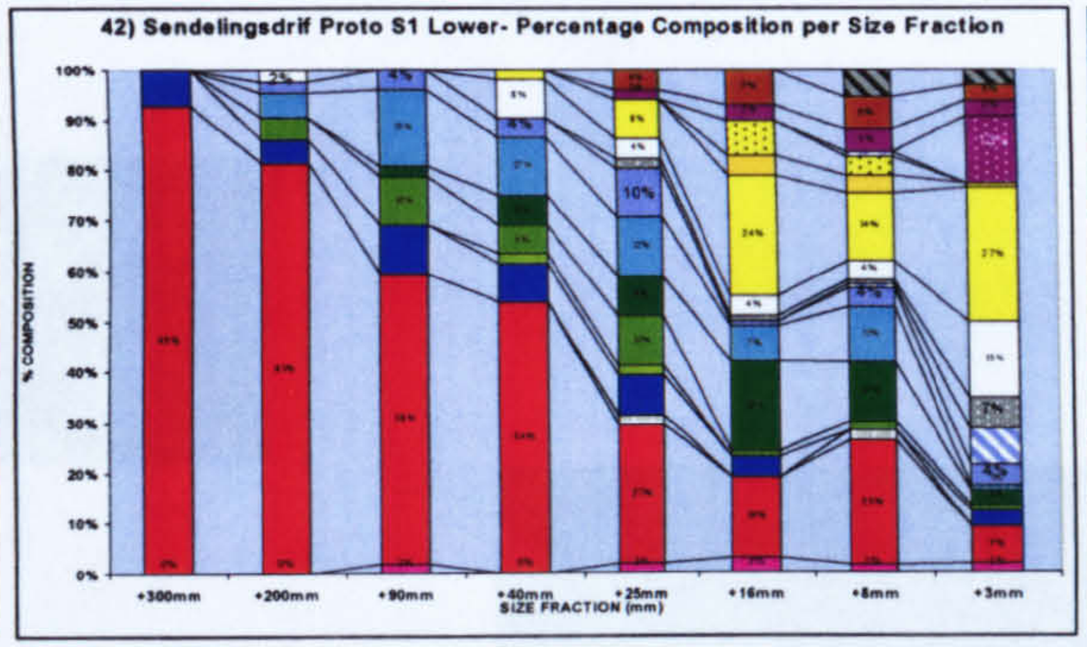

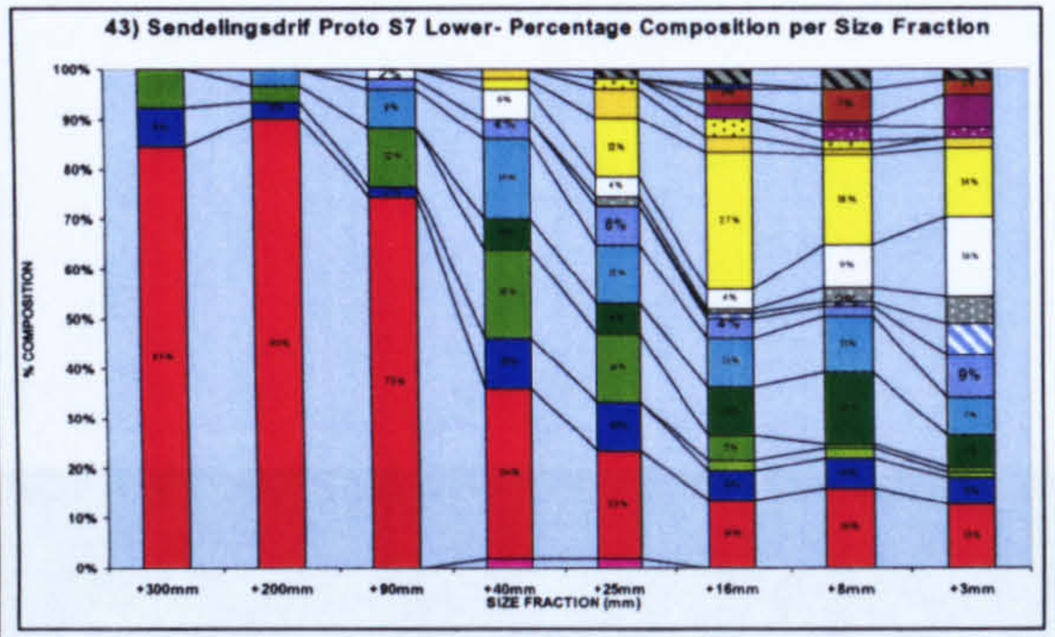

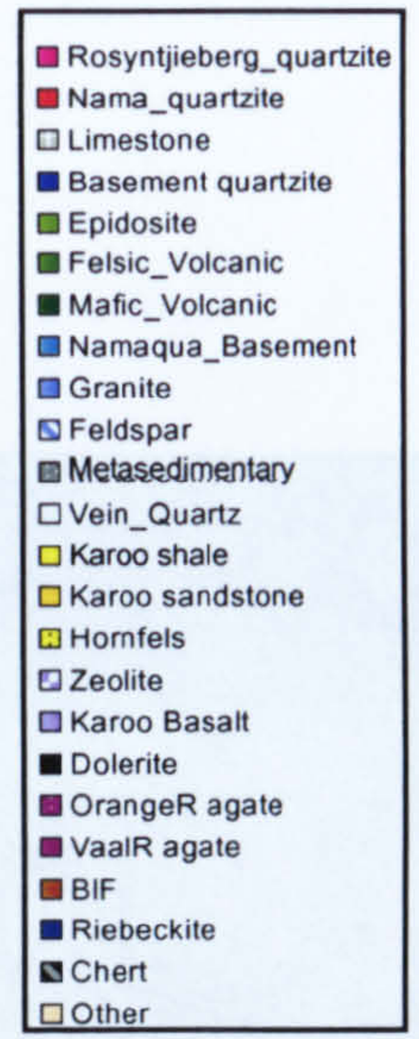

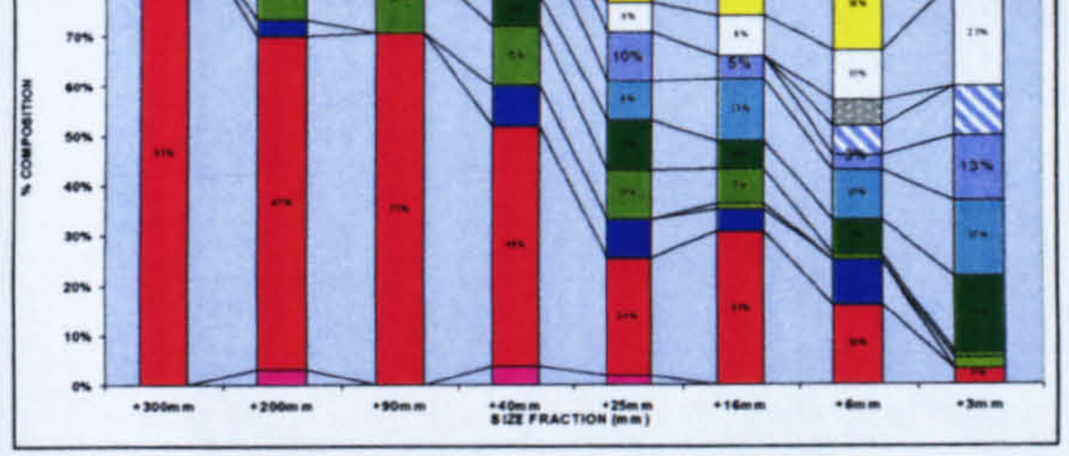

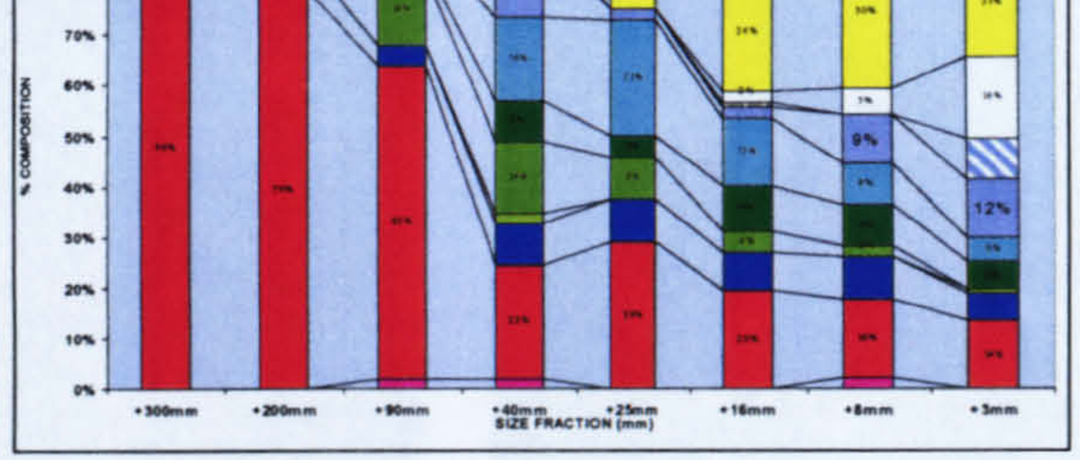

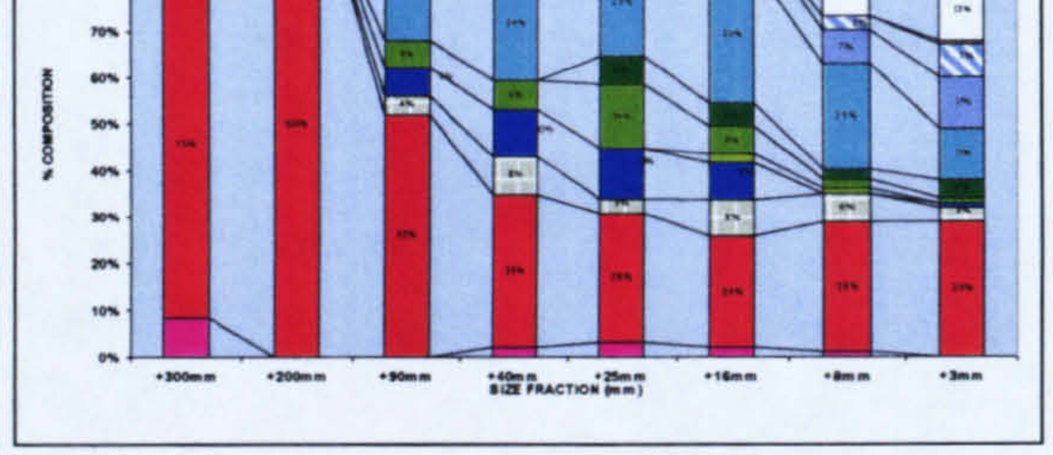

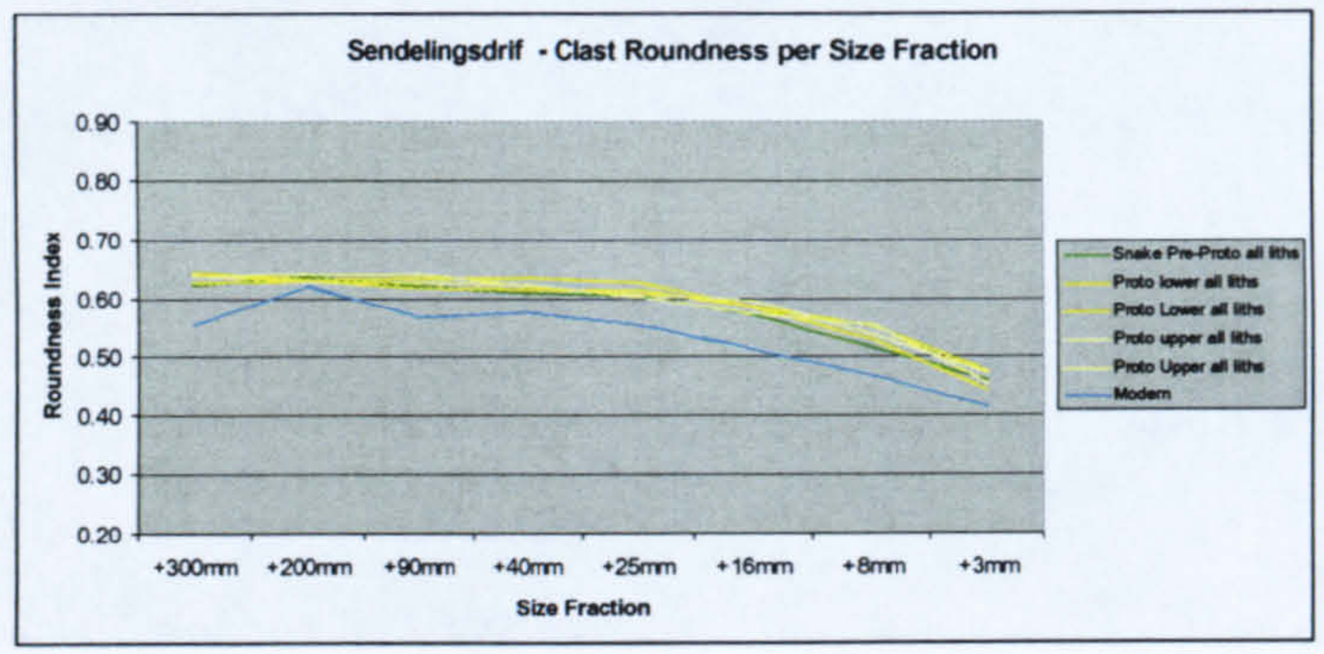

Figure 6.25 Clast type proportions per size fraction and average clast roundness per size fraction for samples in the Sendelingsdrif area.

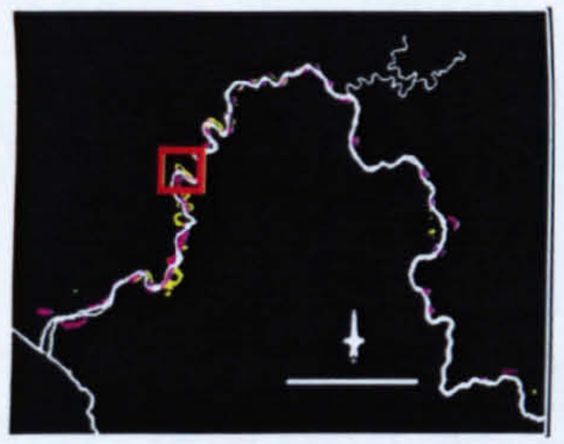

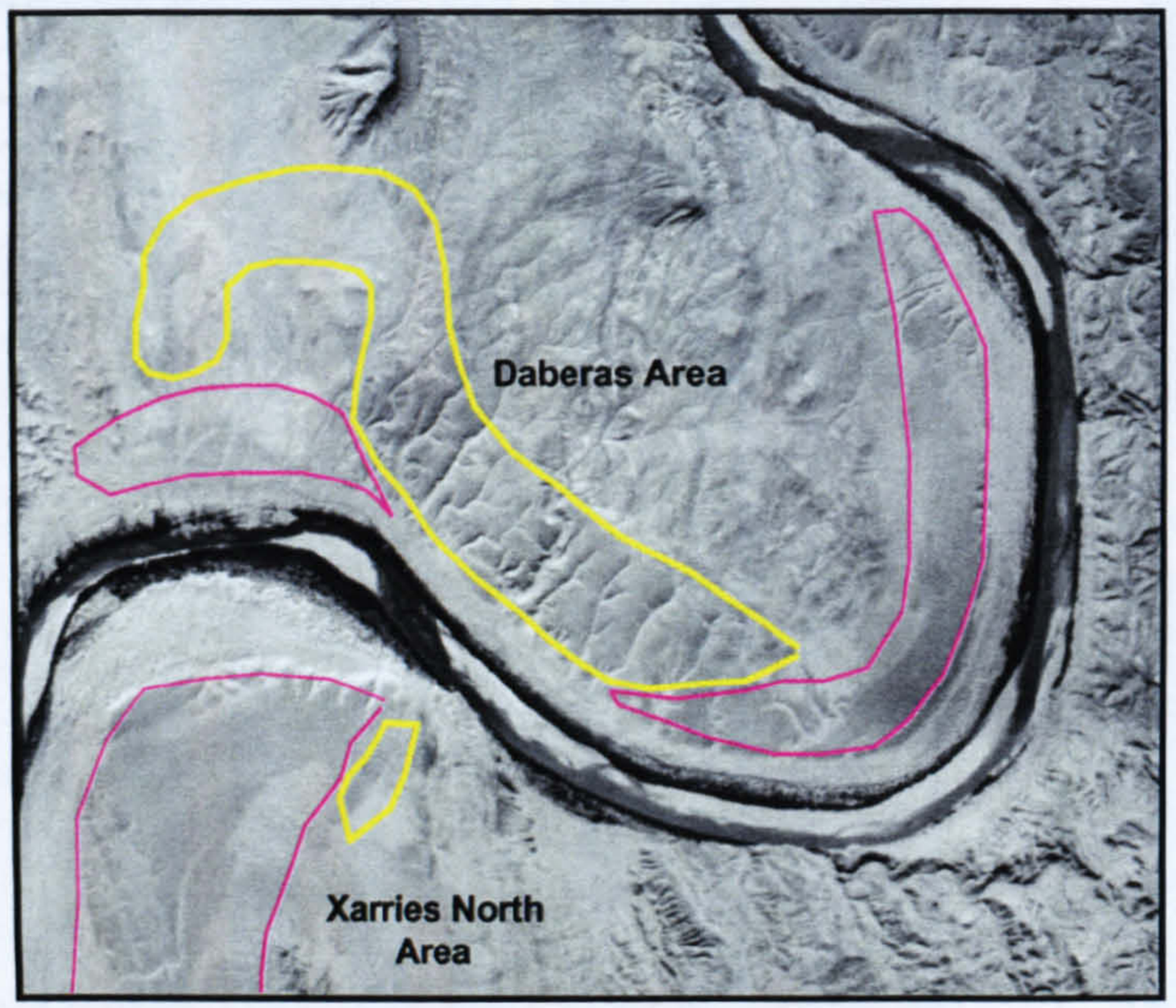

Figure 6.26 Distribution of Proto and Meso terraces in the Daberas area.

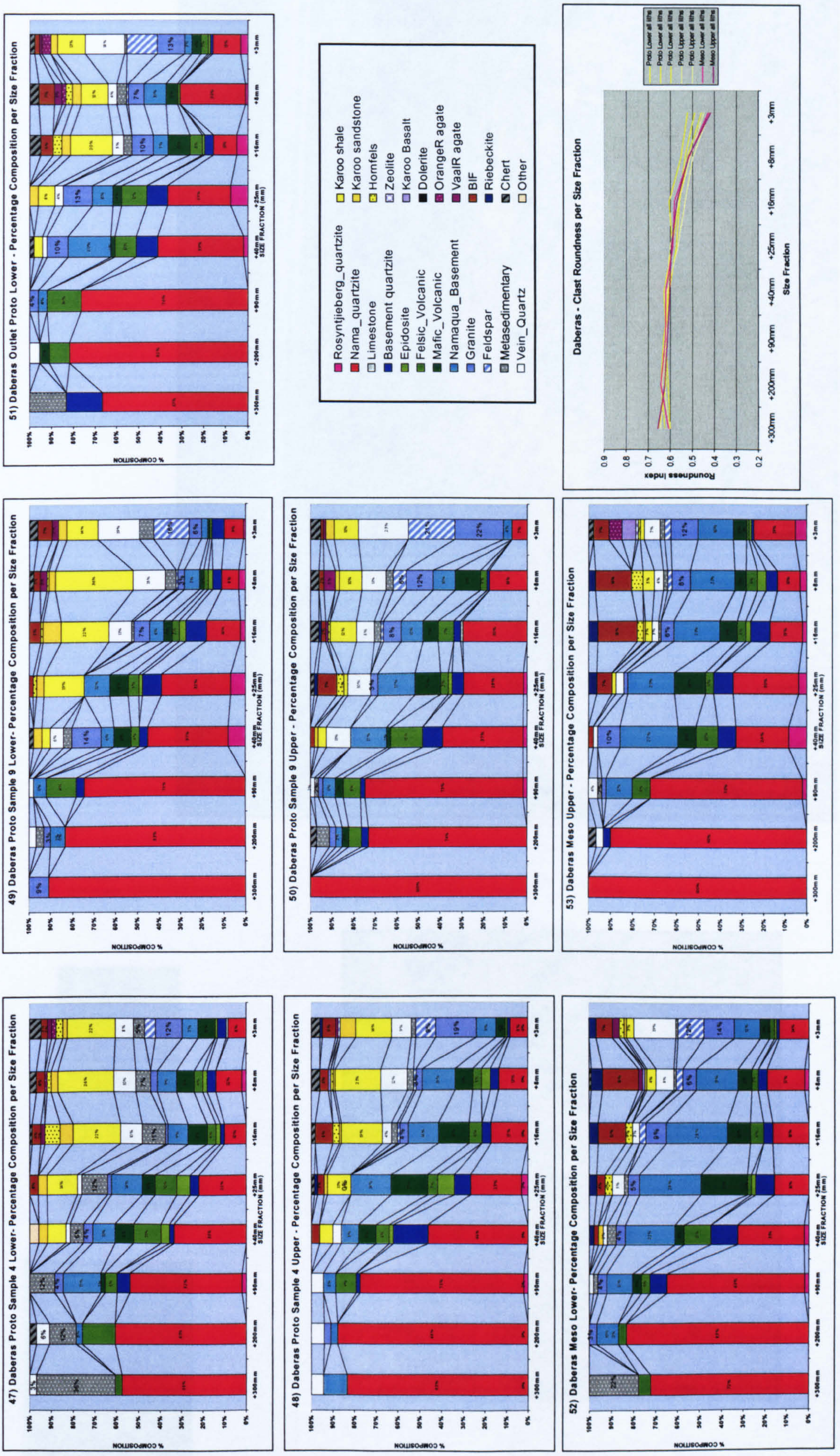

Figure 6.27 Clast type proportions per size fraction and average clast roundness per size fraction for samples in the Daberas area.

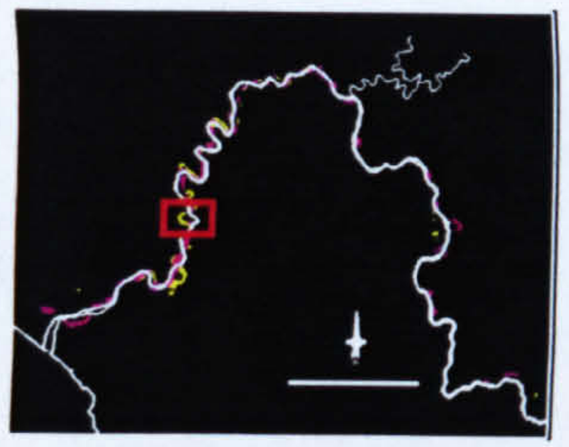

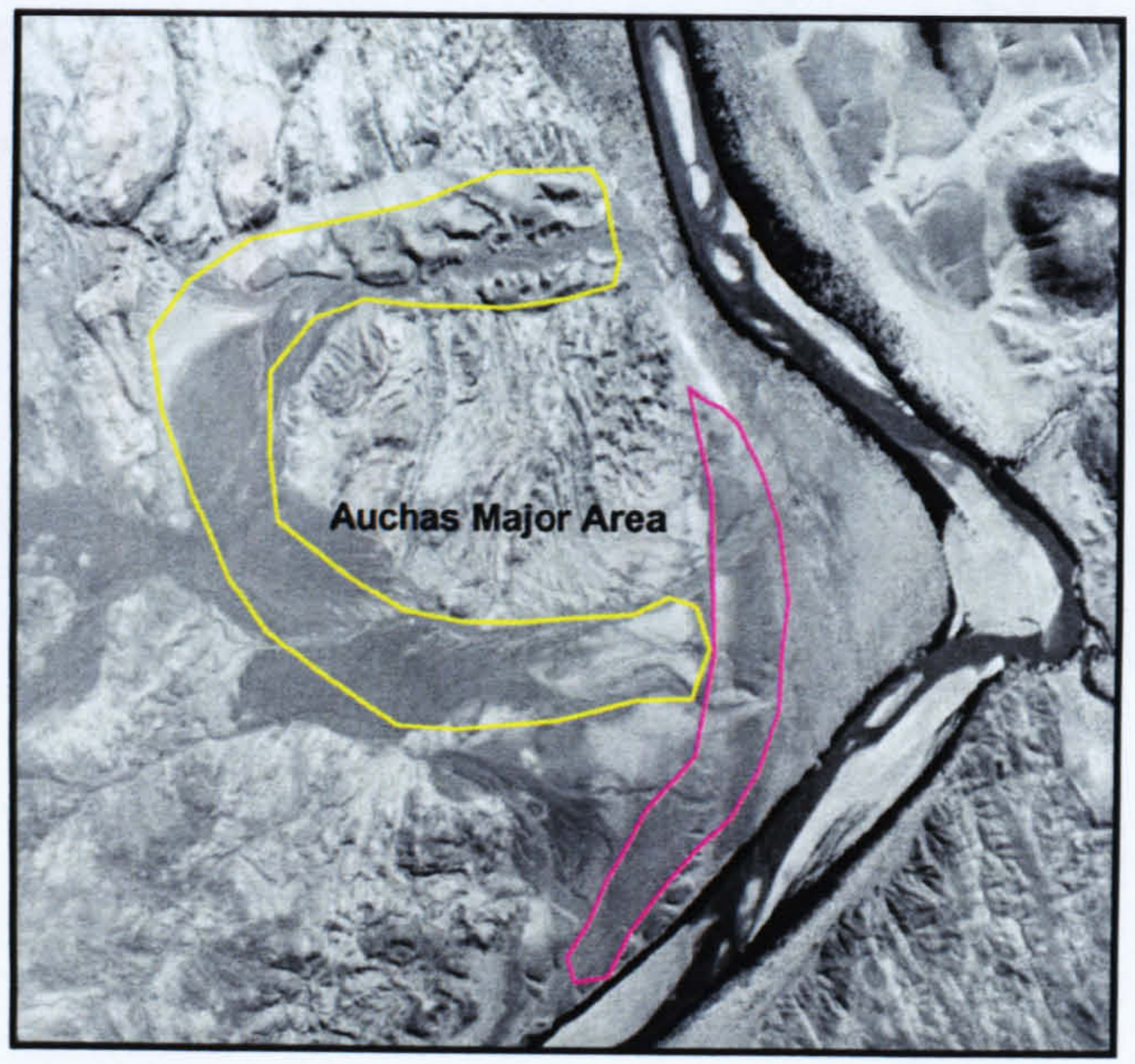

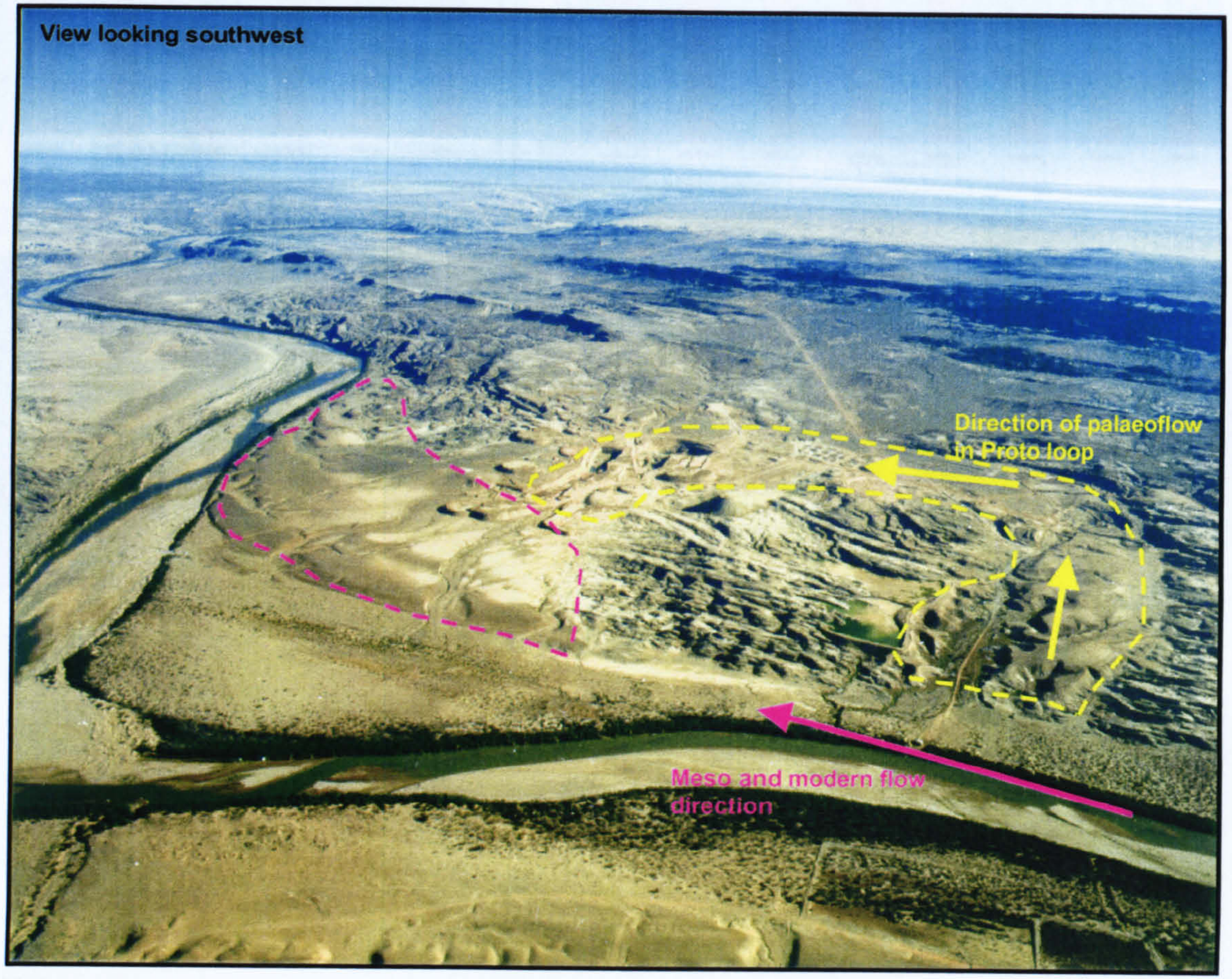

Figure 6.28 Distribution of Proto and Meso terraces in the Auchas Major area.

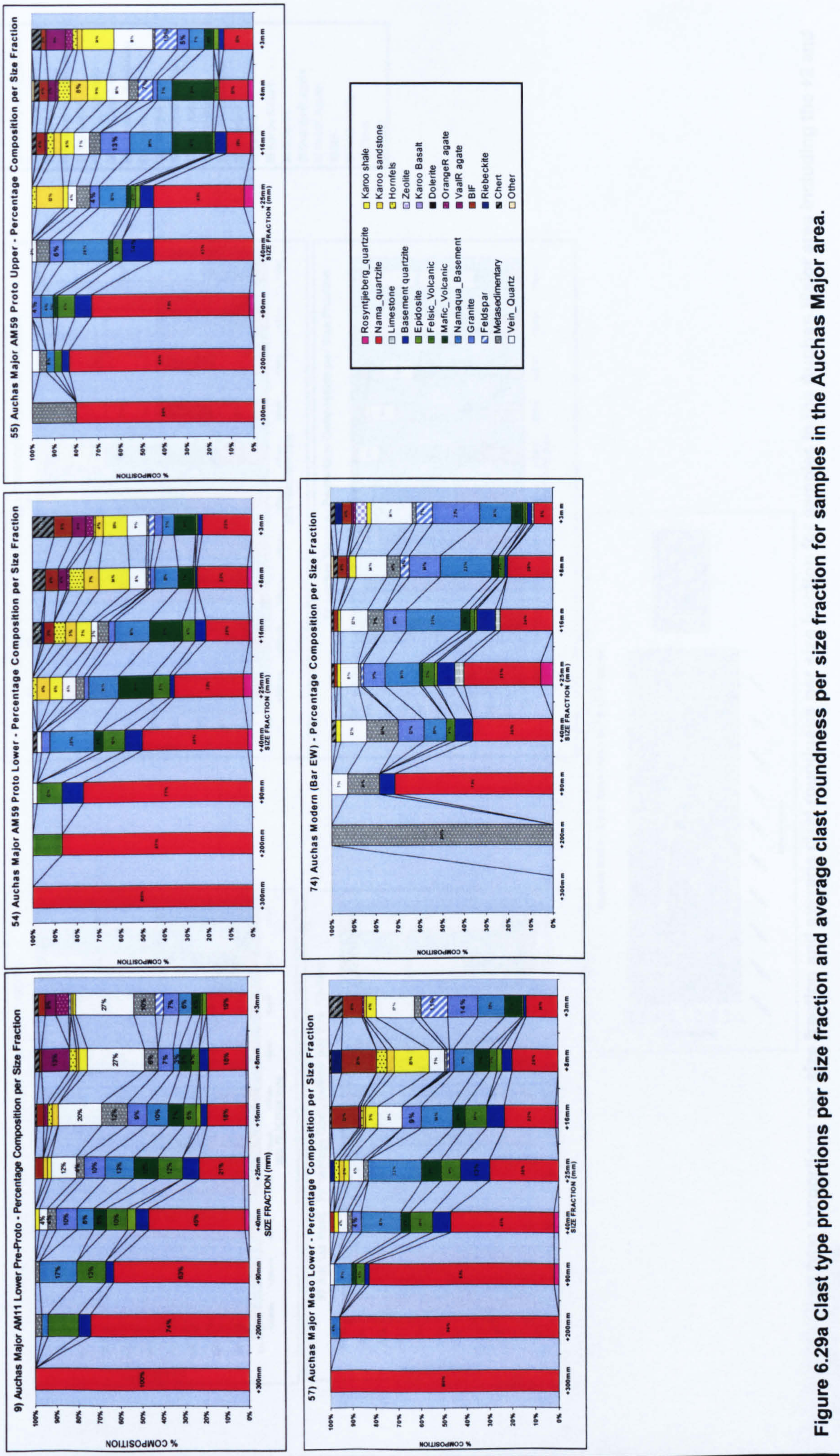

Figure 6.29a Clast type proportions per size fraction and average clast roundness per size fraction for samples in the Auchas Major area.

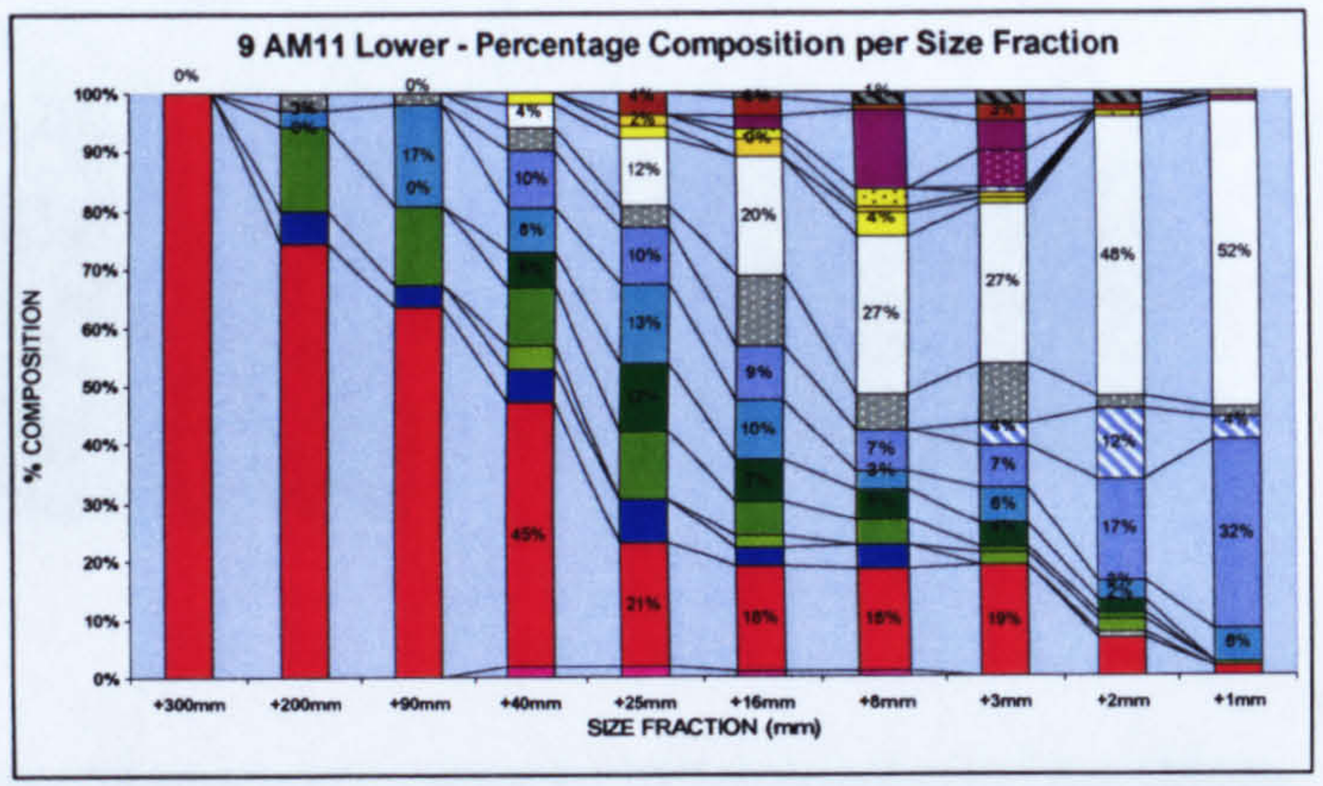

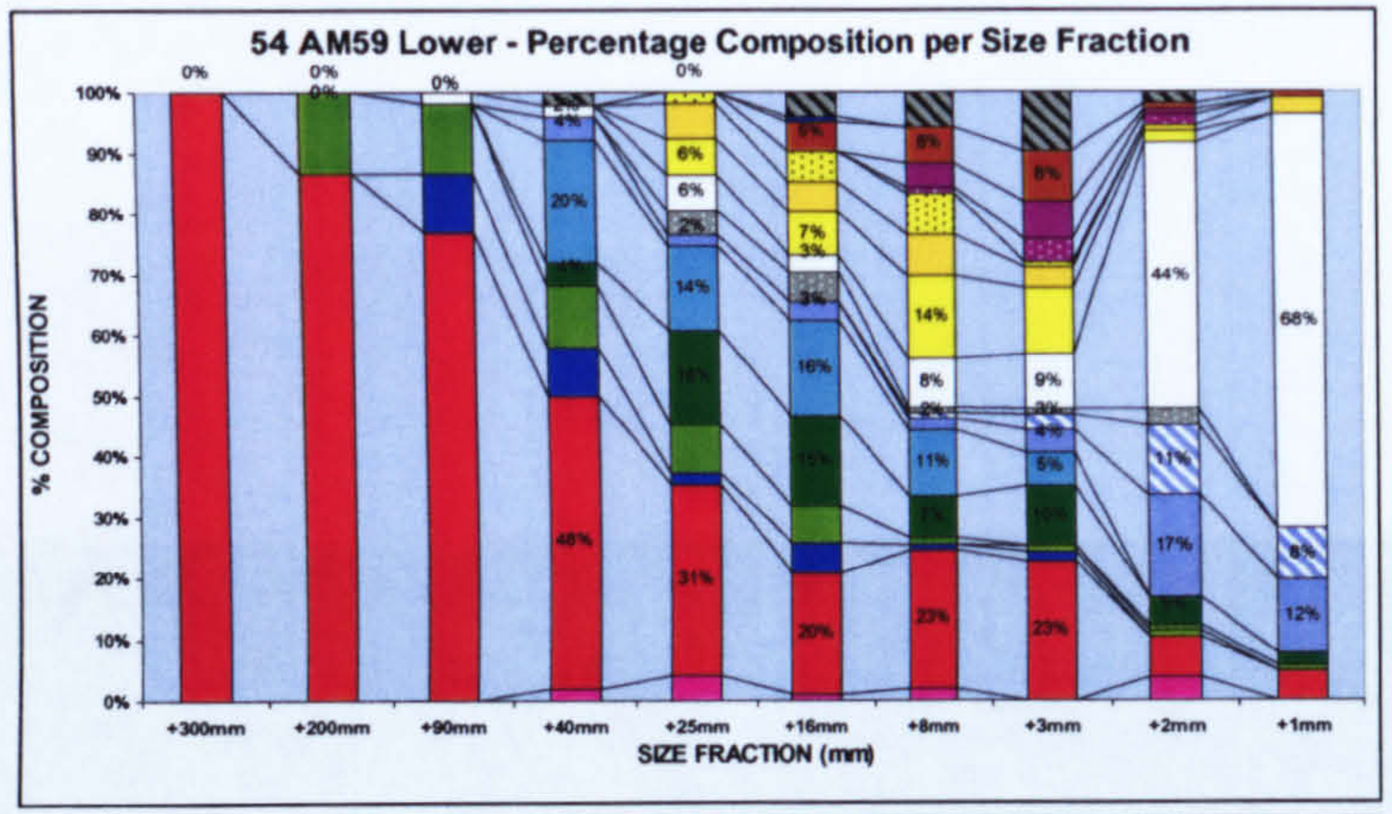

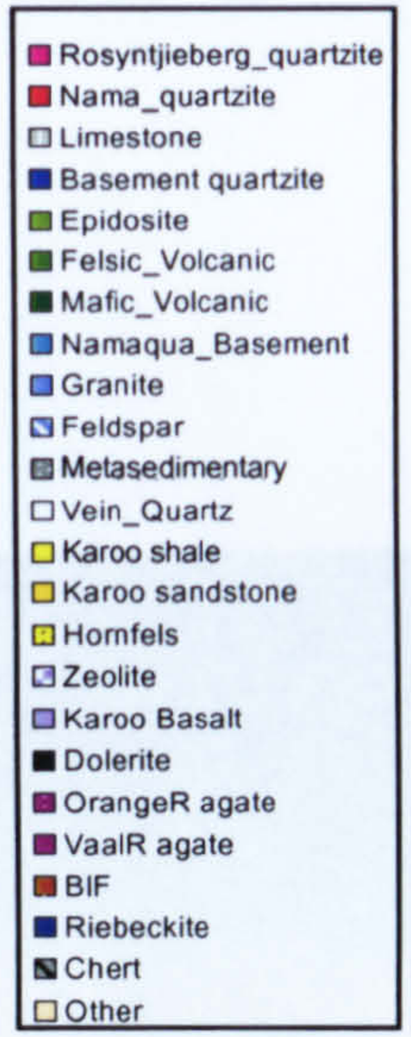

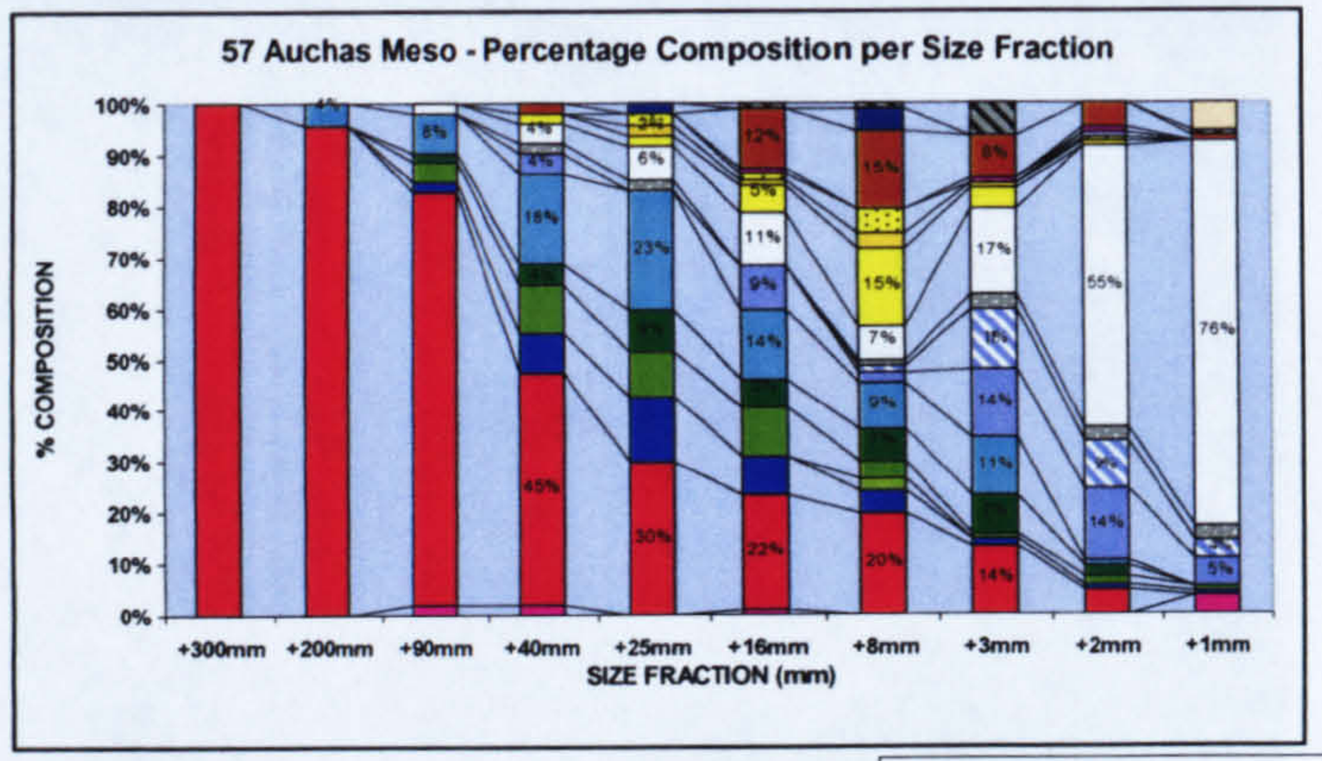

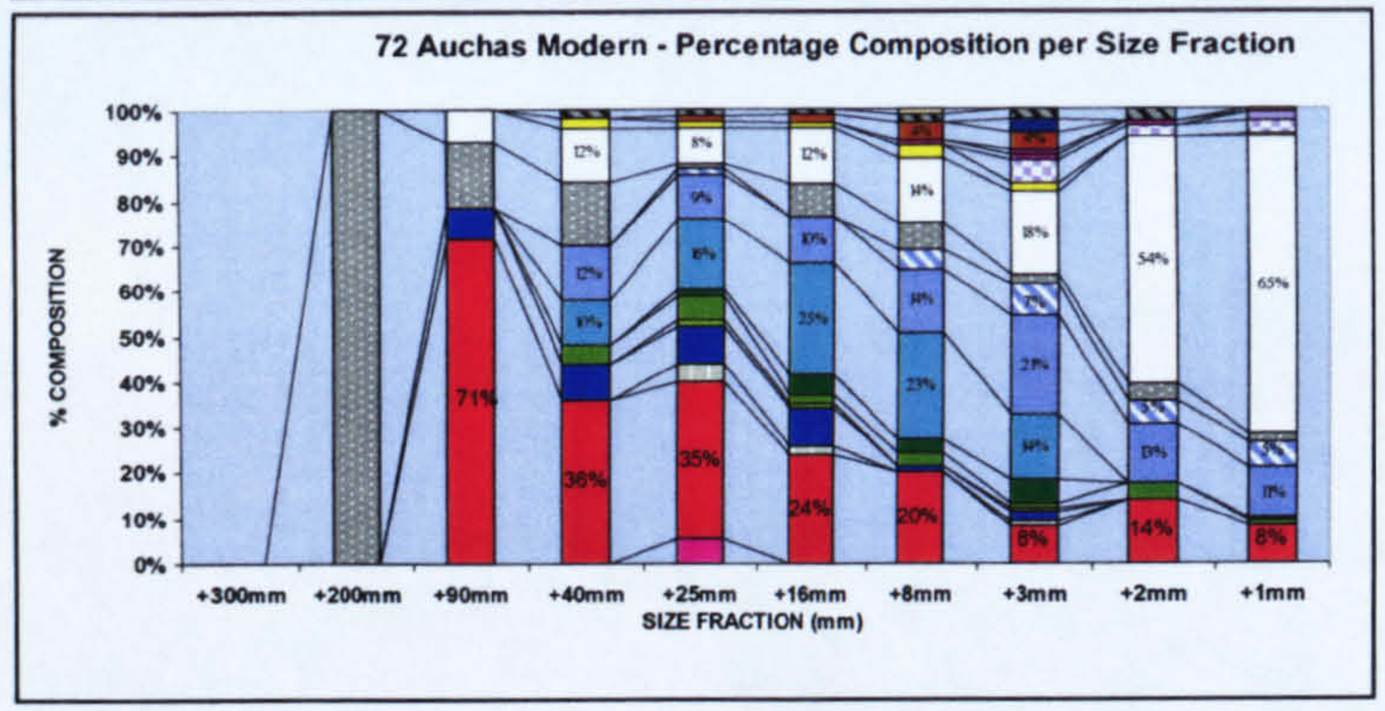

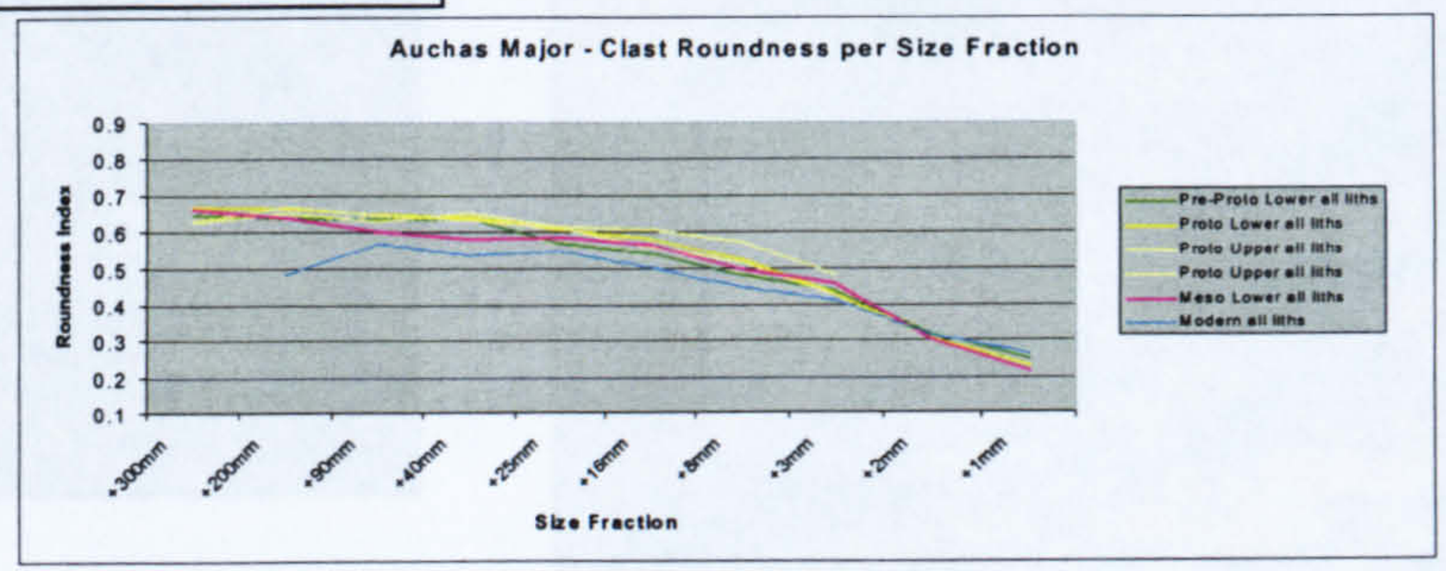

Figure 6.29b Clast type proportions per size fraction and average clast roundness per size fraction for samples in the Auchas Major area including the +2 and +1mm sand fractions.

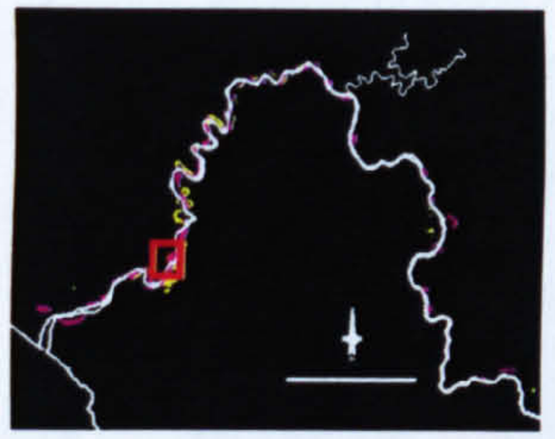

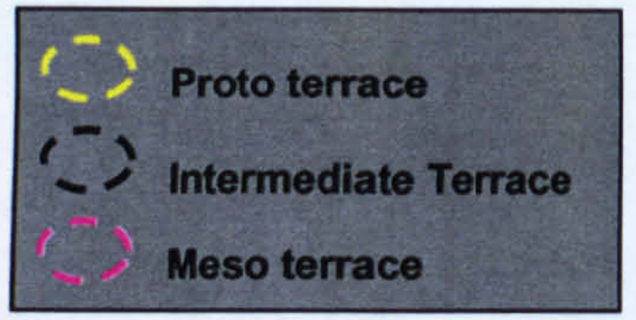

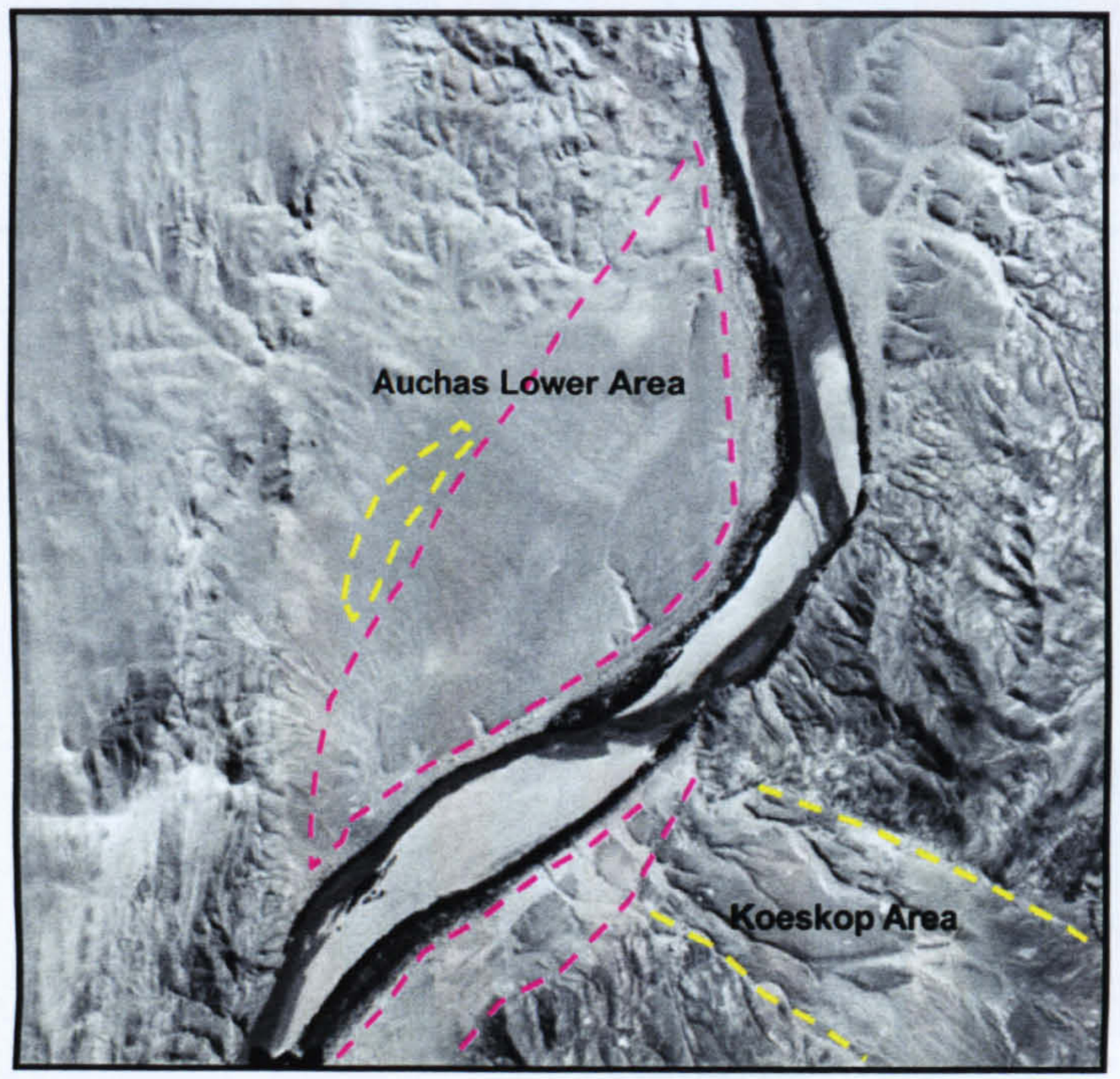

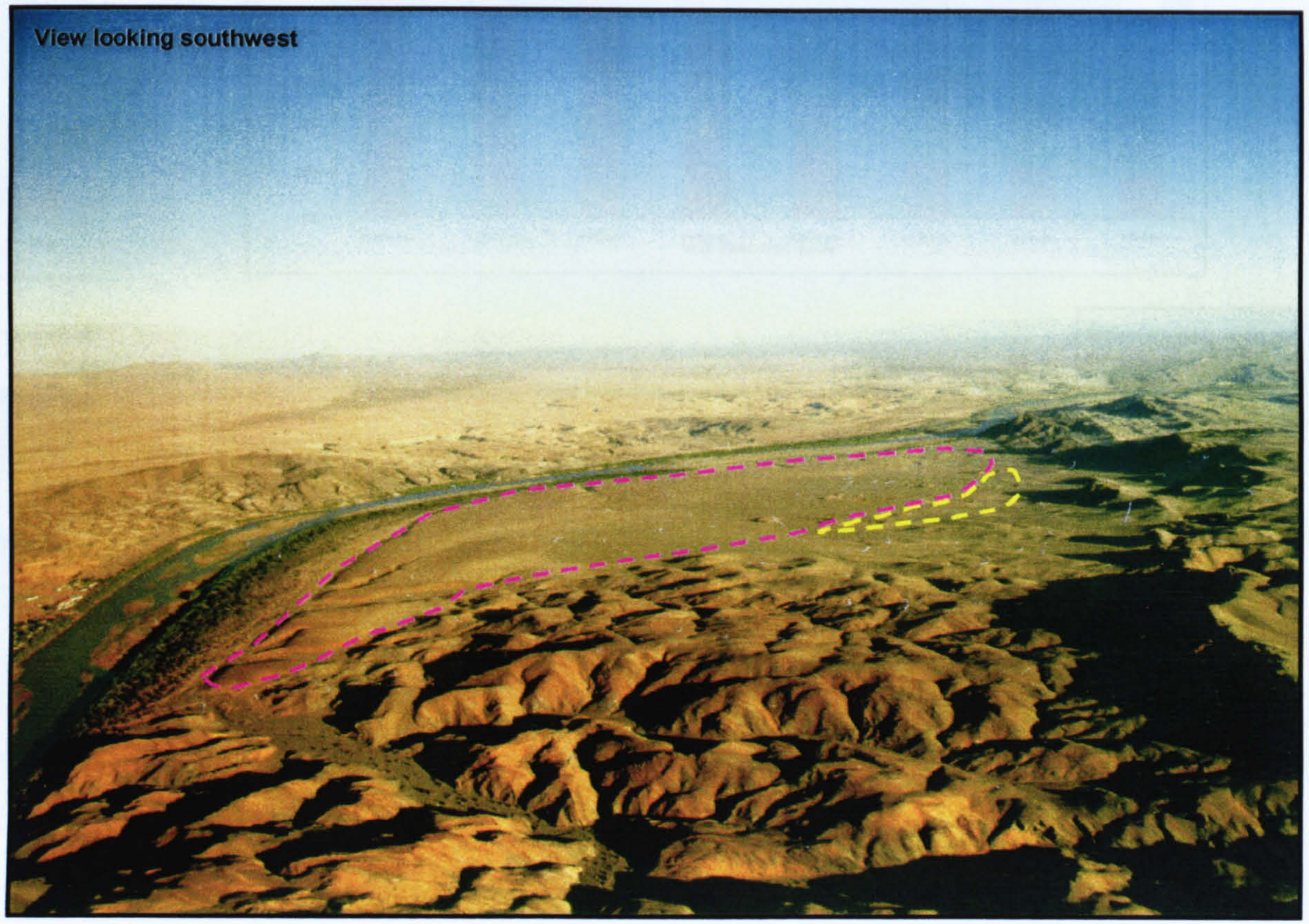

Figure 6.30 Distribution of Proto and Meso terraces in the Auchas Lower area.

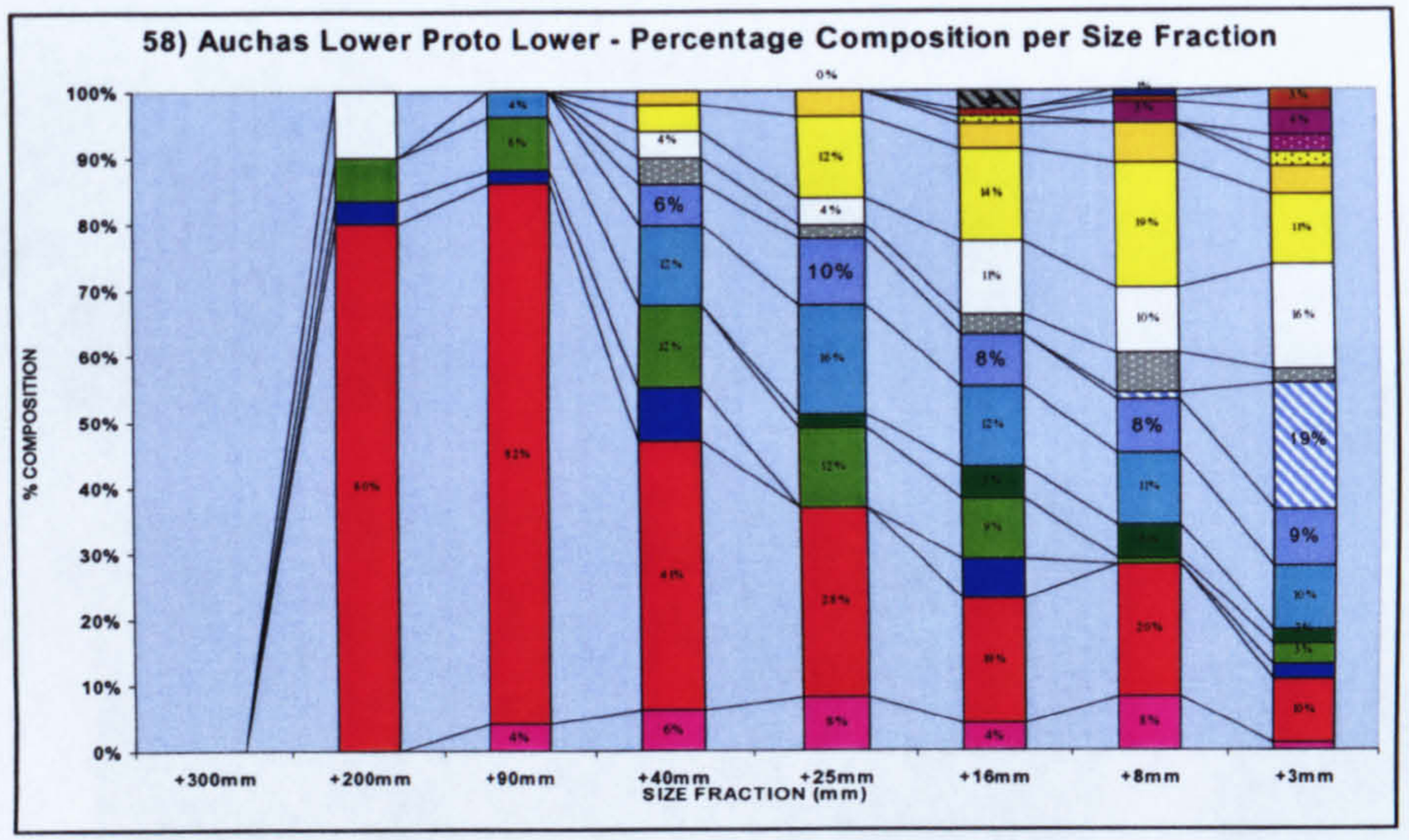

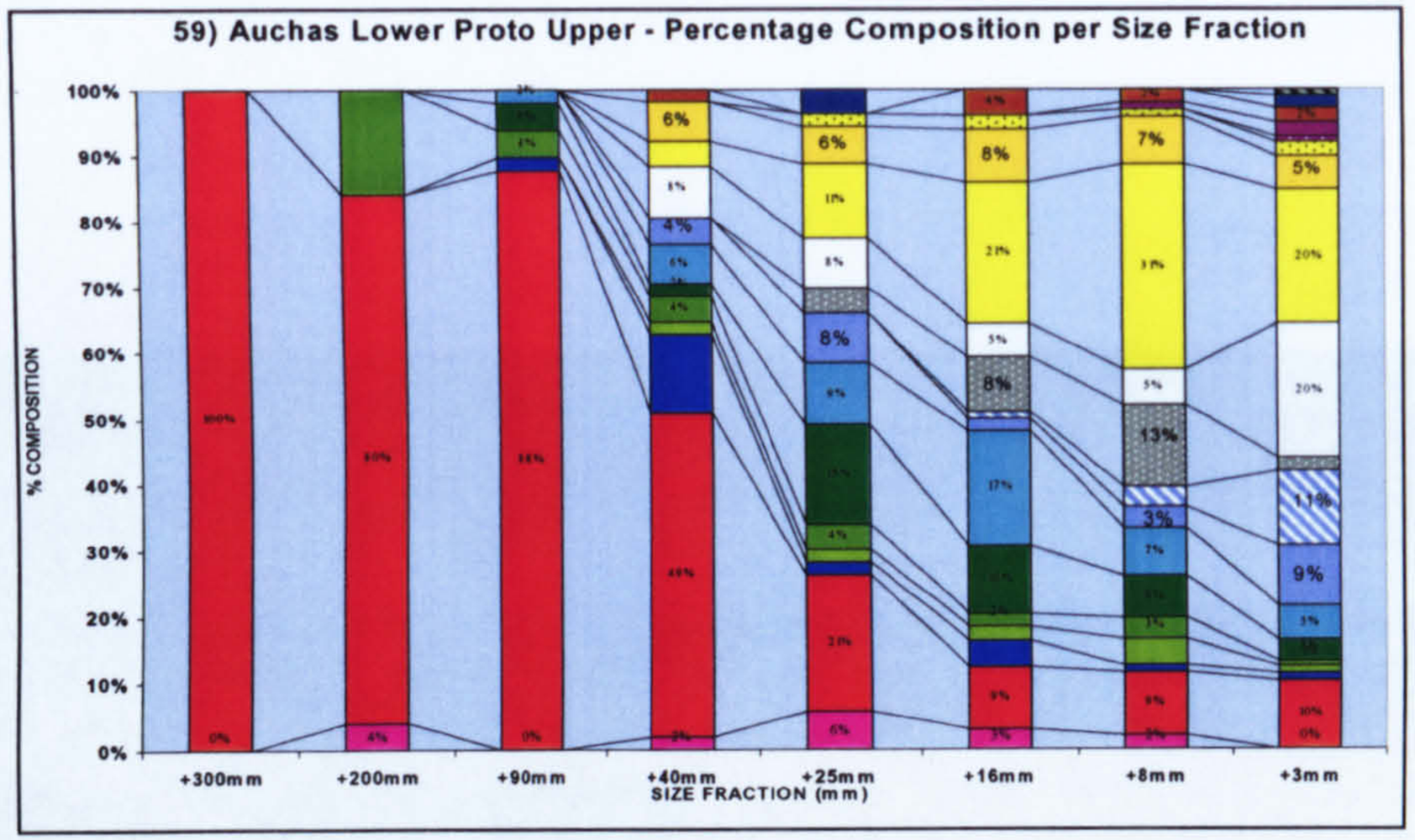

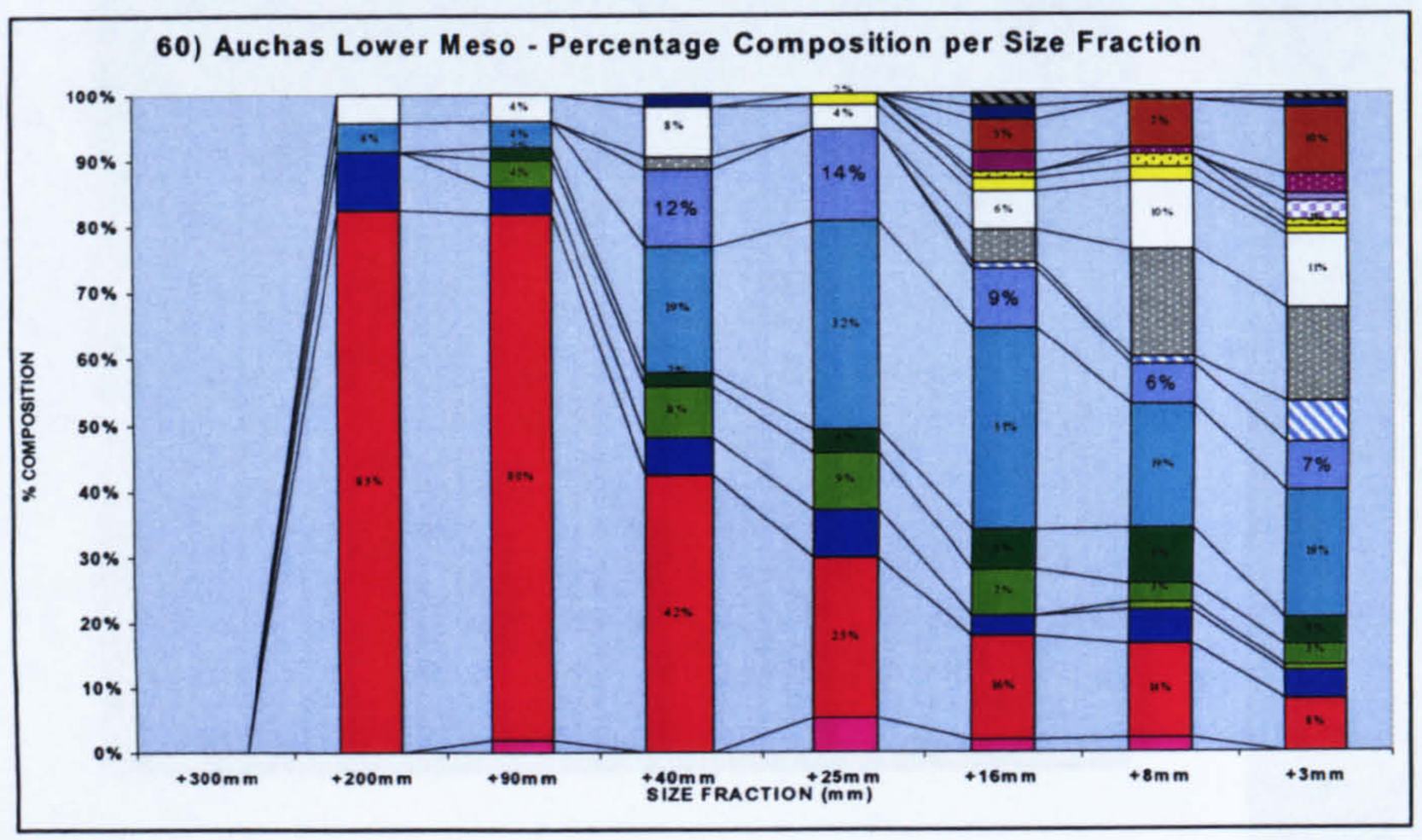

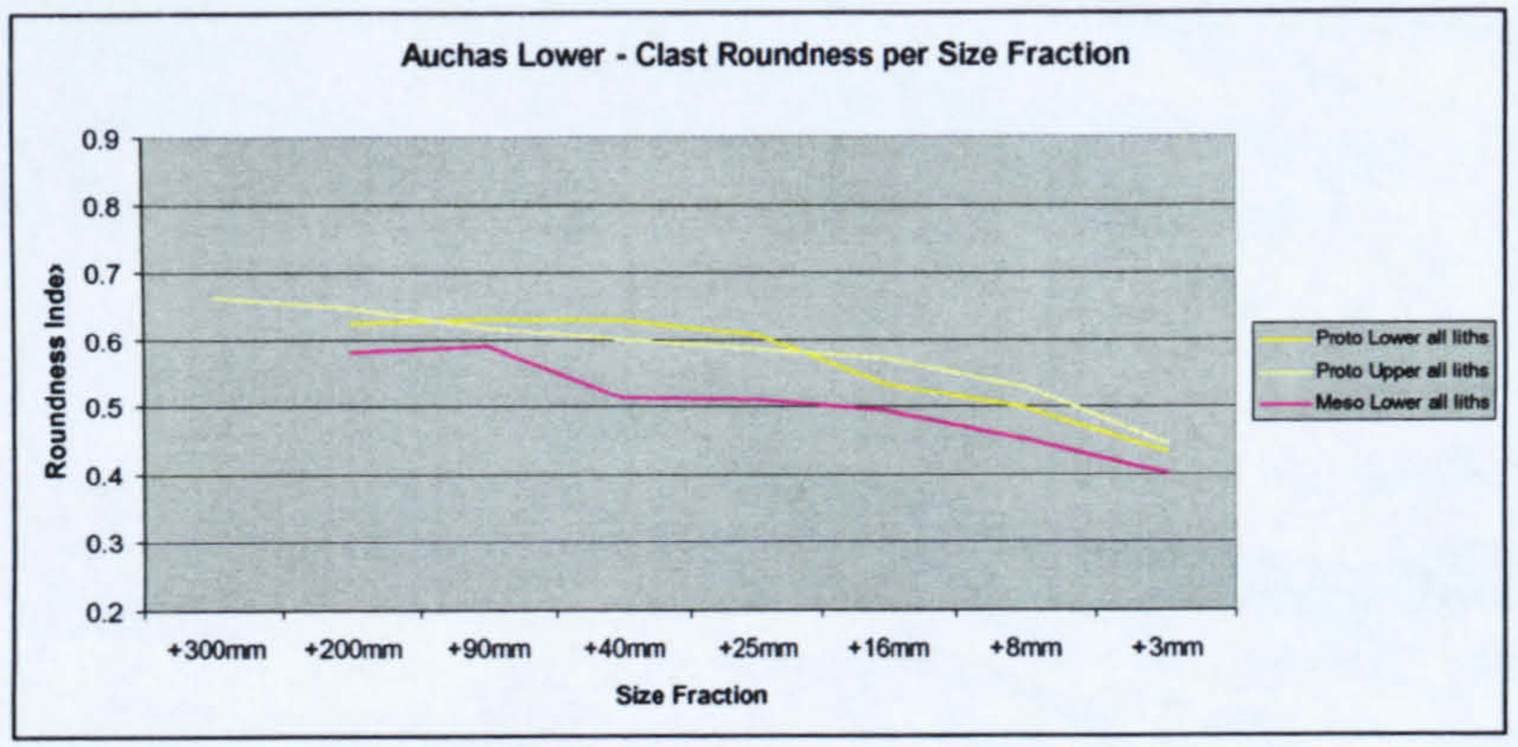

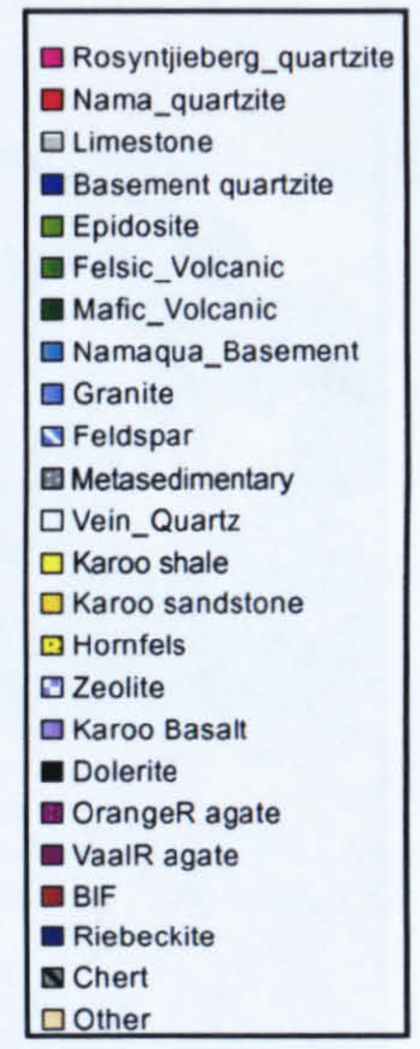

Figure 6.31 Clast type proportions per size fraction and average clast roundness per size fraction for samples in the Auchas Lower area.

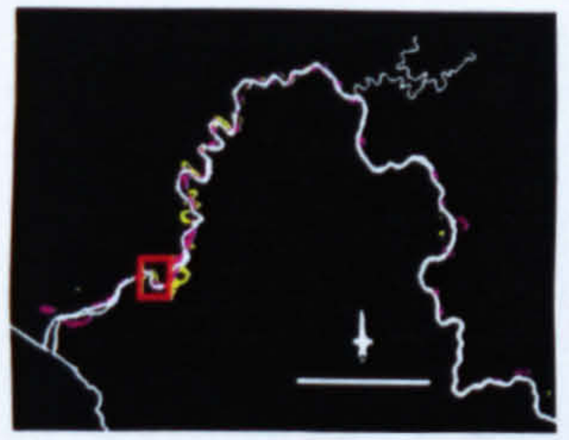

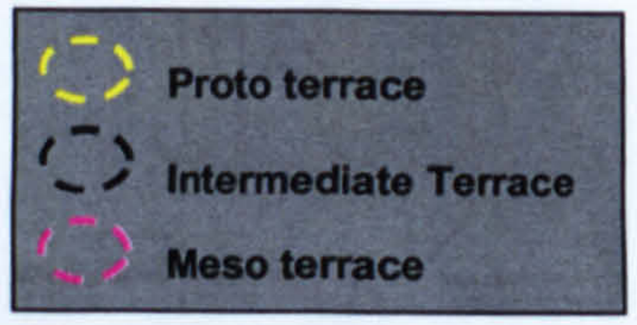

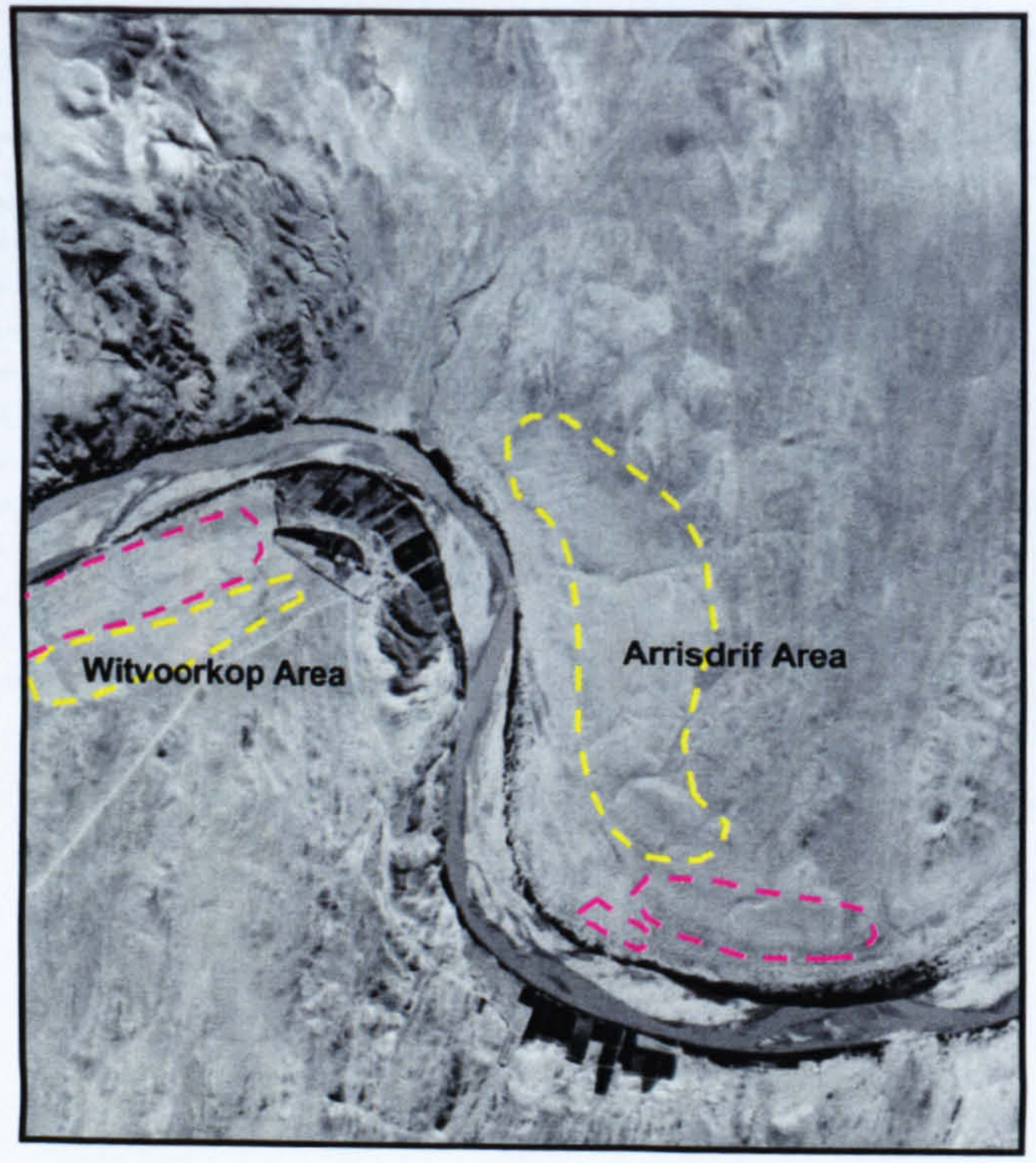

Figure 6.32 Distribution of Proto and Meso terraces in the Arrisdrif area.

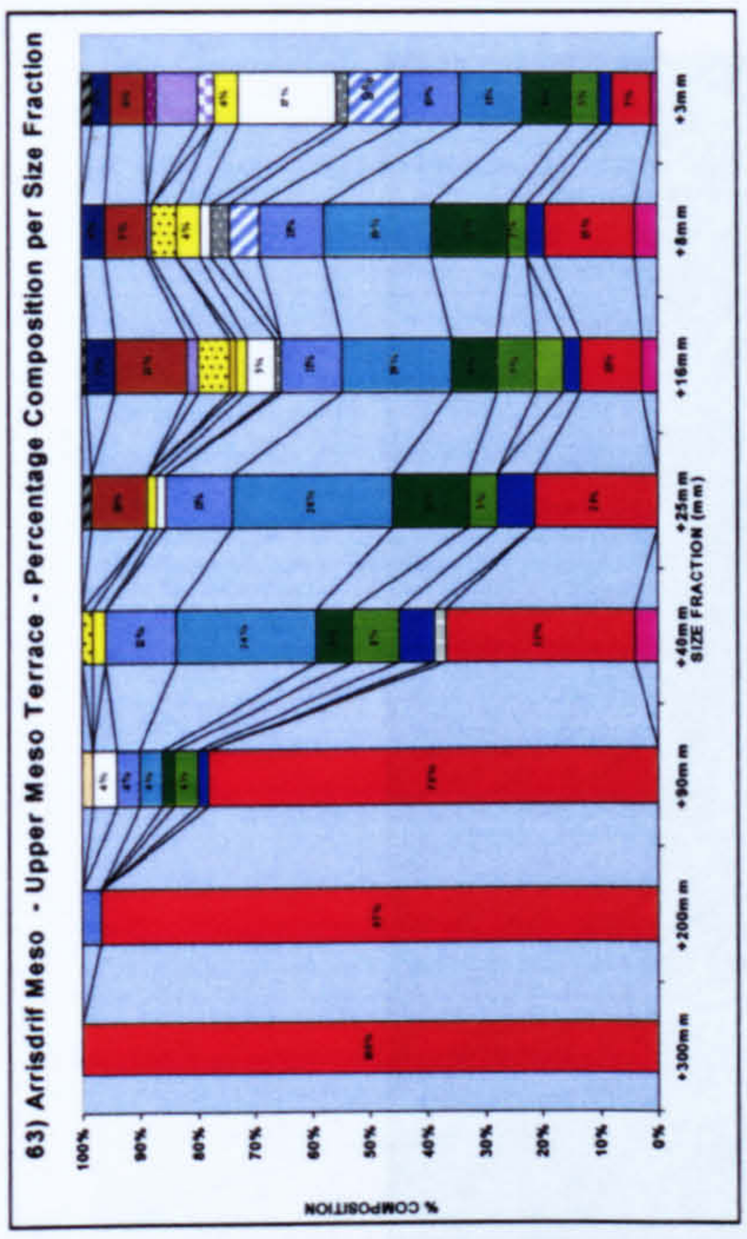

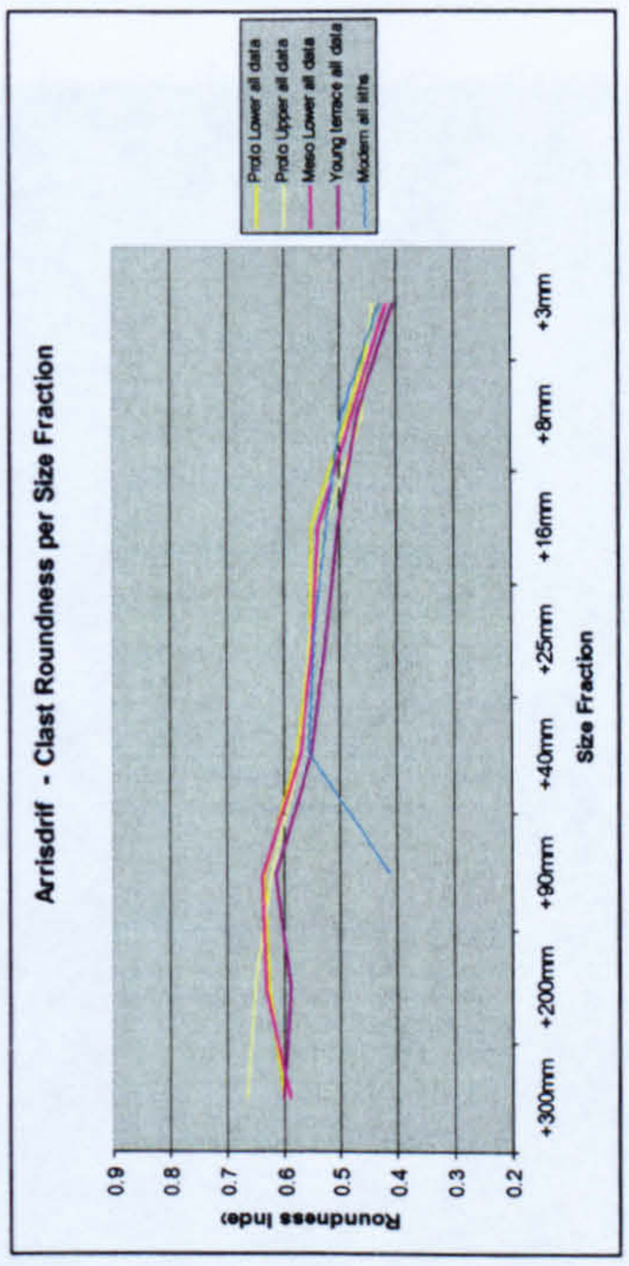

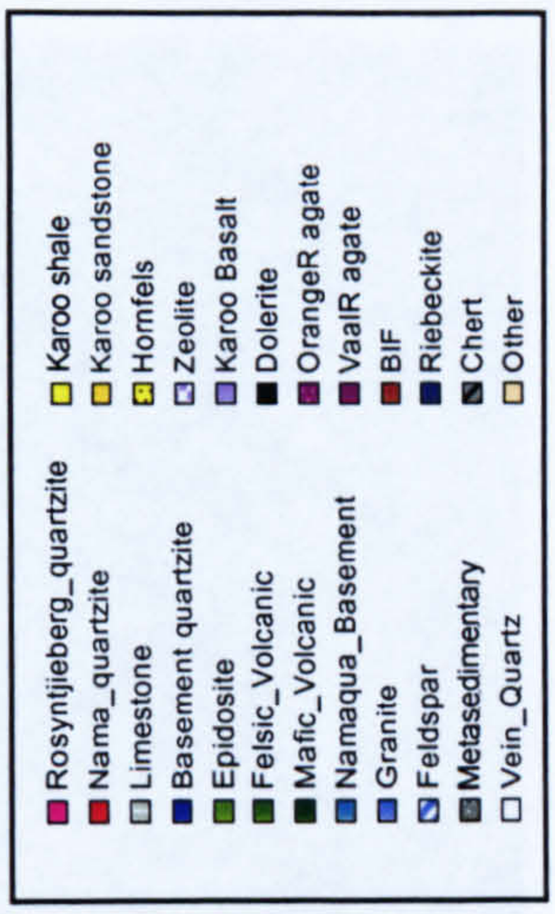

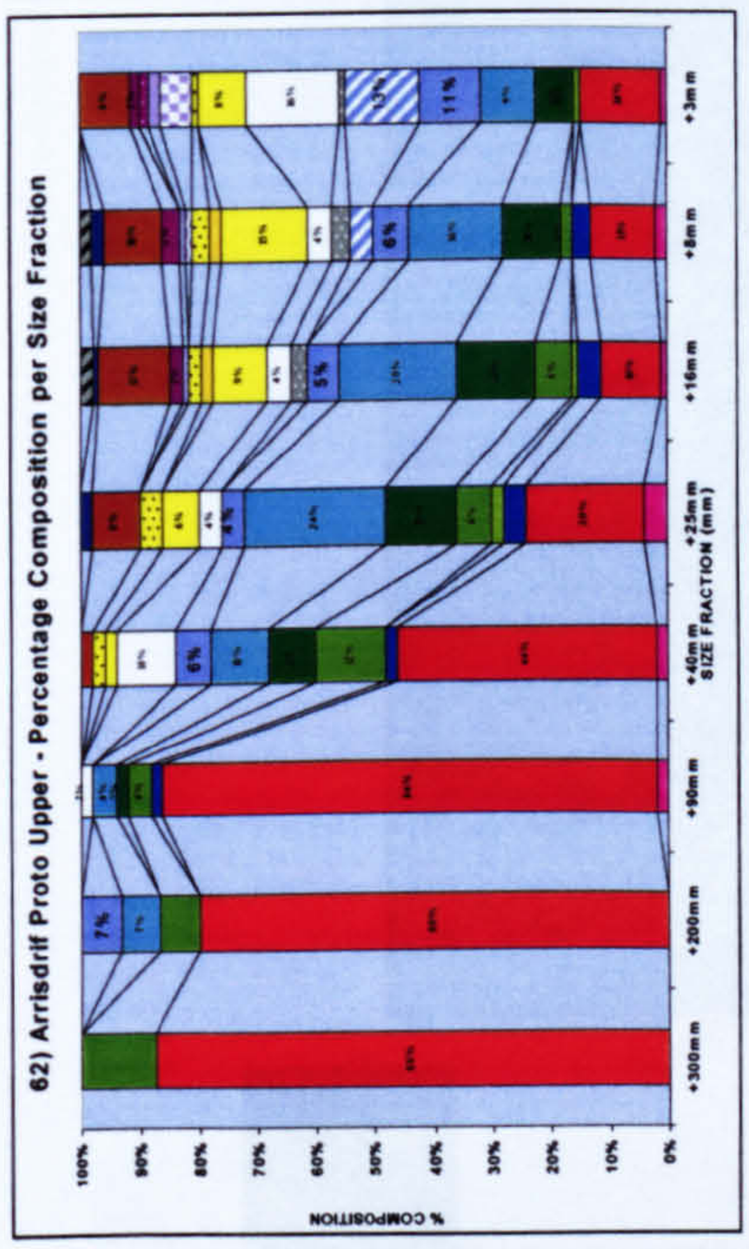

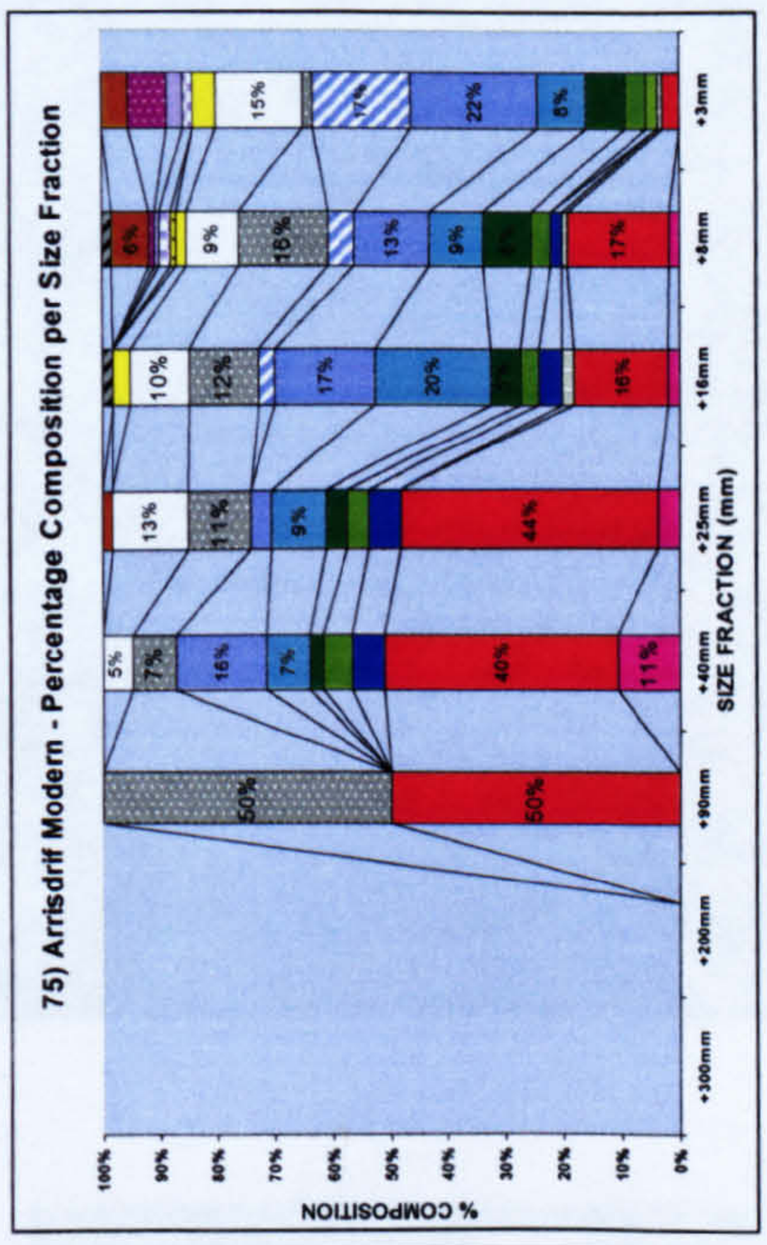

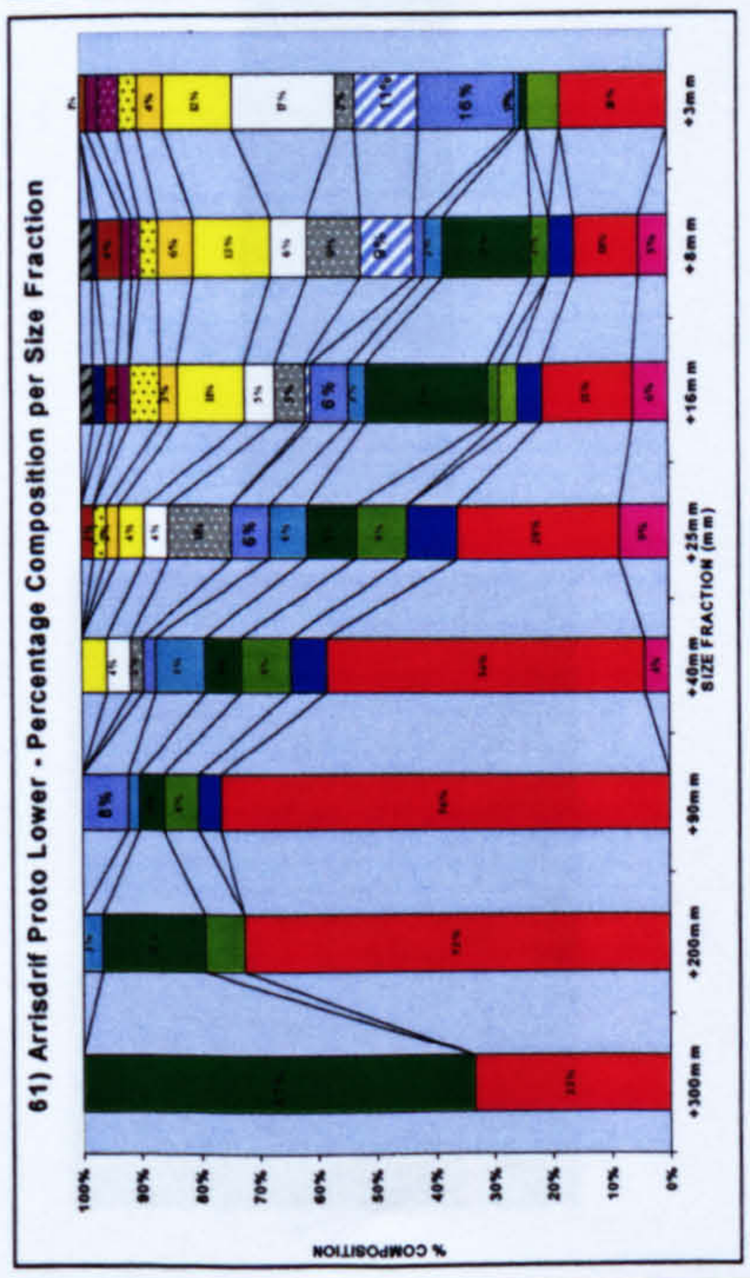

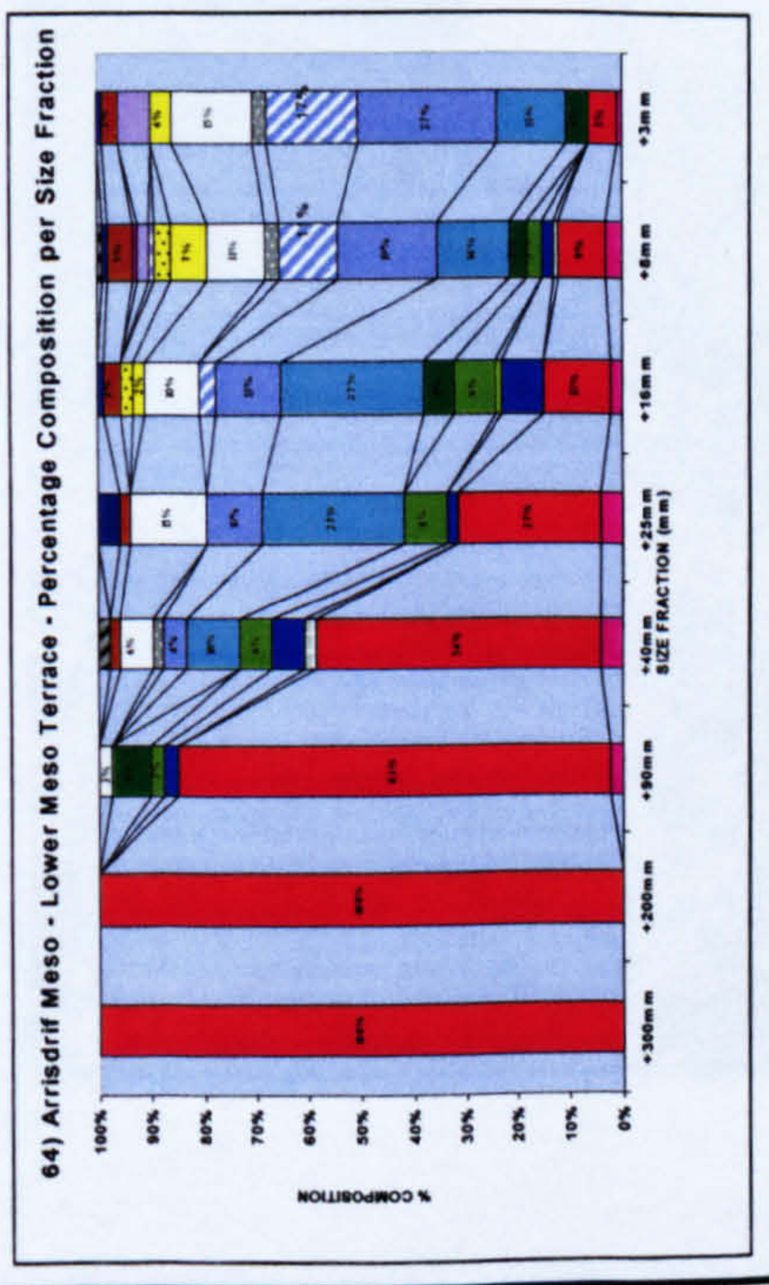

Figure 6.33 Clast type proportions per size fraction and average clast roundness per size fraction for samples in the Arrisdrif area.

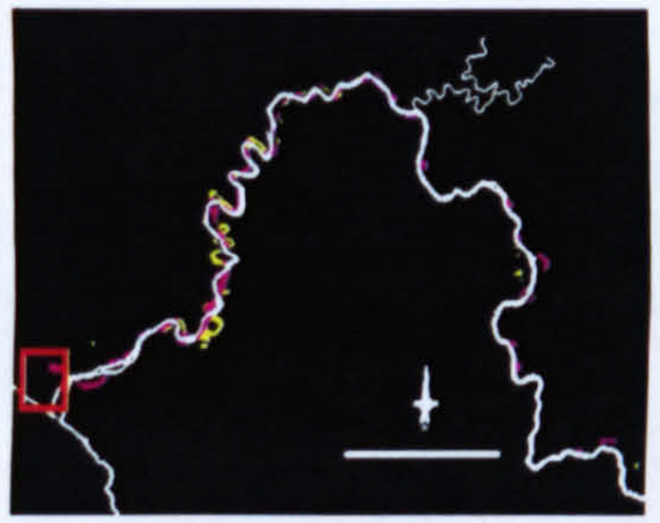

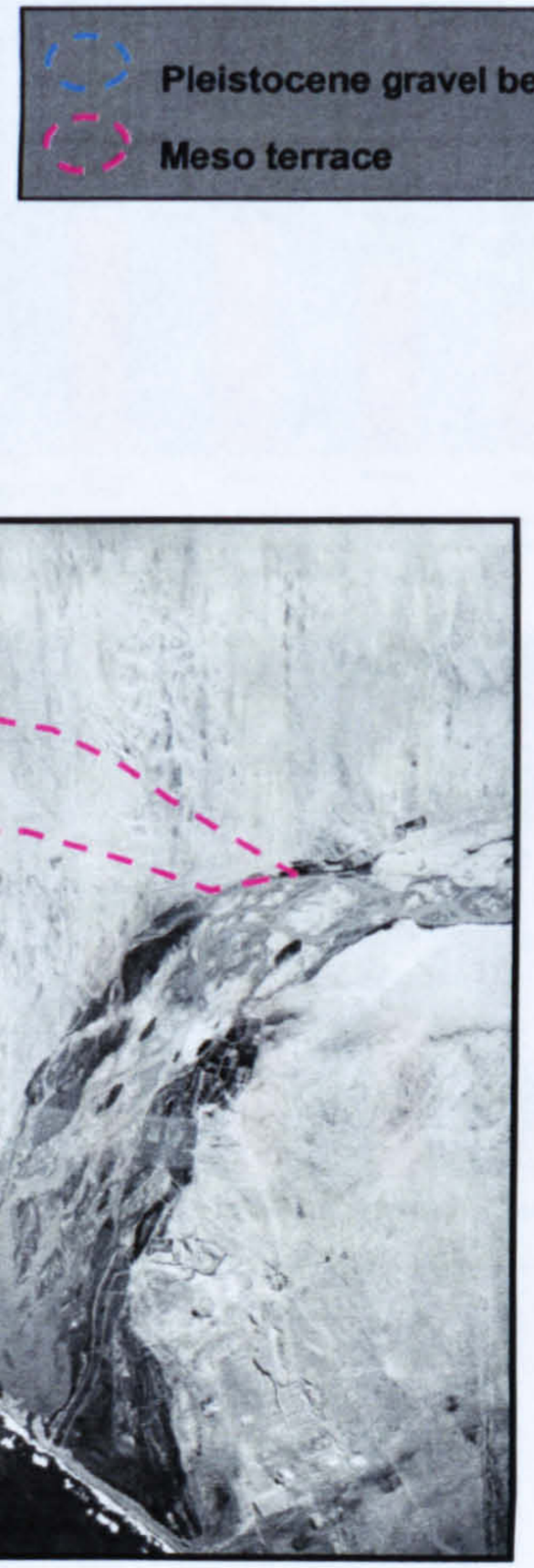

Pleistocene gravel beaches

Meso terrace

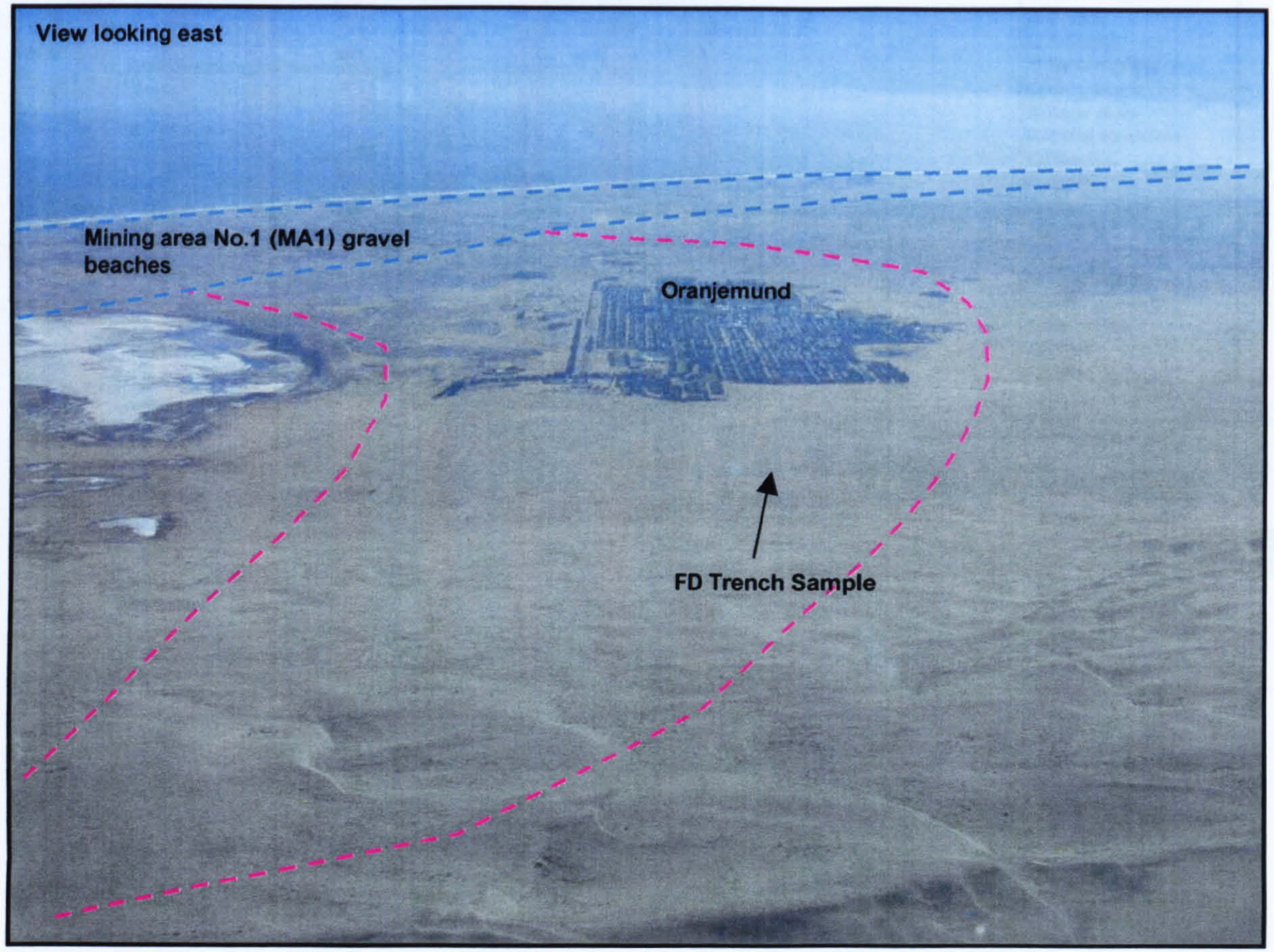

Figure 6.34 Distribution of Proto and Meso terraces in the Oranjemund area.

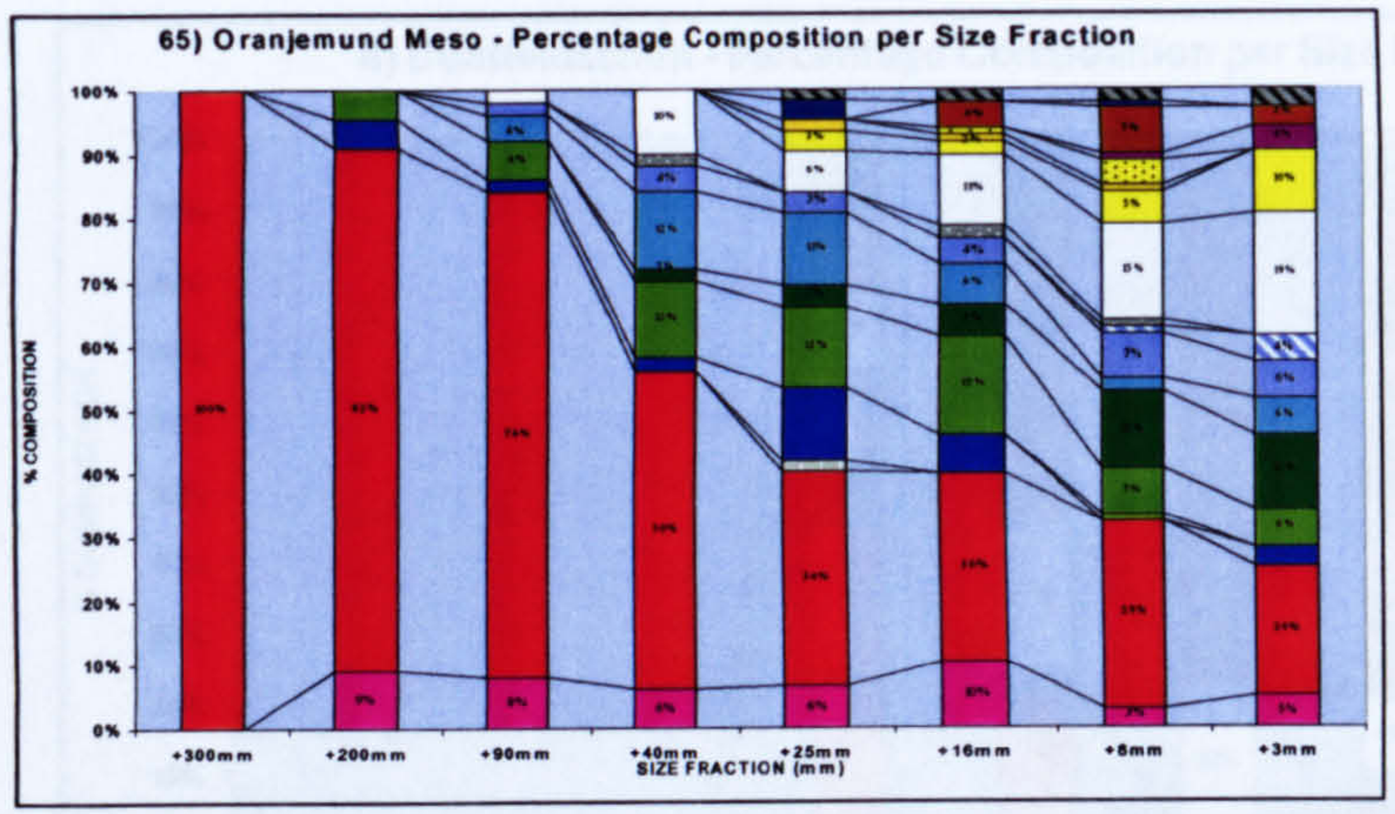

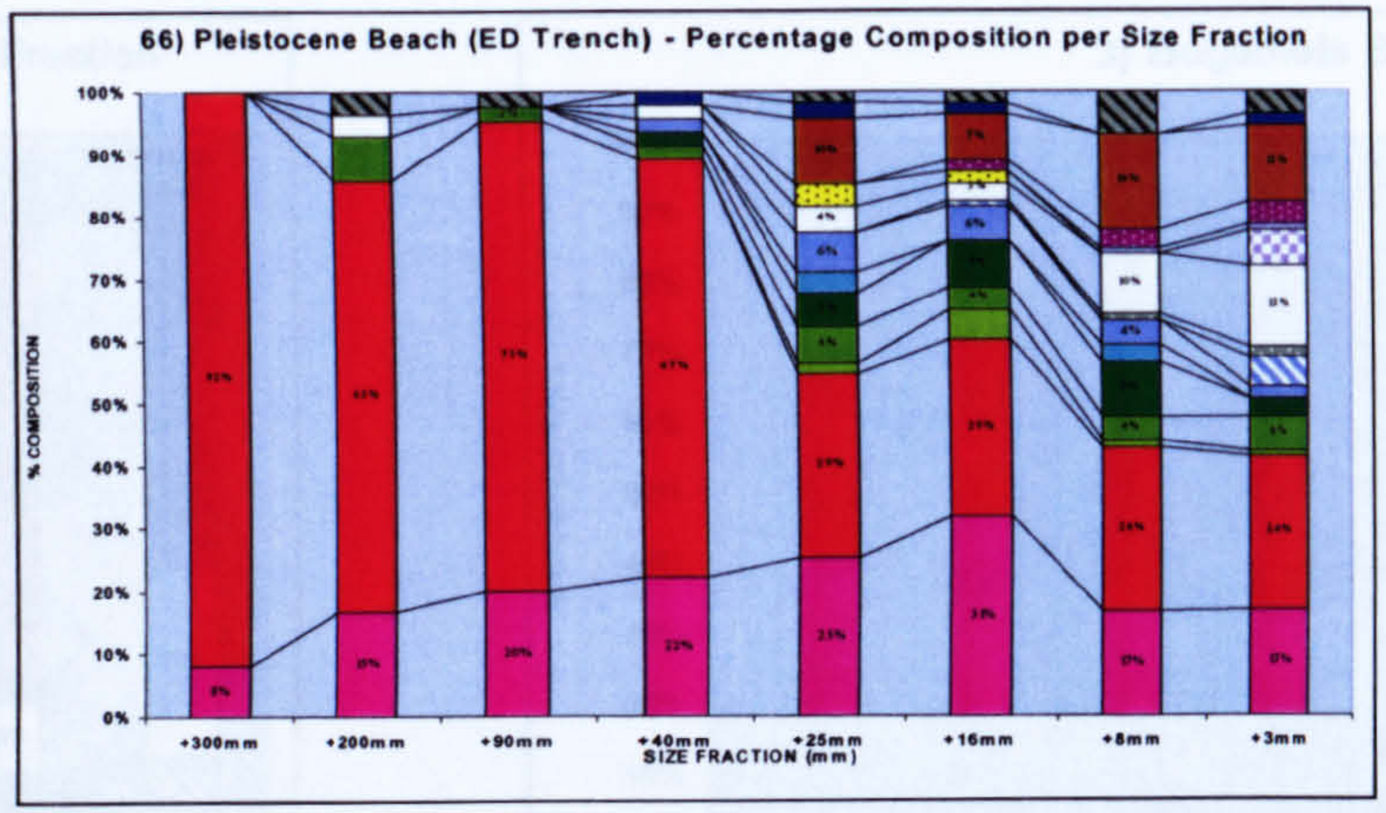

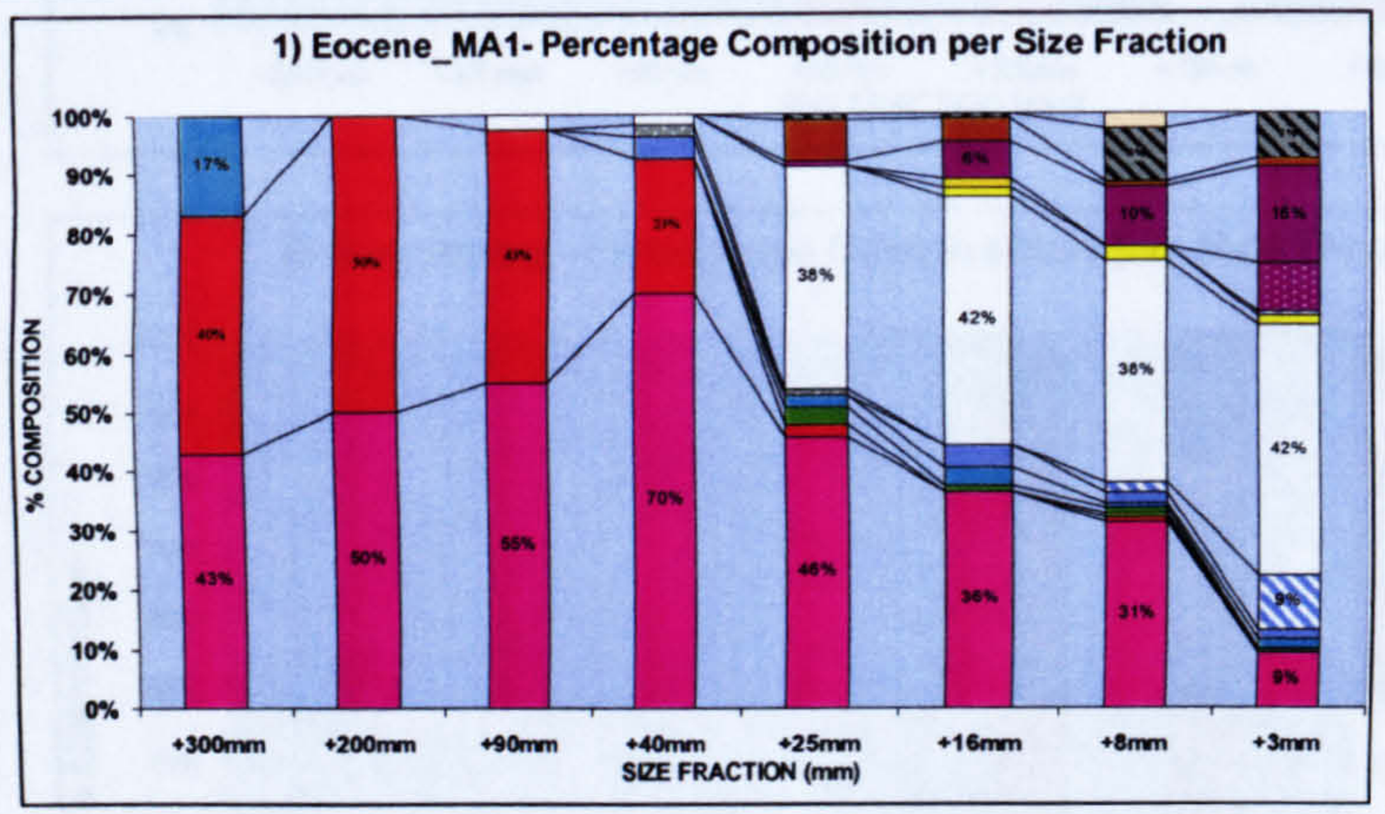

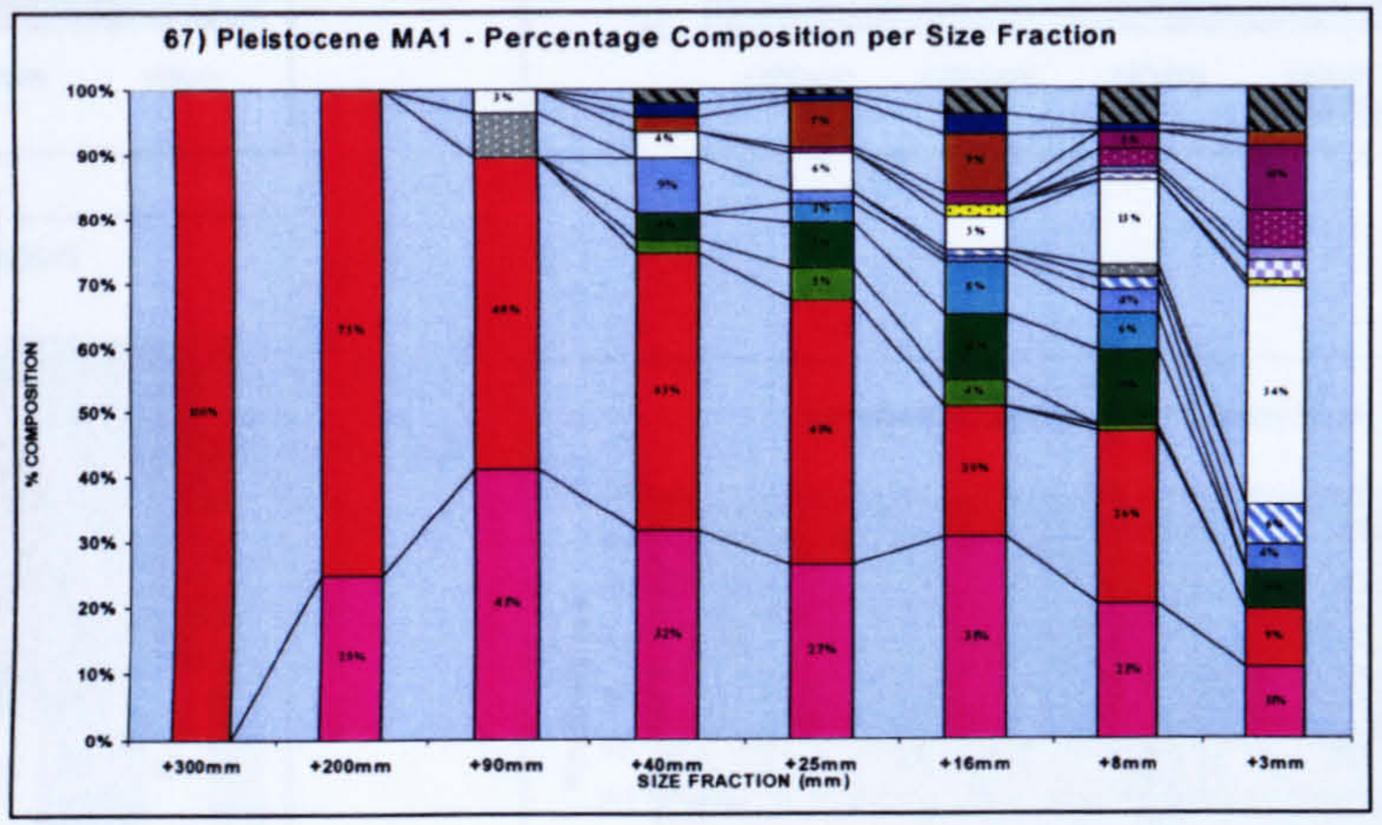

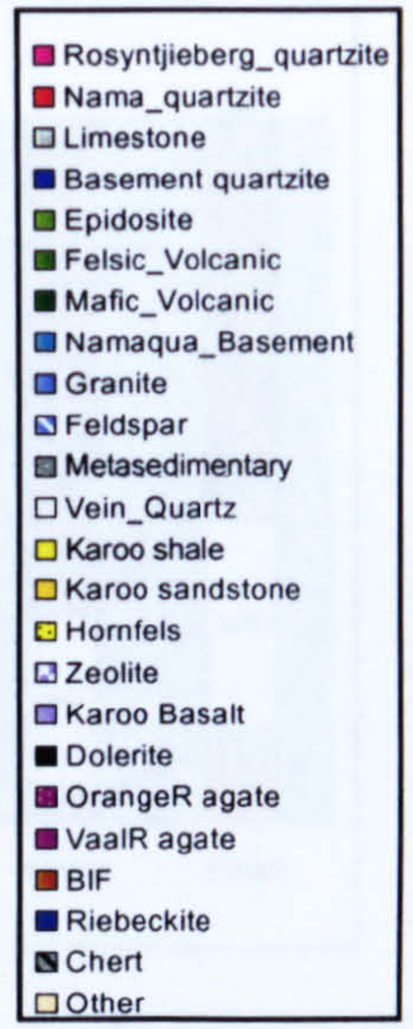

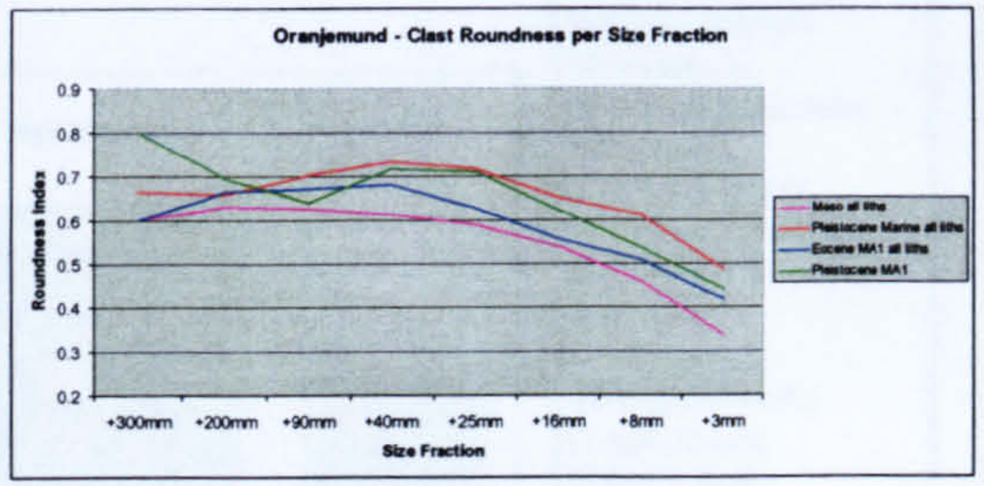

Figure 6.35 Clast type proportions per size fraction and average clast roundness per size fraction for samples in the Oranjemund area.

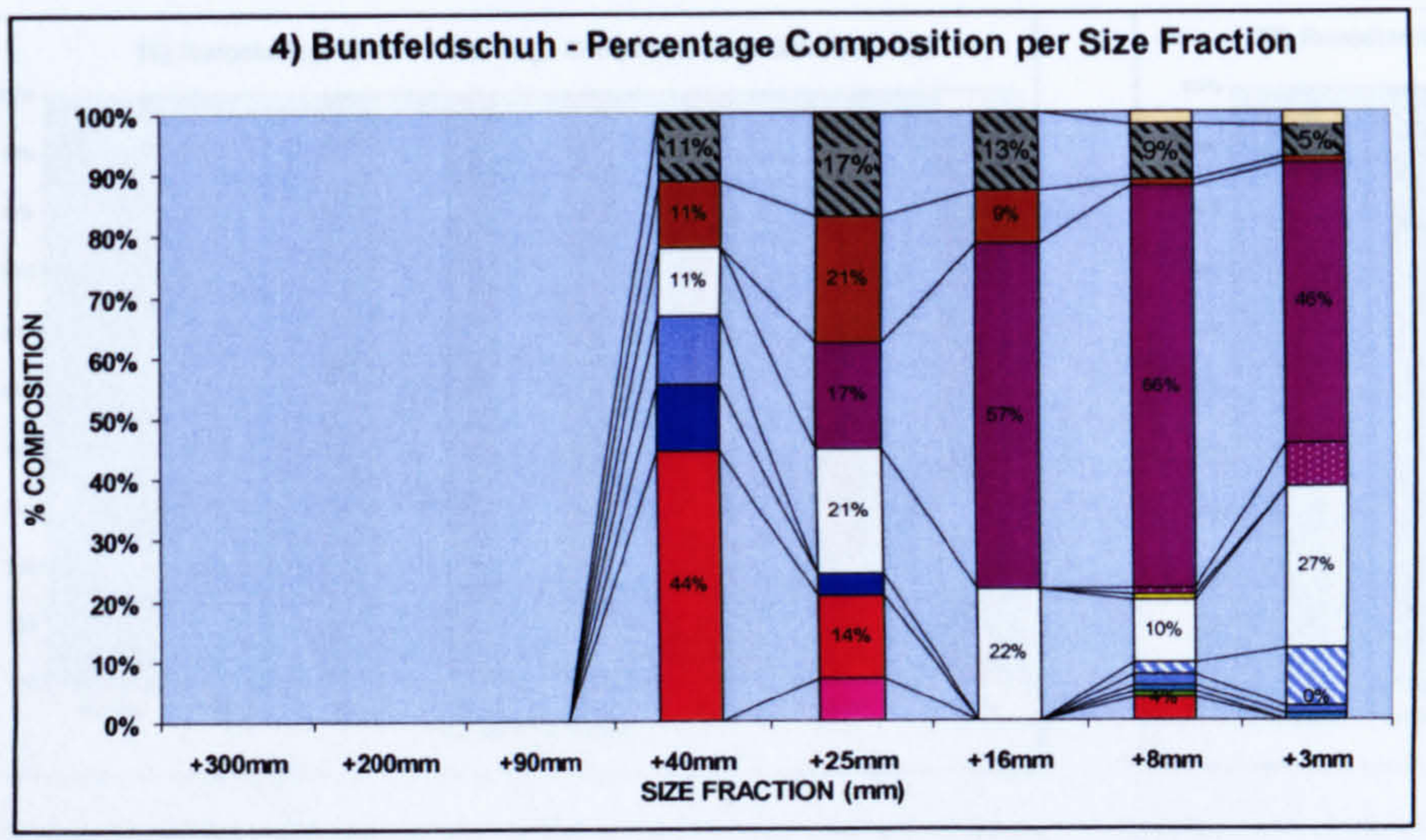

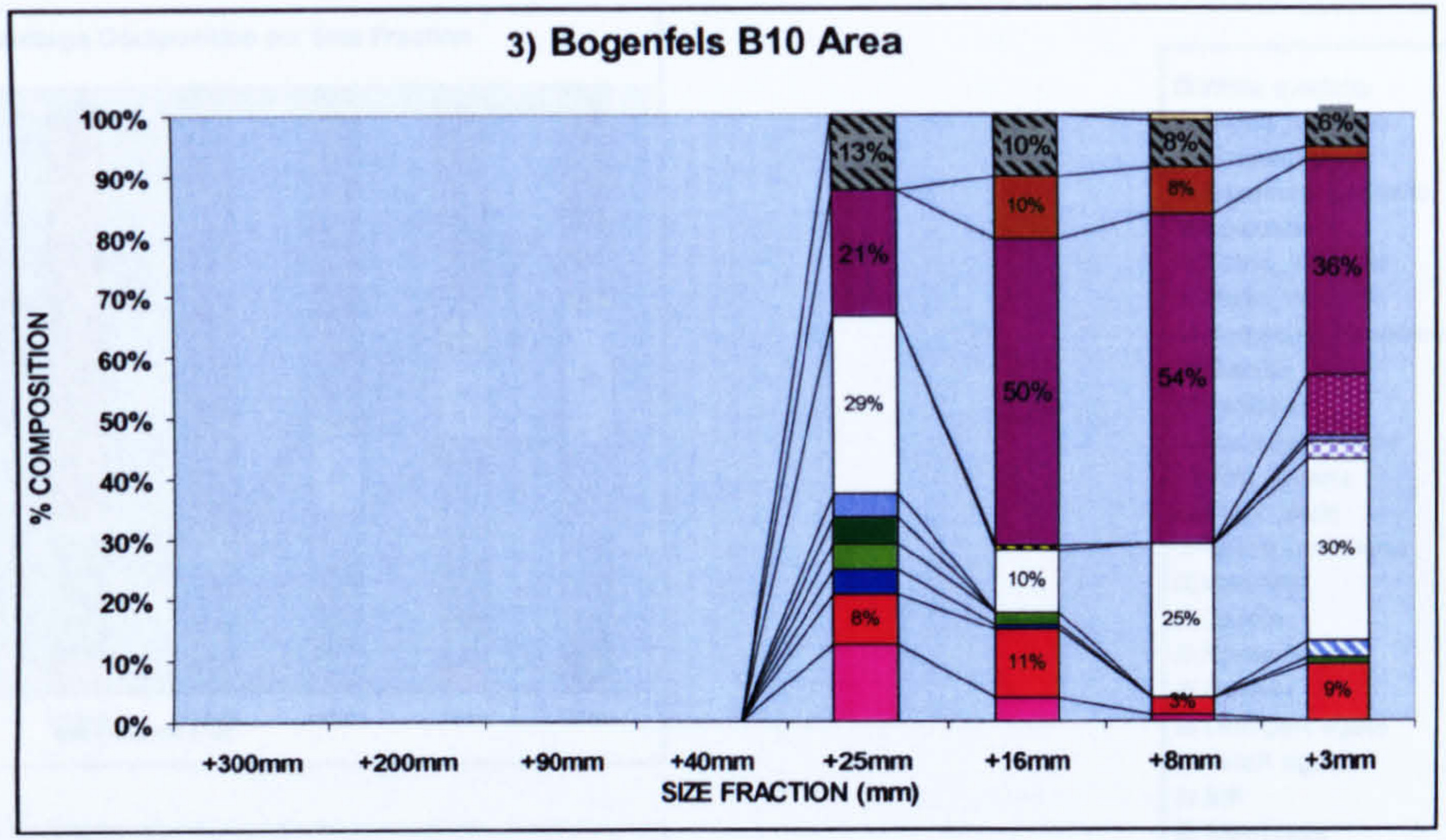

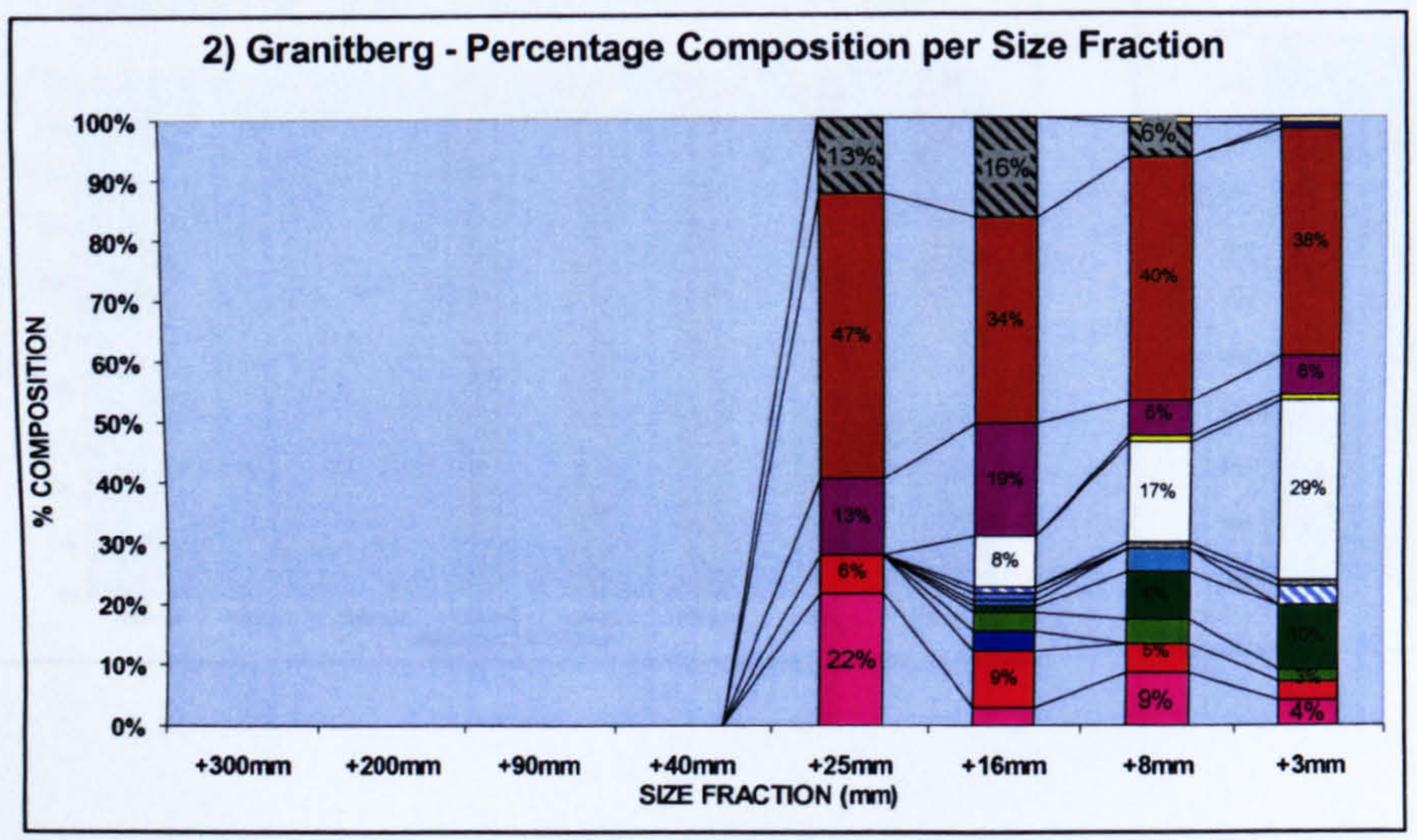

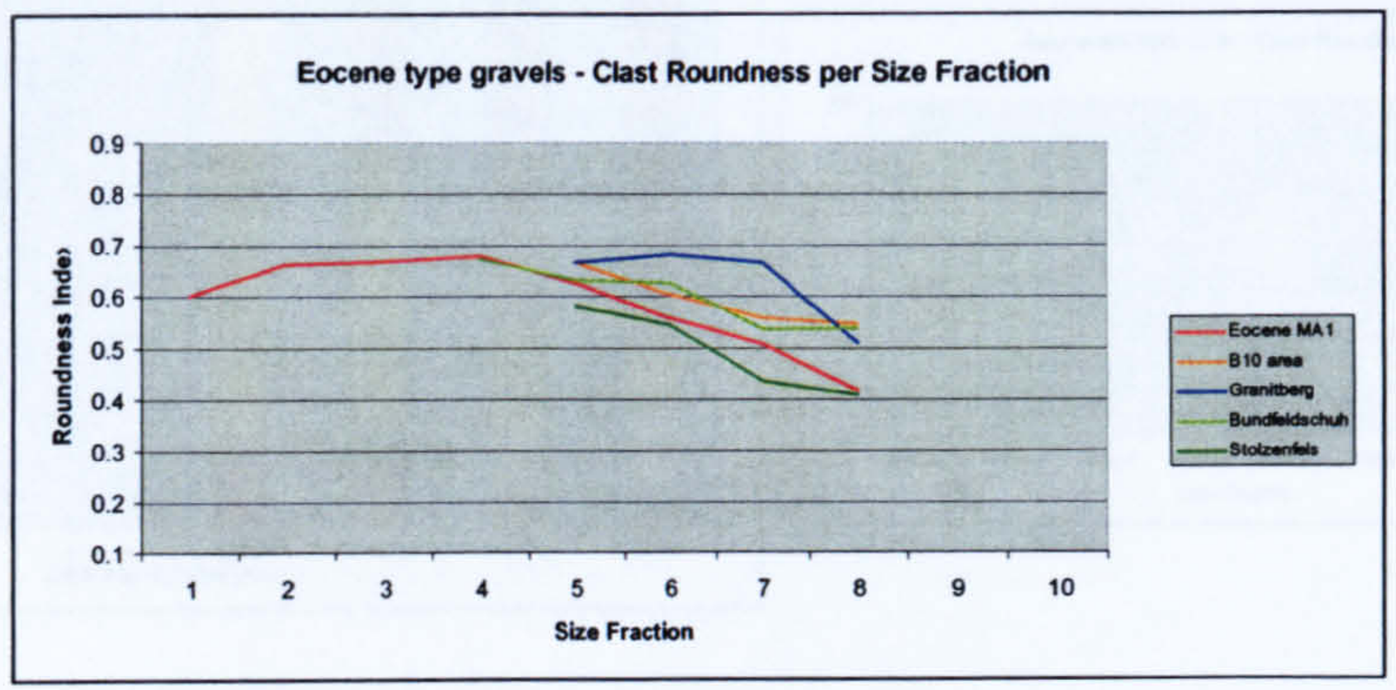

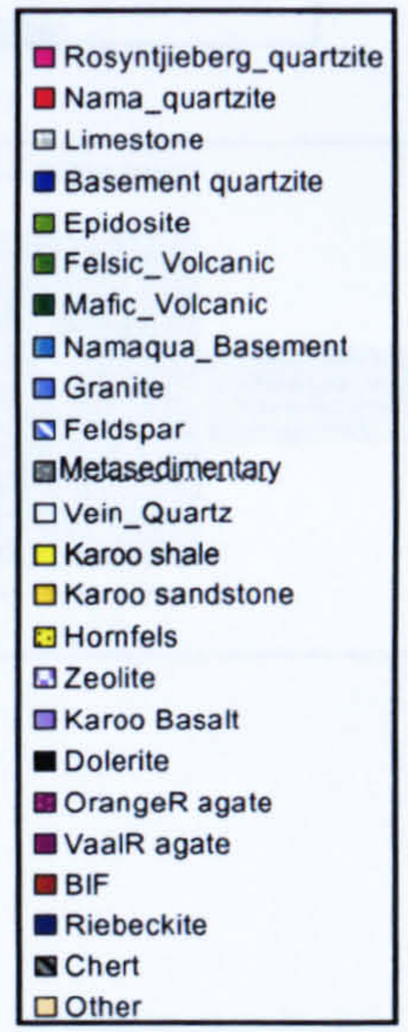

Figure 6.36 Clast type proportions per size fraction and average clast roundness per size fraction for samples in the Buntfeldschuh/Bogenfels area.

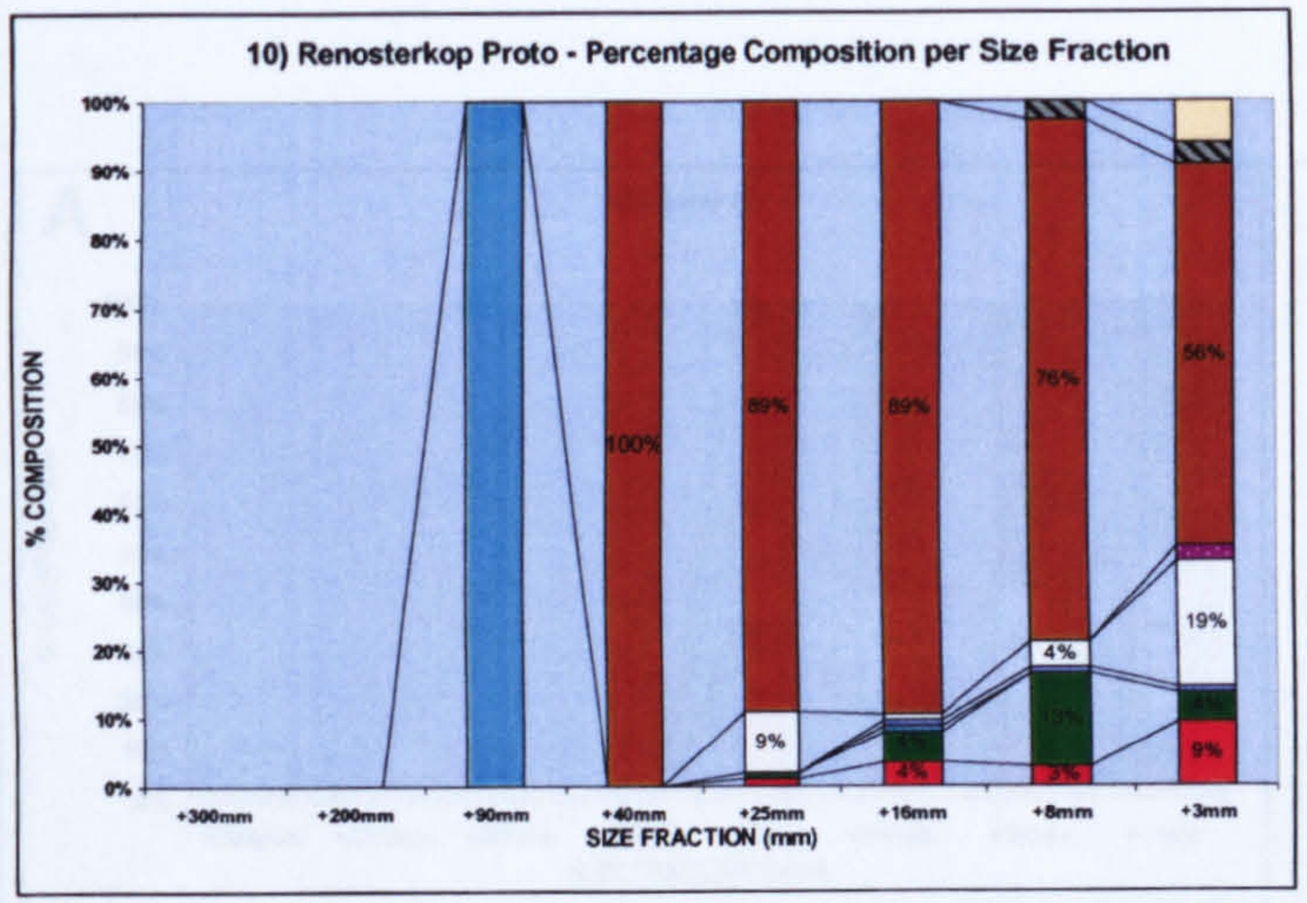

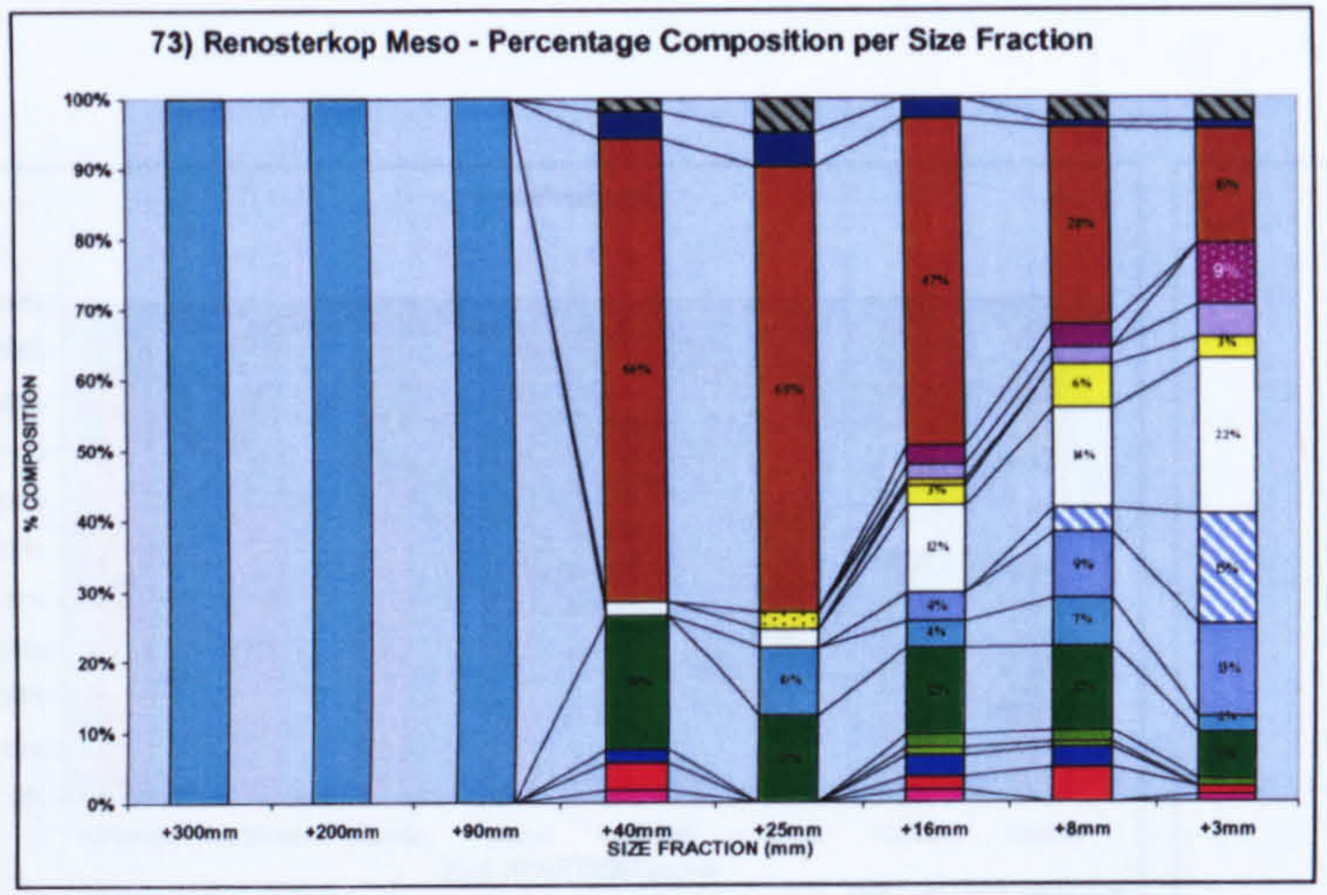

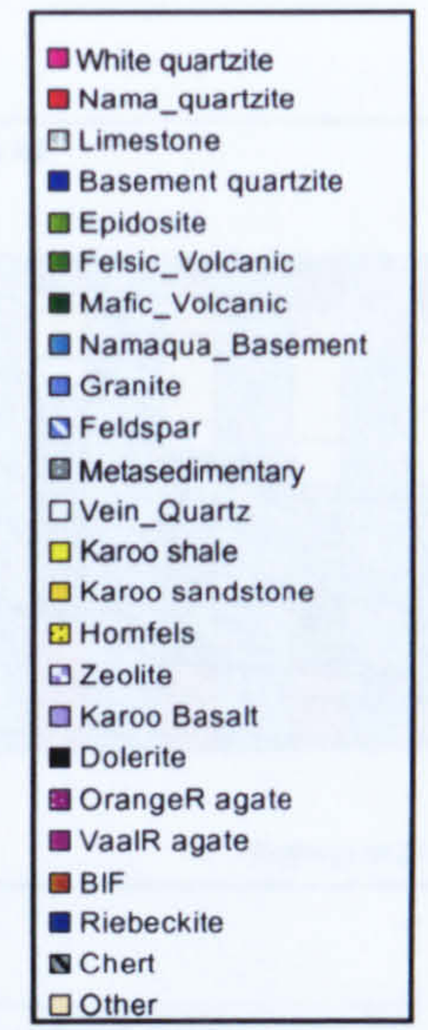

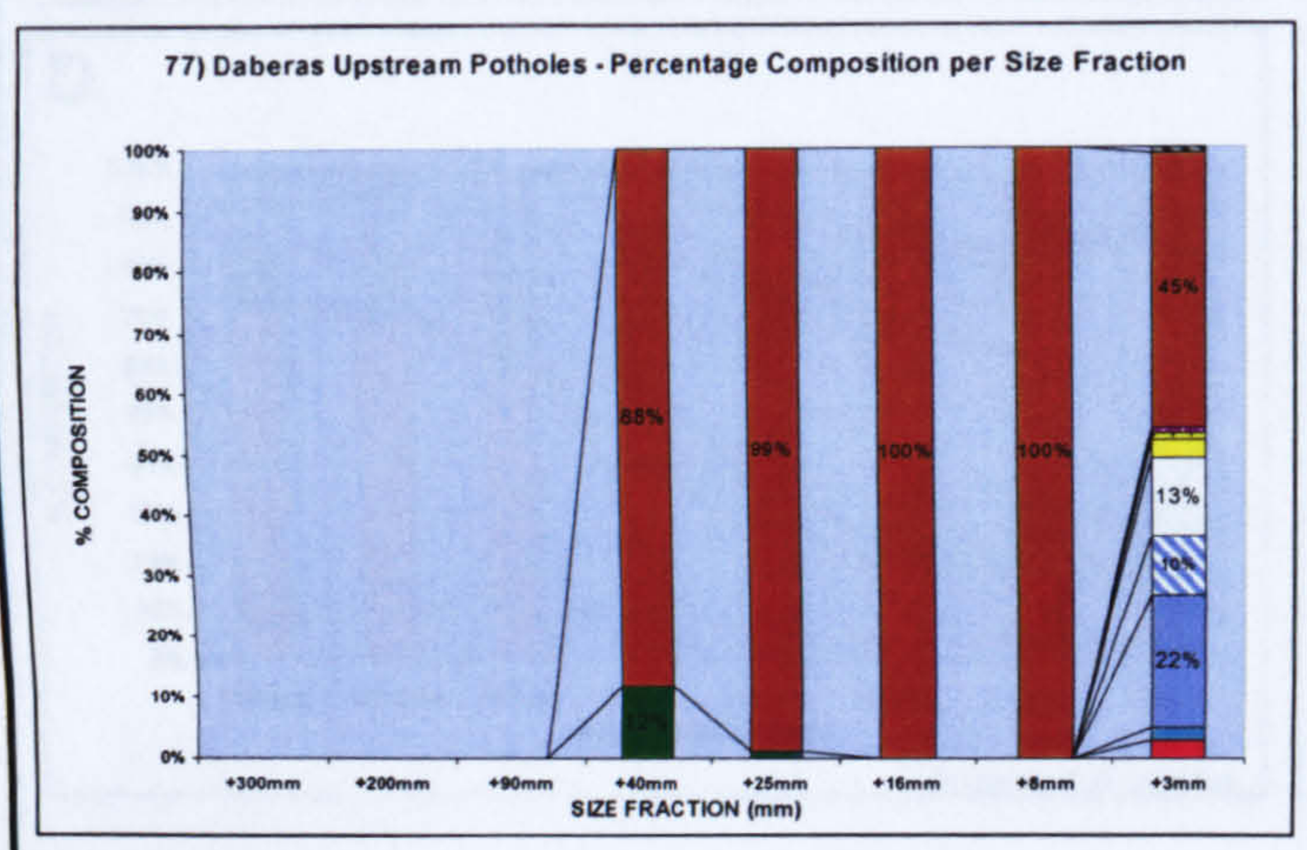

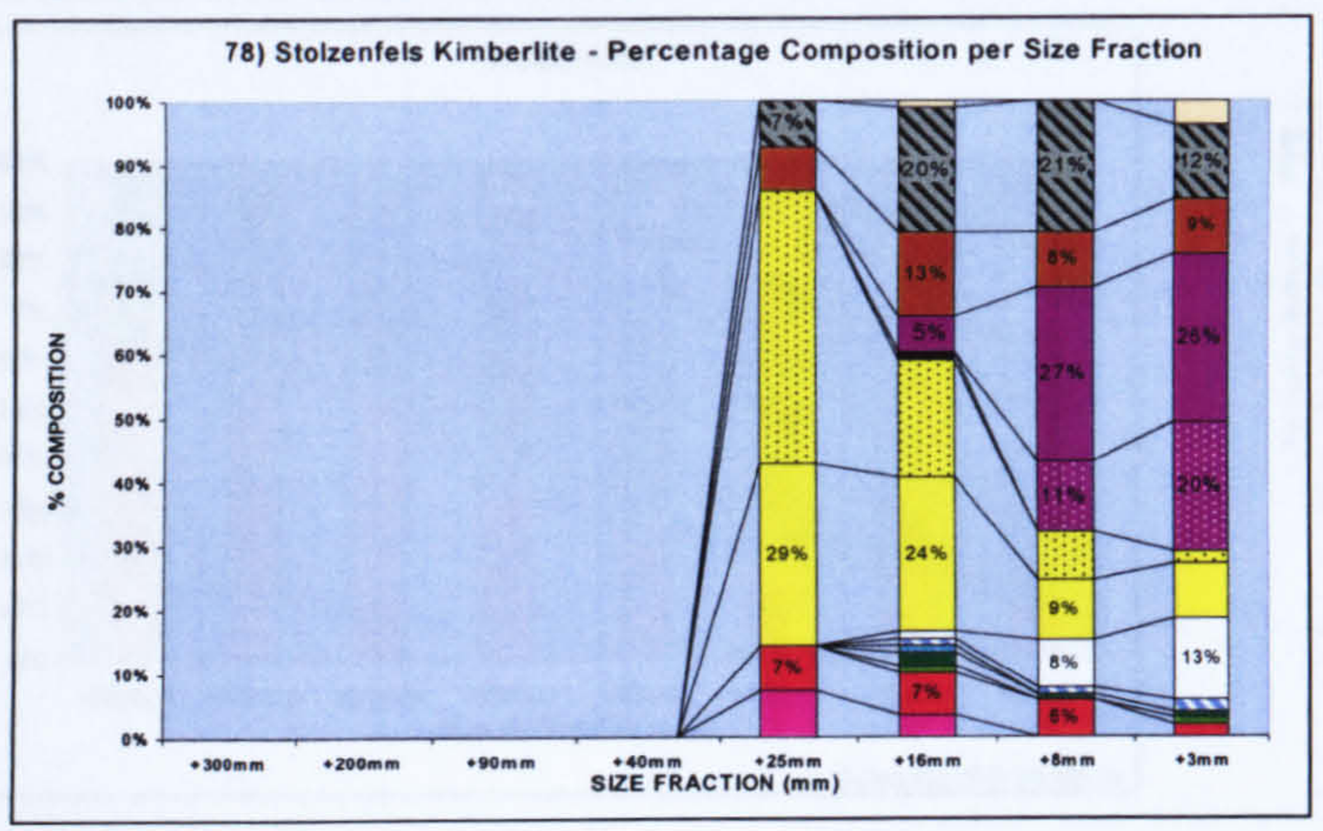

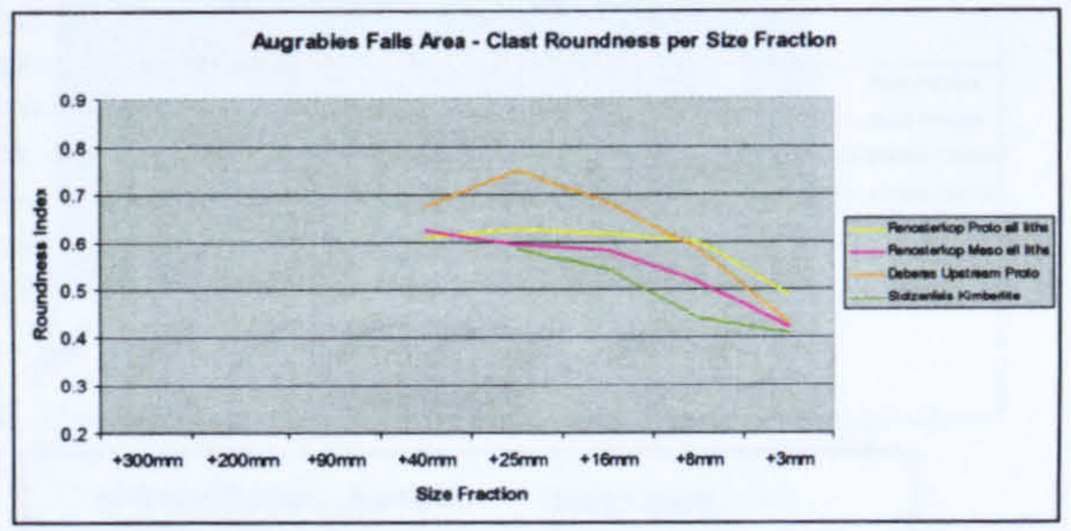

Figure 6.37 Clast type proportions per size fraction and average clast roundness per size fraction for samples in the Augrabies Falls area.

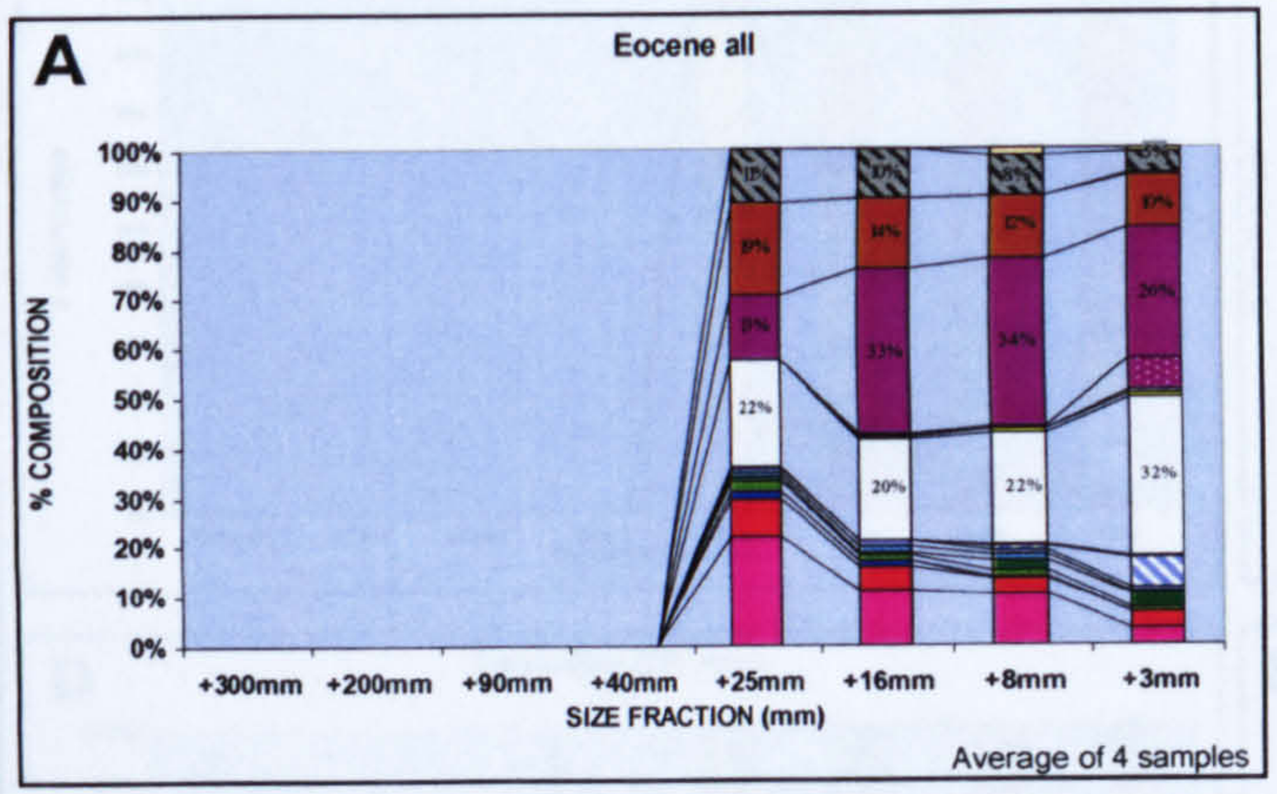

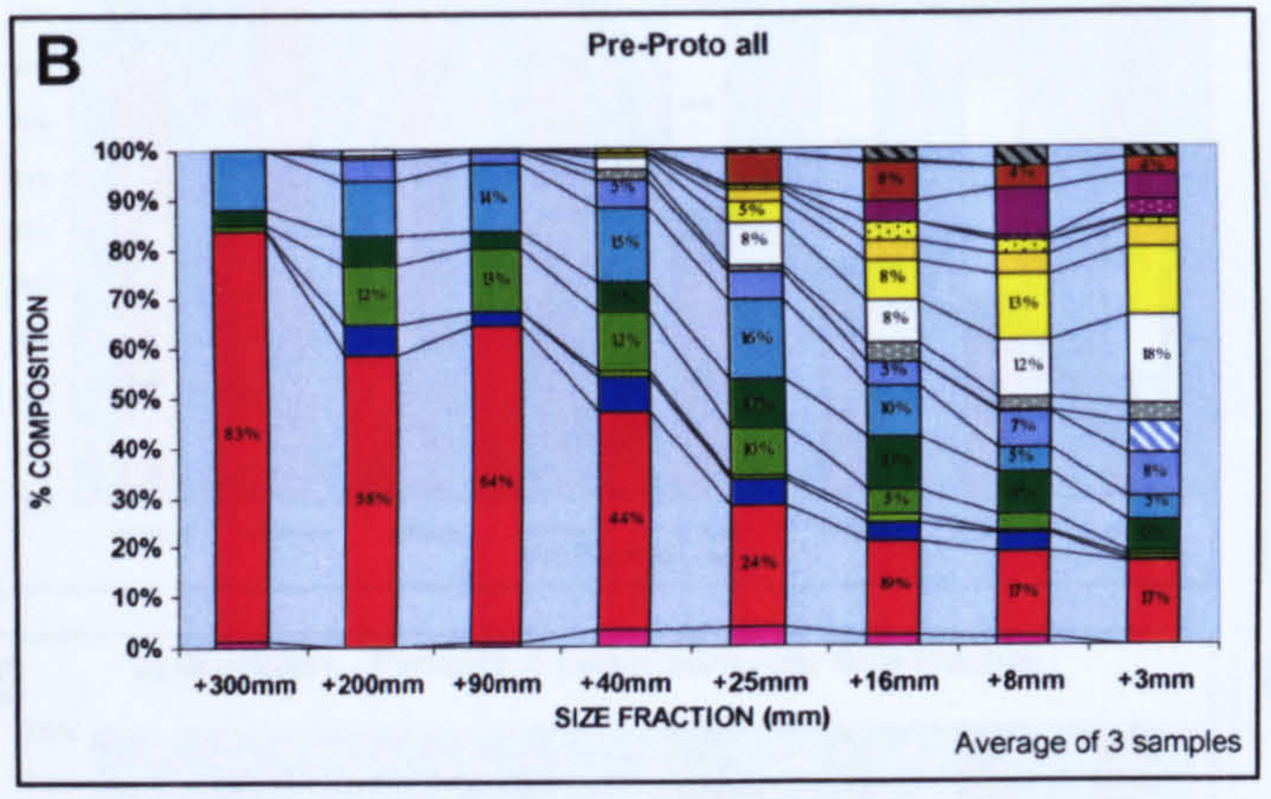

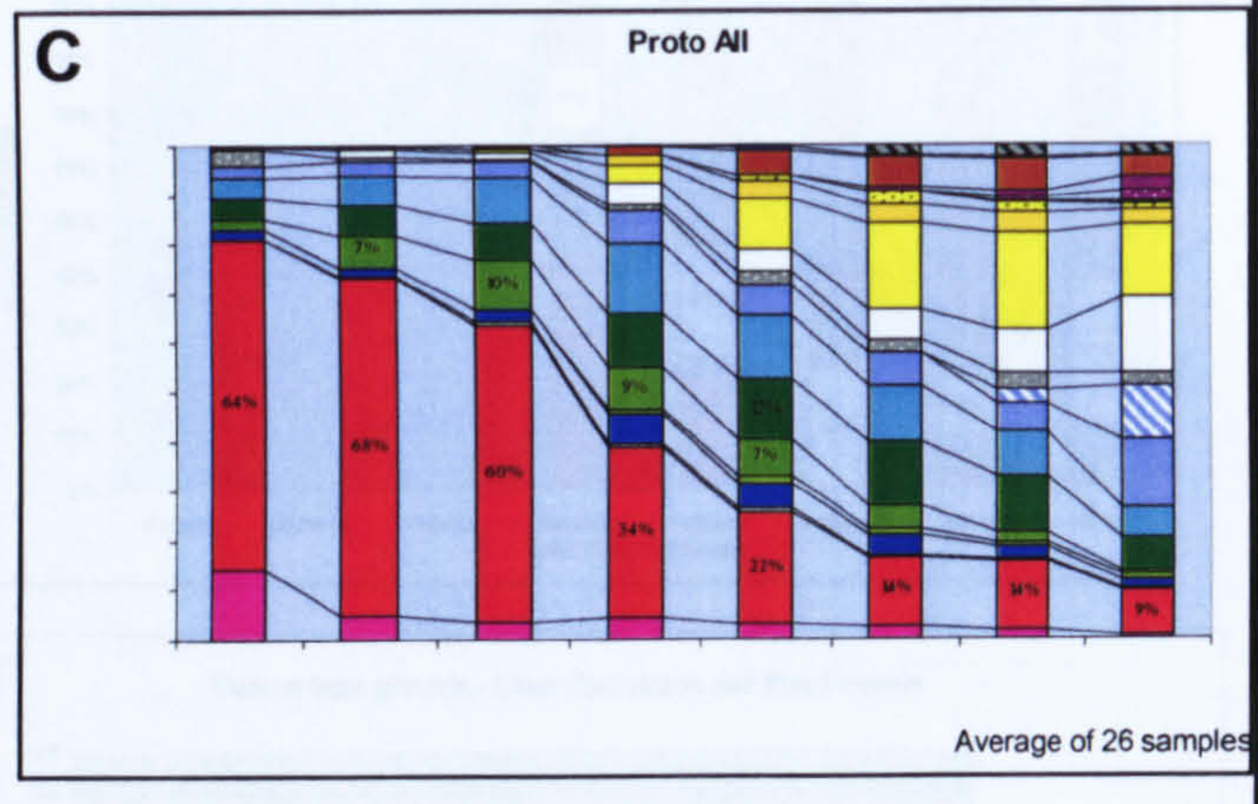

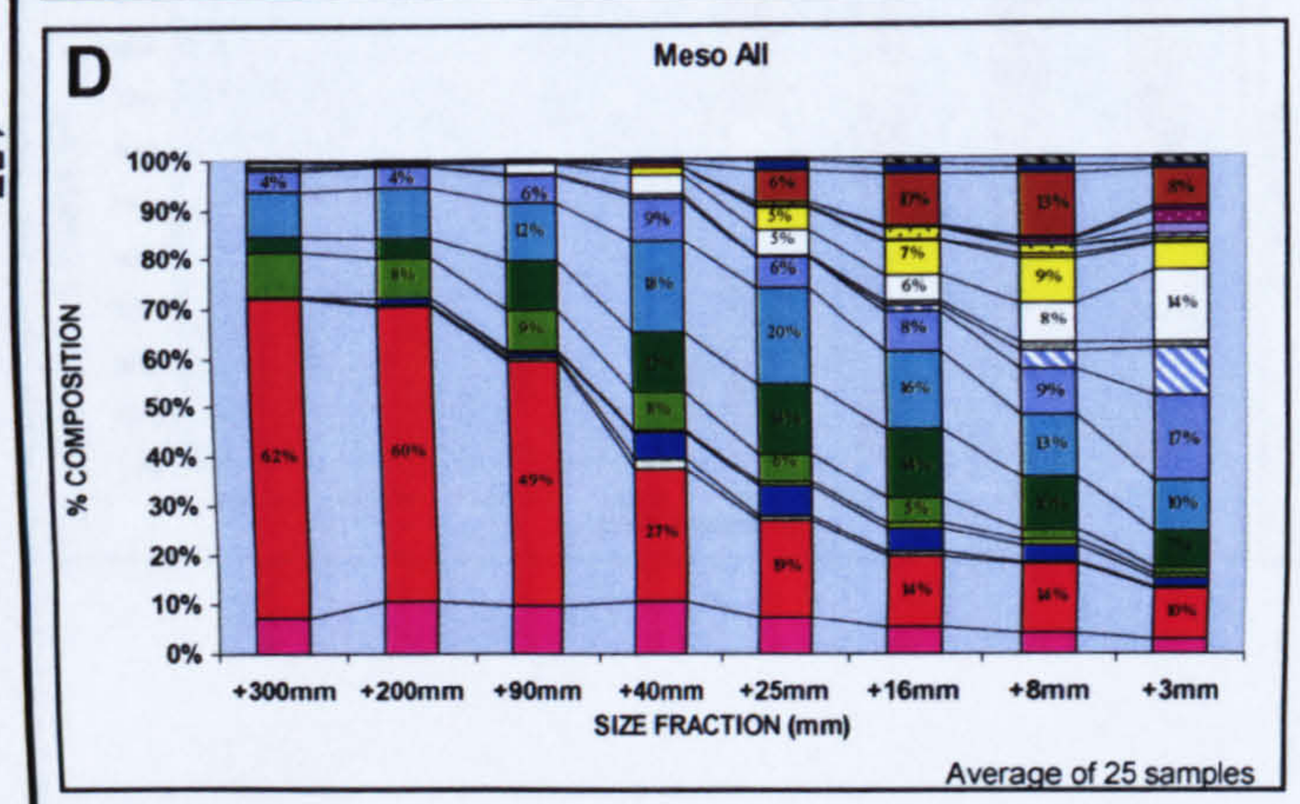

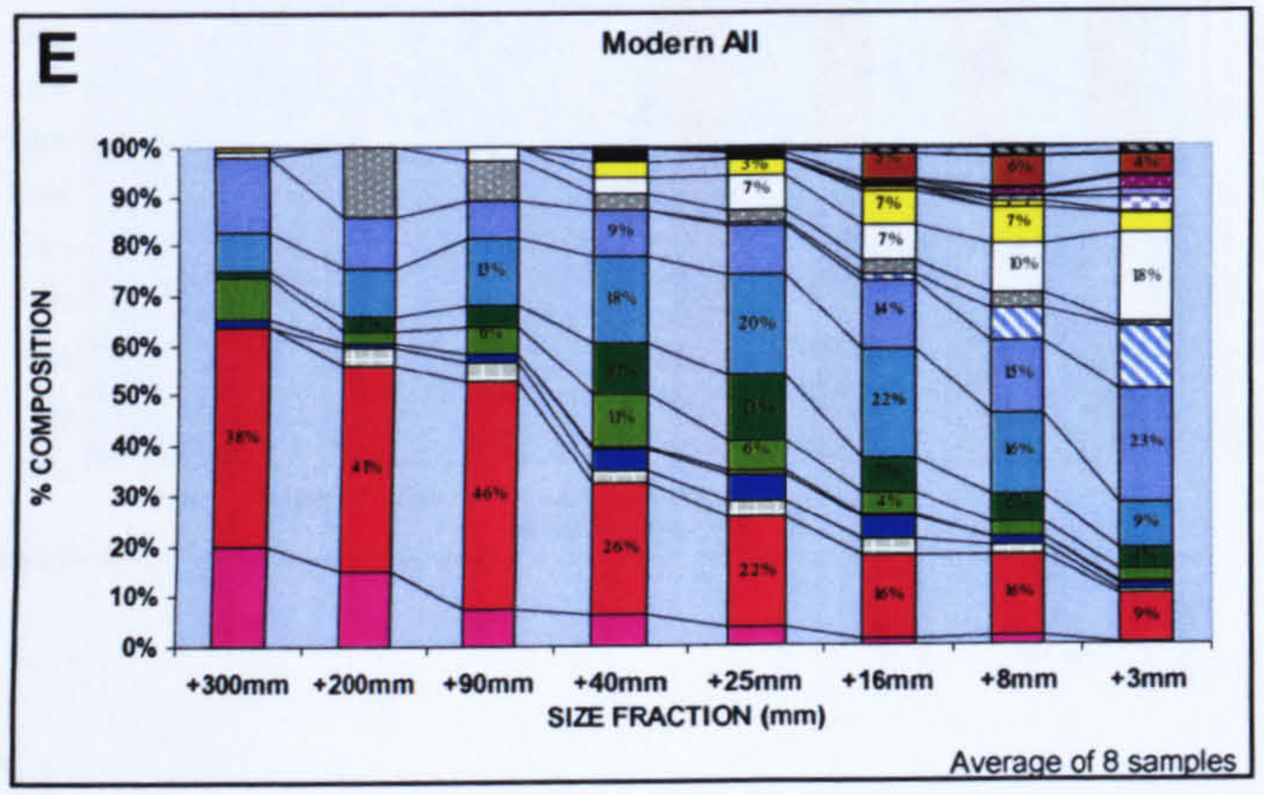

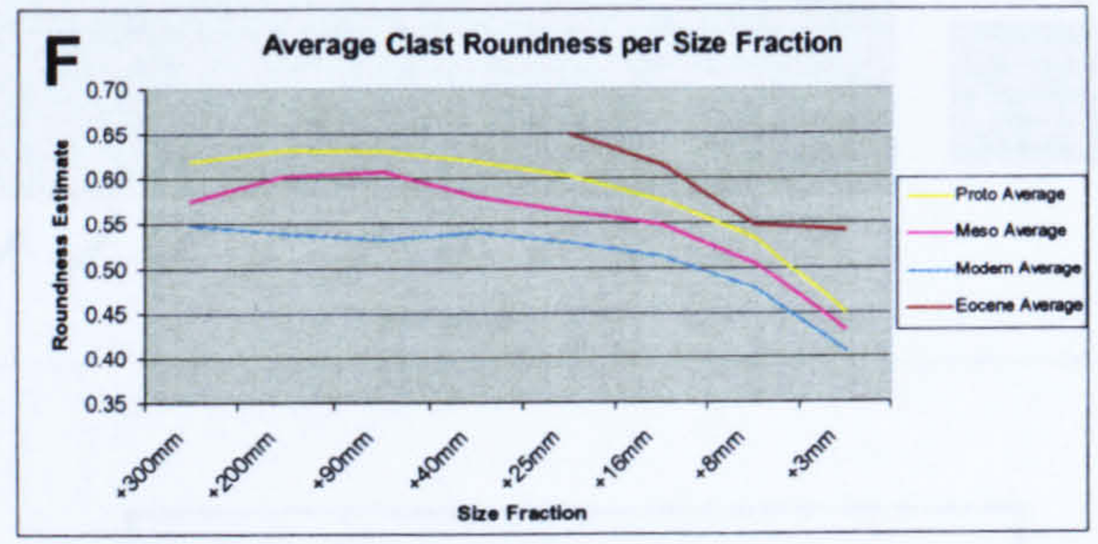

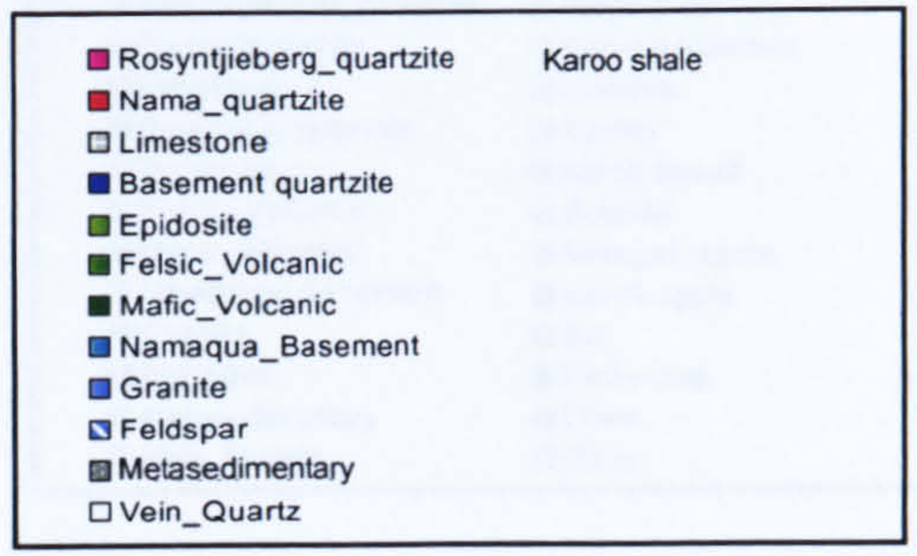

Figure 6.38 Summary of clast assemblages per gravel suite in the study area.

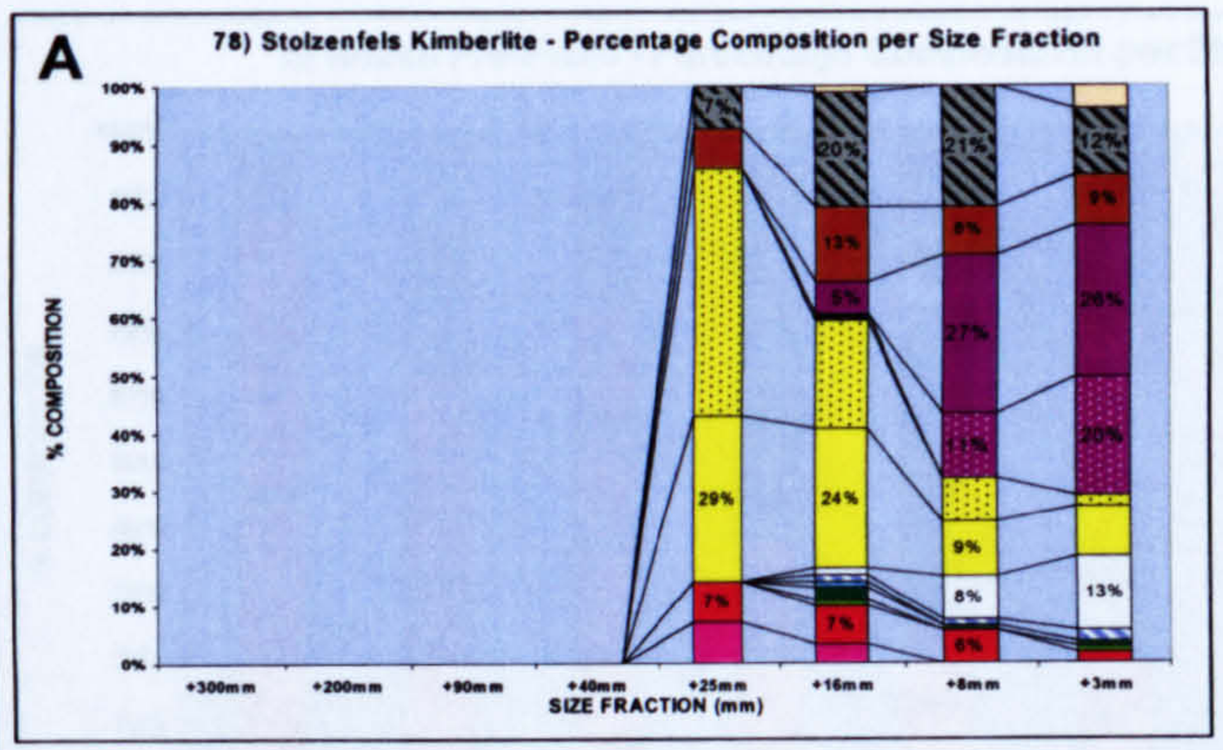

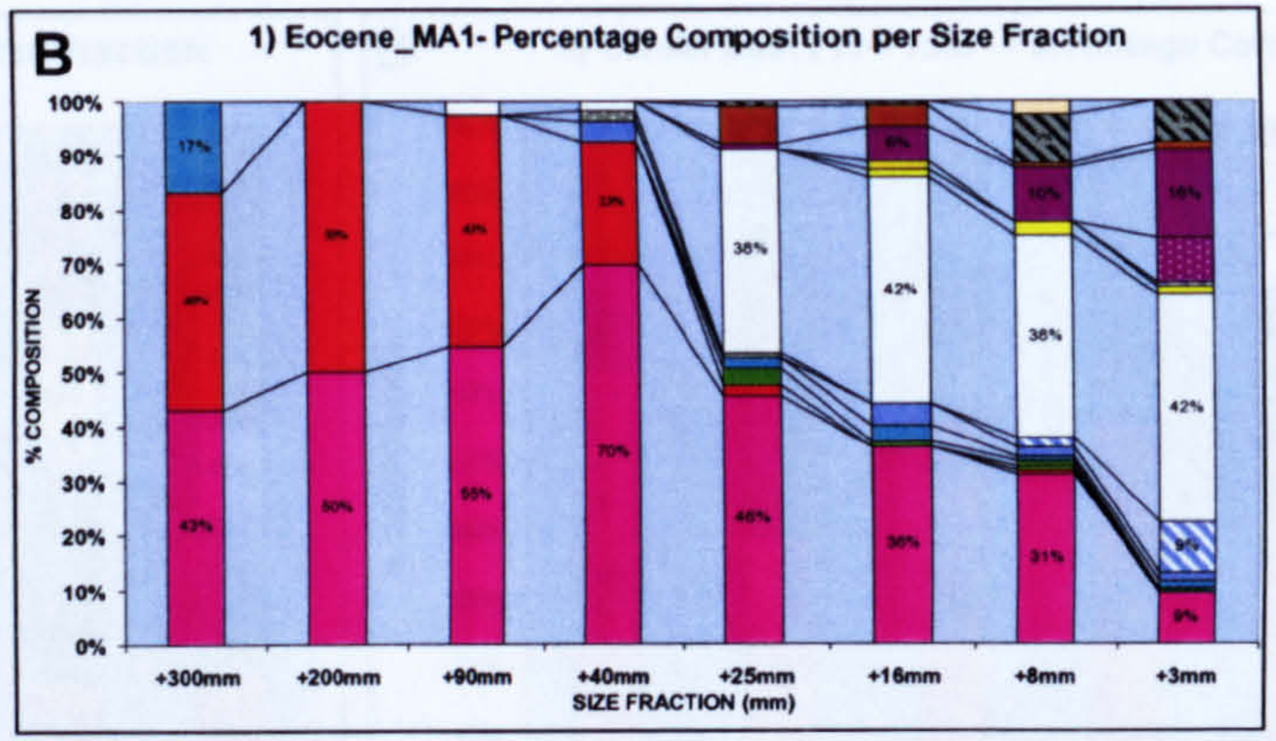

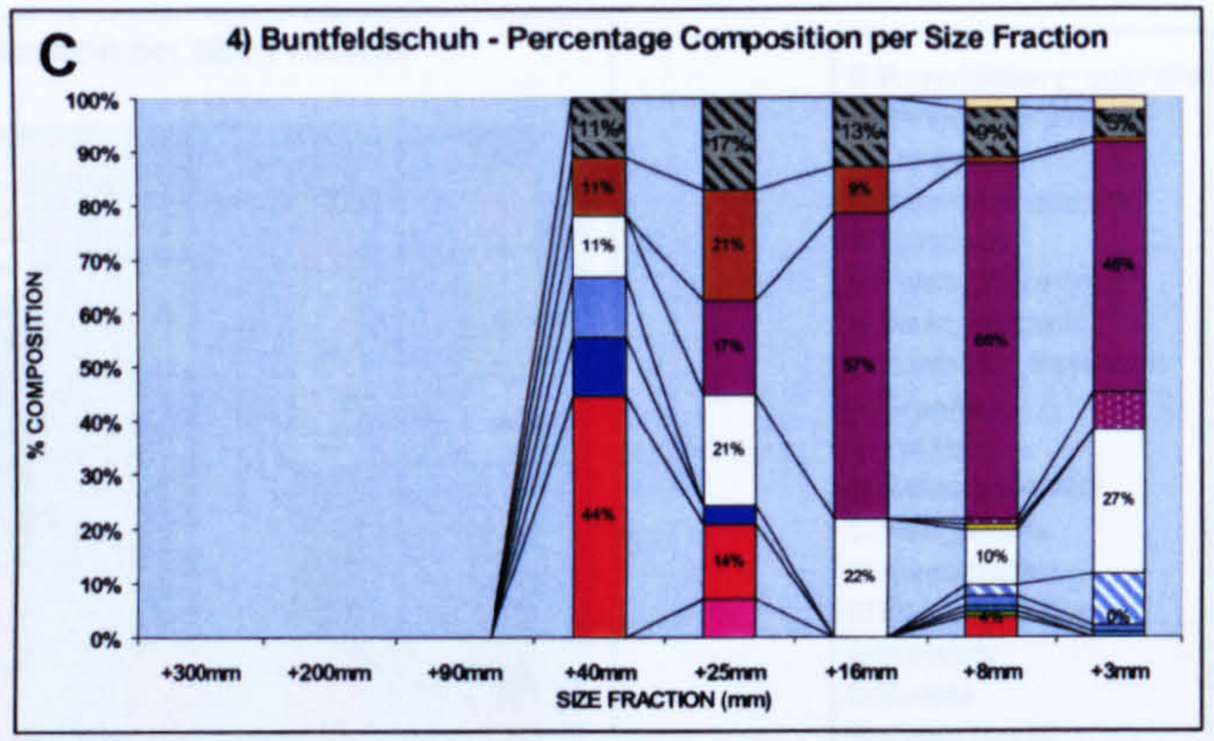

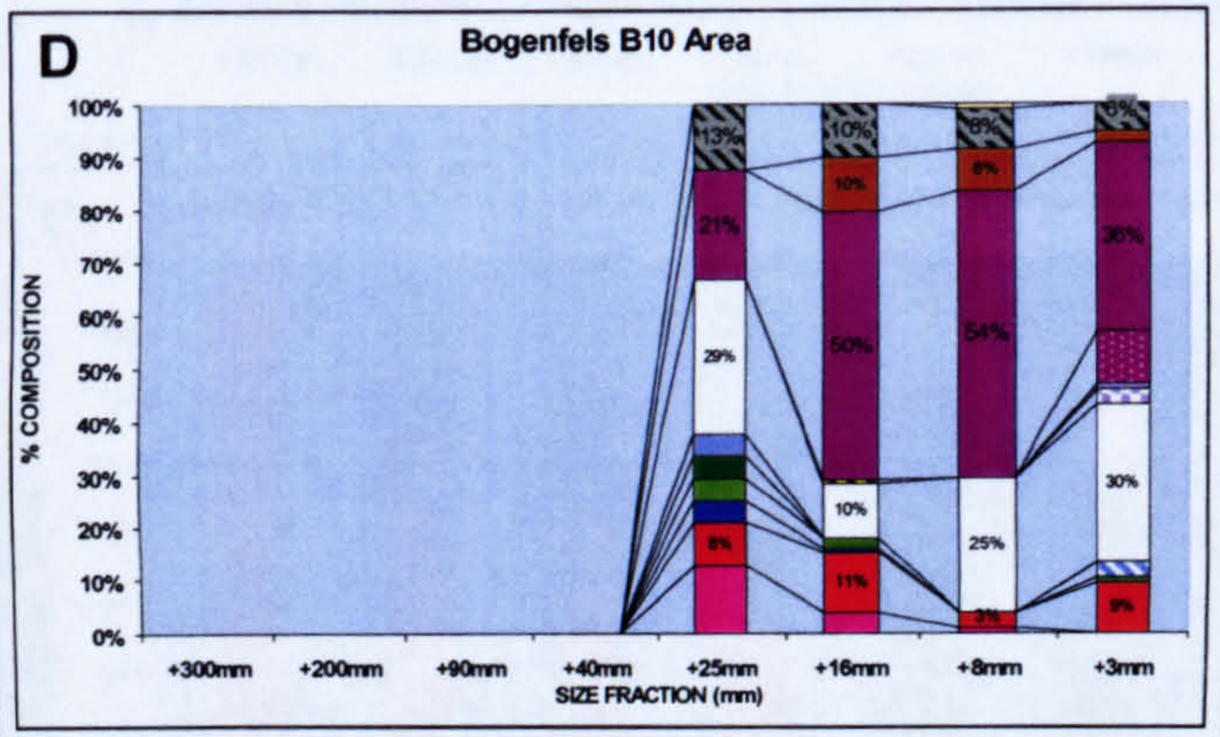

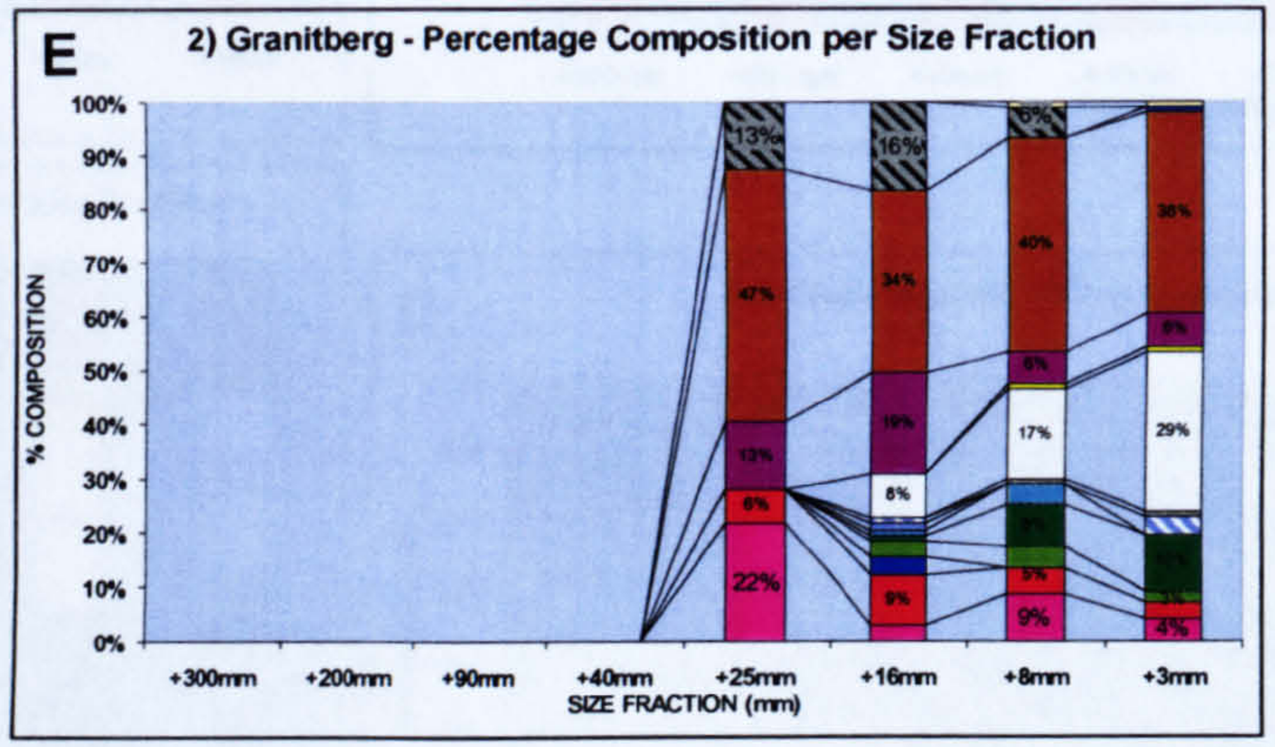

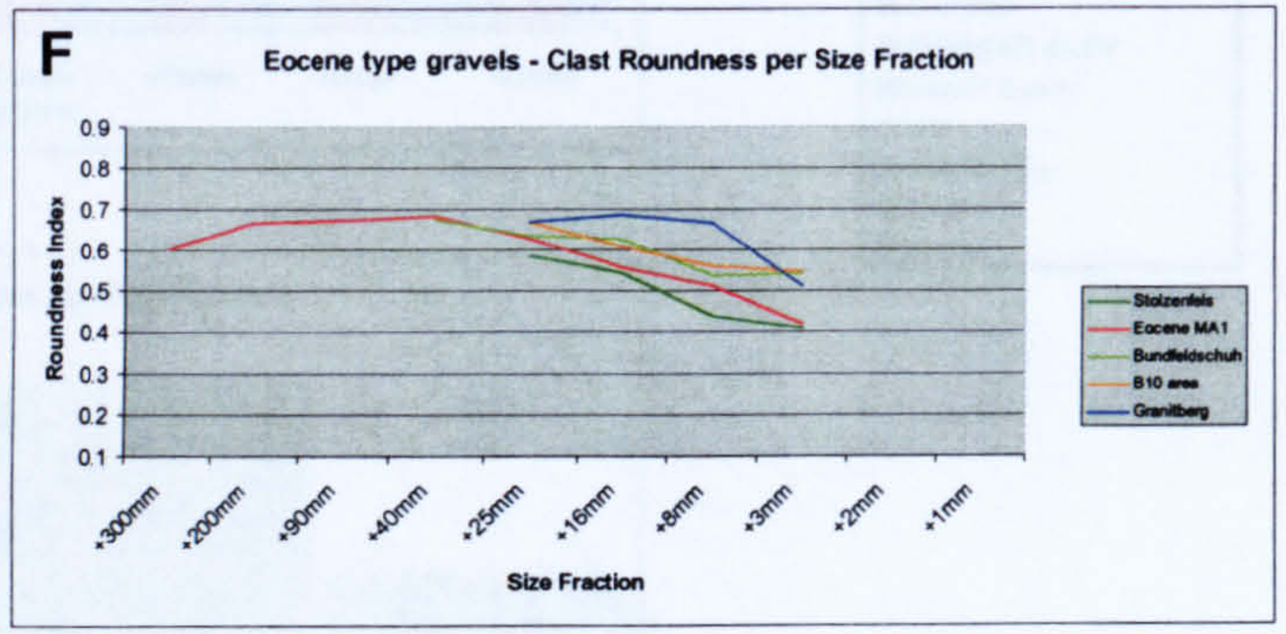

Figure 6.39 Clast assemblage and roundness changes in the Eocene suite of gravels.

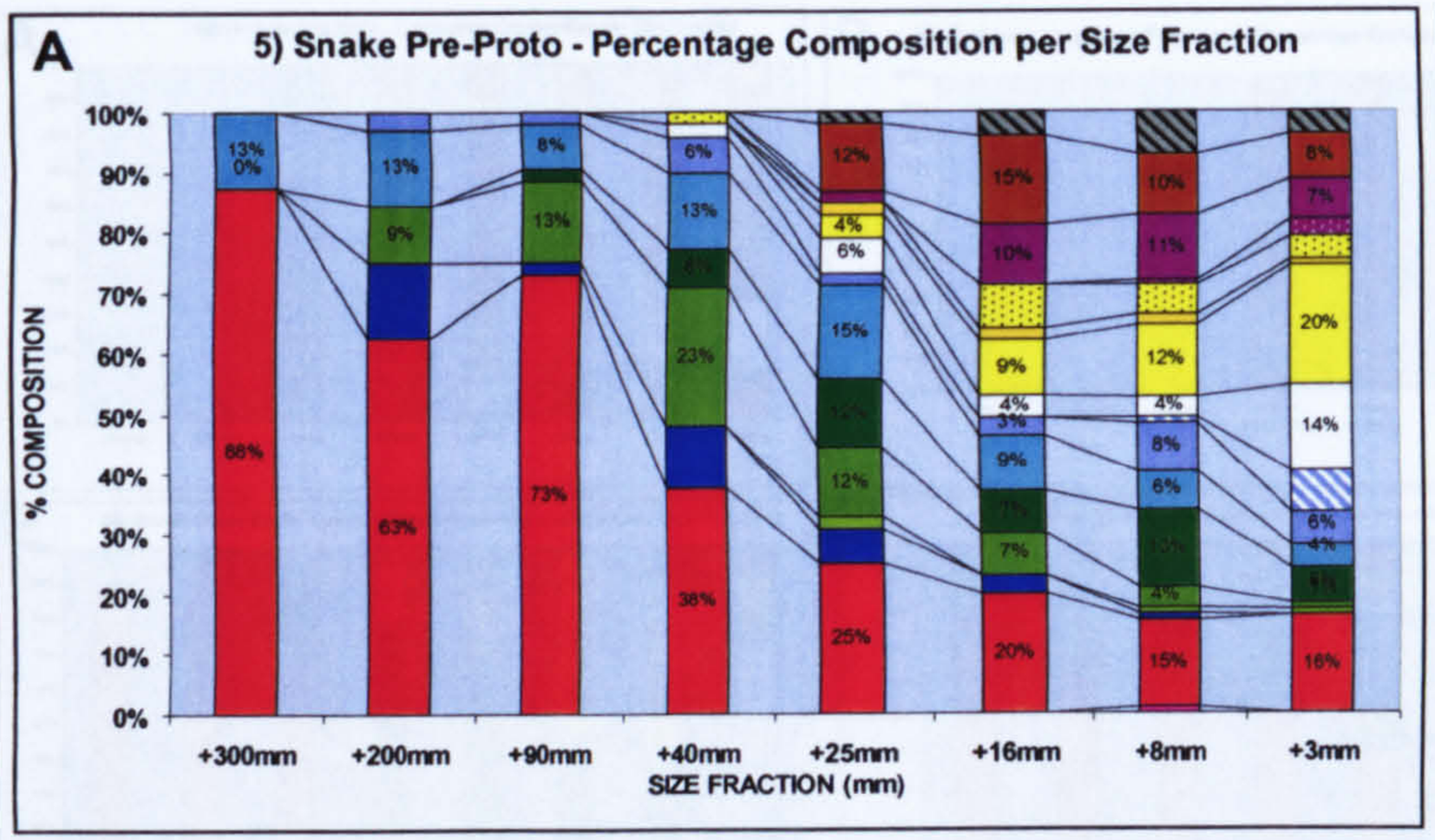

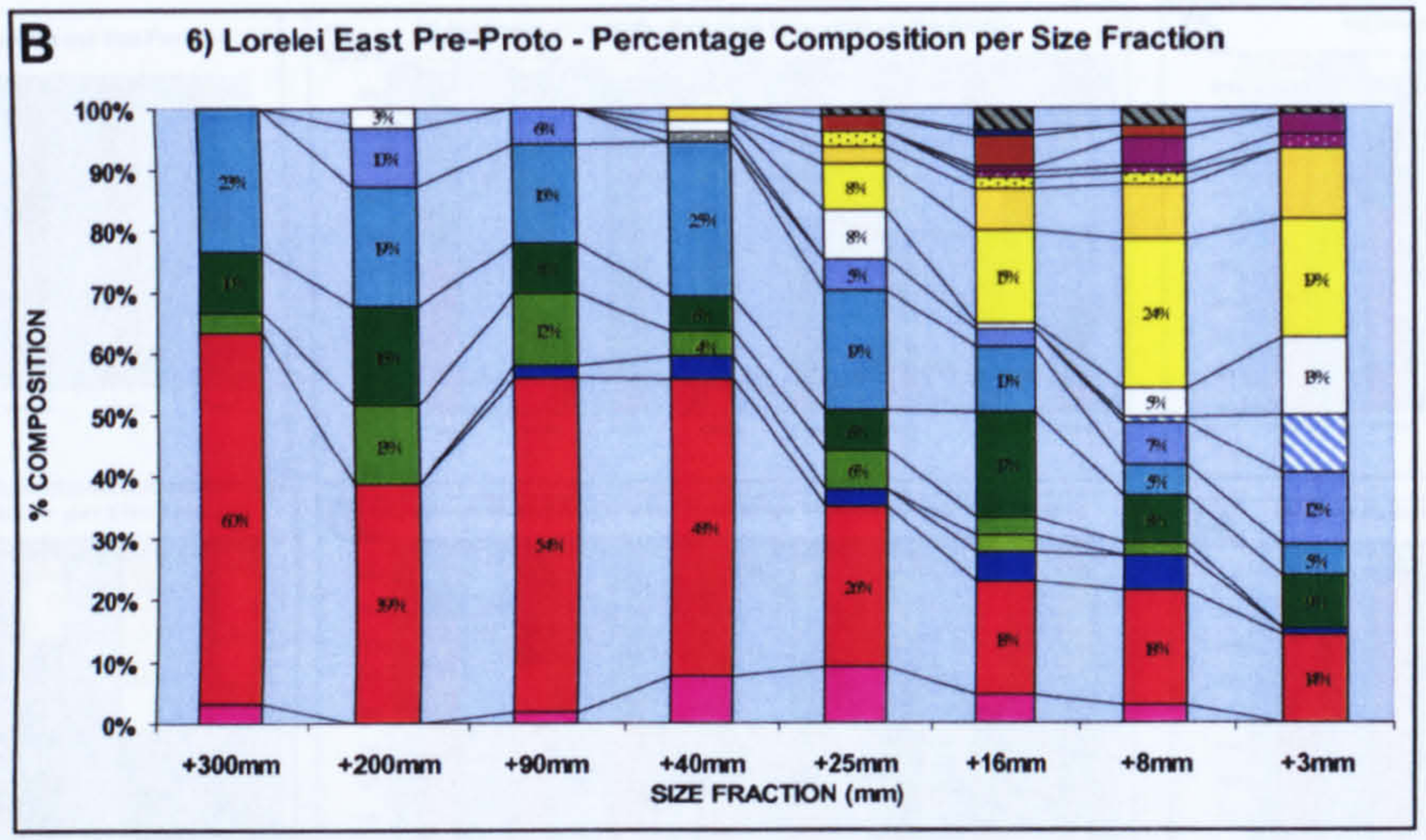

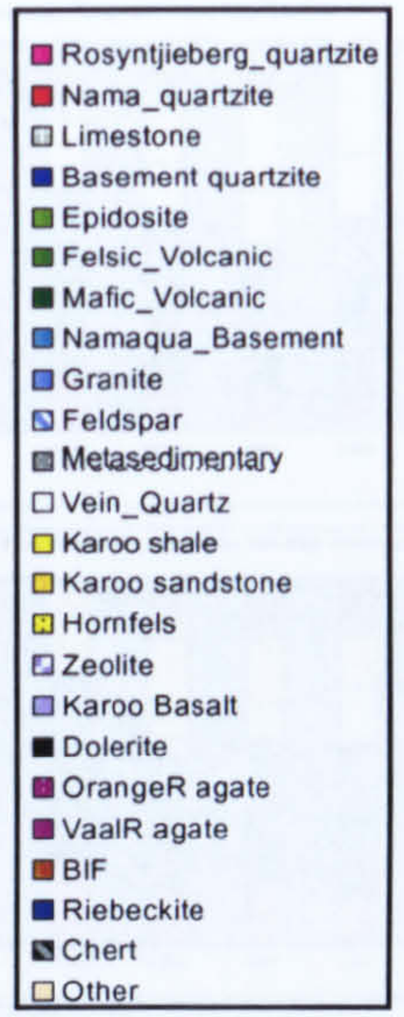

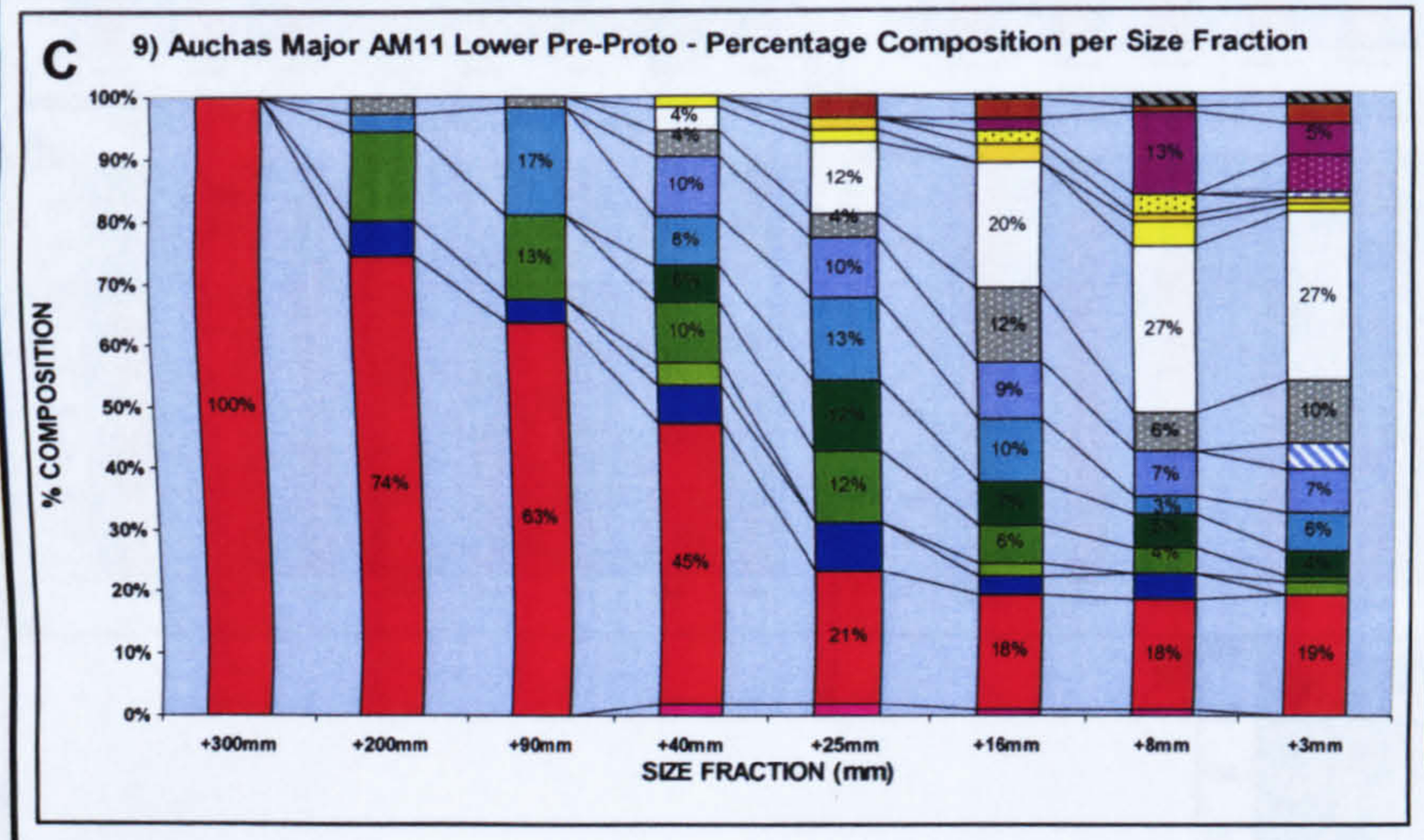

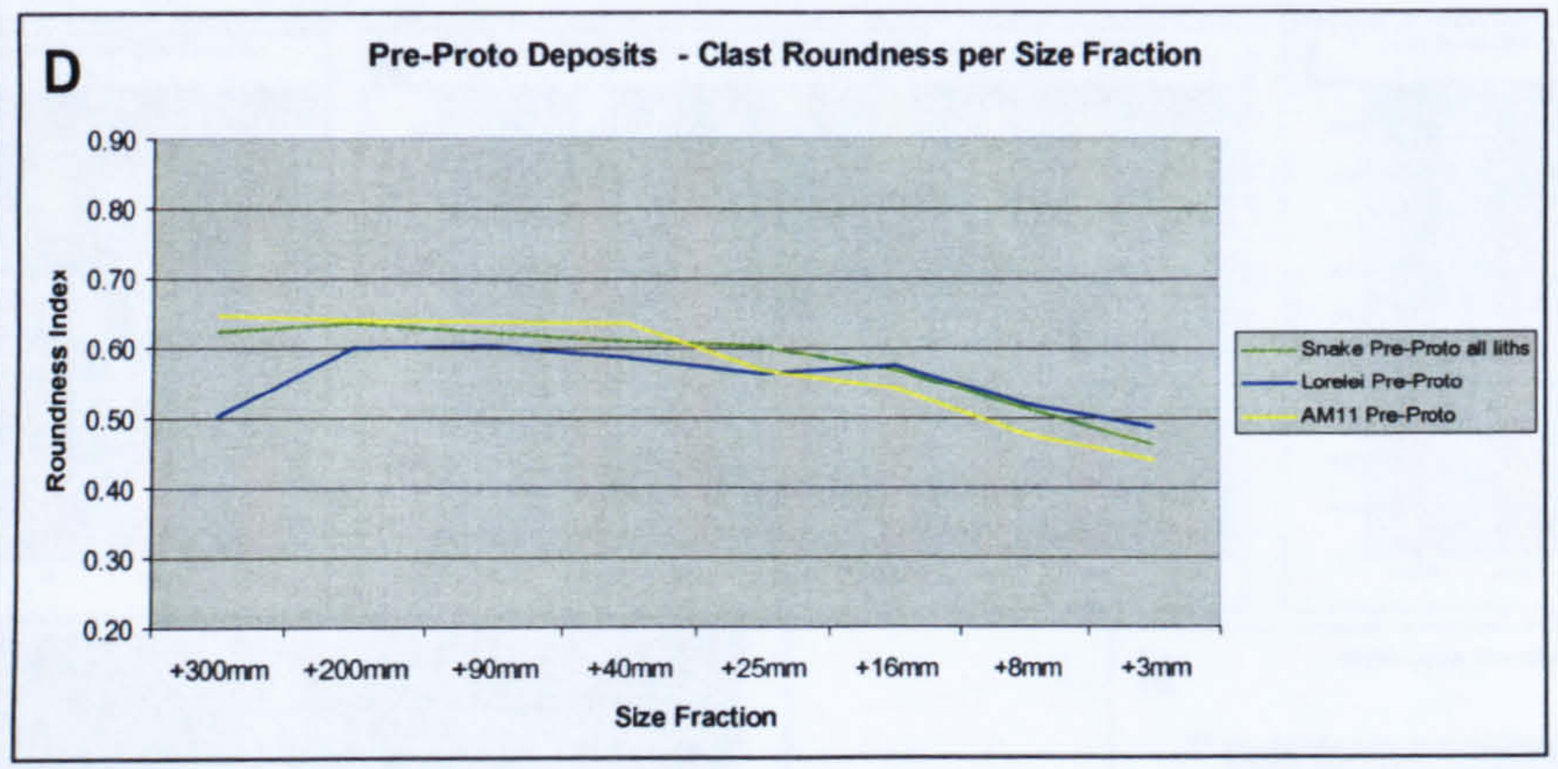

Figure 6.40 Clast assemblage and roundness changes in the Pre-Proto deposits.

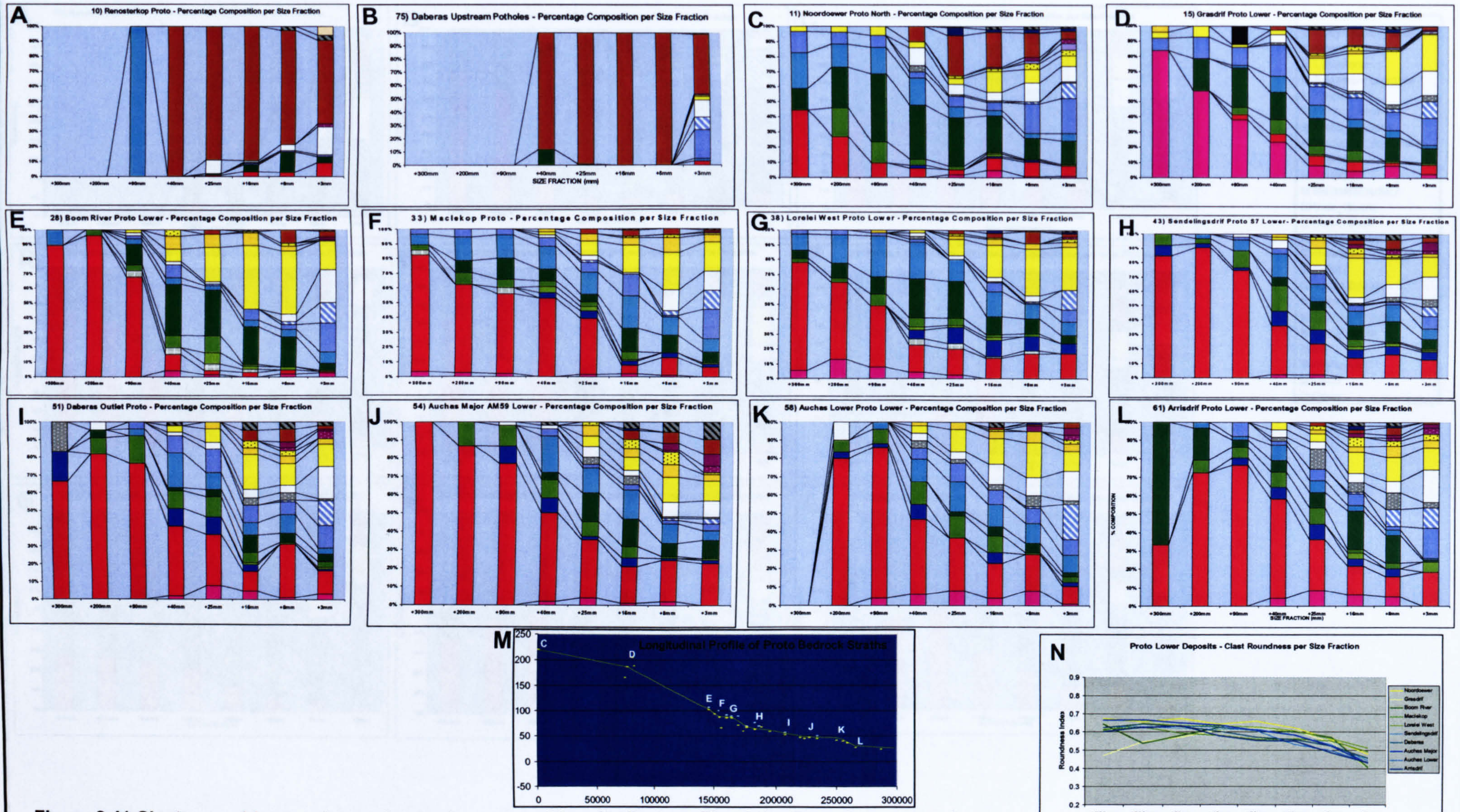

Figure 6.41 Clast assemblage and roundness changes and longitudinal profile of the Proto lower gravels.

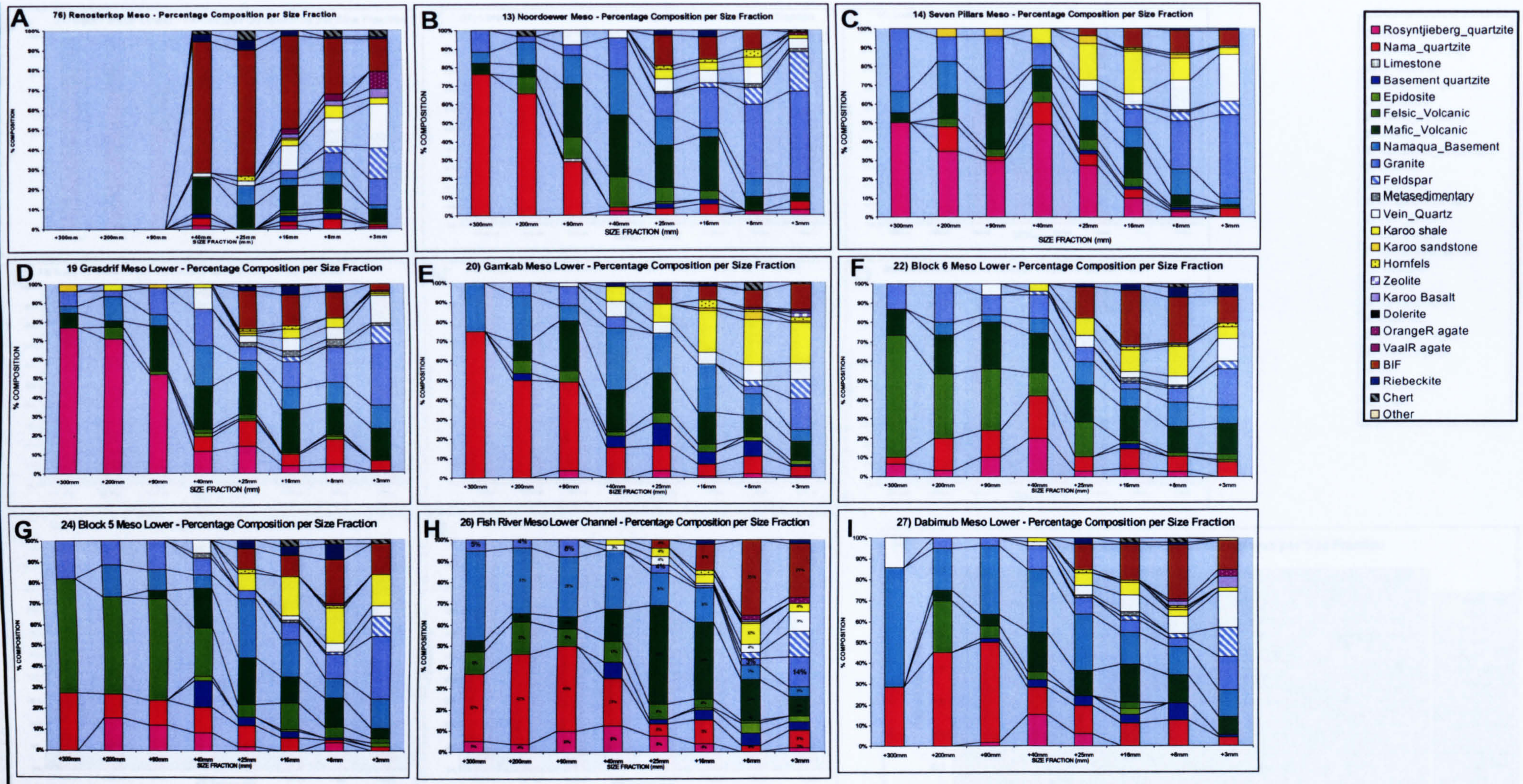

Figure 6.42 A-I Clast assemblage and roundness changes in the Meso deposits.

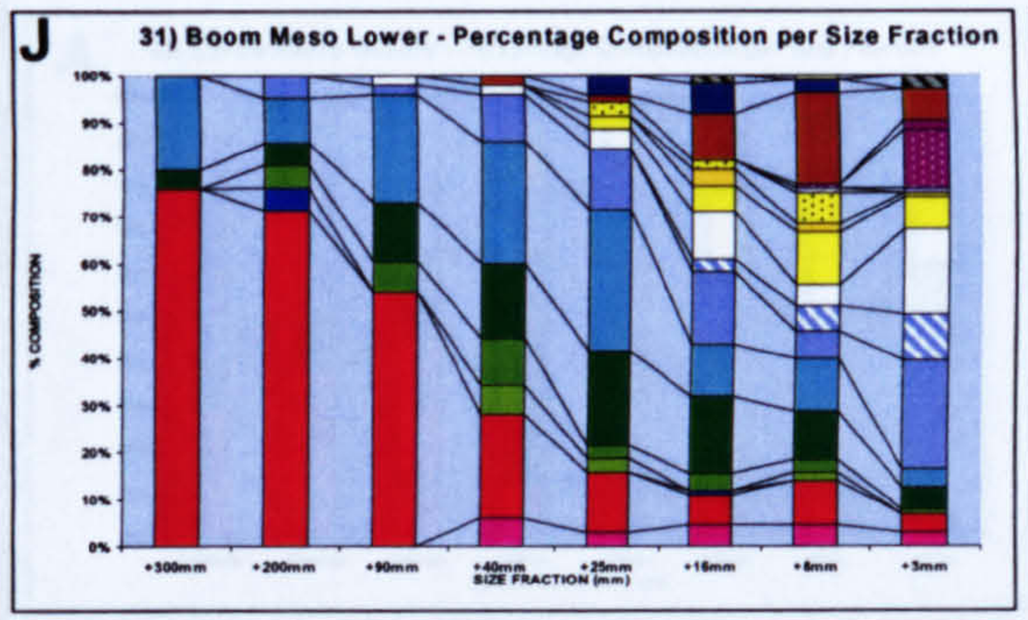

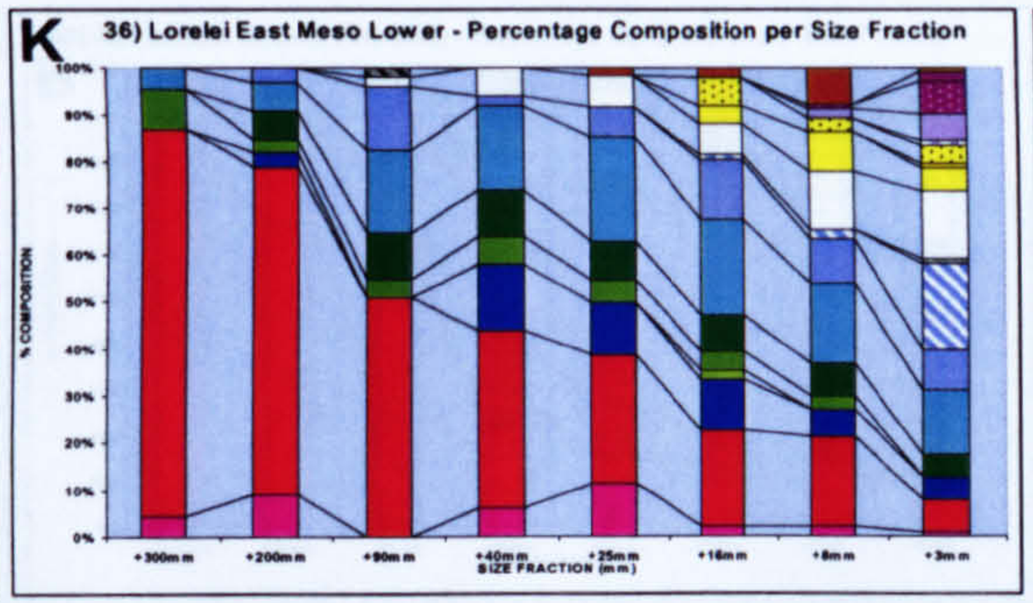

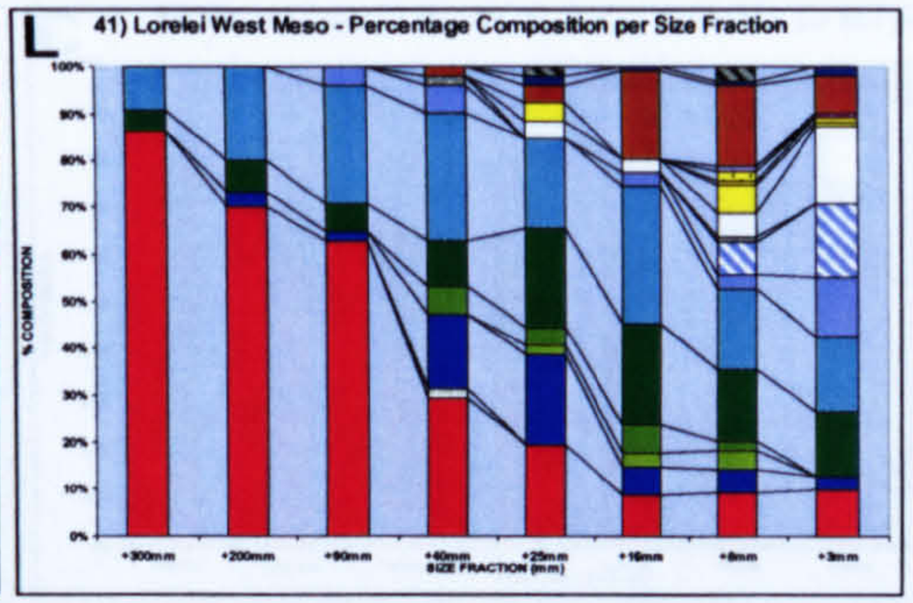

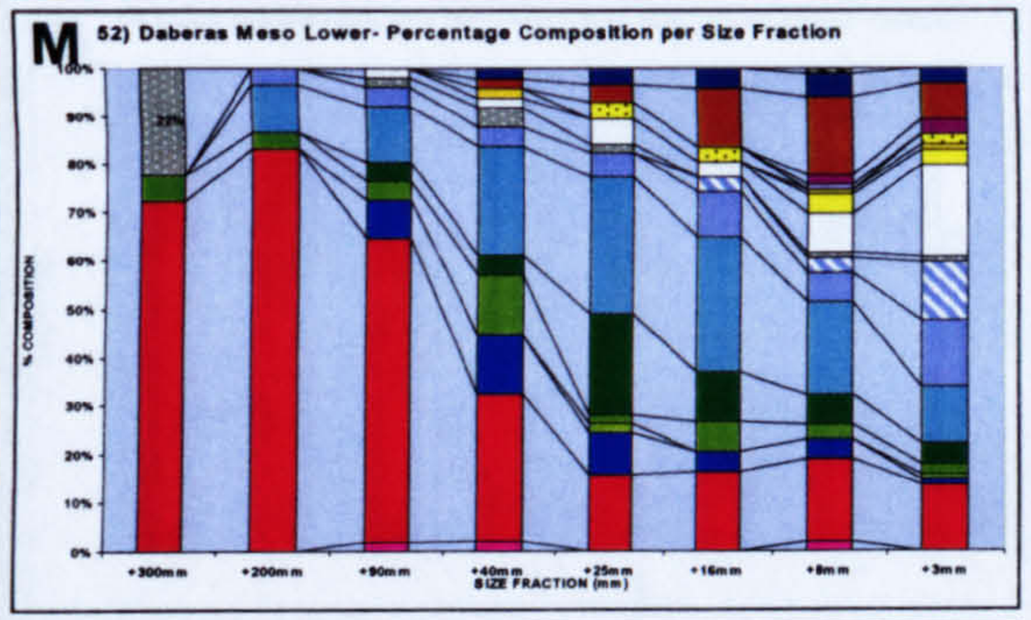

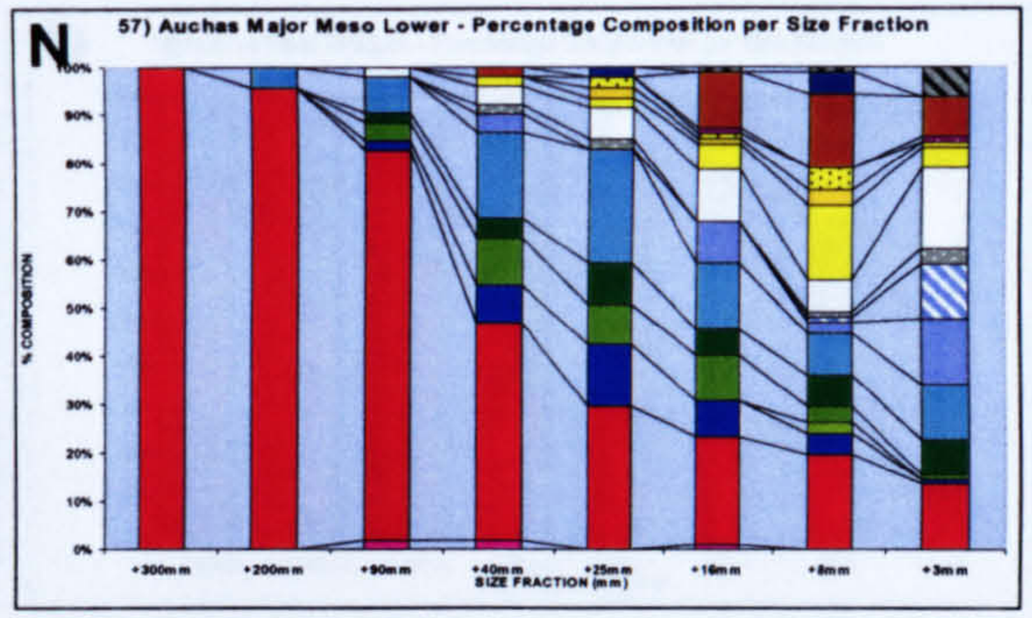

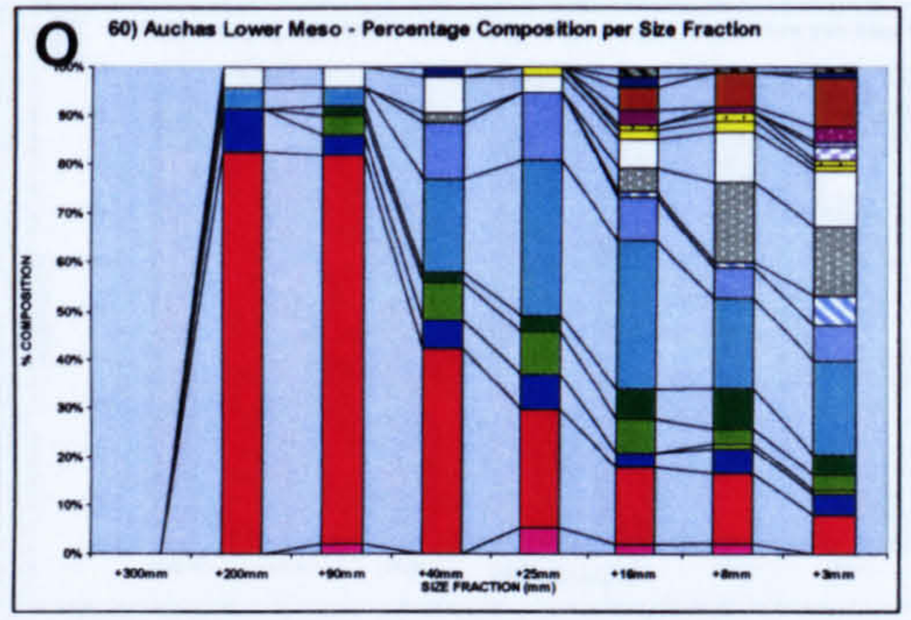

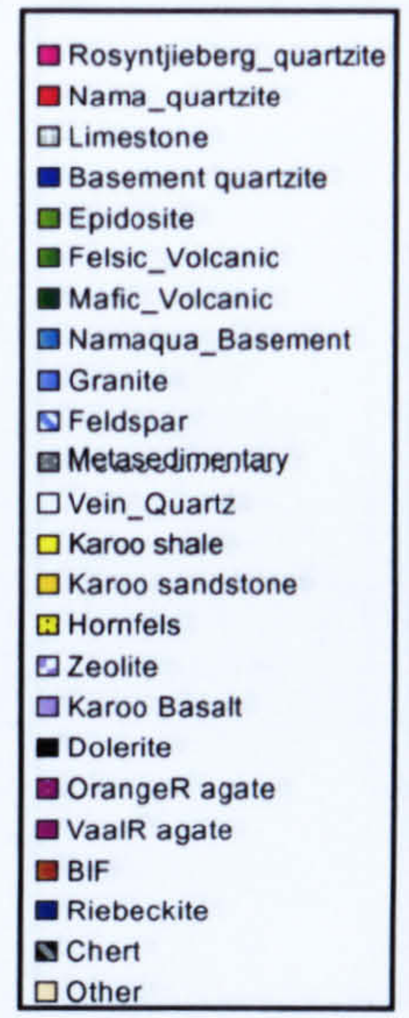

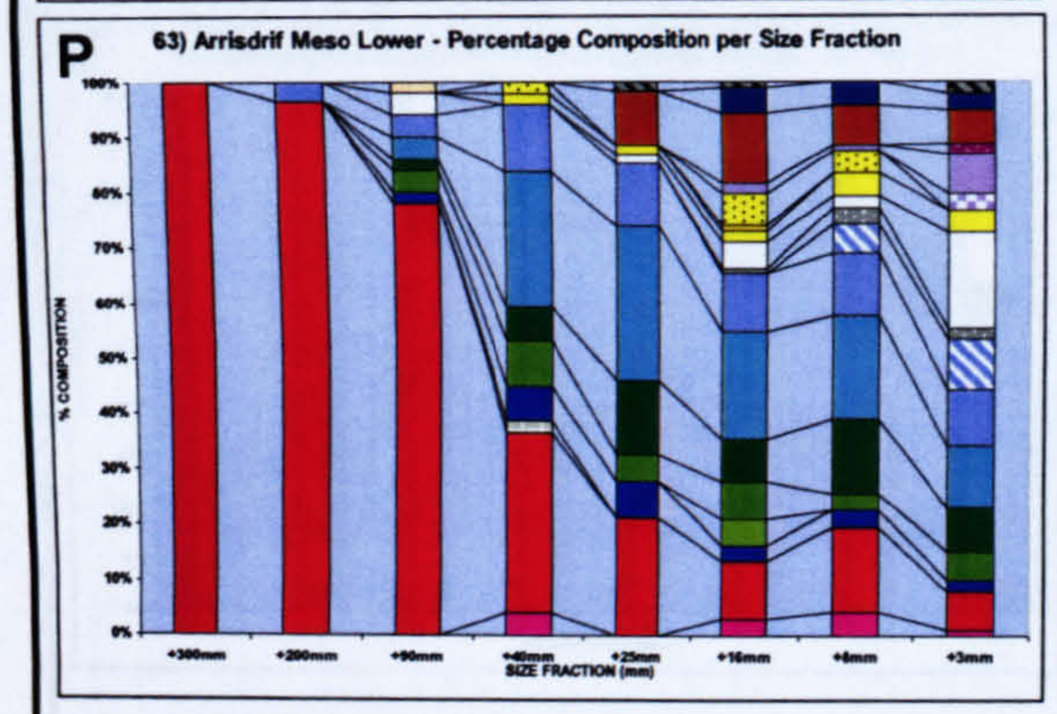

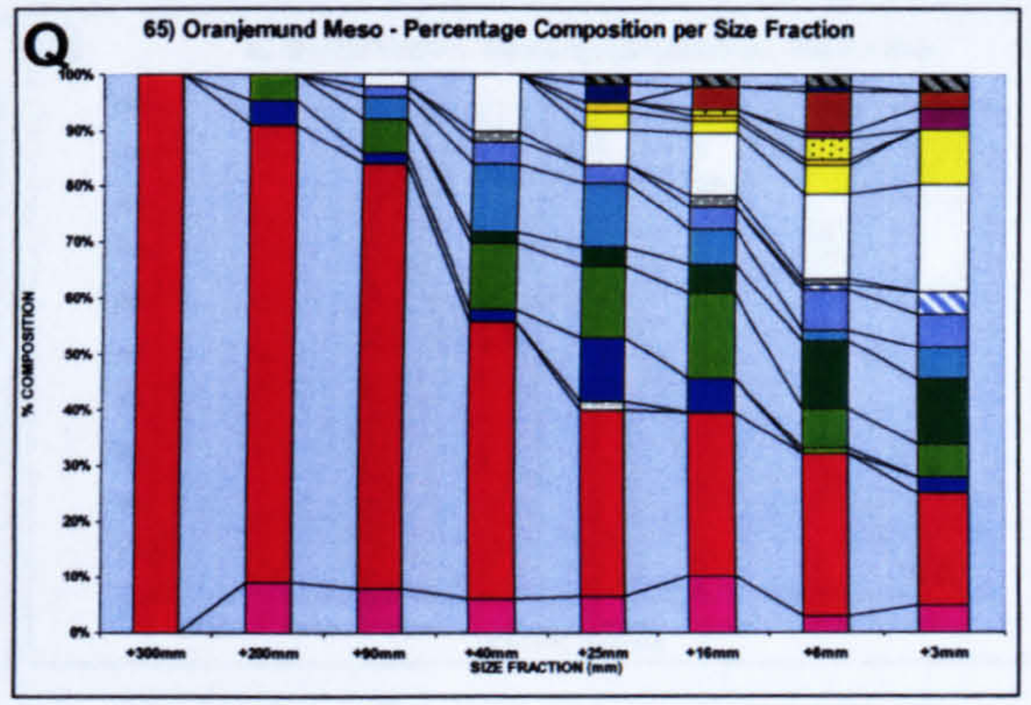

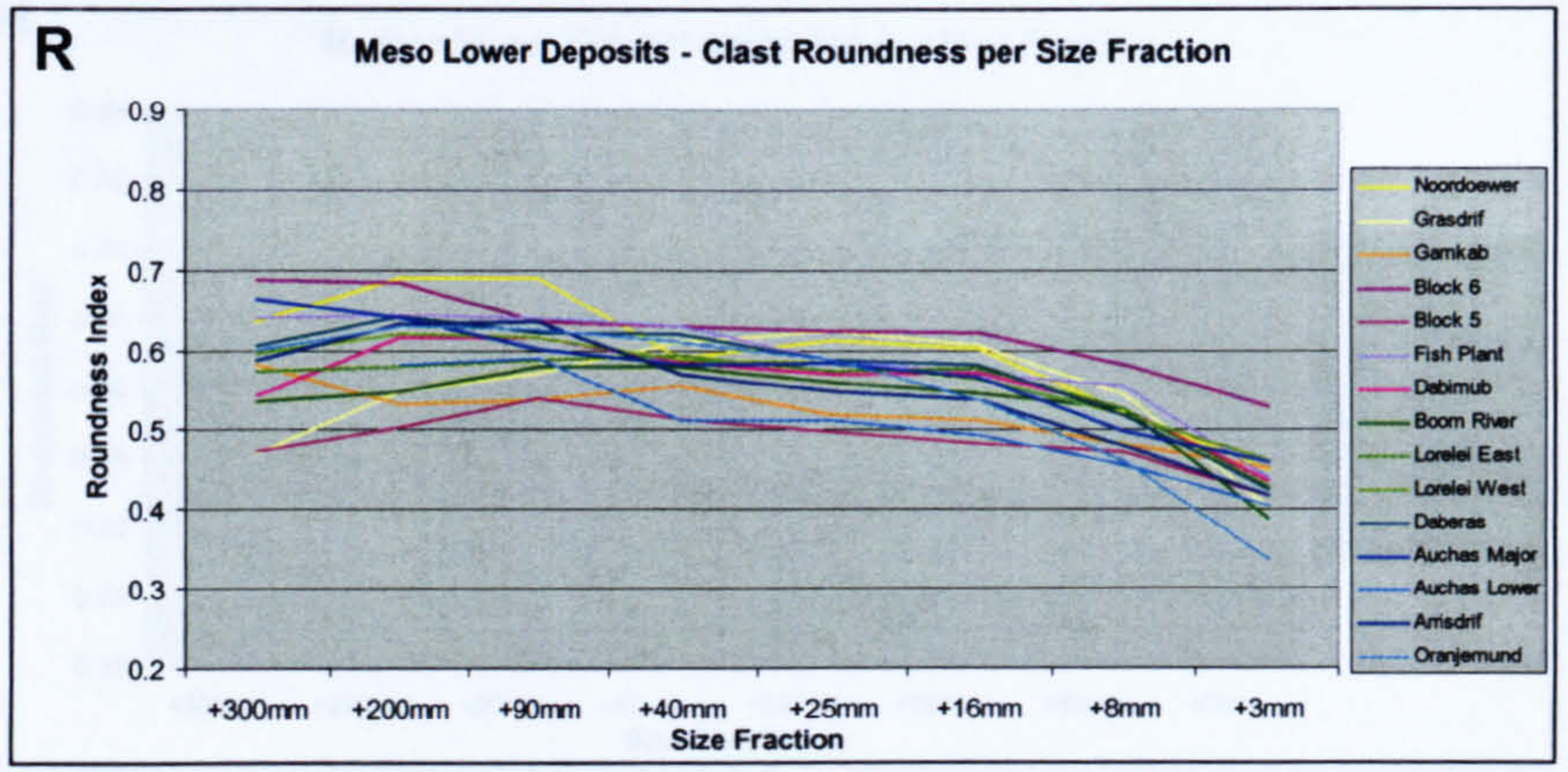

Figure 6.42 J-Q Clast assemblage and roundness changes in the Meso deposits.

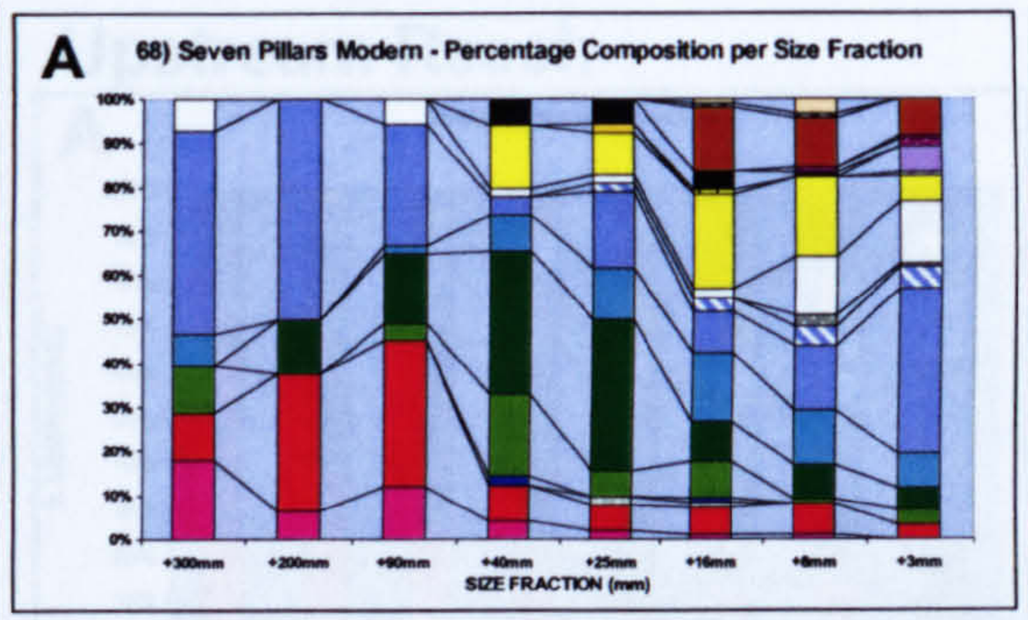

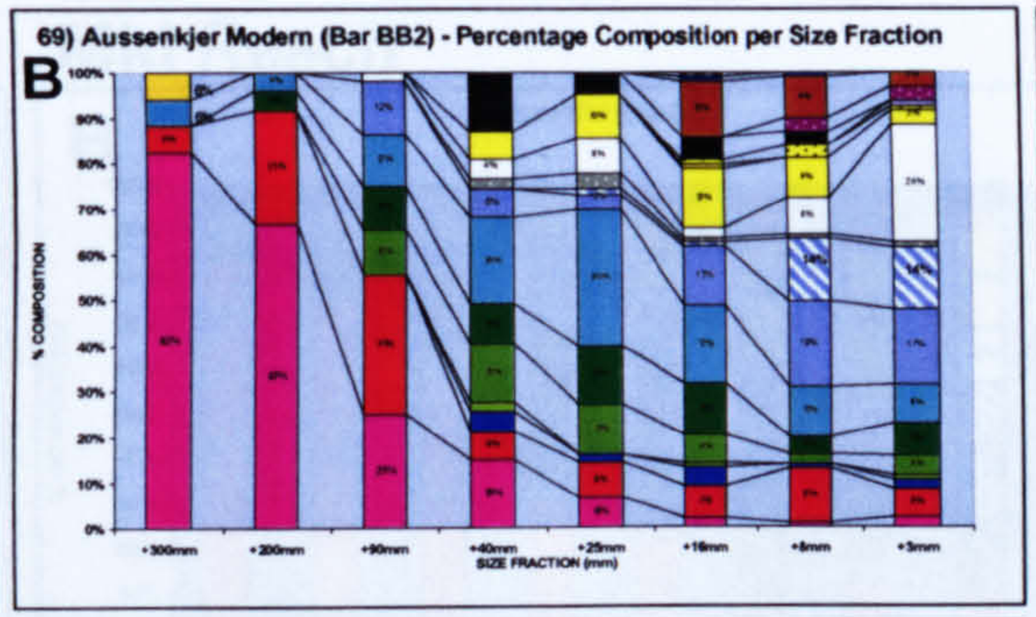

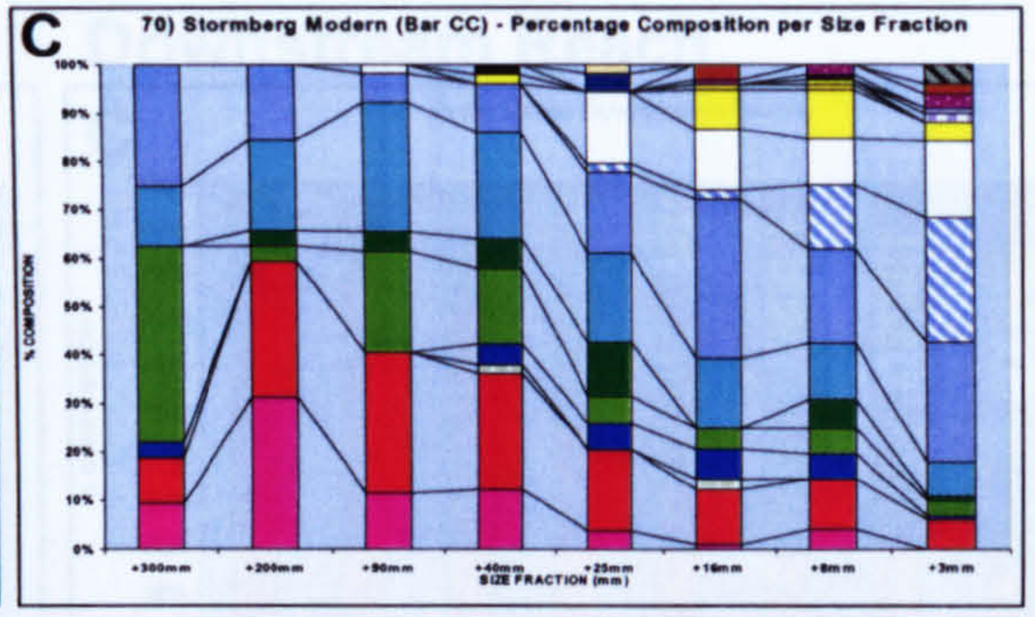

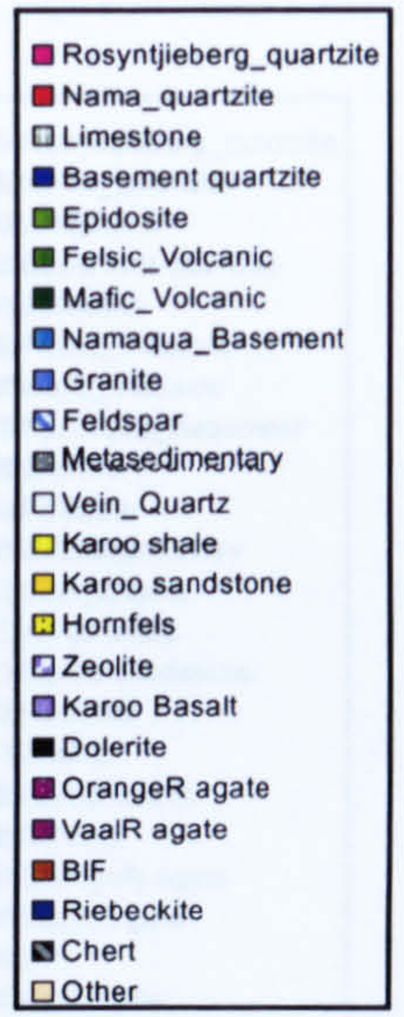

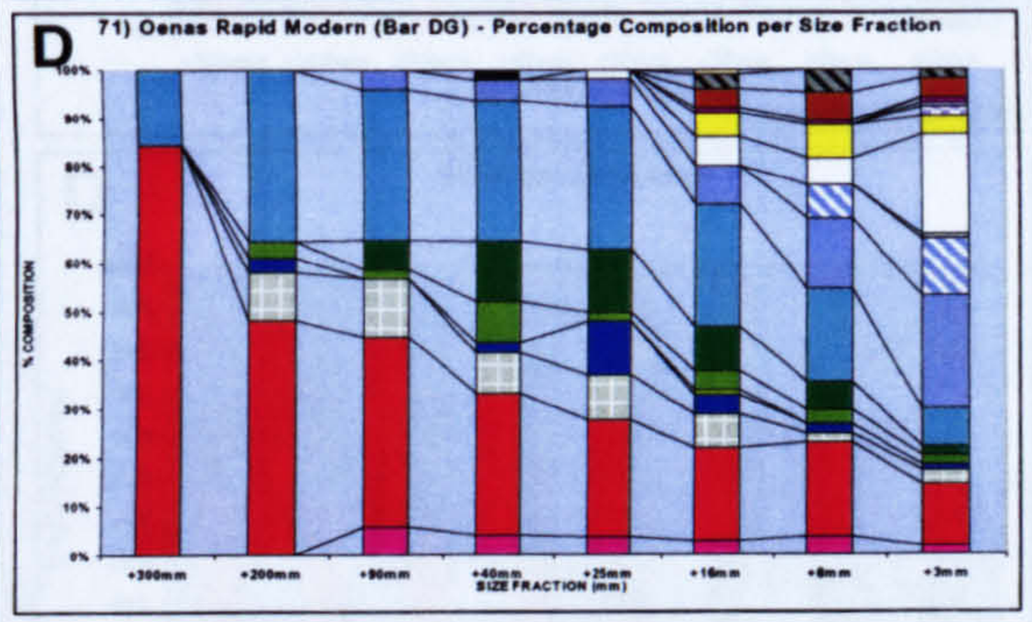

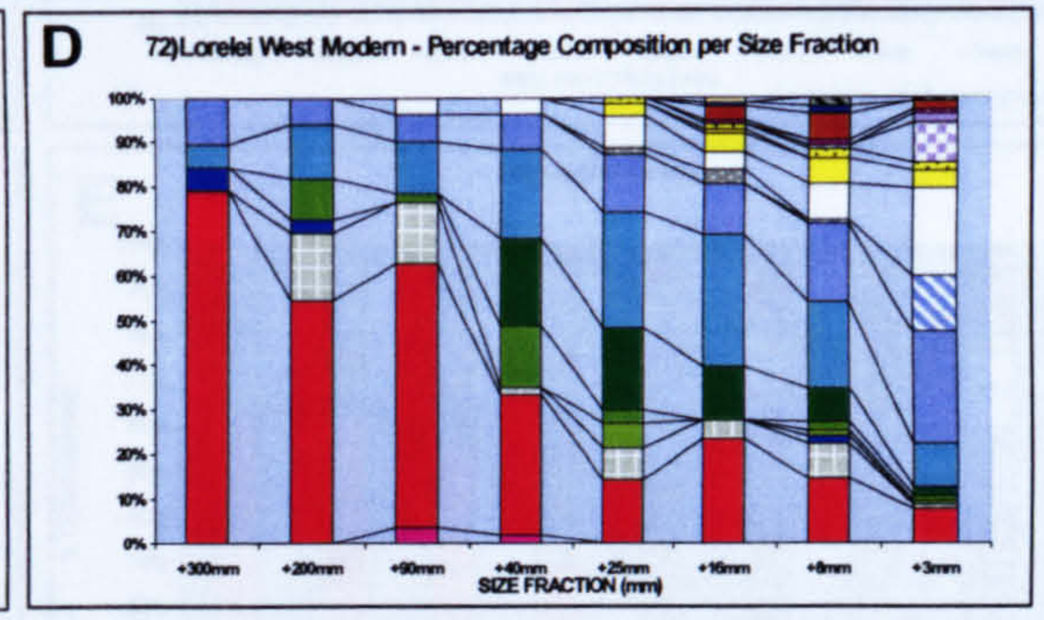

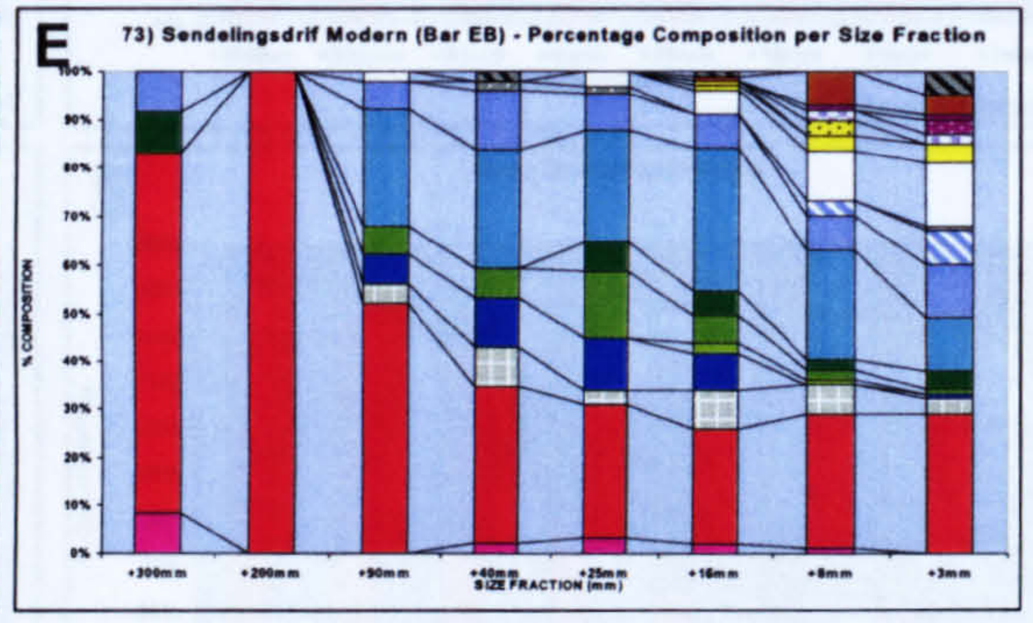

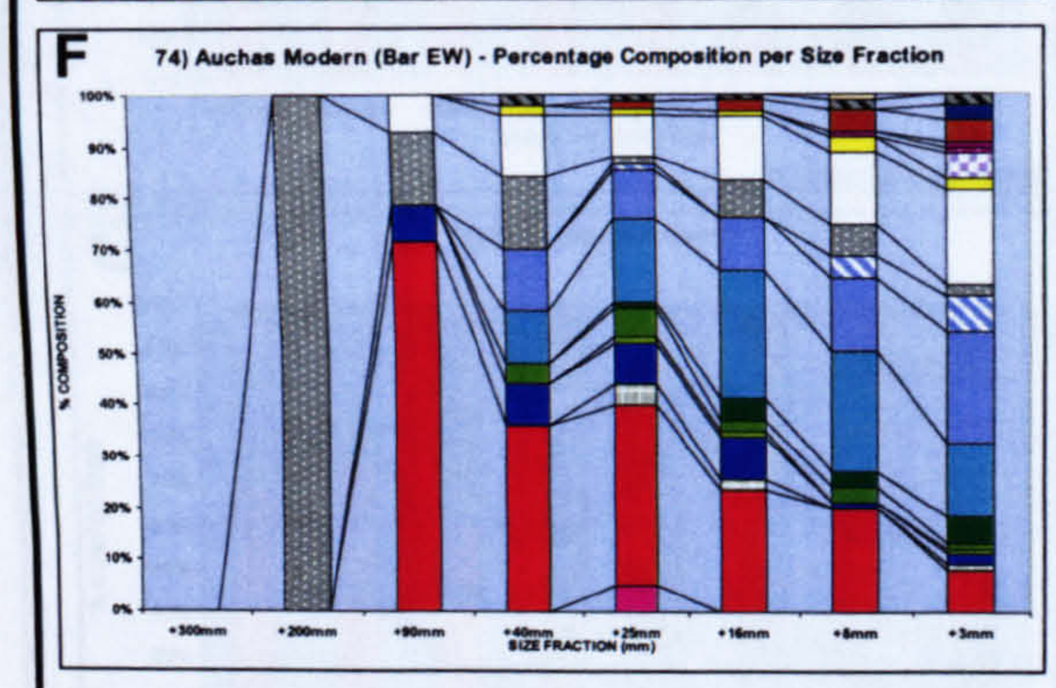

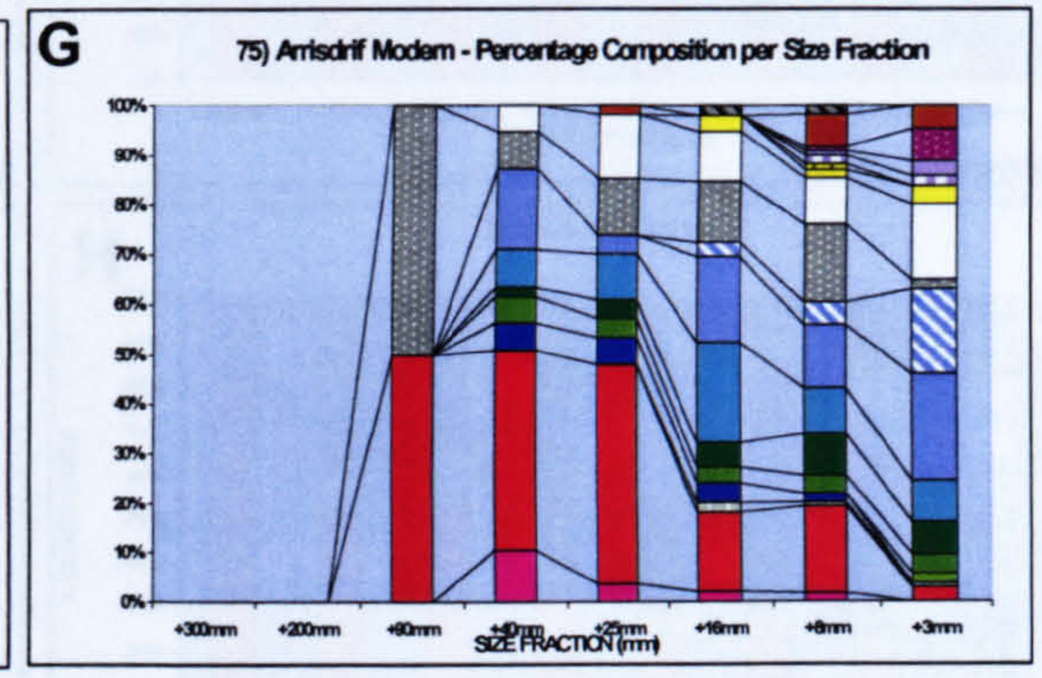

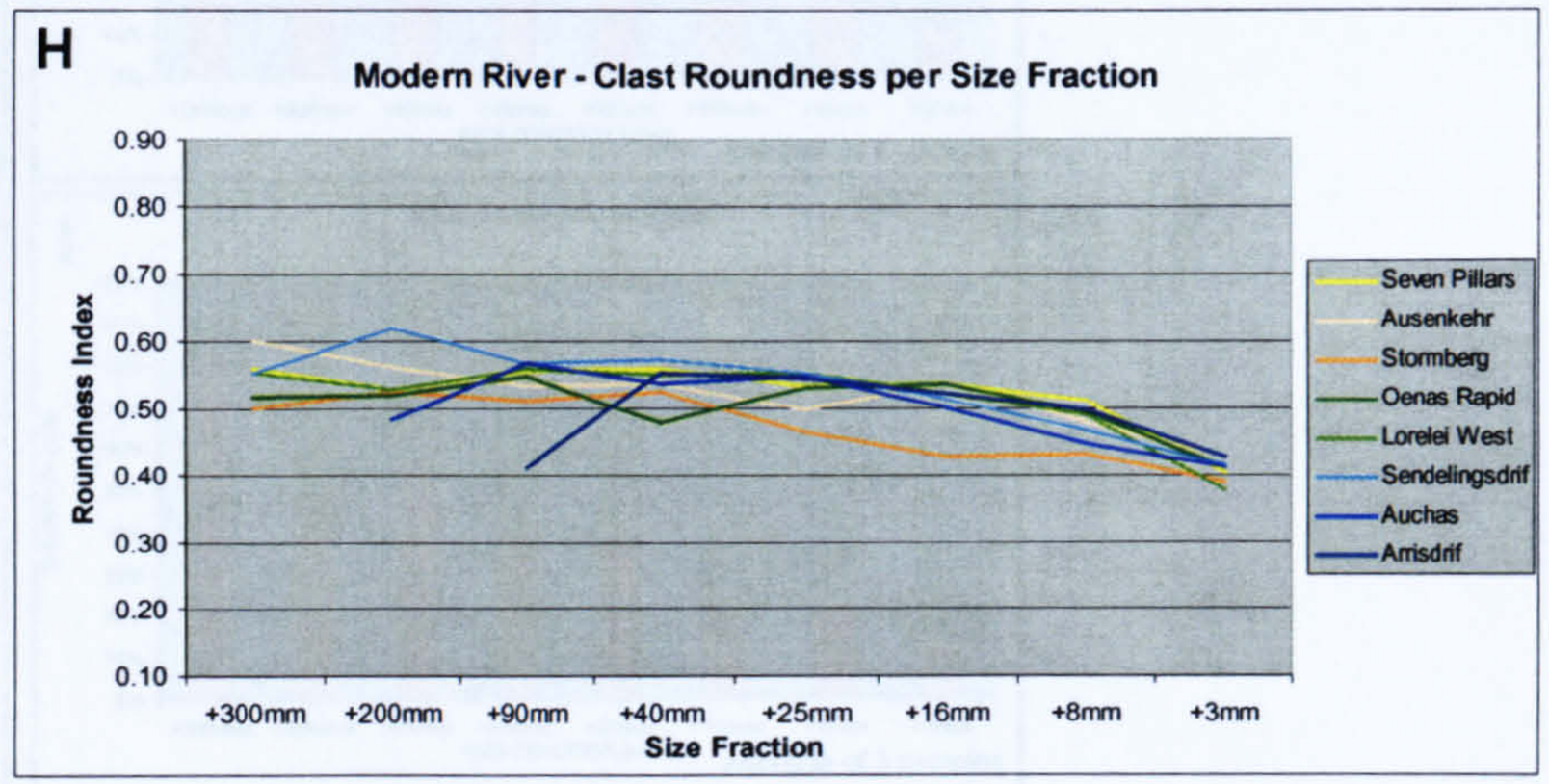

Figure 6.43 Clast assemblage and roundness changes in the Modern deposits.

Upstream Reach

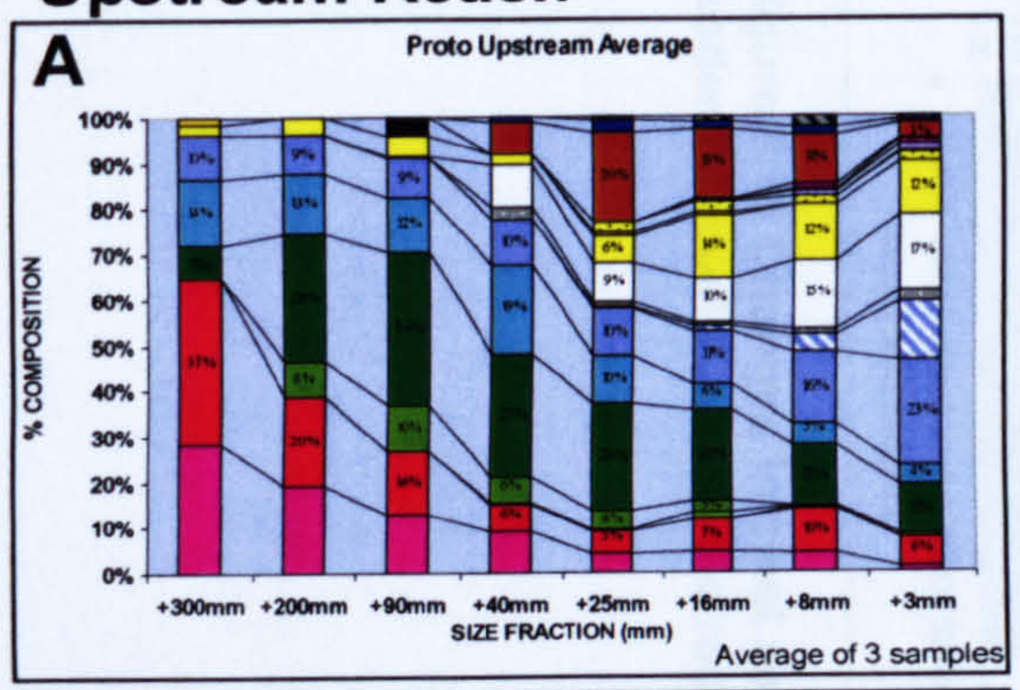

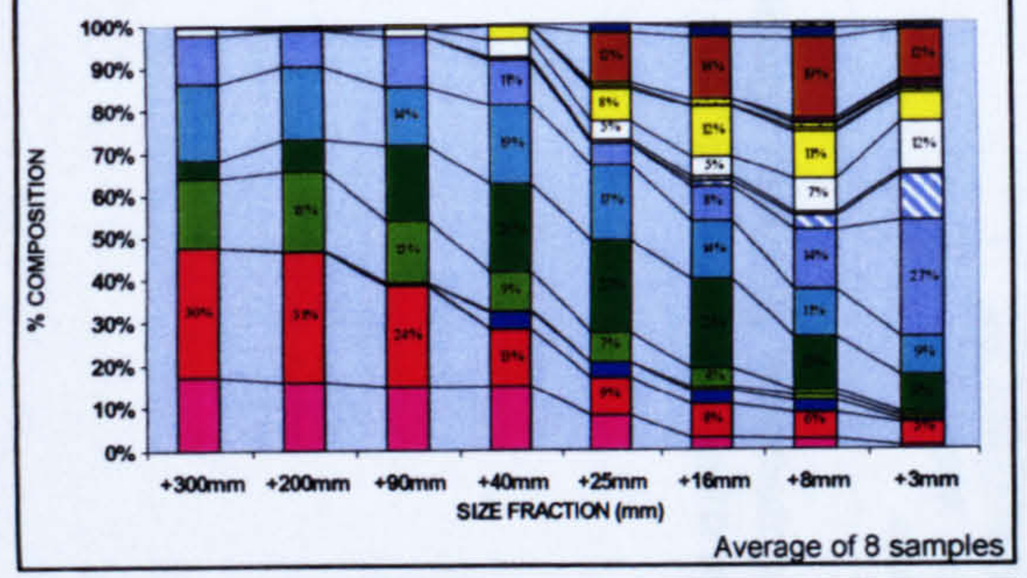

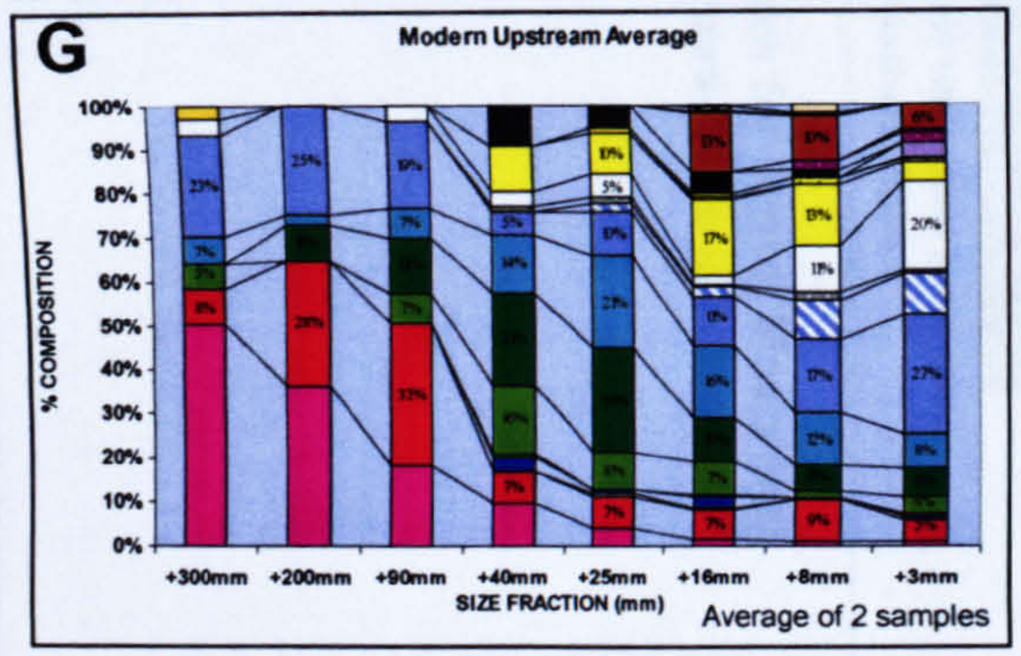

Mid Reach

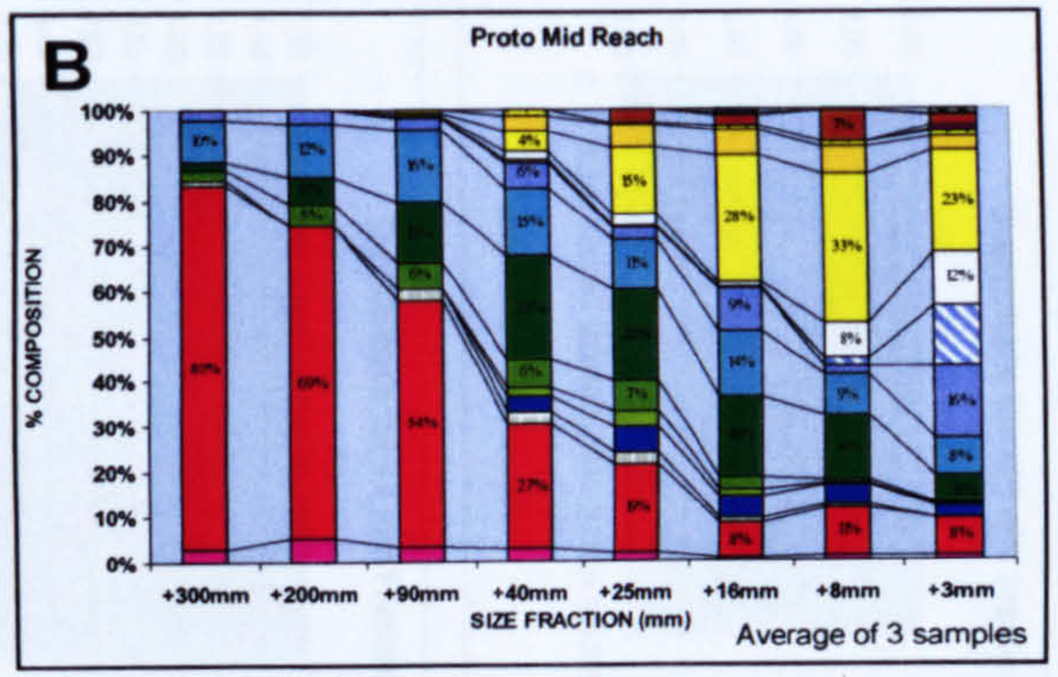

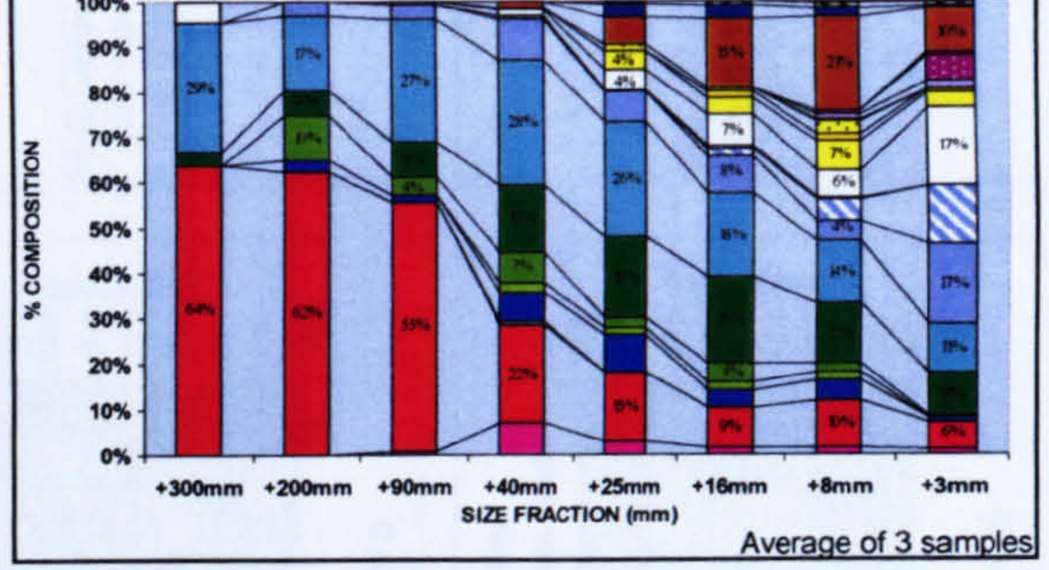

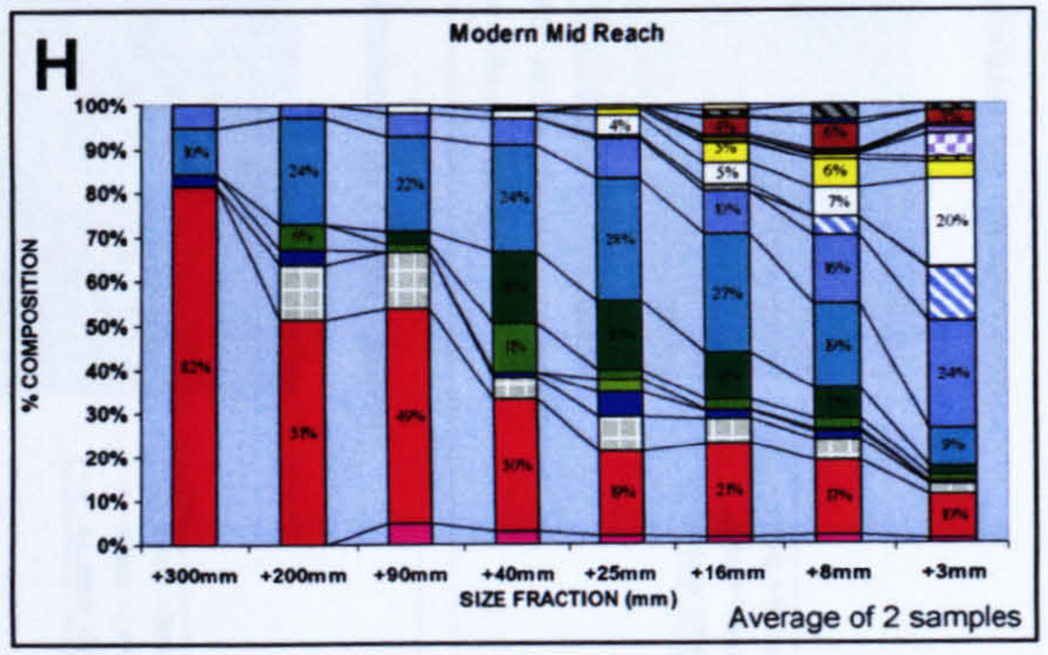

Downstream Reach

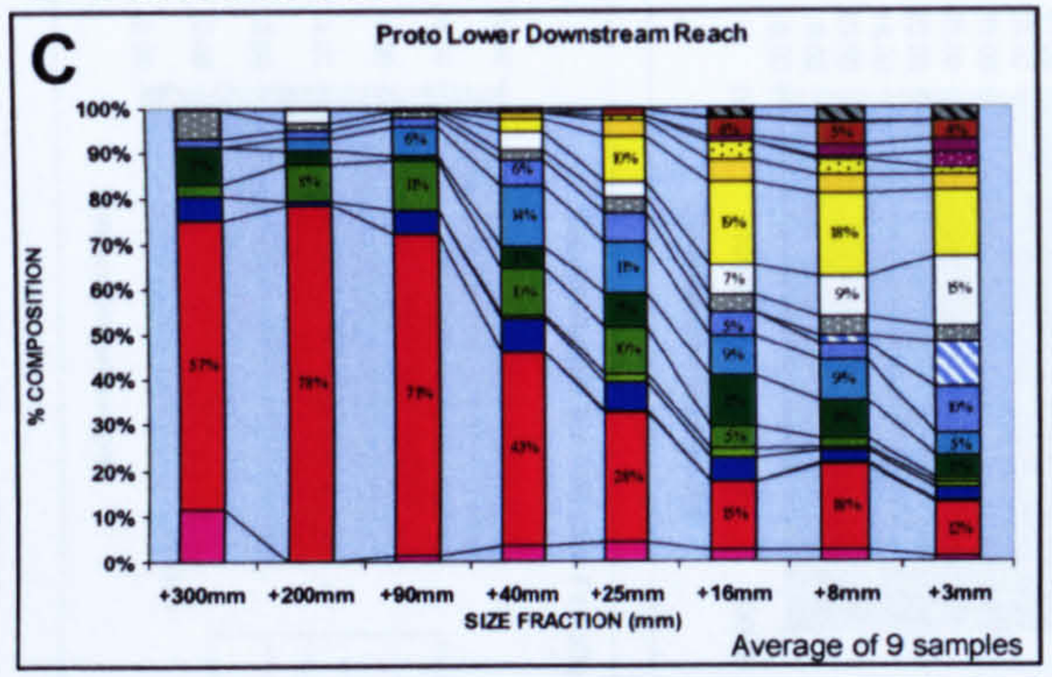

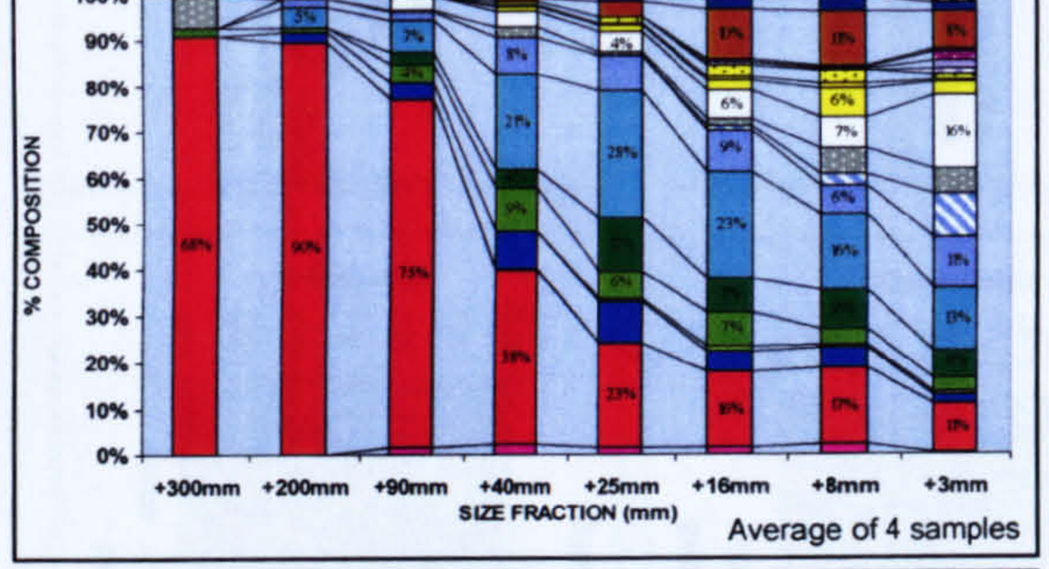

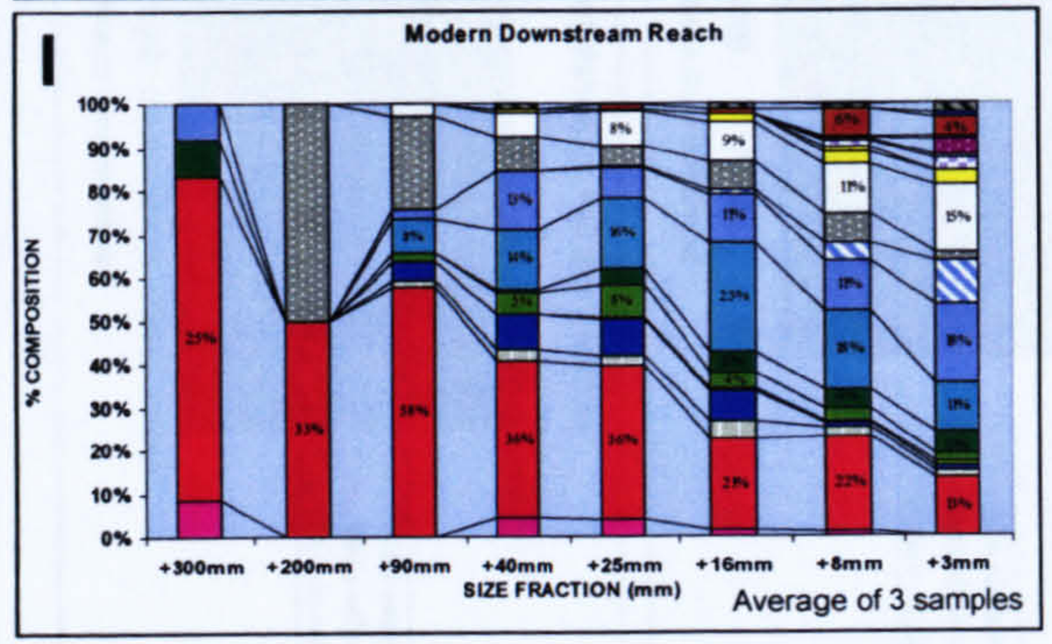

Figure 6.44 Summary of clast assemblage changes per terrace suite within the study area, grouped into upstream, mid and downstream reaches.

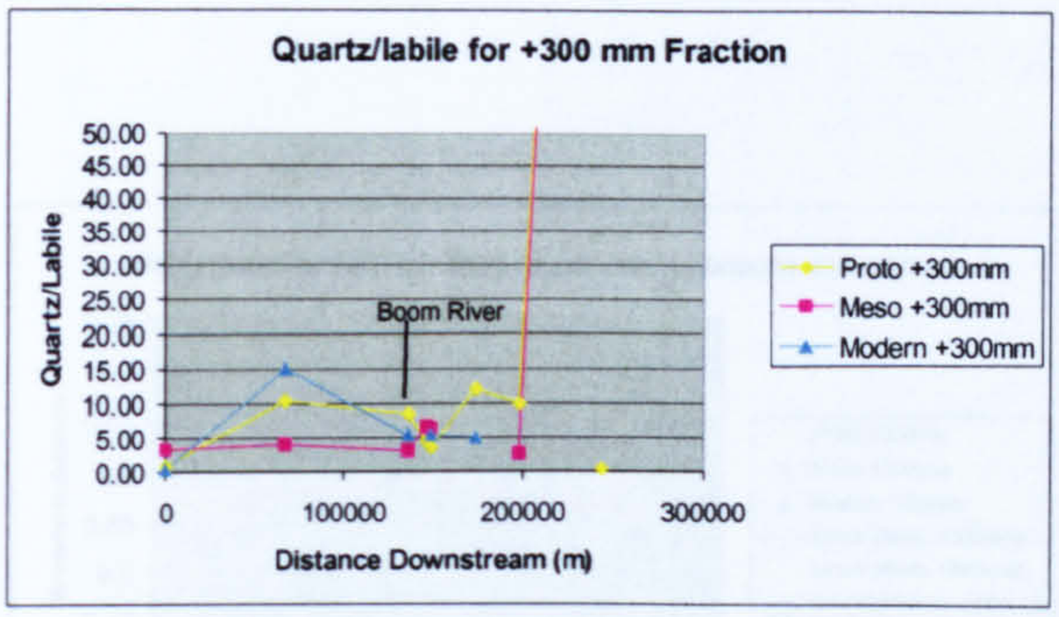

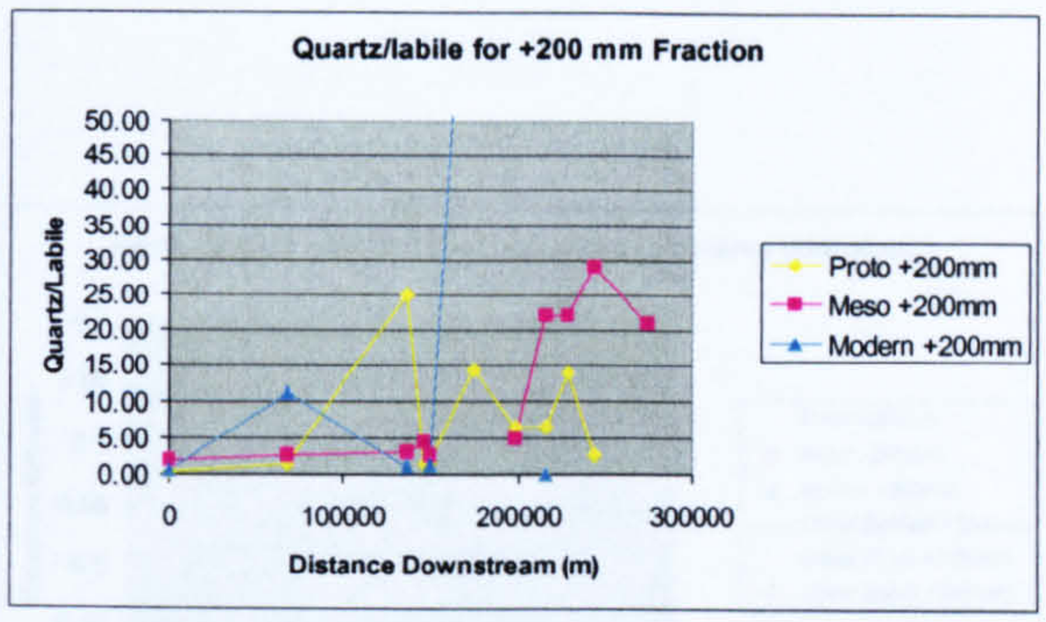

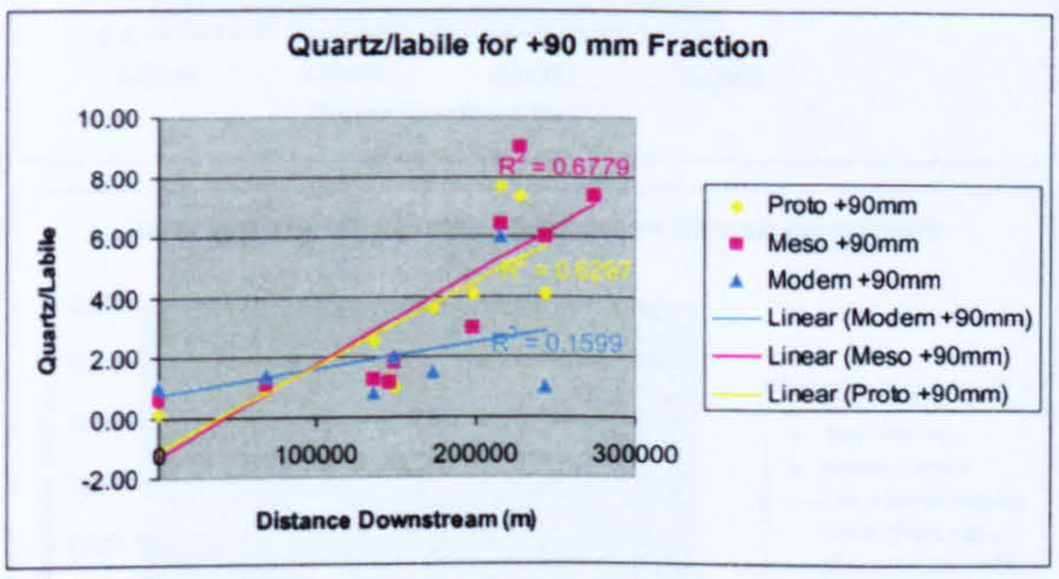

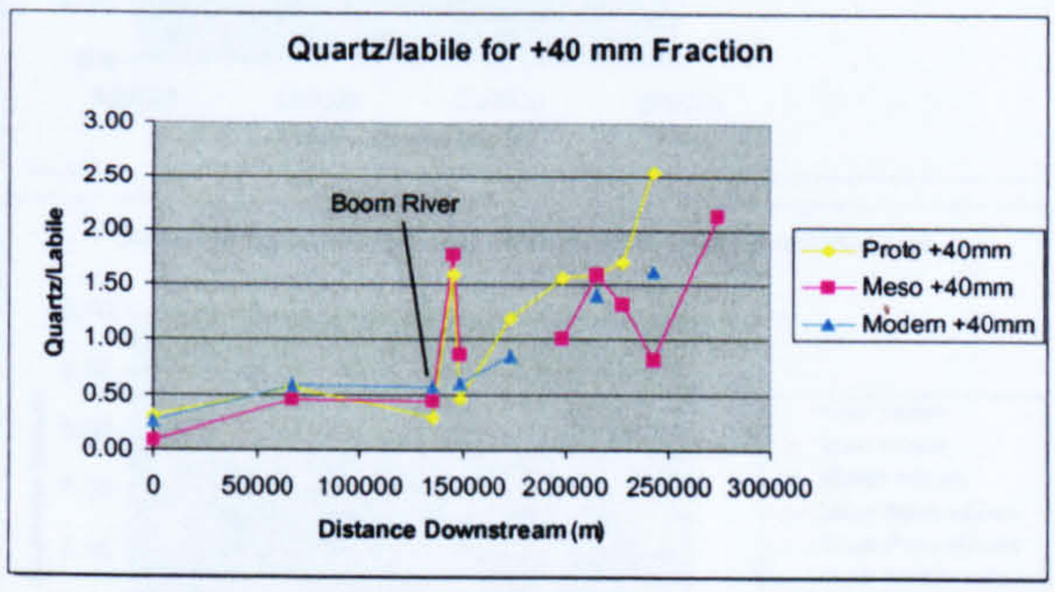

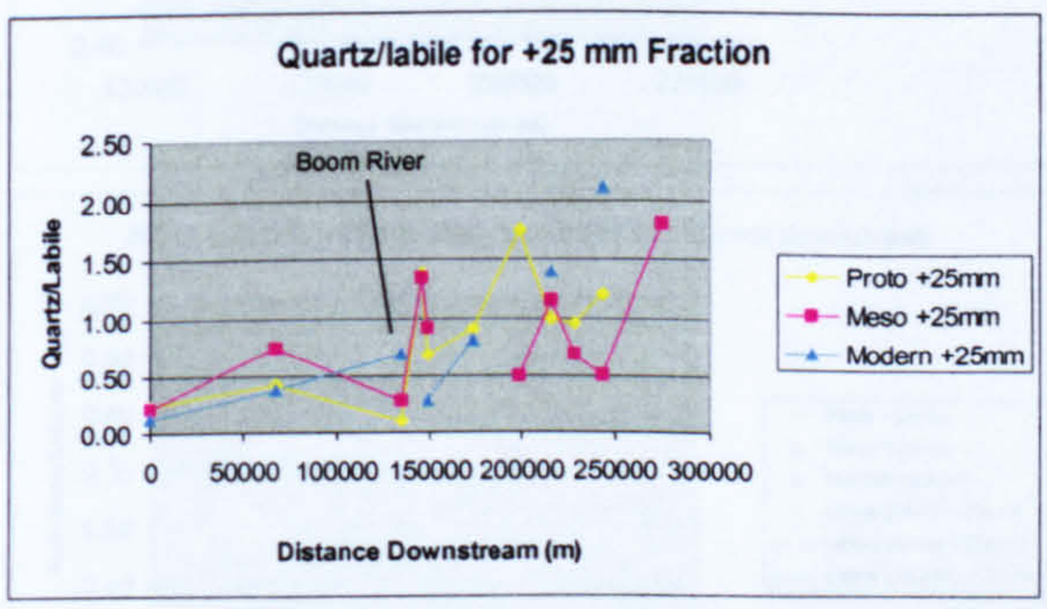

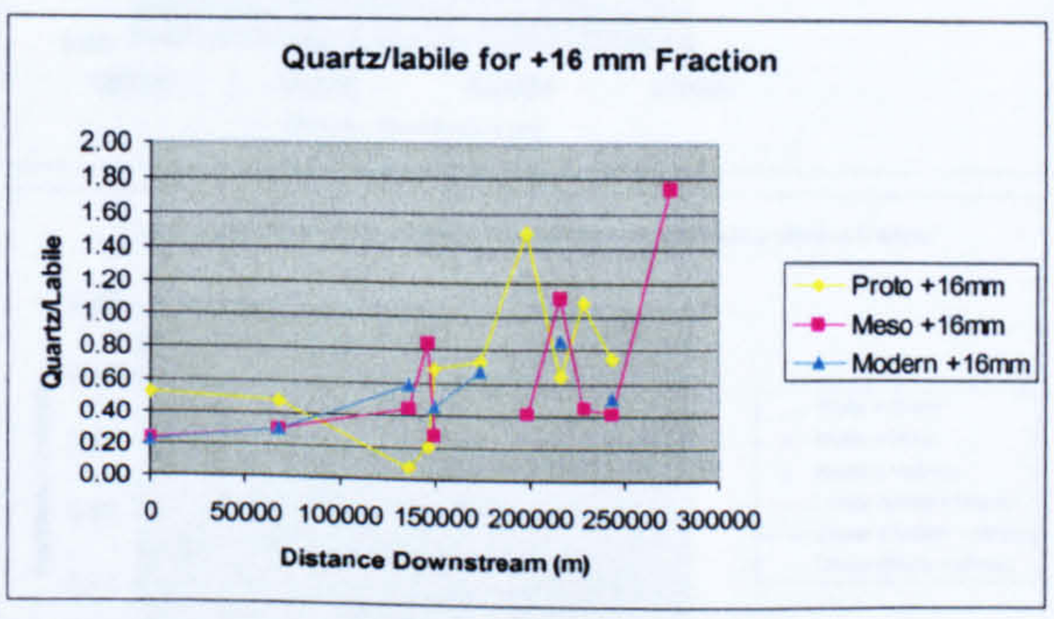

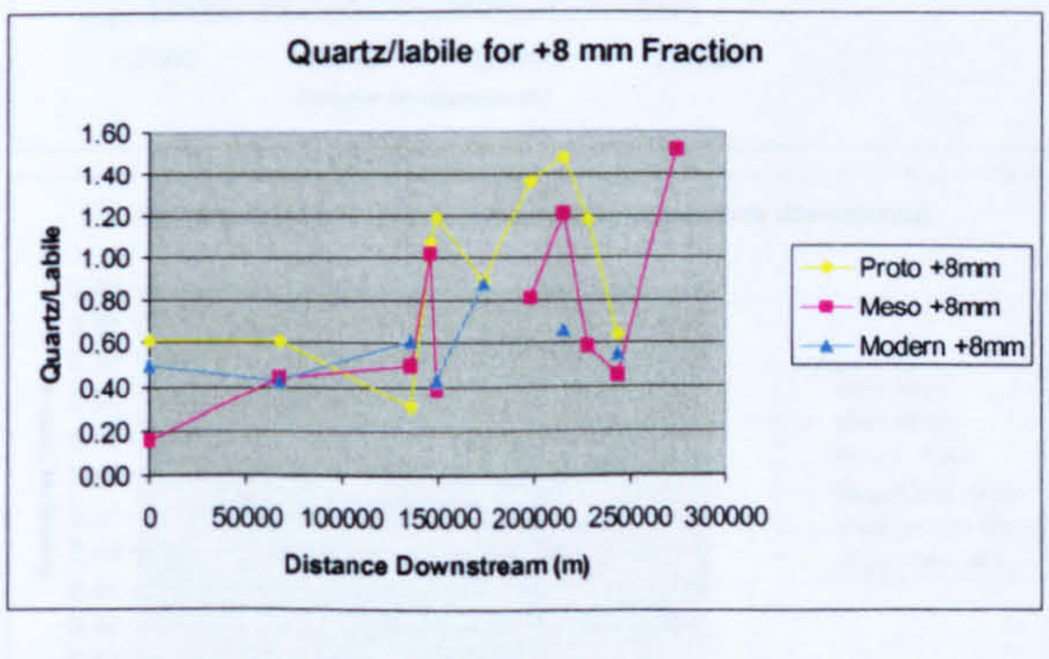

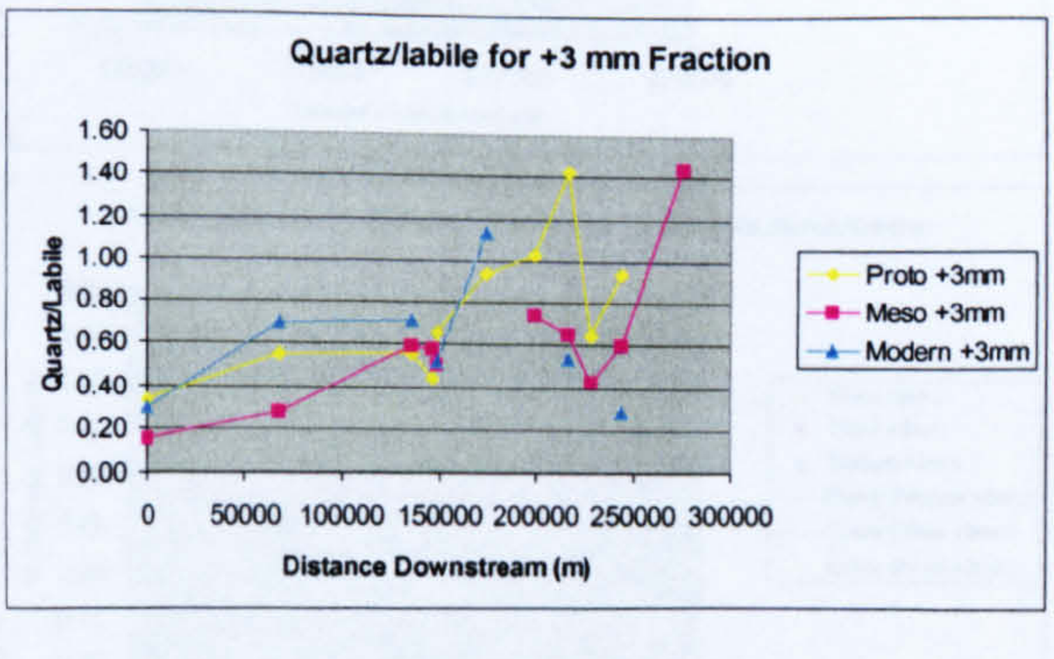

Figure 6.45 Changes in clast assemblage maturity downstream for Proto, Meso and modern deposits, using the ratio of quartzite and quartz to more labile lithologies.

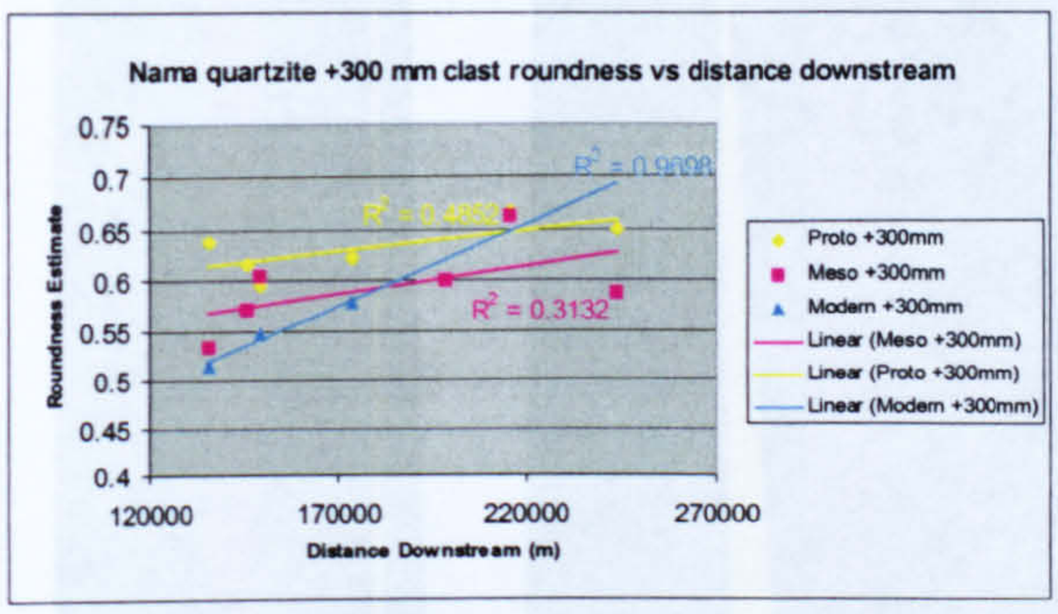

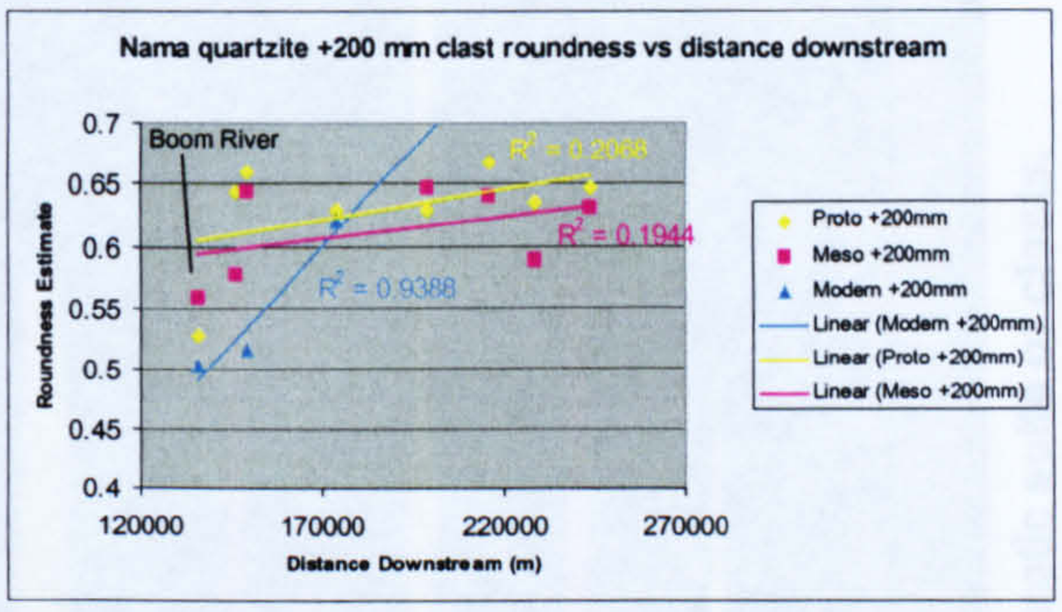

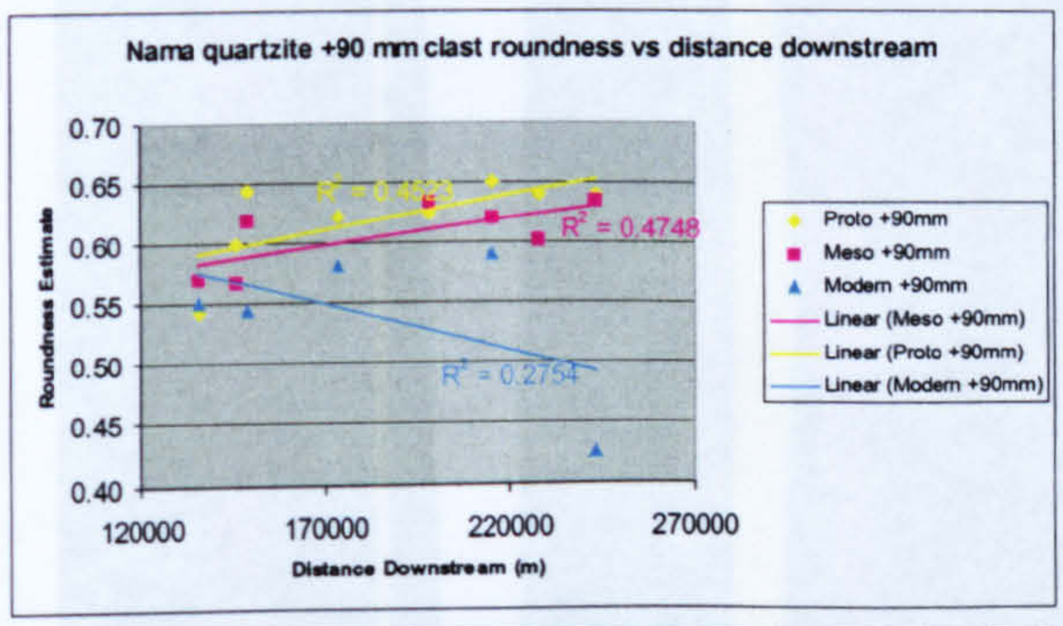

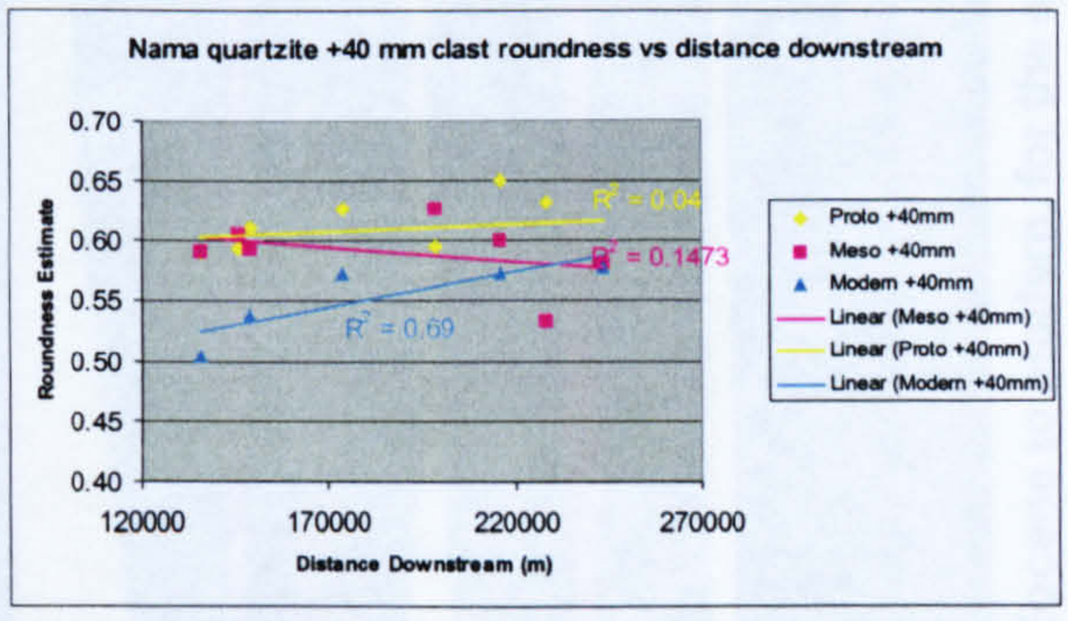

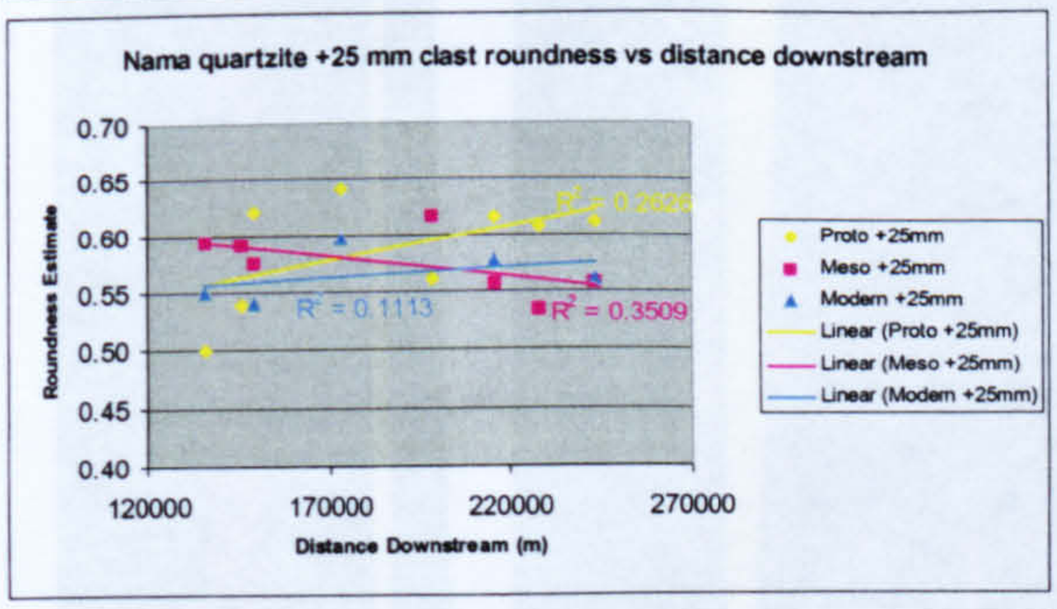

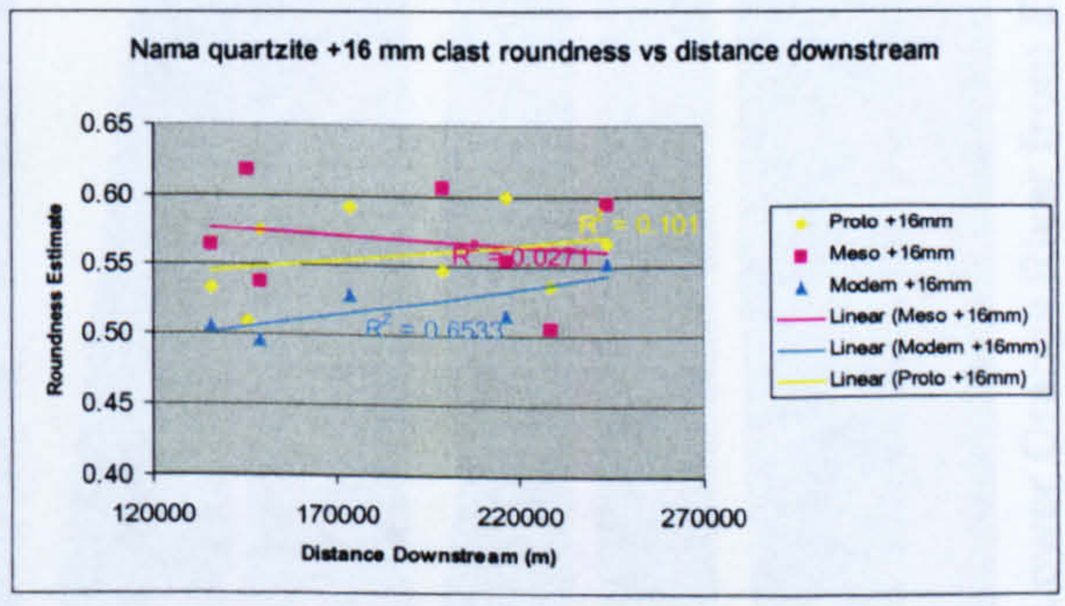

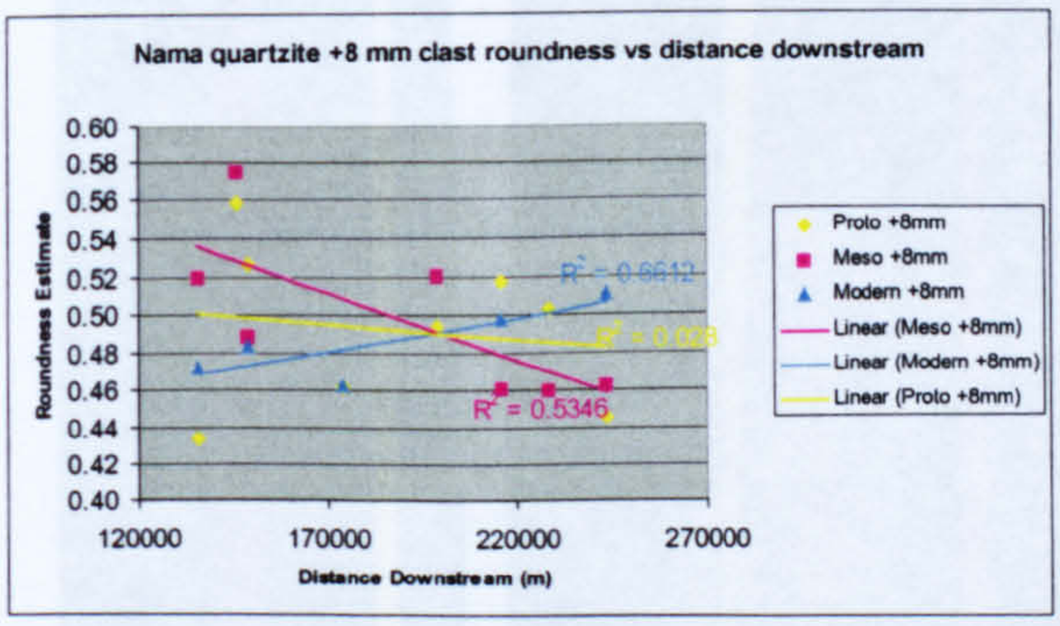

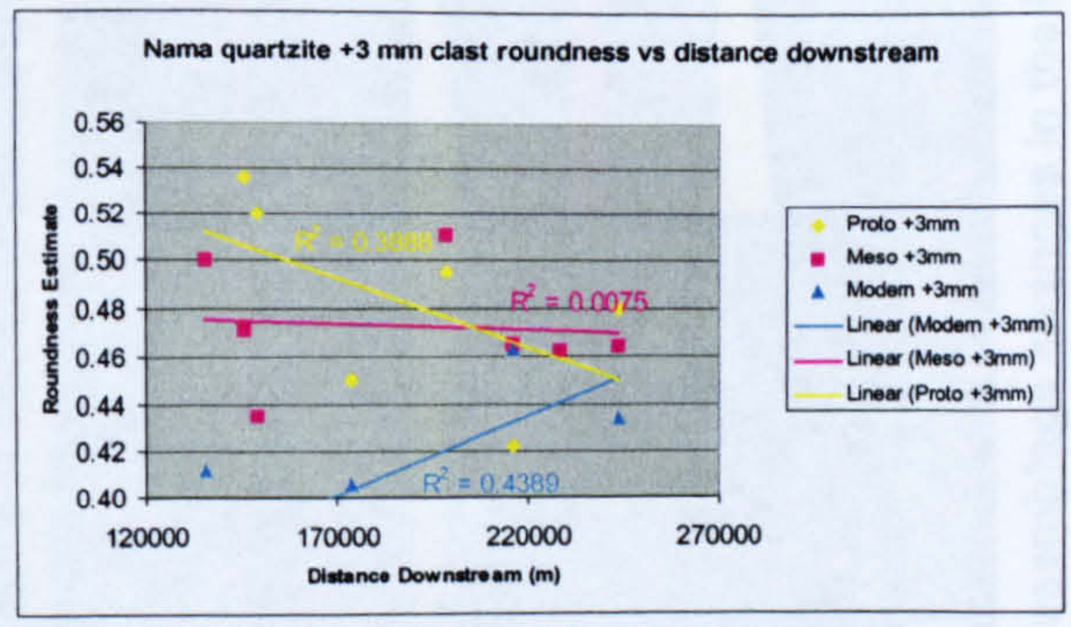

Figure 6.46 Nama quartzite roundness vs distance downstream for Proto, Meso and modern deposits between the Boom River and the mouth.

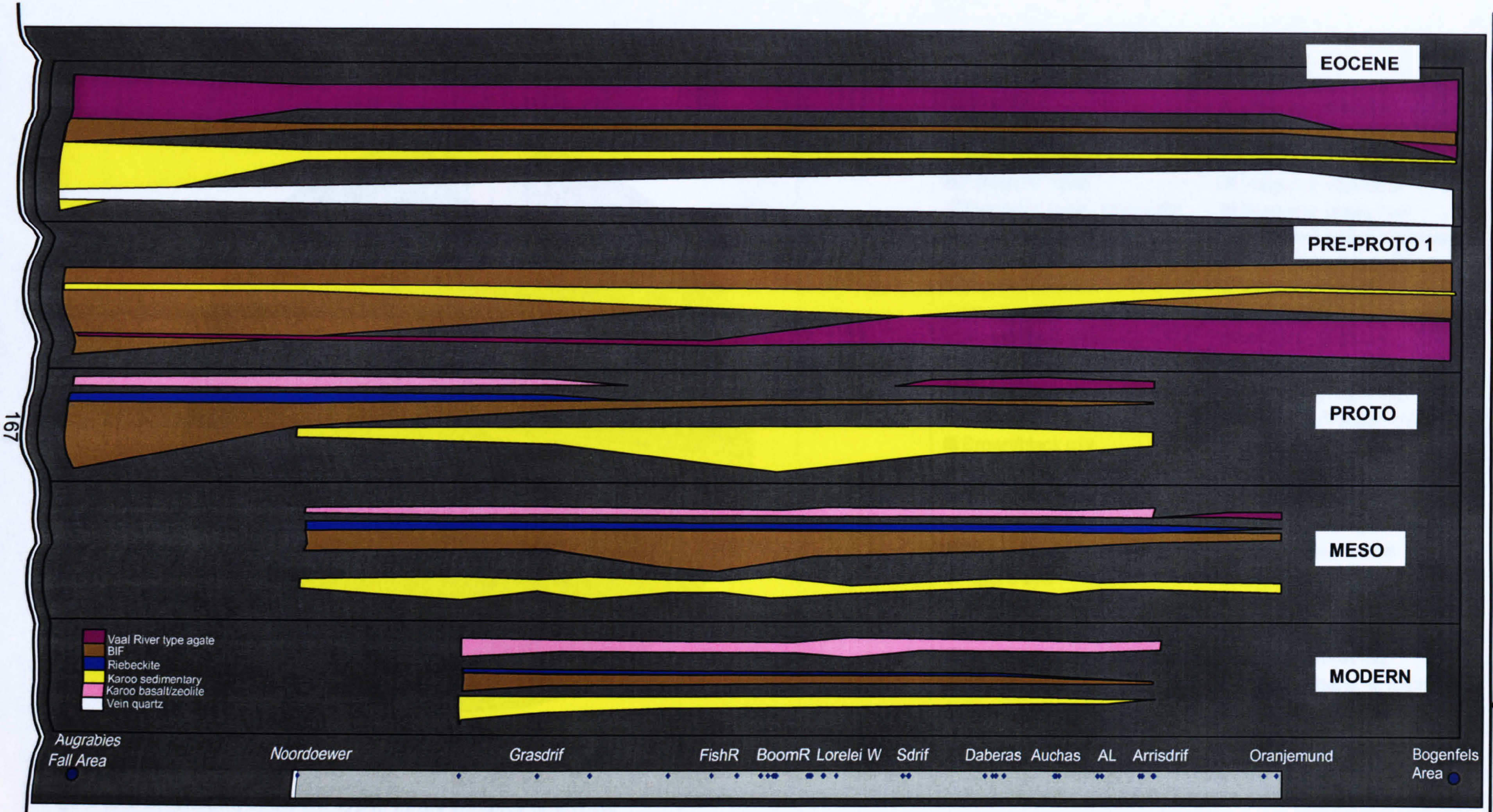

Figure 6.47 Summary of clast asemblage changes in the Lower Orange River from Eocene to modern, for the exotic suite of clasts.

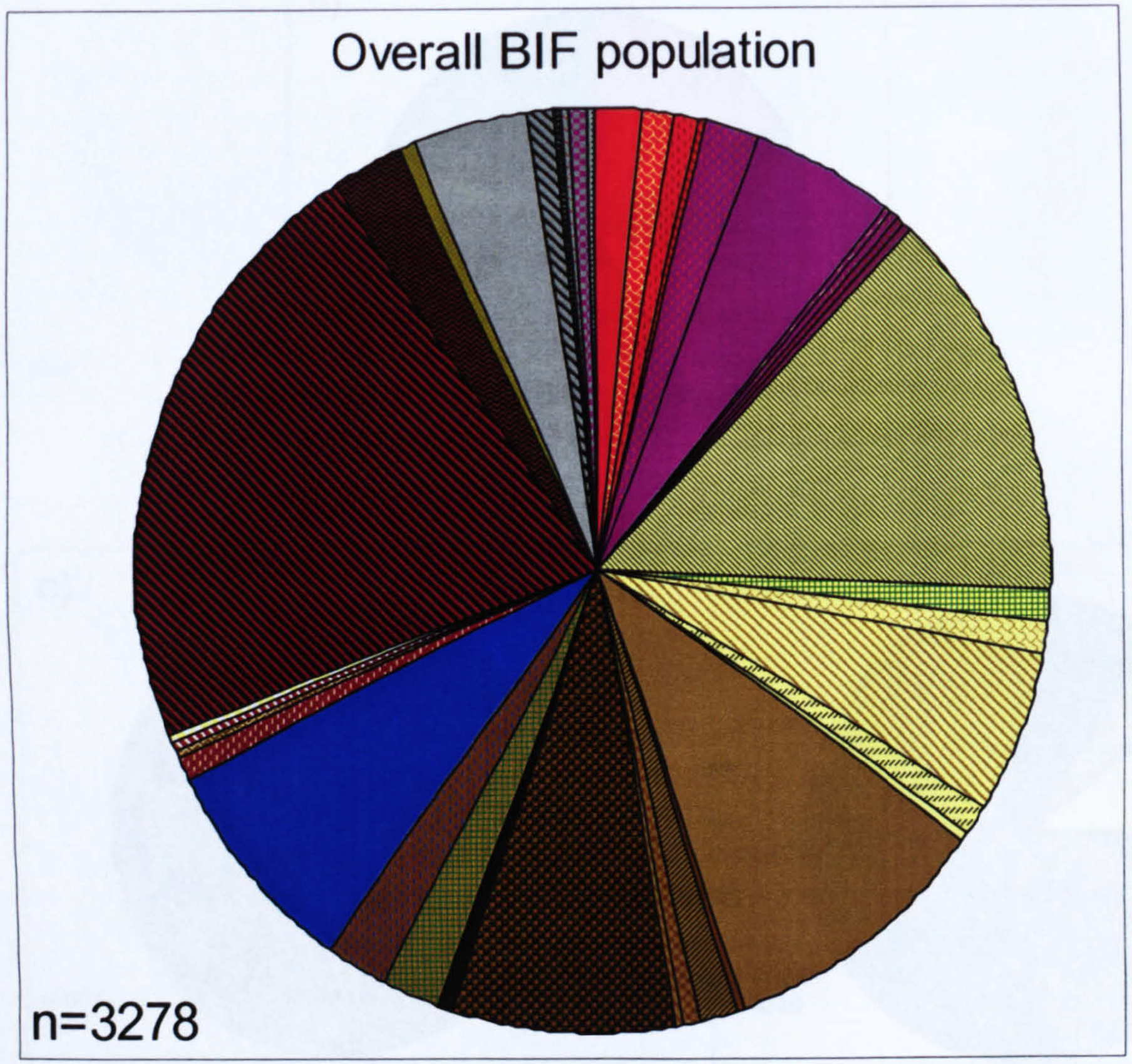

Figure 6.48 Breakdown of the BIF types in the samples analysed.

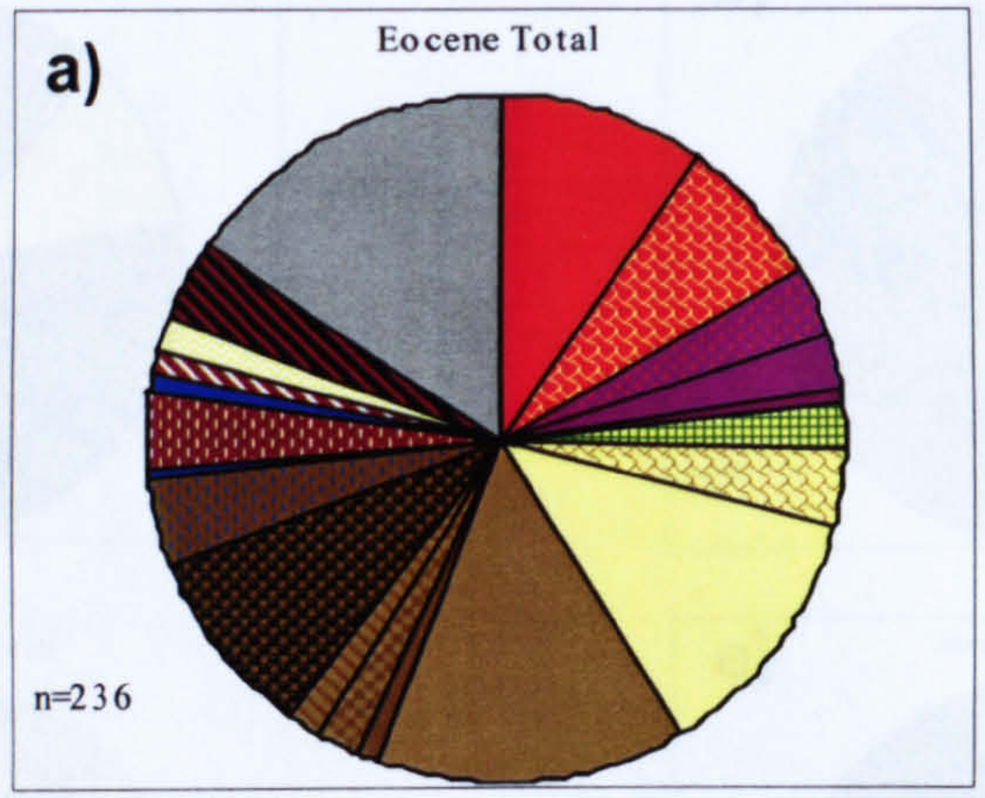

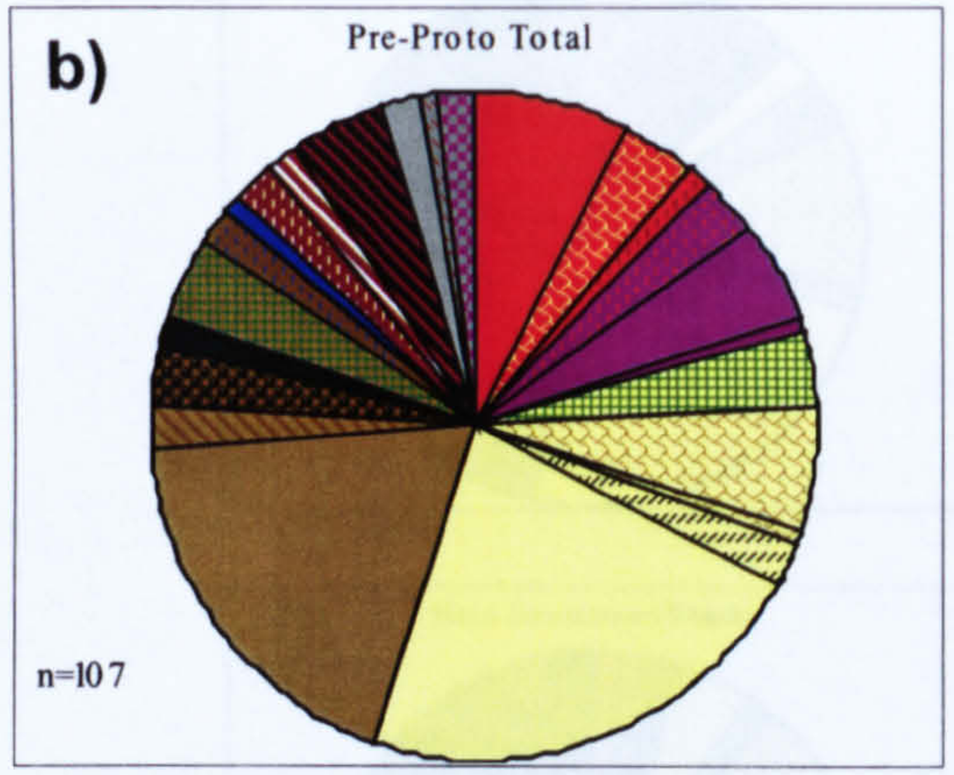

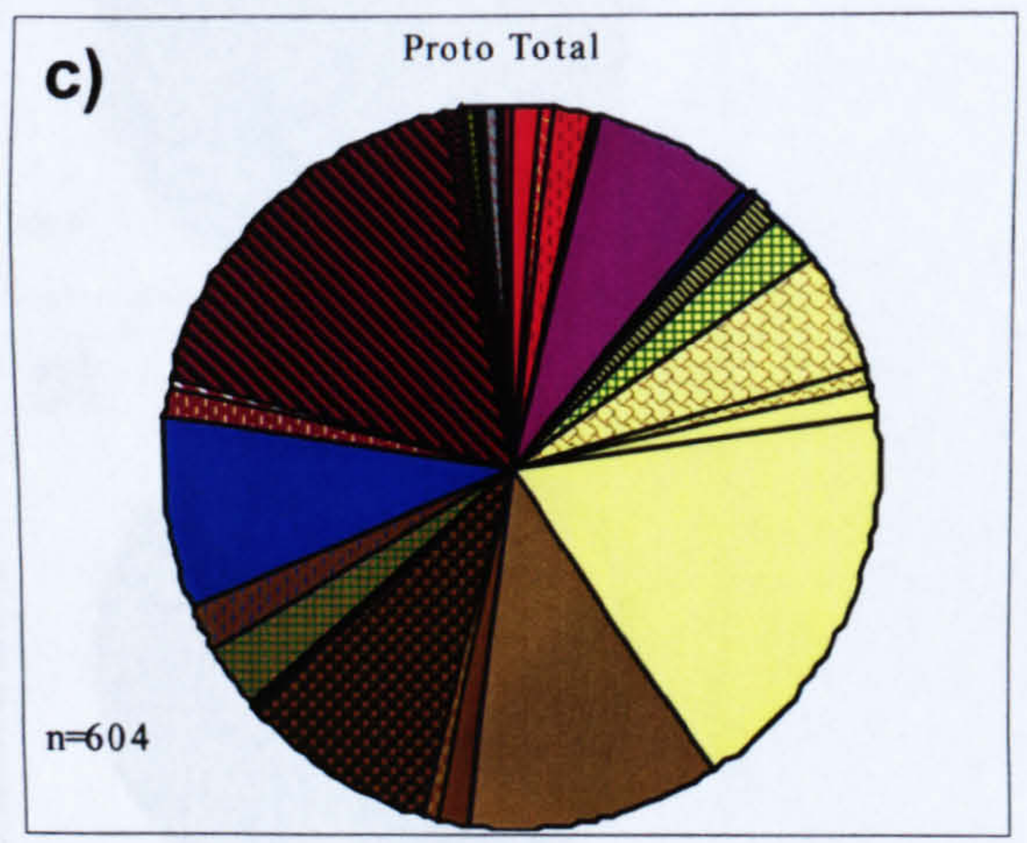

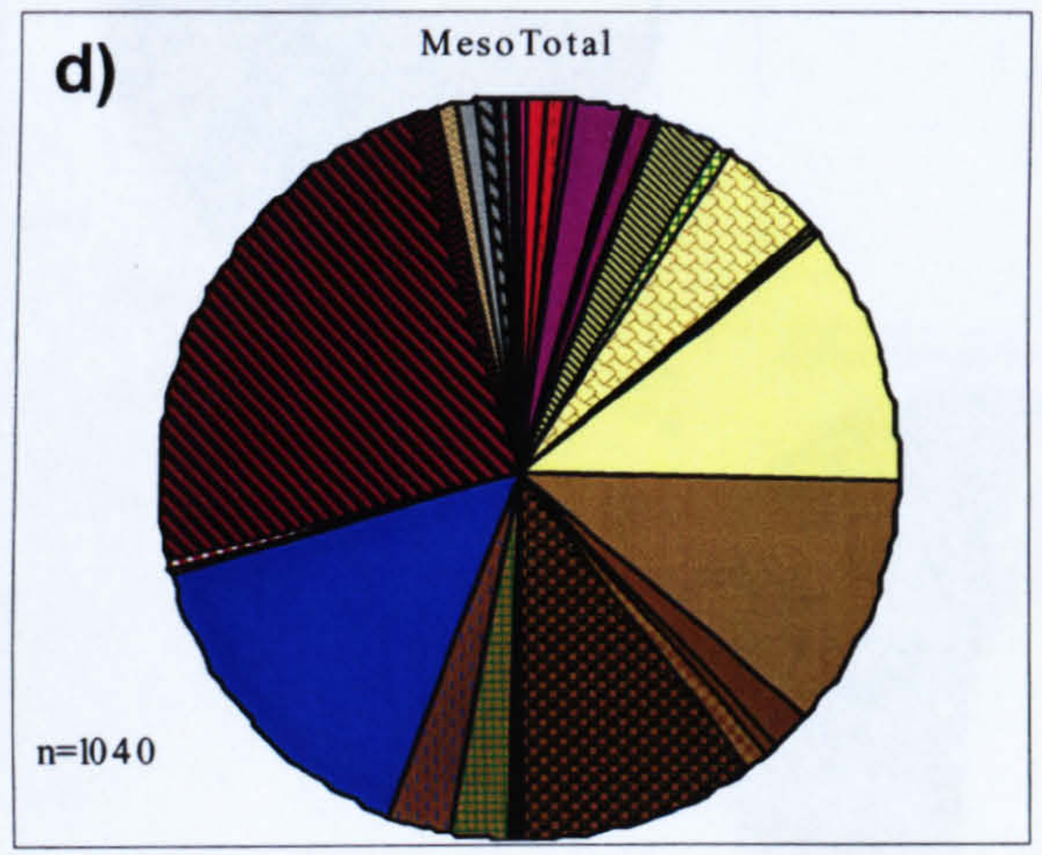

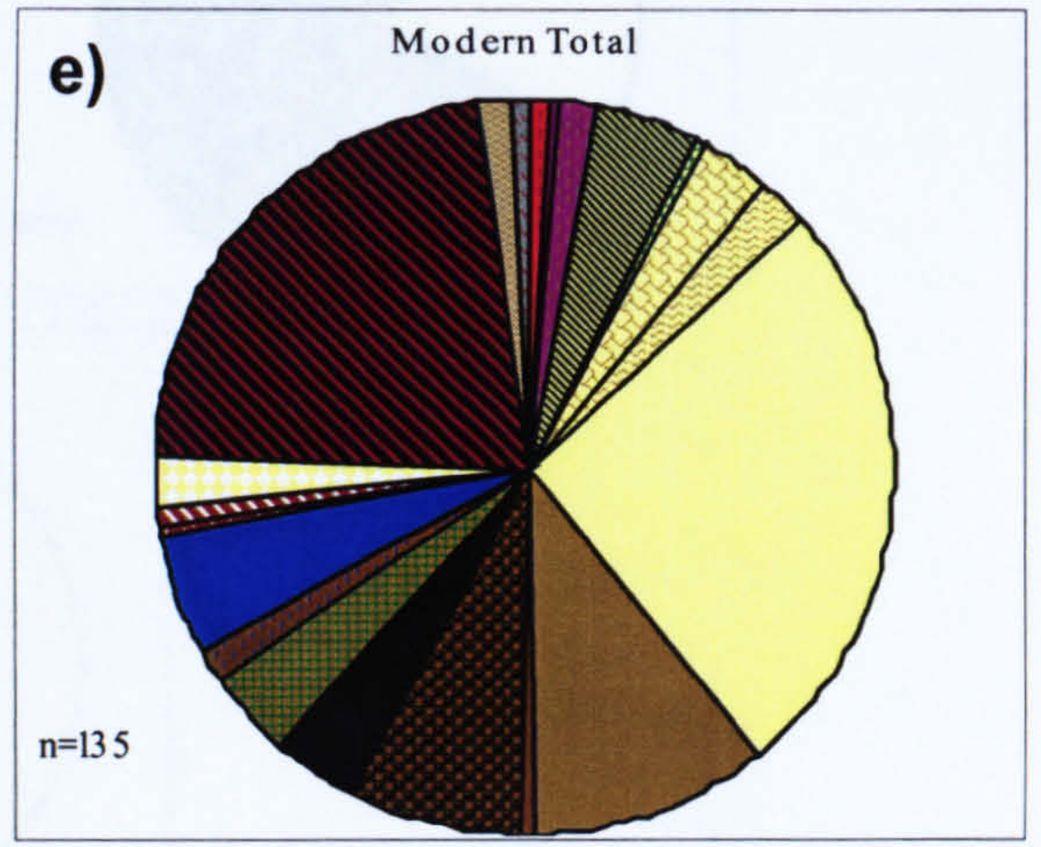

Figure 6.49 Distribution of BIF types in the a) Eocene b) Pre-Proto c) Proto d) Meso and e) Modern samples (legend is in figure 6.48).

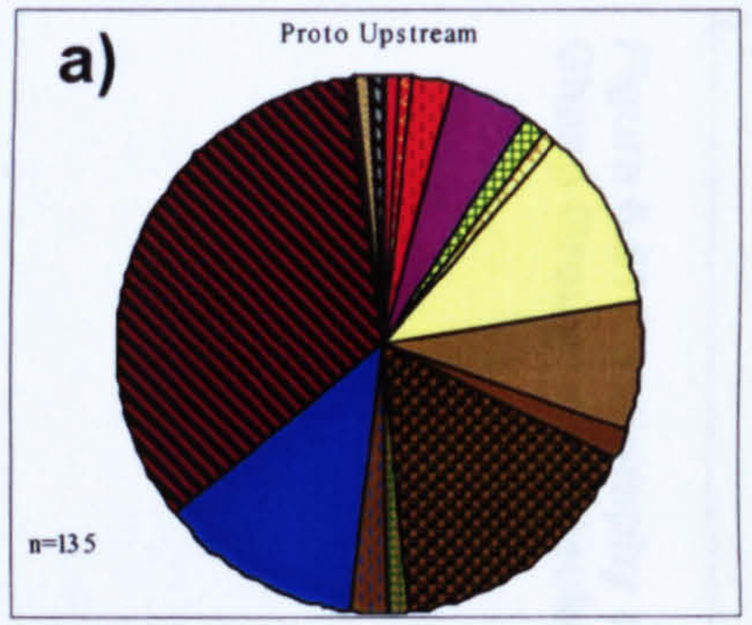

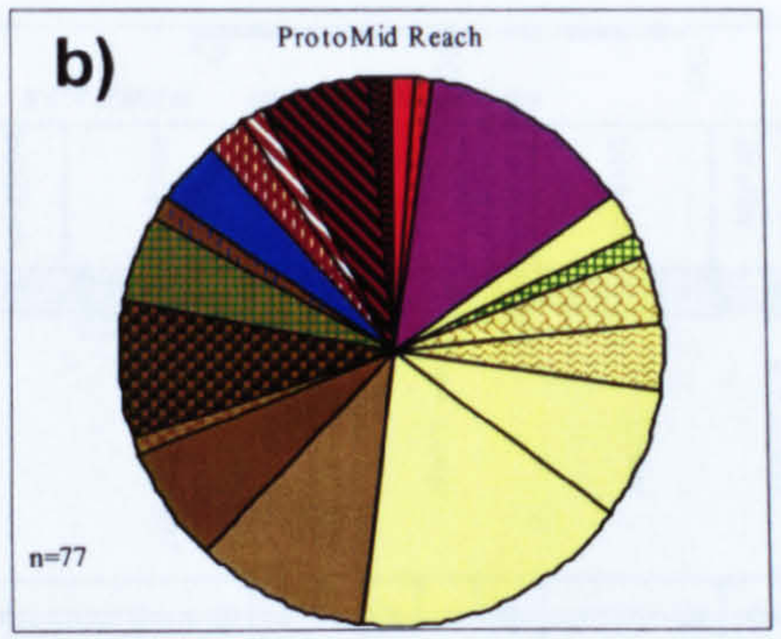

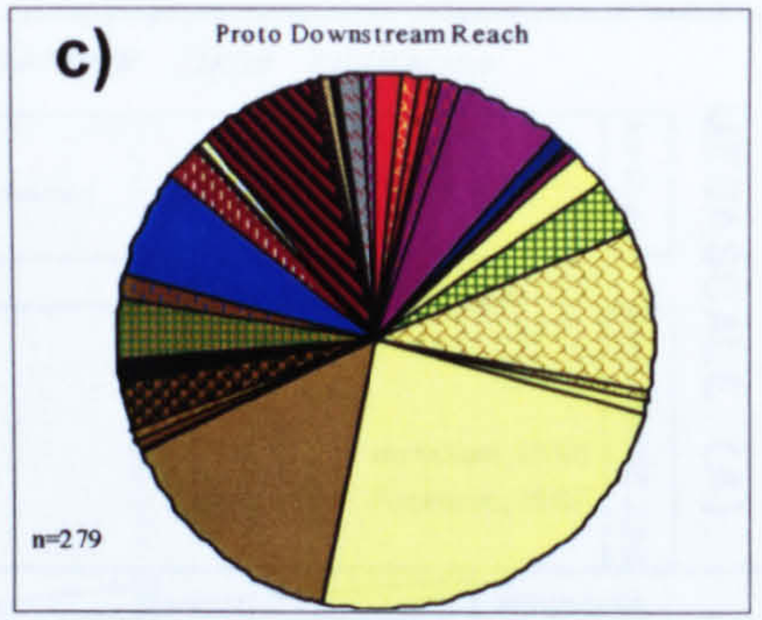

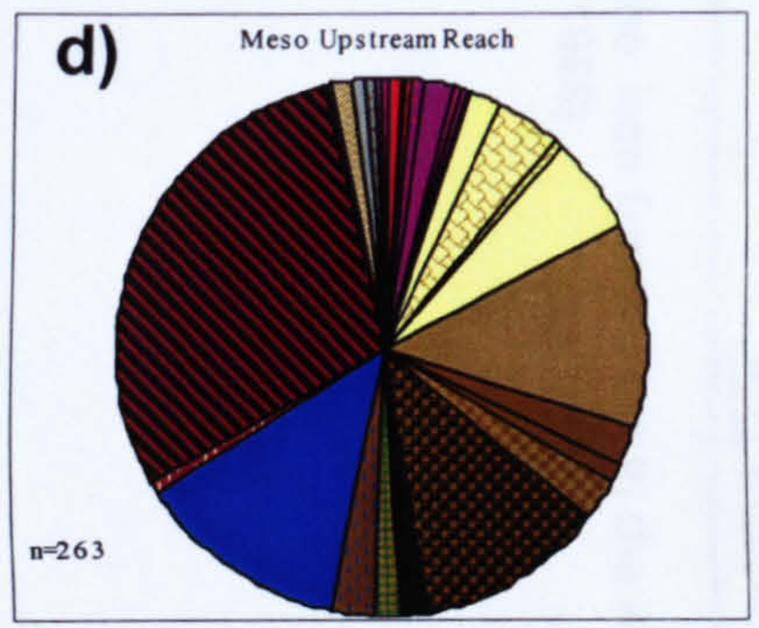

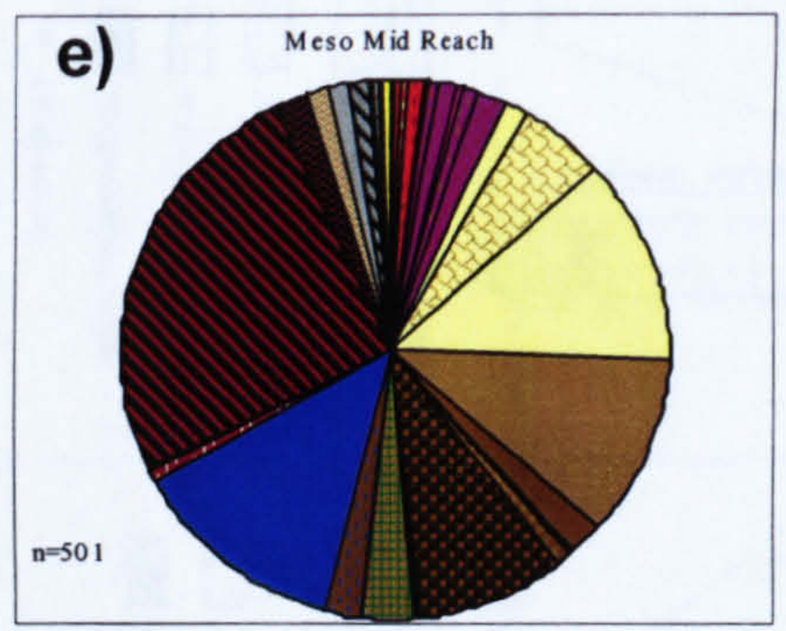

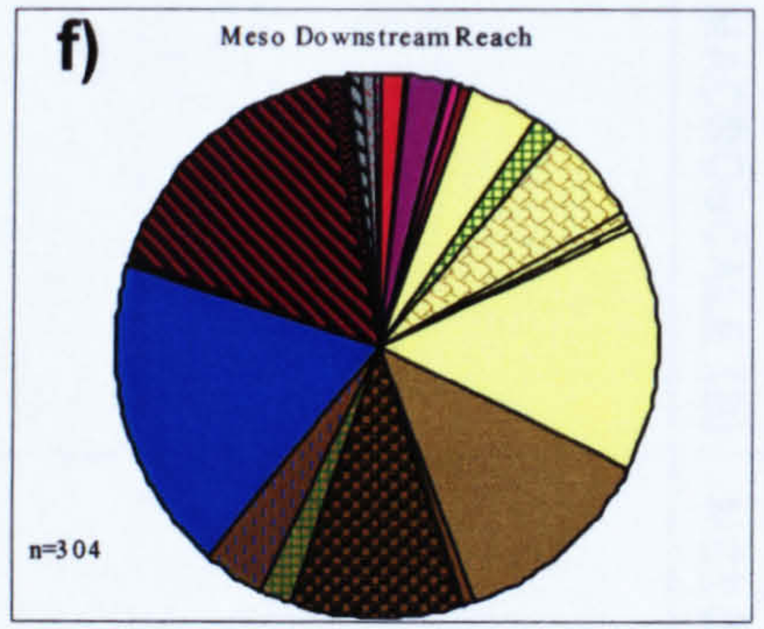

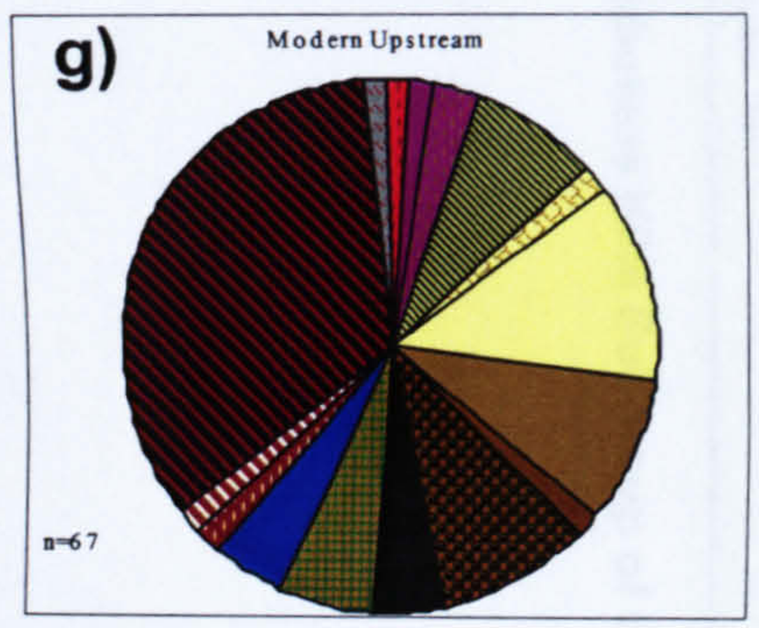

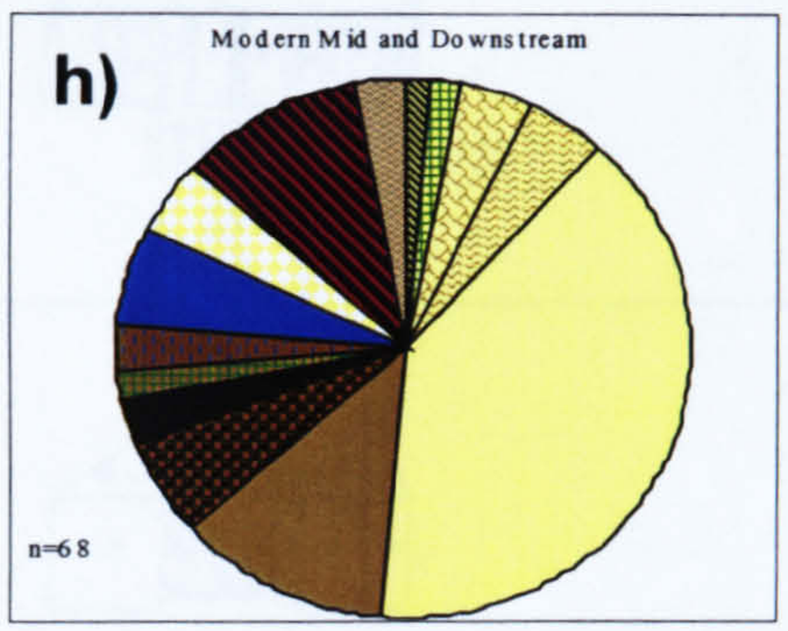

Figure 6.50 Downstream changes in the BIF assemblages of the Proto, Meso and modern deposits within the study reach (legend is in figure 6.48).

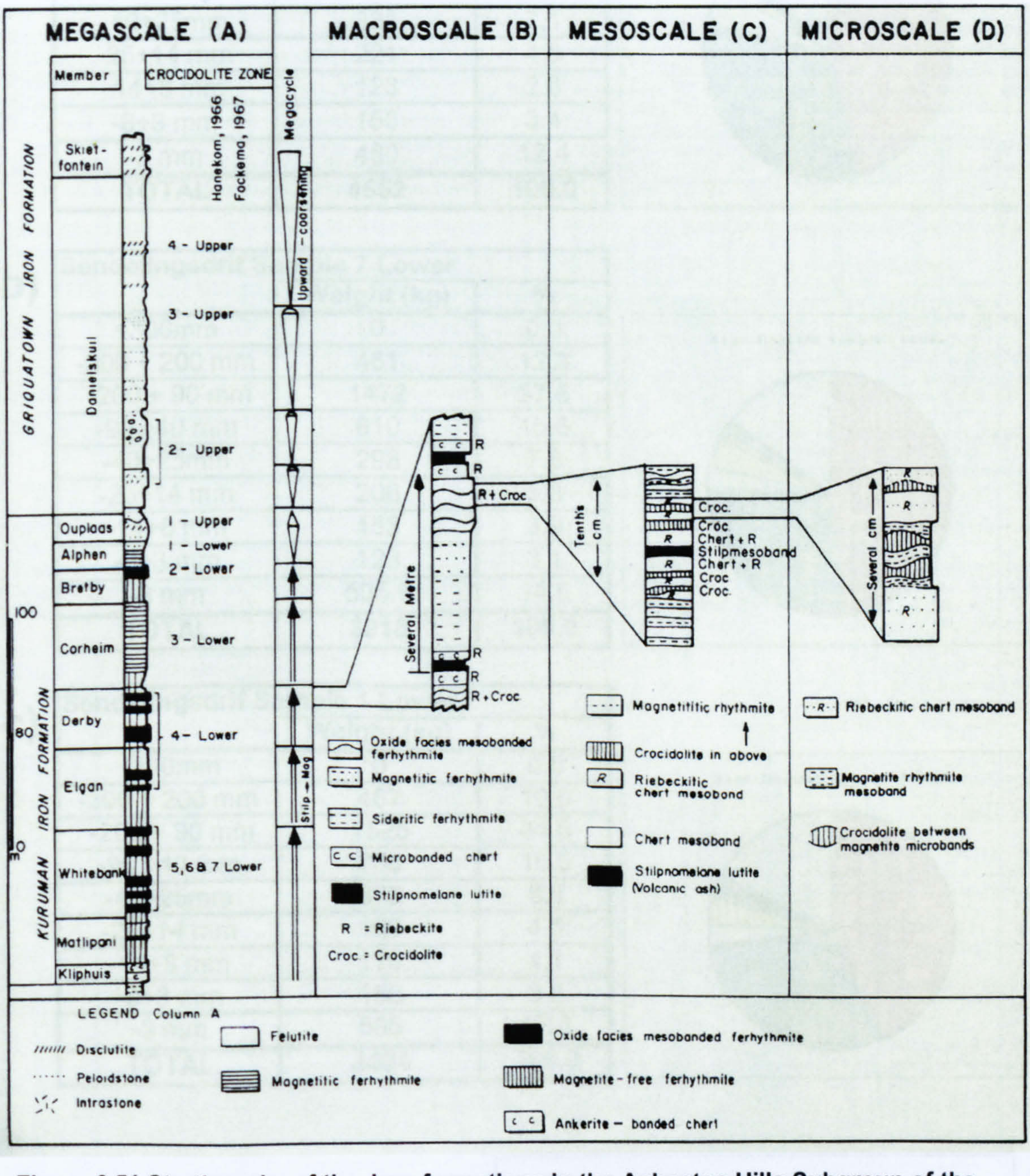

Figure 6.51 Stratigraphy of the iron formations in the Asbestos Hills Subgroup of the Ghaap Group (after Beukes 1986).

a)

Sendelingsdrif Sample 5 Lower		
	Weight (kg)	**%**
+300mm	0	0.0
-300 + 200 mm	389	8.4
-200 + 90 mm	2115	45.5
-90 +40 mm	741	15.9
-40+25mm	331	7.1
-25+14 mm	221	4.8
-14+8 mm	123	2.6
-8+3 mm	156	3.4
-3 mm	480	12.4
TOTAL	**4652**	**100.0**

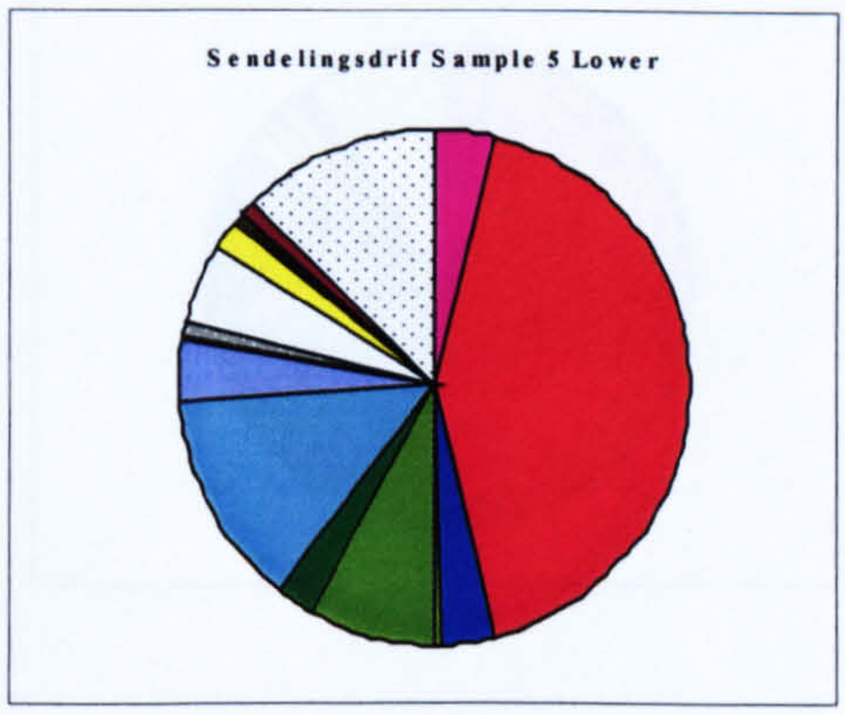

b)

Sendelingsdrif Sample 7 Lower		
	Weight (kg)	**%**
+300mm	0	0.0
-300 + 200 mm	481	12.3
-200 + 90 mm	1472	37.6
-90 +40 mm	610	15.6
-40+25mm	298	7.6
-25+14 mm	208	5.3
-14+8 mm	153	3.9
-8+3 mm	123	3.1
-3 mm	505.6	14.6
TOTAL	**3918**	**100.0**

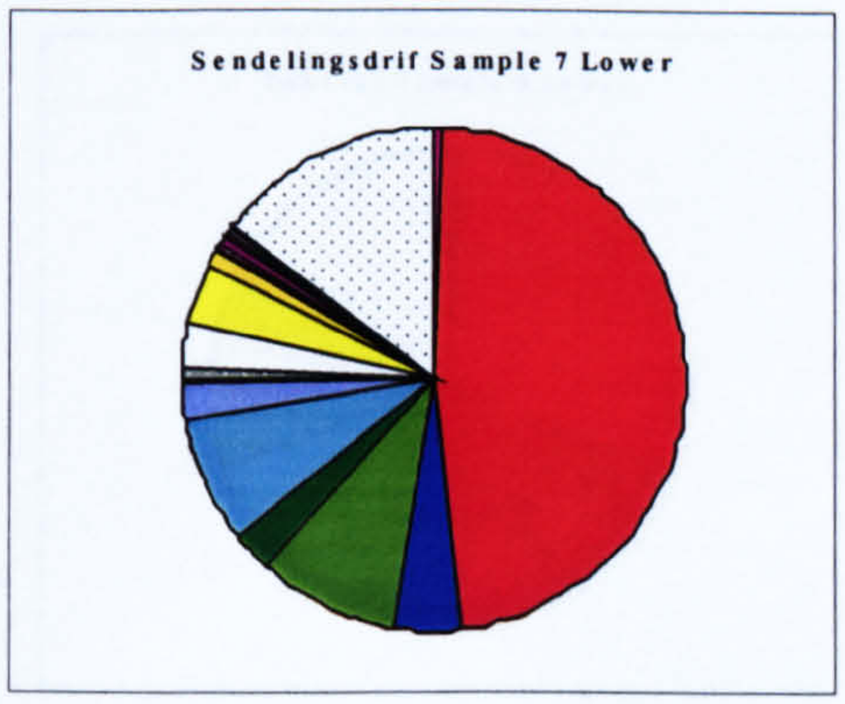

c)

Sendelingsdrif Sample 1 Lower		
	Weight (kg)	**%**
+300mm	0	0.0
-300 + 200 mm	467	10.6
-200 + 90 mm	1525	34.6
-90 +40 mm	730	16.6
-40+25mm	373	8.5
-25+14 mm	199	4.5
-14+8 mm	179	4.1
-8+3 mm	158	3.6
-3 mm	595	17.6
TOTAL	**4404**	**100.0**

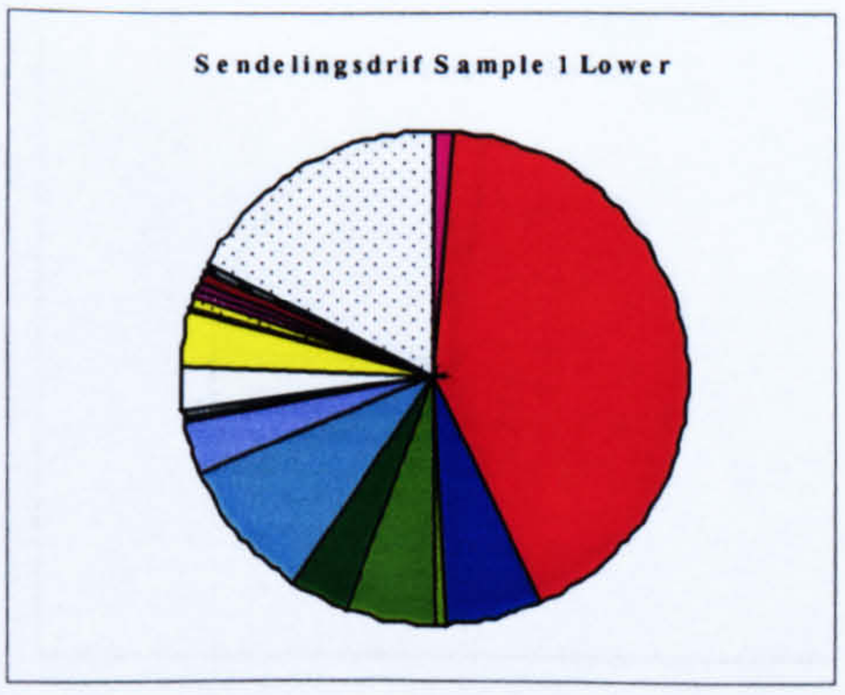

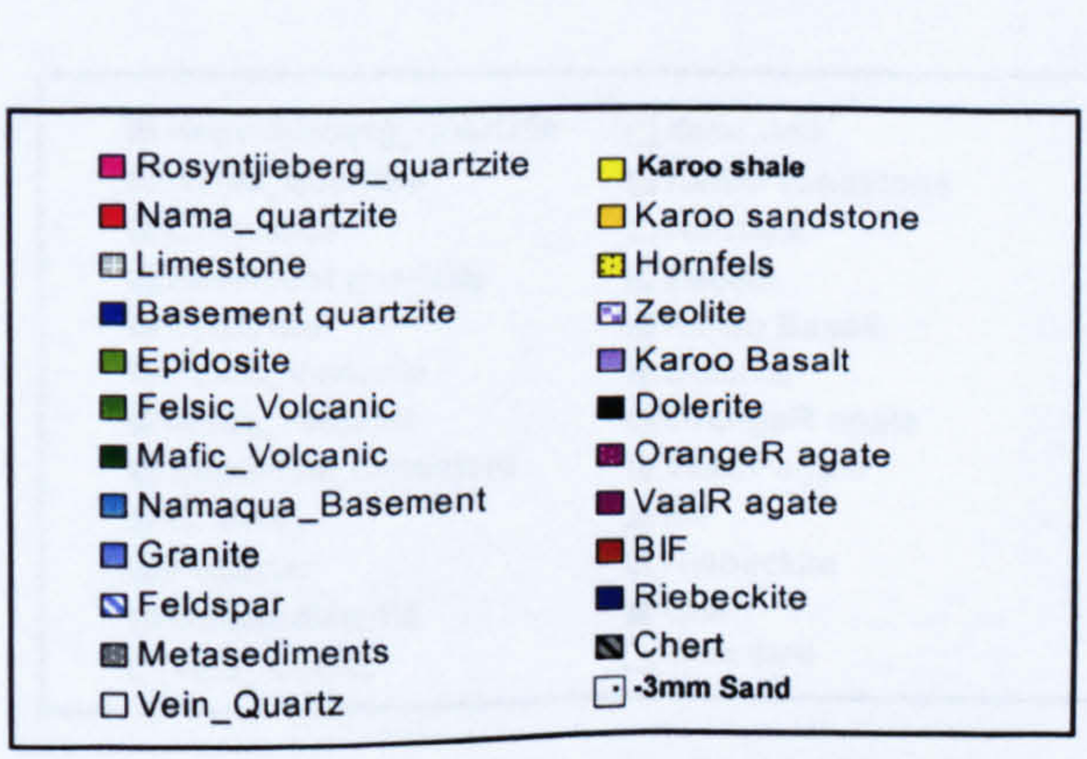

Figure 6.52 a-c Gravel composition, based on the weight percentage of gravel.

d)

Sendelingsdrif Sample 2 Lower		
	Weight (kg)	**%**
+300mm	45	0.6
-300 + 200 mm	1771	23.3
-200 + 90 mm	2920	38.4
-90 +40 mm	1022	13.4
-40+25mm	378	5.0
-25+14 mm	261	3.4
-14+8 mm	196	2.6
-8+3 mm	255	3.4
-3 mm	565	9.9
TOTAL	**7601**	**100.0**

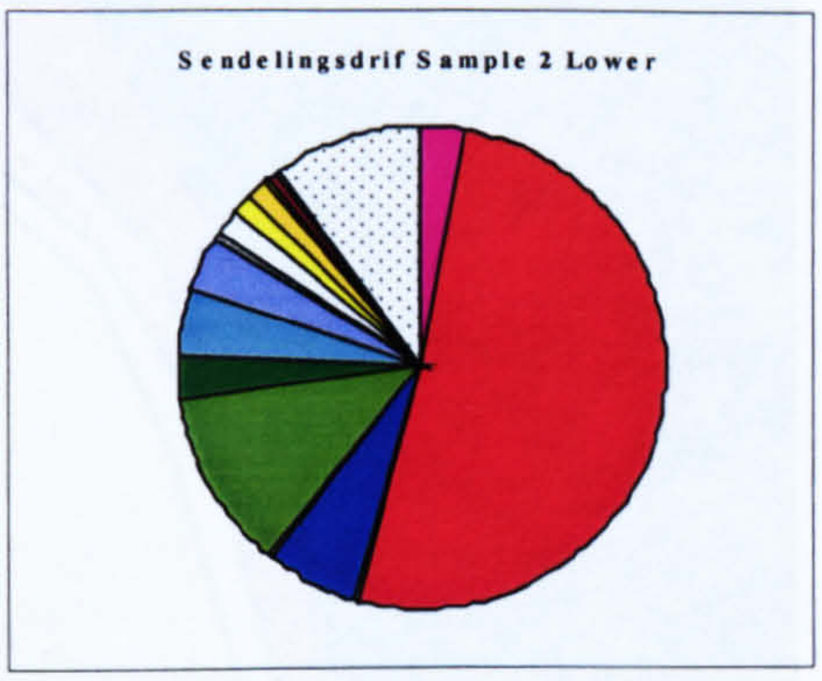

e)

Daberas Sample 4 Lower		
	Weight (kg)	**Wt. %**
+300mm	221	3.1
-300 + 200 mm	1310	18.4
-200 + 90 mm	1028	14.5
-90 +40 mm	1001	14.1
-40+25mm	748	10.5
-25+14 mm	609	8.6
-14+8 mm	514	7.2
-8+3 mm	583	8.2
-3 mm	753	15.3
TOTAL	**7102**	**100.0**

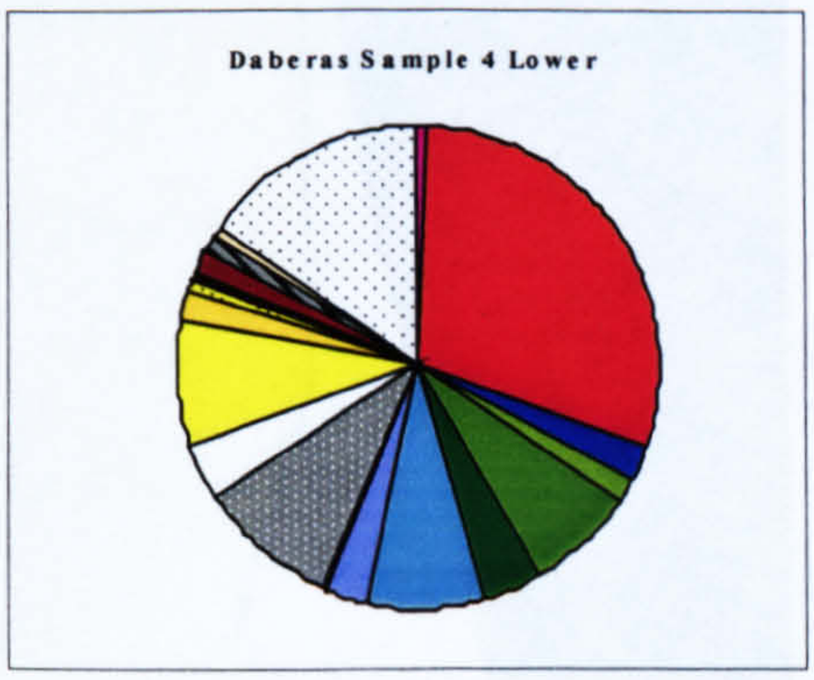

f)

Daberas Sample 9 Lower		
	Weight (kg)	**%**
+300mm	48	0.8
-300 + 200 mm	353	5.8
-200 + 90 mm	2148	35.0
-90 +40 mm	1224	19.9
-40+25mm	443	7.2
-25+14 mm	294	4.8
-14+8 mm	181	2.9
-8+3 mm	166	2.7
-3 mm	1164	20.9
TOTAL	**6138**	**100.0**

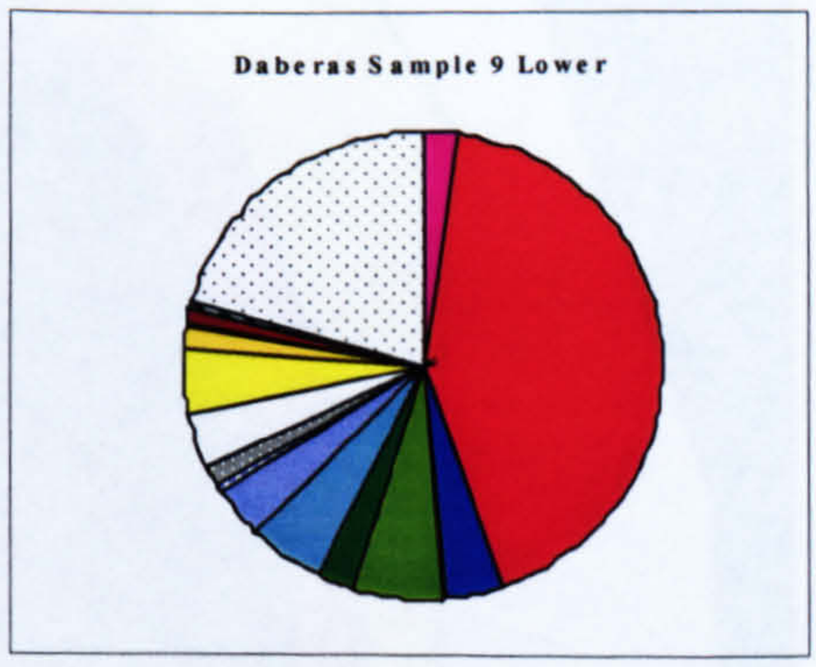

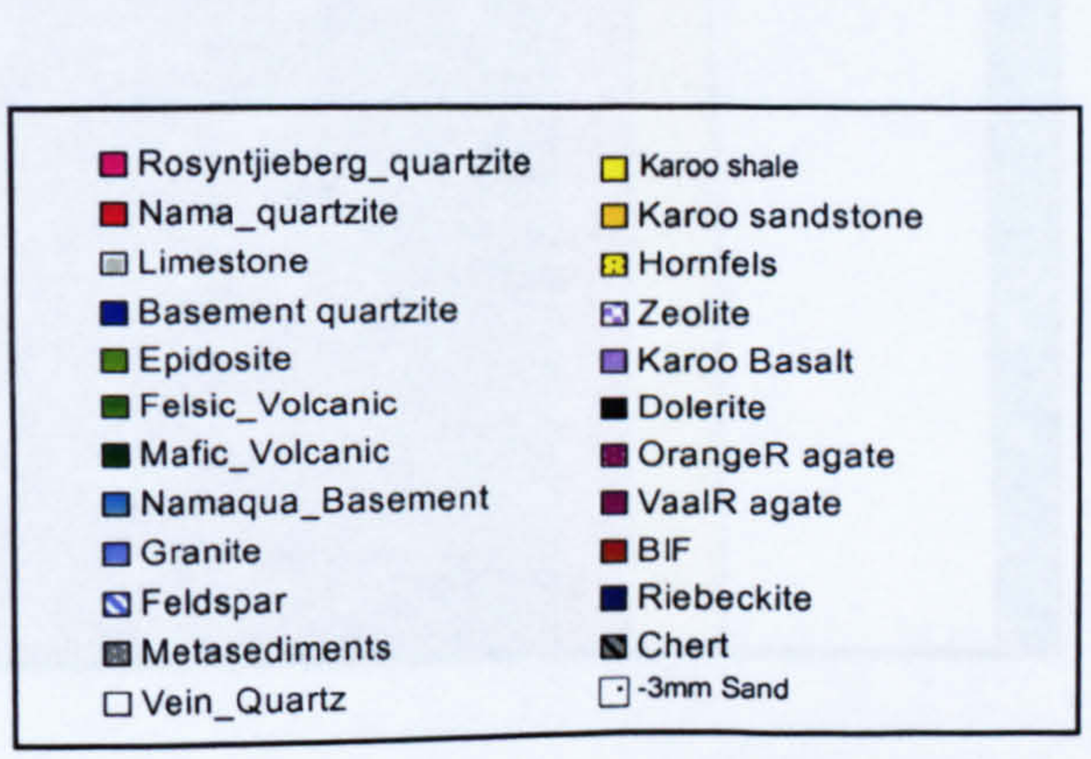

Figure 6.52 d-f Gravel composition, based on the weight percentage of gravel.

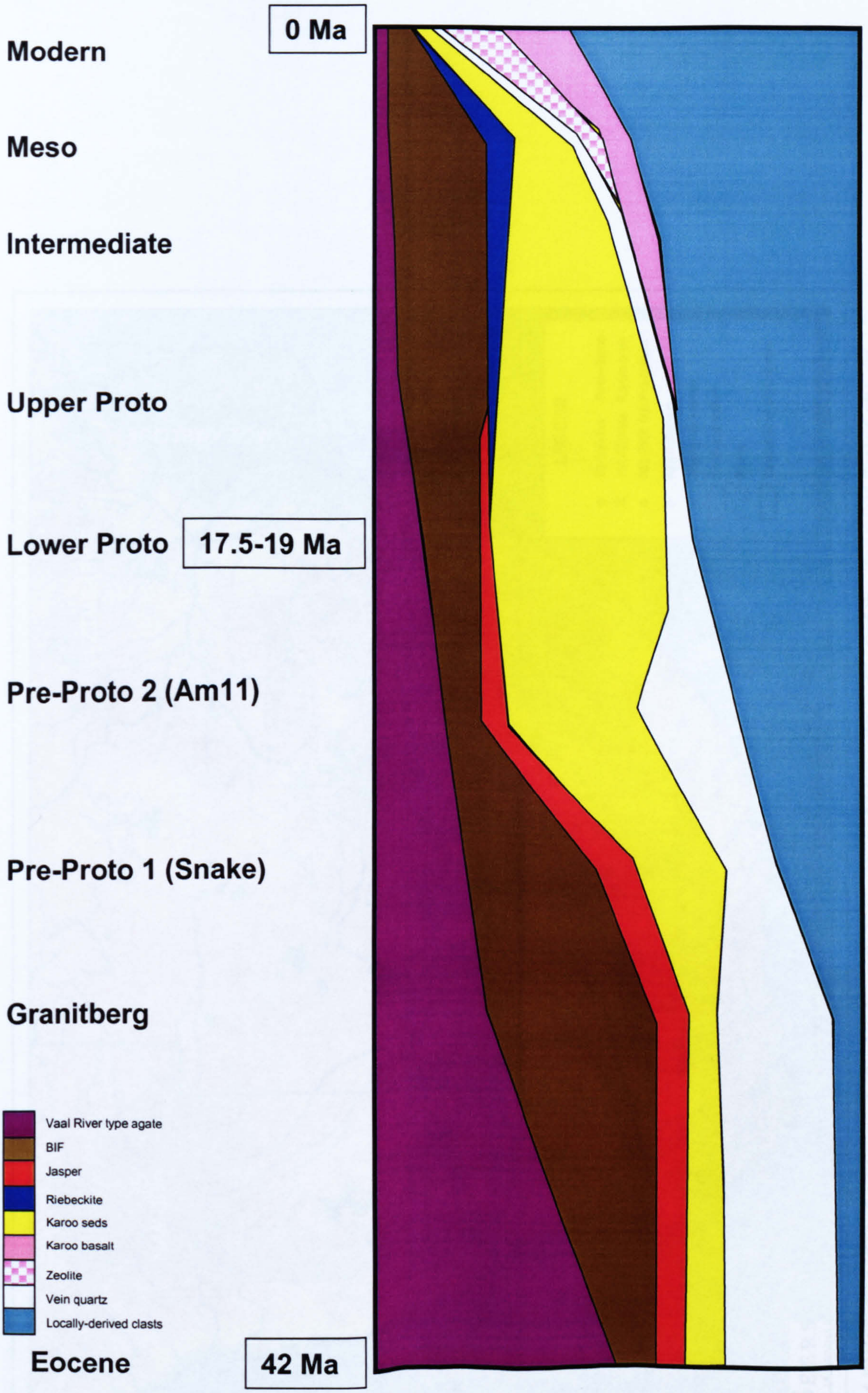

Figure 6.53 Summary of clast assemblage changes through time in the study reach.

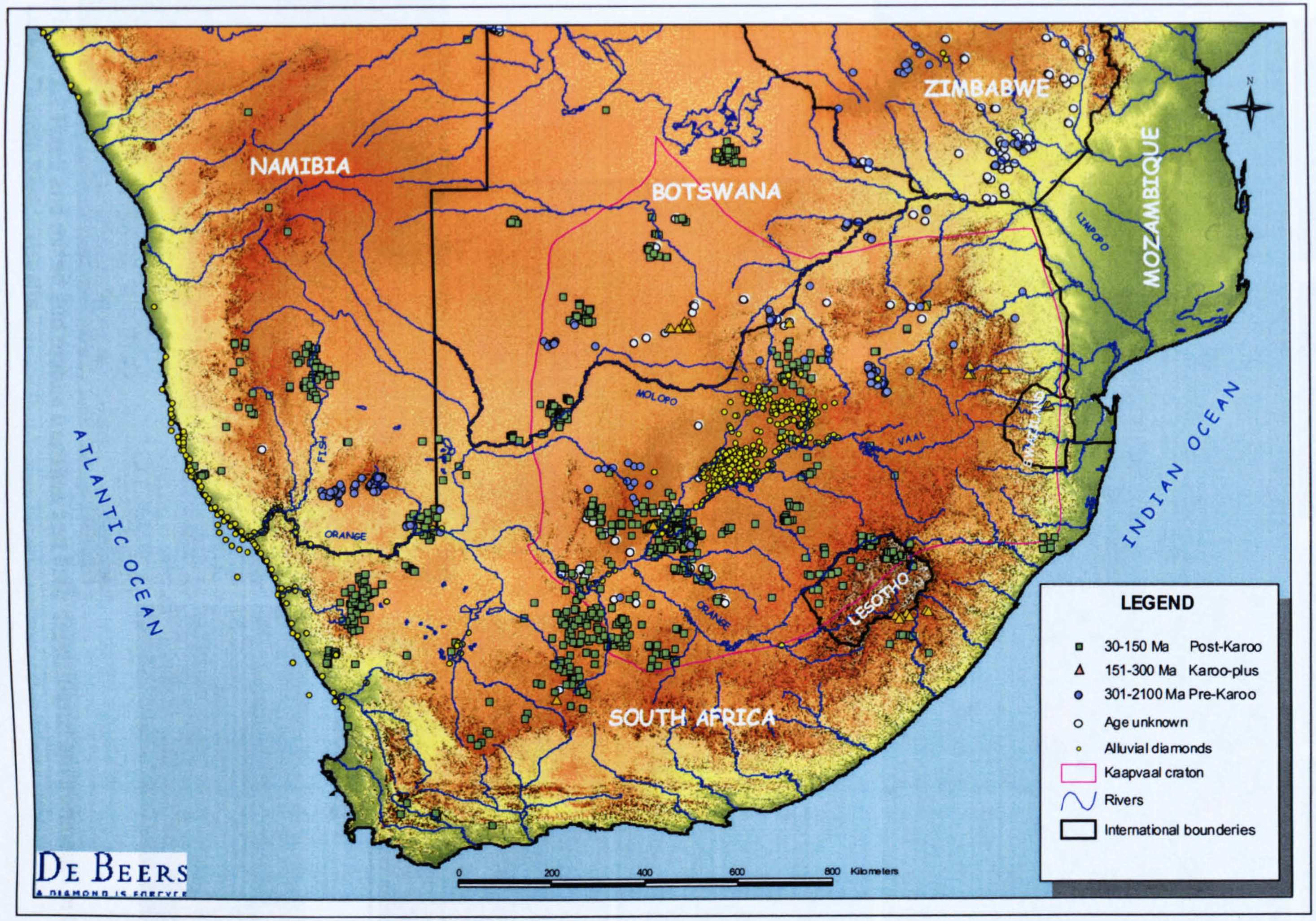

Figure 7.1 Distribution of kimberlites and alluvial deposits in southern Africa with outline of the Kaapvaal Craton shown.

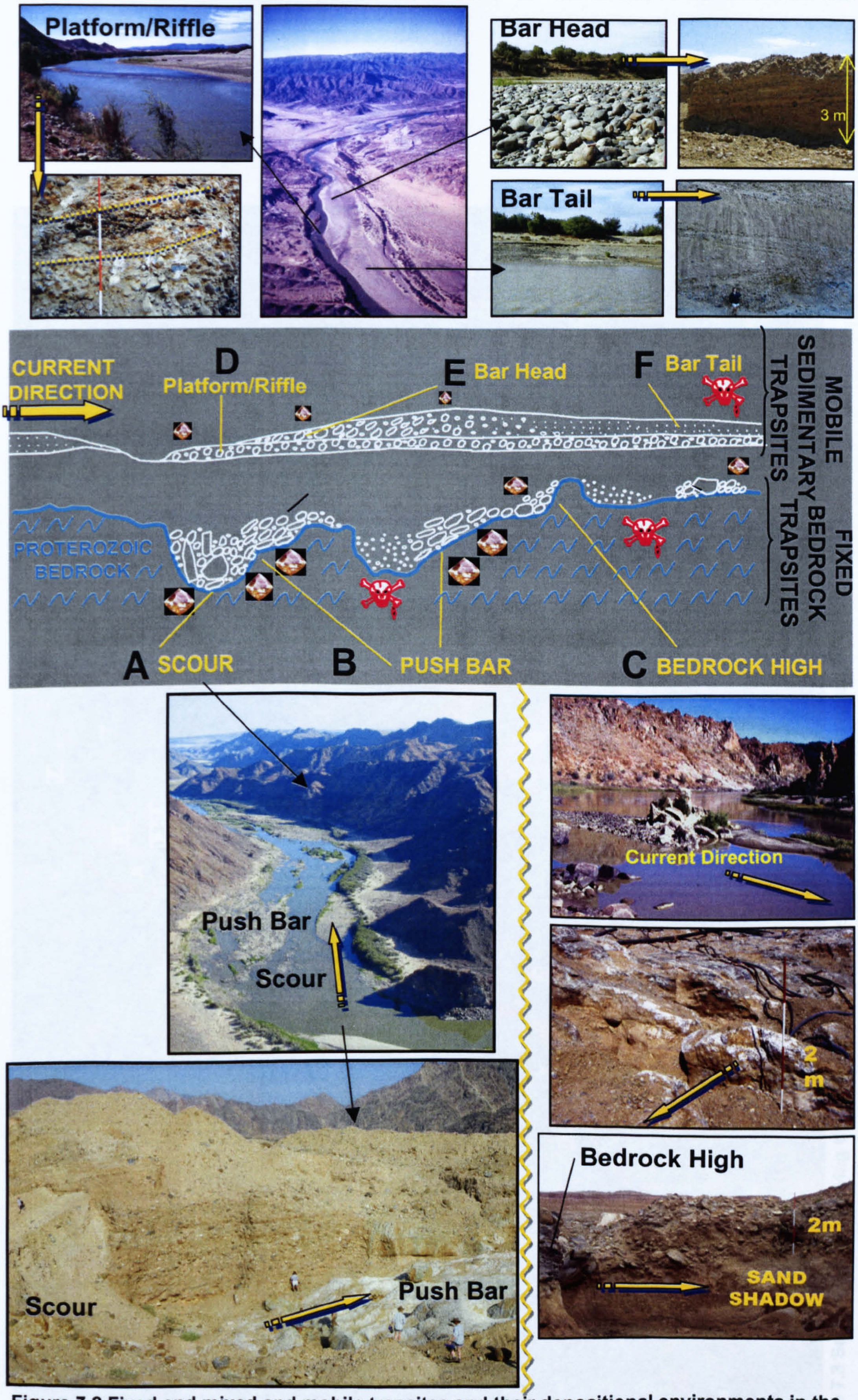

Figure 7.2 Fixed and mixed and mobile trapsites and their depositional environments in the Lower Orange River deposits.

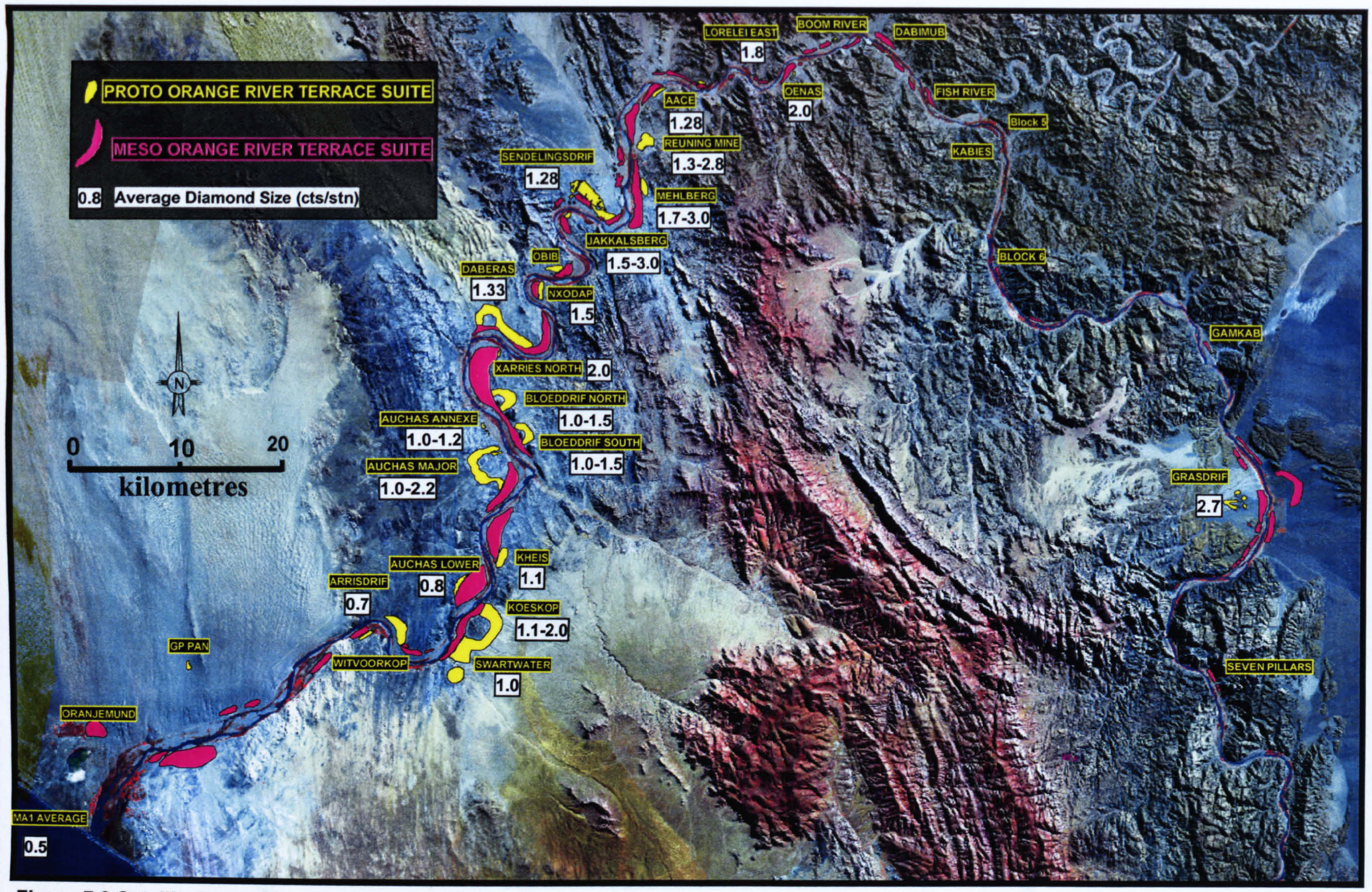

Figure 7.3 Satellite image showing the average diamond size per deposit where available.

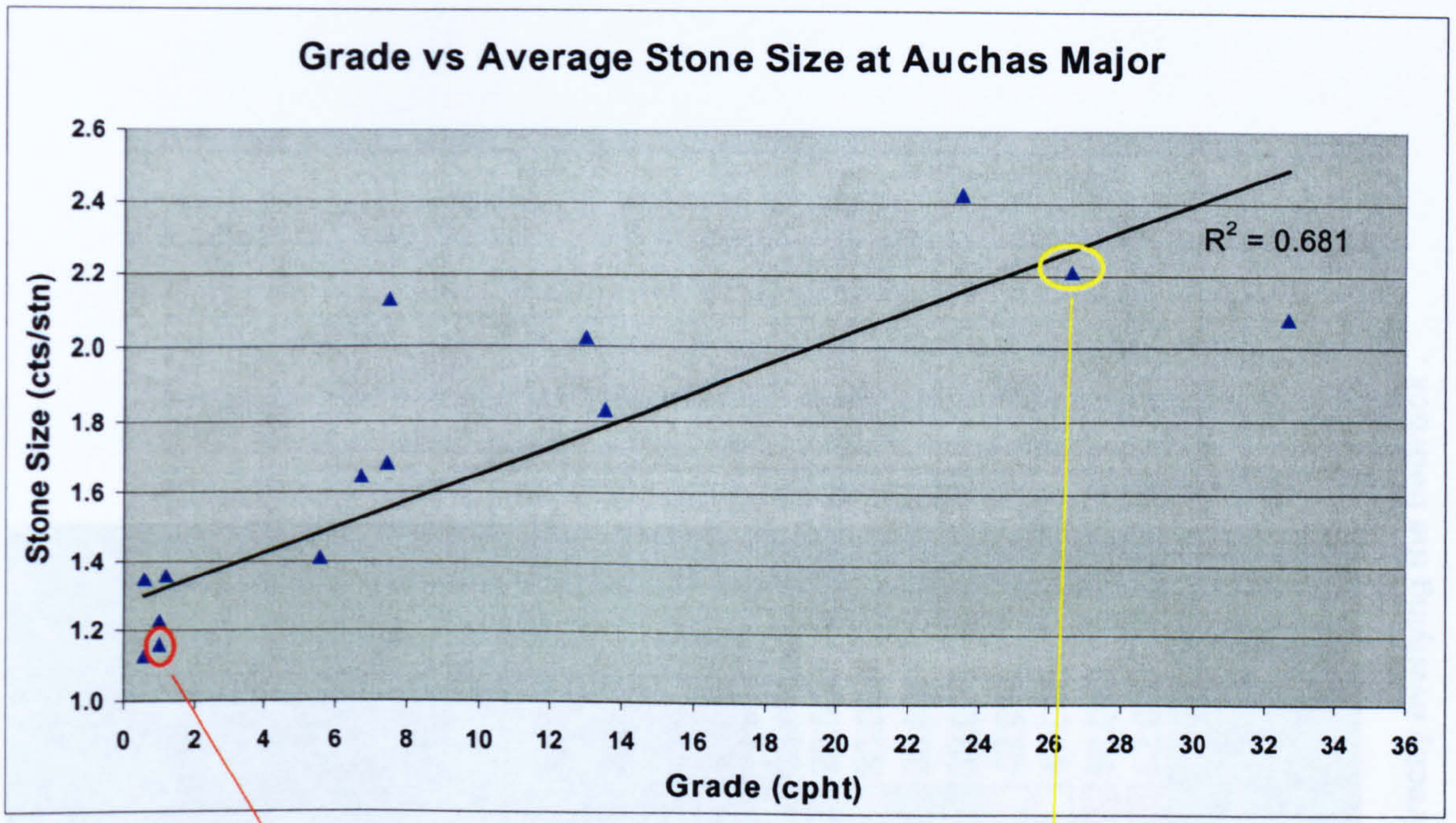

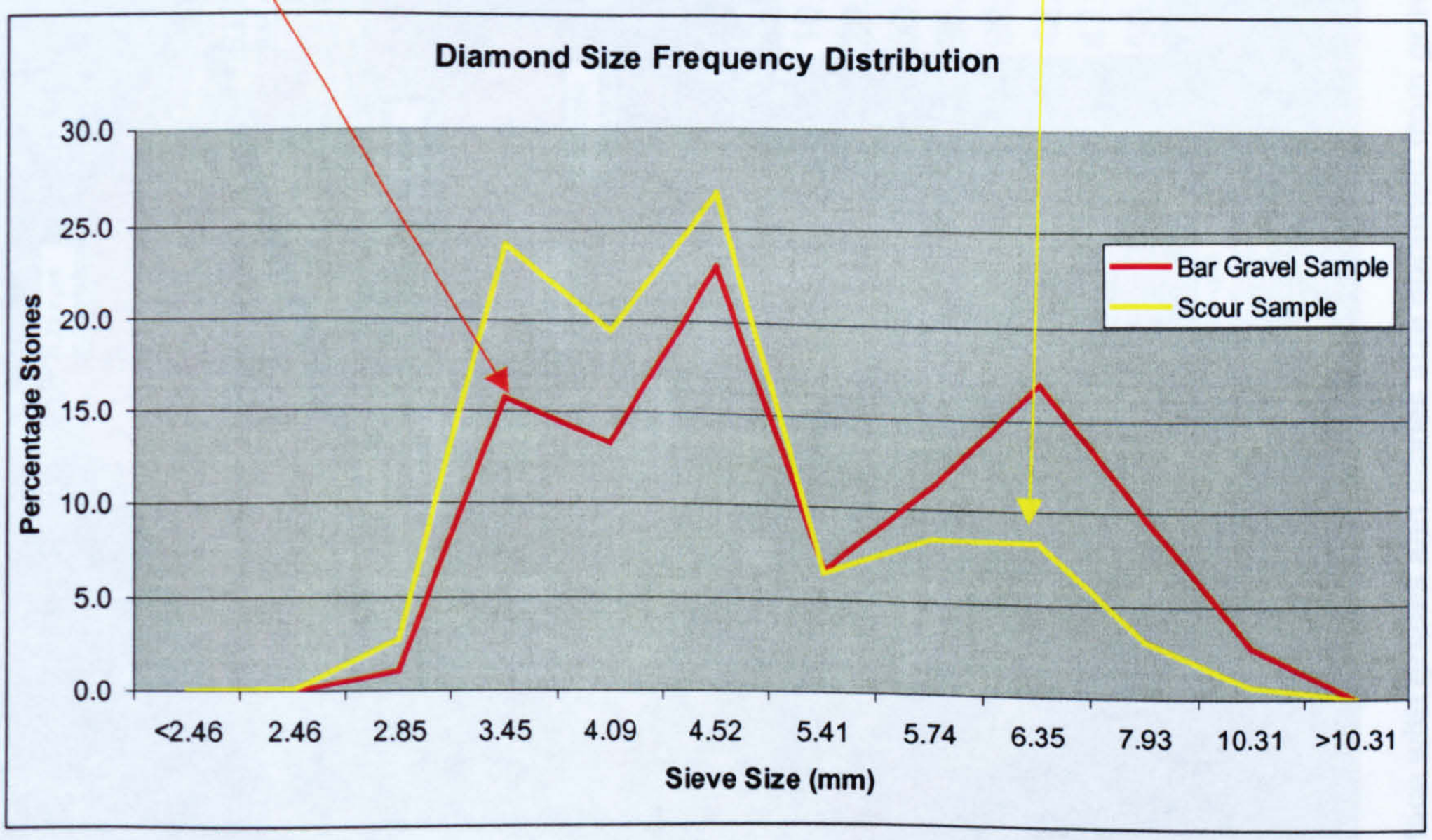

AREA	TONS	CARATS	STONES	GRADE	AVE STONE SIZE
Auchas Bar Gravel Sample	399588	4082.32	3525	**1.02**	**1.16**
Auchas Scour Sample	9884	2629.28	1191	**26.60**	**2.21**

Figure 7.4 a) Grade vs average stone size plot at Auchas Major locality. b) Size frequency distribution of Auchas bar and channel samples.

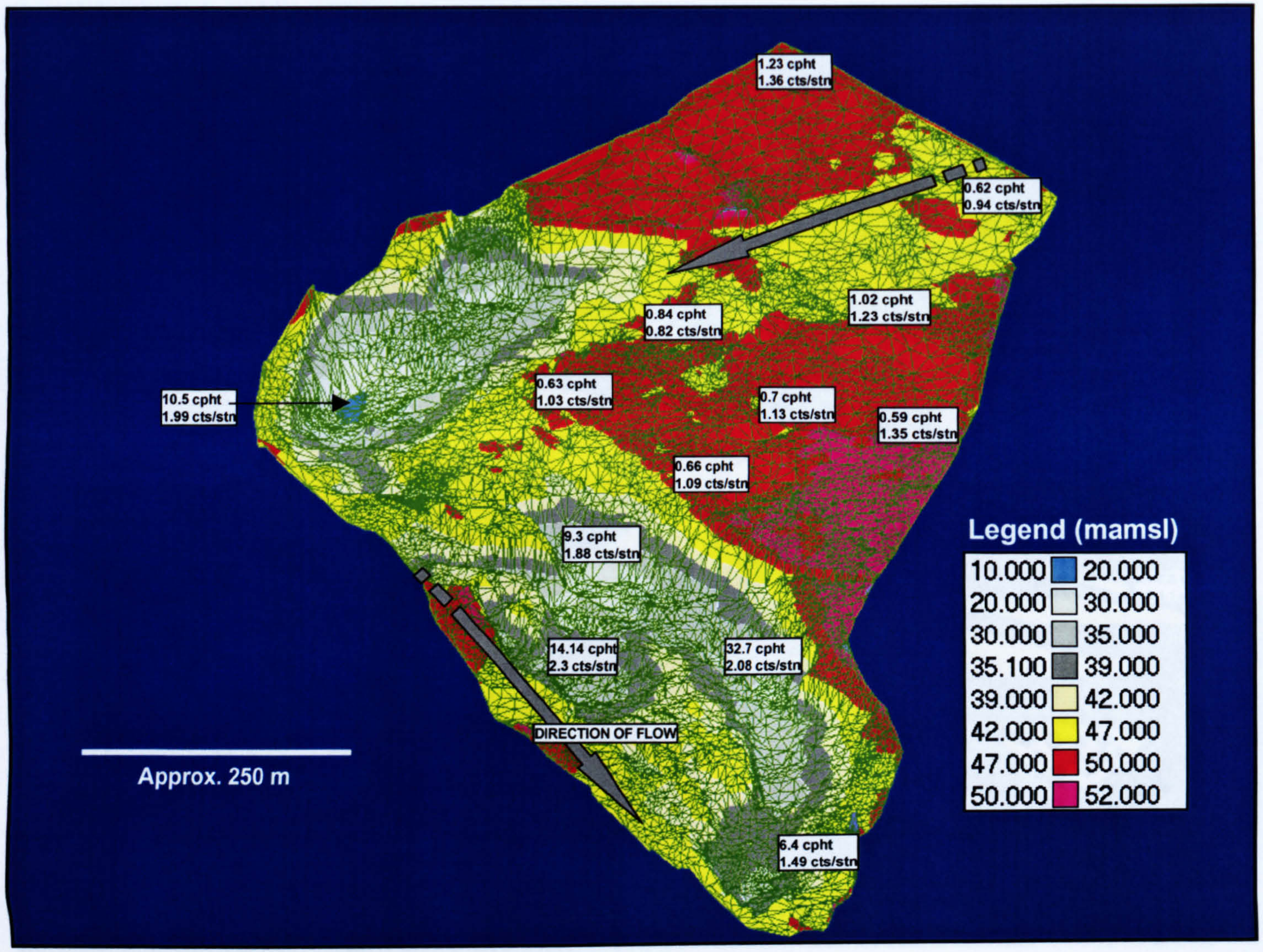

Figure 7.5 Auchas Mine actual bedrock surface with grades and stones size obtained from gravel directly overlying the bedrock .

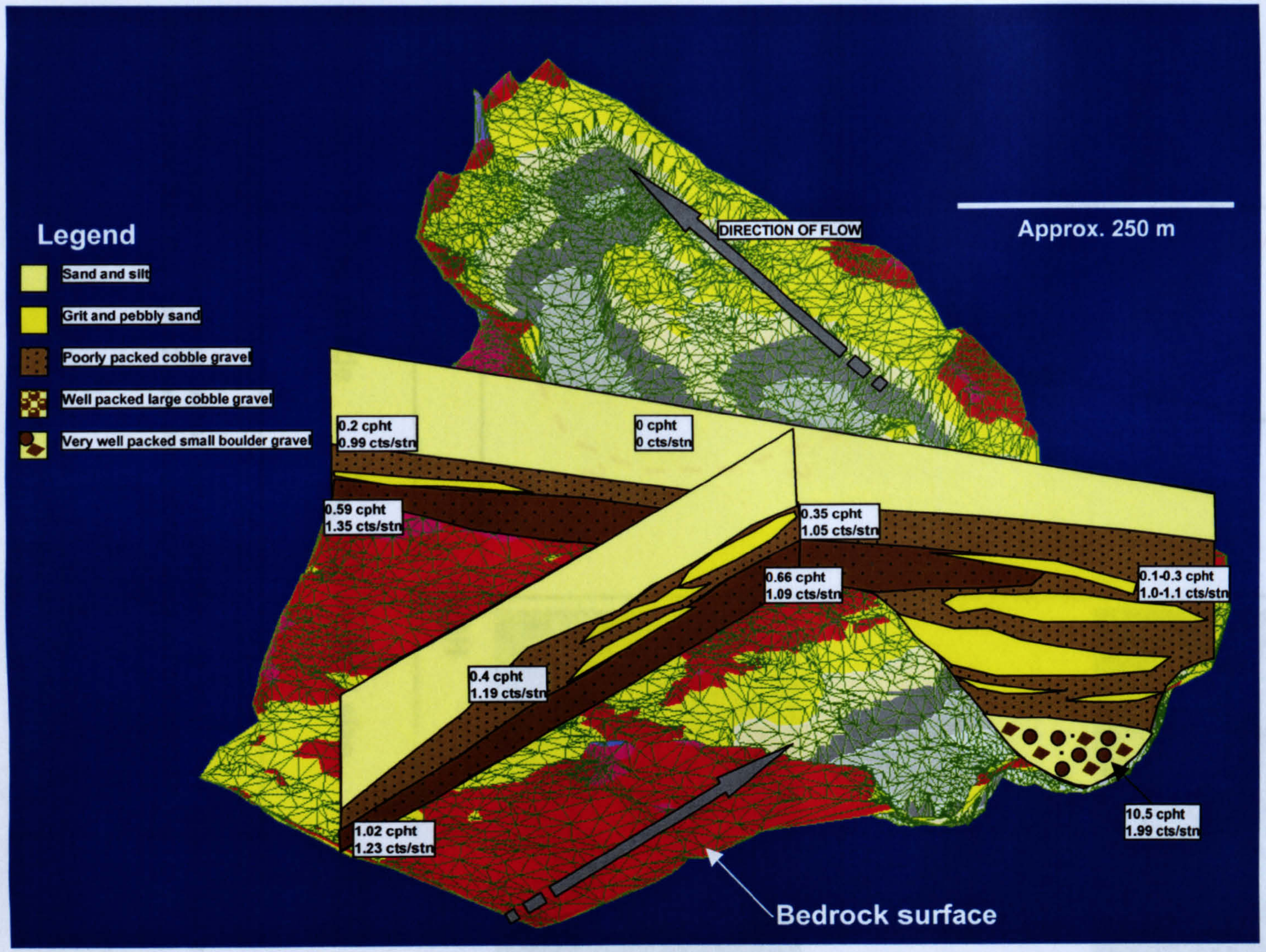

Figure 7.6 Sections through the Auchas Mine deposit showing grades obtained from mining operations in the upper units of the deposit.

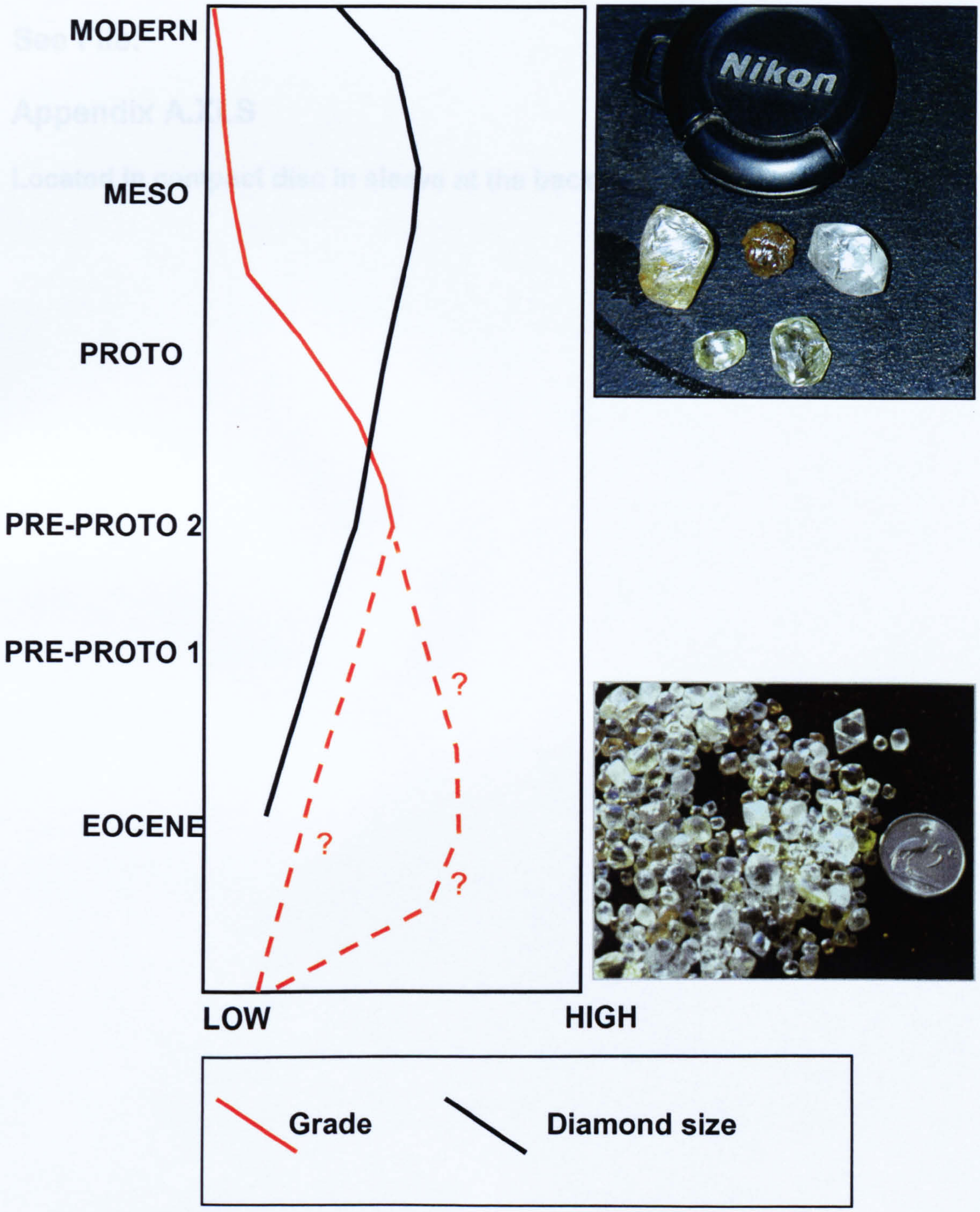

Figure 7.7 Summary of grade and stone size changes in the study area. Grade data in deposits older than Pre-Proto 2 not comparable, hence the uncertainty.

Appendix A

Surface and bottom profile survey of the modern Orange River

See File:

Appendix A.XLS

Located in compact disc in sleeve at the back cover of this volume.

Thesis contains

damaged CDs/DVDs

unable to copy

Appendix B

Terrace levels data.

DEPOSIT	Dist Along Modern Course (m)	Dist. From Mouth (m)	Dist Along Proto Course (m)	PRE-PROTO 1 Topo	PRE-PROTO 1 Bedrock Strath	PRE-PROTO 2 Bedrock Scour	PROTO Bedrock Strath	PROTO Bedrock Upper Strath	PROTO Topo	UPP MESO Bedrock Scour	UPP MESO Bedrock Strath	UPP MESO Topo	L Meso Bedrock Strath	L Meso Topo	INT Bedrock Strath	INT Topo	Proto Local Bedrock	Proto Local Topo	Meso Local Bedrock	Meso local Topo
MOUTH	277766	0.000	305590							-64										
EOCENE MA1	274706	3059.883																		
Oranjemund		5224.000	297707								10	24								
KORTDORING	267210	10555.869	293407			-39				-60	5	20								
ORV holes		12555.869																		
Skilpad			289107			-25														
GP PAN	264159	13606.883	286227			-10	24		80											
HOHENFELS	259224	18541.923	7821							-15	10	20	-6	10						
WITVOORKOP	247061	30705.506	268704																	
ARRISDRIF	243707	34059.444	264807			16	28	39	60		25	36								
SWARTWATER	234926	42839.760	257741				36		50											
KOESKOP	232293	45473.137	254258	88	80	30	40		84											
AUCHAS LOWER	231118	46648.156	249032				42		63	12	27	34	18							
KHEIS	227132	50634.272	244322																	
AUCHAS	216160	61606.086	232895			19.5	45	50	80		35	47	22.568	38.47						
BLOEDDRIF SOUTH	214355	63411.355	226252				47		83	6										
AUCAS ANNEXE	212363	65403.082	222266				45		78											
BLOEDDRIF NORTH	210913	66853.122	218815			1	47		83											
XARRIES	206985	70781.108	215570			17				14	37		25							
DABERAS	202204	75562.467	206133			15	52	57	86											
DAB MESO	198082	79684.294	7821							23	40	55								
NXODAP	189815	87950.953	197114							18										
OBIB	186295	91470.876	194201			52	59		80	27	42	65	32	57						
JAKKALSBERG	177095	100671.489	187659			47.0	68.0		84.0						55.0	70.0				
SD MESO SCOUR	177095	100671.489	7821.000							6.0										
SD Scours	176383	101383	185802			34.0		70.0												
SENDELINGSDRIF	174730	103036	182448	107.5	104.0		63.0	77.0	91.0		46.0	60.0								
SUIDHEK	171023	106743	7821							-0.6			38.0	50.0						
MEHLBERG	167949	109818	176411			52.0	67.0	70.0	82.0	15.2	49.0	58.0	40.0	50.0						
DREIGAT	166322	111444	173395			47.0	60.0			15.0	48.0	64.0	37.0	50.0						
REUNING	163937	113829	169363			43.0	72.0	90.0	110.0	37.7	48.0	59.9								
DREIGRATDRIF	162506	115260	7821							4.6			41.0	50.5						
VLIEGVELD	160664	117102	7821							33.6	45.0	58.0								
AACE	156913	120853	164468				86.0	90.0	105.0	25.8	50.0	58.0			65.0	77.2				
Lorelei West Downstream	155687	122079	7821								56.1	63.1								
LORELEI WEST	152718	125048	160485				86.2	92.0												
LORELEI WEST INT UPSTREAM	151881	125885	7821												62.1	76.0				
SWARTPOORT	149966	127800	7821												73.0	84.0				
LORELEI EAST DOWNSTREAM	148889	128877	7821											51.7						
LORELEI PREPROTO	148498	129268	155859			50.3	65.9		79.4											
LORELEI EAST MESO	147854	129912	7821										51.4	59.9						
ZEBRASFONTEIN PROTO LOCA	147456	130311	154339														115.9	106.7		
WITKOP	147456	130311	154339			74.9	87.1												73.1	78.1
MACLEKOP	146245	131521	153618					99.8											62.9	78.1
OENAS T2	142664	135103	150255			82.0	93.0		112.0											
BOOM RIVER MESO	138397	139370	7821								64.1	84.7								
BOOM RIVER PROTO	137918	139848	145739				101.8	106.4	126.8											
BOOM PROTO LOCAL	136274	141492	144095														134.0	145.6	78.4	88.2
SANDBERG	136274	141492	144095																	
DABIMUB MESO	134330	143437	142151										58.8	68.9						
FISHPLANT MESO	127764	150002	135585							60.9	69.3	74.0	60.9							
Fish Plant Upstream	126556	151210	134377								71.1	75.0								
BLOCK 5	120293	157473	128114								74.8	81.5								
BLOCK 6 Downstream	109248	168518	117069								89.5	93.5								
BLOCK 6 Mid	107774	169993	115595								85.1	94.8								
BLOCK 6 Mid Upstream	107148	170618	114969								88.1	95.0								
Site B downstream	103677	174089	111498																	
SITE B	102513	175253	110334								91.5	97.2								
GAMKAB	84218	193548	92039								105.2	117.7								
KWARTJIE	74982	202784	82803				189.2		194.6											
Proto Remnant	73307	204459	81128				205.0		213.4											
AUSENKEHR MESO	72048	205718	79869								100.0	112.1								
K Terrace	72048	205718	79869								105.0	124.9								
I terrace	69235	208531	77056								106.0	119.5								
AUSENKEHR INTERMEDIATE	68764	209002	76585												134.0	141.0				
GRASDRIF PROTO	68446	209320	76267				186.9		199.9											
F Terrace	67038	210728	74859								108.0	122.7								
GRASDRIF INTERMEDIATE	66587	211179	74408				165.2		176.7						165.2	176.7				
E Terrace	66008	211758	73829								111.0	125.9								
D Terrace	64338	213428	72159										112.2	119.8						
C TERRACE	63237	214529	71058								120.3	129.6								
B Terrace	62534	215232	70355								117.8	131.5								
SEVEN PILLARS	46443	231323	54264								139.0	146.6								
Sambok Ext	43055	234711	50876								149.0	153.5								
FELIX MESO	715	277051	8536								169.2	173.5								
MODDERDRIF MESO	-2196	279962	5625								180.3	186.3								
NOORDOEWER PROTO	-7821	285587	0				221.0		227.3		178.0	184.0								
NOORDOEWER MESO	-10247	288013										173.3								
STOLZENFELS KIMBERLITE		597849			555.0															
Daberas Modern		629557																		
DABERAS UPSTREAM POTHOLES		632946				528.0	528.0		533.0											
AUGRABIES MESO		713537								661.0	661.0	663.0								
RENOSTERKOP		715468				677.0	677.0		683.0	657.0	657.0	664.0								

Appendix C

Maximum clast size dataset

See File:

Appendix C.XLS

Located in compact disc in sleeve at the back cover of this volume.

Appendix D

Clast assemblage with grain size data

Table 1

See Files:

Figures 1-78 (see files "Appendix D Figs 1-78.ppt")
For individual pictures and clast assemblages of samples.

and

"Appendix D Data.XLS"
for raw data from all samples.

Located in compact disc in sleeve at the back cover of this volume.

Table 1 Position of clast assemblage samples.

	SAMPLE NAME	LAT	LONG
	EOCENE		
1	EOCENE MA1	-28.583200	16.413750
2	GRANITBERG EOCENE	-27.340673	15.383192
3	B10 AREA	-27.385949	15.421636
4	BUNDFELDSCHUH	-27.588552	15.569658
	PRE-PROTO 1		
5	SNAKE	-28.162520	16.871820
	PRE-PROTO 2		
6	LORELEI PUSH BAR LOWER	-28.056370	16.984550
9	AM11 LOWER	-28.367280	16.772360
	PROTO		
7	DREIGAT PROTO (PUSH)	-28.139540	16.875680
8	SENDELINGSDRIF SAMPLE 5 LOWER	-28.152940	16.855170
11	NOORDOEWER PROTO SOUTH	-28.723300	17.632233
12	NOORDOEWER PROTO NORTH	-28.721000	17.629111
13	GRASDRIF PROTO LOWER	-28.384528	17.384917
14	GRASDRIF PROTO UPPER	-28.384867	17.384783
15	BOOM PROTO LOCAL	-28.029370	17.070230
16	BOOM PROTO LOWER	-28.037972	17.060583
17	BOOM PROTO UPPER	-28.038222	17.061889
18	MACLEKOP PROTO	-28.069070	16.999570
19	ZEBRASFONTEIN PROTO LOCAL	-28.064240	16.995500
20	LORELEI PUSH BAR UPPER	-28.056500	16.984990
21	LORELEI WEST PROTO	-28.072090	16.948860
22	SENDELINGSDRIF SAMPLE 1 LOWER	-28.163445	16.867843
23	SENDELINGSDRIF SAMPLE 5 UPPER	-28.152680	16.855340
24	SENDELINGSDRIF SAMPLE 7 LOWER	-28.147058	16.849513
25	SENDELINGSDRIF SAMPLE 8 UPPER	-28.149930	16.847890
26	DABERAS SAMPLE 4 LOWER	-28.265400	16.800150
27	DABERAS SAMPLE 4 UPPER	-28.264220	16.799450
28	DABERAS SAMPLE 9 LOWER	-28.258710	16.795991
29	DABERAS SAMPLE 9 UPPER	-28.258540	16.793340
30	DABERAS OUTLET	-28.248640	16.764890
31	AM59 LOWER	-28.365050	16.767140
32	AM59 UPPER	-28.364980	16.766920
33	AM 11 UPPER	-28.366880	16.772000
34	AUCHAS LOWER PROTO LOWER	-28.442580	16.750580
35	AUCHAS LOWER PROTO UPPER	-28.443010	16.751090
36	ARRISDRIF PROTO LOWER	-28.476360	16.706050
37	ARRISDRIF PROTO UPPER	-28.473930	16.702710
	INTERMEDIATE		
38	AUSENKEHR SAMPLE	-28.377440	17.429870
39	GRASDRIF INTERMEDIATE	-28.396500	17.397917
40	LORELEI WEST INTERMEDIATE UPPER	-28.073860	16.948840
41	LORELEI WEST INTERMEDIATE LOWER	-28.074110	16.945000
42	SENDELINGSDRIF SAMPLE 2 LOWER	-28.163807	16.861259
	MESO		
43	NOORDOEWER MESO	-28.690667	17.552889
44	SEVEN PILLARS MESO	-28.517560	17.373230
45	GRASDRIF MESO LOWER	-28.421500	17.393267
46	GAMKAB MESO UPPER	-28.264270	17.361790
47	GAMKAB MESO LOWER	-28.264530	17.361350
48	BLOCK 6 MESO UPPER	-28.212833	17.188278
49	BLOCK 6 MESO LOWER	-28.212806	17.187417
50	BLOCK 5 (KJ TERRACE)	-28.105790	17.195310
51	FISH PLANT MESO UPPER CHANNEL	-28.084030	17.134270
52	FISH PLANT MESO LOWER CHANNEL	-28.084710	17.133480
53	DABIMUB MESO LOWER	-28.036350	17.093790
54	BOOM MESO UPPER	-28.040889	17.055528
55	BOOM MESO LOWER	-28.040972	17.057333
56	LORELEI EAST MESO LOWER	-28.062700	16.988170
57	LORELEI EAST MESO UPPER	-28.062920	16.988630
58	LORELEI WEST MESO	-28.062650	16.921620
59	DABERAS MESO LOWER	-28.271770	16.815310
60	DABERAS MESO UPPER	-28.270930	16.815000
61	AUCHAS OUTLET MESO TRENCH (AMOT)	-28.371330	16.782730
62	AUCHAS LOWER MESO	-28.457890	16.747250
63	ARRISDRIF MESO	-28.493190	16.710760
64	ARRISDRIF YOUNG TERRACE	-28.495500	16.709660
65	FD TRENCH	-28.555780	16.453080
66	ED1	-28.576320	16.407780
67	BROWN PLEISTOCENE IN EOCENE PIT	-28.583200	16.413750
	MODERN		
68	SEVEN PILLARS MODERN	-28.542264	17.376667
69	ENTRANCE BAR	-28.244950	17.271770
70	CUTTING	-28.312810	17.375030
71	OENAS RAPID BAR	-28.052470	17.029660
72	LORELEI WEST MODERN	-28.068950	16.923780
73	SENDELINGSDRIF MODERN	-28.165180	16.886980
74	AUCHAS MODERN	-28.359020	16.808770
75	ARRISDRIF MODERN	-28.502110	16.710570
	UPSTREAM		
10	RENOSTERKOP PROTO	-28.678410	20.455190
76	RENOSTERKOP MESO	-28.684667	20.451556
77	DABERAS UPSTREAM	-28.453000	19.935583
78	STOLZENFELS KIMBERLITE	-28.504389	19.656222

GLASGOW
UNIVERSITY
LIBRARY